RTA

ISSN 1932-2321

JOURNAL IS REGISTERED IN THE LIBRARY OF THE U.S. CONGRESS

RELIABILITY: THEORY & APPLICATIONS

INTERNATIONAL GROUP ON RELIABILITY

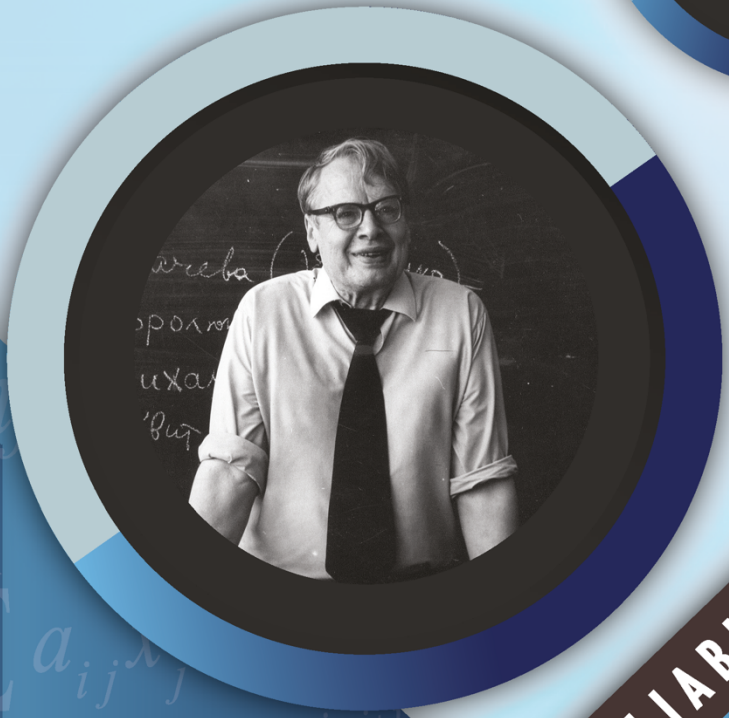

RELIABILITY
RISK ANALYSIS
MAINTENANCE
SAFETY

GNEDENKO FORUM PUBLICATIONS

#3

(69) VOL.17

SEPTEMBER

2022

SAN DIEGO

ISSN 1932-2321

http://www.gnedenko.net/Journal/index.htm



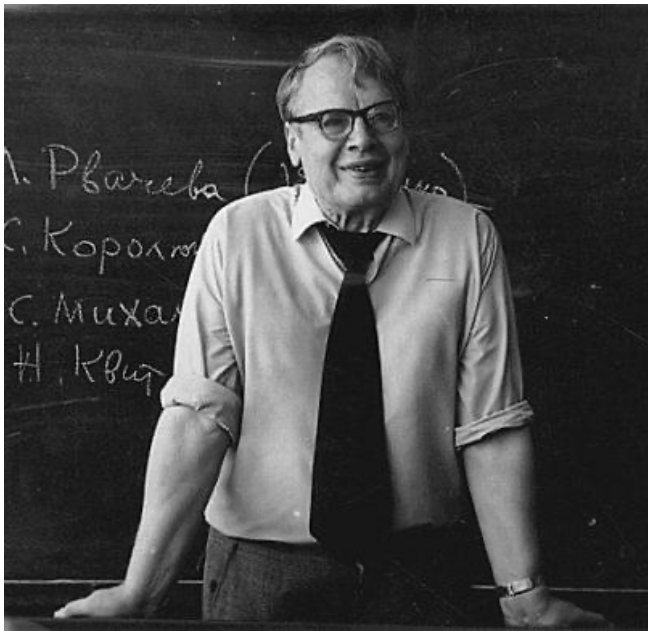

RELIABILITY:

THEORY & APPLICATIONS

Vol.17 No.3 (69),
September 2022

San Diego
2022

Editorial Board

e-Journal ***Reliability: Theory & Applications*** publishes papers, reviews, memoirs, and bibliographical materials on Reliability, Quality Control, Safety, Survivability and Maintenance.

Theoretical papers must contain new problems, finger practical applications and should not be overloaded with clumsy formal solutions.

Priority is given to descriptions of case studies.
General requirements for presented papers

1. Papers must be presented in English in MS Word or LaTeX format.
2. The total volume of the paper (with illustrations) can be up to 15 pages.
3. A presented paper must be spell-checked.
4. For those whose language is not English, we kindly recommend using professional linguistic proofs before sending a paper to the journal.

The manuscripts complying with the scope of journal and accepted by the Editor are registered and sent for external review. The reviewed articles are emailed back to the authors for revision and improvement.

The decision to accept or reject a manuscript is made by the Editor considering the referees' opinion and considering scientific importance and novelty of the presented materials. Manuscripts are published in the author's edition. The Editorial Board are not responsible for possible typos in the original text. The Editor has the right to change the paper title and make editorial corrections.

The authors keep all rights and after the publication can use their materials (re-publish it or present at conferences).

Publication in this e-Journal is equal to publication in other International scientific journals.

Papers directed by Members of the Editorial Boards are accepted without referring.
The Editor has the right to change the paper title and make editorial corrections.

The authors keep all rights and after the publication can use their materials (re-publish it or present at conferences).

Send your papers to Alexander Bochkov, e-mail: a.bochkov@gmail.com

Table of Contents

In Memoriam: Nozer D. Singpurwalla

(1939-2022)

•

Editorial

Nozer D. Singpurwalla died on July 22, 2022 at his home in Washington, DC, surrounded by family. We, the Advisory Board of the Gnedenko Forum, were astonished, deeply sad and broken from the news about the loss of our dear colleague and friend Nozer Singpurwalla. And we are sure, the same feelings share the entire world of probability specialists, statisticians, applied statisticians, Bayesians, reliability researchers, and everyone who new him, ever met or read his works.

Nozer was born in Hubli, India. As a young man, he immigrated to the United States, where he obtained a M.S. in Engineering from Rutgers University, and a Ph.D. in Engineering from New York University. He met Norah Jackson, who had recently immigrated from England, at a dance at Disneyland, and they married in 1969. Nozer and Norah lived most of their married life in Arlington, Virginia, where they raised their two children, Rachel and Darius. Nozer had a curious and creative mind and took much pleasure in his long and happy career as an academic. He spent most of his career at The George Washington University, where he was Distinguished Research Professor and Professor of Statistics. He published a wide variety of books and articles focusing on reliability theory, Bayesian statistics, and risk analysis. He supervised many PhD students and received numerous professional awards, including recognitions as a Fellow of the Institute of Mathematical Statistics, the American Statistical Association, and the American Association for the Advancement of Science, and an Elected Member of the International Statistical Institute. Nozer had a way with words and always enjoyed a spirited debate. He loved classical music, history and politics, and world travel with his family. He is survived by his wife, Norah (née Jackson), his sister, Khorshed Tantra, and her family, his children, Rachel (Peter) and Darius (Jennifer), and his beloved grandchildren, Veronika and Cyrus. There will be a private family memorial in his honor.

Nozer Singpurwalla has been the President of the Gnedenko Forum from 2011 to 2012. During his tenure here, Nozer expressed himself as a delightful person. He showed his wide range of interests, a great sense of humor, and wonderful interpersonal skills. It was always a joy for us to get together with him, discuss and collaborate. Nozer has been very active in the Gnedenko Forum and our academic journal RTA. With his direct participation, meetings were organized with the leadership of the City University of Hong Kong, the president of Way Kuo. The meetings were held in Moscow. We discussed the journal's development strategy, the expansion of contacts among the Gnedenko Forum participants, and the attraction of new participants. Nozer's position has always been distinguished by now Secretary A. Bochkov: "…met him, I was always amazed at his erudition. I do not agree with everything about the concept of risk he developed, but his conversations and

correspondence on this subject made me think about a lot and certainly enriched me".

Every one of us at Cnedenko Forum has great memories about Nozer. Here are the memories shared by the current president of the Gnedenko Forum Dimitrov Boyan: "…me cannot resist to share some if my memories about Nozer. I knew about him long before we met, from Richard Barlow at a meeting in Germany in 1978. We talked about Bayesian approach in statistics, and Barlow then recommended me to talk about this with Noser Singpurwalla. And I met Noser first time ay another ASA International Conference at Oakland University in Michigan. At the end we were seating (12 participant's) on a round table. Nozer was impressive, center of the discussion, making fun of every situation. During his tenure as a Gnedenko Forum Presidency we started a discretion about probability distributions in reliability with periodic failure rates. He said that "such animal" in reliability does not exist. I was well prepared and showed him some examples. He understood and agreed. I believe, since then he started respect me and we started regular communications. These distributions are named Almost Lack of Memory distributions and are used in many applications.

Maybe for this reason Nozer took part in our Flint International Conference (FISC) at Kettering University in the Year of Statistics 2014. I remember his immediate and natural reactions. For instance, when our former colleague Ernest Fokoue (professor of RIT) finished his expiration talk, Nozer exploded: "How you could lose such igniting teacher? If I was you, I immediately would try to bring him back with double the wage he has now there."

At the end we organized a party in our backyard (49 participants from US, Canada, UK, Spain, Germany, Italy, France, South Africa, Bulgaria, Moldova). Nozer was here, with us, and we all enjoyed his attendance. I cannot ever forget that event. We periodically shared news between us. Last our correspondence dates December 26, 2-21. I miss him a lot".

Everybody, who knew Nozer Singpurwalla in live may write interesting things from these meetings. We excerpt just some of thoughts written about Nozer, without showing the authors:

"…I knew Nozer more than 30 years. He was a hilarious, smart, cooperative, sincere friend. We exchanged ideas and results all the time. I cannot believe, Nozer is not with us anymore".

"…I was very saddened to read the news that Nozer had passed away. I met Nozer in the 1990's and I have always treasured the two-day visit that he made to my department. I remember him as energetic, supportive, optimistic, full of zeal and energy, simply a wonderful guy, and I wish I had kept in touch with him more often. I learnt much from him".

"…Nozer and I crossed swords in intellectual discussion more than once and ask one point he indicated that he wasn't sure what I thought of him. I replied, "When I signed up for a second

doctoral seminar with you, that should have answered the question." As often happens, we found a basis for friendship in acquiring a few enemies in common. A great and good man".

"…I just got the news and am deeply saddened. Nozer was a prolific scholar and a great mentor to his students. He put me on the right academic path and remained a friend who was always ready to meet over a glass of wine. In later years his energy and enthusiasm were an inspiration".

MSU, conference dedicated to the 100th anniversary of the birth of B.V. Gnedenko (26-30.06.2012).

"…We met in one of Nozer's reliability classes and were reconnected with each other when both of us were working on our dissertations with Nozer. He never claimed credit for being our matchmaker, but we are grateful for his efforts 32 years ago and for his guidance in our academic careers. It is sad to hear that our friend Nozer Singpurwalla has passed away. I pray that his soul will rest in the eternal peace of God".

We of Gnedenko Forum Advisory Board share all the feelings if our colleagues who knew our remarkable star Professor Nozer Singpurwalla. Let his flight among the stars be peaceful and bright as his life on the Earth. We miss him and will never forget. Our hearts, prays and thoughts are with your family and friends. Our world is impoverished not only by the loss of a young man but also by all that he would have done if he had remained alive a little longer, if he had been among us. ideas, resolutions, students we can't even imagine.

Rest in peace our dear friend.

INVENTORY MODEL WITH EXPONENTIAL DETERIORATION AND SHORTAGES FOR SEVERAL LEVELS OF PRODUCTION

A. Lakshmana Rao[1], S. Arun Kumar[2] and K. P. S. Suryanarayana[3]

•

Department of Mathematics[1,2,3], Aditya Institute of Technology and Management, Tekkali, India
agatamudi111@gmail.com[1], arunkumarsaripalli9788@gmail.com[2], suryanarayana.kornu@gmail.com[3]

Abstract

The EPQ models are mathematical models which represent the inventory situation in a production or manufacturing system. In production and manufacturing units, the EPQ model is extremely significant and also be utilized for scheduling the optimal operating policies of market yards, warehouses, godowns, etc. In this research study, we provide inventory model of economic production for deteriorating commodities at multiple levels, in which various production stages are mentioned as well as deterioration rates follow exponential distributions. After a specific period of time, it is feasible to swap production rates from one to another, which is advantageous by starting with a production of low rate, an enormous amount of manufacturing articles is avoided at the outset, resulting in lower holding costs. Variation in output level allows for customer happiness as well as potential profit. The goal of this study is to determine the best production time solution so as to reduce total cost of the entire cycle. Finally, numerical illustrations and parameter sensitivity analyses have been used to validate proposed inventory system's results.

Keywords: EPQ, optimal operating policies, Exponential distribution, multiple levels of production, cycle time.

1. Introduction

Inventory system plays a leading role in many real applications at certain places such as production processes, manufacturing units, transportation, market yards, ware houses, assembly lines etc. One of the vital sections of operations research is inventory management, which is used for determining the optimal operating policies for inventory management and control. Inventory models provide the basic frame work for analyzing several production systems. The inventory models are broadly categorized into two groups namely, (i) Economic Order Quantity models (EOQ models) and (ii) Economic Production Models (EPQ models). The EPQ models are more common in production and manufacturing processes, warehouses, etc. Recently much emphasis was given for analyzing EPQ models for deterioration items. Deterioration is a natural phenomenon of several commodities over time. For commodities like glassware, hardware, and steel, deterioration can be quite minor at times, causing deterioration to be taken into account when determining economic lot sizes. In general, some commodities decay at a faster pace than others, such as medicine, gasoline, strawberries, fish, blood, and food grains, which must be taken into account when determining the size of a production lot.

Damage, decay, spoiling, evaporation, and obsolescence are all examples of deterioration. In modern years, the issue of decaying inventory has gotten a lot of attention. The majority of studies on deteriorating inventory assumed a constant rate of deterioration. In general the exponential delivery is commonly used to describe a product in stock that deteriorates over interval. The rate of deterioration rises with age, therefore the longer an object is left unused, the faster it will fail. Many commodities decay in real life due to their inherent nature, such as fruits, vegetables, food items, seafood, agricultural products, textiles, chemicals, medicines, electronic components, cement, fertilisers, oils, gas, and so on, which are held in inventory at various locations.

The first economic quantity model was developed by Harris [1]. The inventory model of a decaying item at the end of a scarcity period was studied by Wagner and Whitin [2]. As a result, deterioration functions come in a variety of shapes and sizes, including constant and time-dependent functions. We used the Exponential as the function of deterioration in our proposed model. Berrotoni [3] explored that the leakage failure of both dry batteries and ethical drugs life expectancy may be described as an exponential distribution. In some circumstances, the deterioration rate rises with time. The longer an object is left unused, the faster it deteriorates. This study prompted Covert and Philip [4] to create an inventory model for deteriorating items with varying rates. It was made use of two variables the Weibull distribution will deteriorate as a time distribution.

Balki and Benkherouf [5] also proposed a model as such but with a stock-dependent and time-varying demand rate across a finite time horizon. Chang [6] improved previous model by accounting for profit in the inventory system. Additionally, Begam et al [7] devised an instantaneous replacement policy. They used a three-parameter Weibull distribution to time based model inventory deterioration rate. Begam et al [8] re-examined the previous model, ignoring scarcity and assuming demand to be a linear function of price. Rubbani et al [9] proposed an integrated methodology for deteriorating item pricing and inventory control. For decaying products, Sivasankari and Panayappan [10] suggested a production inventory model that considers two different degrees of output. Cardenas-Barron et al [11] projected substitute heuristic algorithm for a multi-product EPQ (Economic Production Quantity) a vendor-buyer cohesive model with JIT view point and a budget constraint. Sarkar et al. [12], in his investigation on EPQ model with rework in a manufacturing system of single-stage with scheduled backorders, and produced 3 different inventory models for 3 different density functions of distribution like Triangular , Uniform, and Beta. Cardenas-Barron et al [13] determined the ideal replenishment lot size and dispatch strategy for an EPQ inventory model with multiple deliveries and rework. When using a multi-shipment policy, Taleizadeh et al [14] presented study work addresses the problem of determining price for sale, lot size of replenishment, and shipments quantity for a model of economic quantity with rework for defective goods. Karthikeyan and Viji [15] modified this model by using the Exponential distribution for deterioration.

Determining the ideal quantity of production boxes for different periods as an aim in order to reduce total inventory costs. Lately, Viji and Karthikeyan [16] have established an inventory model of economic production quantity for constantly deteriorating products that takes into account three levels of manufacturing. Researchers have established an economic production inventory model for many levels of production with exponential distribution deterioration, demand is time dependent and continuous, and multiple rates of production are examined in this research. The following is a breakdown of the paper's structure. The assumptions as well as notations are presented in Section 2. The third section is dedicated to mathematical modelling. Section 4 includes a numerical example as well as a sensitivity analysis. The paper comes to a conclude with Section 5.

2. Assumptions

For developing the model the following assumptions are made:

- Multiple production rates are taken into account.
- The demand rate is continuous and linear which is $D(t) = \alpha + \beta t$ (1)
- The production system has a limited time horizon.
- Shortages are permitted, as are entire backlogs.
- The exponential distribution governs the time it takes for an item to deteriorate, which is
$$f(t) = \theta e^{-t\theta}, \theta > 0, t > 0 \quad (2)$$
- Consequently, the instantaneous rate of production is
$$h(t) = \frac{f(t)}{1-F(t)} = \theta, \theta > 0 \quad (3)$$
- Production rate (K), which is greater than demand rate(R).
The following notions are used to developing this model.
K is the production rate in units @ unit time.
R is the demand rate in units@ unit time.
The holding cost @ unit of time is denoted by the C_1
The shortages cost @ unit of time is denoted by C_2
The ordering cost @ unit of time is denoted by C_3
The production cost @unit of time is denoted by C_p
S is the shortage level.
Q is the optimum production quantity.
Q_1, Q_2, Q_3 and Q_4 are the maximum possible inventory level at time t_1, t_2, t_3 and t_4.
T is the total cycle length.

3. Mathematical formulation of the model

The following is a description of Figure 1.

Let's the production be assumed to begin at t = O and finishes at t = T. Let the rate of production be 'K' and the rate of demand be 'R' during the time interval [0, t1], where R is less than K. At time t = t1, the stock reaches a level Q1. Through the gaps of time [t_1, t_2], [t_2, t_3] and [t_3, t_4]. Let's call the rate of growth a1(K-R), a2(K-R), and a3(K-R), where a1, a2, and a3 are constants. At times t2, t3, and t4, the inventory level reaches levels Q2, Q3, and Q4, respectively. The product turns into technically superseded or else, customer taste changes during the decline time T. It is important to keep an eye on the product's stock levels. Due to demand, inventory levels begin to decline at a rate of R. To consume all units Q at the demand rate, it will take time T.

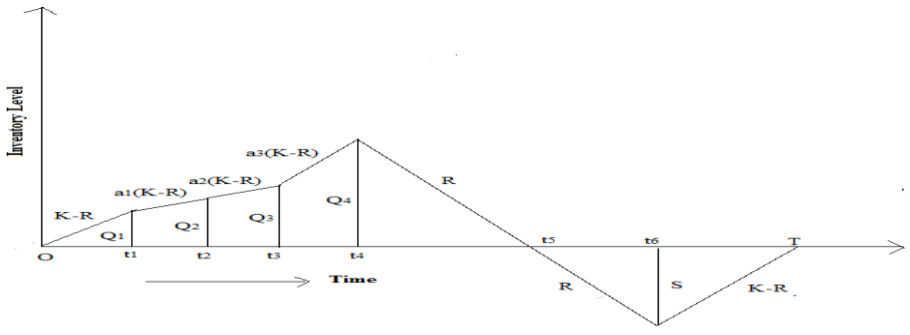

Figure1: Schematic diagram of the inventory level

The model governs distinguished equations as follows.

$$\frac{d}{dt}I(t) + \theta I(t) = (K - R) - (\alpha + \beta t), 0 \le t \le t_1 \quad (4)$$

$$\frac{d}{dt}I(t) + \theta I(t) = a_1(K - R) - (\alpha + \beta t), t_1 \le t \le t_2 \quad (5)$$

$$\frac{d}{dt}I(t) + \theta I(t) = a_2(K - R) - (\alpha + \beta t), t_2 \le t \le t_3 \quad (6)$$

$$\frac{d}{dt}I(t) + \theta I(t) = a_3(K - R) - (\alpha + \beta t), t_3 \le t \le t_4 \quad (7)$$

$$\frac{d}{dt}I(t) + \theta I(t) = -R, t_4 \le t \le t_5 \quad (8)$$

$$\frac{d}{dt}I(t) = -R, t_5 \le t \le t_6 \quad (9)$$

$$\frac{d}{dt}I(t) = (K - R), t_6 \le t \le T \quad (10)$$

I(0) = 0, I(t1) = Q1, I(t2) = Q2, I(t3) = Q3, I(t4) = Q4, I(t5) = 0, I(t6) = S, and I(T) = 0 are the initial conditions.

The solutions of equations (4) - (10), using the initial conditions, the on-hand inventory at time'*t*' is calculated as follows:

$$I(t) = \frac{K - R}{\theta} - \frac{\alpha}{\theta} - \frac{\beta t}{\theta} + \frac{\beta}{\theta^2}\left(1 - e^{-\theta t}\right), 0 \le t \le t_1 \quad (11)$$

$$I(t) = \frac{a_1(K - R)}{\theta} - \frac{\alpha}{\theta} - \frac{\beta t}{\theta} + \frac{\beta}{\theta^2}\left(1 - e^{-\theta t}\right), t_1 \le t \le t_2 \quad (12)$$

$$I(t) = \frac{a_2(K - R)}{\theta} - \frac{\alpha}{\theta} - \frac{\beta t}{\theta} + \frac{\beta}{\theta^2}\left(1 - e^{-\theta t}\right), t_2 \le t \le t_3 \quad (13)$$

$$I(t) = \frac{a_3(K - R)}{\theta} - \frac{\alpha}{\theta} - \frac{\beta t}{\theta} + \frac{\beta}{\theta^2}\left(1 - e^{-\theta t}\right), t_3 \le t \le t_4 \quad (14)$$

$$I(t) = \frac{-R}{\theta}\left(1 - e^{\theta(t_5 - t)}\right), t_4 \le t \le t_5 \quad (15)$$

$$I(t) = -R(t - t_5), t_5 \le t \le t_6 \quad (16)$$

$$I(t) = (K - R)(t - T), t_6 \le t \le T \quad (17)$$

Maximum inventories Q_1, Q_2, Q_3 and Q_4:

The maximum inventories are estimated using $I(t_1) = Q_1$, $I(t_2) = Q_2$, $I(t_3) = Q_3$, and $I(t_4) = Q_4$ during the times t_1, t_2, t_3, and t_4 and equations (11) – (14).

We have omitted the second and higher powers of in the $e^{-\theta t}$ for θ values

Therefore

$$Q_1 = \theta t_1\left(\frac{K - R}{\theta} - \frac{\alpha}{\theta} - \frac{\beta t}{\theta} + \frac{\beta}{\theta^2}\right) \quad (18)$$

$$Q_2 = \theta t_2\left(\frac{a_1(K - R)}{\theta} - \frac{\alpha}{\theta} - \frac{\beta t}{\theta} + \frac{\beta}{\theta^2}\right) \quad (19)$$

$$Q_3 = \theta t_3\left(\frac{a_2(K - R)}{\theta} - \frac{\alpha}{\theta} - \frac{\beta t}{\theta} + \frac{\beta}{\theta^2}\right) \quad (20)$$

$$Q_4 = \theta t_4\left(\frac{a_3(K - R)}{\theta} - \frac{\alpha}{\theta} - \frac{\beta t}{\theta} + \frac{\beta}{\theta^2}\right) \quad (21)$$

Shortage level S:

From equations (16) and (17) and using $I(t_6) = S$, we get,

$I(t_6) = S \Rightarrow I(t_6) = -R(t_6 - t_5) = S$ and

$I(t_6) = S \Rightarrow (K - R)(t_6 - T) = S$

Therefore $-R(t_6 - t_5) = (K - R)(t_6 - T)$

On simplification

Therefore

$$t_6 = \frac{R}{K}(t_5 - T) + T \tag{22}$$

As a result, total cost equals to the entirety of production, ordering, holding, deteriorating and shortage costs.

The overhead costs independently

(i) Production cost per unit time = $R\,C_P$

(ii) Ordering cost per unit time = C_3/T

(iii) Holding cost per unit time

$$= \frac{C_1}{T}\left(\int_0^{t_1} I(t)dt + \int_{t_1}^{t_2} I(t)dt + \int_{t_2}^{t_3} I(t)dt + \int_{t_3}^{t_4} I(t)dt + \int_{t_4}^{t_5} I(t)dt\right)$$

$$= \frac{C_1}{T}\left[\int_0^{t_1} \frac{K-R}{\theta} - \frac{\alpha}{\theta} - \frac{\beta t}{\theta} + \frac{\beta}{\theta^2}\left(1 - e^{-\theta t}\right)dt + \int_{t_1}^{t_2} \frac{a_1(K-R)}{\theta} - \frac{\alpha}{\theta} - \frac{\beta t}{\theta} + \frac{\beta}{\theta^2}\left(1 - e^{-\theta t}\right)dt\right.$$

$$+ \int_{t_2}^{t_3} \frac{a_2(K-R)}{\theta} - \frac{\alpha}{\theta} - \frac{\beta t}{\theta} + \frac{\beta}{\theta^2}\left(1 - e^{-\theta t}\right)dt + \int_{t_3}^{t_4} \frac{a_3(K-R)}{\theta} - \frac{\alpha}{\theta} - \frac{\beta t}{\theta} + \frac{\beta}{\theta^2}\left(1 - e^{-\theta t}\right)dt$$

$$\left. + \int_{t_4}^{t_5} \frac{-R}{\theta}\left(1 - e^{\theta(t_5 - t)}\right)dt\right]$$

We have simplified the expansion of $e^{-\theta t}$ for small values of θ by ignoring the second and higher powers of in the expansion of $e^{-\theta t}$.

Holding cost per unit time

$$= \frac{C_1}{T}\left[(K-R)\left((1-a_1)\frac{t_1^2}{2} + (a_1 - a_2)\frac{t_2^2}{2} + (a_2 - a_3)\frac{t_3^2}{2} + a_3\frac{t_4^2}{2}\right)\right.$$

$$\left. -\left(\alpha - \frac{\beta}{\theta} + R\right)\frac{t_4^2}{2} - R\left(\frac{t_5^2}{2} - t_4 t_5\right) - \beta\frac{t_4^3}{3}\right] \tag{23}$$

Deteriorating cost per unit time

$$= \frac{C_P}{T}\left(\int_0^{t_1} h(t)I(t)dt + \int_{t_1}^{t_2} h(t)I(t)dt + \int_{t_2}^{t_3} h(t)I(t)dt + \int_{t_3}^{t_4} h(t)I(t)dt + \int_{t_4}^{t_5} h(t)I(t)dt\right)$$

, where h(t) = θ

$$= \frac{C_P}{T}\left[\int_0^{t_1} \theta\left(\frac{K-R}{\theta} - \frac{\alpha}{\theta} - \frac{\beta t}{\theta} + \frac{\beta}{\theta^2}\right)\left(1 - e^{-\theta t}\right)dt + \int_{t_1}^{t_2} \theta\left(\frac{a_1(K-R)}{\theta} - \frac{\alpha}{\theta} - \frac{\beta t}{\theta} + \frac{\beta}{\theta^2}\right)\left(1 - e^{-\theta t}\right)dt\right.$$

$$+ \int_{t_2}^{t_3} \theta\left(\frac{a_2(K-R)}{\theta} - \frac{\alpha}{\theta} - \frac{\beta t}{\theta} + \frac{\beta}{\theta^2}\right)\left(1 - e^{-\theta t}\right)dt + \int_{t_3}^{t_4} \theta\left(\frac{a_3(K-R)}{\theta} - \frac{\alpha}{\theta} - \frac{\beta t}{\theta} + \frac{\beta}{\theta^2}\right)\left(1 - e^{-\theta t}\right)dt$$

$$\left. + \int_{t_4}^{t_5} \theta\left(\frac{-R}{\theta}\left(1 - e^{\theta(t_5 - t)}\right)\right)dt\right]$$

We have simplified the expansion of $e^{-\theta t}$ for small values of θ by ignoring the second and higher powers of in the expansion of $e^{-\theta t}$

Deteriorating cost per unit time

$$= \frac{C_P}{T}\left[\theta(K-R)\left((1-a_1)\frac{t_1^2}{2} + (a_1 - a_2)\frac{t_2^2}{2} + (a_2 - a_3)\frac{t_3^2}{2} + a_3\frac{t_4^2}{2}\right)\right.$$

$$\left. + (\beta - \theta\alpha - R\theta)\frac{t_4^2}{2} - R\theta\left(\frac{t_5^2}{2} - t_4 t_5\right) - \beta\theta\frac{t_4^3}{3}\right] \quad (24)$$

Shortage cost per unit time

$$= \frac{C_2}{T}\left[\int_{t_5}^{t_6} I(t)dt + \int_{t_6}^{T} I(t)dt\right]$$

$$= \frac{C_2}{T}\left[\int_{t_5}^{t_6} -R(t - t_5)dt + \int_{t_6}^{T} (K-R)(t-T)dt\right]$$

On simplification

$$\frac{C_2}{T}\left[R\left(\frac{T^2}{2} - \frac{t_5^2}{2} + t_5 t_6\right) - K\left(T t_6 - \frac{T^2}{2} - \frac{t_6^2}{2}\right)\right] \quad (25)$$

Substitute t_6 value in (25) from (22) and on simplification, we have
Shortage cost

$$= \frac{C_2}{T}\left[\frac{R^2 t_5^2}{K} + (K-R)T^2 + \frac{(2+K)RT^2}{2K} - \frac{KT^2}{2} - \frac{R^2 T t_5}{2} + RT t_5 - \frac{R t_5^2}{2} - \frac{R^2 T^2}{2K}\right] \quad (26)$$

Optimum quantity of the model:

$$Q = \int_0^{t_1} h(t)dt + \int_{t_1}^{t_2} h(t)dt + \int_{t_2}^{t_3} h(t)dt + \int_{t_3}^{t_4} h(t)dt + \int_{t_6}^{T} h(t)dt$$

$$Q = Q_1 + Q_2 + Q_3 + Q_4 + \theta(T - t_6)$$

On simplification

$$Q = Q_1 + Q_2 + Q_3 + Q_4 + \theta\frac{R}{K}(t_5 - T) \tag{27}$$

Therefore, total cost is the sum of the costs pertaining to Production, Setup, Holding, Deteriorating and Shortage.

$$TC(t_1, t_2, t_3, t_4, t_5, T) = RC_P + \frac{C_3}{T} + \frac{C_1}{T}\Bigg[(K-R)\Bigg((1-a_1)\frac{t_1^2}{2} + (a_1 - a_2)\frac{t_2^2}{2}$$

$$+(a_2 - a_3)\frac{t_3^2}{2} + a_3\frac{t_4^2}{2} - \left(\alpha - \frac{\beta}{\theta} + R\right)\frac{t_4^2}{2} - R\left(\frac{t_5^2}{2} - t_4 t_5\right) - \beta\frac{t_4^3}{3}\Bigg]$$

$$+\frac{C_P}{T}\Bigg[\theta(K-R)\Bigg((1-a_1)\frac{t_1^2}{2} + (a_1 - a_2)\frac{t_2^2}{2} + (a_2 - a_3)\frac{t_3^2}{2} + a_3\frac{t_4^2}{2}\Bigg)$$

$$+(\beta - \theta\alpha - R\theta)\frac{t_4^2}{2} - R\theta\left(\frac{t_5^2}{2} - t_4 t_5\right) - \beta\theta\frac{t_4^3}{3}\Bigg]$$

$$+\frac{C_2}{T}\left[\frac{R^2 t_5^2}{K} + (K-R)T^2 + \frac{(2+K)RT^2}{2K} - \frac{KT^2}{2} - \frac{R^2 T t_5}{2} + RTt_5 - \frac{Rt_5^2}{2} - \frac{R^2T^2}{2K}\right] \tag{28}$$

Let us consider that $t_1 = u\ t_5$, $t_2 = v\ t_5$, $t_3 = w\ t_5$ and $t_4 = x\ t_5$

Therefore total cost becomes from (28)

$$TC(t_5, T) = RC_P + \frac{C_3}{T} + \frac{C_1}{T}\Bigg[(K-R)\Bigg((1-a_1)\frac{u^2 t_5^2}{2} + (a_1 - a_2)\frac{v^2 t_5^2}{2}$$

$$+(a_2 - a_3)\frac{w^2 t_5^2}{2} + a_3\frac{x^2 t_5^2}{2} - \left(\alpha - \frac{\beta}{\theta} + R\right)\frac{x^2 t_5^2}{2} - R\left(\frac{t_5^2}{2} - x{t_5}^2\right) - \beta\frac{x^3 t_5^3}{3}\Bigg]$$

$$+\frac{C_P}{T}\Bigg[\theta(K-R)\Bigg((1-a_1)\frac{u^2 t_5^2}{2} + (a_1 - a_2)\frac{v^2 t_5^2}{2}$$

$$+(a_2 - a_3)\frac{w^2 t_5^2}{2} + a_3\frac{x^2 t_5^2}{2} + (\beta - \theta\alpha - R\theta)\frac{x^2 t_5^2}{2} - R\theta\left(\frac{t_5^2}{2} - x{t_5}^2\right) - \beta\theta\frac{x^3 t_5^3}{3}\Bigg]$$

$$+\frac{C_2}{T}\left[\frac{R^2 t_5^2}{K} + (K-R)T^2 + \frac{(2+K)RT^2}{2K} - \frac{KT^2}{2} - \frac{R^2 T t_5}{2} + RTt_5 - \frac{Rt_5^2}{2} - \frac{R^2T^2}{2K}\right] \tag{29}$$

Since $TC(t_5, T)$ is minimum so that differentiating (29) with regard to t_5 and T likening to zero that is $\frac{\partial TC(t_5,T)}{\partial t_5} = 0$ and $\frac{\partial TC(t_5,T)}{\partial T} = 0$ also satisfy the condition $\left\{\left(\frac{\partial^2 TC(t_5,T)}{\partial {t_5}^2}\right)\left(\frac{\partial^2 TC(t_5,T)}{\partial T^2}\right) - \left(\frac{\partial^2 TC(t_5,T)}{\partial t_5 \partial T}\right)\right\} > 0$ and then solving to get t_5 and T.

MATHCAD is used to find the optimum solution to equation (29).

4. Numerical Illustration

The following numerical illustration analyses the above stated model by considering the values of the following. K= 1000, R = 500, C_1 = 5, C_2 = 0.5, C_3 = 50, $a_1 = a_2 = a_3$ = 10, θ = 2, α = 0.2, β = 2, u = 0.2, v = 0.4, w=0.6 and x= 0.8. The optimum values are found as T_5 = 0.9 and T = 6.049, production cost = 25000, Holding cost = 198, setup cost = 8.333, deteriorating cost = 4.08, shortage cost = 8.825 and total cost = 364500.
Table 1 and 2 shows when there is an increase in rate of deterioration, the Cycle Time (T), Order Quantity (Q), and Total Cost (TC) increases. All increase as the rate of demand parameter increases.

Table 1: *Parameter variations on optimal values*

Parameters		Optimum values					
		t_1	t_2	t_3	t_4	t_5	T
C_1	**5.0**	0.18	0.37	0.56	0.74	0.893	6.049
	5.25	0.176	0.352	0.53	0.704	0.88	6.293
	5.50	0.17	0.339	0.51	0.679	0.848	6.682
	5.75	0.166	0.332	0.49	0.664	0.831	6.922
C_2	**0.5**	0.18	0.37	0.56	0.74	0.893	6.049
	0.525	0.517	1.033	1.55	2.066	1.051	8.27
	0.550	0.519	1.037	1.56	2.074	1.327	10.21
	0.575	0.526	1.053	1.58	2.105	1.501	11.1
C_3	**50**	0.18	0.37	0.56	0.74	0.893	6.049
	55	0.222	0.445	0.67	0.89	1.591	7.272
	60	0.516	1.033	1.55	2.066	2.282	8.52
	65	0.518	1.036	1.55	2.071	2.609	10.17
C_P	**50**	0.18	0.37	0.56	0.74	0.893	6.049
	55	0.203	0.407	0.61	0.813	1.017	6.476
	60	0.204	0.409	0.61	0.818	1.022	6.993
	65	0.205	0.41	0.62	0.821	1.026	7.462
θ	**2**	0.18	0.37	0.56	0.74	0.893	6.049
	2.1	0.22	0.44	0.66	0.879	1.098	7.621
	2.2	0.265	0.531	0.79	1.062	1.327	9.2
	2.3	0265	0531	0.80	1.062	1.327	9.2
α	**0.2**	0.18	0.37	0.56	0.74	0.893	6.049
	0.21	0.225	0.451	0.68	0.901	1.127	7.574
	0.22	0.248	0.496	0.74	0.992	1.440	10.59
	0.23	0.367	0.734	1.10	1.468	1.836	11.75
β	**2**	0.18	0.37	0.56	0.74	0.893	6.049
	2.1	0.308	0.617	0.93	1.233	1.241	8.768
	2.2	0.318	0.637	0.96	1.274	1.592	9.071
	2.3	0.354	0.708	1.06	1.416	1.770	8.48

Table 2: *Parameter variations on optimal values*

		Optimum values					
Parameters		Q_1	Q_2	Q_3	Q_4	Q	TC
	5.0	629.98	12610	18910	25210	57340	127000
	5.25	615.63	12320	18470	24630	56040	116300
	5.50	593.62	11880	17810	23750	54030	101400

		Optimum values					
Parameters		Q_1	Q_2	Q_3	Q_4	Q	TC
C_1	**5.75**	581.18	11630	17440	23250	52910	98420
C_2	**0.5**	629.98	12610	18910	25210	57340	127100
	0.525	1807	36160	54240	72310	61500	156300
	0.550	1814	36300	54440	72590	65100	170100
	0.575	1841	36840	55260	73680	67600	200700
C_3	**50**	629.98	12610	18910	25210	57340	127100
	55	778.32	15570	23360	31140	60850	156100
	60	1807	36150	54220	72290	63500	182400
	65	1812	36240	54360	72480	67900	215500
C_P	**50**	629.98	12610	18910	25210	57340	127100
	55	711.45	14230	21350	28470	60760	189100
	60	715.25	14310	21460	28620	62110	234700
	65	717.88	14360	21540	28720	65350	272700
θ	**2**	629.98	12610	18910	25210	57340	127100
	2.1	768.4	15370	23060	30750	64950	158100
	2.2	928.59	18580	27870	37160	72530	187100
	2.3	932.58	18780	27970	37260	78730	198100
α	**0.2**	629.98	12610	18910	25210	57340	127100
	0.21	788.49	15770	23660	31550	69770	152600
	0.22	867.58	17360	26040	34710	78970	172400
	0.23	1284	25700	38540	51390	84900	213100
β	**2**	629.98	12610	18910	25210	57340	127100
	2.1	1079	21580	32370	43160	58180	145700
	2.2	1114	22290	33430	44580	60020	152500
	2.3	1239	24790	37180	49570	62200	183700

5. Sensitivity analysis

The sensitivity analysis is carried out to effect the change in parameters -15% to 15%, the optimum values are varied to identify the relation between the parameters and optimum values of the production schedule are shown in Figure 2. The true solution with model parameters which are considered to be stationary at its value, in turn is the total cost function. It makes sense to investigate the sensitivity, or the effect of changing model parameters over a given optimum solution.

I. The optimal quantity (Q), production times t_1, t_2, t_3, and t_4, cycle time (T), maximum inventories Q_1, Q_2, Q_3, and Q_4, and total cost (TC) all increase when the value of the deteriorating parameter θ increases.

II. The optimal quantity (Q), production times t_1, t_2, t_3, and t_4, cycle time (T), maximum inventories Q_1, Q_2, Q_3, and Q_4, and total cost (TC) all increases when the value of ordering cost per unit (C3) increases.

III. The optimal quantity (Q), production times t_1, t_2, t_3, and t_4, maximum inventories Q_1, Q_2, Q_3, and Q_4, and total cost (TC) fall when the value of holding cost per unit (C1) decreases, but cycle time (T) increases.

IV. The optimal quantity (Q), production times t_1, t_2, t_3, and t_4, cycle time (T), maximum inventory Q_1, Q_2, Q_3, and Q_4, and total cost (TC) all increases when the value of shortage cost per unit (C2) increases.

V. The optimal quantity (Q), production times t_1, t_2, t_3, and t_4, cycle time (T), maximum inventory Q_1, Q_2, Q_3, and Q_4, and total cost (TC) increases as the value of demand parameters (α, β) increases.

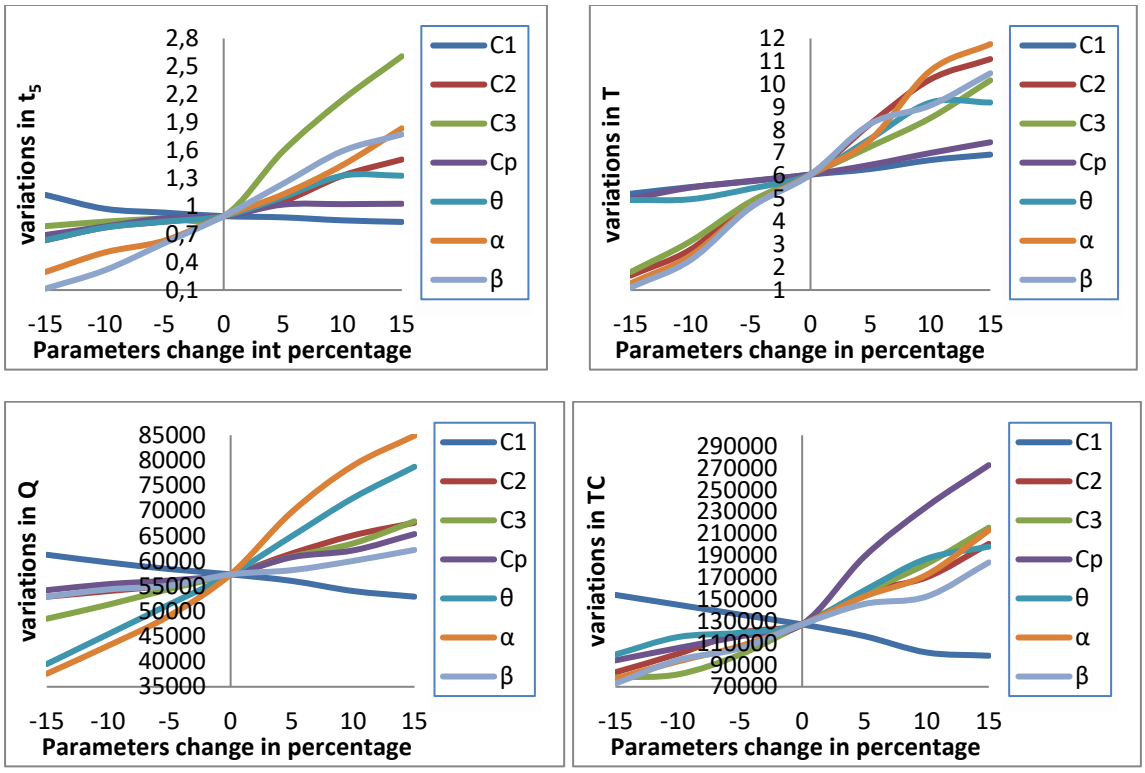

Figure 2: *Relationship between parameters and optimal values (t_5, T, Q, TC)*

6. Conclusion

The study explored an inventory model intended to deteriorating items that takes into account many levels of manufacturing. Researchers supposed that the rate of demand is reliant on time and which is linear and rate of deterioration is follows exponential distribution. The projected model is appropriate for the products introduced newly which have a consistent harmony up to a certain point in time. Such circumstances are beneficial, because, by starting at a modest production rates, a significant quantity of manufacturing goods will be avoided at the outset, resulting in a reduction in holding costs. As a result, we will receive customer happiness as well as possible profit. We developed a solution through mathematical model for this problem. Numerical illustration and sensitivity analysis are contributed to demonstrate the model. The suggested inventory model shall help manufacturers as well as retailers to indeed calculate the best order quantity, cycle time, and total inventory cost. This model is extended in a variety of ways for additional research, including demand with selling price, power demand, on-hand inventory demand etc.

Funding

No funding was provided for the research.

Declaration of Conflicting Interests

The Authors declare that there is no conflict of interest.

References

[1] Harris, F.W, "How many parts to make at once", Magazine of Management, Vol. 10, No.6, pp.135–136, 1913.

[2] Wagner, H.M. Whitin T. M, "Dynamic version of economic lot size model", Management Science, Vol.5, No.1, pp.89–96, 1958.

[3] Berrotoni, J.N, "Practical application of Weibull distribution", In: ASQC Technical Conference Transaction, pp. 303–323, 1962.

[4] Covert R.B. Philip G.S, "An EOQ model with Weibull distribution deterioration", AIIE Transactions, Vol. 5, No.4, pp. 323–326, 1975.

[5] Balki, Z.T, Benkherouf L, "On an inventory model for deteriorating items with stock dependent and time varying demand rates", Computers & Operations Research, Vol. 31, No. 2, pp. 223–240, 2004.

[6] Chang, C. T. Goyal S. K. Teng J. T, "On an EOQ model for perishable items under stock dependent selling rate and time dependent partial backlogging by Dye and Ouyang", Europian Journal of Operational Research, Vol. 174, No.2, pp. 923–929, 2006.

[7] Begam, R, Sahoo R. R. Sahu S. K. Mishra M, "An EOQ model for varying item with weibull distributions deterioration and price- dependent demand", Journal of Scientific Research, Vol. 2, No.1, pp. 24–36, 2010.

[8] Begam, R, Sahoo R. R. Sahu S. K, "A replenishment policy for items with price dependent demand, time-proportional deterioration and no shortage", International Journal of Systems Science, Vol. 43, No.5, pp. 903–910, 2011.

[9] Rubbani Mosand, Zia Nadia Pour mohamonad, Rafiei Hamed, "Optimal dynamic pricing and replenishment policies for deteriorating items", International Journal of Industrial Engineering Computation, Vol. 5, No.4, pp. 621–30, 2014.

[10] Sivasankari, C. K, Panayappan S, "Production inventory model for two – level production with deteriorative items and shortage", International Journal of Advanced Manufacturing Technology, Vol. 76, pp. 2003–2014, 2014.

[11] Cardenas-Barron, L. E. Chung K. J. Trevino-Garza G, "Celebrating a century of the economic order quantity model in honour of Ford Whitman Harris", International Journal of Production Economics, Vol.155, pp. 1–7, 2014.

[12] Sarkar, B, Cardenas-Barron L. E. Sarkar M, Singgih M. L, "An economic Production quantity model with random defective rate rework process and backorder for a single stage production system", Journal of Manufacturing Systems, Vol. 33, No. 3, pp. 423–435, 2014.

[13] Cardenas-Barron, L. E. Trevino-Garza G, Taleizadeh A. A, Pandian V, "Determining replenishment lot size shipment policy for an EPQ inventory model with delivery and rework", Mathematical Problems in Engineering, Vol. 2015, ID. 595498, 2015.

[14] Taleizadeh, A. A. Kalantari S. S. Cardenas-Barron L. E, "Determining optimal price, replenishment lot size and number of shipment for an EPQ model with rework and multiple shipments", Journal of Industrial & Management Optimization, Vol. 11, No. 4, pp. 1059–1071, 2015.

[15] Karthekeyan K, Viji G, "Economic production quantity model for three levels of production with deteriorative item", International Journal of Applied Engineering Research, Vol. 10, pp. 3717-3722, 2015.

[16] Vijji G, Karthikeyan K, "An economic production quantity model for three levels of production with Weibull distribution deterioration and shortages", Ain Shams Engineering Journal, Vol. 9, No.4, pp. 1481-1487, 2018.

SOFTWARE CONTRIBUTION TO THE AVAILABILITY OF MICROPROCESSOR-BASED RELAY PROTECTION

M. I. Uspensky
•
Komi SC UB RAS, Syktyvkar, Russian Federation.
uspensky@energy.komisc.ru

Abstract

An important characteristic of relay protection functioning is availability of microprocessor relay protection software. An approach to estimation of such parameter and correlation between it and hardware availability on the example of 110/35/10 kV distribution network microprocessor protection is considered in the paper. The behavioral nature of the availability under research, reasons and a share of various kinds of the error leading to failure of program execution, variants of program volume definition, some solution approaches to the task at hand, including methods of Jelinsky-Moranda, and also examples of assessing the ratio of these availabilities are considered. An algorithm for the software evaluation used is presented. The influence of different conditions on such evaluation is shown. Applications of different approaches to software readiness estimation for the above types of protection based on data during debugging of protection programs are given.

***Key words*:** reliability, availability, software, relay protection module.

I Introduction

The reliability index is an important characteristic of relay protection and automatics (RPA) functioning. Many authors, including us [1, 2], noted that such characteristic of modern digital protections is convenient to divide into components: hardware or technical reliability, connected with failure (destruction) of relay protection device elements; traffic reliability, defined by temporary loss or distortion of data without failure of process bus element; program reliability due to errors in development of execution programs; and resistance to external purposeful influence on transmitted information. In [3], the behavior of the first component on the reliability indicator was given and shown by the example of the 110/35/10 kV distribution network protection system. Here we will consider the approach to software reliability characterization, and on the example of the same system, we will evaluate the contribution of this component to the total availability of the aforementioned protections.

II Specifics of software reliability

It is known that software failure is associated with its inadequacy to the set tasks. There are many definitions of software failure. Most definitions of a software error come down to [4]: *Software reliability is the probability that a program will work without failures for a certain period of time taking into account the degree of their influence on the output results*. The frequency of errors from statistical data, reduced to 100% errors is given in Table 1, and the position "Incomplete or erroneous task" is disclosed in more detail.

On the one hand, software is not subject to wear and tear and its reliability is determined only by development errors. Thus, this indicator should increase with time, if correction of detected errors does not introduce new errors. On the other hand, many programmers' experience shows that in a large software, no matter how much you test it, some errors will remain. Due to the testing that simulates almost all the real modes, the errors of incorrect software operation are corrected, but there always remains a set of data that occurs due to some, usually external conditions, for example, interference or erroneous human actions, which cannot be foreseen and which will lead the software to work incorrectly. The next dilemma to solve here is how to optimize the quality/cost ratio so as not to lose market priority, or customer confidence. It is important to remember that we are here examining the readiness of the software to work.

Table 1. Frequency of occurrence of some error types [4]

Cause of error	**Frequency**, %
Task deviation	12
Ignorance of programming rules	10
Erroneous data sample	10
Erroneous logic or operation sequence	12
Erroneous arithmetic operations	9
Insufficient time to solve	4
Improper interrupt handling	4
Incorrect constants or input data	3
Inaccurate writing	8
Incomplete or erroneous assignment	28
⇓	
Errors in numerical values	12
Insufficient accuracy requirements	4
Erroneous characters or symbols	2
Mistakes in the design	15
Incorrect description of hardware	2
Incomplete or inaccurate design basis	52
Ambiguity of requirements	13

The manifestation of an error in the software system is reflected in a failure situation, which leads the program either to a hang (stopping while waiting for the next command, which does not really exist) or to incorrect calculations, leading to erroneous actions.

The specificity of relay protection programs is that often the application programs are prepared in the languages of programmable logic controllers (PLCs) [5], which reduces the probability of program errors. However, the operating environment is written in more traditional software languages such as C, Java, etc. A system of programs written in different programming languages when estimating its reliability, is reduced to the average assembler equivalent per 1000 lines through "KAELOC - K of Assembler Equivalent Lines of Code", where K is 1000 lines of code [6] (see Table 2).

Table 2. Conversion factors

Programming language	Factor
Assembler, macroassembler	1
C	2.5
C++	11
Fortran	3
Pascal	3.5
LISP	1.5
Ada	4.5
Forth	5
Query languages (like SQL)	25
Object-oriented 4th generation languages	16
PLC languages	10 … 33

Basically, software bugs are tried to remove when writing and debugging, and a lot of programs are created to detect bugs at the debugging stage. But it is expected that some (small) number of errors is present in the program. The detection programs are tuned for specific external conditions (which group of people prepares the program under test, the temperature and electromagnetic environment, etc.) What to do with the remaining errors? 1. The salesperson continues to test and identify errors, which are corrected in customers. 2. Buyers identify bugs and turn them over to the creators for correction. 3. Change the vendor.

III Evaluating the software's contribution to availability by programming averages

A fairly rough estimate of software availability can be determined as follows [7]. For responsible applications, which include the RPA software, by the time the system is delivered to the client it may contain from 4 to 15 errors per 100 000 lines of program code [8]. For illustration, let us note that the number of code lines of WINDOWS XP is over 45 million, the NASA program is 40 million, the Linux 4.11 kernel is over 18 million. If we estimate the complex of simultaneously working RPA programs at 1 million code lines, the number of errors at the beginning of software operation $E = (V/100\,000) \cdot 15 = 150$ errors. Then, using the formula of average software MTBF, we get

$$\lambda_{SW} = \beta \frac{E}{V} = 0.01 \frac{150}{10^6} = 1.5 \cdot 10^{-6} \text{ or } t_{SW} = \frac{1}{\lambda_{SW}} = \frac{10^6}{1.5 \cdot 8760} \approx 76 \text{ years}, \quad (1)$$

where E is the number of errors per complex of jointly working programs accepted for operation, V is the size of the complex in code lines, β is the program complexity factor, usually in the range of 0.001...0.01, λ_{SW} is the failure rate and t_{SW} is the MTBF of software, 8760 is the number of hours per year. The size of the RPA application programs is most often limited to thousands of assembler lines because of the requirement for their speed. Then, at the value of 15 errors per 100 000 code lines, adopted for the application software after testing with the volume of code lines $E = 4000 \cdot 15/100{,}000 = 0.6$ errors

$$\lambda_{SW} = \beta \frac{E}{V} = 0.01 \frac{0.6}{4000} = 1.5 \cdot 10^{-6} \text{ or } t_{SW} = \frac{1}{\lambda_{SW}} = \frac{6.67 \cdot 10^5}{8760} \approx 76 \text{ years} \quad (2)$$

or about one failure per 76 years. With a recovery time of t_r = 2 h $A_{SW} = \frac{\mu}{\lambda+\mu} = \frac{4380}{1.5 \cdot 10^{-6} + 4380} = 0.9999999997$.

IV Software contribution to availability according to the Jelinsky-Moranda model

There are a number of models of reliability growth concerning the process of failure detection [9, 10]. The classification of such models divides them into two groups: models that consider the number of failures as a Markov process; models that consider the failure rate as a Poisson process. Let us use the model of the second group.

The Jelinsky-Moranda model is based on the following assumptions: 1) the time to the next failure is exponentially distributed; 2) the failure rate of a program is proportional to the number of errors remaining in the program.

This model assumes that the time elapsed between failures follows an exponential distribution with a parameter that is proportional to the number of remaining errors in the software. Figure 1 shows a stepped curve characteristic of program failure rate changes as a function of its model run time. It can be seen that as each error is detected, the degree of risk decreases by proportionality constant. This indicates that the impact of each fault correction is the same.

According to these assumptions, the probability of program failure as a function of time t_i is

$$P(t_i) = e^{-\lambda_i t_i}, \quad (3)$$

where the failure rate is

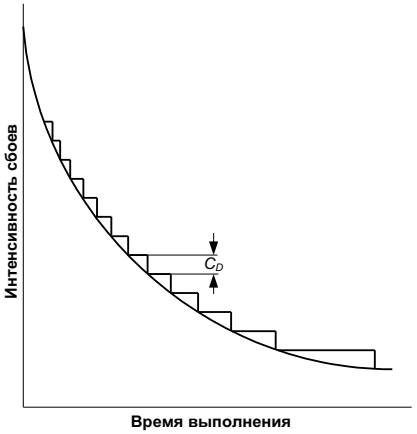

Fig. 1. In the Jelinsky-Moranda model, the failure rate curve decreases from constant CD.

$$\lambda_k = C_D[E_0 - (k-1)]. \quad (4)$$

Here E_0 is the initial number of errors, k is the number of the last observed program failure/fault, C_D is the proportionality factor. The time countdown starts from the penultimate (k – 1) program failure. The disadvantage of the model is that it assumes complete elimination of errors after it detection without introducing new errors.

From model (3) and the maximum likelihood method we can write

$$F = \prod_{i=1}^{k-1} C_D(E_0 - i + 1)\, e^{-C_D(E_0-i+1)t_i}, \quad (5)$$

or logarithmic likelihood function

$$L = \ln F = \sum_{i=1}^{k-1}\{\ln[C_D(E_0 - i + 1)] - C_D(E_0 - i + 1)\}, \quad (6)$$

wherefrom finding the extremum

$$\frac{\partial L}{\partial C_D} = \sum_{i=1}^{k-1}\left[\frac{1}{C_D} - (E_0 - i + 1)t_i\right] = 0, \quad (7)$$

$$\frac{\partial L}{\partial N} = \sum_{i=1}^{k-1}\left[\frac{1}{E_0-i+1} - C_D t_i\right] = 0. \quad (8)$$

From (8) we get

$$C_D = \frac{\sum_{i=1}^{k-1} 1/(E_0-i+1)}{\sum_{i=1}^{k-1} t_i}. \quad (9)$$

Substituting (8) into (7), we obtain

$$(k-1)\frac{\sum_{i=1}^{k-1} t_i}{\sum_{i=1}^{k-1} 1/(E_0-i+1)} = \sum_{i=1}^{k-1}(E_0 - i + 1)t_i, \quad (10)$$

from which we find E_0 by trying its values. Since E_0 is an integer, we find the minimal difference between the left and right parts of (10). The closest integer value E_0, at which the difference between the left and right parts of formula (6) is minimal, is usually given in the range k – 1...2·k, since the initial number of errors is not less than the known value of the number sum of corrected errors, and the error remaining number is usually not greater than the number of detected errors, i.e. the final total value is equal to the doubled detected value.

The manifestation intensity of the remaining errors of the program is determined. According to the methodology in [11], such intensity is calculated by the formula

$$\lambda_k = \frac{\sum_{j=1}^{k} \frac{j}{E_0 - \sum_{i=1}^{j-1} i}}{\sum_{j=1}^{k} t_j}\left(E_0 - \sum_{j=1}^{k} i\right). \quad (11)$$

But this intensity is bound to the volume of lines with errors. In reality, the failure rate is statistically defined as [12]

$$\overline{\lambda}(t) \approx \frac{m(t)}{n(t)\Delta t}, \quad (12)$$

where $m(t)$ is the number of failed elements (lines with errors) in the considered period Δt, $n(t)$ is the average number of equipment elements (in our case, code lines or program commands) work-

ing in this interval. Therefore, the obtained in (9) intensity should be recalculated to the full volume of lines or commands under study software, i.e.

$$\lambda = \lambda_k \frac{E_0}{N_\Sigma}, \tag{13}$$

where N_Σ is the number of lines under study software.

Assuming a constant error rate in accordance with the Jelinsky-Moranda model concept, we calculate the average time to error in the software:

$$t_E = \frac{1}{\lambda}. \tag{14}$$

When the error detection and correction time is assumed to be 2 hours (μ = 0.5), the software availability coefficient is

$$A_{SW} = \frac{\mu}{\lambda+\mu}. \tag{15}$$

The calculation algorithm is shown in Fig. 2. The initial data of this calculation are:
$N_{\Sigma L}$ – number of program lines in programming languages, which are converted by means of Table 2 into N_Σ – number of commands reduced to assembler codes; N_T – number of executed tests; array $[E_i]$ – number of detected and corrected errors at the i-th stage of testing, which time is determined by the array $[t_i]$. DE traces the minimal discrepancy between the left (LP) and the right (RP) part of the formula (10) in the E_0 search. ΣE_i is the sum of errors known from the tests up to position i. Σt_i is the sum of times between tests up to position i. The variable LA corresponds to the manifestation intensity of the remaining program errors (λ). A_{SW} is the software availability index.

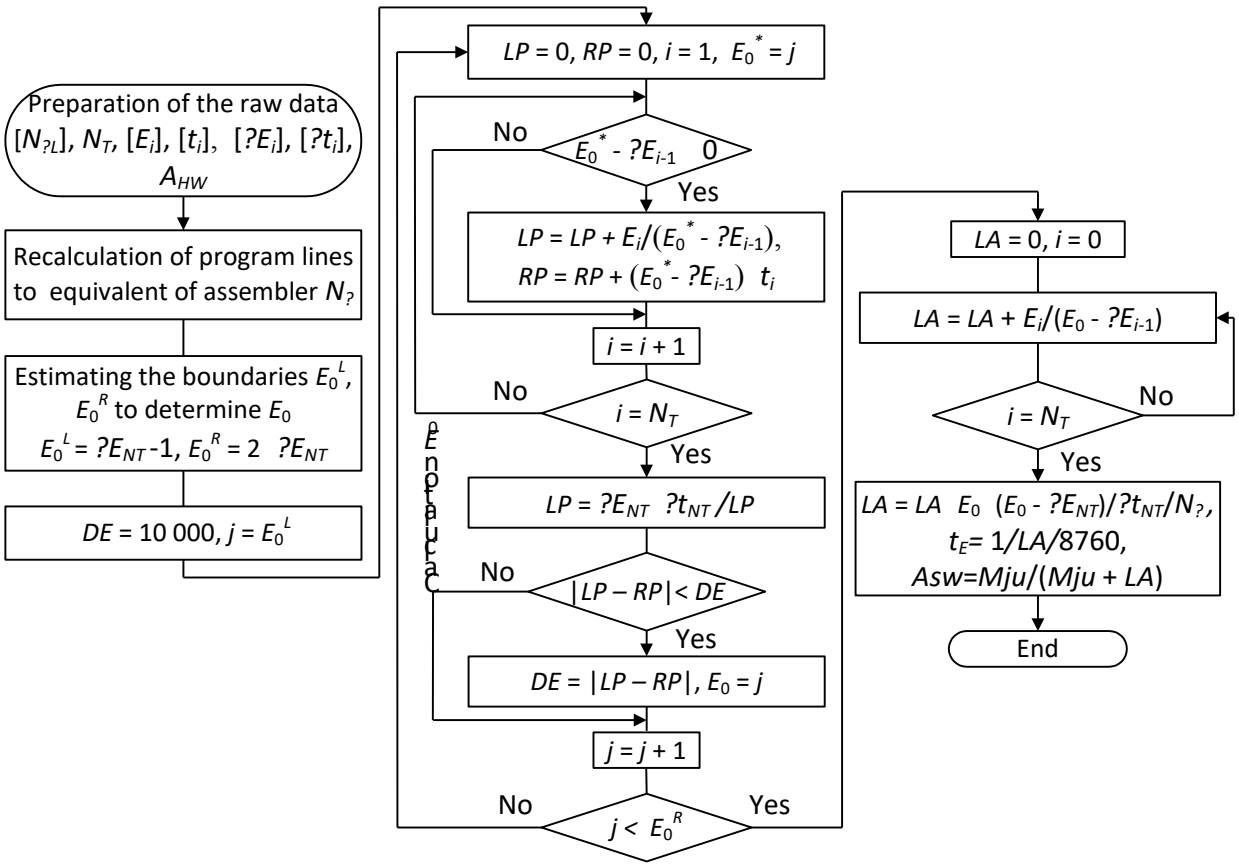

Fig. 2. Calculation algorithm for software availability characteristics.

V Calculation of software contributions to the availability of relay protections

Let's evaluate the software availability of the protection and control modules for the 35 kV bus section and transformer section [3]. The necessary data for the studied modules are presented in Tables 3 and 4. The results of calculations – in Table 5.

Table 3. Transformer section protection and control software module

Initial data	E_i, errors	ΣE_i, errors	t_i, hours	Σt_i, hours
$N_t = 4$	0	0	0	0
$N_\Sigma = 1439_{asm}+200_{C++}$	1	1	77	77
$N_\Sigma = 3639_{asm}$	1	2	63	140
$\mu = 0.5\ h^{-1}$	1	3	7	147
	1	4	187	334
C++ – in codes C++, *asm* – in codes assembler.				

Table 4. 35 kV busbar section protection and control software module

Initial data	E_i, errors	ΣE_i, errors	t_i, hours	Σt_i, hours
$N_t = 3$	0	0	0	0
$N_\Sigma = 1346_{asm}+130_{C++}$	1	1	63	63
$N_\Sigma = 2776_{asm}$	1	2	11	74
$\mu = 0.5\ h^{-1}$	1	3	117	191
C++ – in codes C++, *asm* – in codes assembler.				

Table 5. Calculating results of the software availability characteristics of the modules

Transformer section protection and control module				35 kV busbar section protection and control module				Flexible logic module			
E_0	5	λ, years^{-1}	0.04621	E_0	4	λ, years^{-1}	0.07153	E_0	4	λ, years^{-1}	0.01016
E_i	4	t_E, years	21.64	E_i	3	t_E, years	13.98	E_i	3	t_E, years	98.4
ΔE	1	A_{SW}	0.99998945	ΔE	1	A_{SW}	0.99994558	ΔE	1	A_{SW}	0.99998367

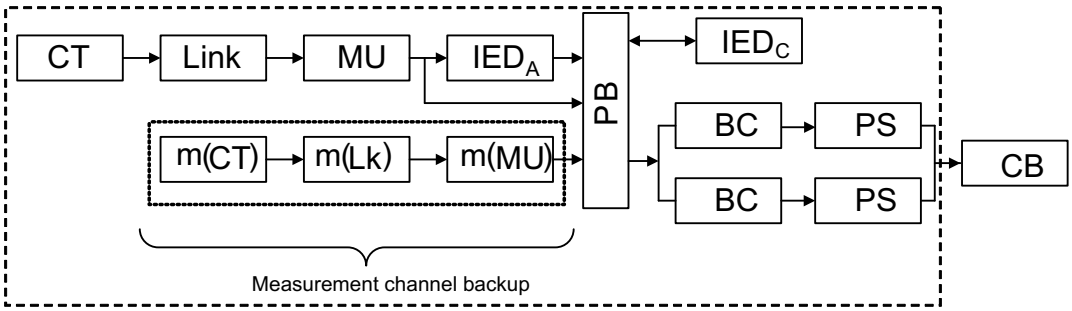

Fig. 3. Reliability block diagram of protection.

According to the protection reliability model (Fig. 3) for the hardware part, presented in [3], and software organization (Fig. 4), we explain that the software part of the model consists of two software protection blocks, autonomous and centralized, included by reliability in parallel with the output to the process bus,

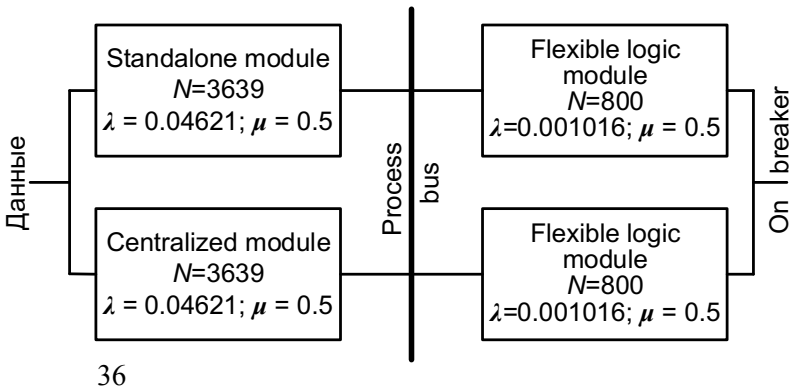

and two parallel blocks of flexible logic program. In the software evaluation of the model, the process bus is not taken into account, because it is taken into account in the hardware.

In accordance with the scheme of Fig. 4 we determine the equivalent failure rate and recovery rate of the corresponding transformer protection programs based on the known relations:
$\lambda_e = \sum_i \lambda_i$; $\mu_e = \lambda_e / \sum_i \frac{\lambda_i}{\mu_i}$ – for series connection and $\mu_e = \sum_i \mu_i$; $\lambda_e = \mu_э / \sum_i \frac{\mu_i}{\lambda_i}$ - for parallel connection. Then for Fig. 4, the equivalent values are:

left-hand side $\mu_{el} = 2 \cdot 0.5 = 1$; $\lambda_{el} = 1/\left(2 \cdot \frac{0.5 \cdot 8760}{0.04621}\right) = 5.2751 \cdot 10^{-6}$ h^{-1};

right-hand side $\mu_{er} = 2 \cdot 0.5 = 1$; $\lambda_{er} = 1/\left(2 \cdot \frac{0.5 \cdot 8760}{0.01016}\right) = 1.1598 \cdot 10^{-6}$ h^{-1};

$\lambda_e = 5.2751 \cdot 10^{-6} + 1.1598 \cdot 10^{-6} = 6.4349 \cdot 10^{-6}$ h^{-1} or 0.05637 years $^{-1}$;

Fig. 4. Reliability model of transformer protection software.

$\mu_e = 6.4349 \cdot 10^{-6} / \left(\frac{5.2751 \cdot 10^{-6} + 1.1598 \cdot 10^{-6}}{0.5}\right) = 0.5$ h^{-1} or 4380 years $^{-1}$.

Consequently, $A_{SW} = \frac{\mu_e}{\lambda_e + \mu_e} = \frac{4380}{0.05637 + 4380} = 0.999987$.

From [3] in the worst case for the hardware model of transformer protection A_{HW} = 0.9999999764, i.e. the contribution to the unavailability of protection from the hardware is essentially less, than from the software, and its total value $A_\Sigma = A_{HW} \cdot A_{SW}$ = 0.9999869, and the average time to failure $t_\Sigma = A_\Sigma / (\mu_e \cdot (1 - A_\Sigma))$ = 17.6 years or 153565 hours.

The scheme of the 35 kV busbar protection software model also corresponds to fig. 4. Equivalent values for the left part: N = 2776 lines of assembler code; λ = 0.007153 years $^{-1}$; μ = 0.5 h^{-1}. The right part is similar to the transformer model. Then the equivalent values of the left part

$\mu_{el} = 2 \cdot 0.5 = 1$; $\lambda_{el} = 1/\left(2 \cdot \frac{0.5 \cdot 8760}{0.07153}\right) = 8.1655 \cdot 10^{-6}$ h^{-1};

$\lambda_e = 8.1655 \cdot 10^{-6} + 1.1598 \cdot 10^{-6} = 9.3253 \cdot 10^{-6}$ h^{-1} or 0.08169 years $^{-1}$;

$\mu_e = 9.3253 \cdot 10^{-6} / \left(\frac{8.1655 \cdot 10^{-6} + 1.1598 \cdot 10^{-6}}{0.5}\right) = 0.5$ h^{-1} or 4380 years $^{-1}$.

Consequently, $A_{SW} = \frac{\mu_e}{\lambda_e + \mu_e} = \frac{4380}{0.08169 + 4380} = 0.999981$.

From [3] in the worst case for the hardware model of busbar protection A_{HW} = 0.999999884, i.e. the contribution to the unavailability of protection also from the hardware is much less, than from the software, and its total value $A_\Sigma = A_{HW} \cdot A_{SW}$ = 0.9999809, and the average time between errors $t_\Sigma = A_\Sigma / (\mu_e \cdot (1 - A_\Sigma))$ = 12.2 years or 106872 hours.

To estimate the contribution of software to the total unavailability of protection, we can use the expression

$$Ctb_{SW} = \frac{n_{E,SW}}{n_{E,SW} + n_{E,HW}} \cdot 100\% = \frac{\lambda_{SW}}{\lambda_{SW} + \lambda_{AHW}} \cdot 100\% = \frac{t_{E,HW}}{t_{E,SW} + t_{E,HW}} \cdot 100\%. \quad (16)$$

Here n_E is the number of failures, t_E is the average time to failure, the index A_{HW} is the availability of the hardware part.

When discussing the results of the presented work, it should be understood that, despite their outward resemblance to a quantitative assessment, they represent only qualitative indicators of software readiness. On the other hand, the obtained results do not take into account the software test control, which improves the studied indicators. Unfortunately, as noted in [13], there are no reliable methods for quantitative software evaluations other than statistics for a significant period of program operation. Nevertheless, they show that software errors can have a significant influence on reliability indicators of microprocessor relay protection.

VI Other approaches to assessing contributions to the availability of relay protections

Let's try to estimate the impact of software on RPA functioning from the following statistics. According to [14], the number of microprocessor-based RPA devices in operation in 2013 was 274062 devices, and in 2014 – 319912 devices (Table 4, [14]). From the data [15] "Distribution of cases of device RPA malfunction by types of technical reasons and device RPA types for the period from 01.01.2020 to 30.06.2020" we know that out of 727 cases of RPA failure 18 cases are related to software failure or malfunction. Then the forecast number of RPA devices for 2020 in relation to 2013 from the formula $d_n = d_1(1+r)^n$ at $r = 100\cdot(d_2 - d_1)/d_1$ %, where d_1 – number of devices of the first year, d_n – number of devices for n year, r – average annual growth of devices, can make

$$d_7 = 274062\left(1 + \frac{319912 - 274062}{274062}\right)^6 = 693328 \text{ devices}$$

Let's take Rosseti's share of RPA as 70% of all devices in [15]. Then a rough estimate of the failure rate $\lambda = \frac{n}{0.7\cdot Nt} = \frac{18\cdot 2}{0.7\cdot 693328} = 7.42\cdot 10^{-5}$ years^{-1}. Here n – the number of devices, failed due to software, for half year (2 in the numerator), $0.7\cdot N$ – the number of all microprocessor protections, t – design period (year). For the recovery time t_r = 2 hours $A_{SW} = \frac{\mu}{\lambda+\mu} = \frac{4380}{7.42\cdot 10^{-5}+4380} = 0.999999983$. And the average time between errors $t_\Sigma = \frac{1}{\lambda} = 13477$ years, which is of course unreal. From the relation $Ctb_{\text{ПО}} = \frac{n_{E,SW}}{n_{E,SW}+n_{E,HW}}\cdot 100\% = \frac{18}{727}\cdot 100\% \approx 2.5\%$ we will note, that the share of failures because of program errors was 2.5%.

One more approach on the basis of data of work [16] where at small sample a share of failures because of software errors in total number of failures can be estimated as (3+1+3+4)/(11+15+18+17) =11/61·100% =18%, where in numerator failures because of software, and in denominator - total failures. Of course, the small sample does not allow us to confidently judge the representativeness of the figures, but, nevertheless, some idea of the ratio is given.

VII Conclusion

The approach according to formulas (1) and (2) gives quite a large uncertainty range, depending on the choice of the error content coefficient per 100 thousand lines of code and the program complexity coefficient. Its result can be considered as an upper bound of A_{SW} under the chosen conditions. An estimation of A_{SW} contribution values showed that software unavailability was 1.3% of the total unavailability.

The Jelinsky-Moranda reliability model can be considered a lower bound for A_{SW} since the initial conditions are more restrictive here.

Calculations of software availability with the Jelinsky-Moranda reliability model showed that the main unavailability of the considered protections is determined by software unavailability, which was 99.8% for transformer protection and 49.8% for busbar protection. Nevertheless, even in this case, the average total error time is more than 150 thousand hours for transformer protection and more than 100 thousand hours for 35 kV busbar protection.

In contrast to the calculated data from statistics [14,15] showed that the error rate due to software is about 2.5%, and from [16] - 18%.

The work was carried out within the framework of the theme "Models and methods of adaptation of power systems in modern conditions".

References

1. Morozov Yu.M. Reliability of hardware and software systems. St. Petersburg, 2011. 136 p. . (In Russian).
2. Uspensky M.I. Contribution of Hardware, Software, and Traffic to the WAMS Communication Network Availability // Reliability: Theory & Applications Vol. 15, No 3. 2020, pp.70-83. DOI:https:// doi.org/10.24411/1932-2321-2020-13007
3. Uspensky M.I. Reliability Assessment of the Digital Relay Protection System // Reliability: Theory & Applications Vol. 14, No 3. 2019, pp. 10-17. DOI: https://doi.org/10.24411/1932-2321-2019-13001.
4. Shklyar VN. Reliability of control systems. Tomsk, Russia: Publishing house of Tomsk Polytechnic University. 2009;126 p. (In Russian).
5. Livshits, Yu. E. Programmable Logic Controllers for Process Control / Minsk: BNTU, 2014, Ch. 1, 206 p. (In Russian).
6. Baranov S.P., Domaratsky A.N., Lastochkin N.K., Morozov V.P. Defects prevention during software products creation // Software Products, #1, 2000, pp. 59-63. (In Russian).
7. Borovikov SM, Dik SS, Fomenko NK. A method for predicting applied software tools at the early stages of their development// Reports of the Belarusian State University of Informatics and Radioelectronics. 2019, #5, pp. 45-51. (In Russian).
8. Chukanov VO, Gurov VV, Prokopyeva EV. Methods of ensuring software and hardware reliability for computing systems// Russia, Presentation of the report at the seminar, pp. 1-44. Available: http://www.mcst.ru/files/5357 ec/dd0cd8/50af39/000000/seminar_metody_ obespecheniya_apparatno-programmnoy_nadezhnosti_vychislitelnyh_sistem.pdf (In Russian). (accessed 12.03.2019)
9. Bubnov V. P., Safonov V. I., Shardakov K. S. Review of existing models of nonstationary service systems and methods of their calculation // Control, Communication and Security Systems. 2020, # 3, pp. 65-121. DOI: 10.24411/2410-9916-2020-10303. (In Russian).
10. Vasilenko N.V., Makarov V.A. Software Reliability Assessment Models // Bulletin of Novgorod State University, 2004, # 28, pp. 126-132. (In Russian).
11. Iyudu K.A. Reliability and diagnostics of computing machines and systems: Textbook on special "Computing machines, complexes, systems and networks" / M.:Vyssh. shk. 1989, 216 p. (In Russian).
12. Shalin A.I. Reliability and diagnostics of relay protection of power systems. Novosibirsk: Publishing house of NSTU, 2002, 384 p. (In Russian).
13. Littlewood B., Strigini L. "Validation of ultra-high dependability…" – 20 years on // BL-LS-SCSS newsletter2011_02_v04distrib.pdf, 5 p. Available: http:// www.staff.city.ac.uk
14. Concept for the Development of Relay Protection and Automation in the Electric Grid Sector // Appendix # 1 to Rosseti's Management Board Protocol # 356pr dated June 22, 2015. M.,2015, 49 p. Available: https://mig-energo.ru›wp-content/uploads/2015/12/rza-fsk.pdf. (In Russian).
15. Distribution of malfunctions of RPA devices by types of technical reasons and types of RPA devices for the period from 01.01.2020 to 30.06.2020// Available: https://www.so-ups.ru/ fileadmin/files/ company/rza/rza_rez_info/rza_rez_vid_teh_1-2k2020.xls. (In Russian).
16. Zakharov O. G. Reliability of Digital Relay Protection Devices. Indicators. Requirements. Estimates. Moscow: Infra-engineering, 2018, 128 p. (In Russian).

A Two Non-Identical Unit Parallel System with Repair and Post Repair Policies of a Failed Unit and Correlated Lifetimes

Pradeep Chaudhary, Surbhi Masih, Rakesh Gupta
•
Department of Statistics
Ch. Charan Singh University, Meerut-250004(India)
pc25jan@gmail.com; 21surbhimasih94@gmail.com; smprgccsu@gmail.com

Abstract

The paper deals with the analysis of a system model consisting of two non-identical units arranged in a parallel configuration. If a unit fails it goes to repair. After its repair, the repaired unit is sent for post repair to complete its repair. A single repairman is always available with the system to repair a failed unit and for post repair of repaired unit. A post repaired unit always works as good as new. Failure time of both the units is assumed to be correlated random variables having their joint distribution as bivariate exponential (B.V.E.). The repair time distribution of both the units are taken as general with different c.d.fs whereas the post repair time distribution of both the units are taken as exponential with different parameters.

Keywords: Transition probabilities, mean sojourn time, bi-variate exponential distribution, regenerative point, reliability, MTSF, availability, expected busy period of repairman, net expected profit.

1. Introduction

Undoubtedly, various actual systems in the field of manufacture, shipment, computation etc. are factitious / unnatural and manufactured by human while there are various natural systems also exist which illustrates that all the systems are manufactured by human and nature and can be simple or complicated. Chopra and Ram [5] studied a two non-identical unit parallel system with two types of failure - common cause failure and partial failure. A repairman is not always available with the system to repair a failed unit i.e. whenever a unit fails, a repairman is called to visit the system and he takes some significant amount of time to reach at the system. This time is known as the waiting time for repairman and during this time the failed unit waits for repair. Pundir et al. [14] investigated a two non-identical unit parallel system where priority is given to first unit in repair. Chandra et al. [4] analysed two different system models in which one consist of two identical units in parallel whereas the other composed of two non-identical units in parallel. They have obtained the reliability characteristics by applying the Semi Markov Process and Regenerative Point Technique. In the above papers, the authors considered a two identical / non-identical unit parallel system. The concept of repair and post repair is not considered in all the above system models.

Goel et al. [6] studied a two unit redundant system in which one unit is operative and the other is a warm standby which replaces the operative failed unit instantaneously. After repair of the operative failed unit it is sent for inspection to decide whether the repaired unit is perfect or not. If the repaired unit is found to be imperfect, it is sent for post repair. Goel et al. [7] investigated a stochastic model of a two unit warm standby system with 'n' failure modes of each unit. Before starting the repair, the failed unit is examined for the type of fault, which decides the failure mode. This process takes a significant random amount of time. After repair, the unit is inspected to decide whether the repair is perfect or not. If the repair is found to be imperfect, the unit is sent for post repair. Agarwal and Mahajan [1] analysed a two-unit degrading system model with repair. After each repair, the unit is tested to see whether the repair meets certain pre-defined specifications. If it does, the unit is put to operation, otherwise it goes to post repair. Pandey et al. [13] discussed a two non-identical unit system with two types of repair, the internal and the external. The external repair is called only when the internal staff fails to do the job. In the case of external repair, there is a provision of inspection, wherein if the repair is found unsatisfactory, it is sent for post repair. Agnihotri et al. [2] analysed a system model consisting of two non-identical parallel units. They have assumed that the repaired unit goes for inspection to decide whether the repair is perfect or not. If the repair is found imperfect then it is sent for post repair. Agnihotri and Satsangi [3] analysed a system model consisting of two non-identical parallel units, in which the one unit gets the priority over the other for repair, inspection and post repair. Mokaddis et al. [12] investigated a two dissimilar unit cold standby redundant system with random interchange of the units. In this system it is assumed that the failure, repair, post repair, interchange of units and inspection times are stochastically independent random variables, each having an arbitrary distribution. The system is analysed by the Semi-Markov Process technique. In all the above system models, the concept of repair and post repair is used. After repair of the operative failed unit, it is sent for inspection to decide whether the repaired unit is perfect or not. If the repaired unit is found to be imperfect then the unit is sent for post repair. The above authors have assumed that time to failure of both the units are uncorrelated random variables.

Gupta and co-workers [8, 9] studied two unit complex / duplicate system by assuming different presumptions. In both these system models the failure and repair times are taken as correlated random variables. The joint distribution of failure and repair times is considered as bivariate exponential in both the models. Gupta and co-workers [10, 11] have also studied two unit active redundant systems by assuming different assumptions. Considering the lifetimes of the units as correlated random variable i.e. the joint distribution of lifetimes of the units is taken as bivariate exponential.

The objective of this paper is devoted to raise the idea of repair and post repair in two non-identical units parallel system assuming that the lifetimes of the units are correlated random variables having their joint distribution as bivariate exponential with joint p.d.f. as follows-

$$f(x_1, x_2) = \alpha_1\alpha_2(1-r)e^{-\alpha_1 x_1 - \alpha_2 x_2} I_0\left(2\sqrt{\alpha_1\alpha_2 r x_1 x_2}\right); \quad x_1, x_2, \alpha_1, \alpha_2 > 0; \quad 0 \le r < 1$$

where, $$I_0(z) = \sum_{k=0}^{\infty} \frac{(z/2)^{2k}}{(k!)^2}$$

is the modified Bessel function of type-I and order zero.

By using regenerative point technique, the following measures of system effectiveness are obtained-

i. Transient-state and steady-state transition probabilities.
ii. Mean sojourn time in various regenerative states.
iii. Reliability and mean time to system failure (MTSF).

iv. Point-wise and steady-state availabilities of the system as well as expected up time of the system during time interval (0, t).

v. The expected busy period of repairman in time interval (0, t).

vi. Net expected profit earned by the system in time interval (0, t) and in steady-state.

2. System Description and Assumptions

1. The system consists of two non-identical units- unit-1 and unit-2. Initially, both the units are operative in parallel configuration.
2. Each unit has two possible modes- Normal (N) and Total failure (F).
3. When a unit fails it goes to repair. After its repair, the repaired unit is sent for post repair.
4. A single repair facility is always available with the system to repair a failed unit and for post repair of repaired unit.
5. A post repaired unit always works as good as new.
6. The repair / post repair discipline is FCFS.
7. Failure time of both the units are assumed to be correlated random variables having their joint distribution as bivariate exponential (B.V.E.) with density function as follows-

$$f(x_1,x_2)=\alpha_1\alpha_2(1-r)e^{-\alpha_1x_1-\alpha_2x_2}\,I_0\left(2\sqrt{\alpha_1\alpha_2 r x_1x_2}\right);\quad x_1,x_2,\alpha_1,\alpha_2>0;\quad 0\le r<1$$

where, $$I_0(z)=\sum_{k=0}^{\infty}\frac{(z/2)^{2k}}{(k!)^2}$$

8. The repair time distribution of both the units are taken as general with different c.d.fs whereas the post repair time distribution of both the units are taken as exponential with different parameters.
9. The system failure occurs when both the units are in total failure mode.
10. A repaired unit always works as good as new.

3. Notations and States of the System

We define the following symbols for generating the various states of the system-

N_o^1, N_o^2:	Unit-1 and Unit-2 in normal (N) mode and operative.
F_r^1, F_r^2 :	Unit-1 and Unit-2 is in failure (F) mode and under repair.
F_{pr}^1, F_{pr}^2 :	Unit-1 and Unit-2 is in failure (F) mode and under post repair.
F_w^1, F_w^2 :	Unit-1 and Unit-2 is in failure (F) mode and waits for repair.

Considering the above symbols in view of assumptions stated in section-2, the possible states of the system are shown in the transition diagram represented by **Figure. 1**. It is to be noted that the epochs of transitions into the state S_3 from S_1, S_4 from S_1, S_5 from S_2 and S_6 from S_2 are non-regenerative, whereas all the other entrance epochs into the states of the systems are regenerative.

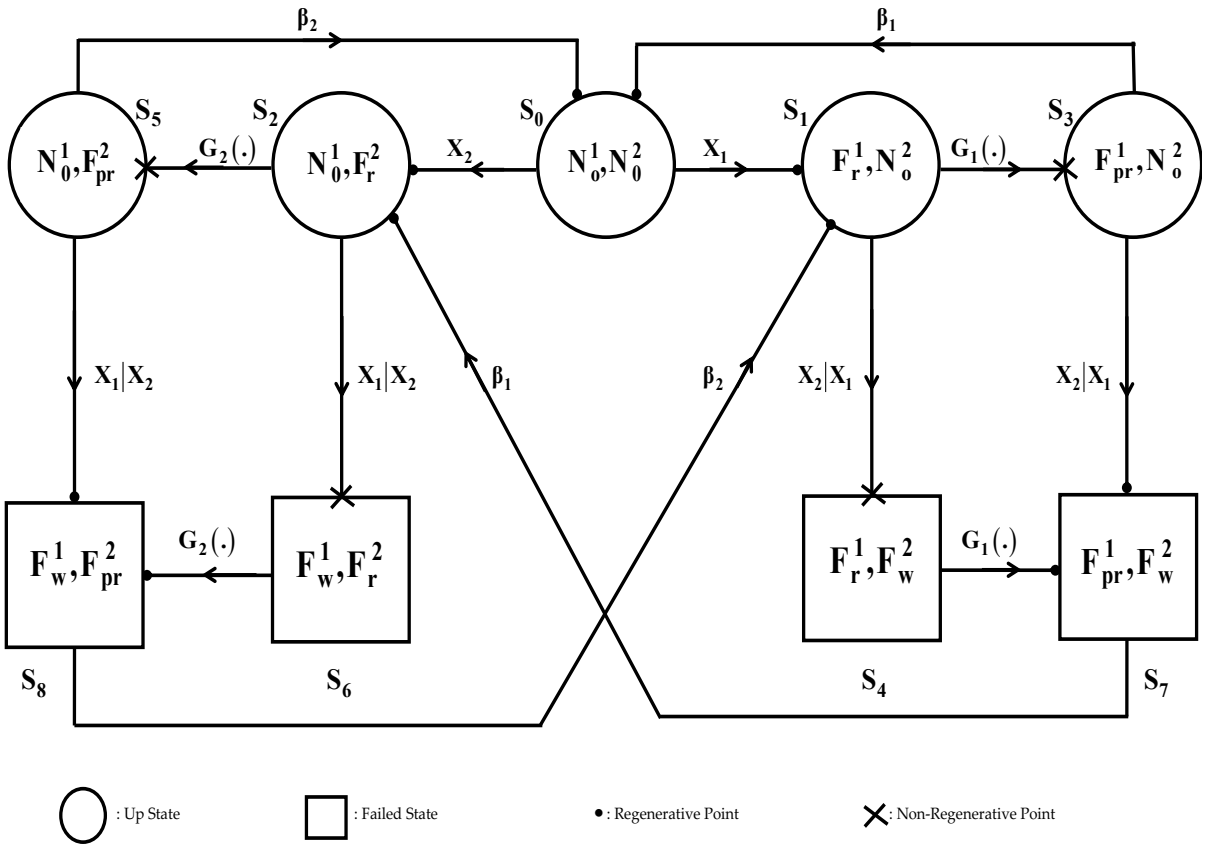

Figure 1: *Transition diagram*

The other notations used are defined as follows:

E : Set of regenerative states.

$X_i\,(i=1,2)$: Random variables representing the failure time of unit-1 in N-mode and unit-2 respectively for i = 1, 2.

$f(x_1,x_2)$: Joint p.d.f. of (x_1,x_2).

$$f(x_1,x_2)=\alpha_1\alpha_2(1-r)e^{-\alpha_1x_1-\alpha_2x_2}\,I_0\left(2\sqrt{\alpha_1\alpha_2rx_1x_2}\right);$$

$$x_1,x_2,\alpha_1,\alpha_2>0\;;\;0\le r<1$$

$$\text{where, } I_0(z)=\sum_{k=0}^{\infty}\frac{(z/2)^{2k}}{(k!)^2}$$

$g_i(x)$: Marginal p.d.f. of $X_i=x$

$$=\alpha_i(1-r_i)e^{-\alpha_i(1-r)x}$$

$k_1(x_1|X_2=x_2)$: Conditional p.d.f. of $X_1|X_2=x$.

$$=\alpha_1e^{-(\alpha_1x_1+\alpha_2rx)}I_0\left(2\sqrt{\alpha_1\alpha_2rxx_1}\right)$$

$k_2(x_2|X_1=x_1)$: Conditional p.d.f. of $X_2|X_1=x$.

$$=\alpha_2e^{-(\alpha_2x_2+\alpha_1rx)}I_0\left(2\sqrt{\alpha_1\alpha_2rxx_2}\right)$$

$K_i(\cdot\,|\,x)$: Conditional c.d.f. of $X_i|X_j=x,\ i\ne j\;;\;i,j=1,2$.

β_1,β_2 : Constant post repair rate of unit-1 and unit-2 respectively.

$G_1(\cdot),G_2(\cdot)$: c.d.f. of repair time of unit-1 and unit-2 respectively.

$q_{ij}(\cdot),q_{ij}^{(k)}(\cdot)$: p.d.f. of transition time from state S_i to S_j and S_i to S_j via S_k.

$p_{ij}, p_{ij}^{(k)}$: Steady-state transition probabilities from state S_i to S_j and S_i to S_j via S_k.

$p_{ij|x}, p_{ij|x}^{(k)}$: Steady-state transition probabilities from state S_i to S_j and S_i to S_j via S_k when it is known that the unit has worked for time x before its failure.

$*$: †Symbol for Laplace Transform i.e. $q_{ij}^{*}(s) = \int e^{-st} q_{ij}(t)\,dt$

$\sim$: Symbol for Laplace Stieltjes Transform i.e. $\tilde{Q}_{ij}(s) = \int e^{-st} dQ_{ij}(t)$

© : Symbol for ordinary convolution i.e.

$$A(t) \copyright B(t) = \int_0^t A(u)B(t-u)\,du$$

4. Transition Probabilities and Sojourn Times

Let $X(t)$ be the state of the system at epoch t, then $\{X(t); t \geq 0\}$ constitutes a continuous parametric Markov-Chain with state space $E = \{S_0 \text{ to } S_5\}$. The various measures of system effectiveness are obtained in terms of steady-state transition probabilities and mean sojourn times in various states. First we obtain the direct conditional and unconditional transition probabilities in terms of

$$\alpha_1' = \frac{\alpha_1}{\alpha_1+\beta_2}, \quad \alpha_1'' = \frac{\alpha_1}{\alpha_1+\lambda_2}, \quad \alpha_2' = \frac{\alpha_2}{\alpha_2+\beta_1} \quad \text{and} \quad \alpha_2'' = \frac{\alpha_2}{\alpha_2+\lambda_1}$$

as follows-

$$p_{01} = \int \alpha_1(1-r)e^{-\{\alpha_1(1-r)+\alpha_2(1-r)\}t}dt = \frac{\alpha_1}{\alpha_1+\alpha_2}$$

Similarly,

$$p_{02} = \frac{\alpha_2}{\alpha_1+\alpha_2}, \qquad p_{72} = \int \beta_1 e^{-\beta_1 t}dt = 1, \qquad p_{81} = \int \beta_2 e^{-\beta_2 t}dt = 1$$

$$p_{10|x}^{(3)} = \int \beta_1 e^{-\beta_1 v}\bar{K}_2(v|x)\left\{\int_0^v e^{\beta_1 u}dG_1(u)\right\}dv, \qquad p_{17|x}^{(3)} = \int e^{-\beta_1 v}\left\{\int_0^v e^{\beta_1 u}dG_1(u)\right\}dK_2(v|x)$$

$$p_{17|x}^{(4)} = \int \bar{G}_1(u)\,dK_2(u|x), \qquad p_{20|x}^{(5)} = \int \beta_2 e^{-\beta_2 v}\bar{K}_1(v|x)\left\{\int_0^v e^{\beta_2 u}dG_2(u)\right\}dv$$

$$p_{28|x}^{(5)} = \int e^{-\beta_2 v}\left\{\int_0^v e^{\beta_2 u}dG_2(u)\right\}dK_1(v|x), \qquad p_{28|x}^{(6)} = \int \bar{G}_2(u)\,dK_1(u|x)$$

The unconditional transition probabilities with correlation coefficient from some of the above conditional transition probabilities can be obtained as follows:

$$p_{10}^{(3)} = \int p_{10|x}^{(3)} g_1(x)\,dx = \int p_{10|x}^{(3)} \{\alpha_1(1-r)e^{-\alpha_1(1-r)x}\}dx$$

Similarly,

$$p_{17}^{(3)} = \int p_{17|x}^{(3)} \{\alpha_1(1-r)e^{-\alpha_1(1-r)x}\}dx, \qquad p_{17}^{(4)} = \int p_{17|x}^{(4)} \{\alpha_1(1-r)e^{-\alpha_1(1-r)x}\}dx = p_{14}$$

$$p_{20}^{(5)} = \int p_{20|x}^{(5)} \{\alpha_2(1-r)e^{-\alpha_2(1-r)x}\}dx, \qquad p_{28}^{(5)} = \int p_{28|x}^{(5)} \{\alpha_2(1-r)e^{-\alpha_2(1-r)x}\}dx$$

$$p_{28}^{(6)} = \int p_{28|x}^{(6)} \{\alpha_2(1-r)e^{-\alpha_2(1-r)x}\}dx = p_{26}$$

It can be easily verified that,

$$p_{01}+p_{02}=1, \quad p_{10}^{(3)}+p_{17}^{(3)}+p_{17}^{(4)}=1, \quad p_{20}^{(5)}+p_{28}^{(5)}+p_{28}^{(6)}=1, \quad p_{72}=p_{81}=1 \qquad (1\text{-}5)$$

[†]The limits of integration are 0 to ∞ whenever they are not mentioned.

5. Mean Sojourn Times

The mean sojourn time ψ_i in state S_i is defined as the expected time taken by the system in state S_i before transiting into any other state. If random variable U_i denotes the sojourn time in state S_i then,

$$\psi_i = \int P[U_i > t]dt$$

Therefore, its values for various regenerative states are as follows-

$$\psi_0 = \int e^{-(\alpha_1+\alpha_2)(1-r)t}\,dt = \frac{1}{(\alpha_1+\alpha_2)(1-r)} \tag{6}$$

$$\psi_{1|x} = \int \bar{G}_1(t)\bar{K}_2(t|x)dt = \int \bar{G}_1(t)\left(\int_t^\infty \alpha_2 e^{-(\alpha_2 u+\alpha_1 rx)}\sum_{j=0}^{\infty}\frac{(\alpha_1\alpha_2 rxu)^j}{(j!)^2}du\right)dt$$

$$\text{so that, } \psi_1 = \int \psi_{1|x} g_1(x)dx = \int \psi_{1|x}\alpha_1(1-r)e^{-\alpha_1(1-r)x}dx \tag{7}$$

$$\psi_{2|x} = \int \bar{G}_2(t)\bar{K}_1(t|x)dt = \int \bar{G}_2(t)\left(\int_t^\infty \alpha_1 e^{-(\alpha_1 u+\alpha_2 rx)}\sum_{j=0}^{\infty}\frac{(\alpha_1\alpha_2 rxu)^j}{(j!)^2}du\right)dt$$

$$\text{so that, } \psi_2 = \int \psi_{2|x} g_2(x)dx = \int \psi_{2|x}\alpha_2(1-r)e^{-\alpha_2(1-r)x}dx \tag{8}$$

$$\psi_{3|x} = \int e^{-\beta_1 t}\bar{K}_2(t|x)dt$$

$$\text{so that, } \psi_3 = \int \psi_{3|x} g_1(x)dx = \frac{1}{\beta_1}\left\{1-\frac{\alpha_2'(1-r)}{(1-r\alpha_2')}\right\} \tag{9}$$

$$\psi_4 = \int \bar{G}_1(t)dt \tag{10}$$

$$\psi_{5|x} = \int e^{-\beta_2 t}\bar{K}_1(t|x)dt$$

$$\text{so that, } \psi_5 = \int \psi_{5|x} g_2(x)dx = \frac{1}{\beta_2}\left\{1-\frac{\alpha_1'(1-r)}{(1-r\alpha_1')}\right\} \tag{11}$$

$$\psi_6 = \int \bar{G}_2(t)dt \tag{12}$$

$$\psi_7 = \int e^{-\beta_1 t}dt = \frac{1}{\beta_1} \tag{13}$$

$$\psi_8 = \int e^{-\beta_2 t}dt = \frac{1}{\beta_2} \tag{14}$$

6. Analysis of Characteristics

6.1. Reliability and MTSF

Let $R_i(t)$ be the probability that the system operates during (0, t) given that at t = 0 system starts from $S_i \in E$. To obtain it we assume the failed states S_4, S_6, S_7 and S_8 as absorbing. By simple probabilistic arguments, the value of $R_0(t)$ in terms of its Laplace Transform (L.T.) is given by

$$R_0^*(s)=\frac{Z_0^*+q_{01}^*\left(Z_1^*+q_{13}^*Z_3^*\right)+q_{02}^*\left(Z_2^*+q_{25}^*Z_5^*\right)}{1-q_{01}^*q_{10}^{(3)*}-q_{02}^*q_{20}^{(5)*}} \tag{15}$$

We have omitted the argument 's' from $q_{ij}^*(s)$ and $Z_i^*(s)$ for brevity. $Z_i^*(s);\ i=0,1,2,3,5$ are the L. T. of

$$Z_0(t)=e^{-(\alpha_1+\alpha_2)(1-r)t}\ ,\qquad Z_1(t)=\bar{G}_1(t)\left\{\int_t^\infty \alpha_2 e^{-(\alpha_2 z+\alpha_1 rx)}I_0\left(2\sqrt{\alpha_1\alpha_2 rxz}\right)dz\right\}g_1(x)dx$$

$$Z_2(t)=\bar{G}_2(t)\left\{\int_t^\infty \alpha_1 e^{-(\alpha_1 z+\alpha_2 rx)}I_0\left(2\sqrt{\alpha_1\alpha_2 rxz}\right)dz\right\}g_2(x)dx$$

$$Z_3(t)=\int e^{-\beta_1 t}\left\{\int_t^\infty \alpha_2 e^{-(\alpha_2 z+\alpha_1 rx)}I_0\left(2\sqrt{\alpha_1\alpha_2 rxz}\right)dz\right\}g_1(x)dx$$

$$Z_5(t)=\int e^{-\beta_2 t}\left\{\int_t^\infty \alpha_1 e^{-(\alpha_1 z+\alpha_2 rx)}I_0\left(2\sqrt{\alpha_1\alpha_2 rxz}\right)dz\right\}g_2(x)dx$$

Taking the Inverse Laplace Transform of (15), one can get the reliability of the system when system initially starts from state S_0.

The MTSF is given by,

$$E(T_0)=\int R_0(t)dt=\lim_{s\to 0}R_0^*(s)=\frac{\psi_0+p_{01}\left(\psi_1+p_{13}\psi_3\right)+p_{02}\left(\psi_2+p_{25}\psi_5\right)}{1-p_{01}p_{10}^{(3)}-p_{02}p_{20}^{(5)}} \tag{16}$$

6.2. Availability Analysis

Let $A_i(t)$ be the probability that the system is up at epoch t, when initially it starts operation from state $S_i\in E$. Using the regenerative point technique and the tools of Laplace transform, one can obtain the value of $A_0(t)$ in terms of its Laplace transforms i.e. $A_0^*(s)$ given as follows-

$$A_0^*(s)=\frac{N_1(s)}{D_1(s)} \tag{17}$$

where,

$$N_1(s)=\left(1-q_{17}^*q_{72}^*q_{28}^*q_{81}^*\right)Z_0^*+\left(q_{01}^*+q_{02}^*q_{28}^*q_{81}^*\right)\left(Z_1^*+q_{13}^*Z_3^*\right)+\left(q_{01}^*q_{17}^*q_{72}^*+q_{02}^*\right)\left(Z_2^*+q_{25}^*Z_5^*\right)$$

and

$$D_1(s)=1-q_{17}^*q_{72}^*q_{28}^*q_{81}^*-\left(q_{01}^*+q_{02}^*q_{28}^*q_{81}^*\right)q_{10}^{(3)*}-\left(q_{01}^*q_{17}^*q_{72}^*+q_{02}^*\right)q_{20}^{(5)*} \tag{18}$$

where, $A_i(t)$, i = 0,1,2,3,5 are same as given in section 6.1.

The steady-state availability of the system is given by

$$A_0=\lim_{t\to\infty}A_0(t)=\lim_{s\to 0}sA_0^*(s) \tag{19}$$

We observe that

$$D_1(0)=0$$

Therefore, by using L. Hospital's rule the steady state availability is given by

$$A_0=\lim_{s\to 0}\frac{N_1(s)}{D_1'(s)}=\frac{N_1}{D_1'} \tag{20}$$

where,

$$N_1=\left(1-p_{17}p_{28}\right)\psi_0+\left(p_{01}+p_{02}p_{28}\right)\left(\psi_1+p_{13}\psi_3\right)+\left(p_{01}p_{17}+p_{02}\right)\left(\psi_2+p_{25}\psi_5\right)$$

and

$$D_1' = (1-p_{17}p_{28})\psi_0 + \left(1-p_{02}p_{20}^{(5)}\right)\{(\psi_1 + p_{13}\psi_3 + p_{14}\psi_4) + p_{17}\psi_7\}$$
$$+\left(1-p_{01}p_{10}^{(3)}\right)\{(\psi_2 + p_{25}\psi_5 + p_{26}\psi_6) + p_{28}\psi_8\} \quad (21)$$

The expected up time of the system in interval (0, t) is given by

$$\mu_{up}(t) = \int_0^t A_0(u)\,du$$

So that, $\mu^*_{up}(s) = \dfrac{A_0^*(s)}{s}$

(22)

6.3. Busy Period Analysis

Let $B_i^1(t)$, $B_i^2(t)$, $B_i^3(t)$ and $B_i^4(t)$ be the respective probabilities that the repairman is busy in the repair of unit-1 and unit-2 and in the post repair of unit-1 and unit-2 at epoch t, when initially the system starts operation from state $S_i \in E$. Using the regenerative point technique and the tools of L.T., one can obtain the values of above four probabilities in terms of their L.T. i.e. $B_i^{1*}(s)$, $B_i^{2*}(s)$, $B_i^{3*}(s)$ and $B_i^{4*}(s)$ as follows-

$$B_i^{1*}(s) = \frac{N_2(s)}{D_1(s)},\ B_i^{2*}(s) = \frac{N_3(s)}{D_1(s)},\ B_i^{3*}(s) = \frac{N_4(s)}{D_1(s)} \text{ and } \quad B_i^{4*}(s) = \frac{N_5(s)}{D_1(s)} \quad (23\text{-}26)$$

where,

$$N_2(s) = \left(q_{01}^* + q_{02}^* q_{28}^* q_{81}^*\right)\left(Z_1^* + q_{14}^* Z_4^*\right)$$
$$N_3(s) = \left(q_{01}^* q_{17}^* q_{72}^* + q_{02}^*\right)\left(Z_2^* + q_{26}^* Z_6^*\right)$$
$$N_4(s) = q_{13}^*\left(q_{01}^* + q_{02}^* q_{28}^* q_{81}^*\right)Z_3^* + \left(q_{01}^* q_{17}^* + q_{02}^* q_{28}^* q_{81}^* q_{17}^*\right)Z_7^*$$
$$N_5(s) = q_{25}^*\left(q_{01}^* q_{17}^* q_{72}^* + q_{02}^*\right)Z_5^* + \left(q_{01}^* q_{17}^* q_{72}^* q_{28}^* + q_{02}^* q_{28}^*\right)Z_8^*$$

and $D_1(s)$ is same as defined by the expression (18) of section 6.2.

Also Z_4^*, Z_6^*, Z_7^* and Z_8^* are the L. T. of

$$Z_4(t) = \bar{G}_1(t),\quad Z_6(t) = \bar{G}_2(t),\quad Z_7(t) = e^{-\beta_1 t},\quad Z_8(t) = e^{-\beta_2 t}$$

The steady state results for the above three probabilities are given by-

$$B_o^1 = \lim_{s\to 0} sB_0^*(s) = N_2/D_1',\quad B_o^2 = N_3/D_1',\quad B_o^3 = N_4/D_1' \text{ and } \quad B_0^4 = N_5/D_1' \quad (27\text{-}30)$$

$$N_2 = \left(1-p_{02}p_{20}^{(5)}\right)(\psi_1 + p_{14}\psi_4)$$
$$N_3 = \left(1-p_{01}p_{10}^{(3)}\right)(\psi_2 + p_{26}\psi_6)$$
$$N_4 = \left(1-p_{02}p_{20}^{(5)}\right)(p_{13}\psi_3 + p_{17}\psi_7)$$
$$N_5 = \left(1-p_{01}p_{10}^{(3)}\right)(p_{25}\psi_5 + p_{28}\psi_8)$$

and D_1' is same as given in the expression (21) of section 6.2.

The expected busy period in repair of unit-1 and unit-2 and post repair of unit-1 and unit-2 during time interval (0, t) are respectively given by-

$$\mu_b^1(t)=\int_0^t B_0^1(u)du,\qquad \mu_b^2(t)=\int_0^t B_0^2(u)du,\qquad \mu_b^3(t)=\int_0^t B_0^3(u)du \text{ and } \qquad \mu_b^4(t)=\int_0^t B_0^4(u)du$$

So that,

$$\mu_b^{1*}(s)=B_0^{1*}(s)/s,\qquad \mu_b^{2*}(s)=B_0^{2*}(s)/s,\qquad \mu_b^{3*}(s)=B_0^{3*}(s)/s \text{ and } \qquad \mu_b^{4*}(s)=B_0^{4*}(s)/s$$

(31-34)

6.4. Profit Function Analysis

The net expected total cost incurred in time interval (0, t) is given by

$P(t)$ = Expected total revenue in (0, t) - Expected cost of repair in (0, t)

$$=K_0\mu_{up}(t)-K_1\mu_b^1(t)-K_2\mu_b^2(t)-K_3\mu_b^3(t)-K_4\mu_b^4(t) \tag{35}$$

Where, K_0 is the revenue per- unit up time by the system during its operation. K_1, K_2, K_3 and K_4 are the amounts paid to the repairman per-unit of time when he is busy in the repair of unit-1 and unit-2 and in the post repair of unit-1 and unit-2 respectively.

The expected total profit incurred in unit interval of time is

$$P=K_0A_0-K_1B_0^1-K_2B_0^2-K_3B_0^3-K_4B_0^4 \tag{36}$$

7. Particular Case

When the time of satisfactory repair of unit-1 and unit-2 also follow exponential with p.d.fs as follows-

$$g_1(t)=\lambda_1e^{-\lambda_1 t},\qquad g_2(t)=\lambda_2e^{-\lambda_2 t}$$

The Laplace Transform of above density function are as given below-

$$g_1^*(s)=\tilde{G}_1(s)=\frac{\lambda_1}{s+\lambda_1},\qquad g_2^*(s)=\tilde{G}_2(s)=\frac{\lambda_2}{s+\lambda_2}$$

Here, $\tilde{G}_1(s)$ and $\tilde{G}_2(s)$ are the Laplace-Stieltjes Transforms of the c.d.fs $G_1(t)$ and $G_2(t)$ corresponding to the p.d.fs $g_1(t)$ and $g_2(t)$.

In view of above, the changed values of transition probabilities and mean sojourn times.

$$p_{10}^{(3)}=1-\frac{\lambda_1}{(\lambda_1-\beta_1)}\frac{\alpha_2'(1-r)}{(1-r\alpha_2')}+\frac{\beta_1}{(\lambda_1-\beta_1)}\frac{\alpha_2''(1-r)}{(1-r\alpha_2'')},\qquad p_{17}^{(3)}=\frac{\lambda_1}{(\lambda_1-\beta_1)}\left[\frac{\alpha_2'(1-r)}{(1-r\alpha_2')}-\frac{\alpha_2''(1-r)}{(1-r\alpha_2'')}\right]$$

$$p_{17}^{(4)}=\frac{\alpha_2''(1-r)}{(1-r\alpha_2'')},\qquad p_{20}^{(5)}=1-\frac{\lambda_2}{(\lambda_2-\beta_2)}\frac{\alpha_1'(1-r)}{(1-r\alpha_1')}+\frac{\beta_2}{(\lambda_2-\beta_2)}\frac{\alpha_1''(1-r)}{(1-r\alpha_1'')}$$

$$p_{28}^{(5)}=\frac{\lambda_2}{(\lambda_2-\beta_2)}\left[\frac{\alpha_1'(1-r)}{(1-r\alpha_1')}-\frac{\alpha_1''(1-r)}{(1-r\alpha_1'')}\right],\qquad p_{28}^{(6)}=\frac{\alpha_1''(1-r)}{(1-r\alpha_1'')}$$

$$\psi_1=\frac{1}{\alpha_2(1-r)+\lambda_1},\qquad \psi_2=\frac{1}{\alpha_1(1-r)+\lambda_2}$$

$$\psi_4=\frac{1}{\lambda_1},\qquad \psi_6=\frac{1}{\lambda_2}$$

8. Graphical Study of Behaviour and Conclusions

For a more clear view of the behaviour of system characteristics with respect to the various parameters involved, we plot curves for **MTSF** and **profit function** in **Fig. 2** and **Fig. 3** w.r.t. α_1 for three different values of correlation coefficient r =**0.16, 0.26** and **0.35** and two different values of repair parameter λ_1 =**0.41** and **0.5** while the other parameters are kept fixed as $\lambda_2 = 0.15,\ \alpha_2 = 0.05,\ \beta_1 = 0.35$ and $\beta_2 = 0.01$. From the curves of **Fig. 2,** we observe that **MTSF** increases uniformly as the values of r and λ_1 increase and it decreases with the increase in α_1. Further, to achieve **MTSF** at least **20** units we conclude from smooth curves that the value of α_1 must be less than **0.2, 0.15 and 0.11** respectively for $r = 0.16$, **0.26** , **0.35** when $\lambda_1 = 0.5$. Whereas from dotted curves we conclude that the value of α_1 must be less than **0.2, 0.16, 0.12** for $r = 0.16$, **0.26** , **0.35** when $\lambda_1 = 0.41$ to achieve at least **12** units of **MTSF**.

Similarly, **Fig. 3** reveals the variations in **profit (P)** w.r.t. α_1 for varying values of r and λ_1, when the values of other parameters are kept fixed as $\lambda_2 = 0.1,\ \alpha_2 = 0.05,\ \beta_1 = 0.35,\ \beta_2 = 0.3, K_0 = 800$, $K_1 = 600, K_2 = 500,\ K_3 = 400$ and $K_4 = 300$. Here also the same trends in respect of α_1 , r and λ_1 are observed as in case of **MTSF**. Moreover, we conclude from the smooth curves that the system is profitable only if α_1 is less than **0.75, 0.5** and **0.37** respectively for $r = 0.25$, **0.35, 0.45** when $\lambda_1 = 0.5$. From dotted curves, we conclude that the system is profitable only if α_1 is less than **0.2, 0.15** and **0.12** respectively for $r = 0.25$, **0.35,** and **0.45** when $\lambda_1 = 0.4$.

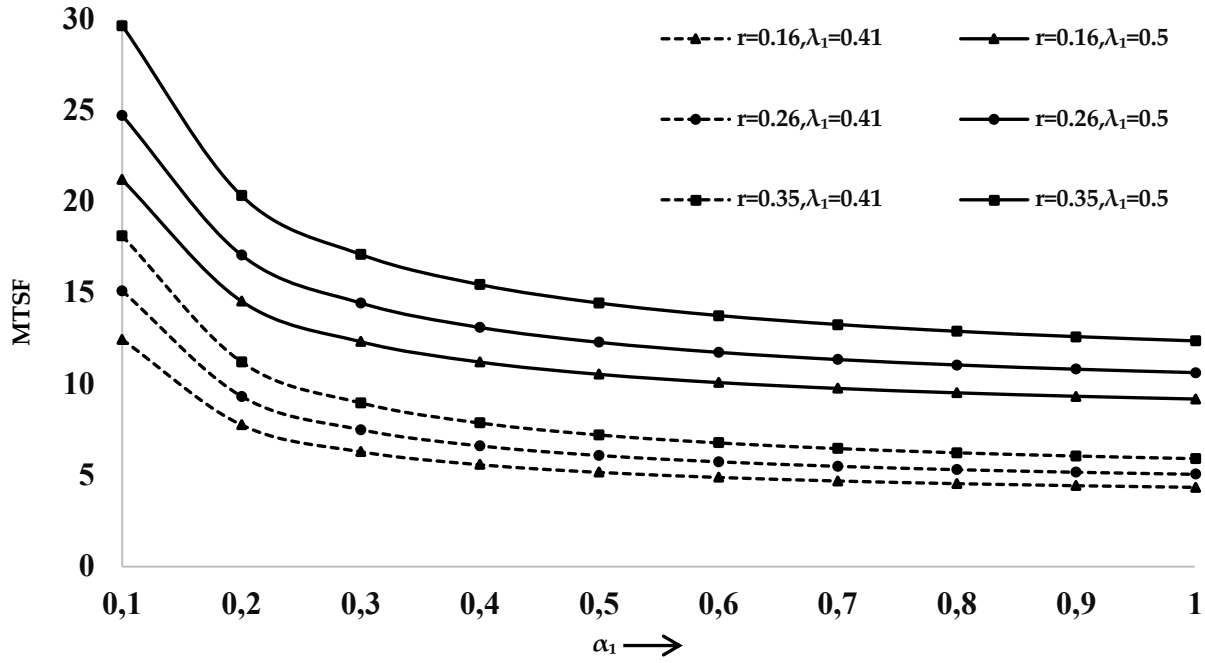

Figure 2: *Behaviour of MTSF w.r.t. α_1 for different values of r and λ_1*

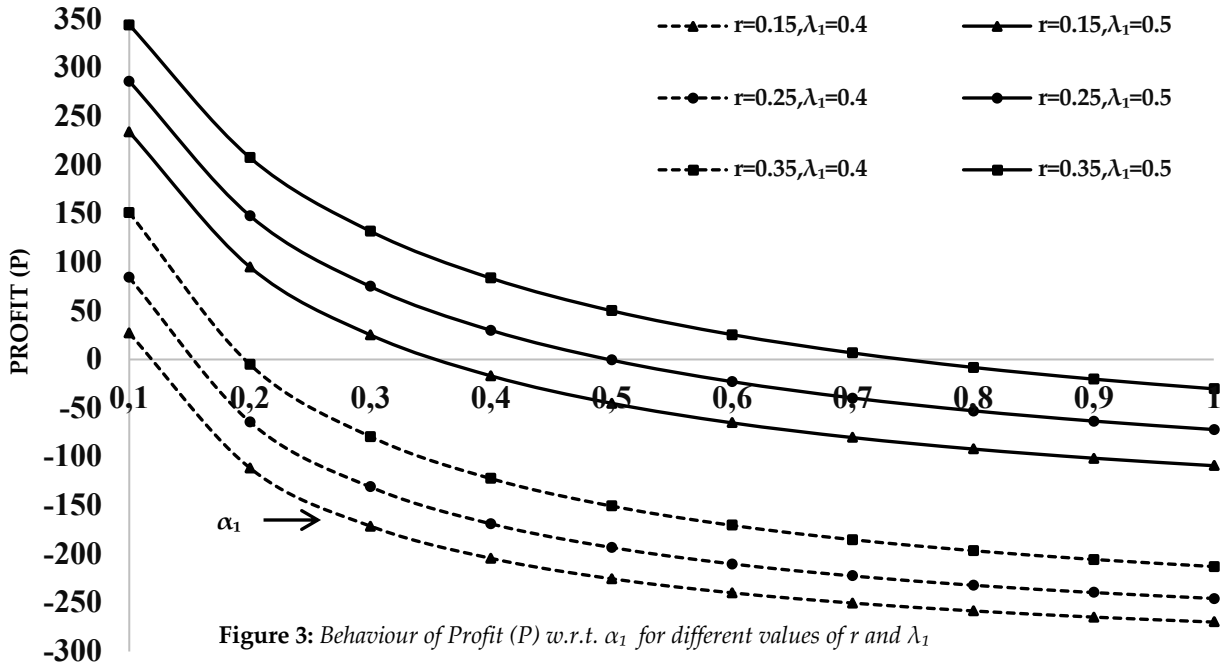

Figure 3: *Behaviour of Profit (P) w.r.t. α_1 for different values of r and λ_1*

9. Acknowledgment

"Author Surbhi Masih thanks to University Grants Commission, Maulana Azad National Fellowship for providing funding support during my Ph.d Course."

References

[1] Agarwal, A. and Mahajan, M. (1993). Performance-related reliability-measures for a repairable 2-unit gracefully degrading system. *Microelectronics and Reliability*, 33(7):921-927.

[2] Agnihotri, R.K., Satsangi, S.K. and Agrawal, S.C. (1995). 2 non-identical operative unit system with repair and inspection. *Microelectronics and Reliability*, 35(5):869-874.

[3] Agnihotri, R.K. and Satsangi, S.K. (1996). Two non-identical unit system with priority based repair and inspection. *Microelectronics and Reliability*, 36(2):279-282.

[4] Chandra, A., Naithani, A., Gupta, S. and Jaggi, C.K. (2020). Reliability and cost analysis comparison between two-unit parallel systems with non-identical and identical consumable units. *Journal of Critical Reviews*, 7(7):695-702.

[5] Chopra, G. and Mangey, R. (2017). Stochastic analysis of two non-identical unit parallel system incorporating waiting time. *International Journal of Quality and Reliability Management*, 34(6):817-832.

[6] Goel, L.R., Agnihotri, R.K. and Gupta, R. (1991). 2-unit redundant system with inspection and adjustable rates. *Microelectronics and Reliability*, 31(1):11-14.

[7] Goel, L.R., Agnihotri, R.K. and Gupta, R. (1991). A single server 2-unit warm standby system with n-failure modes, fault detection and inspection. *Microelectronics and Reliability*, 31(5):841-845.

[8] Gupta, R. and Kumar, K. (2008). A two unit complex system with correlated failure and repair times. *Pure and Applied Matheka Sci.*, LXVII(1-2):23-34.

[9] Gupta, R. and Shivakar (2010). Cost-benefit analysis of a two unit parallel system with correlated failure and repair times. *IAPQR Transactions*, 35(2):117-140.

[10] Gupta, R., Sharma, P. and Sharma, V. (2010). Cost-benefit analysis of a two unit duplicate parallel system with repair/replacement and correlated life time of units. *Journal of Rajasthan Academy and Physical Sciences*, 9(4):317-330.

[11] Gupta, R., Sharma, P.K. and Shivakar (2013). A two-unit active redundant system with two physical conditions of repairman and correlated life times. *Journal of Ravishankar University*, b-24-26:40-51.

[12] Mokaddis, G.S., Tawfek, M.L. and Elhssia, S.A.M. (1997). Analysis of a two dissimilar unit cold standby redundant system subject to inspection and random change in units. *Microelectronics and Reliability,* 37(2):329-334.

[13] Pandey, D., Tyagi, S.K. and Jacob, M. (1995). Profit evaluation of a 2-unit system with internal and external repairs, inspection and post repair. *Microelectronics and Reliability,* 35(2):259-264.

[14] Pundir, P.S., Patawa, R. and Gupta, P.K. (2018). Stochastic outlook of two non-identical unit parallel system with priority in repair. *Cogent Mathematics*, 5(1).

ESTIMATION OF STRESS-STRENGTH RELIABILITY FOR AKASH DISTRIBUTION

Akhila K Varghese, V. M. Chacko
•
Department of Statistics
St. Thomas' College (Autonomous)
Thrissur, Kerala, 680 001, India
akhilavarghesek@gmail.com
chackovm@gmail.com

Abstract

In this paper, we consider the estimation of the stress–strength parameter R = P[Y < X], when X and Y are following one-parameter Akash distributions with parameter θ_1 and θ_2 respectively. It is assumed that they are independently distributed. The maximum likelihood estimator (MLE) of R and its asymptotic distribution are obtained. Asymptotic distributions of the maximum likelihood estimator is useful for constructing confidence interval of P[Y < X]. The Bootstrap confidence interval of P[Y < X] is also computed. The illustrative part consists of the analysis of two real data sets, (i) simulated and (ii) real.

Keywords: stress–strength model; maximum-likelihood estimator; bootstrap confidence intervals; asymptotic distributions

I. Introduction

In reliability analysis, estimation of stress-strength reliability is one of the important and difficult but tractable problem, while using various distributions. In the statistical literature, estimating the stress–strength parameter, R, is quite useful. For example, if X is a measure of a system's strength when it is subjected to a stress Y, then R is a measure of system performance that naturally occurs in a system's mechanical dependability. The system fails if and only if the applied stress exceeds its strength at any point. In reliability analysis, a variety of lifespan distributions are used. In dependability analysis, terms like exponential, Weibull, log-Normal, and their generalizations are frequently used. A number of academics have recently proposed several distributions, with the new ones demonstrating a superior fit than current well-known distributions. While using better fitted models in stress-strength analysis, one may have to inspect its estimation procedure, since, if the estimation procedure fails with available techniques, one may not be able to solve the problem with new models. So estimation of various reliability parameters is vital and researchers have to give more concentration of estimation while using better fitted models.

The estimation of reliability or survival probability of a stress-strength model when X and Y have specified distributions has been discussed in literature. The survival probabilities of a single component stress-strength (SSS) model have been considered by several authors for different

distributions, see Raqab and Kundu [13], Kundu and Gupta [9,10], Constantine and Karson [6] and Downtown [7]. Several authors have studied the problem of estimating R. Church and Harris [5] derived the MLE of R when X and Y are independently Normally distributed. The MLE of R, when X and Y have bivariate exponential distributions has been considered by Awad et. al. [2]. Awad and Gharraf [3] provided a simulation study to compare three estimates of R when X and Y are independent but not identically distributed Burr random variables. Ahmad et. al. [1} and Surles and Padgett [15,14] provided estimates for R when X and Y are having Burr Type X distribution.

In this paper, we consider the problem of estimating the stress–strength reliability parameter R = P(Y < X), when X and Y be independent strength and stress random variables having Akash distribution with parameters θ_1 and θ_2 respectively. Rama Shanker [12] introduced Akash distribution by considering a two-component mixture of an Exponential distribution having scale parameter θ and a Gamma distribution having shape parameter 3 and scale parameter θ. The probability density function (pdf) of Akash distribution can be defined as

$$f(x;\theta) = \frac{\theta^3}{\theta^2+2}(1+x^2)e^{-\theta x}; x > 0, \theta > 0.$$

The corresponding cumulative distribution function (cdf) is given by

$$F(x) = 1 - \left[1 + \frac{\theta x(\theta x+2)}{\theta^2+2}\right]e^{-\theta x}; x > 0, \theta > 0.$$

The estimation of the stress–strength parameter R = P[Y < X], when X and Y are having one-parameter Akash distributions with parameter θ_1 and θ_2 respectively, is an unsolved problem. Statistical inference on stress-strength parameters is important in reliability analysis. It is observed that the maximum likelihood estimators can be obtained implicitly by solving two nonlinear equations, but they cannot be obtained in closed form. So, MLE's of parameters are derived numerically. It is not possible to compute the exact distributions of the maximum likelihood estimators, and we used the asymptotic distribution and we constructed approximate confidence intervals of the unknown parameters.

The rest of the paper is organized as follows. In Section 2, the MLE of R is computed. The asymptotic distribution of the MLEs are provided in Section 3. Bootstrap confidence interval is presented in Section 4. In Section 5, simulation study is given. Theoretical results are verified by analyzing one data set in Section 6 and conclusions are given in Section 7.

II. Maximum Likelihood Estimator of R

In this section, the procedure of estimating the reliability of P[Y<X] models using Akash distributions, is considered. It is clear that

$$R = P(Y < X) = \int_{X<Y} f(x,y)dxd\,y = \int_0^\infty f(x;\theta_1)F(x;\theta_2)dx$$

where f (x,y), is the joint pdf of random variables X and Y, having Akash distributions. If the r.v's X and Y are independent, then f (x, y) = f (x) g(y), where f (x) and g(y) are the marginal pdfs of X and Y, so that

$$R = \int_0^\infty \frac{\theta_1^3}{\theta_1^2+2}(1+x^2)e^{-\theta_1 x}1 - \left[\frac{1+\theta_2 x(\theta_2 x+2)}{\theta_2^2+2}\right]e^{-\theta_2 x}dx.$$

On simplification we get.

$$R = 1 - \frac{\theta_1^3[\theta_2^6+4\theta_1\theta_2^5+6\theta_1^2\theta_2^4+4\theta_1^3\theta_2^3++22\theta_1\theta_2^3+\theta_1^4\theta_2^2+22\theta_1^2\theta_2^2+4\theta_1^2+2\theta_1^4+20\theta_1\theta_2+10\theta_2^3\theta_2+40\theta_2^2+8\theta_2^4]}{(\theta_1^2+2)\left(2+\theta_2^2\right)(\theta_1+\theta_2)^5}$$

If we have two ordered random samples representing strength (X1,X2,...,Xn) and stress (Y1, Y2,...,Ym) of sizes n and m respectively, following Akash distribution with parameters θ_1 and θ_2, respectively. Then the likelihood function of the combined random sample can be obtained as follows

$$L = \prod_{i=1}^{n} \frac{\theta_1^3}{\theta_1^2+2}(1+x_i^2)e^{-\theta_1 x_i} \prod_{i=1}^{m} \frac{\theta_2^3}{\theta_2^2+2}\left(1+y_j^2\right)e^{-\theta_2 y_j}.$$

The log-likelihood function is

$$l = logL = 3n\ log\ \theta_1 - (\theta_1^2+2) - \theta_1\sum_{i=1}^{n}x_i + \sum_{i=1}^{n} log\ (1+x_i{}^2) + 3m\ log\ \theta_2 - mlog\ (\theta_2^2+2) - \theta_2\sum_{i=1}^{m}y_i + \sum_{i=1}^{m} log\left(1+y_j^2\right). \text{----------(1)}$$

The solution of the following non-linear equations yield the MLE of the parameters θ_1 and θ_2. Differentiating (1) with respect to parameters θ_1 and θ_2, we get

$$\frac{\partial l}{\partial \theta_1} = \frac{3n}{\theta_1} - \frac{n2\theta_1}{(\theta_1^2+2)} - \sum_{i=1}^{n}x_i$$

and

$$\frac{\partial l}{\partial \theta_2} = \frac{3m}{\theta_2} - \frac{m2\theta_2}{(\theta_2^2+2)} - \sum_{i=1}^{m}y_j.$$

The second partial derivatives of (1) with respect to parameters θ_1 and θ_2, are

$$\frac{\partial^2 l}{\partial \theta_1^2} = \frac{-3n}{\theta_1^2} - \frac{2n(2-\theta_1^2)}{(\theta_1^2+2)^2}$$

and

$$\frac{\partial^2 l}{\partial \theta_2^2} = \frac{-3m}{\theta_2^2} - \frac{2m(2-\theta_2^2)}{(\theta_2^2+2)^2}$$

MLE of R is obtained as

$$\hat{R} = 1 - \frac{\hat{\theta}_1^3[\hat{\theta}_2^6+4\hat{\theta}_1\hat{\theta}_2^5+6\hat{\theta}_1^2\hat{\theta}_2^4+4\hat{\theta}_1^3\hat{\theta}_2^3++22\hat{\theta}_1\hat{\theta}_2^3+\hat{\theta}_1^4\hat{\theta}_2^2+22\hat{\theta}_1^2\hat{\theta}_2^2+4\hat{\theta}_1^2+2\hat{\theta}_1^4+20\hat{\theta}_1\hat{\theta}_2+10\hat{\theta}_2^3\hat{\theta}_2+40\hat{\theta}_2^2+8\hat{\theta}_2^4]}{(\hat{\theta}_1^2+2)\left(2+\hat{\theta}_2^2\right)(\hat{\theta}_1+\hat{\theta}_2)^5}$$

This can be used in estimation of stress-strength for the given data.

III. Asymptotic Distribution and Confidence Intervals

In this section, the asymptotic distribution and confidence interval of the MLE of R are obtained. To find an asymptotic variance of the MLE $\hat{R}^{ML}$, let us denote the Fisher information

matrix of $\theta = (\theta_1, \theta_2)$ as $I(\theta) = [I_{ij}(\theta); i, j = 1,2]$, i.e.,

$$I(\theta) = E\begin{bmatrix} \frac{-\partial^2 l}{\partial \theta_1^2} & \frac{-\partial^2 l}{\partial \theta_1 \partial \theta_2} \\ \frac{-\partial^2 l}{\partial \theta_2 \partial \theta_1} & \frac{-\partial^2 l}{\partial \theta_2^2} \end{bmatrix}$$

To establish the asymptotic Normality, we define

$$d(\theta) = \left(\frac{\partial R}{\partial \theta_1}, \frac{\partial R}{\partial \theta_2}\right)' = (d_1, d_2)',$$

where

$$\frac{\partial R}{\partial \theta_1} = -\left\{\left(\frac{\theta_1^3}{(\theta_1^2+2)(\theta_2^2+2)(\theta_1+\theta_2)^5}\right)(4\theta_2^5 + 12\theta_1\theta_2^4 + 12\theta_1^2\theta_2^3 + 22\theta_2^3 + 4\theta_1^3\theta_2^2 + 44\theta_1\theta_2^2 + 30\theta_1^2 + 20\theta_2 + 8\theta_1^3 + 8\theta_1) + \left(\frac{(\theta_1^2+2)(\theta_2^2+2)(\theta_1+\theta_2)^5 3\theta_1^2 - \theta_1^3(\theta_2^2+2)[(\theta_1^2+2)5(\theta_1+\theta_2)^4 + 2\theta_1]}{(\theta_1^2+2)^2(\theta_2^2+2)^2(\theta_1+\theta_2)^{10}}\right)(\theta_2^6 + 4\theta_1\theta_2^5 + 6\theta_1^2 + \theta_2^4 + 8\theta_2^4 + 4\theta_1^3\theta_2^3 + 22\theta_1\theta_2^3 + \theta_1^4\theta_2^2 + 22\theta_1^2\theta_2^2 + 40\theta_2^2 + 10\theta_1^3\theta_2 + 20\theta_1\theta_2 + 2\theta_1^4 + 4\theta_1^2)\right\}$$

$$\frac{\partial R}{\partial \theta_2} = \left\{\left(\frac{\theta_1^3}{(\theta_1^2+2)(\theta_2^2+2)(\theta_1+\theta_2)^5}\right)(6\theta_2^5 + 20\theta_1\theta_2^4 + 24\theta_1^2\theta_2^3 + 32\theta_2^3 + 12\theta_1^3\theta_2^2 + 66\theta_1\theta_2^2 + 2\theta_1^4\theta_2 + 44\theta_1^2\theta_2 + 80\theta_2 + 10\theta_1^3 + 20\theta_1) + \left(\frac{-\theta_1^3(\theta_1^2+2)[(\theta_2^2+2)5(\theta_1+\theta_2)^4 + (\theta_1+\theta_2)2\theta_2]}{(\theta_1^2+2)^2(\theta_2^2+2)^2(\theta_1+\theta_2)^{10}}\right)(\theta_2^6 + 4\theta_1 + \theta_2^5 + 6\theta_2^2 + 22\theta_2^2 + 8\theta_2^2 + \theta_2^2 + +\theta_1^3\theta_2^3 + 22\theta_1\theta_2^3 + \theta_2^2 + 10\theta_1^3\theta_2 + 20\theta_1\theta_2 + 2\theta_1^4 + 4\theta_1^2)\right\}.$$

We obtain the asymptotic distribution of $\hat{R}^{ML}$ as

$$\sqrt{n+m}(\hat{R}^{ML} - R) \to^d N(0, d'(\theta)I^{-1}(\theta)d(\theta)).$$

The asymptotic variance of $\hat{R}^{ML}$ is obtained as

$$AV(\hat{R}^{ML}) = \frac{1}{n+m} d'(\theta)^{-1} I(\theta) d(\theta).$$

$$i.e., AV(\hat{R}^{ML}) = V(\hat{\theta}_1)d_1^2 + V(\hat{\theta}_1)d_2^2 + 2d_1d_2(\hat{\theta}_1, \hat{\theta}_1).$$

Asymptotic $100(1-\gamma)\%$ confidence interval for R can be obtained as

$$\hat{R}^{ML} \pm Z_{\frac{\gamma}{2}}\sqrt{AV\left(\hat{R}^{ML}\right)}.$$

IV. Bootstrap Confidence Intervals

In this section, we use confidence intervals based on the parametric percentile bootstrap methods (we call it from now on as Boot-p), Kundu et. al. [11]. Bootstrapping is a statistical approach that resamples a single dataset in order to build up a huge proportion of simulated samples. To estimate confidence intervals of R in this methods, the following steps are used.

1.Estimate θ and ,say $\hat{\theta}$, from the sample using maximum likelihood estimate method
2. Generate a bootstrap sample $(x_{1:n,}x_{2:n,}, x_{2:n,}, \dots x_{n:n,})$ using $\hat{\theta}$, where $x_{i:n}$ represents the ith observation when there are n observations in the experiment. Obtain the bootstrap estimate of θ, say $\hat{\theta}*$ using the bootstrap sample.
3. Repeat Step [2] NBOOT times.
4. Let $CD\bar{F}(x) = P\left(\hat{\theta}^{*} \leq x\right)$, be the cumulative distribution function of $\hat{\lambda}^{*}$. Define $\hat{\theta}_{Boot-p}(x) = \widehat{CD}F^{-1}(x)$ for a given x. The approximate $100(1-\alpha)\%$ confidence interval for θ is given by

$$\left(\hat{\theta}_{Boot-p}\left(\frac{\alpha}{2}\right), \hat{\theta}_{Boot-p}\left(1-\frac{\alpha}{2}\right)\right)$$

V. SIMULATION STUDY

In this section, we present some results based on inversion method to assess the performance of estimators of R. For this purpose, we have generated 1000 samples from independent Akash (θ_1) and Akash (θ_2) distributions. We considered sets of parameter values 1.25 and 1.75 which correspond to the R values 0.6491261. The bias and the mean square error (MSE) of the parameter estimates are calculated. In Tables 1, Maximum likelihood estimate of R (R(ML)), the average biase, MSE, asymptotic confidence Intervals (AS(CI)) and Bootstrap confidence interval (BT(CI)) corresponding to different (n,m) values are calculated by the method explained in section 3.

Table 1

(n,m)	$R(ML)$	$BIAS$	MSE	AS(CI)	BT(CI)
$(7,7)$	0.712703	0.06357	0.007773	0.5929103,0.8324957	0.6775518,0.8844710
$(15,15)$	0.714086	0.06495	0.006078	0.6295406,0.7986314	0.6777669,0.8394092
$(30,30)$	0.713589	0.06446	0.005118	0.652743,0.7744354	0.64231680.7997702
$(30,35)$	0.713068	0.06399	0.004900	0.6571613,0.7689664	0.5521229,0.7371387
$(40,40)$	0.713401	0.06426	0.004835	0.6614061,0.7654101	0.6363909,0.7394242
$(50,50)$	0.713477	0.06341	0.004699	0.667147,0.7598043	0.6572927,0.7705276

From the simulation results, it is observed that as the sample size (n,m) increases the biases and the MSEs decrease. Thus the consistency properties of all the methods are verified.

VI. DATA ANALYSIS

In this section, we consider two real data sets of the breaking strengths of jute fiber at two different gauge lengths (see Xia et. al. [16]). Two sets of real data are shown as follows.

Data set I: Breaking strength of jute fiber length 10 mm (variable X) 693.73, 704.66, 323.83, 778.17, 123.06, 637.66, 383.43, 151.48, 108.94, 50.16, 671.49, 183.16, 257.44, 727.23, 291.27, 101.15, 376.42, 163.40, 141.38, 700.74, 262.90, 353.24, 422.11, 43.93, 590.48, 212.13, 303.90, 506.60, 530.55, 177.25.

Data set II: Breaking strength of jute fiber length 20 mm (variable Y) 71.46, 419.02, 284.64, 585.57, 456.60, 113.85, 187.85, 688.16, 662.66, 45.58, 578.62, 756.70, 594.29, 166.49, 99.72, 707.36, 765.14, 187.13, 145.96, 350.70, 547.44, 116.99, 375.81, 581.60, 119.86, 48.01, 200.16, 36.75, 244.53, 83.55

These data were first used by Xia et al. [16] and later by Saracoglu et. al. [4]. Shahsanaei and Daneshkhah [8] used the data to study the estimation of stress-strength parameter for generalized linear failure rate distribution (GLFRD) under progressive type-II censoring and studied the validity of GLFRD for both data sets.

The table 2 gives the result of goodness of fit test. The test used to check whether the considered distribution is a good fit to the data.

Table 2

PLANE	MLEs	K-S Statistic	P-value
length 10 $mm(X)$	0.00831404	0.13641	0.5847
length 20 $mm(Y)$	0.00880360	0.20925	0.1248

MLEs of parameters of Akash (θ_1) and Akash (θ_2) distributions are 0.00831404 and 0.00880360. Reliability P(Y<X) value for the data is 0.526798. The 95% asymptotic interval of R is (0.36446, 0.7335) and 95% bootstrap confidence interval is (0.376799,0.676798).

VII. CONCLUSION

In this paper, we considered the problem of estimation of P(Y<X) using Akash distribution. The MLE of SSS reliability, R is obtained. Also, asymptotic $100(1-v)\%$ CI for the reliability parameter is computed. Bootstrap confidence interval is also obtained. When the sample size is increased, MSE caused by the estimates comes nearer to zero by extensive simulation. Finally, real data sets are analyzed.

Acknowledgement

The authors are thankful for the comments of referees and editors which helped to improve the paper.

References

[1] Ahmad, K.E., Fakhry, M.E. and Jaheen, Z.F.(1997). Empirical Bayes Estimation of P(Y<X) and characterizations of the Burr-Type X Model, Journal of Statistical Planning and Inference 64, 297-308.

[2] Awad, A.M., Azzam, M.M. and Hamdan, M.A. (1981). Some Inference Results in P(Y <X) in the Bivariate Exponential Model, Communications in Statistics-Theory and Methods 10, 2515-2524.

[3] Awad, A.M. and Gharraf, M.K. (1986). Estimation of P(Y<X) in the Burr Case: A

Comparative Study, Communications in Statistics-Simulation and Computation 15, 389- 402.

[4] B. Saracoglu, I. Kinaci and D. Kundu, On estimation of R = P(Y < X) for exponential distribution under progressive type-II censoring, Journal of Statistical Computation and Simulation 82(5) (2012), 729-744.

[5] Church, J.D. and Harris, B. (1970). The Estimation of Reliability from Stress Strength Relationships, Technometrics 12, 49-54.

[6] Constantine, K. and Karson, M. (1986), "The estimation of P(Y < X) in gamma case", Communications in Statistics - Computations and Simulations, vol. 15, 365 - 388.

[7] Downtown, F. (1973), "The estimation of P(X > Y) in the normal case", Technometrics, vol. 15, 551 - 558.

[8] F. Shahsanaei and A. Daneshkhah, Estimation of stress strength model in generalized linear failure rate distribution (2013), ArXiv Preprint 1312:0401 v1.

[9] Gupta, R. D. and Kundu, D. (2003). Closeness of Gamma and Generalized Exponential Distribution, Communications in Statistics - Theory and Methods 32(4), 705-721.

[10] Kundu, D. and Gupta, R.D. (2005). Estimation of P(Y < X) for Generalized Exponential Distribution, Metrika, vol. 61(3), 291-308.

[11] Kundu, D., Kannan, N. and Balakrishnan, N. (2004), "Analysis of progressively censored competing risks data", Handbook of Statistics, vol. 23, eds., Balakrishnan, N. and Rao, C.R., Elsevier, New York.

[12] Rama Shakar. (2015), Akash distribution and its applications, International Journal of Probability and Statistics, 4(3),65-75.

[13] Raqab, M.Z. and Kundu, D. (2005). Comparison of different estimators of P(Y < X) for a scaled Burr Type X distribution, Communications in Statistics - Simulation and Computation, vol. 34(2), 465-483.

[14] Surles, J.G. and Padgett, W. J. (2001). Inference for P(Y < X) in the Burr-Type X Model, Journal of Applied Statistical Sciences 7, 225-238.

[15] Surles, J.G. and Padgett, W. J. (1998). Inference for Reliability and Stress-Strength for a Scaled Burr-Type X Distribution, Lifetime Data Analysis 7, 187-200.

[16] Z. P. Xia, J. Y. Yu, L. D. Cheng, L. F. Liu and W. M. Wang, Study on the breaking strength of jute fibers using modified Weibull distribution, Journal of Composites Part A: Applied Science and Manufacturing 40 (2009), 54-59.

Estimation of reliability characteristics for linear consecutive k-out-of-n: F systems based on exponentiated Weibull distribution

M. Kalaivani[1,2] and R. Kannan[1]

•

Department of Statistics, Annamalai University, Chidambaram, Tamil Nadu, India
Department of Mathematics and Statistics, SRM Institute of Science and Technology, Kattankulathur, Tamil Nadu, India
kalaivam1@srmist.edu.in, statkannan@gmail.com

Abstract

The focus of this paper is to estimate the reliability characteristics of a linear consecutive k-out-of-n: F system with n linearly ordered components. The components are independent and identically distributed with exponentiated Weibull lifetimes. The system fails if and only if at least k successive components fail. In such a system, the reliability function and mean time to system failure are obtained by maximum likelihood estimation method using uncensored failure observations. The asymptotic confidence interval is determined for the reliability function. The results are obtained by Monte Carlo simulation to compare the performance of the systems using various sample sizes and combination of parameters. The procedure is also illustrated through a real data set.

Keywords: Maximum Likelihood Estimation (MLE), Reliability function, Mean Time to System Failure (MTSF), Asymptotic confidence interval and Exponentiated Weibull distribution

1. Introduction

Redundancy can be used to increase the system reliability. The most popular type of redundancy is k-out-of-n system structure which find the wide applications in both industry and defense systems. The consecutive k-out-of-n system is a special type of redundancy in fault-tolerant systems such as oil pipeline systems, street illumination systems, street parking, communication relay stations batch sampling-based quality control systems, computer networks and multi-pump system in hydraulic control system. These systems are characterized as physical or logical connections between the system components that are arranged in line or circle. Pham [16] proposed two basic aspects that have been used to obtain better reliability of a system. The first is to use redundancy such as parallel system, k-out-of-n system and the second one is a manufactured a high reliable system product. Let n components be linearly connected in such a way that the system fails if and only if at least k consecutive components fail. Figure 1 shows a linear consecutive 3-out-of-7: F system. Whenever the number of consecutive failures reaches 3 the signal flow is interrupted from source to sink and the system fails. Chao et al. [3] emphasized that $Lin/Con/k/n/F$ system has a much higher reliability than series system and is often cheaper than the parallel system. In this paper, we are considering

$Lin/Con/k/n: F$ system redundancy and develop ways to obtain the maximum likelihood estimate of reliability and MTSF of the proposed system, where the components are independent and identically distributed $(i.i.d)$ with exponentiated Weibull lifetimes

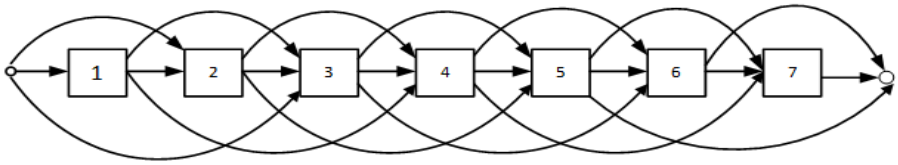

Figure 1: *Linear consecutive* 3*-out-of-*7: F *system*

First, the consecutive k-out-of-n system have been studied by Kontoleon [11]. Chiang and Ni [4] have giving special attention to the reliability of this system. Extensive review of consecutive k-out-of-n and related systems can be found in Hwang [9], Derman and Ross [6], Kuo and Zuo [20] and Eryilmaz [7]. The reliability estimation of a consecutive k-out-of-n: F system has received little attention in the literature. Shi et al. [18] discussed the classical and Bayes approach to study the performance of m-consecutive-k-out-of-n: F system with Burr XII components. Madhumitha and Vijayalakshmi [12] have proposed the Bayesian estimation for reliability and mean time to system failure for Linear (Circular) $Con/k/n: F$ using exponential distribution. Recently, Kalaivani and Kannan [10] estimated the reliability function and MTSF of k-out-of-n system using Weibull failure time model by MLE and Bayes estimation. Demiray and Kizilaslan [5] investigated the point and interval estimates of stress-strength reliability in a consecutive k-out-of-n: G system when stress and strength variable follow the proportional hazard rate model. The reliability estimation is studied under both classical and Bayes estimates. In reliability analysis, Weibull family of distribution is mostly used for modeling consecutive k-out-of-n systems with monotone failure rates.

The exponentiated Weibull distribution introduced by Mudholkar and Srivastava [14] provides a good fit to lifetime datasets that exhibit bathtub shaped as well as unimodal failure rates. The performance of the product may involve high initial failure rate and possible high failure rates due to wear out and aging, reflecting a bathtub failure rate. Pathak and Chaturvedi [15] obtained the ML estimator of the reliability function $P(X > t)$ and $P(X > Y)$ using exponentiated Weibull distribution. Srinivasa Rao et al. [19] have estimated the multicomponent stress-strength of a system when stress and strength follow two parameter exponentiated Weibull distribution with different shape parameters and common scale parameter. Alghamdi and Percy [2] studied the reliability equivalence factors of a series-parallel system with each component has an exponentiated Weibull distribution. Méndez-González et al. [13] analyzed the reliability of an electronic component using exponentiated Weibull model and inverse power law.

According to Hong and Meeker [8], components and system structure determine the reliability of the system. When the component level data is available, it can be used to estimate system reliability. Confidence intervals (CIs) are essential to assess the statistical uncertainty in the estimations. Yet, the best estimation of the redundant consecutive k-out-of-n systems would still be of interest due to recent practical applications of the complex systems. This paper establishes the reliability function, mean time to system failure and asymptotic confidence interval at 95% level of significance for linear consecutive k-out-of-n: F system based on three parameter exponentiated Weibull model that provides a better approach to fit monotone as well as non-monotone failure rates which are quite common in reliability analysis.

This paper is organized as follows. In the introductory section the motivation for the present study and brief review on $Lin/Con/k/n: F$ systems. In Section 2, description of system reliability characteristics and assumptions are given. Section 3 devoted to reliability function, mean time to

failure and the asymptotic confidence interval of the proposed system. In section 4, the results based on simulation study and real data set are illustrated. Finally, the paper ends with a concluding remark are presented in Section 5.

2. Background of System Reliability Characteristics

Assumptions

- Each component and the system are either good or failed state
- The components of the system fail statistically independently of each other
- All component lifetimes are independently and identically distributed
- Life time of the component follows exponentiated Weibull distribution with unknown parameters α, β and θ
- The system fails if and only if at least k consecutive components fail, where $1 \leq k \leq n$

Notation

n	Number of components in a system
k	Minimum number of consecutive components whose failures cause system to failure
$Lin/Con/k/n: F$	Linear consecutive k-out-of-n: F
$R(t)$	Component reliability function. All the components have iid lifetimes
$R_S^L(t)$	System reliability function of $Lin/Con/k/n: F$ system
μ	Component mean time to failure
μ_S^L	Mean time to system failure
$\hat{R}(t)$	MLE of $R(t)$
$\hat{R}_S^L(t)$	MLE of $R_S^L(t)$
$\hat{\mu}$	MLE of μ
$\hat{\mu}_S^L$	MLE of μ_S^L
$\lfloor a \rfloor$	Largest integer less than or equal to a
$i.i.d.$	Independent and identically distributed

A consecutive k-out-of-n system consists of n linearly ordered components where the system fails if and only if a minimum of k components fail. This type of structure is called the linear $con/k/n: F$ system shortly represented by $Lin/con/k/n: F$. Here it is commonly assumed that $1 \leq k \leq n$, and for $k = 1$, the $Lin/con/k/n: F$ system becomes the series system and when $k = n$, the proposed system becomes a parallel system.

The reliability function $R_S^L(t)$ of a $Lin/Con/k/n: F$ system is

$$R_S^L(t) = \sum_{j=0}^{m} N(j,k,n)\ p^{n-j}\, q^j \tag{1}$$

When the components are $i.i.d.$ replacing p and q with $R(t)$ and $1 - R(t)$ in (1), we get the following reliability function for $Lin/Con/k/n: F$ system

$$R_S^L(t) = \sum_{j=0}^{m} \sum_{i=0}^{j} (-1)^i\, N(j,k,n) \binom{j}{i}\ (R(t))^{n-j+i} \tag{2}$$

where

$$m = \begin{cases} n - \left(\frac{n+1}{k}\right) + 1 & if\ n+1\ is\ multiple\ of\ k \\ n - \left\lfloor \frac{n+1}{k} \right\rfloor & if\ n+1\ is\ not\ multiple\ of\ k \end{cases}$$

and

$$N(j,k,n) = \begin{cases} \binom{n}{j}, & 0 \le j \le k-1 \\ \sum_{l=0}^{\left\lfloor \frac{j}{k} \right\rfloor} (-1)^i \binom{n-j+1}{l} \binom{n-lk}{n-j}, & k \le j \le n \\ 0, & j > m \end{cases}$$

and m represents the maximum number of failed components that may exist in the system without causing the system to fail. But $N(j,k,n)$ is the number of ways arranging j failed components in a line such that no k or more failed components are consecutive.

Let T be the lifetime of each component following Exponentiated Weibull Distribution (EWD) with probability density function (pdf)

$$f(t,\alpha,\beta,\theta) = \frac{\alpha\beta}{\theta}\left(\frac{t}{\theta}\right)^{\beta-1}\left[1 - e^{-\left(\frac{t}{\theta}\right)^{\beta}}\right]^{\alpha-1} e^{-\left(\frac{t}{\theta}\right)^{\beta}}, \qquad t > 0, \alpha, \beta, \theta > 0 \tag{3}$$

where θ is scale parameter, α and β are shape parameters and are unknown.

Failure rate (hazard rate) function, is an important function in lifetime modeling is given by

$$h(t) = \frac{f(t)}{R(t)} = \frac{\frac{\alpha\beta}{\theta}\left(\frac{t}{\theta}\right)^{\beta-1}\left[1 - e^{-\left(\frac{t}{\theta}\right)^{\beta}}\right]^{\alpha-1} e^{-\left(\frac{t}{\theta}\right)^{\beta}}}{1 - \left[1 - e^{-\left(\frac{t}{\theta}\right)^{\beta}}\right]^{\alpha}} \tag{4}$$

It is pertinent to note that the $h(t)$ is:

i. Constant $= \beta^{-1}$ if $\beta = \theta = 1$
ii. Increasing (decreasing) FR if $\beta \ge 1$ and $\alpha\beta \ge 1$ ($\beta \le 1$ and $\alpha\beta \le 1$)
iii. Bathtub shaped FR if $\beta > 1$ and $\alpha\beta < 1$
iv. Upside-down bathtub shaped (unimodal) FR if $\beta < 1\ and\ \alpha\beta > 1$

From (3), we know that the EWD includes many distributions as special cases. If $\beta = 1$, it reduced to exponentiated exponential distribution (EED). If $\beta = 2$, it becomes exponentiated Rayleigh distribution (ERD). If $\theta = 1$, it deduced as the standard 2-parameter Weibull distribution (WD). The particular case for $\beta = 2$ and $\theta = 1$ is the Rayleigh distribution. If $\beta = 1$ and $\theta = 1$, it becomes the one-parameter exponential distribution.

The component reliability for mission time t is given by

$$R(t) = 1 - \left[1 - e^{-\left(\frac{t}{\theta}\right)^{\beta}}\right]^{\alpha}, t > 0 \tag{5}$$

and mean time to component failure is expressed as

$$\mu = \int_0^{\infty} R(t)\ dt = \theta\left[\left(1 + \frac{1}{\beta}\right)\sum_{i=0}^{s} (-1)^i \binom{\alpha}{i} i^{-\left(\frac{1}{\beta}\right)}\right. \tag{6}$$

The reliability function of a $Lin/Con/k/n{:}\ F$ system is obtained as

$$R_S^L(t) = \sum_{j=0}^{m}\sum_{i=0}^{j} (-1)^i N(j,k,n) \binom{j}{i} \left(1 - \left[1 - e^{-\left(\frac{t}{\theta}\right)^{\beta}}\right]^{\alpha}\right)^{n-j+i} \tag{7}$$

Using $R_S^L(t)$, we have the following expression for the mean time to system failure (MTSF) of a $Lin/Con/k/n: F$ system

$$\mu_S^L = \int_0^\infty R_S^L(t)\,dt = \sum_{j=0}^{m}\sum_{i=0}^{j}(-1)^i N(j,k,n)\binom{j}{i}\int_0^\infty (R(t))^{n-j+i}\,dt$$

Now,

$$\int_0^\infty [R(t)]^{n-j+i}\,dt = \int_0^\infty \left[1-\left(1-e^{-\left(\frac{t}{\theta}\right)^\beta}\right)^\alpha\right]^{n-j+i} dt$$

$$= \sum_{r=0}^{n-j+i}(-1)^r\binom{n-j+i}{r}\int_0^\infty \left[\left(1-e^{-\left(\frac{t}{\theta}\right)^\beta}\right)^{r\alpha}\right]dt$$

$$= \sum_{r=0}^{n-j+i}(-1)^r\binom{n-j+i}{r}\sum_{l=0}^{s}(-1)^l\binom{r\alpha}{l}\int_0^\infty \left(e^{-l\left(\frac{t}{\theta}\right)^\beta}\right)dt$$

Hence from (7), we have

$$\mu_S^L = \theta\left[\left(1+\frac{1}{\beta}\right)\sum_{j=0}^{m}\sum_{i=0}^{j}(-1)^i N(j,k,n)\binom{j}{i}\sum_{r=0}^{n-j+i}(-1)^r\binom{n-j+i}{r}\sum_{l=0}^{s}(-1)^l\binom{r\alpha}{l}l^{-\left(\frac{1}{\beta}\right)}\right. \quad (8)$$

where $s = \begin{cases} 1,2,3,\ldots if\ r\alpha\ \ is\ integer \\ \infty\ \ if\ r\alpha\ is\ non-integer \end{cases}$

3. Reliability and MTSF Estimation

In this section, we have obtained the ML estimator of $R_S^L(t)$ and the MTSF, μ_S^L for a $Lin/Con/k/n: F$ system. Let n units are put on test and the test ends when all the units have failed. Let $t_1, t_2, \ldots, t_n$ be the random failure times and assume they follow an exponentiated Weibull distribution with density function given in (3). The log likelihood function of the parameters is

$$L = L(\alpha,\beta,\theta) = nlog\alpha + nlog\beta + (\beta-1)\sum_{i=1}^{n} logt_i - n\beta log\theta - \sum_{i=1}^{n}\left(\frac{t_i}{\theta}\right)^\beta$$
$$+(\alpha-1)\sum_{i=1}^{n} log\left[1-\exp\left(-\left(\frac{t_i}{\theta}\right)^\beta\right)\right]$$

Then the maximum likelihood estimator (MLE) of α, β and θ say $\hat{\alpha}, \hat{\beta}$ and $\hat{\theta}$ respectively can be obtained by solving the following simultaneous nonlinear equations using numerical methods

$$\frac{\partial L}{\partial \alpha} = \frac{n}{\alpha} + \sum_{i=1}^{n} log\left[1-e^{-\left(\frac{t_i}{\theta}\right)^\beta}\right] = 0 \quad (9)$$

$$\frac{\partial L}{\partial \beta} = \frac{n}{\beta} + \sum_{i=1}^{n} logx_i - nlog\theta - \sum_{i=1}^{n}\left(\frac{t_i}{\theta}\right)^\beta log\left(\frac{t_i}{\theta}\right) + (\alpha-1)\sum_{i=1}^{n}\left[\frac{\left(\frac{t_i}{\theta}\right)^\beta log\left(\frac{t_i}{\theta}\right)e^{-\left(\frac{t_i}{\theta}\right)^\beta}}{1-e^{-\left(\frac{t_i}{\theta}\right)^\beta}}\right] = 0 \quad (10)$$

$$\frac{\partial L}{\partial \theta} = -n + \sum_{i=1}^{n}\left(\frac{t_i}{\theta}\right)^\beta - (\alpha-1)\sum_{i=1}^{n}\left[\frac{\left(\frac{t_i}{\theta}\right)^\beta e^{-\left(\frac{t_i}{\theta}\right)^\beta}}{1-e^{-\left(\frac{t_i}{\theta}\right)^\beta}}\right] = 0 \quad (11)$$

By applying the invariance property of MLE, the MLE of the reliability function and mean time to failure of components and $Lin/Con/k/n: F$ system is obtained by substituting $\hat{\alpha}, \hat{\beta}\ and\ \hat{\theta}$ in (5), (6), (7) and (8).

4. Asymptotic Confidence Interval of $R_S^L(t)$

The Fishers information matrix for $\lambda = (\alpha, \beta, \theta)$ is

$$I = I(\lambda) = -E\begin{bmatrix} \frac{\partial^2 L}{\partial \alpha^2} & \frac{\partial^2 L}{\partial \alpha \partial \beta} & \frac{\partial^2 L}{\partial \alpha \partial \theta} \\ \frac{\partial^2 L}{\partial \beta \partial \alpha} & \frac{\partial^2 L}{\partial \beta^2} & \frac{\partial^2 L}{\partial \beta \partial \theta} \\ \frac{\partial^2 L}{\partial \theta \partial \alpha} & \frac{\partial^2 L}{\partial \theta \partial \beta} & \frac{\partial^2 L}{\partial \theta^2} \end{bmatrix} = \begin{bmatrix} I_{11} & I_{12} & I_{13} \\ I_{21} & I_{22} & I_{23} \\ I_{31} & I_{32} & I_{33} \end{bmatrix}$$

where

$$I_{22} = -\frac{n}{\beta^2} - \sum_{i=1}^{n} \left(\frac{t_i}{\theta}\right)^{\beta} log^2\left(\frac{t_i}{\theta}\right) + (\alpha - 1) \times \sum_{i=1}^{n} \left[\frac{\left(1 - e^{-\left(\frac{t_i}{\theta}\right)^{\beta}}\right) T_1 - e^{-2\left(\frac{t_i}{\theta}\right)^{\beta}} \left(\frac{t_i}{\theta}\right)^{2\beta} log^2\left(\frac{t_i}{\theta}\right)^{\beta}}{\left(1 - e^{-\left(\frac{t_i}{\theta}\right)^{\beta}}\right)^2} \right]$$

$$I_{33} = \frac{n\beta}{\theta^2} - \sum_{i=1}^{n} \frac{\beta}{\theta^2} \left(\frac{t_i}{\theta}\right)^{\beta} + \left(\frac{\beta}{\theta}\right)^2 \left(\frac{t_i}{\theta}\right)^{\beta} - (\alpha - 1) \sum_{i=1}^{n} \left[\frac{\left(1 - e^{-\left(\frac{t_i}{\theta}\right)^{\beta}}\right) T_2 + \left(\frac{\beta}{\theta}\right)^2 \left(\frac{t_i}{\theta}\right)^{2\beta} e^{-\left(\frac{t_i}{\theta}\right)^{2\beta}}}{\left(1 - e^{-\left(\frac{t_i}{\theta}\right)^{\beta}}\right)^2} \right]$$

$$I_{12} = I_{21} = \sum_{i=1}^{n} \left[\frac{\left(\frac{t_i}{\theta}\right)^{\beta} \left(\frac{t_i}{\theta}\right)^{\beta} log\left(\frac{t_i}{\theta}\right)}{1 - e^{-\left(\frac{t_i}{\theta}\right)^{\beta}}} \right]$$

$$I_{13} = I_{31} = -\sum_{i=1}^{n} \frac{\left(\frac{\beta}{\theta}\right) e^{-\left(\frac{t_i}{\theta}\right)^{\beta}} \left(\frac{t_i}{\theta}\right)^{\beta}}{1 - e^{-\left(\frac{t_i}{\theta}\right)^{\beta}}}$$

$$I_{23} = I_{32} = -\frac{n}{\theta} + \sum_{i=1}^{n} \left[\frac{1}{\theta} \left(\frac{t_i}{\theta}\right)^{\beta} + \left(\frac{\beta}{\theta}\right) \left(\frac{t_i}{\theta}\right)^{\beta} log\left(\frac{t_i}{\theta}\right) \right] + \sum_{i=1}^{n} \left[\frac{\left(1 - e^{-\left(\frac{t_i}{\theta}\right)^{\beta}}\right) T_3 + \left(\frac{\beta}{\theta}\right) \left(\frac{t_i}{\theta}\right)^{2\beta} log\left(\frac{t_i}{\theta}\right) e^{-2\left(\frac{t_i}{\theta}\right)^{\beta}}}{\left(1 - e^{-\left(\frac{t_i}{\theta}\right)^{\beta}}\right)^2} \right]$$

and

$$T_1 = \left[e^{-\left(\frac{t_i}{\theta}\right)^{\beta}} \left(\frac{t_i}{\theta}\right)^{\beta} log^2\left(\frac{t_i}{\theta}\right)^{\beta} - e^{-\left(\frac{t_i}{\theta}\right)^{\beta}} \left(\frac{t_i}{\theta}\right)^{2\beta} log^2\left(\frac{t_i}{\theta}\right)^{\beta} \right]$$

$$T_2 = \left(\frac{\beta}{\theta}\right)^2 e^{-\left(\frac{t_i}{\theta}\right)^{\beta}} \left(\frac{t_i}{\theta}\right)^{2\beta} - \frac{\beta}{\theta^2} \left(\frac{t_i}{\theta}\right)^{\beta} e^{-\left(\frac{t_i}{\theta}\right)^{\beta}} - \left(\frac{\beta}{\theta}\right)^2 e^{-\left(\frac{t_i}{\theta}\right)^{\beta}} \left(\frac{t_i}{\theta}\right)^{\beta}$$

$$T_3 = \left(\frac{\beta}{\theta}\right) \left(\frac{t_i}{\theta}\right)^{2\beta} log\left(\frac{t_i}{\theta}\right) e^{-\left(\frac{t_i}{\theta}\right)^{\beta}} + \frac{1}{\theta} \left(\frac{t_i}{\theta}\right)^{\beta} e^{-\left(\frac{t_i}{\theta}\right)^{\beta}} - \left(\frac{\beta}{\theta}\right) \left(\frac{t_i}{\theta}\right)^{\beta} log\left(\frac{t_i}{\theta}\right) e^{-\left(\frac{t_i}{\theta}\right)^{\beta}}$$

The MLE of $R_S^L(t)$, $\hat{R}_S^L(t)$ is asymptotically normal with mean $R_S^L(t)$, and variance

$$\sigma^2_{R_S^L(t)} = \sum_{j=1}^{3} \sum_{i=1}^{3} \frac{\partial R_S^L(t)}{\partial \lambda_i} \frac{\partial R_S^L(t)}{\partial \lambda_j} I_{ij}^{-1}$$

where I_{ij}^{-1} is the $(i,j)th$ element of $I(\lambda)$ (see Rao[17]). Then,

$$\sigma_{R_{S(t)}^L}^2 = \left(\frac{\partial R_S^L(t)}{\partial \alpha}\right)^2 I_{11}^{-1} + \left(\frac{\partial R_S^L(t)}{\partial \beta}\right)^2 I_{22}^{-1} + \left(\frac{\partial R_S^L(t)}{\partial \theta}\right)^2 I_{33}^{-1} + 2\frac{\partial R_S^L(t)}{\partial \alpha}\frac{\partial R_S^L(t)}{\partial \beta} I_{12}^{-1} + 2\frac{\partial R_S^L(t)}{\partial \alpha}\frac{\partial R_S^L(t)}{\partial \theta} I_{13}^{-1} + 2\frac{\partial R_S^L(t)}{\partial \beta}\frac{\partial R_S^L(t)}{\partial \theta} I_{23}^{-1}$$

where

$$\frac{\partial R_S^L(t)}{\partial \alpha} = -log\left[1 - e^{-\left(\frac{t}{\theta}\right)^\beta}\right]\left[1 - e^{-\left(\frac{t}{\theta}\right)^\beta}\right]^\alpha h$$

$$\frac{\partial R_S^L(t)}{\partial \beta} = -\alpha\left(\frac{t}{\theta}\right)^\beta e^{-\left(\frac{t}{\theta}\right)^\beta} log\left(\frac{t}{\theta}\right)\left[1 - e^{-\left(\frac{t}{\theta}\right)^\beta}\right]^{\alpha-1} h$$

$$\frac{\partial R_S^L(t)}{\partial \beta} = \frac{\alpha\beta}{\theta}\left(\frac{t}{\theta}\right)^\beta e^{-\left(\frac{t}{\theta}\right)^\beta}\left[1 - e^{-\left(\frac{t}{\theta}\right)^\beta}\right]^{\alpha-1} h$$

and

$$h = \sum_{j=0}^{m}\sum_{i=0}^{j}(-1)^i N(j,k,n)\binom{j}{i}(n-j+i)(R(t))^{n-j+i-1}$$

Therefore, an asymptotic $100(1-\gamma)\%$ confidence interval of $R_{S(t)}^L$ is given by

$$R_S^L(t) \in \left(\hat{R}_S^L(t) \pm Z_{\gamma/2}\right)$$

where $Z_{\gamma/2}$ is the upper $\gamma/2$th quantile of the standard normal distribution and $\hat{\sigma}_{R_S^L(t)}$ is the value of $\sigma_{R_S^L(t)}$ at the MLE of the parameters.

5. Simulation Study and Data Analysis

In this section, a simulation study is carried out along with the application of the $Lin/Con/k/n$: F system and a real data set to the estimate system reliability and mean time to system failure when samples are drawn from EWD.

5.1. Simulation Study

We study some results based on Monte Carlo simulation to compare the performance of $R_S^L(t)$ μ_S^L and asymptotic confidence interval using different sample sizes $n = 30$ and 50 for combination of parameters $(\alpha, \beta, \theta) = (0.5,0.5,1)$, $(0.5,1.5,1)$, $(0.5,2.5,1)$, $(1.5,0.5,1)$ and $(2.5,0.5,1)$ and are evaluated using R software.

i. For each combination of α, β, θ and sample size n, we can derive the random samples from the EWD by inverting the cumulative distribution of (3).
$X = \theta\left[-log\left(1 - U^{1/\alpha}\right)\right]^{1/\beta}$, $U \sim U(0,1)$

ii. Based on the data and using (9), (10) and (11), we estimate the MLE of α, β and θ, $R_S^L(t)$, μ_S^L and asymptotic confidence interval.

iii. Repeat step (i) and (ii) over 3000 times and the mean square errors for the estimators are calculated.

iv. The above steps are repeated for $Lin/Con/k/n$: F system by taking $n = 10$ and $k = 3$ and 6. The results are presented in Table 1, 2 and 3.

Table 1: *Reliability Estimation of $Lin/Con/3/10$: F system*

Parameters	t	$R_S^L(t)$	$n = 30$				$n = 50$			
			$\hat{R}_S^L(t)$	MSE	Asymptotic CI		$\hat{R}_S^L(t)$	MSE	Asymptotic CI	
					LL	UL			LL	UL
$\alpha = 0.5$, $\beta = 0.5$, $\theta = 1$	0.2	0.297747	0.303069	0.018713	0.249567	0.355806	0.297385	0.011802	0.264664	0.329299
	0.4	0.162046	0.176572	0.011650	0.137303	0.214943	0.169849	0.007063	0.146110	0.192815
	0.6	0.100745	0.116668	0.007394	0.087137	0.145560	0.110241	0.004283	0.092532	0.127299
	0.8	0.067312	0.082330	0.004848	0.059416	0.104628	0.076508	0.002686	0.062907	0.089549
	1.0	0.047150	0.060606	0.003270	0.042428	0.078231	0.055435	0.001737	0.044833	0.065699
$\alpha = 0.5$, $\beta = 1.5$, $\theta = 1$	0.2	0.854684	0.831226	0.008891	0.789136	0.873496	0.833757	0.005326	0.807877	0.859582
	0.4	0.546503	0.537213	0.021241	0.474321	0.599168	0.531110	0.013585	0.492483	0.569434
	0.6	0.281312	0.294728	0.018049	0.241666	0.346063	0.283371	0.011144	0.251503	0.314827
	0.8	0.122807	0.143560	0.009532	0.109112	0.176196	0.132677	0.005272	0.112644	0.152358
	1.0	0.047150	0.063644	0.003753	0.044633	0.081262	0.055754	0.001731	0.045140	0.066163
$\boldsymbol{\alpha = 0.5}$, $\boldsymbol{\beta = 2.5}$, $\boldsymbol{\theta = 1}$	0.2	0.983359	0.973400	0.000761	0.962288	0.984654	0.976043	0.000371	0.969691	0.982422
	0.4	0.830987	0.805319	0.010896	0.759474	0.851011	0.808428	0.006486	0.780539	0.836273
	0.6	0.505575	0.493241	0.022685	0.430379	0.555143	0.490158	0.014306	0.451895	0.528157
	0.8	0.197713	0.210763	0.014190	0.166860	0.253530	0.202739	0.008425	0.176460	0.228638
	1.0	0.047150	0.061131	0.003794	0.042884	0.078609	0.054835	0.001680	0.044332	0.065048
$\alpha = 1.5$, $\beta = 0.5$, $\theta = 1$	0.2	0.934871	0.915864	0.004256	0.889625	0.942087	0.919800	0.002230	0.904357	0.935242
	0.4	0.815863	0.788815	0.013581	0.740635	0.836936	0.792504	0.007750	0.763610	0.821397
	0.6	0.693397	0.667344	0.020847	0.607435	0.727154	0.669078	0.012392	0.632893	0.705262
	0.8	0.582536	0.561714	0.024429	0.497174	0.626124	0.561157	0.014812	0.522036	0.600278
	1.0	0.487040	0.472712	0.025109	0.407868	0.537404	0.470101	0.015345	0.430729	0.509473
$\alpha = 2.5$, $\beta = 0.5$, $\theta = 1$	0.2	0.996454	0.992783	0.000106	0.989188	0.996379	0.993912	0.000045	0.992011	0.995813
	0.4	0.976451	0.965417	0.001186	0.952008	0.978826	0.968151	0.000583	0.960528	0.975774
	0.6	0.937420	0.918920	0.004066	0.892858	0.944981	0.922706	0.002155	0.907477	0.937936
	0.8	0.883603	0.859445	0.008437	0.820951	0.897940	0.863512	0.004693	0.840678	0.886346
	1.0	0.820477	0.793148	0.013325	0.744110	0.842186	0.796827	0.007664	0.767454	0.8262

Table 2: *Reliability Estimation of $Lin/Con/6/10$: F system*

Parameters	t	$R_S^L(t)$	$n = 30$				$n = 50$			
			$\hat{R}_S^L(t)$	MSE	Asymptotic CI		$\hat{R}_S^L(t)$	MSE	Asymptotic CI	
					LL	UL			LL	UL
$\alpha = 0.5,$ $\beta = 0.5,$ $\theta = 1$	0.2	0.878187	0.854031	0.009330	0.820145	0.887532	0.861369	0.005120	0.841135	0.881186
	0.4	0.767127	0.742157	0.017567	0.695727	0.787805	0.750602	0.010092	0.722402	0.778081
	0.6	0.676749	0.654458	0.022542	0.602294	0.705814	0.663003	0.013098	0.630975	0.694176
	0.8	0.602410	0.583262	0.025178	0.528435	0.637110	0.591528	0.014681	0.557627	0.62446
	1.0	0.540364	0.524086	0.026268	0.468303	0.578803	0.531901	0.015332	0.497441	0.565671
$\alpha = 0.5,$ $\beta = 1.5,$ $\theta = 1$	0.2	0.997601	0.995090	4.75E-05	0.992582	0.997590	0.995899	0.000018	0.994557	0.997237
	0.4	0.965283	0.952884	0.001772	0.937312	0.968168	0.955734	0.000925	0.946606	0.964788
	0.6	0.868454	0.849576	0.008993	0.814768	0.883334	0.852847	0.005244	0.831893	0.873555
	0.8	0.714275	0.698971	0.019396	0.648864	0.747063	0.701058	0.011516	0.670576	0.731087
	1.0	0.540364	0.532961	0.025731	0.476643	0.586475	0.533617	0.014971	0.499182	0.567542
$\alpha = 0.5,$ $\beta = 2.5,$ $\theta = 1$	0.2	0.999975	0.999860	0.000000	0.999752	0.999970	0.999913	0.000000	0.999869	0.999958
	0.4	0.996649	0.993299	0.000084	0.990042	0.996534	0.994407	0.000033	0.992675	0.996134
	0.6	0.956381	0.940101	0.002694	0.921477	0.958424	0.944680	0.001395	0.933970	0.955323
	0.8	0.804664	0.779584	0.014721	0.736400	0.821867	0.786669	0.008520	0.760821	0.81225
	1.0	0.540364	0.524527	0.025982	0.468467	0.579204	0.530556	0.015108	0.496113	0.564469
$\alpha = 1.5,$ $\beta = 0.5,$ $\theta = 1$	0.2	0.999574	0.998694	0.000008	0.997905	0.999481	0.999065	0.000002	0.998704	0.999426
	0.4	0.995942	0.991603	0.000156	0.987592	0.995609	0.993213	0.000050	0.991174	0.995252
	0.6	0.986857	0.977439	0.000723	0.968280	0.986586	0.980672	0.000282	0.975772	0.985572
	0.8	0.971944	0.957120	0.001876	0.941835	0.972381	0.961952	0.000820	0.953511	0.970392
	1.0	0.951824	0.932068	0.003592	0.910394	0.953705	0.938280	0.001691	0.926041	0.950519
$\alpha = 2.5,$ $\beta = 0.5,$ $\theta = 1$	0.2	0.999999	0.999986	0.000000	0.999974	0.999999	0.999993	0.000000	0.999989	0.999997
	0.4	0.999949	0.999760	0.000000	0.999586	0.999935	0.999847	0.000000	0.999777	0.999918
	0.6	0.999608	0.998782	0.000007	0.998018	0.999546	0.999126	0.000002	0.998780	0.999473
	0.8	0.998523	0.996374	0.000039	0.994360	0.998388	0.997205	0.000011	0.996229	0.998182
	1.0	0.996166	0.991969	0.000142	0.987952	0.995987	0.993500	0.000047	0.991461	0.99554

Table 3: *Estimation of mean time to system failure (MTSF)*

Parameters		$\alpha = 0.5,$ $\beta = 0.5,$ $\theta = 1$	$\alpha = 0.5,$ $\beta = 1.5,$ $\theta = 1$	$\alpha = 0.5,$ $\beta = 2.5,$ $\theta = 1$	$\alpha = 1.5,$ $\beta = 0.5,$ $\theta = 1$	$\alpha = 2.5,$ $\beta = 0.5,$ $\theta = 1$
$Lin/Con/3/10: F$ system						
Sample size	μ_S^L	0.233168	0.475392	0.614456	1.338123	2.431575
$\boldsymbol{n = 30}$	$\hat{\mu}_S^L$	0.265047	0.483305	0.620654	1.364669	2.435709
	MSE	0.0278	0.014594	0.151323	0.234167	0.460743
$\boldsymbol{n = 50}$	$\hat{\mu}_S^L$	0.250012	0.473758	0.608595	1.336523	2.405559
	MSE	0.014272	0.006604	0.004345	0.13133	0.264359
$Lin/Con/6/10: F$ system						
Sample size	μ_S^L	2.564288	1.134486	1.051981	6.084472	8.497633
$\boldsymbol{n = 30}$	$\hat{\mu}_S^L$	3.520812	1.140934	1.112734	6.36528	8.728028
	MSE	373.2682	0.173304	10.29648	7.102796	9.147431
$\boldsymbol{n = 50}$	$\hat{\mu}_S^L$	2.844258	1.12965	1.044834	6.247015	8.627549
	MSE	7.607097	0.022023	0.007051	3.34101	4.402205

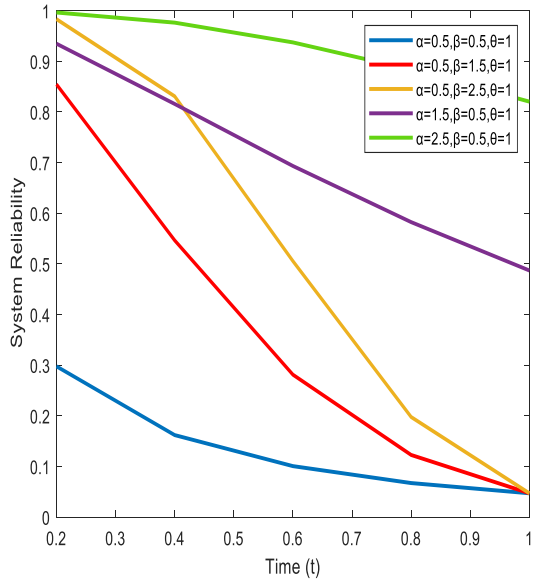

Figure 2: *Reliability of $Lin/Con/3/10: F$ system*

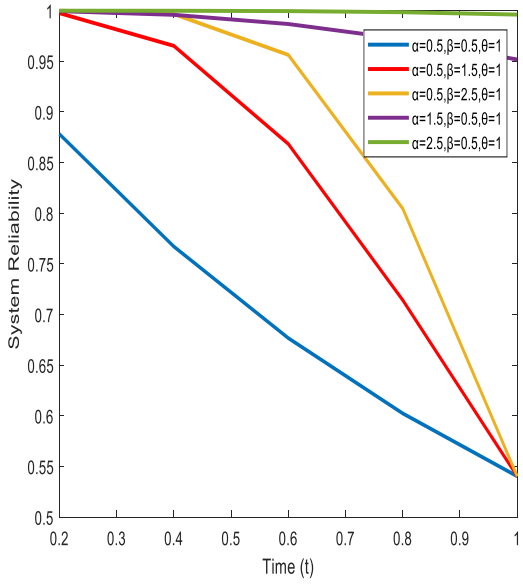

Figure 3: *Reliability of $Lin/Con/6/10: F$ system*

According to Table 1, 2 and 3, the MSEs for estimate of reliability and average lifetime of the system decreases as the sample size increases. The expected length of the confidence interval reduces as sample size increases at 95% level of significance for all combinations of parameters. By comparing the system reliabilities and MTSFs for $k = 3$ and $k = 6$, we can see that the system reliability and MTSF are increase when the number of consecutive failed components, k increases from 3 to 6 and other parameters are kept unchanged. The results are consistent with the definition of the consecutive k-out-of-n: F system. Further, it is observed that the time increases the reliability of the system declines, as expected. In addition, the length of the confidence interval of the $Lin/Con/6/10: F$ larger than the $Lin/Con/3/10: F$ system for the all combinations of parameters.

Figure 2 and 3 show the true value of reliability in $Lin/Con/3/10: F$ and $Lin/Con/6/10: F$. $R_S^L(t)$ is low when $\alpha < 1$, $\beta < 1$ and $\alpha\beta < 1$, the components of the system having initial failure rate. On the other hand, for $\alpha < 1, \beta > 1$ and $\alpha\beta < 1$, the performance of the system is improved, the

system's components are in bath tub failure mode. When, $\alpha < 1, \beta > 1$ and $\alpha\beta > 1$, $R_S^L(t)$ declines quickly because the components are in the increasing failure rate. If $\alpha > 1, \beta < 1$ and $\alpha\beta < 1$, the reliability improved well when compare with first one even though the components are in the decreasing failure rate. Suppose $\alpha > 1, \beta < 1$ and $\alpha\beta > 1$, the performance of the system is high, because the system's components possessing unimodal failure rate.

From Table 3, it is seen that the MSEs of MTSF of $Lin/Con/6/10:F$ is more as compare with $Lin/Con/3/10:F$ system. This is due the number of consecutive failed components is large. The MTTF of each component are same. Therefore, it can be concluded that the failure rate of the distribution will affect the average failure time of the system. However, the influence is dependent on the values of the parameters.

5.2. Data Analysis

In this section, the model proposed in (3) is applied to estimate the lifetimes of 18 electronic devices shown in Table 4. The presented data were taken from Ahmad and Ghazal [1] as a lifetime distribution having bathtub shaped failure rate. The MLE of α, β, θ and their standard errors are given below

$$\hat{\alpha} = 0.144884\ (0.008049) \qquad \hat{\beta} = 5.285692\ (0.275845) \qquad \hat{\theta} = 373.218\ (9.72593)$$

The ML estimates of reliability and MTSF for a $Lin/Con/k/10:F$ system has been evaluated with $n = 10$ and $k = 3\ and\ 6$.

Table 4: *Lifetime of 18 electronic devices*

5	11	21	31	46	75	98	122	145	165
196	224	245	293	321	330	350	420		

Table 5: *Reliability, MTSF and asymptotic confidence intervals at 95% level of significance*

t	$Lin/Con/3/10:F$ system $\hat{\mu}_S^L = 154.3145$			$Lin/Con/6/10:F$ system $\hat{\mu}_S^L = 289.8265$		
	$\hat{R}_S^L(t)$	Asymptotic CI		$\hat{R}_S^L(t)$	Asymptotic CI	
		LL	UL		LL	UL
0	1	-	-	1	-	-
50	0.936522	0.895956	0.977088	0.999596	0.999051	1.000142
100	0.747427	0.652674	0.84218	0.991666	0.984417	0.998914
150	0.497669	0.387101	0.608237	0.95448	0.927456	0.981504
200	0.265821	0.179307	0.352334	0.858565	0.801264	0.915866
250	0.106003	0.05878	0.153227	0.686347	0.602146	0.770548
300	0.028072	0.010935	0.045209	0.457671	0.366109	0.549232
350	0.004127	0.000463	0.007791	0.236461	0.161964	0.310958
400	0.000257	-0.00011	0.00062	0.08773	0.043646	0.131815

From Table 5, it can be seen that the reliability and MTSF of the consecutive k-out-of-n the failure rate of the distribution when time increases the reliability of the system decreases, as expected. The system parameter k increases the reliability and expected life time increase. In addition, the length of the confidence interval decreases when the number of consecutive failure components decreases. These can be seen in the simulation study results.

6. Conclusions

In this paper, we have proposed a $Lin/Con/k/n:F$ system which composed of n independent and identically distributed components having exponentiated Weibull lifetimes with three unknown parameters and studied the reliability characteristics. This distribution has the ability to model the non-monotonic and monotonic failure rate. The reliability and mean time to system failure are estimated based on simulated observations by maximum likelihood estimation for various combination of parameters. Asymptotic confidence intervals were also constructed. The MSEs of $R_S^L(t)$, MTSF and length of the confidence interval decrease as sample size increases for $Lin/Con/3/10:F$ and $Lin/Con/6/10:F$ In addition, MSEs of MTSF as well as the mean length of the confidence interval increases as the number consecutive failed components k increases. A real-life data set was used to show the entire approach.

References

[1] Abd EL-Baset, A. A., and Ghazal, M. G. M. (2020). Exponentiated additive Weibull distribution. *Reliability Engineering & System Safety*, *193*, 106663.

[2] Alghamdi, S. M., and Percy, D. F. (2014). Reliability equivalence factors for a series-parallel system assuming an exponentiated Weibull distribution.

[3] Chao, M. T., Fu, J. C., and Koutras, M. V. (1995). Survey of reliability studies of consecutive-k-out-of-n: F and related systems. *IEEE Transactions on reliability*, *44*(1), 120-127.

[4] Chiang, D. T., and Niu, S. C. (1981). Reliability of consecutive-k-out-of-n: F system. *IEEE Transactions on Reliability*, *30*(1), 87-89.

[5] Demiray, D., and Kızılaslan, F. (2022). Stress–strength reliability estimation of a consecutive k-out-of-n system based on proportional hazard rate family. *Journal of Statistical Computation and Simulation*, *92*(1), 159-190.

[6] Derman, C., Lieberman, G. J., and Ross, S. M. (1982). On the consecutive-k-of-n: F system. *IEEE Transactions on Reliability*, *31*(1), 57-63.

[7] Eryilmaz, S. (2010). Review of recent advances in reliability of consecutive k-out-of-n and related systems. *Proceedings of the Institution of Mechanical Engineers, Part O: Journal of Risk and Reliability*, *224*(3), 225-237.

[8] Hong, Y., and Meeker, W. Q. (2014). Confidence interval procedures for system reliability and applications to competing risks models. *Lifetime data analysis*, *20*(2), 161-184.

[9] Hwang, F. K. (1986). Simplified reliabilities for consecutive-k-out-of-n systems. *SIAM Journal on Algebraic Discrete Methods*, *7*(2), 258-264.

[10] Kalaivani, M., and Kannan, R. (2022). Estimation of reliability function and mean time to system failure for k-out-of-n systems using Weibull failure time model. *International Journal of System Assurance Engineering and Management*, 1-13.

[11] Kontoleon, J. M. (1980). Reliability determination of a r-successive-out-of-n: F system. *IEEE Transactions on Reliability*, *29*(5), 437-437.

[12] Madhumitha, J., and Vijayalakshmi, G. (2020). Bayesian Estimation of Linear/Circular Consecutive k-out-of-n: F System Reliability. *International Journal of Performability Engineering*, *16*(10).

[13] Méndez-González, L. C., Rodríguez-Picón, L. A., Valles-Rosales, D. J., Alvarado Iniesta, A., and Carreón, A. E. Q. (2019). Reliability analysis using exponentiated Weibull distribution and inverse power law. *Quality and Reliability Engineering International*, *35*(4), 1219-1230.

[14] Mudholkar, G. S., and Srivastava, D. K. (1993). Exponentiated Weibull family for analyzing bathtub failure-rate data. *IEEE transactions on reliability*, *42*(2), 299-302.

[15] Chaturvedi, A., and Pathak, A. (2012). Estimation of the Reliability Function for Exponentiated Weibull Distribution. *Journal of Statistics & Applications*, *7*.

[16] Pham, H. (2010). On the estimation of reliability of k-out-of-n systems. *International Journal of Systems Assurance Engineering and Management*, *1*(1), 32-35.

[17] Rao, C. R., and Statistiker, M. (1973). *Linear statistical inference and its applications* (Vol. 2, pp. 263-270). New York: Wiley.

[18] Shi, Y. M., Gu, X., and Sun, Y. D. (2011, July). Reliability evaluation for m-consecutive-k-out-of-n: F system with Burr XII components. In *2011 International Conference on Multimedia Technology* (pp. 2314-2317). IEEE.

[19] Srinivasa Rao, G., Aslam, M., and Arif, O. H. (2017). Estimation of reliability in multicomponent stress–strength based on two parameter exponentiated Weibull Distribution. *Communications in Statistics-Theory and Methods*, *46*(15), 7495-7502.

[20] Kuo, W., and Zuo, M. J. (2003). *Optimal reliability modeling: principles and applications*. John Wiley & Sons.

RT&A, No 3 (69)
Volume 17, September 2022

A Numerical Study of the Damage Mechanisms of the Specimens (SENT, SENB, CT, and DENT) used for P265 GH steel

Mohammed Lahlou *

•

Chouaib Doukkali University of El Jadida, Natl Sch Appl Sci, Sci Engineer Lab Energy, El Jadida, Morocco, lahloumohammed89@gmail.com

Bouchra Saadouki

•

Laboratory of Control and Mechanical Characterization of Materials and Structures, National Higher School of Electricity and Mechanics, BP 8118 Oasis, Hassan II University, Casablanca, Morocco, bouchra.saadouki@gmail.com

Abderrazak En-naji

•

Department of Physics, Laboratory M3ER, Faculty of Sciences and Technology, Moulay Ismail University, Meknes, Morocco, abdenaji14@gmail.com

Fatima Majid

•

Laboratory of Nuclear, Atomic, Molecular, Mechanical and Energetic Physics, University Chouaib Doukkali, El jadida, Morocco, majidfatima9@gmail.com

Nadia Mouhib

•

Higher Institute of Maritime Studies ISEM, Casablanca, Morocco
mouhib.nadia@gmail.com

Abstract

During operation, most mechanical structures are subjected to time-varying stresses, which leads to their failure of serious accidents. The lifetime of a mechanical structure is broken down into three stages: stage I; the initiation, stage II; the slow propagation and stage III; the brutal propagation. The objective of this paper is to determine the damage and the lifetime of a pressure equipment by establishing a numerical modeling by finite elements on different specimens (SENT, SENB, DENT, CT) using the calculation code CASTEM. The material studied is P265GH steel commonly used as boiler plate and pressure vessels. The results show that the damage severity of the SENT specimen is more important, followed by the DENT specimen, then the CT specimen and finally SENB.

Keywords: Pressure vessels; Finite element model; Mechanical behaviors; Damage; Tensile test; Maintenance.

RT&A, No 3 (69)
Volume 17, September 2022

1. Introduction

The computer has become an essential tool in our lives, specifically in the industrial sectors. For reasons of competitiveness and development, companies are looking to predict the durability and consider solutions in the design and maintenance of parts and structures. The finite element method can be used to solve these problems, more precisely mechanical problems [1].

All materials have defects on a microscopic scale (heterogeneities, inclusions, manufacturing defects, etc.), and all mechanical parts present section changes or rough surface states. Since these conditions favor the appearance of stress concentrations, we should often consider the possibility of crack initiation as well as its propagation when calculating a structure. For this reason, the designers of structures or any element subjected to cyclic loadings should not only take into account the possibility of cracking, but also estimate the velocity of crack propagation, to ensure that these cracks do not reach the critical length, which will inevitably lead to failure [2-7].

Behavior simulation with FEM has been presented by many authors with the aim of improving the knowledge of predicting trends. H. Yoshihara [8] presented the critical stress intensity factor on the SENT specimen. Saffih [9] studied the harmfulness of circumferential or axisymmetric semi-elliptical cracks in a cylindrical shell with a thickness transition. A. Hachim [10] presented a finite element based approach to simulate a Double Edge Notch Tension specimen of S355 Steel; he studied the behavior of the material in the presence of defects.

The finite element method adopted in this paper is the most commonly used for real applications to provide a robust solution for most industrial problems.

This work is based on the finite element analysis of various specimens (SENT, SENB, DENT, CT) using the calculation code CASTEM to classify the criticality of these specimens.

2. Expérimentation

To extract the mechanical characteristics of the P265GH steel used in our program, tensile tests on standard specimens (Figure 1) were conducted in different directions of roll (longitudinal and transversal) [11]. The test curves showing the stress versus strain are given in figure 2.

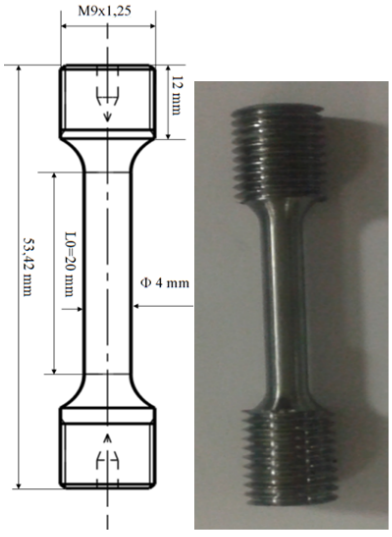

Figure 1 : *Dimensions of the tensile test specimen*

RT&A, No 3 (69)
Volume 17, September 2022

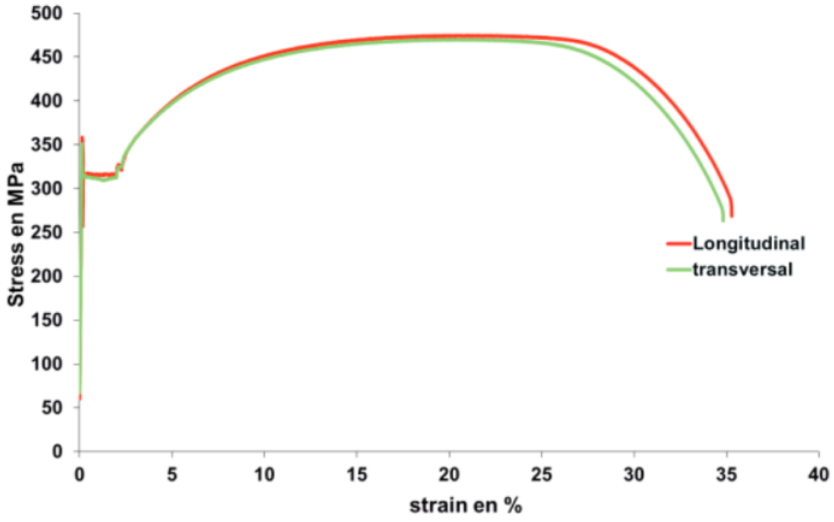

Figure 2 : *Traction curve*

By comparing the mechanical characteristics of specimens in both rolling directions, it is found that there is a negligible difference between tensile test curves. The mechanical characteristics of P265GH steel at the ambient temperature are reported in Table 1[12].

Table 1: Mechanical properties of the material

Young's modulus *E (MPa)*	elastic limit σ_e (MPa)	Breaking stress: σ_g (MPa)	Elongation %	Poisson's ratio ν
2.10^5	320	470	35	0,3

We notice that the elongation is about 35%, which is higher than the 14% required by the CODAP [13]. Therefore, this P265GH steel used is well adapted for pressurized structures.

3. Numerical modeling

The Cast3m [14] calculation code is used to create a finite element model for the analysis of the different specimens (SENT, SENB, DENT, CT).

3.1. Geometry

The geometries and dimensions of the specimens are shown in Figure 3. The study is restricted to mode I.

RT&A, No 3 (69)
Volume 17, September 2022

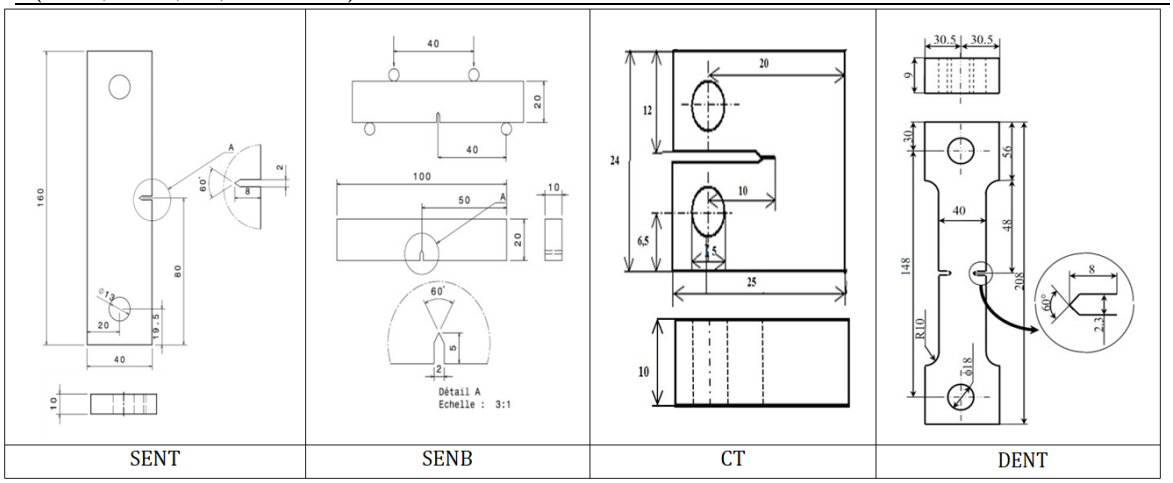

Figure 3 : The geometry of the specimens

3.2. Mesh, boundary conditions and Loading

For the DENT specimen, there are two planes of symmetry. Therefore, only a quarter of this specimen is modeled [15]. On the other hand, for the specimens (SENT, CT, and SENB), only one plane of symmetry appears, so half of the parts are modeled.

The numerical results are intended for analysis of fracture mechanics. Special attention is paid to mesh principally in the crack and its vicinity (Mesh Refinement using Barsoum elements) [16]. Details of the mesh are illustrated in figure 4.

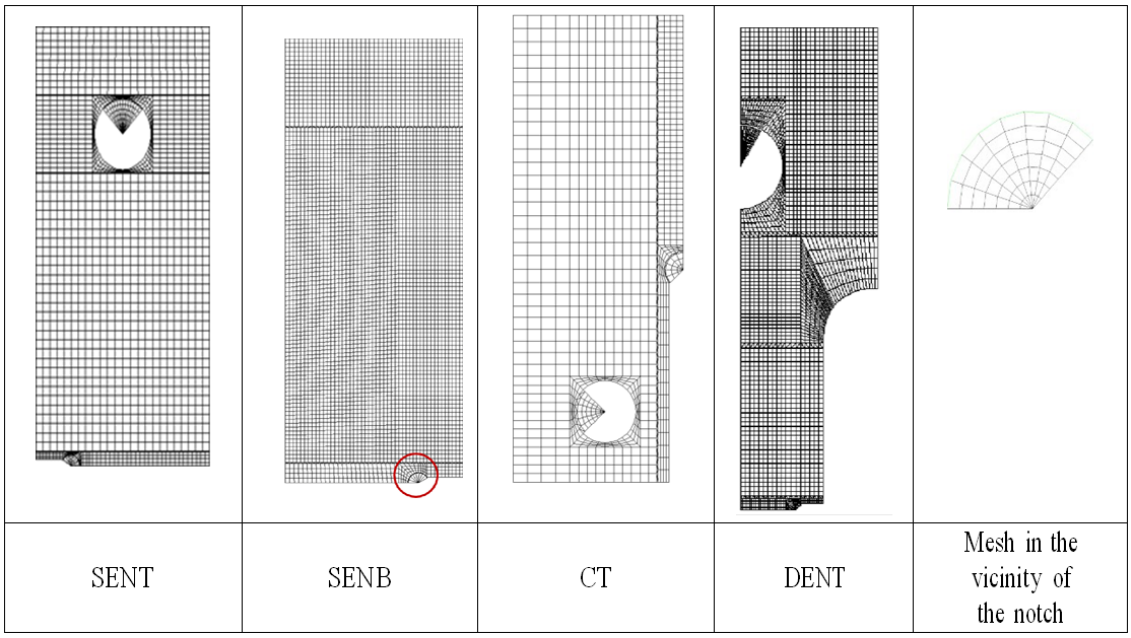

Figure 4 : The mesh of test pieces

RT&A, No 3 (69)
Volume 17, September 2022

4. Results and discussion

For all specimens, the life fraction (β) is the notch length over the specimen width (β=a/w) [17]. For each notch depth, we determine the stress that leads to failure. This stress is called the ultimate residual stress (σ_{ur}). And (σ_u) is the value of the ultimate stress in the initial state;

The curves in Figure 5 show the evolution of the dimensionless stress [18] (σ_{ur} /σ_u) as a function of the life fraction for the SENT, DENT, SENB, and CT specimens.

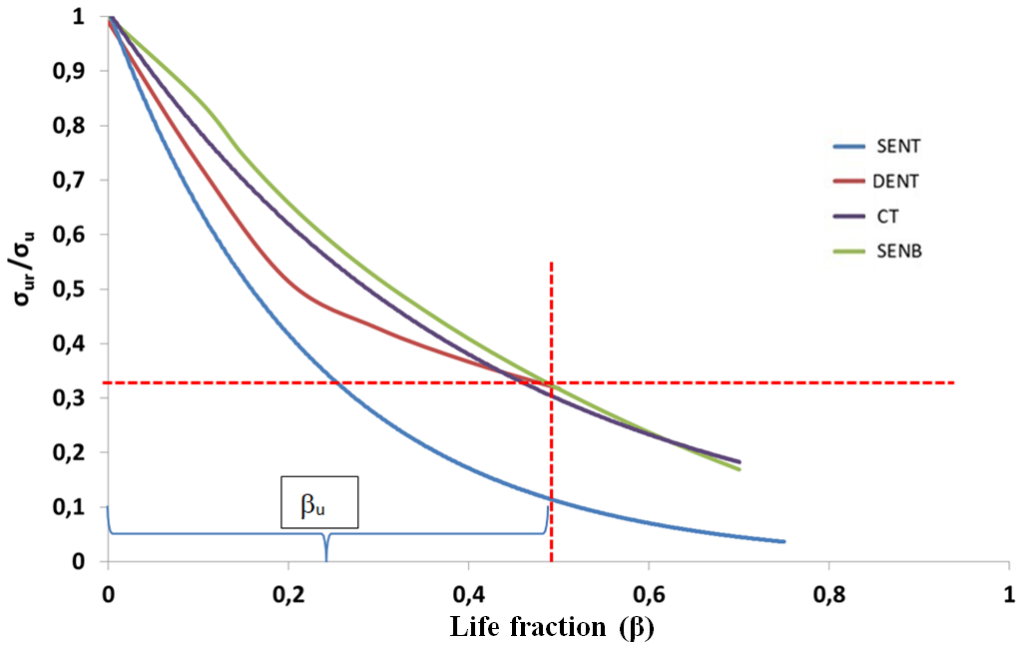

Figure 5 : Dimensional stress as a function of life fraction for SENT, DENT, SENB and CT specimens

The analysis of the curve in Figure 5 shows that the dimensionless stress decreases as a function of the fraction of life. We note that the stress loss is very aggressive for the SENT specimen, followed by the DENT specimen, the CT specimen, and finally the SENB specimen.

We also note that, from life fraction, the dimensionless stress of all specimens is less than 33% (a safety factor equal to 3). Therefore, we define the useful life fraction ($\beta u=a/w_u$) as the ratio of the notch length and the width of the useful specimens (with a safety factor equal to 3).

4.1. Quantification of the static damage

The static damage model is based on the residual stress evolution according to the equation (1) [19,20].

$$D = \frac{1-\frac{\sigma_{ur}}{\sigma_u}}{1-\frac{\sigma_a}{\sigma_u}} \quad (1)$$

with:

- σ_u: Value of the ultimate stress in the initial state ;
- σ_{ur} : Value of the residual ultimate stress ;
- σ_a : Stress just before break in the useful zone.

The boundary conditions are shown below:

In the initial state	$\beta_u = 0$	➔	$\sigma_{ur} = \sigma_u$	➔ D = 0
In the final state	$\beta_u = 1$	➔	$\sigma_{ur} = \sigma_a$	➔ D = 1

The variation of damage as a function of useful life fraction βu for the specimens (SENT, DENT, SENB, and CT) is illustrated by the curves in Figure 6:

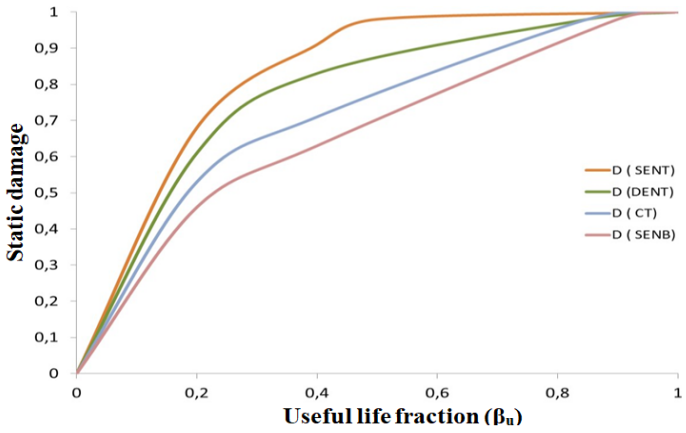

Figure 6 : Static damage to residual stress as a function of the useful life fraction

The increase in damage causes an increase in the static tensile strength loss of the specimens. From the curves in Figure 6, we observe that the damage evolution of the tensile specimen (SENT) is the most critical for the same fraction of service life (β_u), while the damage of the bending specimen (SENB) is the less critical.

Reliability is the inverse of damage, and equation (2) shows the ratio between damage and reliability [21]:

$$R(\beta_u) + D(\beta_u) = 1 \quad (2)$$

The equation obtained is used to draw the curve of the reliability variation with the damage curve (Figure 7) for the SENT, DENT, CT, and SENB specimens.

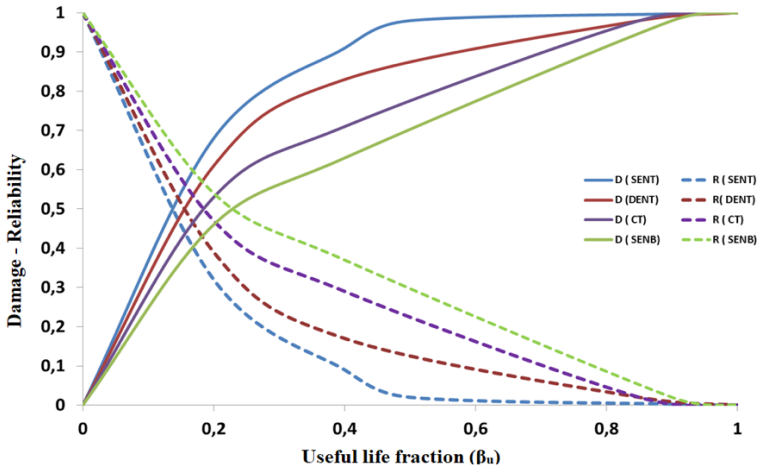

Figure 7 : Damage - Reliability as a function of the usual life fraction

The Reliability-Damage curves for each specimen intersect at a β_{ui} intersection point. This point of intersection is coincident with a reversal of the situation. Indeed, the reliability that was initially higher than the damage decreases beyond this point. This corresponds to the acceleration of damage. The damage becomes critical and uncontrollable when the damage value exceeds 80%, this value is named the critical life fraction β_{uc}.

Damage is generally described by the following three stages:

- Stage I [0, β_{ui}]: Corresponds to the initiation of damage where reliability is higher than damage.
- Stage II [β_{ui}, β_{uc}]: Corresponds to progressive damage where predictive maintenance is required.
- Stage III [β_{uc}, 1]: Corresponds to the brutal damage. At this stage of damage, the specimen is declared failed.

The table 2 recapitulates the stages of damage and the criticality of the damage for each of the specimens studied.

Table 2: Damage stage results

Specimens	**SENT**	**DENT**	**CT**	**SENB**
Stage I	[0 0,16]	[0 0,17]	[0 0,19]	[0 0,22]
Stage II	[0,16 0,27]	[0,17 0,35]	[0,19 0,53]	[0,22 0,63]
Stage III	[0,27 1]	[0,35 1]	[0,53 1]	[0,63 1]
Criticality of the damage	Important	Less important	Moderate	Minimal

4.2. Quantification of damage by unified theory

The loading level applied on the material influences the progression and the behavior of its damage. The various theories representing this damage are given by the linear model initiated by Miner's law according to which the damage evolves linearly as a function of the life fraction.

By analogy, with the unified theory, an empirical relation describing the damage is proposed (equation (3)) [22]:

$$D_{th} = \frac{\beta_u}{\beta_u + (1-\beta_u)\left[\frac{\gamma - \left(\frac{\gamma}{\gamma_u}\right)^8}{\gamma - 1}\right]} \quad (3)$$

With

$\beta_u = \frac{a}{w_u}$, $\gamma = \frac{\sigma_{ur}}{\sigma_0}$ and $\gamma_u = \frac{\sigma_u}{\sigma_0}$

$\sigma_0 = \alpha\sigma_u$ is the endurance limit of the virgin material, with $\alpha = \frac{1}{factor\ of\ safety} = 0.33$

In this unified theory, many curves are drawn. Each curve is associated with a loading level defined with σ_a.

Figure 8 show the damage curves by the unified theory for the specimens SENT, DENT, CT, and SENB:

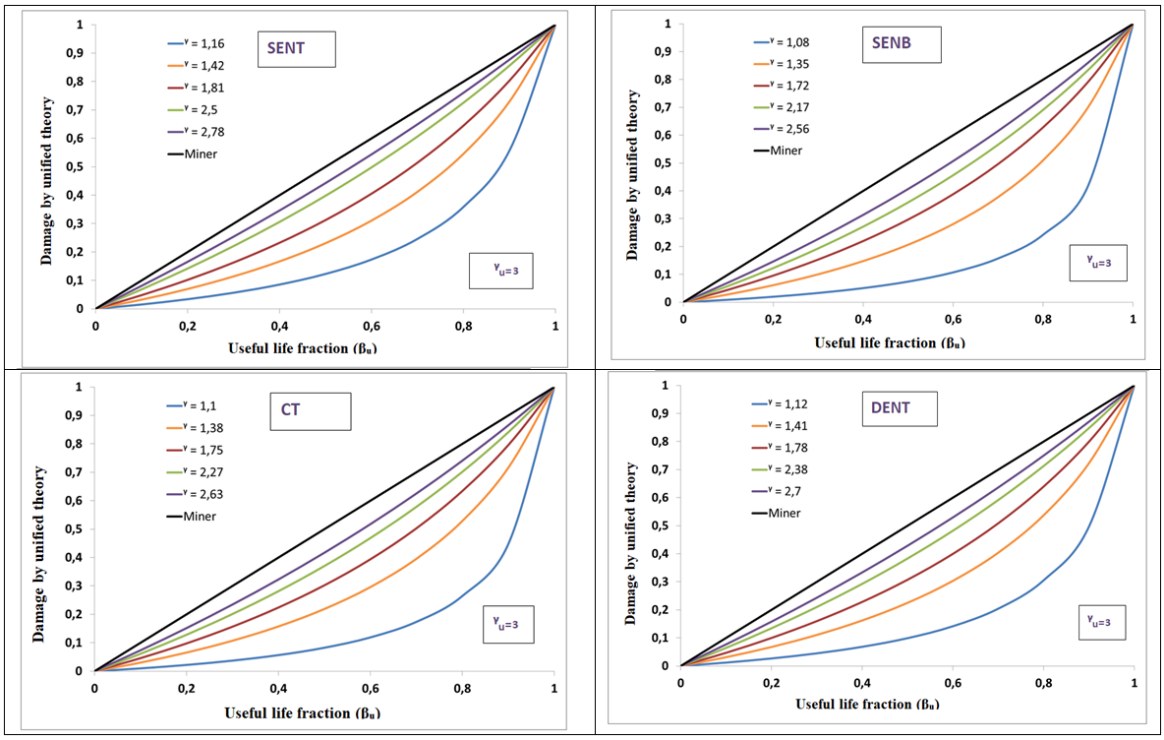

Figure 8 : Evolution of Damage by unified theory and Miner law in function of the life fraction

The analysis of the curves shows that the damage curve is gradually approaching the bisector (Miner's linear rule) as a function of βu for high loading levels.

The damage curves by unified theory are below the Miner's law curve. Therefore, Miner's law presents more simplicity to the user than the unified theory. For this reason, many researchers adopted this law for the study of damage.

5. Conclusion

In risky structures such as pressure equipment and in the presence of cracks, for safety reasons, it is fundamental to know precisely the degree of damage of the failure. Numerical modeling by the finite element method is a very effective tool to resolve this problem. The analysis of the results shows that the damage evolution of the tensile specimen (SENT) is the most critical for the same fraction of life, while the damage of the bending specimen (SENB) is the less dangerous.

References

[1] Lahlou, M., Hachim, A., Mouhib, N., Ouaomar, H., Rachik, M., & El Ghorba, M. (2015). Numerical modeling and analytical validation of stress intensity factor and crack velocity for SENT tensile specimen of. International Journal of Research, 2(6), 489-494.

[2] Damien Fournier, (2011) Analyse et Développement de Méthodes de Rafinement hp en Espace pour l'Equation de Transport des Neutrons, Mémoire de thèse doctorat Université de Provence Marseille,

[3] LAHLOU, M., et al. "Numerical modeling and analytical validation of stress and stress intensity factor for SENT tensile specimen of P265GH steel material."IPASJ International Journal of Mechanical Engineering (IIJME):Volume 3, Issue 4, April 2015 pp. 042–048

[4] Zekriti, Najat et al." Mode I stress intensity factors of printed and extruded specimens based on Digital Image Correlation method (DIC): case of ABS material". Procedia Structural Integrity. 28. 1745-1754. (2020). DOI : 10.1016/j.prostr.2020.10.149.

[5] Majid, Fatima et al. "Mechanical behavior and crack propagation of ABS 3D printed specimens". Procedia Structural Integrity. 28. 1719-1726. (2020). DOI : 10.1016/j.prostr.2020.10.147.

[6] En-Naji, Abderrazak & Lahlou, M. & Ghorba, M. & Mouhib, Nadia. "Change of experimental elongations with increasing temperature for an abs material subjected to tensile test". International Journal of Mechanical Engineering and Technology. 9. 932-944.2018

[7] Fatima Majid, Rajaa Rhanim, Mohammed Lahlou, Hassan Rhanim, Mohammed Ezzahi, Mohamed Elghorba, "Maintainability and reliability of high density polyethylene pipes through experimental and theoretical models", Procedia Structural Integrity, Volume 25, 2020, Pages 430-437, ISSN 2452-3216, https://doi.org/10.1016/j.prostr.2020.04.048

[8] Yoshihara, H., 2013: "Mode II critical stress intensity factor of medium-density fi berboard measured by asymmetric four- point bending tests and analyses of kink crack formation". BioResources 8 (2): 1771-1789.

[9] A. Saffih, S. Hariri, Numerical study of elliptical cracks in cylindrers with a thickness transition, International Journal of Pressure Vessels and Piping, Vol 83, No. 1, pp. 35-41, 2006.

[10] A. HACHIM, (2012) Numerical evaluation of stress triaxiality at the top of notch for a specimen steel notched bi-S355, International Journal of Engineering and Science, Vol. 1, Issue 1, PP 088-93

[11] LAHLOU, M. et al. Numerical modeling and analytical validation of stress and stress intensity factor for SENB bending specimen of P265GH steel material. International Journal of Research, [S.l.], v. 2, n. 6, p. 468-472, jun. 2015.

[12] CODAP: Code de Construction des Appareils à Pression non soumis à la flame 2005

[13] Lahlou, Mohammed et al . "Numerical Study of Internal Radius Effect on Mechanical Behavior of P265GH Material". Periodica Polytechnica Mechanical Engineering. 60. 233-237.(2016). DOI : 10.3311/PPme.8978.

[14] LAHLOU, M., HACHIM, A., OUAOMAR, H., MOUHIB, N., & EL GHORBA, M. (2015). Procedure for the numerical modeling of the specimen (SENB) using CAST3M calculation code. International Journal of Innovation and Scientific Research, 19(2), 259-266.

[15] Cast3M, code d'éléments finis, CEA. (Cast3M, finite element code.) [Online]. Available from: http://www-cast3m.cea.fr/ [Accessed: 2013] (in French)

[16] Barsoum, R. S. "Further application of quadratic isoparametric finite ele-ments to linear fracture mechanics of plate bending and general shells." International Journal of Fracture. 11(1), pp. 167-169. 1975. DOI: 10.1007/BF00034724

[17] N.MOUHIB "Static tests of a steel wire strand (1+6 wires) containing 3/7 damaged wires and prediction of its life time" International Journal of Mechanical Engineering, Vol3 (2015):pp.30-35.

[18] M. LAHLOU, Etude numérique de l'endommagement des éprouvettes (SENT, SENB, CT et DENT) en acier P265GH, IXèmes Journées d'Etudes Techniques – JET'2016 Les 03, 04 & 05 Mai 2016, Hammamet – Tunisie

[19] H.Ouaomar, N. Mouhib, M. Lahlou, A .Barakat and M. El Ghorba ,Study of specific energy in elastic phase of the different elements of a low voltage underground power cable' Int. J. Adv. Res. Sci. Technol. Volume 4, Issue 6, 2015, pp.406-408.

[20] N.Mouhib, H.Ouaomar, M.Lahlou, M.Barakat and M. El Ghorba' Application of Student and Weibull statistical distributions on experimental tensile test results of steel wires extracted from antigyratory wire rope (19x7)'. Int. J. Adv. Res. Sci. Technol. Volume 4, Issue 6, 2015, pp.498-501.

[21] Mouhib, N., Ouaomar, H., Lahlou, M., & El Ghorba, M. ,'Characterization of residual energy loss and Damage Prediction of 7-wire strand extracted from a steel wire rope and subjected to a static test' . International Journal of Research, 2015, vol. 2, no 6, p. 473-478.

[22] E. Boudlal,M. Barakat,N. Mouhib,M. Lahlou,M.El Ghorba,H. Ouaomar, "Mechanical Behaviour Of Damaged Central Core Strand Constituting A Steel Wire Rope Hoist Under The Effect Of A Static Load", International Journal of Mechanical Engineering and Technology(IJMET), 2016, 7(3), PP.360-367

EPQ MODELS WITH GENERALIZED PARETO RATE OF PRODUCTION AND WEIBULL DECAY HAVING DEMAND AS FUNCTION OF ON HAND INVENTORY

D.Madhulatha[1], K. Srinivasa Rao[2], B.Muniswamy[3]

•

Department of Statistics[1], Andhra Loyola College, Vijayawada, India
Department of Statistics [2,3], Andhra University, Visakhapatnam, India
madhulatha.dasari@gmail.com[1], ksraoau@yahoo.co.in[2], munistats@gmail.com[3]

Abstract

Economic production quantity (EPQ) models are more important for scheduling production processes in particular batch production in which the production uptime and production downtime are decision variables. This paper addresses the development and analysis of an EPQ model with random production and Weibull decay having stock dependent demand. The random production is more appropriate in several production processes dealing with deteriorated items. The instantaneous state of on hand inventory is derived. With appropriate cost considerations the total cost function is derived and minimized for obtaining optimal production uptime, production downtime and production quantity. The model sensitivity with respect to changes in parameters and costs is also studied and observe that the production distribution parameters and deteriorating distribution parameters have significant influence on optimal operating policies of the model. This model is extended to the case of without shortages and observed that allowing shortages reduce total product cost. It is further observed that the demand being a function of on hand inventory can reduce inventory cost than other patterns of demand.

Keywords: Stochastic production, on hand inventory, Weibull decay, Generalized Pareto distribution, Production Schedules, Sensitivity analysis.

I. Introduction

In production scheduling problems the on hand inventory plays a dominant role. To have efficient decisions on when to start production and when to stop production the EPQ models provide the basic frame work. In developing the EPQ models the major string is on nature of the product. The product may be subjective deterioration or decay depending upon various random factors. Much work has been reported in literature regarding EPQ models for deteriorating items. The literature on inventory models for deteriorating items are reviewed by Pentico and Drake [1], Ruxian Lie et al [2], Goyal and Giri [3], Raafat [4] and Nahmias [5].

In addition to the nature of the commodity another important factor for developing EPQ models is demand. Several authors developed various models with different patterns of demand. Among them the inventory models with stock dependent demand gained importance due to this applicability in many places. Silver et al. [6] mentioned that the demand for many consumer items is directly proportional to the stock on hand. Gupta et al. [7] have pointed the inventory models with inventory models with stock dependent demand. Later Panda et al. [8], Roy et al. [9], Uma Maheswara Rao et al. [10] and others have developed inventory models for deteriorating items with stock dependent demand. Yang et al. [11], Srinivasa Rao et al. [12], Santanu Kumar Ghosh et al. [13] have developed an inventory model for deteriorating items with Weibull replenishment

and generalized Pareto decay. Brojeswar et al. [14], Srinivasa Rao et al[15], Lakshmana Rao et al [16], Srinivasa Rao et al [17], Ardak and Borade [18], Anindya Mandal, Brojeswar Pal and Kripasindhu Chaudhuri [19], Sunit Kumar, Sushil Kumar and Rachna Kumari [20]. and Jyothsna et al. [21] studied a production inventory system for deteriorating items. In all these papers the authors assumed that the production is either instantaneous or finite rate.

However, in many production processes the production is random due to various random factors such as availability of raw material, skill level of the manpower, tool wear, environmental conditions and availability of power (electricity). Very little work has been reported regarding EPQ models with random production for deteriorating items except the works of Sridevi et al. [22], Srinivasa Rao et al [23] who developed EPQ models with Weibull production and constant rate of deterioration. In reality, many products may not have constant rate of deterioration but will have a variable rate of deterioration can be well characterized by Weibull decay. The generalized Pareto rate of production can characterize the time dependent production. Hence, in this paper we develop and analyze an EPQ model with the assumption that the production process is characterized by generalized Pareto distribution and the lifetime of the commodity follows a Weibull distribution. It is further assumed that the demand is a linear function of on hand inventory. This type of model is much useful in textile industry where the lifetime of the government is random and may have decreasing or increasing or constant rates of deterioration and production is random.

Using the differential equations the instantaneous state of inventory at different states of production are derived. The total cost function is obtained with appropriate cost considerations. Assuming shortages are allowed and fully backlogged, the optimal operating policies of the production schedule such as production downtime and production uptime are derived. The optimal production quantity is also obtained. The effect of change in parameters on optimal production schedule and optimal production quantity are studied in sensitivity analysis. The case of without shortages is also discussed. The conclusions are given at the end.

II. Assumptions

For developing the model the following assumptions are made:

- The demand rate is a function of on hand inventory.
  i.e. $\lambda(t) = \phi_1 + \phi_2 I(t)$ (*1*)
- The production is random and follows a Generalized Pareto distribution. The instantaneous rate of production is
  $K(t) = \frac{1}{\alpha - \gamma t} \quad ; 0 < t < \frac{\alpha}{\gamma}$ (*2*)
- Lead time is zero.
- Cycle length is T. It is known and fixed.
- Shortages are allowed and fully backlogged.
- A deteriorated unit is lost.
- The life time of the item is random and follows a two parameter Weibull distribution with probability density function
  $f(t) = \theta\eta t^{\eta-1} e^{-\theta t^{\eta}} \quad ; \theta, \eta > 0, \quad t > 0$

Therefore the instantaneous rate of deterioration is

$$h(t) = \frac{f(t)}{1-F(t)} = \theta\eta t^{\eta-1} \quad ; \theta, \eta > 0, \quad t > 0 \qquad (3)$$

The following notations are used for developing the model.

Q: Production quantity.

A: Setup cost.

C: Cost per unit.

h: Inventory holding cost per unit per unit time.
π: Shortages cost per unit per unit time.

III. EPQ Model with Shortages

Consider a production system in which the stock level is zero at time $t = 0$. The stock level increases during the period $(0, t_1)$, due to production after fulfilling the demand and deterioration. The production stops at time t_1 when stock level reaches *S*. The inventory decreases gradually due to demand and deterioration in the interval (t_1, t_2). At time t_2 the inventory reaches zero and backorders accumulate during the period (t_2, t_3). At time t_3 the production again starts and fulfills the backlog after satisfying the demand. During (t_3, T) the backorders are fulfilled and inventory level reaches zero at the end of cycle *T*. The Schematic diagram representing the inventory level is given in Figure 1.

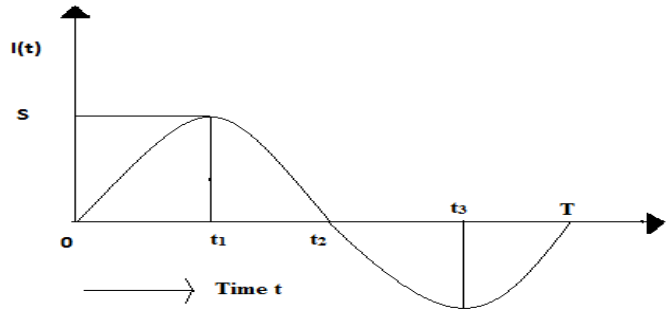

Figure 1: *Schematic Diagram representing the inventory level*

Let *I(t)* be the inventory level of the system at time '*t*' ($0 \le t \le T$). The differential equations governing the instantaneous state of *I(t)* over the cycle of length are:

$$\frac{d}{dt}I(t) + h(t)I(t) = \frac{1}{\alpha - \gamma t} - \left(\phi_1 + \phi_2 I(t)\right) \quad ; \quad 0 \le t \le t_1 \qquad (4)$$

$$\frac{d}{dt}I(t) + h(t)I(t) = -\left(\phi_1 + \phi_2 I(t)\right) \quad ; \quad t_1 \le t \le t_2 \qquad (5)$$

$$\frac{d}{dt}I(t) = -\left(\phi_1 + \phi_2 I(t)\right) \quad ; \quad t_2 \le t \le t_3 \qquad (6)$$

$$\frac{d}{dt}I(t) = \frac{1}{\alpha - \gamma t} - \left(\phi_1 + \phi_2 I(t)\right) \quad ; \quad t_3 \le t \le T \qquad (7)$$

Where, h(t) is as given in equation (3), with the initial conditions I(0) = 0, $I(t_1) = S$, $I(t_2) = 0$ and I(T) = 0. Substituting h(t) in equations (4) and (5) and solving the differential equations, the on hand inventory at time ' t ' is obtained as

$$I(t) = Se^{\theta\left(t_1^{\eta} - t^{\eta}\right) + \phi_2(t_1 - t)} - e^{-(\theta t^{\eta} + \phi_2 t)} \int_t^{t_1} \left(\frac{1}{\alpha - \gamma u} - \phi_1\right) e^{(\theta u^{\eta} + \phi_2 u)}\, du \; ; \quad 0 \le t \le t_1 \qquad (8)$$

$$I(t) = Se^{\theta\left(t_1^{\eta} - t^{\eta}\right) + \phi_2(t_1 - t)} - \phi_1 e^{-(\theta t^{\eta} + \phi_2 t)} \int_{t_1}^{t} e^{(\theta u^{\eta} + \phi_2 u)}\, du \quad ; \quad t_1 \le t \le t_2 \qquad (9)$$

$$I(t) = \frac{\phi_1}{\phi_2}\left(e^{\phi_2(t_2 - t)} - 1\right) \quad ; \quad t_2 \le t \le t_3 \qquad (10)$$

$$I(t) = e^{-\phi_2 t}\left[\int_{t_3}^{t} \left(\frac{1}{\alpha - \gamma u} - \phi_1\right) e^{\phi_2 u}\, du + \int_{t_3}^{T} \left(\frac{1}{\alpha - \gamma u} - \phi_1\right) e^{\phi_2 u}\, du\right] \quad ; \quad t_3 \le t \le T \qquad (11)$$

Production quantity Q in the cycle of length T is

$$Q = \int_0^{t_1} K(t)dt + \int_{t_3}^{T} K(t)dt = \frac{1}{\gamma}\log\left(\frac{\alpha\,(\alpha-\gamma t_3)}{(\alpha-\gamma t_1)(\alpha-\gamma T)}\right) \quad (12)$$

From equation (8) and using the initial condition I(0) = 0, we obtain the value of 'S' as

$$S = e^{-(\theta t_1^{\eta}+\phi_2 t_1)} \int_0^{t_1}\left(\frac{1}{\alpha-\gamma u}-\phi_1\right)e^{(\theta u^{\eta}+\phi_2 u)}du \quad (13)$$

When t = t_3, then equations (10) and (11) become

$$I(t_3) = \frac{\phi_1}{\phi_2}\left(e^{\phi_2(t_2-t_3)}-1\right) \text{ and} \quad (14)$$

$$I(t_3) = e^{-\phi_2 t_3}\int_{t_3}^{T}\left(\frac{1}{\alpha-\gamma u}-\phi_1\right)e^{\phi_2 u}\,du \quad \text{respectively.} \quad (15)$$

Equating the equations (14) & (15) and on simplification, one can get

$$t_2 = t_3 + \frac{1}{\phi_2} ln\left[1+\frac{\phi_2}{\phi_1}e^{-\phi_2 t_3}\int_{t_3}^{T}\left(\frac{1}{\alpha-\gamma u}-\phi_1\right)e^{\phi_2 u}\,du\right] = x(t_3) \quad (say) \quad (16)$$

Let $K(t_1, t_2, t_3)$ be the total production cost per unit time. Since the total production cost is the sum of the set up cost, cost of the units, the inventory holding cost. Hence the total production cost per unit time becomes

$$K(t_1,t_2,t_3) = \frac{A}{T}+\frac{CQ}{T}+\frac{h}{T}\left[\int_0^{t_1} I(t)dt + \int_{t_1}^{t_2} I(t)dt\right] + \frac{\pi}{T}\left[\int_{t_2}^{t_3} -I(t)dt + \int_{t_3}^{T} -I(t)dt\right] \quad (17)$$

Substituting the values of I(t) and Q in equation (17), we can obtain $K(t_1, t_2, t_3)$ as

$$\begin{aligned} K(t_1,t_2,t_3) = {} & \frac{A}{T}+\frac{C}{\gamma T}\log\left(\frac{\alpha\,(\alpha-\gamma t_3)}{(\alpha-\gamma t_1)(\alpha-\gamma T)}\right) + \frac{h}{T}\left[\int_0^{t_1}\left[Se^{\theta(t_1^{\eta}-t^{\eta})+\phi_2(t_1-t)}\right.\right. \\ & \left.-e^{-(\theta t^{\eta}+\phi_2 t)}\int_t^{t_1}\left(\frac{1}{\alpha-\gamma u}-\phi_1\right)e^{(\theta u^{\eta}+\phi_2 u)}\,du\right]dt \\ & + \int_{t_1}^{t_2}\left[Se^{\theta(t_1^{\eta}-t^{\eta})+\phi_2(t_1-t)} - \phi_1 e^{-(\theta t^{\eta}+\phi_2 t)}\int_{t_1}^{t} e^{(\theta u^{\eta}+\phi_2 u)}\,du\right]dt\Bigg] \\ & + \frac{\pi}{T}\left[\frac{\phi_1}{\phi_2}\int_{t_2}^{t_3}\left(1-e^{\phi_2(t_2-t)}\right)dt - \int_{t_3}^{T}\left[e^{-\phi_2 t}\left[\int_{t_3}^{t}\left(\frac{1}{\alpha-\gamma u}-\phi_1\right)e^{\phi_2 u}\,du\right.\right.\right. \\ & \left.\left.\left.+\int_{t_3}^{T}\left(\frac{1}{\alpha-\gamma u}-\phi_1\right)e^{\phi_2 u}\,du\right]\right]dt\Bigg] \end{aligned} \quad (18)$$

0n integration and simplification one can get

$$\begin{aligned} K(t_1,t_2,t_3) = {} & \frac{A}{T}+\frac{C}{\gamma T}\log\left(\frac{\alpha\,(\alpha-\gamma t_3)}{(\alpha-\gamma t_1)(\alpha-\gamma T)}\right) + \frac{h}{T}\left[e^{(\theta t_1^{\eta}+\phi_2 t_1)}\int_0^{t_2} Se^{-(\theta t^{\eta}+\phi_2 t)}dt\right. \\ & \left.-\int_0^{t_1}\left[e^{-(\theta t^{\eta}+\phi_2 t)}\int_t^{t_1}\left(\frac{1}{\alpha-\gamma u}-\phi_1\right)e^{(\theta u^{\eta}+\phi_2 u)}\,du\right]dt\right. \end{aligned}$$

$$-\phi_1\int_{t_1}^{t_2}\left[e^{-(\theta t^{\eta}+\phi_2 t)}\int_{t_1}^{t}e^{(\theta u^{\eta}+\phi_2 u)}\,du\right]dt\Bigg]+\frac{\pi}{T}\left[\frac{\phi_1}{\phi_2}\left(t_3-t_2-\frac{1}{\phi_2}\left(1-e^{\phi_2(t_2-t_3)}\right)\right)\right.$$
$$\left.-\int_{t_3}^{T}\left[e^{-\phi_2 t}\left[\int_{t_3}^{t}\frac{e^{\phi_2 u}}{\alpha-\gamma u}du+\int_{t_3}^{T}\frac{e^{\phi_2 u}}{\alpha-\gamma u}du\right]dt+\frac{\phi_1}{\phi_2}\left(e^{\phi_2(T-t)}-1\right)\right]dt\right] \quad (19)$$

Substituting the values of S and t_2 in equation (19), one can obtain

$$K(t_1,t_3)=\frac{A}{T}+\frac{C}{\gamma T}\log\left(\frac{\alpha\,(\alpha-\gamma t_3)}{(\alpha-\gamma t_1)(\alpha-\gamma T)}\right)$$
$$+\frac{h}{T}\left[\int_0^{x(t_3)}\left[e^{-(\theta t^{\eta}+\phi_2 t)}\int_0^{t_1}\left(\frac{1}{\alpha-\gamma u}-\phi_1\right)e^{(\theta u^{\eta}+\phi_2 u)}du\right]dt\right.$$
$$-\int_0^{t_1}\left[e^{-(\theta t^{\eta}+\phi_2 t)}\int_t^{t_1}\left(\frac{1}{\alpha-\gamma u}-\phi_1\right)e^{(\theta u^{\eta}+\phi_2 u)}\,du\right]dt$$
$$\left.-\phi_1\int_{t_1}^{x(t_3)}\left[e^{-(\theta t^{\eta}+\phi_2 t)}\int_{t_1}^{t}e^{(\theta u^{\eta}+\phi_2 u)}\,du\right]dt\right]$$
$$+\frac{\pi}{T\phi_2}\left[e^{-\phi_2 t_3}\int_{t_3}^{T}\left(\frac{1}{\alpha-\gamma u}-\phi_1\right)e^{\phi_2 u}\,du-\phi_1[t_3-T\right.$$
$$\left.\left.-\frac{1}{\phi_2}\left[1-e^{\phi_2(T-t_3)}-ln\left[1+\frac{\phi_2}{\phi_1}e^{-\phi_2 t_3}\int_{t_3}^{T}\left(\frac{1}{\alpha-\gamma u}-\phi_1\right)e^{\phi_2 u}\,du\right]\right]\right]$$
$$-\phi_2\int_{t_3}^{T}e^{-\phi_2 t}\left[\int_{t_3}^{t}\frac{e^{\phi_2 u}}{\alpha-\gamma u}du+\int_{t_3}^{T}\frac{e^{\phi_2 u}}{\alpha-\gamma u}du\right]dt\Bigg] \quad (20)$$

IV. Optimal Production Schedules of the Model

In this section we obtain the optimal policies of the system under study. To find the optimal values of t_1 and t_3, we obtain the first order partial derivatives of $K(t_1,t_3)$ given in equation with respect to t_1 and t_3 and equate them to zero. The condition for minimization of $K(t_1,t_3)$ is

Where D is the Hessian matrix

$$D=\begin{vmatrix}\dfrac{\partial^2 K(t_1,t_3)}{\partial {t_1}^2} & \dfrac{\partial^2 K(t_1,t_3)}{\partial t_1\partial t_3}\\ \dfrac{\partial^2 K(t_1,t_3)}{\partial t_1\partial t_3} & \dfrac{\partial^2 K(t_1,t_3)}{\partial {t_3}^2}\end{vmatrix}>0$$

Differentiating $K(t_1,t_3)$ given in equation (20) with respect to t_1 and equating to zero, we get

$$\frac{C}{\alpha-\gamma t_1}+he^{(\theta t_1^{\eta}+\phi_2 t_1)}\left[\left(\frac{1}{\alpha-\gamma t_1}-\phi_1\right)\left[\int_0^{x(t_3)}e^{-(\theta t^{\eta}+\phi_2 t)}\,dt\right.\right.$$
$$\left.\left.-\int_0^{t_1}e^{-(\theta t^{\eta}+\phi_2 t)}\,dt\right]+\phi_1\int_{t_1}^{x(t_3)}e^{-(\theta t^{\eta}+\phi_2 t)}\,dt\right]\quad=0 \quad (21)$$

Differentiating $K(t_1,t_3)$ with respect to t_3 and equating to zero, we get

$$\frac{-C}{\alpha-\gamma t_3}+he^{-\left[\theta(x(t_3))^{\eta}+\phi_2 x(t_3)\right]}y(t_3)\left[\int_0^{t_1}\left(\frac{1}{\alpha-\gamma u}-\phi_1\right)e^{(\theta u^{\eta}+\phi_2 u)}du\right.$$
$$\left.-\phi_1\int_{t_1}^{x(t_3)}e^{(\theta u^{\eta}+\phi_2 u)}du\right]+\frac{\pi}{\phi_2}\left[\left(\frac{3-2e^{\phi_2(t_3-T)}}{\alpha-\gamma t_3}\right)\right.$$

$$-\phi_1\left[1-e^{\phi_2(T-t_3)}+\frac{1}{(\alpha-\gamma t_3)\left[\phi_1+\phi_2 e^{-\phi_2 t_3}\int_{t_3}^{T}\left(\frac{1}{\alpha-\gamma u}-\phi_1\right)e^{\phi_2 u}\,du\right]}\right]=0 \tag{22}$$

$$\text{where,}\quad x(t_3)=t_2=\ t_3+\frac{1}{\phi_2}ln\left[1+\frac{\phi_2}{\phi_1}e^{-\phi_2 t_3}\int_{t_3}^{T}\left(\frac{1}{\alpha-\gamma u}-\phi_1\right)e^{\phi_2 u}\,du\right]$$

$$y(t_3)=\frac{\partial}{\partial t_3}x(t_3)=\frac{1}{(\alpha-\gamma t_3)\left[\phi_1+\phi_2 e^{-\phi_2 t_3}\int_{t_3}^{T}\left(\frac{1}{\alpha-\gamma u}-\phi_1\right)e^{\phi_2 u}\,du\right]}-1$$

Solving the equations (21) and (22) simultaneously, we obtain the optimal time at which production is stopped t_1^* of t_1 and the optimal timet_3^* of t_3 at which the production is restarted after accumulation of backorders. The optimum production quantity Q^* of Q in the cycle of length T is obtained by substituting the optimal values of t_1^*, t_3^* in equation (12) as

$$Q^*=\frac{1}{\gamma}\log\left(\frac{\alpha\,(\alpha-\gamma t_3{}^*)}{(\alpha-\gamma t_1{}^*)(\alpha-\gamma T)}\right) \tag{23}$$

V. Numerical Illustration

The numerical illustration is carried to explore the effect of changes in model parameters and costs on the optimal policies, by varying each parameter (-15%, -10%, -5%, 0%, 5%, 10%, 15%) at a time for the model under study. The results are presented in Table 1. The relationships between the parameters and the optimal values of the production schedule are shown in Figure 2.

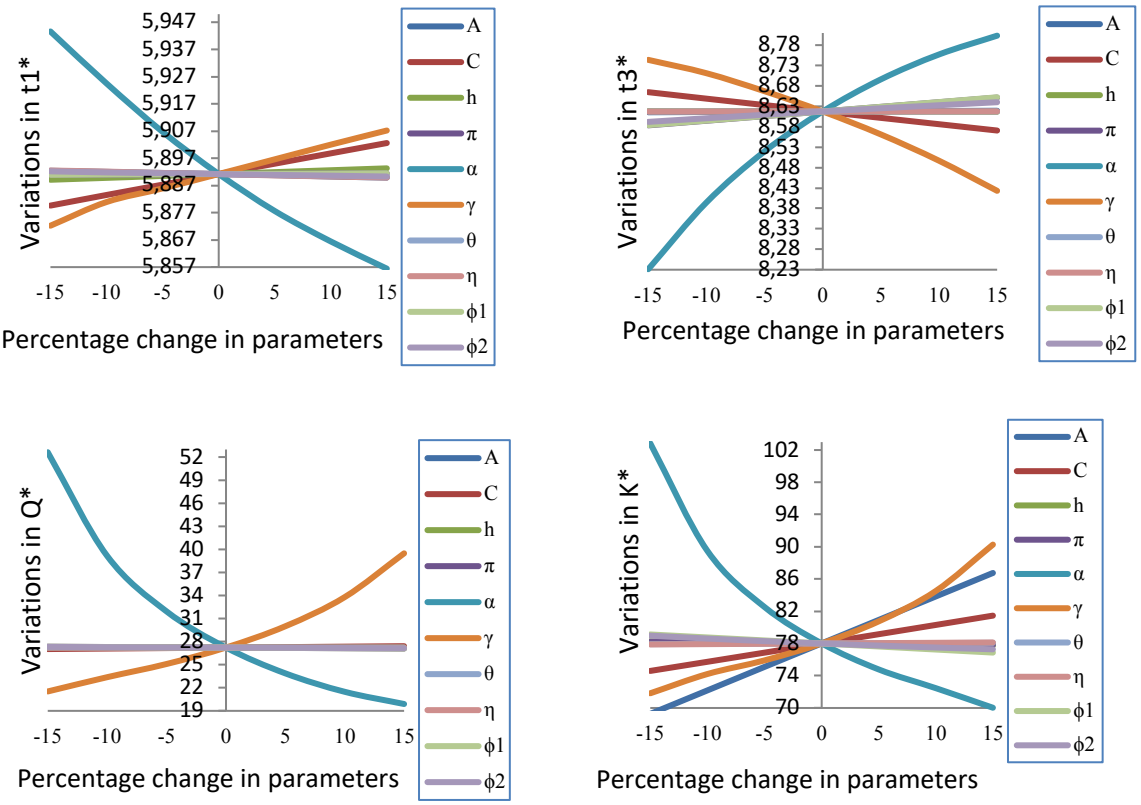

Figure 2: *Relationship between parameters and optimal values with shortages*

Table 1: *Numerical Illustration of the Model - With Shortages*

Variation Parameters	Optimal Policies	-15%	-10%	-5%	0%	5%	10%	15%
A	t_1^*	5.8924	5.892	5.8916	5.8912	5.8908	5.8903	5.8899
	t_3^*	8.6156	8.6162	8.6169	8.6175	8.6181	8.6187	8.6193
	Q^*	27.2344	27.2313	27.2281	27.225	27.2219	27.2187	27.2156
	K^*	69.2564	72.1721	75.0877	78.0034	80.919	83.8347	86.7503
C	t_1^*	5.8796	5.8835	5.8873	5.8912	5.895	5.8988	5.9026
	t_3^*	8.6648	8.6489	8.6332	8.6175	8.6018	8.5863	8.5708
	Q^*	27.0359	27.0993	27.1623	27.225	27.2872	27.3491	27.4106
	K^*	74.5927	75.7248	76.8617	78.0034	79.1498	80.3009	81.4566
h	t_1^*	5.8891	5.8898	5.8905	5.8912	5.8919	5.8926	5.8933
	t_3^*	8.6181	8.6179	8.6177	8.6175	8.6173	8.6171	8.6169
	Q^*	27.218	27.2203	27.2226	27.225	27.2273	27.2297	27.232
	K^*	78.2736	78.1835	78.0934	78.0034	77.9133	77.8233	77.7334
π	t_1^*	5.8909	5.891	5.8911	5.8912	5.8913	5.8914	5.8914
	t_3^*	8.5835	8.5948	8.6061	8.6175	8.6288	8.6402	8.6515
	Q^*	27.3403	27.3019	27.2635	27.225	27.1864	27.1477	27.109
	K^*	78.1961	78.1288	78.0646	78.0034	77.9451	77.8898	77.8375
α	t_1^*	5.9436	5.9245	5.9067	5.8912	5.8776	5.8664	5.8564
	t_3^*	8.2309	8.3944	8.5196	8.6175	8.6961	8.7571	8.8032
	Q^*	52.6288	39.1438	31.9239	27.225	23.8626	21.4632	19.8741
	K^*	102.832	89.4855	82.5151	78.0034	74.7664	72.4419	70.0115
γ	t_1^*	5.8722	5.8809	5.8859	5.8912	5.8966	5.902	5.9072
	t_3^*	8.7439	8.7112	8.6671	8.6175	8.5612	8.4968	8.423
	Q^*	21.5134	23.3696	25.0854	27.225	29.9954	33.7873	39.4837
	K^*	71.8131	74.203	75.8954	78.0034	80.7391	84.512	90.2701
θ	t_1^*	5.8921	5.8918	5.8915	5.8912	5.8909	5.8906	5.8904
	t_3^*	8.6173	8.6174	8.6174	8.6175	8.6175	8.6176	8.6177
	Q^*	27.2277	27.2268	27.2259	27.225	27.2241	27.2233	27.2225
	K^*	77.9196	77.9484	77.9763	78.0034	78.0296	78.0549	78.0796
η	t_1^*	5.8925	5.8921	5.8916	5.8912	5.8907	5.8903	5.8899
	t_3^*	8.6172	8.6173	8.6174	8.6175	8.6176	8.6177	8.6178
	Q^*	27.2292	27.2278	27.2264	27.225	27.2236	27.2222	27.2208
	K^*	77.8796	77.9207	77.962	78.0034	78.0449	78.0864	78.128
ϕ_1	t_1^*	5.8909	5.891	5.8911	5.8912	5.8913	5.8914	5.8915
	t_3^*	8.5841	8.5951	8.6062	8.6175	8.6289	8.6405	8.6523
	Q^*	27.338	27.3009	27.2633	27.225	27.1861	27.1465	27.1062
	K^*	79.1187	78.7492	78.3773	78.0034	77.6275	77.25	76.8709
ϕ_2	t_1^*	5.8922	5.8918	5.8915	5.8912	5.8909	5.8906	5.8903
	t_3^*	8.592	8.6009	8.6094	8.6175	8.6253	8.6328	8.6402
	Q^*	27.3141	27.2828	27.2532	27.225	27.1978	27.1713	27.1455
	K^*	78.9696	78.6124	78.2924	78.0034	77.7405	77.4996	77.2776

VI. Observations

The major observations drawn from the numerical study are:

- It is observed that the costs are having a significant influence on the optimal production quantity and production schedules.
- As the setup cost 'A' decreases, the optimal production downtime t_1^* and the optimal production quantity Q^* are increasing and the total production cost per unit time K^* and the optimal production up time t_3^* are decreasing.
- As the cost per unit 'C' decreases, the optimal production up time t_3^* increases and the optimal production downtime t_1^*, the optimal production quantity Q^* and the total cost per unit time K^* are decreasing.
- As the holding cost 'h' decreases, the optimal production up time t_3^* and the total production cost per unit time K^* are increasing, the optimal production downtime t_1^* and the optimal production quantity Q^* are decreasing.
- As shortage cost 'π' decreases the optimal production downtime t_1^*, the optimal production quantity Q^* and the total production cost per unit time K^* are increasing and the optimal production up time t_3^* decreases.
- As the production rate parameter 'γ' decreases, the optimal production up time t_3^* increases and the optimal production downtime t_1^*, the optimal production quantity Q^* and the total production cost per unit time K^* are decreasing.
- Another production rate parameter 'α' decreases, the optimal production downtime t_1^*, the optimal production quantity Q^* and the total production cost per unit time K^* are increasing and the optimal production up time t_3^* decreases.
- As deteriorating parameter θ decreases, the optimal production downtime t_1^* and the total production cost per unit time K^* are increasing and the optimal production up time t_3^* and the optimal production quantity Q^* are decreasing.
- Another deteriorating parameter η decreases the optimal production downtime t_1^* and the optimal production quantity Q^* are increasing and the optimal production up time t_3^* and the total cost production per unit time K^* are decreasing.
- As demand rate parameter ϕ_1 decreases, the optimal production quantity Q^* and the total production cost per unit time K^* are increasing and the optimal production downtime t_1^* and the optimal production up time t_3^* are decreasing.
- Another demand rate parameter ϕ_2 increases, the optimal production quantity Q^* and the total production cost per unit time K^* are decreasing, the optimal production downtime t_1^* and the optimal production up time t_3^* are increasing.

Finally, from the numerical illustrations we can observe that the parameters are having tremendous influence on the optimal policies of the system.

VII. EPQ Model without Shortages

In this section the inventory model for deteriorating items without shortages is developed and analyzed. Here, it is assumed that shortages are not allowed and the stock level is zero at time $t=0$. The stock level increases during the period $(0, t_1)$ due to excess production after fulfilling the demand and deterioration. The production stops at time t_1 when the stock level reaches S. The inventory decreases gradually due to demand and deterioration in the interval (t_1, T) . At time T the inventory reaches zero. The schematic diagram representing the instantaneous state of inventory is given in Figure 3.

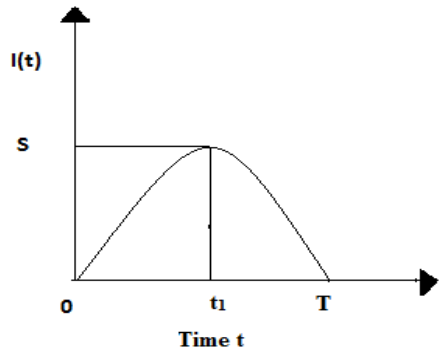

Figure 3: *Schematic diagram representing the inventory level*

Let *I(t)* be the inventory level of the system at time 't' *(0 ≤ t ≤ T).* Then the differential equations governing the instantaneous state of *I(t)* over the cycle of length *T* are:

$$\frac{d}{dt}I(t) + h(t)I(t) = \frac{1}{\alpha-\gamma t} - \left(\phi_1 + \phi_2 I(t)\right) \quad ; \quad 0 \le t \le t_1 \tag{24}$$

$$\frac{d}{dt}I(t) + h(t)I(t) = -\left(\phi_1 + \phi_2 I(t)\right) \quad ; \quad t_1 \le t \le T \tag{25}$$

where, h(t) is as given in equation (3), with the initial conditions I(0) = 0, $I(t_1) = S$ and I(T) = 0.

Substituting h(t) in equations (24) and (25) and solving the differential equations, the on hand inventory at time 't ' is obtained as

$$I(t) = Se^{\theta\left(t_1^{\eta}-t^{\eta}\right)+\phi_2(t_1-t)} - e^{-(\theta t^{\eta}+\phi_2 t)} \int_t^{t_1} \left(\frac{1}{\alpha-\gamma u} - \phi_1\right) e^{(\theta u^{\eta}+\phi_2 u)}\, du \; ; \quad 0 \le t \le t_1 \tag{26}$$

$$I(t) = Se^{\theta\left(t_1^{\eta}-t^{\eta}\right)+\phi_2(t_1-t)} - \phi_1 e^{-(\theta t^{\eta}+\phi_2 t)} \int_{t_1}^{t} e^{(\theta u^{\eta}+\phi_2 u)}\, du \; ; \quad t_1 \le t \le T \tag{27}$$

Production quantity Q in the cycle of length T is

$$Q = \int_0^{t_1} K(t)dt \quad = \frac{1}{\gamma}\log\left(\frac{\alpha}{(\alpha-\gamma t_1)}\right) \tag{28}$$

From equation (26) and using the initial conditions I(0) = 0, we obtain the value of 'S' as

$$S = e^{-(\theta t_1^{\eta}+\phi_2 t_1)} \int_0^{t_1} \left(\frac{1}{\alpha-\gamma u} - \phi_1\right) e^{(\theta u^{\eta}+\phi_2 u)} du \tag{29}$$

Let $K(t_1)$ be the total production cost per unit time. Since the total production cost is the sum of the set up cost, cost of the units, the inventory holding cost. Therefore the total production cost per unit time becomes

$$K(t_1) = \frac{A}{T} + \frac{CQ}{T} + \frac{h}{T}\left[\int_0^{t_1} I(t)dt + \int_{t_1}^{T} I(t)dt\right] \tag{30}$$

Substituting the values of I(t) and Q in equation (30), one can obtain K(t_1) as

$$K(t_1) = \frac{A}{T} + \frac{C}{\gamma T}\log\left(\frac{\alpha}{\alpha-\gamma t_1}\right)$$

$$+ \frac{h}{T}\left[\int_0^{t_1}\left[Se^{\theta\left(t_1^{\eta}-t^{\eta}\right)+\phi_2(t_1-t)} - e^{-(\theta t^{\eta}+\phi_2 t)} \int_t^{t_1}\left(\frac{1}{\alpha-\gamma u} - \phi_1\right) e^{(\theta u^{\eta}+\phi_2 u)}\, du\right] dt\right.$$

$$\left. + \int_{t_1}^{T}\left[Se^{\theta\left(t_1^{\eta}-t^{\eta}\right)+\phi_2(t_1-t)} - \phi_1 e^{-(\theta t^{\eta}+\phi_2 t)} \int_{t_1}^{t} e^{(\theta u^{\eta}+\phi_2 u)}\, du\right] dt\right] \tag{31}$$

0n simplification, one can get

$$K(t_1) = \frac{A}{T} + \frac{C}{\gamma T}\log\left(\frac{\alpha}{\alpha - \gamma t_1}\right) + \frac{h}{T}\left[e^{(\theta t_1^{\eta} + \phi_2 t_1)} \int_0^T S e^{-(\theta t^{\eta} + \phi_2 t)} dt \right.$$
$$- \int_0^{t_1} \left[e^{-(\theta t^{\eta} + \phi_2 t)} \int_t^{t_1} \left(\frac{1}{\alpha - \gamma u} - \phi_1\right) e^{(\theta u^{\eta} + \phi_2 u)}\, du\right] dt$$
$$\left. - \phi_1 \int_{t_1}^{T} \left[e^{-(\theta t^{\eta} + \phi_2 t)} \int_{t_1}^{t} e^{(\theta u^{\eta} + \phi_2 u)}\, du\right] dt\right] \quad (32)$$

Substituting the value of S in equation (32), one can obtain

$$K(t_1) = \frac{A}{T} + \frac{C}{\gamma T}\log\left(\frac{\alpha}{\alpha - \gamma t_1}\right)$$
$$+ \frac{h}{T}\left[\int_0^T \left[e^{-(\theta t^{\eta} + \phi_2 t)} \int_0^{t_1} \left(\frac{1}{\alpha - \gamma u} - \phi_1\right) e^{(\theta u^{\eta} + \phi_2 u)} du\right] dt \right.$$
$$- \int_0^{t_1} \left[e^{-(\theta t^{\eta} + \phi_2 t)} \int_t^{t_1} \left(\frac{1}{\alpha - \gamma u} - \phi_1\right) e^{(\theta u^{\eta} + \phi_2 u)}\, du\right] dt$$
$$\left. - \phi_1 \int_{t_1}^{T} \left[e^{-(\theta t^{\eta} + \phi_2 t)} \int_{t_1}^{t} e^{(\theta u^{\eta} + \phi_2 u)}\, du\right] dt\right] \quad (33)$$

VIII. Optimal Production Schedules of the Model

In this section we obtain the optimal policies of the inventory system under study. To find the optimal values of t_1, we equate the first order partial derivatives of $K(t_1)$ with respect to t_1 equate them to zero. The condition for minimum of $K(t_1)$ is

$$\frac{\partial^2 K(t_1)}{\partial {t_1}^2} > 0$$

Differentiating $K(t_1)$ with respect to t_1 and equating to zero, we get

$$\frac{C}{\alpha - \gamma t_1} + h e^{(\theta t_1^{\eta} + \phi_2 t_1)} \left[\left(\frac{1}{\alpha - \gamma t_1} - \phi_1\right)\left[\int_0^T e^{-(\theta t^{\eta} + \phi_2 t)}\, dt \right.\right.$$
$$\left.\left. - \int_0^{t_1} e^{-(\theta t^{\eta} + \phi_2 t)}\, dt\right] + \phi_1 \int_{t_1}^{T} e^{-(\theta t^{\eta} + \phi_2 t)}\, dt \quad = 0 \quad (34)$$

Solving the equation (34), we obtain the optimal time t_1^* of $t_1$at which the production is to be stopped.

The optimal production quantity Q^* of Q in the cycle of length T is obtained by substituting the optimal values of t_1 in equation (28).

IX. Numerical Illustration

The numerical illustration is carried to explore the effect of changes in model parameters and costs on the optimal policies, by varying each parameter (-15%, -10%, -5%, 0%, 5%, 10%, 15%) at a time for the model under study. The results are presented in Table 2.

The relationship between the parameters and the optimal values of the production schedule is shown in Figure 4.

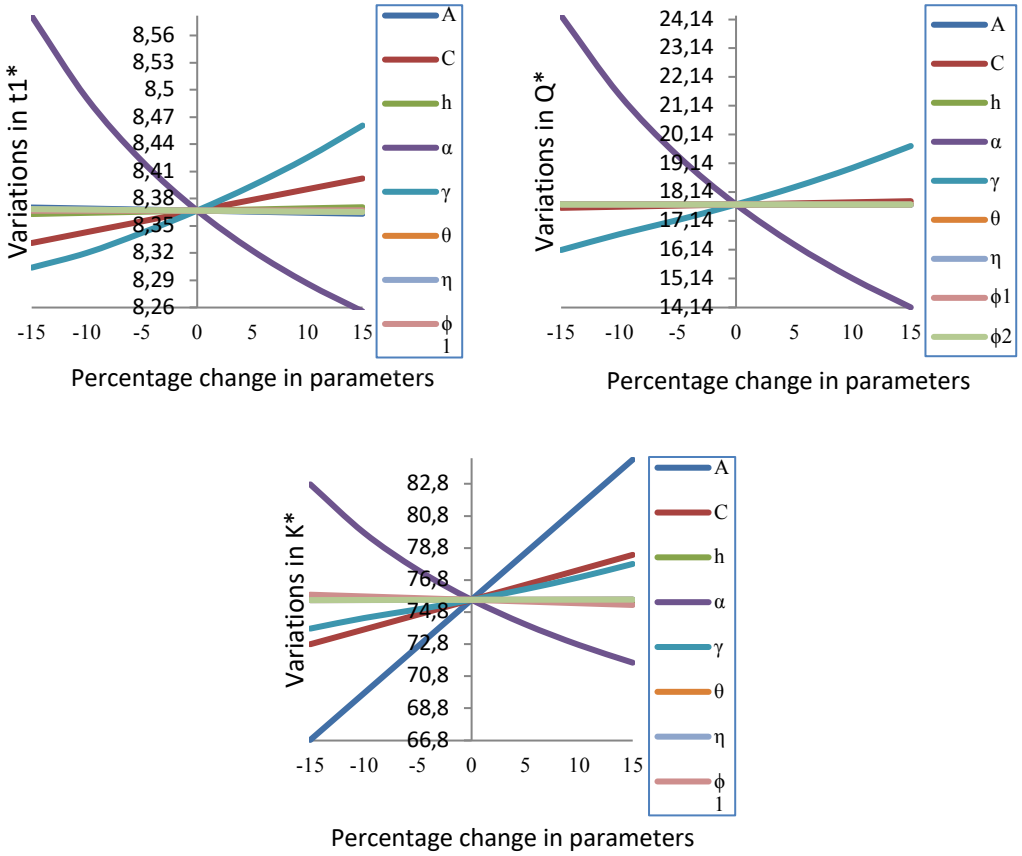

Figure 4: *Relationship between parameters and optimal values without shortages*

Table 2: Numerical illustration *of the model - Without Shortages*

Variation Parameters	Optimal Policies	-15%	-10%	-5%	0%	5%	10%	15%
A	t_1^*	8.3703	8.3692	8.368	8.3669	8.3657	8.3645	8.3634
	Q^*	17.7291	17.7253	17.7215	17.7177	17.7139	17.7101	17.7062
	K^*	66.83	69.7424	72.6549	75.5674	78.4798	81.3923	84.3047
C	t_1^*	8.3311	8.3431	8.355	8.3669	8.3787	8.3905	8.4023
	Q^*	17.6011	17.64	17.6789	17.7177	17.7565	17.7952	17.8339
	K^*	72.7991	73.718	74.6408	75.5674	76.4978	77.432	78.37
h	t_1^*	8.3631	8.3644	8.3656	8.3669	8.3681	8.3694	8.3706
	Q^*	17.7055	17.7096	17.7136	17.7177	17.7218	17.7258	17.7299
	K^*	75.6268	75.6069	75.5871	75.5674	75.5476	75.528	75.5083
α	t_1^*	8.5814	8.4906	8.4214	8.3669	8.3227	8.2863	8.2556
	Q^*	24.275	21.5265	19.4117	17.7177	16.3216	15.1462	14.1399
	K^*	82.7598	79.7446	77.4251	75.5674	74.0371	72.7491	71.6467
γ	t_1^*	8.3039	8.3202	8.3423	8.3669	8.3944	8.4254	8.4607
	Q^*	16.1354	16.6849	17.1767	17.7177	18.3176	18.9892	19.7498
	K^*	73.7729	74.4309	74.9721	75.5674	76.2279	76.967	77.8039
θ	t_1^*	8.3679	8.3676	8.3672	8.3669	8.3665	8.3662	8.3659
	Q^*	17.7212	17.72	17.7188	17.7177	17.7166	17.7155	17.7145
	K^*	75.55	75.5561	75.5619	75.5674	75.5726	75.5776	75.5823
η	t_1^*	8.3685	8.368	8.3674	8.3669	8.3663	8.3657	8.3651
	Q^*	17.7231	17.7213	17.7195	17.7177	17.7158	17.7139	17.712
	K^*	75.5454	75.5529	75.5602	75.5674	75.5743	75.5811	75.5877
ϕ_1	t_1^*	8.3667	8.3667	8.3668	8.3669	8.367	8.3671	8.3672
	Q^*	17.7173	17.7174	17.7176	17.7177	17.7178	17.718	17.7181
	K^*	75.888	75.7811	75.6742	75.5674	75.4605	75.3536	75.2467
ϕ_2	t_1^*	8.3685	8.3679	8.3674	8.3669	8.3663	8.3658	8.3654
	Q^*	17.7231	17.7213	17.7194	17.7177	17.716	17.7144	17.7128
	K^*	75.5528	75.5578	75.5626	75.5674	75.572	75.5765	75.5809

X. Observations

The major observations drawn from the numerical study are:

- It is observed that the costs are having a significant influence on the optimal production quantity and production schedules.
- As the setup cost 'A' decreases, the optimal production time t_1^* and the optimal production quantity Q^* are increasing and the total production cost per unit time K^* decreases.
- As the cost per unit 'C' decreases, the optimal production time t_1^*, the optimal production quantity Q^* and the total production cost per unit time K^* are decreasing.
- As the holding cost 'h' decreases, the total production cost per unit time K^* increases and the optimal production time t_1^* and the optimal production quantity Q^* are decreasing.
- As the production rate parameter 'γ' decreases, the optimal production time t_1^*, the optimal production quantity Q^* and the total production cost per unit time K^* are decreasing.
- As the production rate parameter 'α' decreases, the optimal production time t_1^*, the optimal production quantity Q^* and the total production cost per unit time K^* are increasing.
- As deteriorating rate parameter θ decreases, the total production cost per unit time K^* decreases and the optimal production time t_1^* and the optimal production quantity Q^* are increasing.
- As deteriorating parameter η decreases, the total cost per unit time K^* decreases and the optimal production time t_1^* and the optimal production quantity Q^* are increasing.
- As demand rate parameter ϕ_1 decreases, the total production cost per unit time K^* increases and the optimal production time t_1^* and the optimal production quantity Q^* are decreasing.
- Another demand rate parameter ϕ_2 decreases, the total production cost per unit time K^* decreases and the optimal production time t_1^* and the optimal production quantity Q^* are increasing.

Finally, from the numerical illustration we can observe that the parameters are having tremendous influence on the optimal policies of the system.

XI. Conclusions

This paper addresses the derivation of optimal ordering policies of an EPQ model with the assumption that the production process is random and follows a generalized Pareto distribution. Further it is assumed that the lifetime of the commodity is random and follows a Weibull distribution. The generalized Pareto distribution characterizes the production process more close to the reality. The Weibull rate deterioration can include increasing/decreasing/constant rates of deterioration for different values of parameters. The sensitivity analysis of the model reveals that the replenishment distribution parameters have significant influence on the optimal values of the production uptime, production downtime, production quantity and total cost per a unit time. The deterioration distribution parameters also influencing the optimal values of the model. The replenishment and deterioration distributions can be estimated by using historical data. With the distributional data the production and deterioration distributions parameters can be estimated and the analysis of the production process can obtain the optimal production downtime and uptime. This model also includes some of the earlier models as particular cases for specific or limiting values of the parameters. This model can be extended for the cases of changing money value (inflation) and multicommodity production systems which will be taken elsewhere.

Funding

No funding was provided for the research.

Declaration of Conflicting Interests

The Authors declare that there is no conflict of interest.

References

[1] Pentico, D. W. and Drake, M. J, "A survey of deterministic models for the EOQ and EPQ with partial backordering", European Journal of Operational Research, Vol. 214, Issue. 2, pp. 179-198, 2011.

[2] Ruxian, LI., Lan, H. and Mawhinney, R. J, "A review on deteriorating inventory study", Journal of Service Science Management, Vol. 3, No. 1, pp. 117-129, 2010.

[3] Goyal, S. K and Giri, B. C, "Recent trends in modeling of deteriorating inventory", European Journal of operational Research, Vol. 134, No.1, pp. 1-16, 2001.

[4] Raafat, F. "Survey of literature on continuously deteriorating inventory models", Journal of the Operational Research Society, Vol. 42, No. 1, pp. 27-37, 1991.

[5] Nahmias, S, "Perishable inventory theory: A review", OPSEARCH, Vol. 30, No. 4, pp. 680-708, 1982.

[6] Silver, E.A. and Peterson, R., Decision systems for inventory management and production planning, John Wiley & Sons, New-York, 2, pp.1- 6, 1985.

[7] Gupta, R. and Vrat, P., Inventory model for stock dependent consumption rate, OPSEARCH, Vol.23, pp.19-24, 1986.

[8] Panda, S., Senapati, S and Basu, M., A single cycle perishable inventory model with time dependent quadratic ramp-type demand and partial backlogging, International Journal of Operational Research, Vol.5, No.1, pp.110-129, 2009.

[9] Roy, A., Maitai, M, K., Kar, S and Maitai, M., An inventory model for a deteriorating item with displayed stock dependent demand under fuzzy inflation and time discounting over a random planning horizon, Applied Mathematical Modelling, Vol.33, No.2, pp.744-759, 2009.

[10] Uma Maheswara Rao, S. V., Venkata Subbaiah, K. and Srinivasa Rao.K., Production inventory models for deteriorating items with stock dependent demand and Weibull decay, IST Transaction of Mechanical Systems-Theory and Applications, Vol.1, Issue.2, pp. 13-23, 2010.

[11] Yang, C. T., Ouyang, L. Y., Wu, K. S and Yen, H. F., An optimal replenishment policy for deteriorating items with stock-dependent demand and relaxed terminal condition under limited shortage space, Central European Journal of Operational Research, Vol.19, No.1, pp.139.153, 2011.

[12] Srinivasa Rao, K and Essey Kebede Muluneh,, Inventory models for deteriorating items with stock dependent production rate and Weibull decay, International Journal of Mathematical Archive, Vol.3, No.10), pp. 3709-3723, 2012.

[13] Santanu Kumar Ghosh, Jamia Sarkar and Kripasindhu, A Multi items inventory model for deteriorating items in limited storage space with stock dependent demand, American Journal of Mathematical and Management Sciences, Vol.34, No.2, pp.147-161, 2015.

[14] Brojeswar Pal, Shib Shankar Sana and Kripasindhu Chaudhuri, A stochastic production inventory model for deteriorating items with products, finite life-cycle, RAIRO Operations Research, Vol.51, No.3, pp.669-684, 2017.

[15] Srinivasa Rao, K., Nirupama Devi, K. and Sridevi, G, "Inventory model for deteriorating items with Weibull rate of production and demand as function of both selling price and time", Assam Statistical Review, Vol. 24, No.1, pp.57-78, 2010.

[16] Lakshmana Rao, A. and Srinivasa Rao, K, "Studies on inventory model for deteriorating items with Weibull replenishment and generalized Pareto decay having demand as function of on hand inventory", International Journal of Supply and Operations Management, Vol. 1, Issue. 4, pp. 407-426, 2015.

[17] Srinivasa Rao et al, "Inventory model for deteriorating items with Weibull rate of replenishment and selling price dependent demand", International Journal of Operational Research, Vol. 9(3), pp. 329-349, 2017.

[18] Ardak, P.S. and Borade, A.B, "An economic production quantity model with inventory dependent demand and deterioration", International journal of engineering and technology, Vol.9, No.2, pp. 955-962, 2017.

[19] Anindya Mandal, Brojeswar Pal and Kripasindhu Chaudhuri, "Unreliable EPQ model with variable demand under two-tier credit financing", Journal of Industrial and Production Engineering, Vol.37, No. 7, pp. 370–386, 2020.

[20] Sunit Kumar, Sushil Kumar and Rachna Kumari, "An EPQ model with two-level trade credit and multivariate demand incorporating the effect of system improvement and preservation technology", Malaya Journal of Matematik, Vol. 9, No. 1, pp. 438-448, 2021.

[21] Sai Jyothsna Devi.V, Srinivasa Rao.K, EPQ models with mixture of Weibull production Exponential decay and constant demand, Reliability theory and applications, Vol.16, No.4, pp.167-185, 2021

[22] Sridevi, G., Nirupama Devi, K. and Srinivasa Rao, K., Inventory model for deteriorating items with Weibull rate of replenishment and selling price dependent demand, International Journal of Operational Research, Vol.9, No.3, pp.329-349, 2010.

[23] Srinivasa Rao, K., Nirupama Devi, K. and Sridevi, G., Inventory model for deteriorating items with Weibull rate of production and demand as function of both selling price and time, Assam Statistical Review, Vol.24, No.1, pp.57-78, 2010.

SELECTION OF SKIP-LOT SAMPLING PLAN OF TYPE SkSP-T USING SPECIAL TYPE DOUBLE SAMPLING PLAN AS REFERENCE PLAN BASED ON FUZZY LOGIC TECHNIQUES USING R PROGRAMMING LANGUAGE

S. Suganya
•
Assistant Professor, Department of Statistics,
PSG College of Arts & Science,
Coimbatore, Tamil Nadu, India
suganstat@gmail.com

K. Pradeepa Veerakumari
•
Assistant Professor, Department of Statistics,
Bharathiar University,
Coimbatore, Tamil Nadu, India
pradeepaveerakumari@buc.ac.in

Abstract

This paper justify the scheming technique of new system of skip-lot sampling plan of type SkSP-T with Special type Double Sampling plan as Reference plan Using Fuzzy Logic Techniques. The designing methodology includes the evaluation of Acceptable Quality Level, Limiting Quality Level, Operating ratio and the Operating Characteristic (OC) Curves are constructed for using various Fuzzy parametric values. Also draw the Fuzzy OC Band for new proposed plan. FOC band specify the fuzzy probability of acceptance value with corresponding fraction of nonconforming items of this sampling plan.

Keywords: Fuzzy logic, FOC band, incoming and outgoing quality levels, STDSP, SkSP-T.

I. Introduction

Acceptance sampling plan by attributes is a familiar quality control approach for attaining quality stability in procured products. In AS, performance measures, procedures and tables are given for the preference of sampling schemes, sampling systems and sampling plans to analyze the acceptability of manufactured goods. The acceptance sampling plan have been extensively used in industries for sustain the high quality level of the product at the least inspection cost. Acceptance sampling plans specify the judgment (accept or reject) concerning the submitted lots on the system of sample information selected from the lot. Consequently, there is a possibility of rejecting a good lot is known as producer's risk and accepting a bad lot is known as consumer's risk. This new skip-

lot sampling plan is designed to reduce these two (producer's and consumer's) risks. Skip-lot sampling plans have been extensively used in industries to minimize the inspection troubles when products have good quality reports. These systems are identified as economically superior and advantageous to reduce the inspection cost of the terminal lots.

The concept of skip-lot sampling plan of type SkSP-1 was initially introduced by Dodge [8]. Skip-lot sampling plan is a bulk material (or goods, components, products) made within consecutive lots. The SkSP-1 sampling procedure is a scheme that extends only the theoretical approach of the CSP-1 plan, without considering any reference plan concept. Perry [20] introduced the new skip-lot sampling plan, which is designated as SkSP-2. Perry discussed the application of SkSP-2 using the Poisson distribution with markov chain techniques. The SkSP-2 is characterized as an individual with the purpose of applying a present lot inspection plan by the method of attributes, called the Reference Plan. The idea of skip-lot sampling plan of type SkSP-3 was introduced by Soundararajan and Vijayaraghavan [26]. SkSP-3 is based on the concept of Continuous Sampling Pan of type CSP-2 of Dodge and Terry [14]. Its performance measures are derived by using power series approach. Vijayaraghavan [28] developed and extended the concept of SkSP-3 plan, then the operating characteristics functions are obtained by markov chain approach. Skip-lot sampling plan of type SkSP-V was introduced by Balamurali and Chi-Hyuck Jun (2010). In SkSP-V is based on the idea of Continuous Sampling Plan of type CSP-V. Saminathan Balamurali, Muhammad Aslam and Chi-Hyuck Jun [25] introduced new method of skip lot sampling plan of Resampling (SkSP-R) concept.

Lieberman and Solomon [11] introduced some multilevel continuous sampling plan. Derman, Littauer and Solomon [7] developed tightened multi-level continuous sampling plan using basic continuous sampling plans and Lieberman and Solomon [11] concepts. Tightened multilevel plans that include three levels designed by Fordice [10]. Kandasamy and Govindaraju [17] used Markov Chain techniques to find the characteristics function of CSP-T plan. Balamurali and Govindaraju [4] developed a modified tightened two level continuous sampling plan of MMLP-T-2. Balamurali [2] proposed Modified Tightened Three level Continuous sampling plan. Balamurali and Chi-Hyuck Jun [3] proposed a modified CSP-T sampling procedure.

Pradeepa Veerakumari and Suganya [21] introduced the Skip-lot sampling plan of a new type of tightened Skip-lot sampling plan, which is designated as SkSP-T. This new method is found on the approach (both theoretical and derivational) of the continuous sampling plan of type CSP-T, CSP-M, modified tightened three level continuous sampling plans and skip-lot sampling plan of type SkSP-2. Sampling levels are fixed by using CSP-M procedure; sampling fractions are taken from the CSP-T procedure and other concepts are taken by modified CSP-T and SkSP-2 procedures. The main advantage of skip-lot sampling plan of type SkSP-T is that whenever a defect is found in skipping level, there is a normal inspection in that fraction level. In SkSP-T sampling plan, the sampling frequency (f) is minimized by every skipping inspection level. The Operating Characteristic functions for this SkSP-T plan are also derived using the reference plan of the single sampling plan. SkSP-T plan vary among normal inspection and skipping inspection with three levels. Skip-lot sampling plan starts with the normal inspection using various reference plans. In skipping inspection entire lots in the structure of construction are continuing. The number of consecutive conforming lots or batches reaches some pre-specified clearances number i and continue to normal inspection. If i consecutive lots are cleared with normal inspection, using skipping inspection with fraction f, then continue the skipping inspection. If another i consecutive conforming lots are passed under fractional inspection, the fraction (f) is bisected to f/2, and then to f/4 provided no non-conforming is found. If the non-conforming lots are found in skipping inspection, then the system goes to normal inspection. Pradeepa veerakumari and Suganya [22] introduced skip-lot sampling plan of type SkSP-T with DSP as reference plan using Fuzzy techniques. Pradeepa veerakumari and Suganya [23] developed skip-lot sampling plan of type SkSP-T used special type double sampling plan as reference plan. Suganya and Pradeepa veerakumari [24] derived skip-lot sampling plan of type SkSP-T for life test based on the percentiles of Exponentiated Rayleigh Distribution.

Govindaraju [12] introduced the new attribute lot-by-lot sampling plan it is named as Special Type Double Sampling Plan, which is designated as STDSP. In special type double sampling plan in which arrangements are made to apply only small acceptance numbers c=0 and c=1, and to inspect the submitted lot by study a second sample even if the first sample contains zero defective item (or) zero nonconforming item. STDSP is better discriminating power over single sampling plan and using only the smaller acceptance numbers c=0 and c=1. Govindaraju also derived two important operating characteristic functions of STDSP. 1. Probability of acceptance ($P_a(p)$) and 2. Average Sample Number (ASN). STDSP is enforced under the common conditions 1. The manufacturing process must be balanced. 2. The lots assemble from the process are identical as possible. 3. Process fluctuation is not existing. 4. The probability of producing nonconforming units or lots are consistent. 5. Random samples are drawn from homogeneous lots resulted from a stable process.

Lotfi A. Zadeh [18] has introduced Fuzzy set theory. The fuzzy set theory proposed formation of the membership functions; it will operate over the range of real numbers 0 and 1. The approach of fuzzy probability is well defined from that of second order probability, then the probability value which is portrayed by its probability distribution. In recent years fuzzy with statistical theory (Acceptance Sampling plan) and statistical application based problems are derived by many authors, Kanagawa and Ohta [16], Tamaki, Kanagawa and Ohta [27], Hrniewicz [15], Chakraborty [6], Grzegorzewski [13], Buckley [5], Bahram Sadeghpour-Gildeh et.al [1], Ezzatallah Baloui Jamkhaneh et.al [9], Zdenek karpisek, petr stepanek and petr jurak., [29] and Malathi and Muthulakshmi [29].Application of fuzzy theory can be used in Acceptance Sampling, Artificial Intelligent (AI), Computer Science, Decision making theory, Intelligent retrieval, Machine learning, Neural Networks, Operations Research, Pattern Recognition, Robotics. Fuzzy expansion contains superior to an extremely standard and be still forthcoming nowadays.

II. Operating Procedure of STDSP

Considering a lot, select a random sample of n_1 units and the total number of defectives (damaged items) d_1. If d_1 is greater than or equal to 0 ($d1 \geq 0$) then the lot is rejected. If d_1 is equal to 0 ($d_1=0$), then select a second random sample of n_2 units and the number of defectives (damaged items) d_2. If d_2 less than or equal to 1 ($d_2 \leq 1$) then the lot is accepted. Otherwise d_2 is greater than or equal to 2 (if $d_2 \geq 2$), then the lot is rejected.

III. Operating Characteristics Function of STDSP

Govindaraju [12] derived the Special Type Double Sampling plan operating characteristic functions. There is no defective found in the first sample of size n_1 would be $e^{-n_1 p}$. And there exist a one defects or less than one defects found in the second sample of size n_2 would be $e^{-n_2 p} + n_2 p e^{-n_2 p}$. When the sampling plan is accepted there is no defective found in the first sample of size n_1 and one defects or less than one defects found in the second sample of size n_2. The operating characteristics function of STDS plan is given by

$$P_a(p) = e^{-n_1 p}(e^{-n_2 p} + n_2 p e^{-n_2 p})$$
$$P_a(p) = e^{-(n_1+n_2)p} + n_2 p e^{-(n_1+n_2)p}$$

After some substitutions, we get

$$P_a(p) = e^{-np}(1 + \phi np)$$

Where $\phi = n_2/n$ and $n = n_1 + n_2$

Although this plan is valid under general conditions for applications of attribute sampling inspection. This will be especially useful to product characteristics involving costly or destructive testing.

Preliminary facts and definitions

Definition 1: (*fuzzy set*)

Let B be a non void set. A fuzzy set B in Y is characterized by its membership function

$$\mu_B = Y \rightarrow [0,1]$$

Where, $\mu_B(y)$ is explained as the degree of membership of element y in fuzzy set B for each $y \in Y$.

Definition 2: (*normal fuzzy set*)

A fuzzy subset B of a classical set Y is called normal if ∃ any $y \in Y$: B(y) = 1. Otherwise B is subnormal.

Definition 3: (α - *cut*)

An α-level set of a fuzzy set B of Y is a non-fuzzy set denoted by $[B]^\alpha$ and is defined by

$$[B]^\alpha = \begin{cases} \{k \in Y \mid B(k) \geq \alpha\} & , \quad if\ \alpha > 0 \\ cl(suppB) & , \quad if\ \alpha = 0 \end{cases}$$

where *cl (suppB)* denotes the closure of the support of B.

Definition 4: (*fuzzy number*)

A fuzzy number B is a fuzzy set of the real line with a normal, (fuzzy) convex and continuous membership function of bounded support. The family of fuzzy numbers will be denoted by F.

Definition 5: (*triangular fuzzy number*)

A fuzzy set B is called triangular fuzzy number with peak (or center) c, left, width $\alpha > 0$ and right width $\beta > 0$ if its membership function has the following form

$$A(t) = \begin{cases} 1 - \frac{c-k}{\alpha} & , \quad if\ c - \alpha \leq k \leq c \\ 1 - \frac{c-a}{\beta} & , \quad if\ c \leq k \leq c + \beta \\ 0 & otherwise \end{cases}$$

Let A = (c, α, β). It can easily be verified that

$$[B]^\gamma = [c - (1-\gamma)\alpha, c + (1-\gamma)\beta], \forall\ \gamma \in [0,1].$$

The support of B is $(c - \alpha, d + \beta)$.

The triangular fuzzy number with center "a" may be seen as a fuzzy quantity.

Definition 6:

Random variable X having the probability mass function of the Poisson distribution

$P(x, \lambda) = \frac{e^{-\lambda}\lambda^x}{x!}$, for x=0, 1, 2… and Poisson parameter $\lambda > 0$.

λ is exchanged as $\tilde{\lambda}$. The fuzzy number $\tilde{\lambda}$ is greater than zero ($\tilde{\lambda} > 0$), and P (x) is exchanged by $\tilde{P}(x)$. After substituting α-cut for the fuzzy number as

$$\tilde{P}(x)[\alpha] = \{\frac{e^{-\lambda}\lambda^x}{x!} | \lambda \in \lambda[\alpha]\}$$

$\forall\ \alpha \in [0,1]$ Such that $\exists\ \widetilde{P}[\alpha]$. The fuzzy parameter $\tilde{P}(x)[\alpha]$ is substituted by $\tilde{P}[a,b][\alpha]$.

$\tilde{P}[a,b][\alpha] = \left\{\sum_{x=a}^{b} \frac{e^{-\lambda}\lambda^x}{x!} | \lambda \in \lambda[\alpha]\right.$

IV. Operating Procedure for SkSP-T

Operating procedure of the SkSP-T plan is stated as follows:

- Initiate SkSP-T procedure with normal inspection using the special type double sampling plan as reference plan.
- When *i* successive lots are received on normal inspection, terminate the normal inspection and change to skipping inspection.
- On skipping inspection, inspect only a fraction *f* of the lots selected at random, level 1.
- After i consecutive lots in succession has been found without a non-conforming at level 1, the system then switches to skipping inspection with a fraction of *f*/2, level 2.
- After *i* consecutive lots in succession has been found without a non-conforming at level 2, the system then switches to skipping inspection with a fraction of *f*/4, level 3.
- If a non-conforming lot is found on either skipping level, the system reverts to normal inspection.

V. Skip Lot Sampling Plan of Type SkSP-T with Fuzzy Poisson Distribution

The Operating Characteristic function for SkSP-T plan is given as

$$\text{Pa (p)} = \frac{\text{P}^{\text{i}}(\text{f}_2\text{f}_3(1-\text{P}^{\text{i}}) + \text{f}_1\text{f}_3\text{P}^{\text{i}}(1-\text{P}^{\text{i}}) + \text{f}_1\text{f}_2\text{P}^{2\text{i}})}{\text{f}_1\text{f}_2\text{f}_3(1-\text{P}^{\text{i}}) + \text{P}^{\text{i}}(\text{f}_2\text{f}_3(1-\text{P}^{\text{i}}) + \text{f}_1\text{f}_3\text{P}^{\text{i}}(1-\text{P}^{\text{i}}) + \text{f}_1\text{f}_2\text{P}^{2\text{i}})}$$

Where, i-clearance number, f-sampling fraction and P- Special Type Double Sampling Plan as reference plan using fuzzy parameters. From STDSP, n_1 is the first random sample size, n_2 is the second random sample size, d- represented the number of defective in the sample, and p-proportion defective. Considering a lot, select a random sample of n_1 units and the total number of defectives (damaged items) d_1. If d_1 is greater than or equal to 0 ($d1 \geq 0$) then the lot is rejected. If d_1 is equal to 0 ($d_1=0$), then select a second random sample of n_2 units and the number of defectives (damaged items) d_2. If d_2 less than or equal to 1 ($d_2 \leq 1$) then the lot is accepted. Otherwise d_2 is greater than or equal to 2 (if $d_2 \geq 2$), then the lot is rejected. Poisson distribution parameter λ = np. The Probability of acceptance of STDSP is as follows

$$P_a(p) = e^{-n_1 p}(e^{-n_2 p} + n_2 p e^{-n_2 p})$$
$$P_a(p) = e^{-(n_1+n_2)p} + n_2 p e^{-(n_1+n_2)p}$$
$$P_a(p) = e^{-(n_1+n_2)p}(1 + n_2 p)$$

After some substitutions, we get

$$P_a(p) = e^{-np}(1 + \phi np)$$

Where $\phi=n_2/n$ and $n=n_1+n_2$

If the sample size is large then the proportion defective items are not easily calculated. In these situations fuzzy parameters with fuzzy number $\tilde{P}$ is introduced as $\tilde{P} = (a_1, a_2, a_3)$. After Poisson distribution parameters are converted into fuzzy parameters, the poisson parameter λ is modified as $\tilde{\lambda}$ such that $\tilde{\lambda} = n\tilde{p}$. Fuzzy probability with fuzzy number is used in STDSP and the function is modified and as follows

$$\tilde{P}[\alpha] = [P^L[\alpha] P^U[\alpha]]$$
$$P^L[\alpha] = min\{e^{-\lambda}(1 + \phi\lambda) \mid \lambda \in \tilde{\lambda}[\alpha]\}$$
$$P^U[\alpha] = max\{e^{-\lambda}(1 + \phi\lambda) \mid \lambda \in \tilde{\lambda}[\alpha]\}$$

Also the probability of acceptance $P_a(p)$ is defined by fuzzy probability of acceptance $\tilde{P_a}(p)$ and it is given as

$$\tilde{P_a}(p) = \{e^{-\lambda}(1 + \phi\lambda) | \lambda \in \tilde{\lambda} = n\tilde{p}[\alpha]\}$$
$$\tilde{P_a}(p) = [P^L[\alpha] P^U[\alpha]]$$
$$P^L[\alpha] = min\{e^{-\lambda}(1 + \phi\lambda) | \lambda \in \tilde{\lambda} = n\tilde{p}[\alpha]\}$$
$$P^U[\alpha] = max\{e^{-\lambda}(1 + \phi\lambda) | \lambda \in \tilde{\lambda} = n\tilde{p}[\alpha]\}$$

I. R programming

R (programming language) is an open source programming language and software environment for statistical computing and graphical techniques, including linear and nonlinear modeling, classical statistical tests, classification and others. Also R has stronger Object-Oriented Programming facilities than most statistical computing languages. In this paper, R-programming is used to construct the table of Upper and Lower limit of Fuzzy OC Band and draw the Fuzzy Operating characteristic curve and Fuzzy Probability of Acceptance curve.

II. Numerical illustration

The following illustrations derive the new system of skip lot sampling plan of type SkSP-T with Special type Double Sampling Plan as reference plan using Fuzzy Parameters of Fuzzy

Probability of Acceptance, Fuzzy Operating Characteristic (FOC) Curve, Fuzzy Average Sample Number (FASN), Fuzzy Average Outgoing Quality (FAOQ) and Fuzzy Average Total Inspection (FATI). The Fuzzy, SkSP-T and STDSP parameters n_1-the first random sample size, n_2-the second random sample size, i – clearance interval, f- sampling frequency, N- lot size, p - proportion or fraction defective, $P_a(p)$ - Probability of Acceptance and m – fuzzy proportion defective.

III. Example 1: Calculating the Fuzzy Probability of Acceptance

Skip lot sampling plan of type SkSP-T with special type double sampling plan as reference plan using fuzzy parameters. The proportion of defective items is calculated by using fuzzy number $\tilde{p} = [0.0001, 0.005, 0.01]$. Also consider the sample sizes (n1, n2), and fuzzy poisson parameter $(\tilde{\lambda})$ as follows:

n1=30, n2=60 $\tilde{p} = [0, 0.005, 0.01]$

$\tilde{\lambda}_1 = n_1\tilde{p}$, $\tilde{\lambda}_2 = n_2\tilde{p}$. Then the proportion defective $\tilde{p}$ take three values.

Hence $\tilde{\lambda}_1 = [30 * \tilde{p}, 30 * \tilde{p}, 30 * \tilde{p}]$ and $\tilde{\lambda}_2 = [60 * \tilde{p}, 60 * \tilde{p}, 60 * \tilde{p}]$

After using α – cut it becomes

$$\tilde{\lambda}[\alpha] = \tilde{\lambda}_1[\alpha] + \tilde{\lambda}_2[\alpha]$$

$$\tilde{\lambda}[\alpha] = [(a_2 - a_1)\alpha + a_1, a_3 - (a_3 - a_2)\alpha]$$

Hence $$\tilde{\lambda}[\alpha] = [0.441\alpha + 0.009, 0.9 - 0.45\alpha]$$

The probability of acceptance

$$\tilde{P_a}(p) = \{e^{-\lambda}(1 + \phi\lambda) | \lambda \epsilon \tilde{\lambda} = n\tilde{p}[\alpha]\}$$

The probability of acceptance $\tilde{P_a}(p)$ is defined by upper and lower bound values. $\tilde{P_a}(p)$ is calculated by the sustaing formula

$$\tilde{\lambda}[\alpha] = [\, e^{-((a_3-(a_3-a_2)\alpha))}\,(1 + \phi * (a_3 - (a_3 - a_2)\alpha))),$$
$$e^{-((a_2-a_1)\alpha+a_1)}(1 + \phi * ((a_2 - a_1)\alpha + a_1))]$$

Put different values of α in [0, 1]. For $\alpha = 0$,

$$\tilde{P_a}(p) = [0.99, 1]$$

$\tilde{P_a}(p)$ values of acceptance special type double sampling plan with fuzzy parameter using poisson distribution are compared that of STDSP plan using fuzzy parameters. It is concluded that SkSP-T with STDSP as reference plan using fuzzy logic is better than the other. Figure 1 and Table 1 represent the fuzzy probability of acceptance values of skip-lot sampling plan of type SkSP-T with STDSP as reference plan using fuzzy parameters. $\tilde{P_a}(p) = [0.99,1]$, it is expected that for every 100 lots in such a process, 99 to 100 lots will be accepted. For acceptance STDSP with fuzzy poisson process 98 to 100 is accepted. The skip lot sampling plan of type SkSP-T with STDSP fuzzy set gives the better result. Also it minimizes the producer's and consumer's risk.

IV. Example 2: Calculating the Fuzzy Operating Characteristic Curve

The operating characteristic curve is drawn for SkSP-T with STDSP as reference plan using fuzzy parameter. The Operating Characteristics curve represents the Probability of Acceptance (P_a (p)) and proportion defective (p). Operating Characteristics Curve is used in Discriminant of sampling plan among good lots and bad lots. An ideal Operating Characteristics Curve can be attained through 100% inspection. Usually the OC Curve considers certain level of risks. The consumer reject a product that satisfies the established conditions (i.e., the product quality is good). In this risk is called as producer's risk. The consumer accept a product that does not meet the conditions (i.e., the product quality is bad). In this risk is called consumer's risk. For calculating the proportion defective, a fuzzy parameter of the upper and lower band may be used. If the Upper and Lower band values are equal, then it is called as superior state. Consider the fuzzy number $\tilde{p}$ and the proportion defective p to defined

$$\tilde{P_a} = (m, a_2 + m, a_3 + m)$$

Consider, $\tilde{\lambda} = n\tilde{p}$, then

$$n\tilde{p} = (\, nm, na_2 + nm, na_3 + nm)$$

Where, m is the domain of [0, 1-a_3]. Then OC band is calculated as

$$\tilde{p}[\alpha] = [p_1[\alpha], p_2[\alpha]]$$

$$[p_1[\alpha], p_2[\alpha]] = [m + a_2\alpha, a_3 + m - (a_3 - a_2)\alpha]$$

The above fuzzy probability condition is extended to $\tilde{\lambda}[\alpha]$ and$\tilde{P}_a[\alpha]$. For the above example, define a_2 = 0.001, a_3 = 0.002 and α = 0. These values are substituted in the fuzzy poisson upper and lower band equation and find these values are tabulated below. Characteristic curve used for the purpose of Probability of Acceptance depends upon the fraction defective and also conclude the producer risk (α) and consumer risk (β). From Figure 2 it is observed that has proportion defective (p) increases as the Probability value (P_a (p)) decreases. It is concluded that as sample size increase, producer risk is minimized and consumer risk maximized. However, sample size is minimized thus safeguarding the consumer.

Table 1: *Comparison of SkSP-T with Special Type Double Sampling Plan as reference plan using fuzzy parameters with Acceptance single sampling plan with fuzzy parameter with the using of Poisson distribution [fuzzy probability of acceptance table]*

M	$\tilde{p}$	$\tilde{P}_a$ [Acceptance special type double sampling plan with fuzzy parameter with the using of poisson distribution]	$\tilde{P}_a$ [SkSP-T with STDSP as reference plan using Fuzzy parameters]
0	[0,0.01]	[0.8889,0.9851]	[0.9950,1]
0.01	[0.01,0.02]	[0.7683,0.8889]	[0.9823, 0.9950]
0.02	[0.02,0.03]	[0.6505,0.7683]	[0.9513, 0.9823]
0.03	[0.03,0.04]	[0.5421,0.6505]	[0.9028, 0.9513]
0.04	[0.04,0.05]	[0.4462,0.5421]	[0.8345, 0.9028]
0.05	[0.05,0.06]	[0.3636,0.4462]	[0.7483, 0.8345]
0.06	[0.06,0.07]	[0.2938,0.3636]	[0.6504, 0.7483]
0.07	[0.07,0.08]	[0.2358,0.2938]	[0.5497, 0.6504]
0.08	[0.08,0.09]	[0.1860,0.2358]	[0.4540,0.5497]
0.09	[0.09,0.10]	[0.1476,0.1860]	[0.3645,0.4540]
0.10	[0.10,0.11]	[0.1166,0.1476]	[0.2921,0.3645]

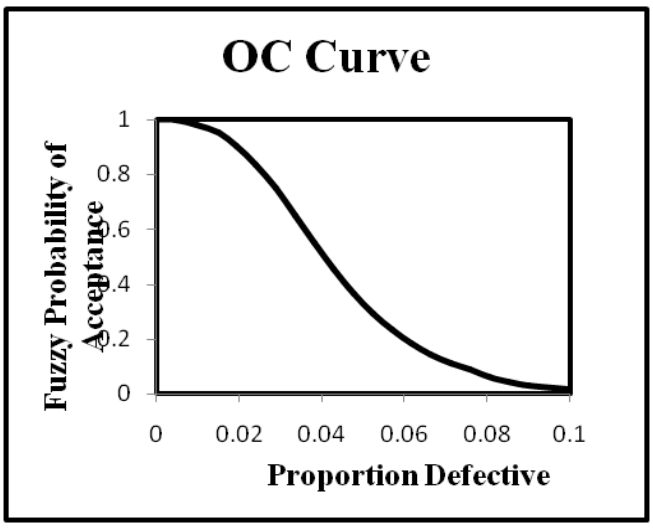

Figure 1: Curve for Probability of Acceptance of SkSP-T with STDSP as reference plan using Fuzzy Parameters

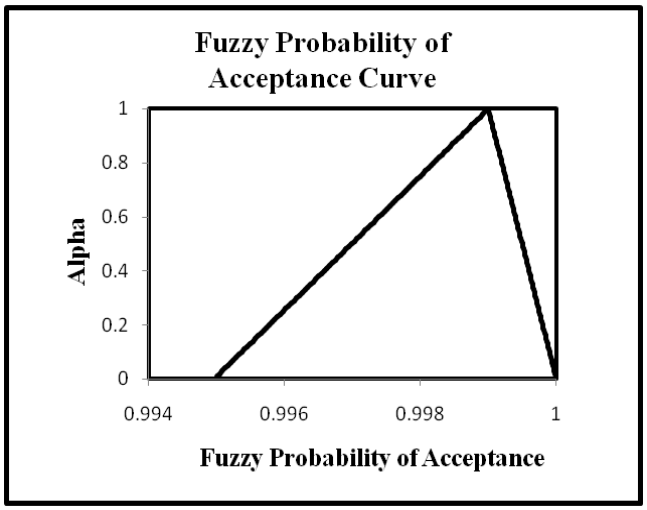

Figure 2: Operating Characteristic Curve for of SkSP-T with STDSP as reference plan using Fuzzy Parameters

VI. CONCLUSION

In this paper, designing for a skip lot sampling plan of type SkSP-T with Special Type Double Sampling Plan as Reference plan using Fuzzy Parameters. In general skip lot sampling plans are reducing the frequency of sampling inspection and overall inspection cost. Comparison of STDSP with Fuzzy Poisson and skip-lot sampling plan of type SkSP-T with STDSP using Fuzzy Parameter, it concludes that SkSP-T with STDSP using Fuzzy logic has a high probability of acceptance and good quality level. From these illustrations it is noted that the sample size is more for an optimum plan (SkSP-T plan), then the producer and consumer risks are reduced while compared with traditional SSP that is a crucial objective for any good sampling plans.

References

[1] Bahram Sadeghpour-Gideh, Gholamhossein Yari and Ezzatallah Baloui Jamkhaneh (2008): Acceptance Double Sampling plan with fuzzy parameter, *Proceedings of the 11th joint conference in information sciences*.

[2] Balamurali, S., (2002). Modified Tightened Three level Continuous sampling plan, *Economic Quality Control*, 17: 221-234.

[3] Balamurali, S., and Chi-Hyuck Jun, (2004). Modified CSP-T sampling procedures for continuous production process, *Quality Technology and Quantitative Management* 1(2):175-188.

[4] Balamurali S. and Govindaraju (2000). Modified Tightened two-level continuous sampling plans, *Journal of Applied Statistics,* 27(4):397-409.

[5] Buckley, J. J. (2003): Fuzzy probability: New approach and application, physica-velage, Heidelberg, Germany.

[6] Chakraborty T.K. (1992): A class of single sampling plan based on fuzzy Optimization, *Opsearch*, 29(1):108-126.

[7] Derman, C., Littauer, S and Solomon, H. (1957). Tightened multi-level continuous sampling Plans, *Annals of Mathematical Statistics*, 28(2):395-404.

[8] Dodge H.F, (1955): Skip-Lot sampling plan, *Industrial Quality Control*, 11(5):3-5.

[9] Ezzatallah Baloui Jamkhaneh et. Al., (2009): Acceptance Single Sampling Plan with fuzzy parameter with the using of Poisson distribution, *International journal of mathematical, computational, physical, electrical and Computer Engineering*, 3(1).

[10] Fordice, J.J. (1972). A Tightened Multi-Level Continuous Sampling Plan CSP-T, Report No.QEM 21230-10, *Ammunition Procurement and Supply Agency*, Joliety, Illinois.
[11] G. J. Lieberman and H. Solomon (1954). Multi-level continuous sampling plans, *Technical Report No. 17, Applied Mathematics and Statistics Laboratory*, Stanford University.
[12] Govindaraju. K (1984): Contributions to the study of certain special purpose plans, *PhD Thesis*, Bharathiar University, Coimbatore.
[13] Grzegorzewski P. (1998): A soft design of acceptance sampling by attributes, Proceedings of the VIth International Workshop on Intelligent statistical quality control. Wurzburg, September 14-16:29-38.
[14] H. F. Dodge and M. N. Torrey (1951). Additional continuous sampling inspection plans, *Industrial Quality Control*, 7 (1951): 7-12.
[15] Hrniewicz. O.,(1994): Statistical acceptance sampling with uncertain information from a sample and fuzzy quality criteria, Working Paper of SRI PAS, Warsaw,(in Polish).
[16] Kanagawa A. And Otha H. (1990): A design for single sampling attribute plan based on Fuzzy Set Theory, *Fuzzy Sets and Fuzzy system*, 37: 173-181.
[17] Kandasamy, C. and Govindaraju, K., (1993). Selection of CSP-T plans, *Communication in Statistics - Simulation and Computation*, 22(1): 265-283.
[18] L.A Zadeh (1965), Fuzzy Sets, *Information and Control*, 8:338-353.
[19] Malathi and Muthulakshmi (2012): Special Double Sampling Plan with Fuzzy Parameter, *Indian Journal of Applied Research*, 2(1).
[20] Perry. R. L, (1973): Skip lot Sampling Plans, *Journal of Quality Technology*, 5 (3):123-130.
[21] Pradeepa Veerakumari. K and Suganya. S (2016). A New System of SkSP-T with Single Sampling Plan as Reference Plan, *Research Journal of Mathematics and Statistics*, 4 (4):1-6.
[22] Pradeepa veerakumari and Suganya (2017): SkSP-T with Double Sampling Plan (DSP) as Reference Plan using Fuzzy Logic Optimization Techniques, *International Journal of Pure and Applied Mathematics*, 117(12):409-418.
[23] Pradeepa veerakumari and Suganya (2019), Characteristic Evaluation of SkSP-T with special type double sampling plan as reference plan, *International Journal of Productivity and Quality Management*, 28(3):360-371.
[24] Suganya and Pradeepa veerakumari (2020), Skip-lot sampling plan of type SkSP-T for life tests based on percentiles of exponentiated Rayleigh distribution, *Life cycle Reliability and Safety Engineering*, 9:247-251.
[25] Saminathan Balamurali, Muhammad Aslam, and Chi-Hyuck Jun (2014). A New System of Skip-Lot Sampling Plans including Resampling, The *Scientific World Journal*, 1-6.
[26] Soundararajan, V and Vijayaraghavan, R (1989): A new system of skip-lot inspection plans of type SkSP-3, *Quality for Process and Development, Wiley Eastern*.
[27] Tamaki f., Kanagawa a. And Ohta h., (1991): A Fuzzy Design of Sampling Inspection plans by Attributes, *Japanese journal of fuzzy theory and systems*, 315-327.
[28] Vijayaraghavan R (2000). Design and evaluation of skip-lot sampling plans of type SkSP-3, *Journal of Applied Statistics*, 27 (7): 901-908.
[29] Zdenek karpisek, petr stepanek and petr jurak.,(2010): Weibull fuzzy probability distribution for reliability of concrete structures, *Engineering MECHANICS*, 17(5/6): 363-372.

Selection of Skip-Lot Sampling Plan of Type SkSP-T Using Special Type Double Sampling Plan as reference Plan Based on Fuzzy Logic Techniques Using R programming Language

R CODING

```
> n1=30;
> n1
> n2=60;
> n2
> n= n1+n2;
> n
> p1=0.001;
> p1
> p2=0.005;
> p2
> p3=0.01;
> p3
> lam1=n1*p1;
> lam 1
> lam2=n1*p2;
> lam2
> lam3=n1*p3;
> lam3
> lam11=n2*p1;
> lam11
> lam12=n2*p2;
> lam12
> lam13=n2*p3;
> lam13
> alpha=seq(0.01,1,length=100);
> alpha
> a1=lam1+lam11
> a2=lam2+lam12
> a3=lam3+lam13
> phi=n2/(n)
> phi
> lambda1(alpha)=exp^(-(a3-((a3-a2)*alpha)));
> lambda1(alpha)
> lambda11(alpha)=1+(phi*((a3-((a3-a2)*alpha))));
> lambda11(alpha)
> value(P1)=lambda1(alpha)*lambda11(alpha);
> value(P1)
> lambda2=exp^(-((a2-a1)*alpha)+alpha);
> lambda2
> lambda22=1+(phi*((a2-a1)*alpha)+a1);
> lambda22
> value(P2)=lambda2*lambda22;
> value(P2)
> i=1
> f1=1/2
> f2=(f1/2)
> f3=(f1/4)
>uppernum=(f2*f3*(1-(value(P1)^i))*(value(P1)^i))+(f1*f3*(value(P1)^i)*(1-(value(P1)^i))*(value(P1)^i))+(f1*f2*(
value(P1)^(3*i)));
> uppernum
> upperden=(((f1*f2*f3*(1-( value(P1)^i)))+uppernum));
> upperden
> upperbound=cbind(uppernum/upperden)
>lowernum=(f2*f3*(1-(value(P2)^i))*(value(P2)^i))+(f1*f3*(value(P2)^i)*(1-(value(P2)^i))*( value(P2)^i))+(f1*f2*(
value(P2)^(3*i)));
```

```
> lowernum
> lowerden=(((f1*f2*f3*(1-( value(P2)^i)))+lowernum));
> lowerden
> lowerbound=cbind(lowernum/lowerden)
> cbind(alpha,ubin,lbin);
> plot(alpha, lowerbound,upperbound)
```

Using the code for combinations of OC Curves

```
plot(p, Pa(p),type = 'l',lty=2,lwd=3,pch=2,lend=0,ljoin=2,lmitre=2,bg="black", lab ="Proportion defective,p",
ylab="Probability of acceptance Pa(p)",main="OC Curve");
lines(p, Pa(p)(changing n value),ity=3,lwd=3,pch=2,bg="black");
lines(p, Pa(p)(changing n value),ity=3,lwd=3,pch=2,bg="black");
```

n1- first sample of size
n2-second sample of size
n-combined sample of size
P1-special type double sampling upper bound value
P2-special type double sampling lower bound value
exp-expectation
phi=ϕ
num=numerator
den=denominator
cbind-column representation

OPTIMAL ECONOMIC AGE REPLACEMENT MODELS FOR NON-REPAIRABLE SYSTEMS WITH SUDDEN BUT NON-CONSTANT FAILURE RATE

Nse Udoh
●
Department of Statistics, University of Uyo, Nigeria
nsesudoh@uniuyo.edu.ng

Iniobong Uko
●
Department of Statistics, University of Uyo, Nigeria
iniobonguko144@gmail.com

Akaninyene Udom
●
Department of Statistics, University of Nigeria, Nsukka, Nigeria
akaninyene.udom@unn.edu.ng

Abstract

Proper maintenance of non-repairable systems is essential for optimum utilization of systems to prevent lost production runs, cost inefficiencies, defective output which leads to customer dissatisfaction and unavailability of the facility for future use. This work proposes new preventive replacement maintenance models with constant-interval preventive replacement time with associated cost of replacement maintenance. Improved results of economic values with respect to optimal replacement time at minimum cost were obtained for radio transmitter system with sudden but non-constant failure rate when compared to some existing models. Other parameters and maintenance probabilities of the system were also obtained including; reliability, hazard rate and availability to ascertain the operational condition of the system.

Keywords: *Birnbaum-Saunders distribution, Radio Transmitter Systems, Reliability, Replacement model, Availability, Optimum replacement time and cost*.

I. Introduction

The failure behaviour in time of a system could be examined by the failure rate of the system. The failure rate is also a function of time, which is also known as the hazard rate. In reliability studies, systems can be classified into two main categories which are repairable and non-repairable system. A repairable system is one which can be restored to satisfactory operation by any maintenance action, including parts replacement or changes to adjustable settings. Examples of such systems are mechanical systems like the generators, grinding machines, welding machines, etc. while a non-repairable system is one in which its component or the entire system is always replaced during any

form of maintenance. Examples of these systems are mainly electronic systems like stabilizers, refrigerators, transmitters and many more. It is characterized by the failure time distribution such as the cumulative distribution function of its time to failure, whereas a repairable system's behavior is described by a stochastic point process, and so must be characterized differently, for example by using the rate of occurrence of failures (ROCOF) or the expected number of failures for a given time period.

According to [1] and [2], maintenance can be defined as "the combination of all technical and associated administrative actions intended to retain an item or system, or restore it to a state in which it can perform its required function." Maintenance does not only improve the cost-efficiency of operating a system but it can also significantly reduce the probability of catastrophic failure of the system, [3]. Therefore, maintenance managers must plan the maintenance actions, so that a balance is achieved between the expected benefits and corresponding expected potential consequences, [4]. On the contrary, poor maintenance of production facilities can result in defective end-product and customer dissatisfaction, lost production runs, cost inefficiencies, and sometimes, unavailability of the facility for future use, [5]. It was further observed by [6] that "facility maintenance is the effort in connection with different technical and administrative action to keep a physical asset, or restore it to a condition where it can perform a require function". Maintenance can be classified according to its type and its degree: corrective maintenance (CM) and preventive maintenance (PM). Corrective maintenance are all maintenance actions performed after a system has failed with the objective of restoring its functionality while preventive maintenance refers to planned maintenance actions performed while the system is operational with the objective of maintaining the system over a desired operational time horizon by preventing or delaying failures. For instance, in an age replacement maintenance policy a unit is replaced at failure (CM) or at PM time, T where T is a constant, [7] and [8]. The principle of age replacement model was applied by [9] in developing a periodic replacement policy for a two-unit system with failure rate interaction between units.

Preventive maintenance policies are perhaps one of the most studied maintenance policies in the literature, [10]. Furthermore, the expected replacement costs per unit time and the age that minimizes this value was used to provide the optimal maintenance interval, [11]. These fixed time frames are established ahead of time and remain in place regardless of when actual failures occur. This means that if a failure occurs just before reaching the fixed time frame, the unit will be replaced both at the failure and immediately again at the time interval. Replacement models of expected cost rates and optimal replacement times were obtained by [12] for a required availability level and were optimized. A theory for non-random preventive replacement (and corrective replacement only for units with exponential failure) and modification of age replacement was established for the situation when the life cycle of the unit is a random variable with probability distribution. The history and development of replacement model from the earliest work to the general replacement model was considered by [13]. They combined age and random replacement models and treated replacement first, replacement last, replacement overtime, replacement overtime first and replacement overtime last. These made up the general replacement models with n replacement times which were obtained by formulating the distributions of replacement times with n variables. The performances of seven optimization models of age replacement policy were evaluated by [14]. The performances were evaluated from perspectives; cost (or availability) and reliability. Furthermore, three performance measures that correspond to cost, reliability and overall performance, respectively, were developed for evaluating the performances of the models. A survey on age replacement model involving minimal repair was conducted by [15] by considering a parallel-series system with two subsystems. Age replacement models (involving minimal repair) that determine the optimal replacement time of the parallel-series system based on two different policies (Policy 1 and Policy 2) were formulated and compared using numerical example.

It is on this premise that this work seeks new perspectives by formulating new preventive replacement models characterized by failure and hazard distribution functions of the system that would provide optimal replacement time and minimum cost of maintenance.

The remainder of this paper shall consider methods in section II on the concept of formulating and optimizing age preventive replacement models and its application to the maintenance of radio transmitter system. Section III deals with numerical analysis based on the failure time distribution and maintenance probabilities of the radio transmitter system. Results would also be discussed in this section. The paper is concluded in section IV.

II. Methods

1 Formulation of Preventive Replacement Model

In developing a replacement model, the decision criterion is defined by $E[c(t)]$, which is the expected cost/cycle time of replacing a part of the system in cycle period (0,t). It was shown in [16] that the expected number of failures occurring in the cycle period (0,t) is equal to the probability of occurrence of failures before time, t, denoted by F(t). The number of failures occurring during the period (0,t) is defined as N(t), which is a discrete random variable. Its probability distribution function is defined as;

$$P[N(t) = n] = G(n); n = 0,1,2, \ldots$$

Its expected value is then equal to;

$$E[N(t)] = \sum_{N(t)=0}^{N(t)=n} N(t) \times G[N(t)]$$

Where $G[N(t)]$ is the failure distribution function of N(t) occurring in the period (0, t). It is assumed that each interval is made as short as the need may be so that the probability of having more than one failure is negligible. In this situation, the probability of having two failures is small compared to having a single failure and so on. That is;

$$P[N(t) = 2] < P[N(t) = 1]$$

and the probability of having three failures is smaller compared to having two failures;

$$P[N(t) = 3] < P[N(t) = 2], \text{ etc.}$$

Therefore,

$$P[N(t) = 1] < P[N(t) = 2] > \cdots$$

In the case of preventive replacement at τ, the expected number of failures in the period (0, τ), denoted by $E[N(\tau)]$can be estimated from the following;

$$G(1) = P[N(t) = 1] \approx F(\tau) and G(0) = P[N(t) = 0 \approx 1 - F(\tau)]$$

Then,

$$E[N(\tau)] = \sum_{n=0}^{\infty} n \times G(n) = 0 \times [1 - F(\tau)] + 1 \times F(\tau)$$

$$E[N(\tau)] = F(\tau) \quad (1)$$

Therefore, $E[N(\tau)]$ is equal to the probability of occurrence of a failure before time, τ and F(τ) is the cumulative failure function. Let C_{fr} be the total cost of failure replacement, C_{pr} be the total cost of preventive replacement maintenance and τ is the replacement time. The total expected cost per cycle for preventive replacement maintenance at replacement time, τ is defined as;

$$E[N(\tau)] = \frac{total\ expected\ cost}{replacement\ time} = \frac{C_{pr} + C_{fr}\{N(\tau)]}{\tau} \quad (2)$$

Therefore;

$$E[C(\tau)] = \frac{C_{pr} + C_{fr}F(\tau)]}{\tau} \quad (3)$$

Also, [17] stated that the mean number of failures occurring during the cycle (0,τ] is equal to the cumulative hazard rate at time, τ using the concept of non-homogeneous Poisson process. Hence, the expected cost per unit time for preventive replacement maintenance is given by;

$$E[C(\tau)] = \frac{C_{pr}+C_{fr}H(\tau)]}{\tau} \quad (4)$$

Where H(τ) is the cumulative hazard function. The objective is to determine the time necessary for preventive replacement maintenance in order to minimize the total expected replacement cost per unit time.

2 The propose age replacement models

Let C_r be the replacement maintenance costs for each failed unit (RM), let C_p be the preventive maintenance cost for each non-failed unit, where $C_p < C_r$. Also, let $N_1(t)$ denote the number of failures in the interval (0, t] and $N_2(t)$ denote the number of non-failed units that are preventively maintained in the interval (0, t]. Therefore, the expected cost during (0, t] is expressed as:

$$\hat{C}(T) = C_r E\{N_1(t)\} + C_p E\{N_2(t)\}$$

Based on the renewal reward theorem, [18], the expected cost per unit time (expected cost rate) for an infinite time span is;

$$\hat{C}(T) \equiv \lim_{T\to\infty} \frac{\hat{C}(T)}{t} = \frac{Expected\ cost\ of\ one\ cycle}{mean\ time\ of\ one\ cycle}$$

Let **T**, $(0 < T \leq \infty)$ be the time for a planned replacement of a component with failure time, τ; the expected cost on a cycle as obtained in [19] is expressed as;

$$C_r P(\tau \leq T) + C_p P(\tau > T) = C_r F(T) + C_p F^{/}(T)$$

where $$F^{/}(T) = 1 - F(T)$$

The mean time of a cycle is denoted by τ, where a cycle refers to the interval from the start of the system to the completion of repair maintenance action or replacement maintenance. Hence, our propose expected cost function is given in (5). An optimal policy can be found by obtaining the value of τ that minimizes this cost function.

$$\hat{C}(T) = \frac{C_r F(T)+C_p F^{/}(T)}{\tau} \quad (5)$$

Similarly, if we also assume that the mean number of failures occurring during the cycle (0, τ] is equal to the cumulative hazard rate at time, τ using the concept of non-homogeneous Poisson process as in [17]; the expected cost per unit time for preventive replacement maintenance is given by;

$$\hat{C}(T) = \frac{C_r F(T)+C_p H^{/}(T)}{\tau} \quad (6)$$

2.1 Minimization of the expected cost functions:

Taking the partial derive of (2) with respect to τ yields;

$$\tau^* = \frac{\frac{C_{pr}}{C_{fr}}+E[N(\tau)]}{\frac{d}{d\tau}E[N(\tau)]} \quad (7)$$

To obtain τ^* for the models in (3) and (4), we respectively have;

$$E[N(\tau)] = \frac{d}{d\tau}E[N(\tau)] = \frac{d}{d\tau}F(\tau) = f(t)$$

$$\tau^* = \frac{\frac{C_{pr}}{C_{fr}}+F(\tau)}{f(t)} \quad (8)$$

and

$$E[N(\tau)] = H(t);\ \frac{d}{d\tau}E[N(\tau)] = \frac{d}{d\tau}H(\tau) = h(t)$$

$$\therefore \tau^* = \frac{\frac{c_{pr}}{c_{fr}} + H(\tau)}{h(t)} \quad (9)$$

Similarly, we also obtain τ^* respectively from (5) and (6), as;

$$\tau^* = \frac{F(\tau)}{f(t)} + \frac{c_p}{(c_r - c_p) f(T)} \quad (9)$$

$$\tau^* = \frac{H(\tau)}{h(t)} + \frac{c_p}{(c_r - c_p) h(T)} \quad (10)$$

3. Limiting Availability of a System

Availability is the probability that a system will work as required during a particular period of time.

Let A(τ*) denote the availability of a system at optimal time, τ^*

E[Up] is the expected uptime at optimal time, τ^*

E[Down] is the expected downtime at optimal time, τ^*

D_{pr} is the average downtime for preventive replacement

D_{fr} is the average downtime for failure replacement

R(τ*) is the reliability at optimal time, τ^*

F(τ*) is the cumulative failure at optimal time, τ^*

According to [17];

$$E[Up] = \int_0^\infty t f(t) dt + \tau^* R(\tau^*)$$

where

$$\int_0^\infty t f(t) dt = \tau^* f(\tau^*) - 0 \times f(0) = \tau^* \times f(\tau^*)$$

$$E[Down] = D_{pr} F(\tau^*) + D_{fr} R(\tau^*)$$

where

$$D_{fr} = \frac{\sum_{i=1}^{n} D_i}{n} \text{ and } D_{pr} = \frac{\sum_{j=1}^{m} D_i}{m}$$

$$A(\tau^*) = \frac{E(UP)}{E(Up) + E(Down)} = \frac{\tau^* f(\tau^*) + \tau^* R(\tau^*)}{\tau^* f(\tau^*) + \tau^* R(\tau^*) + \left(D_{pr} F(\tau^*) + D_{fr} R(\tau^*)\right)} \quad (12)$$

4. Application of Replacement models to the maintenance of radio transmitter system

4.1 The Birnbaum-Saunders (Fatigue Life) Failure Distribution

The Birnbaum Sanders (BS) distribution has appeared in several different contexts, with varying derivations. It was given by Fletcher in 1911, and was formally obtained by [20]. However, it was the derivation by [21] that brought the usefulness of this distribution into a clear focus. Authors in [22] introduced a two-parameter lifetime distribution to model fatigue life of a metal, subject to cyclic stress by making a monotone transformation on the standard normal random variable. Consequently, the distribution is also sometimes referred to as the fatigue-life distribution. Since then, extensive work has been done on this model providing different interpretations, constructions, generalizations, inferential methods, and extensions to bivariate and multivariate cases, [23]. Its application is sought in this work as the best fit probability model to provide parameters estimates and optimal probabilities for inter-failure times of electronic systems with radio transmitter system as a case study. These estimates would be used to obtain optimal replacement policies in existing age preventive replacement maintenance models as well as our propose class of models.

The radio transmitter is a complex electronic device which major components are integrated circuits, diodes and fuses which are replaced after each failure. Hence, it is a non-repairable system. It fails suddenly but at a non-constant rate. The inter-failure times of the transmitter

system was modeled as the Birnbaum-Saunders distribution having a chi-square best fit of rank 1 using Easyfit (5.6) software.

4.1.1 Failure and Cumulative Failure Distributions of the Two-Parameter Birnbaum-Saunders distribution

Consider a material that continually undergoes cycles of stress loads. During each cycle, a dominant crack grows towards a critical length that will cause failure. Under repeated application of **n** cycles of loads, the total extension of the dominant crack can be written as; $W_n = \sum_{j=1}^{n} Y_j$. Let Q be an integer-valued non-negative random variable denoting the smallest number of cycles at which W_n exceeds a critical value ω, which the failure of the material occurs. Clearly, $P(Q \leq n) = P(W_n \geq \omega)$ and this implies that;

$$P(Q \leq n) = 1 - P\left(\sum_{j=1}^{n} Y_j \leq \omega\right) \quad (13)$$

Since Y_j's are assumed to have mean, μ and variance, σ^2, thus the Y_j's can be standardized to give

$$P(Q \leq n) = 1 - P\left(\frac{\sum_{j=1}^{n}(Y_j - \mu)}{\sigma\sqrt{n}} \leq \frac{\omega - n\mu}{\sigma\sqrt{n}}\right)$$

Another assumption is that the Y_j's are independent. Also if **n** is large (a criterion easy to satisfy in fatigue studies), the central limit theorem applies. Hence, by the symmetry of the normal distribution,

$$P(Q \leq n) = 1 - \emptyset\left(\frac{\omega - n\mu}{\sigma\sqrt{n}}\right) = \emptyset\left(\frac{n\mu}{\sigma\sqrt{n}} - \frac{\omega}{\sigma\sqrt{n}}\right); \text{ where } = \emptyset(X) = \int_{-\infty}^{x} \frac{e^{\frac{x^2}{2}}}{\sqrt{2\pi}} ds$$

The above derivation, which involved a non-negative integer-valued random variable Q, can be extended to continuous variables. Let **T**, a continuous non-negative random variable denote the time to failure of the material with a distribution function, F(t). If **T** is viewed as the continuous analog of Q, and **t** as a continuous analog of **n**, then,

$$F(t) = P(T \leq t) = P(Q \leq n) = \emptyset\left(\frac{\mu\sqrt{n}}{\sigma} - \frac{\omega}{\sigma\sqrt{n}}\right) \quad (14)$$

Replacing **n** by **t**, we have;

$$F(t) = \emptyset\left(\emptyset\left(\frac{\mu\sqrt{t}}{\sigma} - \frac{\omega}{\sigma\sqrt{t}}\right)\right)$$

Let

$$\alpha = \frac{\sigma}{\sqrt{\mu\omega}} \; and \; \beta = \frac{\omega}{\mu}$$

Then

$$F(t;\alpha,\beta) = \emptyset\left(\frac{1}{\alpha}\left[\sqrt{\frac{t}{\beta}} - \sqrt{\frac{\beta}{t}}\right]\right) \quad (15)$$

Equation (15) is the two parameter Birnbaum-Saunders failure cumulative distribution function with shape parameter α and scale parameter β. It follows that;

$$Z = \frac{1}{\alpha}\left[\sqrt{\frac{T}{\beta}} - \sqrt{\frac{\beta}{T}}\right] \quad (16)$$

Then, Eq (16) is distributed with mean 0 and variance 1 and that the probability density function of T is;

$$f(t;\alpha,\beta) = \frac{1}{2\sqrt{2\pi\alpha\beta}}\left[\left(\frac{t}{\beta}\right)^{\frac{1}{2}} + \left(\frac{\beta}{t}\right)^{\frac{3}{2}}\right] exp\left[-\frac{1}{2\alpha^2}\left(\frac{t}{\beta} + \frac{\beta}{t} - 2\right)\right]; t > 0; \alpha, \beta > 0 \quad (17)$$

4.1.2 The Mean and Variance of the two-parameter Birnbaum-Saunders Distribution using Monotone Transformation

The mean and variance of **T** can be found in the usual manner by integration. For ease of computation, however, the following alternative approach is adopted. Let a random variable **X** be normally distributed with mean 0 and variance $\alpha^2/4$. It follows that 2X is also normally distributed with mean 0, and variance α. Moreover, since **Z** has a unit normal distribution, αZ is distributed normally with mean 0 and variance α^2. Thus,

$$Z = \frac{2X}{\alpha} \Rightarrow \alpha Z = 2X$$

Hence, from Eq (16);

$$2X = \left(\sqrt{\frac{T}{\beta}} - \sqrt{\frac{\beta}{T}}\right) \tag{18}$$

Squaring both sides we have;

$$4X^2 = \left(\frac{T}{\beta} + \frac{\beta}{T} - 2\right) \times \beta T$$

$$T^2 + \beta^2 - 2T(\beta + 2\beta X^2) = 0 \tag{19}$$

The positive roots yield;

$$T = \beta\left(1 + 2X^2 + 2X(1 + X^2)^{\frac{1}{2}}\right) \tag{20}$$

where **T** is the Birnbaum-Saunders random variable.

The mean of T

$$E[T] = E\left[\beta\left(1 + 2X^2 + 2X(1 + X^2)^{\frac{1}{2}}\right)\right]$$

$$E[T] = \beta\left[E[1] + 2E[X^2] + 2[X]E(1 + X^2)^{\frac{1}{2}}\right] \tag{21}$$

But **X** follows a normal distribution with mean, $\mu = 0$ and variance, $\sigma = {\alpha^2}/{4}$; then we have that;

$$E[X^2] = var(X) = \frac{\alpha^2}{4} \tag{22}$$

$$\therefore E[T] = \beta\left(1 + \frac{2\alpha^2}{4}\right) \tag{23}$$

Variance of T

$$Var(T) = var\left(\beta\left(1 + 2X^2 + 2X(1 + X^2)^{\frac{1}{2}}\right)\right) = \beta^2\left[var(1) + var(2X^2) + var\left(2X(1 + X^2)^{\frac{1}{2}}\right)\right]$$

$$= \beta^2\left(var(1) + 4var(X^2) + 4var\left(X(1 + X^2)^{\frac{1}{2}}\right)\right) \tag{24}$$

From the non-central moment of a normal distribution, we have that;

$$E(X^4) = \mu + 6\mu^2\sigma^2 + 3\sigma^4$$

But

$$\mu = 0, \sigma^2 = \frac{\alpha^2}{4}$$

Then,

$$E(X^4) = \frac{3\alpha^2}{16};\ E(X^2) = var(X) = \frac{\alpha^2}{4}$$

$$\therefore\ var(X^2) = \frac{3\alpha^2}{16} - \left(\frac{\alpha^2}{4}\right)^2 = \frac{2\alpha^4}{16} \tag{25}$$

Let

$$Y = X(1 + X^2)^{\frac{1}{2}}$$

$$Var\left(X(1+X^2)^{\frac{1}{2}}\right) = E\left(\left(X(1+X^2)^{\frac{1}{2}}\right)^2\right) - \left(E\left(X(1+X^2)^{\frac{1}{2}}\right)\right)^2$$

$$E\left(X^2(1+X^2)\right) = E(X^2+X^4) = E(X^2) + E(X^4)$$

$$Var\left(X(1+X^2)^{\frac{1}{2}}\right) = \frac{\alpha^2}{4} + \frac{3\alpha^2}{16} \quad (26)$$

Substitute (25) and (26) into (24), we have;

$$Var(T) = \beta^2\alpha^2\left(1 + \frac{5\alpha^2}{4}\right) \quad (27)$$

4.1.3 Modified moment estimation for the two-parameter Birnbaum-Saunders Distribution

For the usual moment estimators in a two-parameter case, the first and second population moments are equated with the corresponding sample moments. In the case of modified moment estimation (MME), the expectation of the random variable is equated to the sample arithmetic mean and the expectation of the inverse of the random variable is equated to the sample harmonic mean. Let $\{t_1, t_2, t_3 \ldots\}$ be a random sample of size **n** from the Birnbaum–Saunders distribution with the probability density function as given in Eq (17). The sample arithmetic and harmonic means are defined by;

$$S = \frac{\sum_{i=1}^{n} t_i}{n} \quad (28)$$

$$r = \left(\frac{\sum_{i=1}^{n} t_i^{-1}}{n}\right)^{-1} \quad (29)$$

Therefore by MME;

$$S = E(T) \text{ and } r = E(T^{-1})$$

If **T** has a Birnbaum–Saunders distribution with parameters α and β, then T^{-1} also has a Birnbaum–Saunders distribution with the corresponding parameters α and β^{-1} respectively, [21]. Therefore, we readily have;

$$E(T^{-1}) = \beta^{-1}\left(1 + \frac{\alpha^2}{2}\right)$$

$$Var(T^{-1}) = \alpha^2\beta^{-2}\left(1 + \frac{5\alpha^2}{4}\right)$$

Hence;

$$S = \beta\left(1 + \frac{\alpha^2}{2}\right) \quad (30)$$

$$r^{-1} = \beta^{-1}\left(1 + \frac{\alpha^2}{2}\right) \quad (31)$$

$$\frac{S}{r^{-1}} = \frac{\beta\left(1 + \frac{\alpha^2}{2}\right)}{\beta^{-1}\left(1 + \frac{\alpha^2}{2}\right)} = \beta^2$$

$$\therefore \hat{\beta} = \sqrt{Sr} \quad (32)$$

By substituting (28) and (29) in (32), we obtain;

$$\hat{\beta} = \sqrt{\left(\frac{\sum_{i=1}^{n} t_i}{n}\right)\left(\left(\frac{\sum_{i=1}^{n} t_i^{-1}}{n}\right)^{-1}\right)} \quad (33)$$

Substituting (31) into (29), we have;

$$S = \sqrt{Sr}\left(1 + \frac{\alpha^2}{2}\right)$$

$$\hat{\alpha} = \left\{2\left(\frac{S}{\sqrt{Sr}} - 1\right)\right\}^{\frac{1}{2}} = \left\{2\left(\frac{S}{\hat{\beta}} - 1\right)\right\} \quad (34)$$

4.1.4 Reliability Function of Birnbaum- Saunders Distribution

Let R(t) be the reliability function of the Birnbaum – Saunders distribution given as;

$$R(t) = 1 - F(t) = P(T > t); t > 0$$
$$= 1 - \int_0^t f(u)du = \int_t^\infty f(u)du$$

Hence, R(t) is the probability that the item does not fail in the time interval (0,t], or, in other words, the probability that the item survives the time interval (0, t] and is still functioning at time t.
For the two parameter Birnbaum-Saunders distribution, we have;

$$R(t) = 1 - F(t; \alpha, \beta)$$

Recall Eq (15):

$$F(t; \alpha, \beta) = \emptyset\left\{\frac{1}{\alpha}\left(\sqrt{\frac{t}{\beta}} - \sqrt{\frac{\beta}{t}}\right)\right\}$$
$$R(t) = 1 - \emptyset\left\{\frac{1}{\alpha}\left(\sqrt{\frac{t}{\beta}} - \sqrt{\frac{\beta}{t}}\right)\right\}$$

Because of the symmetry of the normal distribution, we have that;

$$R(t) = \emptyset\left\{\frac{1}{\alpha}\left(\sqrt{\frac{\beta}{t}} - \sqrt{\frac{t}{\beta}}\right)\right\} \quad (35)$$

4.1.5 Determination of Hazard Function, h(t)

The probability that an item will fail in the interval $(t, t + \Delta t)$ when we know that the item is functioning at time, **t** is;

$$P(t < T \leq t + \Delta t/T > t) = \frac{P(t < T \leq t + \Delta t)}{P(T > t)} = \frac{F(t + \Delta t) - F(t)}{R(t)}$$

By dividing this probability by the length of the time interval, $\boldsymbol{\Delta t}$, and letting $\boldsymbol{\Delta t \to 0}$, we get the failure rate function, h(t) of the item as;

$$h(t) = \lim_{\Delta t \to 0} \frac{P(t < T \leq t + \Delta t/T > t)}{\Delta t} = \lim_{\Delta t \to 0} \frac{F(t + \Delta t) - F(t)}{\Delta t} \times \frac{1}{R(t)} = \frac{f(t)}{R(t)}$$
$$\therefore R(t) = \frac{f(t)}{R(t)} \quad (36)$$

Note: According to [24], the density of Birnbaum-Saunders failure distribution can be written in a different form as;

$$f(t) = \frac{\left(\sqrt{\frac{t}{\beta}} - \sqrt{\frac{\beta}{t}}\right)}{2\alpha t} \times \emptyset\left\{\frac{1}{\alpha}\left(\sqrt{\frac{t}{\beta}} - \sqrt{\frac{\beta}{t}}\right)\right\}$$
$$Z = \frac{1}{\alpha}\left(\sqrt{\frac{t}{\beta}} - \sqrt{\frac{\beta}{t}}\right)$$

$$\emptyset(Z) = \frac{exp\left(-\frac{Z^2}{2}\right)}{\sqrt{2\pi}}$$

Therefore,

$$R(t) = \emptyset(-Z)$$

and

$$h(t) = \frac{\left(\sqrt{\frac{t}{\beta}} \sqrt{\frac{\beta}{t}}\right)}{2\alpha t} \times \left(\frac{\emptyset(Z)}{\emptyset(-Z)}\right) \quad (37)$$

4.1.6 The Cumulative Hazard function of Birnbaum-Saunders distribution

By definition;

$$f(t) = \frac{d}{dt}F(t) = \frac{d}{dt}\big(1 - R(t)\big) = -R(t)$$

Then

$$h(t) = \frac{R^{/}(t)}{R(t)} = -\frac{d}{dt}lnR(t)$$

Recall

$$\int h(t)\,dt = -lnR(t) = H(t)$$

$$H(t) = -lnR(t) \tag{38}$$

III. Results

I. Estimation of the Birnbaum-Saunders Parameter of the Radio Transmitter System

The modified moment estimators as given in (33) and (34) were used to obtained estimated shape parameter, $\hat{\alpha} = 0.95701$ and scale parameter, $\hat{\beta} = 557.37$ for the inter-failure times of the radio transmitter which follows a two-parameter Birnbaum-Saunders distribution. Easyfit version 5.6 was used for the goodness-of fit test as well as the estimation of parameters.

II. Replacement models and probability functions of radio transmitter systems at respective optimum times

Optimal probability functions in Eqs (15) and (17), availability factor in Eq (12) and expected cost per cycle in Eqs (3) - (6) were obtained in Table 1 at the respective optimum values of the four replacement models under consideration.

Table 1: Optimal probabilities, availability and expected cost functions for replacement models

Probability function	Cumulative Failure-Based Replacement model **A** $\tau^* = 143$	Cumulative Hazard-Based Replacement model **B** $\tau^* = 137$	Proposed Replacement model **C** based on cumulative failures, $\tau^* = 153$	Proposed Replacement model **D** based on cumulative hazard, $\tau^* = 149$
$f(\tau^*)$	0.00115	0.001081	0.001376	0.001145
$F(\tau^*)$	0.06256	0.0560	0.093197	0.069341
$h(\tau^*)$	0.0012	0.0015	0.0015174	0.001231
$R(\tau^*)$	0.93744	0.94407	0.906803	0.930659
$A(\tau^*)$	0.9829	0.98	0.9597	0.95903
$E\left[C\left(\tau^*\right)\right]$	388	392	208	166

IV. Discussion

I. Estimated parameters of the Birnbaum-Saunders distribution

The estimates $\hat{\alpha} = 0.95701$ and $\hat{\beta} = 557.37$ are the respective shape and scale parameters of the Birnbaum-Saunders distribution. The shape of the failure density function and the hazard function are governed by α. Also, the failure density function is unimodal for all values of α. The scale parameter is also known as the median of the distribution. As α increases the hazard rate and the failure density function of the distribution becomes more skewed to the right.

II. Choice of Optimal Replacement Models

The propose replacement maintenance models by the authors yield improved results and are therefore considered the preferred economic optimal model for maintenance policy of the system due to the following reasons;

i. Improved optimal operational time estimate before replacement: The cumulative failure function-based replacement model **A** from [16] in column (2) of Table 1 yields an optimal replacement time of 143 hours versus our propose optimal replacement time of 153 hours based on model **C** with same parameters in column 4. Also, the cumulative hazard function-based replacement model **B** by [17] in column 3 of Table 1 shows that the radio transmitter system has an optimal replacement time of 137 hours versus our propose optimal replacement time of 149 hours from model **D** based on the parameters of the same kind in column 5.
ii. Improved expected minimum cost value for replacement maintenance: The cumulative failure function-based replacement model **A** from [16] in column (2) of Table 1 yields an expected minimum cost value of 388naira versus our propose expected minimum cost value of 208 naira from model **C** based on the same parameters. Also, the cumulative hazard function-based replacement model **B** by [17] in column 3 of Table 1 shows that the radio transmitter system has an expected minimum cost value of 396 naira versus our propose expected minimum cost value of 166 in model **D** based on the same parameters.
iii. Comparative chance of failure occurrence: The cumulative failure based function replacement model **A** from [16] in column (2) of Table 1 yields a 0.12% chance of failure occurrence versus a 0.15% chance of failure occurrence obtained from our propose model **C** of same kind. But, the cumulative hazard function-based replacement model **B** by [17] in column 3 of Table 1 yields a 0.15% chance of failure occurrence versus a lesser percentage of 0.12% chance of failure occurrence obtained from our propose model **D** of the same kind.

The results obtained in this study show that the failure distribution of Radio transmitter system used as a case study follows the Birnbaum-Sanders distribution with best fit parameters: $\hat{\alpha} = 0.95701$ and $\hat{\beta} = 557.37$. Hence, the Birnbaum-Sanders failure distribution is recommended as a good probability model which characterized the failure distribution of transmitter and similar systems. It is also clear from the results that the propose class of replacement maintenance models gives improved results than earlier models by [16] and [17]. Specifically, our second propose cumulative hazard function-based model yields the most economic cost (166 naira) at optimal time $\tau^* = 149$ with competing availability and reliability values and a smaller chance of failure occurrence before replacement maintenance. It is remarkable that the propose models are better in terms of optimal replacement time and minimum expected cost, with comparable variations in the probability of occurrence of failure in the cumulative failure function-based model and an improved result from our cumulative hazard-based replacement models. These provide good reasons for the choice of our propose hazard function-based model as the preferred model in particular and the propose class of models in general for the study.

Consequently, our propose preventive replacement maintenance models are the optimal economic models with respect to time and cost as vital economic factors in formulating replacement maintenance policies for the radio transmitter and similar systems.

References

[1] Jardine, A. K. S and Buzacott, J. A. (1985). Equipment reliability and maintenance. *European Journal of Operational Research*, 19: 285-296.

[2] Dekker, R. (1996). Applications of maintenance optimization models: a review and analysis. *Reliability Engineering and System Safety*, 51: 229-240.

[3] Marais, K. B. and Saleh J. H. (2009). Beyond its cost, the value of maintenance; an analytical framework for capturing its net present value, *Reliability Engineering and System Safety*, 94: 644-657.

[4] Zio, E. Maintainability: A key to Effective and Maintenance Management. John Wiley and Sons, 2009.

[5] Lavy S, Garcia J. A. and Dixit M. K. (2010). Establishment of KPIs for facilities performance measurement: Review of literature. *Facilities*, 28(9/10): 440-464.

[6] Bagshaw K.B., George T. P. (2015). Facility management and organizational effectiveness of manufacturing firms in Rivers State Nigeria. *European Journal of Business Management*, 7(26): 67-89.

[7] Wang, H. and Pham, H. Reliability and Optimal Maintenance. Springer, 2006

[8] Tam, A. S. B, Chan, W. M. and Price, J. W. H. (2007). Optimal maintenance intervals for a multi-component system. *Production planning and control*, 17 (8): 769-779.

[9] Lai, MT. and Chen, Y. C. (2006). Optimal periodic replacement policy for a two-unit system with failure rate interaction. *International Journal of Advance Manufacturing Technology,* 29**:** 367–371.

[10] Das, A. N. and Sarmah, S. P. (2010). Preventive replacement models: An overview and their application in process industries, *European Journal of Industrial Engineering*, 4(3): 280-307.

[11] Jiang, R. Introduction to Quality and Reliability Engineering. Springer Berlin Heidelberg, 2015.

[12] Zhao, X., Al-Khalifa, K. N., Hamouda, A. and Nakagawa, T. (2017). *Reliability Engineering & System Safety*, 161: 95-105.

[13] Nakagawa, T., Chen, M. and Zhao, X. (2018). Note on history of age replacement policies. *International Journal of Mathematical, Engineering and Management Sciences*, 3(2):151-166.

[14] Jiang, R. (2018). Performance evaluation of seven optimization models of age replacement policy," *Reliability Engineering and System Safety*, Elsevier, 180(C): 302-311.

[15] Waziri, T. A. and Yusuf, I. (2020). On age replacement policy of a system involving minimal repair. *Reliability: Theory & Applications*, *15*(4): 54-62.

[16] Bahrami-G, K., Price, J.W.H. and Mathew J. (2000). The constant - interval replacement Model for preventive maintenance: A new perspective. *International Journal of Quality and Reliability Management*, 17(8): 822-838.

[17] Cassady, C. R., Pohl, E. A. and Murdock, W. P. (2003). Selective maintenance modeling for industrial systems, *Journal of Quality in Maintenance Engineering*, 7(2): 104-117.

[18] Ross, S. M. Introduction to Probability Models. Academic Press, 1970.

[19] Udoh, N., Effanga E. and Onwukwe, C. (2020) Complementary optimal age maintenance (COAM) policy for repairable systems. *International Journal of Reliability and Safety*, 14:1–13.

[20] Konstantinowsky, D. (1914). Elektrische Ladungen und Brown'sche Bewegung Sehr Kleiner Metallteilchen in Gasen. *Sitzungsberichte der Kaiserlichen Akademie der Wissenschaften*, 123: 1697- 1752.

[21] Birnbaum, Z. W., Saunders, S. C. (1969a). A new family of life distribution. *Journal of Applied Probability*, 6: 319-327.

[22] Birnbaum, Z. W., Saunders, S. C. (1969b). Estimation for a family of life distributions with applications to fatigue, *Journal of Applied Probability*, 6: 328.

[23] Bhattacharyya, G. K., Fries, A. (1982). Fatigue failure models - Birnbaum-Saunders versus inverse Gaussian. *IEEE Transactions on Reliability*, 31:439-440.

[24] Balakrishnan, N., Saulo, H., Bourguignon, M., Zhu, X. (2017). On moment-type estimators for a class of log-symmetric distributions. *Computational Statistics*, 32: 1339-1355.

Funding: This research received no specific grant from any funding agency in the public, commercial, or not-for-profit sectors.

Declaration of conflict of interest: The Authors declare that there is no conflict of interest.

ANALYSIS OF A TWO-STATE PARALLEL SERVERS RETRIAL QUEUEING MODEL WITH BATCH DEPARTURES

[1]Neelam Singla, [2*]Sonia Kalra

•

[1]Associate Professor, Department of Statistics
Punjabi University Patiala, Punjab (147002)
neelgagan2k3@yahoo.co.in

[2]Assistant Professor, University School of Business
Chandigarh University, Gharuan, Mohali (Punjab) 140413
soniakalra276@gmail.com

Abstract

This paper deals with the transient state behavior of an M/M/1 retrial queueing model contains two parallel servers with departures occur in batches. At the arrival epoch, if all servers are busy then customers join the retrial group. Whereas, if the customers find any of one server is free then they join the free server and start its service immediately. Here, we assume that primary customers arrive according to Poisson process. The retrial customers also follow the same fashion. Service time follows an exponential distribution. Explicit time dependent probabilities of exact number of arrivals and exact number of departures when both servers are free or when one server is busy or when both servers are busy are obtained by solving the difference differential equation recursively. Some important verification and conversion of two-state model into single state are also discussed. Some of the existing results in the form of special cases have been deduced.

Keywords: Retrial, Queueing, Arrivals, Departures, Batch

1. Introduction

In recent years, computer networks and data communication systems are the fastest growing technologies, which have led to significant development in applications such as advance in internet, audio data traffic, video data traffic, etc. Recently there have been significant contributions to retrial queueing system in which arriving customer who finds the server busy upon arrival is require leaving the service area and repeating his demand after some time. Between trials, a blocked customer who remains in a retrial group is said to be in orbit. Retrial queue have applications in telephone switching systems, telecommunication networks and computers are competing to gain service from a central processing unit. Moreover, retrial queues are also used as mathematical models of several computer systems: packet switching networks, shared bus local area networks operating under the carrier-sense multiple access protocol and collision avoidance star local area networks etc. There are enough of literatures available on retrial queues. We referred some of the work like Artalejo and Corral [1], Falin and Templeton [2] and Artalejo [3] etc.

In many queueing systems it is assumed that customers arrive singly at a service facility and depart singly from the service facility. However, this assumption is violated in many other real word situations. Letters arriving at a post office, ships arriving at a port in convoy, people going to a theatre and so on are some examples of queuing in which customers do not arrive and depart singly but in bulk or groups. The size of an arriving group and departing group may be a random variable or a fixed number. Mathematically as well as practically the cases where the size of an arriving group and departing group is a random variable, are more common, and also more difficult to handle.

One can note that the batch arrival queue may not always be given the name 'batch' but instead of this many authors chose to use the term 'bulk'. Predominantly, this reflects two leading strands of applications, where 'bulk' often gives a connotation of transportation settings whereas 'batch' frequently implies applications in communications.

Queueing situations in which arrivals occur singly, but service is in bulk are considered in this research. Bulk service queues have potential applications in many areas e.g. in loading and unloading of cargoes at a seaport, in traffic signal systems, in computer networks where jobs are processed in batches, manufacturing/ production systems, cinema halls, in transportation processes involving buses, airplanes, trains, ships, elevators etc. Bailey [4] introduced the concept of bulk service and the same was later studied by a number of parishioners. Juan [5] obtained a numerical method for the single server bulk service queueing system with variable capacity. Janssen and Leeuwaarden [6] presented an analytic rather than a numerical framework for dealing with discrete time bulk service queue. Goswami et al. [7] analysed a discrete time single server infinite buffer bulk service queues. In this research, the inter-arrival time of successive arrivals and service times of batches are assumed to be independent and geometrically distributed. Al-khedhairi and Tadj [8] investigated the queueing process of a bulk service queueing system under Bernoulli schedule.

The classical transient results for the M/M/1, M/M/c and M/G/1 queue provide little insight into the behavior of a queueing system through a fixed operation time t. The function $P_n(t)$ gives the distribution for the number in the system at time t, but practically provides no information on how the system has regulated up until time t. The question seems to be answered by Pegden and Rosenshine [9]. The analysis of their paper based on M/M/1 queueing model in which the state of the system is given by (i, j), where i is the number of arrivals and j is the number of departures until time t. Kalra and Singla [10] investigated the performance analysis of a two-state retrial queueing model with batch departures. In this paper, they obtained time dependent probabilities of exact number of arrivals in the system and exact number of departures from the system when only one server is free or busy. Garg and Kumar [11] studied a single server retrial queue with impatient customers and obtained time-dependent probabilities of number of exact arrivals and number of exact departures from the orbit.

This research studies a time dependent retrial queueing model by obtaining the explicit probabilities of the exact number of arrivals in the system and the exact number of departures from the system by a given time t wherein the departures occur from the orbit in batches of variable size.

The rest of this paper is organized as follows: Section 2 gives a relatively formal description of the queueing model. In Section 3, we defined the two-dimensional state model and derived the difference-differential equations. The time dependent solution for the model is obtained in section 4. Section 5 presents the some useful performance measures of the system and Section 6 discussed some special cases. The last section ends with a suitable conclusion.

2. Model Description

2.1. Assumption and Notation

The two parallel servers retrial queueing system is considered wherein departures take place in batches of variable size whenever these occur from the orbit. The primary calls follow a Poisson distribution with rate λ. If the server is busy at the arrival time, then the arriving call joins the orbit, whereas if the server is free then the service of arriving call gets started. The behavior of customers in orbit is same as in the main model, i.e. every customer in orbit produces a Poisson flow of repeated calls with rate θ. If a batch of repeated calls finds the server free, it is served and leaves the system after service otherwise, if the server is occupied at that time then the system state does not change. Arrivals occur one by one and departures occur from the orbit in batches of variable size with rate μ. The input flow of primary calls, intervals between repeated trials and service times are mutually independent. For distribution of arrivals, service times and retrials, we make use of the following assumptions and notations:

1) The repeated calls for each server follow a Poisson distribution with parameter θ.
2) In this model the departures occur from the orbit is treated as bulk departures whose capacity is determined afresh before each service which is equal to newly determined capacity of the server or units present in the orbit, whichever is less. In this case capacity of the server is a random variable. The size of the batch is determined at beginning of the each service. The probability that the server can serve a batch of γ units is b_γ so that $\sum_{\gamma=1}^{K} b_\gamma = 1$, where K is the maximum capacity of the server.
3) The Service times for each call depart in batches of variable size and follow an exponential distribution with parameter μ.

Laplace transformation $\bar{f}(s)$ of $f(t)$ is given by

$\bar{f}(s) = \int_0^\infty e^{-st} f(t)\,\mathrm{dt}$, Re (s) > 0

The Laplace inverse of

$\frac{Q(p)}{P(p)}$ is $\sum_{k=1}^{n}\sum_{l=1}^{m_k} \frac{t^{m_k-l} e^{a_k t}}{(m_k-l)!(l-1)!} \times \frac{d^{l-1} Q(p)}{dp^{l-1} P(p)}$ $(p-a_k)^{m_k}$ $\forall$ p= a_k, $a_i \neq a_k$ for i ≠ k.

where,

$P(p) = (p-a_1)^{m_1} (p-a_2)^{m_2} \ldots\ldots\ldots (p-a_n)^{m_n}$

$Q(p)$ is a polynomial of degree < m_1+m_2+m_3 +……m_n-1.

If $L^{-1}\{p(s)\} = P(t)$ and $L^{-1}\{q(s)\} = Q(t)$, then

$L^{-1}\{p(s)\ q(s)\} = \int_0^t P(\mathrm{u}) Q(\mathrm{t}-\mathrm{u})\mathrm{du} = P * Q$, where $P * Q$ is the convolution of P and Q.

3. The Two-Dimensional State Model

3.1. Definitions

$P_{i,j,0}(t)$= Probability that there are exactly i arrivals in the system and j departures from the system by time t when server is idle.
$P_{i,j,k}(t)$= Probability that there are exactly i arrivals in the system and j departures from the system by time t when k servers are busy. $k = 1,2$.
$P_{i,j}(t)$= Probability that there are exactly i arrivals in the system and j departures from the system

by time t.

$$P_{i,j}(t) = P_{i,j,0}(t) + P_{i,j,1}(t) \qquad \forall i, j; \quad i \geq j.$$

Also

$$P_{i,j,1}(t) = 0, i \leq \text{j};\ P_{i,j,0}(t) = 0, i < j.$$

Initially

$$P_{0,0,0}(0) = 1;\ P_{i,j,0}(0) = 0\ \&\ P_{i,j,k}(0) = 0;\ \ \forall i, j \neq 0.\ k = 1,2.$$

3.2. The difference – differential equations governing the system are

$$\frac{d}{dt}P_{i,i,0}(t) = -\lambda\, P_{i,i,0}(t) + \mu \sum_{\gamma=1}^{K}\Big(\sum_{l=\gamma}^{K} b_l\Big) P_{i,i-\gamma,1}(t) \qquad i \geq 0,\ i \geq \text{K} \tag{1}$$

$$\frac{d}{dt}P_{i,j,0}(t) = -(\lambda + (i-j)\theta)P_{i,j,0}(t) + \mu \sum_{\gamma=1}^{K} b_\gamma\, P_{i,j-\gamma,1}(t) \qquad i > j, i > 0;\ j \geq \text{K} \tag{2}$$

$$\frac{d}{dt}P_{1,0,1}(t) = -(\lambda + \mu)P_{1,0,1}(t) + \lambda P_{0,0,0}(t) \tag{3}$$

$$\frac{d}{dt}P_{2,0,2}(t) = -(\lambda + \mu)P_{2,0,2}(t) + \lambda P_{1,0,1}(t) \tag{4}$$

$$\frac{d}{dt}P_{i,j,1}(t) = -(\lambda + \mu + (i-j-1)\theta)P_{i,j,1}(t) + \lambda P_{i-1,j,0}(t) + (i-j)\theta P_{i,j,0}(t) + 2\mu P_{i,j-1,2}(t) \qquad i > 1, i > \text{j} \geq 0 \tag{5}$$

$$\frac{d}{dt}P_{i,j,2}(t) = -(\lambda + 2\mu)P_{i,j,2}(t) + \lambda P_{i-1,j,1}(t) + \lambda\big(1 - \delta_{i-2,j}\big)P_{i-1,j,2}(t) + (i-j-1)\theta P_{i,j,1}(t) \qquad i > 2, i > \text{j} \geq 0 \tag{6}$$

where $\delta_{i-2,j} = \begin{cases} 1, & when\ i-2 = j \\ 0, & otherwise \end{cases}$

Using the Laplace transformation $\bar{f}$ (s) of $f(t)$which is given by

$\bar{f}$ (s) = $\int_0^\infty e^{-st} f(t)$ dt, Re (s) > 0

in the equations (1) - (6) along with the initial conditions, the following equations are obtained:

$$\left.\begin{aligned}(s+\lambda)\bar{P}_{0,0,0}(s) &= P_{0,0,0}(0) \\ (s+\lambda)\bar{P}_{i,i,0}(s) &= \mu \sum_{\gamma=1}^{K}\Big(\sum_{l=\gamma}^{K} b_l\Big)\bar{P}_{i,i-\gamma,1}(s)\end{aligned}\right\} \qquad i > 0,\ i \geq \text{K} \tag{7}$$

$$(s+\lambda+(i-j)\theta)\bar{P}_{i,j,0}(s) = \mu \sum_{\gamma=1}^{K} b_\gamma\, \bar{P}_{i,j-\gamma,1}(s) \qquad i > j, i > 0,\ j \geq \text{K} \tag{8}$$

$$(s+\lambda+\mu)\bar{P}_{1,0,1}(s) = \lambda\, \bar{P}_{0,0,0}(s) \tag{9}$$

$$(s+\lambda+\mu)\bar{P}_{2,0,2}(s) = \lambda\, \bar{P}_{1,0,1}(s) \tag{10}$$

$$(s+\lambda+\mu+(i-j-1)\theta)\bar{P}_{i,j,1}(s) = \lambda\, \bar{P}_{i-1,j,0}(s) + (i-j)\theta\bar{P}_{i,j,0}(s) + 2\mu\bar{P}_{i,j,-1,2}(s) \qquad i > 1, i > j \geq 0 \tag{11}$$

$$(s+\lambda+2\mu)\bar{P}_{i,j,2}(s) = \lambda\, \bar{P}_{i-1,j,1}(s) + \lambda\,\big(1 - \delta_{i-1,j}\big)\bar{P}_{i-1,j,2}(s) + (i-j-1)\theta\bar{P}_{i,j,1}(s) \qquad i > 2, i > j \geq 0 \tag{12}$$

3.3. Solution of the Problem

Solving equations (7) to (12) recursively, the following results are obtained

$$\bar{P}_{0,0,0}(s) = \frac{1}{s+\lambda} \tag{13}$$

$$\bar{P}_{1,1,0}(s) = \frac{\lambda\mu}{(s+\lambda)^2\,(s+\lambda+\mu)} \tag{14}$$

$$\bar{P}_{i,i,0}(s) = \frac{1}{s+\lambda}\mu \sum_{\gamma=1}^{K}\Big(\sum_{l=\gamma}^{K} b_l\Big)\bar{P}_{i,i-\gamma,1}(s) \qquad i > 1 \tag{15}$$

$$\bar{P}_{i,2,0}(s) = \frac{\mu}{(s+\lambda+\mu+(i-2)\theta)}\left[b_1\bar{P}_{i,1,1}(s) + b_2\bar{P}_{i,0,1}(s)\right] \qquad i > 2 \qquad (16)$$

$$\bar{P}_{1,0,1}(s) = \left(\frac{1}{s+\lambda}\right)\left(\frac{\lambda}{s+\lambda+\mu}\right) \qquad (17)$$

$$\bar{P}_{2,1,1}(s) = \frac{\lambda}{(s+\lambda+\mu)}\bar{P}_{1,1,0}(s) + 2\mu\frac{\lambda}{(s+\lambda+2\mu)(s+\lambda+\mu)}\bar{P}_{1,0,1} \qquad (18)$$

$$\bar{P}_{i,1,1}(s) = \frac{2\mu}{(s+\lambda+\mu+(i-2)\theta)}\frac{\lambda^{i-1}}{(s+\lambda+2\mu)^{i-1}}\bar{P}_{1,0,1}(s) \qquad i > 2 \qquad (19)$$

$$\bar{P}_{i,i-1,1}(s) = \frac{\lambda}{(s+\lambda+\mu)}\bar{P}_{i-1,i-1,0}(s) + \frac{\theta}{(s+\lambda+\mu)}\bar{P}_{i,i-1,0}(s) + \frac{2\mu}{(s+\lambda+\mu)}\bar{P}_{i,i-2,2}(s)$$

$$i > 2 \qquad (20)$$

$$\bar{P}_{i,0,2}(s) = \frac{\lambda^{i-1}}{(s+\lambda+2\mu)^{i-1}}\bar{P}_{1,0,1}(s) \qquad i > 1 \qquad (21)$$

$$\bar{P}_{i,j,2}(s) = \left(\sum_{k=1}^{i-j}\left(\frac{\lambda}{s+\lambda+2\mu}\right)^{i-j-k}\eta_k'(s)\bar{P}_{j+k,j,1}(s)\right) \qquad i \geq j+2, j \geq 1 \qquad (22)$$

$$\text{where } \eta_k'(s) = \begin{cases} 1 & for\ k = 1 \\ \left(1 + \frac{(k-1)\theta}{s+\lambda+2\mu}\right) & for\ k = 2\ to\ i-j-1 \\ \frac{(k-1)\theta}{s+\lambda+2\mu} & for\ k = i-j \end{cases}$$

$$\bar{P}_{i,j,1}(s) = \frac{\lambda}{(s+\lambda+\mu+(i-j-1)\theta)}\bar{P}_{i-1,j,0}(s) + \frac{(i-j)\theta}{(s+\lambda+\mu+(i-j-1)\theta)}\bar{P}_{i,j,0}(s)$$
$$\frac{2\mu}{(s+\lambda+\mu+(i-j-1)\theta)}\left(\sum_{k=0}^{i-j}\left(\frac{\lambda}{s+\lambda+2\mu}\right)^{i-j-k}\eta_k'(s)\bar{P}_{j+k,j-1,1}(s)\right)$$

$$i \geq j+2, j \geq 2 \qquad (23)$$

$$where\ \eta_k'(s) = \begin{cases} 1 & for\ k = 0 \\ \left(1 + \frac{k\theta}{s+\lambda+2\mu}\right) & for\ k = 1\ to\ i-j-1 \\ \frac{k\theta}{s+\lambda+2\mu} & for\ k = i-j \end{cases}$$

$$\bar{P}_{i,j,0}(s) = \frac{1}{(s+\lambda+(i-j)\theta)}\left(\mu\sum_{\gamma=1}^{K} b_\gamma\right)\bar{P}_{i,j-\gamma,1}(s) \qquad i > j \geq 3 \qquad (24)$$

Using the Inverse Laplace transformation

$\frac{Q(p)}{P(p)}$ is $\sum_{k=1}^{n}\sum_{l=1}^{m_k}\frac{t^{m_k-l}e^{a_k t}}{(m_k-l)!(l-1)!}\times\frac{d^{l-1}}{dp^{l-1}}\left(\frac{Q(p)}{P(p)}\right)(p-a_k)^{m_k} \quad \forall\ p = a_k,\ a_i \neq a_k$ for $i \neq k$.

where

$P(p) = (p-a_1)^{m_1}(p-a_2)^{m_2}\ldots\ldots\ldots(p-a_n)^{m_n}$

$Q(p)$ is a polynomial of degree $< m_1+m_2+m_3+\ldots\ldots\ldots\ldots m_n - 1$.

If $L^{-1}\{f(s)\} = F(t)$ and $L^{-1}\{g(s)\} = G(t)$, then

$L^{-1}\{f(s)\ g(s)\} = \int_0^t F(u)G(t-u)du = F * G$, F * G is called the convolution of F and G.

and

The Laplace inverse of $\bar{N}^{a,b,c}_{n_1,n_2,n_3}(s) = \frac{1}{(s+a)^{n_1}(s+b)^{n_2}(s+c)^{n_3}}$ is

$$N^{a,b,c}_{n_1,n_2,n_3}(t) = \sum_{l=1}^{n_3}\sum_{m=1}^{l}\frac{e^{-at}\, t^{n_3-l}(-1)^{m+1}\binom{l-1}{m-1}\left(\prod_{g_1=0}^{l-m-1}(n_1+g_1)\right)\left(\prod_{g_2=0}^{m-2}(n_2+g_2)\right)}{(n_3-l)!(m-1)!\,(b-a)^{n_2+m-1}(c-a)^{n_1+l-m}}$$

$$+\sum_{l=1}^{n_2}\sum_{m=1}^{l}\frac{e^{-bt}\, t^{n_2-l}(-1)^{m+1}\binom{l-1}{m-1}\left(\prod_{g_1=0}^{l-m-1}(n_1+g_1)\right)\left(\prod_{g_2=0}^{m-2}(n_3+g_2)\right)}{(n_2-l)!\,(m-1)!\;(a-b)^{n_3+m-1}(c-b)^{n_1+l-m}}$$

$$+\sum_{l=1}^{n_1}\sum_{m=1}^{l}\frac{e^{-ct}\, t^{n_1-l}(-1)^{m+1}\binom{l-1}{m-1}\left(\prod_{g_1=0}^{l-m-1}(n_2+g_1)\right)\left(\prod_{g_2=0}^{m-2}(n_3+g_2)\right)}{(n_1-l)!\,(m-1)!\;(a-c)^{n_3+m-1}(b-c)^{n_2+l-m}}$$

in equations (13) to (24), the following probabilities are

$$P_{0,0,0}(t) = e^{-\lambda t} \tag{25}$$

$$P_{1,1,0}(t) = \lambda\mu(te^{-\lambda t})e^{-(\lambda+\mu)t} \tag{26}$$

$$P_{i,i,0}(t) = \left\{\mu\sum_{\gamma=1}^{K}\left(\sum_{l=\gamma}^{K} b_l\right)e^{-\lambda t}\right\} * P_{1,i-\gamma,1}(t) \qquad i > 1 \tag{27}$$

$$P_{i,2,0}(t) = \mu b_1 e^{-(\lambda+\mu+(i-2)\theta)t} * P_{i,1,1}(t) + \mu b_2 e^{-(\lambda+\mu+(i-2)\theta)t} * P_{i,0,1}(t) \qquad i > 2 \tag{28}$$

$$P_{1,0,1}(t) = \lambda e^{-\lambda t}\left(\frac{1}{\mu} - \frac{e^{-\mu t}}{\mu}\right) \tag{29}$$

$$P_{2,1,1}(t) = \lambda e^{-(\lambda+\mu)t} * P_{1,1,0}(t) + 2\lambda\mu e^{-(\lambda+\mu)t}\left(\frac{1}{2\mu} - \frac{e^{-2\mu t}}{2\mu}\right) * P_{1,0,1}(t) \tag{30}$$

$$P_{i,1,1}(t) = \left[2\mu\lambda^{i-1}e^{-(\lambda+\mu+(i-2)\theta)t}\left\{\frac{1}{(2\mu)^{i-1}} - e^{-2\mu t}\sum_{r=0}^{i-2}\frac{(t)^r}{r!}\frac{1}{(2\mu)^{i-r}}\right\}\right] * P_{1,0,1}(t)$$

$$i > 2 \tag{31}$$

$$P_{i,i-1,1}(t) = \lambda e^{-(\lambda+\mu)t} * P_{i-1,i-1,0}(t) + \theta e^{-(\lambda+\mu)t} * P_{i,i-1,0}(t) + 2\mu e^{-(\lambda+\mu)t} * P_{i,i-2,2}(t) \qquad i > 2 \tag{32}$$

$$P_{i,0,2}(t) = \left(\lambda^{i-1}\frac{t^{i-2}}{(i-2)!}e^{-(\lambda+2\mu)t}\right) * P_{1,0,1}(t) \qquad i > 1 \tag{33}$$

$$P_{i,j,2}(t) = \left(\lambda^{i-j-1}\frac{t^{i-j-2}}{(i-j-2)!}e^{-(\lambda+2\mu)t}\right) * P_{j+1,j,1}(t) +$$

$$\sum_{k=2}^{i-j-1}\left(\lambda^{i-j-k}\frac{t^{i-j-k-1}}{(i-j-k-1)!}e^{-(\lambda+2\mu)t}\right) * P_{j+k,j,1}(t) + \sum_{k=2}^{i-j-1}\left(\lambda^{i-j-k}(\mathrm{k}-1)\theta\frac{t^{i-j-k}}{(i-j-k)!}e^{-(\lambda+2\mu)t}\right) *$$

$$P_{j+k,j,1}(t) + \left((\mathrm{i}-\mathrm{j}-1)\theta e^{-(\lambda+2\mu)t}\right) * P_{i,j,1}(t) \qquad i \geq j+2, j \geq 1 \tag{34}$$

$$P_{i,j,1}(t) = \lambda e^{-(\lambda+\mu+(i-j-1)\theta)t} * P_{i-1,j,0}(t) + (i-j)\theta e^{-(\lambda+\mu+(i-j-1)\theta)t} * P_{i,j,0}(t) +$$

$$2\mu\lambda^{i-j}e^{-(\lambda+\mu+(i-j-1)\theta)t}\left\{\frac{1}{(2\mu)^{i-j}} - e^{-2\mu t}\sum_{r=1}^{i-j-1}\frac{(t)^r}{r!}\frac{1}{(2\mu)^{i-j-r}}\right\} * P_{j,j-1,1}(t) +$$

$$2\mu e^{-(\lambda+\mu+(i-j-1)\theta)t}\sum_{k=1}^{i-j-1}\lambda^{i-j-k}\left\{\frac{1}{(2\mu)^{i-j-k}} - e^{-2\mu t}\sum_{r=0}^{i-j-k-1}\frac{(t)^r}{r!}\frac{1}{(2\mu)^{i-j-k-r}}\right\} * P_{j+k,j-1,1}(t) +$$

$$2\mu e^{-(\lambda+\mu+(i-j-1)\theta)t}\sum_{k=1}^{i-j-1}\lambda^{i-j-k}(\mathrm{k}\theta)\left\{\frac{1}{(2\mu)^{i-j-k+1}} - e^{-2\mu t}\sum_{r=0}^{i-j-k}\frac{(t)^r}{r!}\frac{1}{(2\mu)^{i-j-k+1-r}}\right\} *$$

$$P_{j+k,j-1,1}(t) + 2\mu(i-j)\theta e^{-(\lambda+\mu+(i-j-1)\theta)t}\left(\frac{1}{2\mu} - \frac{e^{-2\mu t}}{2\mu}\right) * P_{i,j-1,1}(t)^{\circledast}$$

$$i \geq j+2, j \geq 2 \quad (35)$$

$$P_{i,j,0}(t) = \left(\mu \sum_{\gamma=1}^{K} b_\gamma e^{-(\lambda+\mu+(i-j)\theta)t}\right) * P_{i,j-\gamma,1}(t) \qquad i > j \geq 3 \quad (36)$$

4. Measures of Effectiveness

4.1. The Laplace transform of the probability $P_{i.}(t)$ that exactly i units arrive by time t is :

$$\bar{P}_{i.}(s) = \sum_{j=0}^{i} \bar{P}_{i,j}(s) = \frac{\lambda^i}{(s+\lambda)^{i+1}} \text{ ;i > 0} \quad (37)$$

And its Inverse Laplace transform is

$$P_{i.}(t) = \frac{e^{-\lambda t}(\lambda t)^i}{i!} \quad (38)$$

The basic assumption on primary arrivals is that it forms a Poisson process and above analysis of abstract solution also verifies the same.

4.2. The probability that exactly j customers have been served by time t. $P_{.j}(t)$ in terms of $P_{i,j}(t)$ is given by:

$$P_{.j}(t) = \sum_{i=j}^{\infty} P_{i,j}(t)$$

4.3. From the abstract solution of our model, we verified that the sum of all possible probabilities is one i.e. taking summation over i and j on equations (15)-(31) and adding, we get

$$\sum_{i=0}^{\infty} \sum_{j=0}^{i} \left\{\bar{P}_{i,j,0}(s) + \bar{P}_{i,j,1}(s) + \bar{P}_{i,j,2}(s)\right\} = \frac{1}{s}$$

Taking inverse Laplace transformation, we get

$$\sum_{i=0}^{\infty} \sum_{j=0}^{i} \left\{P_{i,j,0}(t) + P_{i,j,1}(t) + +P_{i,j,2}(t)\right\} = 1,$$

which is a verification of our results.

4.4. Converting two-state model into single state model:

To convert two-dimensional state model into a single state model probability $Q_{n,k}(t)$ is defined as under:

$Q_{n,k}(t)$ = Probability that there are n customers in the orbit at time t and the servers are free or busy according as $k = 0,1,2$.

The probability of exactly n customers in the system at time t in terms of $P_{i,j,0}(t)$ and $P_{i,j,k}(t)$:

When the server is free, it is defined by probability $Q_{n,0}(t)$

$$Q_{n,0}(t) = \sum_{j=0}^{\infty} P_{j+n,j,0}(t)$$

In this case, the number of customers in the orbit is equal to n which is obtained by using:

n = (number of arrivals – number of departures)

When k servers are busy, it is defined by probability $Q_{n,k}(t)$

$$Q_{n,k}(t) = \sum_{j=0}^{\infty} P_{j+n+k,j,k}(t) \qquad (k = 1,2)$$

where k defines the number of servers.

In this case, the number of customers in the orbit is equal to n which is obtained by using:

n = (number of arrivals – number of departures – k)

Using the above definitions from the equations (1) to (6) the set of equations in statistical equilibrium are:

$$\lambda Q_{0,0} = \mu\left[\sum_{\gamma=1}^{K}\left(\sum_{l=\gamma}^{K} b_l\right)\right]Q_{\gamma,1} \quad (39)$$

$$(\lambda + n\theta)Q_{n,0} = \mu\left(\sum_{l=\gamma}^{K} b_l\right)Q_{n+\gamma,1} \qquad n > 0 \quad (40)$$

$$(\lambda + n\theta + \mu)Q_{n,1} = \lambda Q_{n,} + (n+1)\theta Q_{n+1,0} + 2\mu Q_{n,2,0} \qquad n \geq 0 \quad (41)$$

$$(\lambda + 2\mu)Q_{n,2} = \lambda Q_{n,1} + (n+1)\theta Q_{n+1,1} + \lambda Q_{n-1,2} \qquad n \geq 0 \quad (42)$$

4.5. Special Case:

1. When the units are served singly and considering$K = 1,\ b_1 = 1,\ b_2 = b_3 = b_4 = \cdots = b_K = 0$ in equations (25) to (36), then the probabilities coincide with the results of Singla and Kalra [12].

$$P_{0,0,0}(t) = e^{-\lambda t} \quad (43)$$

$$P_{1,1,0}(t) = \lambda\mu(te^{-\lambda t})e^{-(\lambda+\mu)t} \quad (44)$$

$$P_{i,i,0}(t) = \lambda\mu e^{-\lambda t}\left(\frac{1}{\mu} - \frac{e^{-\mu t}}{\mu}\right) * P_{i-1,i-1,0}(t) + \mu\theta e^{-\lambda t}\left(\frac{1}{\mu} - \frac{e^{-\mu t}}{\mu}\right) * P_{i,i-1,0}(t) + 2\mu^2 e^{-\lambda t}\left(\frac{1}{\mu} - \frac{e^{-\mu t}}{\mu}\right) * P_{i,i-2,2}(t) \qquad i > 1 \quad (45)$$

$$P_{i,2,0}(t) = 2\mu^2 e^{-(\lambda+(i-2)\theta)t}\left(\frac{1}{(\mu+(i-2)\theta)} - \frac{e^{-(\mu+(i-2)\theta)t}}{(\mu+(i-2)\theta)}\right) * P_{i,0,2}(t) \qquad i \geq 3 \quad (46)$$

$$P_{1,0,1}(t) = \lambda e^{-\lambda t}\left(\frac{1}{\mu} - \frac{e^{-\mu t}}{\mu}\right) \quad (47)$$

$$P_{2,1,1}(t) = \lambda e^{-(\lambda+\mu)t} * P_{1,1,0}(t) + 2\lambda\mu e^{-(\lambda+\mu)t}\left(\frac{1}{2\mu} - \frac{e^{-2\mu t}}{2\mu}\right) * P_{1,0,1}(t) \quad (48)$$

$$P_{i,1,1}(t) = \left[2\mu\lambda^{i-1}e^{-(\lambda+\mu+(i-2)\theta)t}\left\{\frac{1}{(2\mu)^{i-1}} - e^{-2\mu t}\sum_{r=0}^{i-2}\frac{(t)^r}{r!}\frac{1}{(2\mu)^{i-r}}\right\}\right] * P_{1,0,1}(t) \qquad i > 2 \quad (49)$$

$$P_{i,i-1,1}(t) = \lambda e^{-(\lambda+\mu)t} * P_{i-1,i-1,0}(t) + \theta e^{-(\lambda+\mu)t} * P_{i,i-1,0}(t) + 2\mu e^{-(\lambda+\mu)t} * P_{i,i-2,2}(t) \qquad i > 2 \quad (50)$$

$$P_{i,0,2}(t) = \left(\lambda^{i-1}\frac{t^{i-2}}{(i-2)!}e^{-(\lambda+2\mu)t}\right) * P_{1,0,1}(t) \qquad i > 1 \quad (51)$$

$$P_{i,j,2}(t) = \left(\lambda^{i-j-1}\frac{t^{i-j-2}}{(i-j-2)!}e^{-(\lambda+2\mu)t}\right) * P_{j+1,j,1}(t) + \sum_{k=2}^{i-j-1}\left(\lambda^{i-j-k}\frac{t^{i-j-k-1}}{(i-j-k-1)!}e^{-(\lambda+2\mu)t}\right) * P_{j+k,j,1}(t) + \sum_{k=2}^{i-j-1}\left(\lambda^{i-j-k}(\mathrm{k}-1)\theta\frac{t^{i-j-k}}{(i-j-k)!}e^{-(\lambda+2\mu)t}\right) * P_{j+k,j,1}(t) + \left((\mathrm{i}-\mathrm{j}-1)\theta e^{-(\lambda+2\mu)t}\right) * P_{i,j,1}(t) \qquad i \geq j+2, j \geq 1 \quad (52)$$

$$P_{i,j,1}(t) = \lambda e^{-(\lambda+\mu+(i-j-1)\theta)t} * P_{i-1,j,0}(t) + (i-j)\theta e^{-(\lambda+\mu+(i-j-1)\theta)t} * P_{i,j,0}(t) + 2\mu\lambda^{i-j}e^{-(\lambda+\mu+(i-j-1)\theta)t}\left\{\frac{1}{(2\mu)^{i-j}} - e^{-2\mu t}\sum_{r=1}^{i-j-1}\frac{(t)^r}{r!}\frac{1}{(2\mu)^{i-j-r}}\right\} * P_{j,j-1,1}(t) + 2\mu e^{-(\lambda+\mu+(i-j-1)\theta)t}\sum_{k=1}^{i-j-1}\lambda^{i-j-k}\left\{\frac{1}{(2\mu)^{i-j-k}} - e^{-2\mu t}\sum_{r=0}^{i-j-k-1}\frac{(t)^r}{r!}\frac{1}{(2\mu)^{i-j-k-r}}\right\} *$$

$$P_{j+k,j-1,1}(t) +$$

$$2\mu e^{-(\lambda+\mu+(i-j-1)\theta)t}\sum_{k=1}^{i-j-1}\lambda^{i-j-k}\,(\mathrm{k}\theta)\left\{\frac{1}{(2\mu)^{i-j-k+1}}-e^{-2\mu t}\sum_{r=0}^{i-j-k}\frac{(t)^r}{r!}\frac{1}{(2\mu)^{i-j-k+1-r}}\right\}*$$

$$P_{j+k,j-1,1}(t)+2\mu(i-j)\theta e^{-(\lambda+\mu+(i-j-1)\theta)t}\left(\frac{1}{2\mu}-\frac{e^{-2\mu t}}{2\mu}\right)*P_{i,j-1,1}(t)$$

$$i\geq j+2, j\geq 2 \qquad (53)$$

$$P_{i,j,0}(t)=\lambda\mu e^{-(\lambda+(i-j)\theta)t}\left(\frac{1}{\mu+(i-j)\theta}-\frac{e^{-(\mu+(i-j)\theta)t}}{\mu+(i-j)\theta}\right)*P_{i-1,j-1,0}(t)+$$

$$\mu(i-j+1)\theta e^{-(\lambda+(i-j)\theta)t}\left(\frac{1}{\mu+(i-j)\theta}-\frac{e^{-(\mu+(i-j)\theta)t}}{\mu+(i-j)\theta}\right)*P_{i,j-1,0}(t)$$

$$+2\mu^2\lambda^{i-j+1}\left[\sum_{l=1}^{i-j+1}\sum_{m=1}^{l}\frac{e^{-(\lambda+(i-j)\theta)t}\;t^{(i-j+1)-l}(-1)^{m+1}\binom{l-1}{m-1}\left(\prod_{g_1=0}^{l-m-1}(1+g_1)\right)\left(\prod_{g_2=0}^{m-2}(1+g_2)\right)}{\big((i-j+1)-l\big)!\,(m-1)!\;(\mu)^m(2\mu-(i-j)\theta)^{1+l-m}}\right.$$

$$\left.-\;\frac{e^{-(\lambda+\mu+(i-j)\theta)t}}{(\mu)^{(i-j+1)}(\mu-(i-j)\theta)}+\frac{e^{-(\lambda+2\mu)t}}{(2\mu-(i-j)\theta)^{(i-j+1)}(\mu-(i-j)\theta)}\right]*P_{j-1,j-2,1}(t)+\;2\mu^2\sum_{k=1}^{i-j}\lambda^{(i-j+1)-k}$$

$$\left[\sum_{l=1}^{(i-j+1)-k}\sum_{m=1}^{l}\frac{e^{-(\lambda+(i-j)\theta)t}\;t^{((i-j+1)-k)-l}(-1)^{m+1}\binom{l-1}{m-1}\left(\prod_{g_1=0}^{l-m-1}(1+g_1)\right)\left(\prod_{g_2=0}^{m-2}(1+g_2)\right)}{(((i-j+1)-k)-l)!(m-1)!\;(\mu)^m(2\mu-(i-j)\theta)^{1+l-m}}-\right.$$

$$\left.\frac{e^{-(\lambda+\mu+(i-j)\theta)t}}{(\mu)^{(i-j+1)-k}(\,\mu-(i-j)\theta)}+\frac{e^{-(\lambda+2\mu)t}}{(2\mu-(i-j)\theta)^{(i-j+1)-k}(\,\mu-(i-j)\theta)}\right]*P_{j+k-1,j-2,1}(t)+\;2\mu^2\sum_{k=1}^{i-j}\lambda^{(i-j+1)-k}\,(k\theta)$$

$$\left[\sum_{l=1}^{((i-j+1)-k)+1}\sum_{m=1}^{l}\frac{e^{-(\lambda+(i-j)\theta)t}\;t^{(((i-j+1)-k)+1)-l}(-1)^{m+1}\binom{l-1}{m-1}\left(\prod_{g_1=0}^{l-m-1}(1+g_1)\right)\left(\prod_{g_2=0}^{m-2}(1+g_2)\right)}{((((i-j+1)-k)+1)-l)!(m-1)!\;(\mu)^m(2\mu-(i-j)\theta)^{1+l-m}}-\right.$$

$$\left.\frac{e^{-(\lambda+\mu+(i-j)\theta)t}}{(\mu)^{((i-j+1)-k)+1}(\mu-(i-j)\theta)}+\frac{e^{-(\lambda+2\mu)t}}{(2\mu-(i-j)\theta)^{((i-j+1)-k)+1}(\mu-(i-j)\theta)}\right]*P_{j+k-1,j-2,1}(t)+2\mu^2\,(i-j+$$

$$1)\theta\left[\frac{e^{-(\lambda+(i-j)\theta)t}}{(\mu)(2\mu-(i-j)\theta)}-\frac{e^{-(\lambda+\mu+(i-j)\theta)t}}{(\mu)(\mu-(i-j)\theta)}+\frac{e^{-(\lambda+2\mu)t}}{(2\mu-(i-j)\theta)(\mu-(i-j)\theta)}\right]*P_{i,j-2,1}(t)$$

$$i>j\geq 3 \qquad (54)$$

2. Letting $K=1,\ b_1=1,\ b_2=b_3=b_4=\cdots=b_K=0$ and $\mu=1$ in (39) to (42), then the following equations are:

$$(\lambda+n\theta)Q_{n,0}=Q_{n,1} \qquad n\geq 0 \qquad (55)$$

$$(\lambda+n\theta+1)Q_{n,1}=\lambda Q_{n,0}+(n+1)\theta Q_{n+1,0}+2Q_{n,2} \qquad n\geq 0 \qquad (56)$$

$$(\lambda+2)Q_{n,2}=\lambda Q_{n,1}+(n+1)\theta Q_{n+1,1}+\lambda Q_{n-1,2} \qquad n\geq 0 \qquad (57)$$

which coincide with the results (2.1) – (2.3) of Falin and Templeton [2].

6. Conclusion

In this study, a two retrial queueing system with bulk departures having two identical parallel servers is investigated. Bulk queueing systems are common in real-life situations such as elevators, loading and unloading cargoes, giant wheel, chemical manufacturing process, communication networks and tourism etc.

Transient probabilities of exact number of arrivals and departures are found by solving difference differential equations recursively when no, one or both servers are busy. Further, some particular

cases of interest are discussed along with special cases. From two-dimensional state queueing model, factors are well understood and quantified.

References

[1] Artalejo, J.R. and Corral, A.G. Retrial Queueing Systems: A Computational Approach, Springer, Berlin-Heidelberg, 2008.

[2] Falin, G.I. and Templeton, J.G.C. Retrial queues, Chapman and Hall, London, 1997.

[3] Artalejo, J.R. (2010). Accessible bibliography on retrial queues: progress in 2000-2009, *Mathematical and Computer Modelling*, 51:1071-1081.

[4] Bailey, N.T. J. (1954). On queueing processes with bulk service, *J.R. Stat. Soc. Ser. B*, 16: 80-87.

[5] Juan, M.T. (2005). Numerical methods for the single-server bulk-service queueing system with capacity, M/ G^Y/1, with discretized service time probability distribution, *International Conference on Operations Research*, Sept. 7-9, Berman, Germany.

[6] Janssen, A.J.E.M. and Van Leeuwaarden, J.S.H. (2005). Analytic computation schemes for the discrete-time bulk service queue, *Queueing Systems*, 50:141-163.

[7] Goswami, V., Mohanty, J.R. and Samanta, S.K. (2006). Discrete-time bulk-service queue with accessible and non-accessible batches, *Applied Mathematics and computation*, 182:898-906.

[8] Al-Khedhairi, A. and Tadj, L. (2007). A bulk service with a choice of service and re-service under bernoulli schedule, *International Journal Contemp. Math. Sciences,* 2:1107-1120.

[9] Pegden, C.D. and Rosenshine, M. (1982). Some new results for the M/M/1 queue, *Mgt Sci,* 28: 821-828.

[10] Kalra, S. and Singla, N (2019). A Two-State Retrial Queueing Model with Batch Departures, *Journal of Gujarat Research Society*, 21:1388-1396.

[11] Garg, P.C. and Kumar, S. (2012). A single server Retrial queues with impatient customers, *Mathematical journal of interdisciplinary sciences,* 1: 67-82.

[12] Singla, N. and Kalra, S. (2018). Explicit Time Dependent Solution of a Two-State Retrial Queueing Model with Two Parallel Servers, *Int. J. Agricult. Stat. Sci,* 14: 419-429.

Fuzzy Project Planning and Scheduling with Pentagonal Fuzzy Number

Adilakshmi Siripurapu[1], Ravi Shankar Nowpada[2]

•

Dept. of Basic Science and Humanities, Vignan's Institute of Information Technology (A), Duvvada, Visakhapatnam, AP, India[1]
slakshmijagarapu@gmail.com

Dept. of Mathematics, Institute of Science, GITAM (Deemed to be University), Visakhapatnam, AP, India[2]
Drravi68@gmail.com

Abstract

In optimization approaches such as assignment issues, transportation problems, project schedules, artificial intelligence, data analysis, network flow analysis, an uncertain environment in organizational economics, and so on, ranking fuzzy numbers is essential. This paper introduces a new fuzzy ranking in Pentagonal fuzzy numbers. Each activity's duration is expressed as a Pentagonal fuzzy number in the project schedule. The new ranking function transforms every Pentagonal fuzzy number into a crisp number (normal number). We calculated the fuzzy critical path using a new algorithm. These approaches are illustrated with a numerical example.

Keywords: Activity duration, centroid, fuzzy ranking, fuzzy critical path, fuzzy number, project schedule.

1. Introduction

The critical path approach is one of the most important concepts in network analysis. It is used to solve project challenges by creating networks and establishing each activity's earliest start and earliest finish date. It is also a scheduling algorithm for a collection of project networks. It is also generally associated mostly with Program Evaluation and Review Technique (PERT).

Zadeh [12] introduced the existence of 'fuzzy logic', which considers inaccuracies and inconsistencies. Several academics have used fuzzy numbers in various forms, such as fuzzy triangular numbers, Trapezoidal fuzzy numbers, etc.

In many practical situations, the variables that define information uncertainty or vagueness are usually triangular or trapezoidal fuzzy numbers. Lee et al. [5] introduced Pentagonal fuzzy numbers and generalized the results of addition, subtraction, multiplication, and division based on Zadeh's extension principle. Pathinadhan et al. [6] proposed a new form of the non-normal generalized pentagonal fuzzy number, and some of its arithmetic operations, centroid, and median were discussed. Siji et al. [8] solved network problems with Pentagonal Intuitionistic fuzzy numbers using the ranking approach. Arokiamary et al. [1] determined the critical path analysis in a project network using the fuzzy TOPSIS method. Uthra et al. [11] defined a Generalized Intuitionistic Pentagonal fuzzy number and developed a new ranking formula.

Sahaya Sudha et al. [7] solved the fuzzy linear programming problem by applying the pentagonal fuzzy ranking function. Uma Maheswari et al. [10] introduced a simple approach for solving fuzzy transportation problems using fuzzy pentagonal numbers. Avishek Chakraborty et al. [2] studied interval-valued pentagonal fuzzy numbers, properties, ranking, and defuzzification. They solved the game problem by using a ranking function in fuzzy pentagonal numbers. Someshwar et al. [9] solved the linear programming problem using the pentagonal fuzzy ranking function. Das et al. [3] suggested a novel pentagonal neutrosophic technique for solving the linear programming problem.

2. Basic Definitions

In this section we look at a few definitions.

2.1 Fuzzy Set [12]

As stated in Zadeh's paper, the formalization of a fuzzy set is:
Let *X* be a space of points (objects), with a generic element of *X* denoted by x. Thus, $X = \{x\}$. A fuzzy set (class) *A* in *X* is characterized by a membership (characteristic function) function $\mu_A(x)$, which associates with each point in *X* a real number in the interval [0,1], with the value of $\mu_A(x)$ at x representing the "grade of membership" of x in *A*. When *A* set in the ordinary sense of the term, its membership function can take on only two values, 0 and 1, $\mu_A(x) = 1\ or\ 0$ according to x does or does not belong to *A*.

2.2 Fuzzy Number [4]

It is a Fuzzy set of the following conditions:

- Convex fuzzy set
- Normalized fuzzy set.
- Its membership function is piece-wise continuous.
- It is defined in the real number.

Fuzzy numbers should be normalized and convex. Here the condition of normalization implies that the maximum membership value is 1.

2.3 Pentagonal Fuzzy Number (PFN) [6]

A pentagonal fuzzy number $\tilde{A}_p = (p_1, p_2, p_3, p_4, p_5)$ where p_1, p_2, p_3, p_4, p_5 real numbers and its membership function is defined by:

$$\mu_{\tilde{A}_p}(x) = \begin{cases} \frac{1}{2}\left(\frac{x-p_1}{p_2-p_1}\right); & p_1 \le x \le p_2 \\ \frac{1}{2}+\frac{1}{2}\left(\frac{x-p_2}{p_3-p_2}\right); & p_2 \le x \le p_3 \\ 1-\frac{1}{2}\left(\frac{x-p_3}{p_4-p_3}\right); & p_3 \le x \le p_4 \\ \frac{1}{2}\left(\frac{p_5-x}{p_5-p_4}\right); & p_4 \le x \le p_5 \\ 0; & otherwiise \end{cases}$$

The Pentagonal Fuzzy Number diagram is represented in Figure 1.

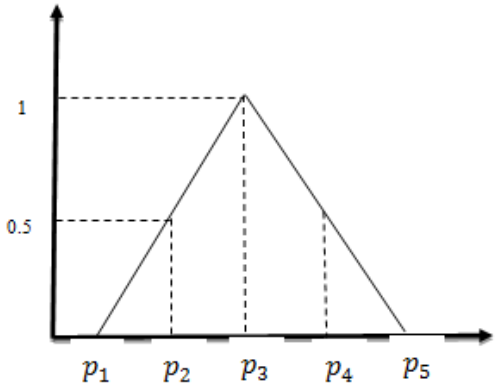

Figure 1: *Pentagonal Fuzzy Number*

2.4 Generalized Pentagonal Fuzzy Number (GPFN) [6]

The generalized pentagonal fuzzy number $\tilde{A}_p = (p_1, p_2, p_3, p_4, p_5;\ \omega)$ its membership function is expressed as;

$$\mu_{\tilde{A}_p}(x) = \begin{cases} \frac{\omega}{2}\left(\frac{x-p_1}{p_2-p_1}\right); & p_1 \le x \le p_2 \\ \frac{1}{2}+\frac{\omega}{2}\left(\frac{x-p_2}{p_3-p_2}\right); & p_2 \le x \le p_3 \\ 1-\frac{\omega}{2}\left(\frac{x-p_3}{p_4-p_3}\right); & p_3 \le x \le p_4 \\ \frac{\omega}{2}\left(\frac{p_5-x}{p_5-p_4}\right); & p_4 \le x \le p_5 \\ 0; & otherwiise \end{cases}$$

The generalized Pentagonal Fuzzy Number diagram is represented in Figure 2.

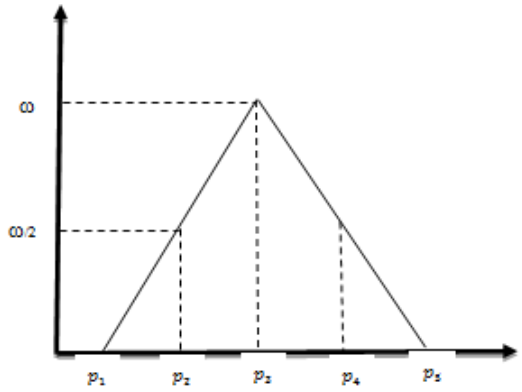

Figure 2: *Generalized Pentagonal Fuzzy Number*

3. Methodology

This section, proposed a new ranking function in Pentagonal fuzzy number.

Divide the pentagon into two triangles and one rectangle. Let G_1, G_2, and G_3 be the centroid of the three plane figures, respectively. The centroid of a fuzzy pentagon number is supposed to indicate the pentagon's balancing point (Figure 3).

The Proposal ranking in the Pentagonal fuzzy number diagram is represented in Figure 3.

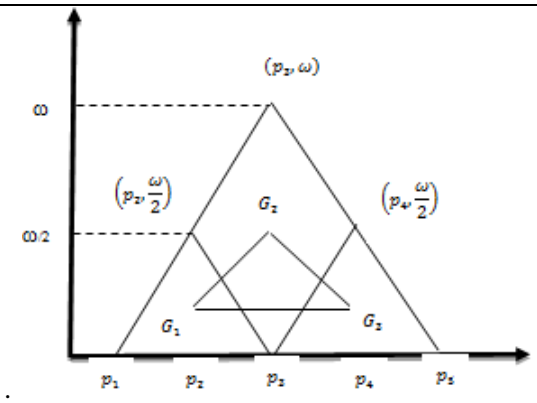

Figure 3: *Proposed Ranking Approach*

To determine the ranking of a generalized pentagon fuzzy number, the in centre of the centroid G_1, G_2, G_3 is used as a point of reference.

Consider the generalized pentagon fuzzy number $\tilde{A}_p = (p_1, p_2, p_3, p_4, p_5, \omega)$

The three plane figures' centroid is$G_1 = \left(\frac{p_1+p_2+p_3}{3}, \frac{\omega}{6}\right)$, $G_2 = \left(\frac{p_2+2p_3+p_4}{4}, \frac{\omega}{2}\right)$, $G_3 = \left(\frac{p_3+p_4+p_5}{3}, \frac{\omega}{6}\right)$ respectively.

The centroid of G_1, G_2 and G_3 is $\left(\frac{4P_1+7P_2+14p_3+7p_4+4P_5}{36}, \frac{5\omega}{36}\right)$.

$$G_{\tilde{A}_p}(x_0, y_0) = \left(\frac{4P_1 + 7P_2 + 14p_3 + 7p_4 + 4P_5}{36}, 5\omega/36\right)$$

The in centre of the centroid with Euclidean distance is;

$$\sqrt{x_0^2 + y_0^2}$$

Consider that the centroid's center with Euclidean distance is a new ranking function in the generalized Pentagonal fuzzy number.

Therefore, a new ranking in the Generalized Pentagonal fuzzy number is;

$$\Re(\tilde{A}_p) = \sqrt{x_0^2 + y_0^2}$$

3.1 Fuzzy Critical Path Analysis

The primary objective of the fuzzy critical path is to estimate the total project duration and assign start and finish dates to all project activities. This makes it possible to compare the actual progress to the estimated duration.

The following fuzzy factors should be known to prepare the project schedule.

(i) Project completion time
(ii) Each activity's earliest and latest times
(iii) Critical activities and the critical path
(iv) Float for each activity (i.e., the time required to complete a non-critical activity can be delayed without affecting the overall project completion time)

3.1.1 Notations

$\tilde{FES}_{ij}$ = Earliest start of time of an activity (i, j)

$\tilde{FLS}_{ij}$ = Latest start time of an activity (i,j)
$\tilde{FEF}_{ij}$ = Earliest finish time of an activity (i,j)
$\tilde{FLF}_{ij}$ = Latest finish time of an activity(i,j)
$\tilde{Ft}_{ij}$ = Total duration of an activity (i,j)
$\tilde{FTF}_{ij}$=Total float of an activity (i,j)

3.1.2 Algorithm for Fuzzy Critical Path

Step1: Construct a fuzzy project network with predecessor and successor events.
Step2: Express every activity time as PFN.
Step3: Transformed every PFN as a crisp number using a new ranking function.
Step4: Calculate earliest start time, $\tilde{FES}_{ij} = \max_{i}\{\tilde{FES}_{ij} + \tilde{t}_{ij}\}, i =$ number of preceding nodes.
Step5: Calculate earliest finish time, $\tilde{FEF}_{ij} = \tilde{FES}_{i} + \tilde{t}_{ij}$.
Step6: Calculate latest finish time $\tilde{FLF}_{ij} = \min_{j}\{\tilde{FLF}_{ij} - \tilde{t}_{ij}\}$, $j =$ number of succeeding nodes
Step7: Calculate latest start time, $\tilde{FLS}_{ij} = \tilde{FLF}_{ij} - \tilde{t}_{ij}$
Step8: Calculate Total float, $\tilde{FTF}_{ij} = \tilde{FLF}_{ij} - \tilde{FEF}_{ij}$ *or* $\tilde{FLS}_{ij} - \tilde{FES}_{ij}$

4 Application of Pentagonal fuzzy numbers in a project schedule

Consider the following fuzzy project network, in which the Pentagonal fuzzy number represents each activity. The fuzzy project network has seven nodes and nine activities. This example shows how to schedule a construction project using a project Network. My objective is to analyze the maximum path that is the essential Critical path for the construction process.

Table 1 represents the activities, their description and duration periods. Figure 4 represents the project network diagram.

Table 1: *Project Network Description*

Activity	Pentagonal fuzzy numbers
1→2	(1,2,3,4,5)
1→3	(6,7,8,9,10)
2→4	(11,12,13,14,15)
3→4	(16,17,18,19,20)
2→5	(21,22,23,24,25)
3→6	(26,27,28,29,30)
4→7	(31,32,33,34,35)
5→7	(36,37,38,39,40)
6→7	(41,42,43,44,45)

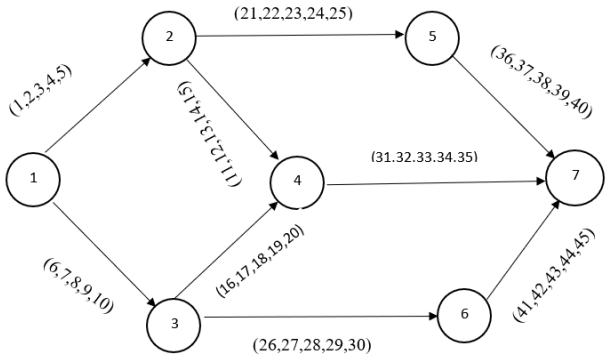

Figure 4: *Project Network*

4.1 Expected time of activities

Pentagonal fuzzy number transformed into activity duration by proposal ranking function. This activity duration is taken as the time between the nodes, and the fuzzy critical path is calculated by applying an algorithm. The expected time of activities is represented in Table 2, and the related diagram is represented in Figure 5.

Table 2: *Expected time of activities*

Activity $i \longrightarrow j$	Pentagonal fuzzy number	Expected time
1→2	(1,2,3,4,5)	3.0032
1→3	(6,7,8,9,10)	8.0012
2→4	(11,12,13,14,15)	13.0007
3→4	(16,17,18,19,20)	18.0005
2→5	(21,22,23,24,25)	23.0004
3→6	(26,27,28,29,30)	28.0003
4→7	(31,32,33,34,35)	33.0002
5→7	(36,37,38,39,40)	38.0002
6→7	(41,42,43,44,45)	43.0002

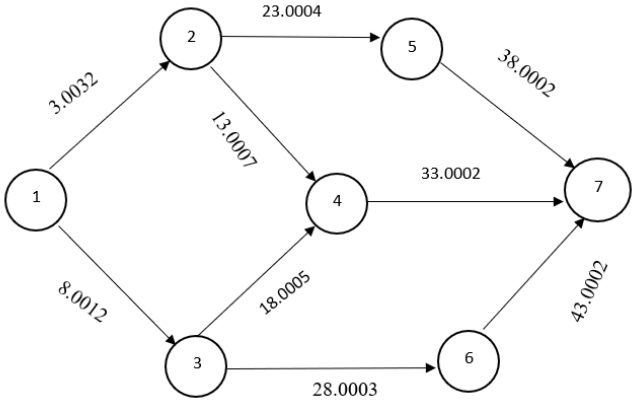

Figure 5: *Expected time of Activities*

4.2 Earliest, latest times and Total float of fuzzy activities

Computed Earliest, latest times and total float using formulas mentioned in procedure step 4, step 5, step6, step7 and step 8, respectively.

The earliest, latest and total float times of fuzzy activities represented in Table 3.

Table 3: *The earliest, latest times and total float of fuzzy activities with defuzzified values of PFN*

$i \longrightarrow j$	$F\tilde{t}_{ij}$	$FE\tilde{S}_{ij}$	$FE\tilde{F}_{ij}$	$FL\tilde{S}_{ij}$	$FL\tilde{F}_{ij}$	$FT\tilde{F}_{ij}$
1→2	3.0032	0	3.0032	14.9979	18.0011	14.9979
1→3	8.0012	0	8.0012	0	8.0012	0*
2→4	13.0007	3.0032	16.0039	33.0008	46.0015	29.9976
3→4	18.0005	8.0012	26.0017	28.001	46.0015	19.9998
2→5	23.0004	3.0032	26.0036	18.0011	41.0015	14.9979
3→6	28.0003	8.0012	36.0015	8.0012	36.0015	0*
4→7	33.0002	26.0017	59.0019	46.0015	79.0017	19.9998
5→7	38.0002	26.0036	64.0038	41.0015	79.0017	14.9979
6→7	43.0002	36.0015	79.0017	36.0015	79.0017	0*

4.3 Results

According to the fuzzy total float, the fuzzy critical activities are 1→3, 3→6, 6→7.
Therefore, the critical path of the fuzzy project network is 1→3→6→7.
Hence, the total duration of the project network is 79.0017≅79 days.

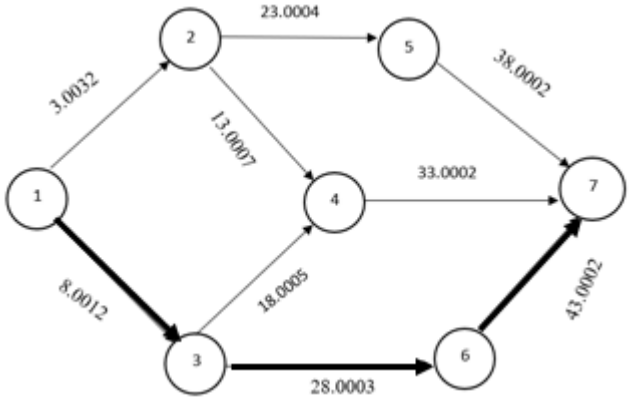

Figure 6: *Fuzzy Critical Path*

5. Conclusion

This paper introduced a new ranking function in Pentagonal fuzzy numbers. The proposed ranking function is derived from the centroid of PFN. In the network, every activity period is expressed by a PFN. The duration of every activity is transformed into the normal number or crisp number by a new ranking function. This normal number is considered the expected time of activity. The fuzzy critical path algorithm was used to identify the fuzzy critical path and project completion time. The proposal ranking can also be applied to more complex project networks in the real world. We can apply the ranking function of PFN to solve game problems and transportation problems.

References

[1] Arokiamary, A., & Jayapalan P. (2016) Fuzzy Critical Path Analysis in a Project Network Using Fuzzy Topsis Method, *International Journal of Mathematics And its Application*, Volume 4, Issue 4, 423-429.

[2] Avishek Chakraborty., Mondal, S. P., Alam, S., Ahmadian, A., Senu, N., De, D., & S. Salahshour. (2019). The fuzzy pentagonal number: its different representations, properties, ranking, defuzzification and application in-game problems. *Symmetry*, *11*(2), 248.

[3] Das, S. K., & Chakraborty, A. (2020). A new approach to evaluate linear programming problem in pentagonal neutrosophic environment. *Complex & intelligent systems*, *7*(1), 101-110.

[4] Kaufmann, A. and Madan M. Gupta (1986). Introduction to fuzzy arithmetic: theory and applications. *Van Nostrand Reinhold,* New York.

[5] Lee. B and Yong Sik Yun, The Pentagonal Fuzzy Numbers, *Journal of the Chungcheong Mathematical Society*, Volume 27, No. 2, May 2014.

[6] Pathinathan. T, Ponnivalvan. K, Ebinesar Mike. (2015). Different Types of Fuzzy Numbers and Certain Properties. *Journal of Computer and Mathematical Sciences*. 6. 631-651.

[7] Sahaya Sudha, S Vimalavirginmary, S Sathya (2017), A Novel approach for Solving Fuzzy Linear Programming Problem using Pentagonal Fuzzy Numbers, *International Journal of Advanced Research in Education & Technology,* Vol.4, Issue 1, ISSN: 2394-6814.

[8] Siji.S, K. Selva Kumari (2016). An Approach for solving Network Problem with Pentagonal Intuitionistic Fuzzy Numbers Using Ranking Technique, *Middle-East Journal of Scientific Research,* 24(9),2977-2980, ISSN:1990-9233.

[9] Someshwar Siddi & Reddy, Y. (2020). Solving Fuzzy LPP for Pentagonal Fuzzy Number Using Ranking Approach, *MuktShabd Journal*, and IX. 2674. ISSN: 2347-3150.

[10] Uma Maheswari & Kandasamy, Ganesan. (2018). Solving fully fuzzy transportation problem using pentagonal fuzzy numbers. *Journal of Physics: Conference Series*. 1000. 012014.

[11] Uthra, G., Thangavelu, K., & Shunmugapriya, S. (2017). Ranking Generalized Intuitionistic Pentagonal Fuzzy Number by Centroidal Approach, *International Journal of Mathematics and Its Applications,* Volume-5, Issue 4-D, 589-593, ISSN: 2347-1557.

[12] Zadeh L.A. (1965) Fuzzy sets, *Information and Control*, Volume 8, Issue 3, 338-353, ISSN: 0019-9958.

Predictive Convolutional Long Short-Term Memory Network for Detecting Anomalies in Smart Surveillance

[1]Priyanka Patel, [2]Dr. Amit Nayak

•

[1]U & P U Patel Department of Computer Engineering,
Chandubhai S Patel Institute of Technology,
Faculty of Technology & Engineering,
Charotar University of Science and Technology (CHARUSAT), Changa, Gujarat, India
priyankapatel.it@charusat.ac.in

[2]Department of Information Technology,
Devang Patel Institute of Advance Technology and Research (DEPSTAR),
Faculty of Technology& Engineering, Charotar University of Science
and Technology (CHARUSAT), Changa, Gujarat, India
amitnayak.it@charusat.ac.in

Abstract

Surveillance is the monitoring of behavior, actions, or information, with the purpose of collecting, influencing, controlling, or guiding evidence. Despite the technical traits of cutting-edge science, it is difficult to detect abnormal events in the surveillance video and requires exhaustive human efforts. Anomalous events in the video remain a challenge due to the occlusions of objects, different densities of the crowd, cluttered backgrounds & objects, and movements in complex scenes and situations. In this paper, we propose a new model called time distributed convolutional neural network long short-term memory Spatiotemporal Autoencoder (TDSTConvLSTM), which uses a deep neural network to automatically learn video interpretation. Convolution neural network is used to extract visual features from spatial and time distributed LSTM use for sequence learning in temporal dimensions. Since most anomaly detection data sets are restricted to appearance anomalies or unusual motion. There are some anomaly detection data-sets available such as the UCSD Pedestrian dataset, CUHK Avenue, Subway entry-exit, ShanghaiTech, street scene, UCF-crime, etc. with varieties of anomaly classes. To narrow down the variations, this system can detect cyclists, bikers, skaters, cars, trucks, tempo, tractors, wheelchairs, and walkers who are walking on loan (off the road) which are visible under normal conditions and have a great impact on the safety of pedestrians. The Time distributed ConvLSTM has been trained with a normal video frame sequence belonging to these mentioned classes. The experiments are performed on the mentioned architecture and with benchmark data sets UCSD PED1, UCSD PED2, CUHK Avenue, and ShanghaiTech. The Pattern to catch anomalies from video involves the extraction of both spatial and temporal features. The growing interest in deep learning approaches to video surveillance raises concerns about the accuracy and efficiency of neural networks. The time distributed ConvLSTM model is good compared to benchmark models.

Keywords: Predictive ConvolutionLSTM, Distributed convolutional neural network, long short-term memory, Spatiotemporal Autoencoder, TDSTConvLSTM, Video Surveillance, Anomaly detection, Machine Learning, Deep Learning, Smart Video Monitoring.

1. Introduction

Anomalies are patterns or observations in the video sequence that do not conform to normal or expected behavior. And the detection of anomaly is an approach to discover the patterns those unexpected behavior. The unexpected behaviors are characterized as outliers, novel or anomalies. Mainly three types of anomalies are there. First is point anomaly, second is contextual anomaly and the third is collective anomaly. The most common type of anomaly is point anomaly and has been a focus of most of the research. It can be defined as an individual entity that is considered abnormal with regard to other data. In Figure-1 point A1, point A2, and points in region A3 are point anomalies as they are outside to the normal region. The contextual anomaly is also known as a conditional anomaly. It can be defined as in some specific context if a data instance is anomalous then it is a contextual anomaly. These types of anomalies are usually found out in spatial data and time-series data. The last one is the collective anomaly; it can be defined as a set of related data instances that is anomalous with regard to the remaining data in the data set. Individual entities may not be anomalies by themselves in collective anomalies but their occurrence to gather is considered anomalous. The aspect of anomaly detection approach, the nature of data and the type of label on instance are shown in [1, 2]. In recent years, the demand for visual surveillance has increased. Large-scale visual surveillance system has been implemented with many high-quality cameras for security concern in private and public zones but at same time it generates large amounts of data every second and which is impossible to monitor and process such a huge amount of information in real-world applications. Therefore, it is commanding to develop autonomous systems that can detect, identify, and predict abnormal articles or events, and then help take early action to avoid threats or unexpected actions. The international border security agencies are also looking for the solution of security in surveillance in each sector. It can also be used in various applications, such as group activity detection, home security, organization Security, restricted area monitoring, traffic analysis, and also Through macro applications (traffic surveillance, building surveillance, city surveillance, and business intelligence), through micro applications (perimeter intrusion detection, pattern recognition, people counting and management, automatic license plate recognition (ALPR), incident detection, face recognition and others including advanced eye recognition and behavior analysis), upon deployment (on premise and in the cloud), by industry (government and transport, BFSI, trade and industry, healthcare, retail and others, including education, housing and hospitality), by region (North, East, West AND South) and competitive landscape covered by Dublin, Nov. 19, 2018 Research Markets[43,49]. Recent research shows that it has received great attention in the research community and has become a major problem to find a better solution in computer vision. However, the implementation of surveillance systems in practical applications brings three main challenges: one is the unlabeled data that is readily available, but training on the labelled data is not offered. The second is Anomalies that are not clearly defined in actual video surveillance. And the third is Video complexity that adds expensive features and makes it difficult

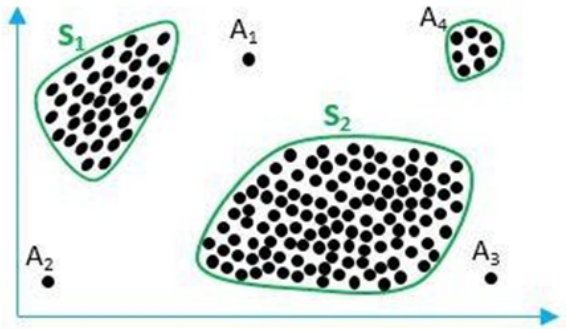

Figure 1: *Example with Normal and anomaly region in Two- Dimensional Data*

to extract manually. According to the exclusive summary by global endowment of international Peace [3]. It is important that AI surveillance is not a stand-alone tool of repression, but part of a set of digital tools of repression: information and communication technologies used to monitor, intimidate, coerce and harass people, and to deter certain people Illegal activities or beliefs. A lot of work has been done in the field of video surveillance, such as detecting objects, tracking them, and recognizing the behavior of objects, but it is still interesting to see rare, novel and unusual objects. The interesting thing to occurrences of the new objects in the video frames and at a same time it is also difficult to spot and detect those new and suspicious behavior in large amount of data sequence. Finding such rare occurrences in a video sequence is a critical task for an autonomous model because the unusual and novel, doesn't keep happening again and again, the model has not been adequately trained with these novel objects (anomalous objects). However, current technology works well [4,5,43,49,78] it gives good results, but at the same time they are all contextual independent. The detection of all types of anomalous objects in all data contexts has yet to be introduced. In the case of video data, this is a challenge due to the high dimensional of input data, the noise it contains and the large number of new types of objects and interactions. These objects are context-independent. For example: walking in a canteen is considered an unusual occurrence, but walking in a playground would be normal.

2. Background

Illustrates anomalies in a simple two-dimensional data-set is shown in Figure-1. In the whole data set, there are two normal regions which are S1 and S2 since most observations lie in these two regions. Points A1, A2 and A3 and A4 are far away from the normal regions S1 and S2. So those A1, A2, A3 & A4 regions are consider as an anomaly as it does not lie under S1 and S2 normal regions. Various examination studies have examined Decision Engine approaches which can be classified in five categories, classification based, Clustering based, knowledge based, combination based and statistical based, as illustrated in Figure-2.

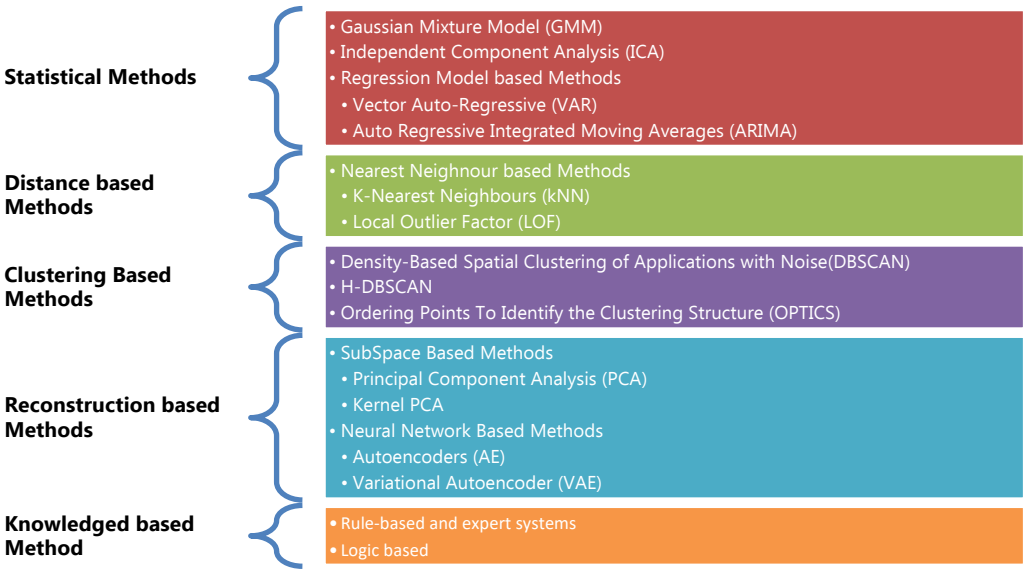

Figure 2: *Taxonomy of Classical Methods in Previous Examinations*

The surveillance may include the use of electronic devices such as closed-circuit television (CCTV) for remote monitoring or the interception of Internet traffic and other electronic transmissions of information. It can also include simple technical methods, such as collecting information and intercepting messages. Object Recognition, Detection, and Localization in Video are broadly discovered by researchers in computer vision and machine learning. Figure-3 shows summarize each technique and its corresponding global implementation level [3]. However, it is a monotonous task to spot a particular object or action which is not expected to be a part of the video sequence is relatively difficult to track. Anomalies in surveillance video are extensively described as activities or sports which might be uncommon and symbolize abnormal behavior. It is an unsupervised method of detecting anomalies. Due to the unclear definition of video events, it is challenging to automatically detect abnormal events in long video sequences.

In computer vision, the detection of anomaly events is one of the most difficult problems and has attracted a great deal of research effort in the last few decades [2, 5-8, 49], whereby common detection methods can be roughly divided into the following three groups. The first category of abnormality detection methods focuses on the hypothesis that abnormalities are rare and that behaviors that differ from normal patterns are considered abnormal. In these methods, regular patterns are coded by various statistical models, z field-based models that combine dynamic models and treat anomalies as outliers. The second category of anomaly detection approaches is sparse reconstruction [12] which is used to learn common patterns. In particular, a dictionary is created using a sparse representation for normal behavior, and those with a high error are recognized as anomalies. Recently, with the promising advancement of deep learning, some researchers are building deep neural networks for anomaly detection, including learning video prediction and learning abstraction features [2, 13-15], The third group is the Hybrid methods of normal and abnormal behavior for modeling [10, 17], in which multi-instance learning (MIL) is used in a weakly monitored environment to model movement patterns [15, 17]. For example, Sultani et al. developed a classifier based on MIL [10] that can detect anomalies. In the meantime, a deep classification model is used to predict anomaly scores. To take advantage of the superiority of Sultan's work, which takes normal and anomalous video into account, in this work reconstruct of the model using weakly labeled supervised learning. The related methods based on autoencoder for abnormality detection are describe in [4, 14, 26-28].

In order to avoid enormous computational effort caused by backtracking in the existing methods, we propose a new and effective three-step method for unsupervised anomaly detection.

AI Surveillance Technique	Description	Global Proliferation (out of 75 countries)
Smart Cities/Safe Cities	Cities with sensors that transmit real-time data to facilitate service delivery, city management, and public safety. Often referred to as "safe cities," they incorporate sensors, facial recognition cameras, and police body cameras connected to intelligent command centers to prevent crime, ensure public safety, and respond to emergencies. Only platforms with a clear public safety focus are incorporated in the index.	56 countries
Facial Recognition Systems	Biometric technology that uses cameras (still images or video) to match stored or live footage of individuals with images from databases. Not all systems focus on database matching; some systems assess aggregate demographic trends or conduct broader sentiment analysis via facial recognition crowd scanning.	64 countries
Smart Policing	Data-driven analytic technology used to facilitate investigations and police response; some systems incorporate algorithmic analysis to make predictions about	53 countries

Figure 3: *Summary of AI Surveillance Techniques and Global Prevalence [3]*

In the first stage, a Convneted auto- encoder is trained to learn the latent space representation of

frame sequence. Latent space representation of each frame is passed to the stacked thereof or stacked LSTM and it's trained to predict whether the sequence of frames contains an anomaly or not. We proposed such a problem by learning collecting features from previous feature maps that can recognize, detect and localize anomalies under the video. We approach end-to-end trainable composite Time Distributed Spatiotemporal Convolutional Long Short-Term Memory (TSConvLSTM).

Basic Convolutional LSTM Architecture:

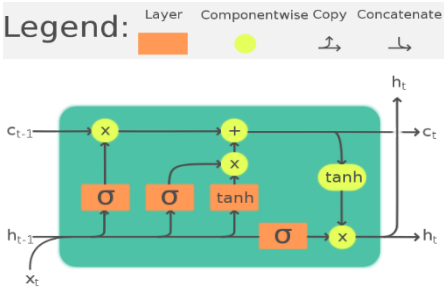

Figure 4: *The LSTM cell can process data sequentially and keep its hidden state through time [15].*

In this section, we have explained the types of LSTM networks as shown in Figures 4, 5, 6, 7, 8 respectively and with the help of that we have designed a new hybridTime Distributed ConvLSTM network. LSTM stands for "Long Short Time Memory", it is a layer that can receive various chronological entries in order to find what is very useful for forecasting. It's a simplified explanation, but it's close to reality. Since we process frames in chronological order, we want to be able to determine the relationship from one frame to another at a specific point in time. Since we have timed inputs, LSTM is very suitable for filtering the useful values from these inputs. Usually there are two options: Before applying LSTM, do a convolution or some other neural Computation. Do the same work after the LSTM. To decide which order to choose, you need to think about what you want to filter. In our example, we need to check for a moving object, so we need to find the object before it can detect movement, so here we need to do convolution before LSTM. Here in LSTM input and state at a timestamp are 1D vectors. Dimensions of the state can be permuted without affecting the overall structure. With the increasing popularity of LSTMs, various changes to the traditional LSTM architecture have been tested to simplify the internal design of cells to operate more efficiently and to reduce computational complexity. Gers et.al,2000 introduced peephole connections that allowed the gate layers to see the state of the cell at all times. Some LSTMs also used a coupled entrance and a forgetting gate instead of two separate gates, which helps to make two decisions at the same time.

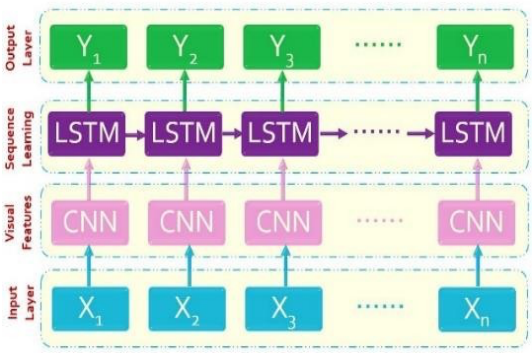

$$i_t = \boldsymbol{\sigma}(W_i \circ x_t + b_{ii} + U_i \circ h_{t-1} + b_{hi}) \quad (1)$$

$$f_t = \boldsymbol{\sigma}\left(W_f \circ x_t + b_{if} + U_f \circ h_{t-1} + b_{hf}\right) \quad (2)$$

$$g_t = \boldsymbol{tanh}\left(W_g \circ x_t + b_{ig} + U_g \circ h_{t-1} + b_{hg}\right) \quad (3)$$

$$o_t = \boldsymbol{\sigma}(W_o \circ x_t + b_{io} + U_o \circ h_{t-1} + b_{ho}) \quad (4)$$

$$c_t = f_t \circ C_{t-1} + i_t \circ g_t \quad (5)$$

$$h_t = o_t \circ \tanh ct \quad (6)$$

Figure 5: *Simple Convolutional LSTM Architecture*

where, $\boldsymbol{\sigma}$ Sigmoid function, i_t input gate, f_t forgot gate, g_t cell gate, o_t output gate, C_t cell state, h_t hiden state, x_t input at time t, W, U, learnable weights, B bias, Hadamard or entry wise product, tanh hyperbolic tangent function.

Anomaly detection is of great importance for video surveillance structures. Most of the

structures that are proposed use techniques like Convolutional Neural Network (CNN) and LSTM (Long Short- Term Memory) networks to efficiently train the machine in an effort to locate the anomalies in each supervised in addition to unsupervised manners. The supervised learning approach emphasizes the use of the present understanding approximately a specific anomaly to teach a machine even as the unsupervised learning approach, on the other hand, attempts to learn normality instead of learning abnormality. This means that if a massive deflection is visible from ordinary behavior, it provokes abnormality. The convolutional LSTM basic Architecture is shown in figure-5.

2. Literature Review

In recent times, many deep convolution neural networks have been proposed [9, 13, 29-32] to extract high-level features by learning the temporal regularity in video clips. Deep cluster-based anomaly detection techniques are introduced in [33-35]. Although deep learning technology has made significant progress in several other fields, there are few reports on deep learning methods used to detect video anomalies. However, for deep learning-based video anomaly detection techniques, such as abnormal activity detection or abnormal object detection, there are few specialized investigations have been made and many researches are already cried out as shown in Table 1.

Table 1: *Summary of Recent work*

Year wise Work proposed	***Broad area and Challenges***
Wan et.al, 2021[37]	*Anomaly Detection in Video Sequences: A Benchmark and Computational Model*
Lu et.al, 2020[21]	*Challenge is providing only Few-Shot Scene and detect anomalies from huge data.*
Bansod et.al,2019 [39]	*Transfer learning for video anomaly detection*
Zhu et.al,2020[51]	*Video Anomaly Detection for Smart Surveillance*
Ramachandra et al.2020[53]	*A Survey of Single-Scene Video Anomaly Detection*
Basora et.al, 2019 [38]	*Recent Advances in Anomaly Detection Methods Applied to Aviation*
Chalapathy et.al, 2019 [40]	*Deep-learning-based anomaly detection techniques for various domains*
Chong et.al,2017[14]	*Abnormal Event Detection in Videos using Spatiotemporal Autoencoder*
Sultani et.al. 2018[17]	*Real-world Anomaly Detection in Surveillance Videos.*
Kiran et.al.2018[18]	*An overview of deep learning-based methods for Unsupervised and semi-supervised anomaly detection in videos.*

The team argue that the low recognition performance of these baselines reveals that the dataset is very challenging and opens more opportunities for future work. Bharathkumar Ramachandra et al, 2020 [53] reported on a survey of single-scene video anomaly detection. VIDEO anomaly detection is the task of localizing anomalies in space and/or time in a video. They have provided a comprehensive review of research in single-view video anomaly detection. The authors built an intuitive taxonomy and situated past research works in relation to each other. The pixel-level criterion of follows: Given the predicted anomaly score map St corresponding to the tth frame of a test video, the frame is counted as a true positive frame. Sijie Zhu (2020) [56] noted that in modern intelligent video surveillance systems, automatic anomaly detection through computer vision analytics plays a pivotal role. Video anomaly detection has been studied for a long time, while this problem is far from being solved. Since real-world anomaly events happen with low probability, it is hard to capture all types of anomalies. This problem is typically formulated as unsupervised

learning, where the models are trained with only normal video frames and validated with both normal and anomaly frames. UCF-Crime is currently the largest anomaly detection dataset with realistic anomalies, which contains thousands of anomalies and normal videos. The analysis involved 5 popular benchmark datasets.

Boyang Wan et al. [37] noted that Anomaly detection aims to distinguish abnormal and normal activities as well as anomaly categories in video sequences. Existing databases only provide video-level labels in training set, which makes it infeasible to learn anomaly detection models in a fully-supervised manner. By tracking all moving objects in a video sequence, the anomaly event is detected by considering different levels of spatiotemporal contexts. 100 video sequences are collected for each abnormal category, making it the largest database for anomaly detection to date. Anomaly detection attempts to automatically predict abnormal/normal events in a given video sequence. In the proposed multi-task deep neural network, the local spatiotemporal features are first extracted by an inflated 3D convolutional network from each video segment.

A group led by Zhuang-Zhuang Wang at the School of Computer Science and Engineering, [20] noted that the process of the proposed small-object detection algorithm is divided into four parts: input, backbone network, neck network, and head. The team continue to use PANet and the spatial pyramid pooling layer structure to fuse the feature information of feature maps of different sizes. It is believed that improving the accuracy of small-target detection by enhancing the resolution of the image will increase the number of calculations of the network. Small- object detection plays a key role in many tasks such as identifying traffic signs or pedestrians that are almost invisible in low-resolution images. This study introduces the FFT module to complete images SR and uses Darknet53 combined with dense block to extract small target features.

MyeongAh Cho et.al [54] reported in 'Unsupervised Video Anomaly Detection via Normalizing Flows with Implicit Latent Features' that surveillance anomaly detection finds abnormal events such as traffic monitoring, accidents, and crime using the petabytes of videos from CCTVs. They suggest distribution learning with normalizing flow models using static and dynamic features obtained from implicit two-path AE. They propose an ITAE that implicitly focuses on static and dynamic features. These two encoders generate a higher reconstruction error than one-path encoder for scenes with abnormal motion or appearance and perform anomaly detection better. Novel method for learning to detect anomalies in videos with only a few frames of video footage, which could have huge potential in real-world applications.

A research team led by Yiwei Lu of the University of Manitoba [21] have introduced a new problem called few-shot scene-adaptive anomaly detection. The group believe this new problem setup is closer to the real-world deployment of anomaly detection systems. Experimental results show that the proposed approach significantly outperforms other alternative methods. They consider the problem of anomaly detection in surveillance videos. Given a video, the goal is to identify frames where abnormal events happen. They learn a model that can quickly adapt to a new scene by using only a few frames from it. The researchers propose to learn few-shot scene-adaptive anomaly detection models. Target Methods K=1 K=5 K=10. Ped1 Fine-tuned 76.99 77.85 78.23 Ours 79.94 80.44 78.88 Ours 80.6 81.42 82.38. Ped2 Fine-tuned 85.64 89.66 91.11 Ours 90.73 91.5 91.11 Ours 91.19 91.8 92.8. Aspects of the findings appear to offer an alternative view to previous work in this subject: "In the train/test split used in, both training and test sets contain videos from the same set of 13 scenes.

4. Challenges in Anomaly Detection

At the abstract level, anomalies are defined as patterns that do not correspond to expected normal behavior. Therefore, an easy way to detect anomalies is to identify region that represent normal behavior and declare any observations in the data that are not related to that normal behavior that region is like an anomaly, but there are several factors that make this apparently simple method very difficult. Here is a list of the challenges we encountered in the research process 1) it is difficult to define a region that comprehends all probably normal behavior. It is due to the boundary between normal and outlying behavior is often not precise. Thus, an anomaly observation situated close to the boundary may be normal or abnormal. 2) While anomaly is arising due to the malicious deed, these malicious rivals often accommodate themselves to appear abnormal behavior as normal so the task of labeling normal behavior region becomes more difficult. 3) Current notion of normal behavior might not be sufficiently represented in the future. Means For different application domains the exact view of anomaly is dissimilar. For example, a small variation in normal reading might be diseases in the medical domain. Whereas, in the stock market domain small variation might be considered normal. This makes it complex to apply a particular domain technique to another domain. 4) The exact notion of an anomaly is different for different video surveillance video data-sets. 5) Availability of labeled data for training/validation. 7) Action pattern variations within the same class Environmental variations and noise Normal behavior keeps evolving. And the Actual Challenges found while performing experiments are: 1) Limited labeled data 2) Ambiguous definition of abnormal 3) Expensive feature engineering steps. 4) Abnormal events are challenging to obtain due to their rarity. Massive variety of abnormal events, manually detecting and labeling such events is a difficult task that requires much manpower. 5) Small objects in the wide data-set may behave like normal objects rather than anomalous.

5. Proposed Time Distributed ConvLSTM

The TDSTConvLSTM model work on context dependent and compare the result with benchmark data-set. The main objective of the research is to detection, localize and identify the anomaly object to provide security in surveillance video. Detecting an anomalous event in long sequence video is challenging. Due to the ambiguity of how strongly such events are defined, the accuracy of the object recognition in the video improves in order to achieve a better result with the reference data set. Achieve a better result with benchmark data-set. Optimize the model parameters and Compare results with benchmark data-set. Achieve better feature identification and representation. Train a model which is able to detect anomalies which are not significantly distinct from normal events.

1) Working of the Model:

A ConvLSTM is a variant of LSTM recurrent network. In ConvLSTM the internal matrix multiplication is replaced by convolutional operation, which allows the data through the ConvLSTM cells to keep the input dimension rather than just a one-dimensional vector with a function. The ConvLSTM also replaces fully connected layer operators with convolution operators [23-25, 41]. Figure-6 shows the final encoding and decoding for prediction network of Time distributed ConvLSTM. ConvLSTM use convolution operators for input to state and state to state connections. By replacing the convolution operators with an LSTM memory cell, the ConvLSTM model can

therefore know which information from the previous state of the cell should be "remembered" or "forgotten" with the help of its forgetting gate. ConvLSTM also determines what information should be saved in the current state of the cell. The ConvLSTM process is described similarly to equations (1-5) is used to calculate the LSTM storage space. We have used these equations of basic Convolution LSTM and created new equations for hybrid Time Distributed ConvLSTM (eq1 -eq6).

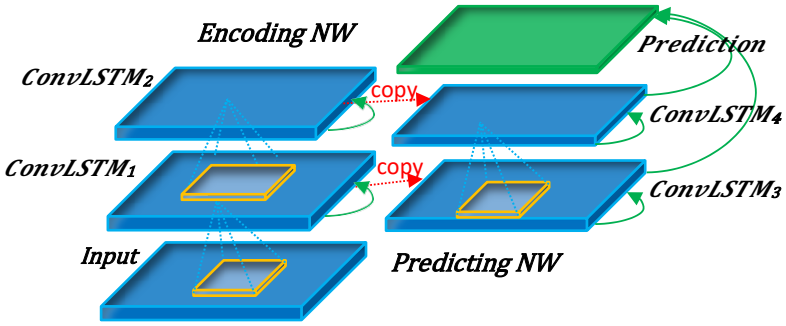

Figure 6: *Time Distributed ConvLSTM encoding and decoding for prediction*

The difference with TimeDistributed ConvLSTM is that the input vector xt is supplied as images (i.2D or 3D matrices), with each weight in the connection being replaced by convolution filters. The intermediate state (of time steps) is analogous to the movement between frames.

2) Algorithm of working model

Algorithm 1 Training algorithm for Time Distributed ConvLSTM Encoder–Decoder

Input: Set of the sequential input range $X = \{\overrightarrow{X_1}, \overrightarrow{X_2}, \vec{X}, \dots, \overrightarrow{X_t}\}$

Output: Set of the sequential output range $Y = \{\vec{Y}, \overrightarrow{Y_2}, \overrightarrow{Y_3}, \dots, \overrightarrow{Y_t}\}$

Initialize network parameters by Xavier initializer

$$W \sim U\left[-\frac{\sqrt{6}}{\sqrt{X_t+X_{t+1}}}, \frac{\sqrt{6}}{\sqrt{X_t+X_{t+1}}}\right]$$

while the loss has not converged do

Compute loss between X and Y using Euclidean distance

$$E(X,Y,t) = \| I(X,Y,t) - fw(I(X,Y,t)) \|_2$$

Update parameters by ADAM optimizer

end while

Here Xavier algorithmic used for weight initialization and Adam optimization used with a learning rate of 0.0001. When the learning loss stops decreasing, we attenuate it to 0.00001 and set the epsilon value to 0.000001. The distance between the frames are matured with the Euclidean distance algorithm. Then after reconstruction cost is calculated.

3) General Architecture:

The TimeDistributed layer provides exactly what we need. The generated allConv2D blocks are trained for the recognition we want, so our frames are processed to recognize things that are not simple object recognition, but things that "change" from frame to another frame. Figure-7 shows the

Time Distributed spatiotemporal ConvLSTM autoencoder. It is a neural network trained to reconstruct the input data. The TSConvLSTM autoencoder consists of two parts, Encoder and decoder. The ConvLSTM Encoder is able to learn a valid representation of the input(X), called $g(\phi)$ encoding. The last layer of the encoder is called the bottleneck(z) and contains the input representation $f(\phi)$. The ConvLSTM Decoder is use bottleneck coding to reconstruct the input data $R = f(g((\phi)) = X'R$.

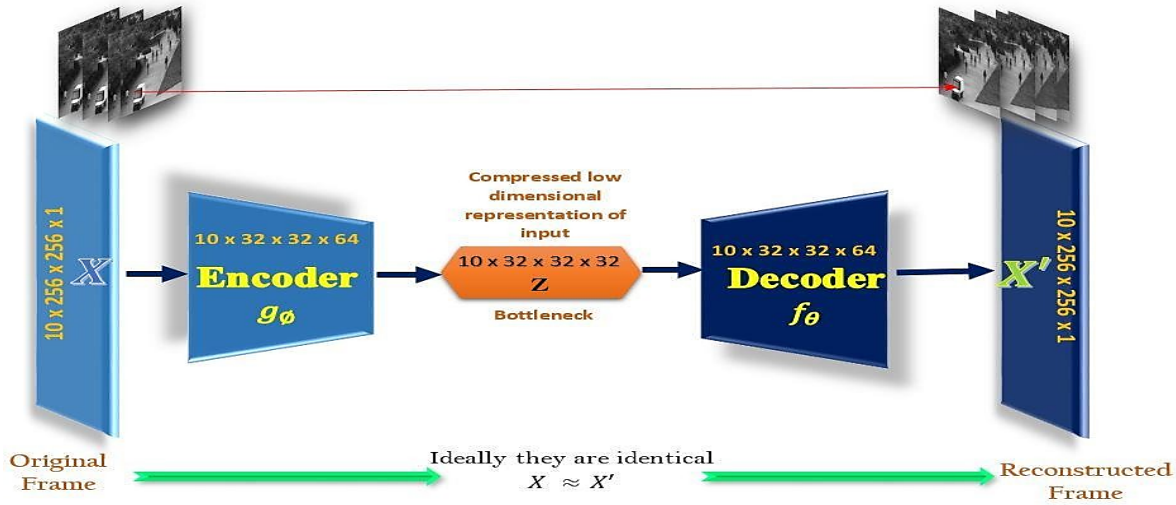

Figure 7: *Framework of Time Distributed spatiotemporal ConvLSTM N/W*

4) Collect Datasets & Analysis

It is expected that the trained anomaly detection model can be directly applied to multiple scenes with different perspectives; however, the existing data sets almost only contain videos recorded with fixed-angle cameras, which lack the diversity of scenes and angles. We summarize all anomaly detection data sets as follows: The data set Pedestrian 1 (Ped1) contains 34 training videos and 36 test videos, including 40 irregular events. All these unusual incidents involve vehicles such as bicycles and cars. Figures-8 and 9 show some examples of anomalies that are available in the UCSD data sets Ped1 and ped2.

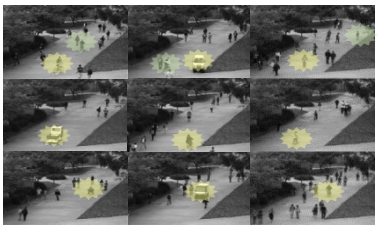

Figure 8: *UCSD PED1 dataset- Unlike normal training video streams, this scene consists of a small cart, Car, tempo, Cyclist, Wheelchair as well as a person skater*

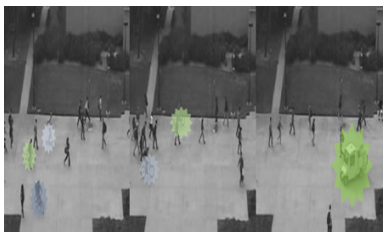

Figure 9: *UCSD PED2 dataset- Unlike normal training video streams, this scene consists of a small cart, Car, tempo, Cyclist, Wheelchair as well as a person skater*

Figure 10: *Shanghaitech dataset with different classes of anomalies*

The data set Pedestrian 2 (Ped2) contains 16 training videos and 12 test videos, including 12 abnormal events. The definition of Ped2 anomaly is the same as Ped1. The ShanghaiTech dataset is a collection of 13 scenes with complex lighting conditions and camera views in Shanghai University

of Technology. It consists of 437 videos, each with an average of 726 frames. The training set contains 330 normal videos, and the test set contains 107 videos and 130 anomalies. Unusual events include unusual patterns on campus, such as cyclists or cars. https://svip-lab.github.io/dataset/campus_dataset. Figure-10 shows some of the available anomaly examples in the ShanghaiTech dataset.

Table 2: *Video Anomaly Detection Dataset*

Dataset	Total Frames	Training Frames	Testing Frames	Anomalous Events	Anomaly Type	Irregularity	Regularity	Ground Truth	Resolution
UCSDPed1	14,000	6,800	7,200	54	5	4,005	9,995	Spatial, Temporal	238 x 158
UCSDPed2	4,560	2,550	2,010	23	5	1,636	2,924	Spatial, Temporal	360 x 240
CUHKAvenue	30,652	15,328	15,324	47	5	3,820	26,832	Spatial, Temporal	640 x 360
Shanghai-Tech	3,17,398	2,74,515	42,883	130	13	17,090	3,00,308	Spatial, Temporal	856 x 480

CUHK Avenue data set contains 16 training videos and 21 test videos, a total of 47 anomalies Incidents, including throwing objects, loitering and running. The size of the person can vary according to the position and angle of the camera. The subway data collection takes a total of 2 hours. There are two categories: entry and exit. Unusual experiences include going in the wrong direction and wandering. More importantly, this data set was recorded indoors, and the above data was recorded outdoors. https://data.world/datasets/subway. The metadata of the benchmark datasets is shown in Table 2 and the distribution of the dataset by domains is shown in Figure-11.

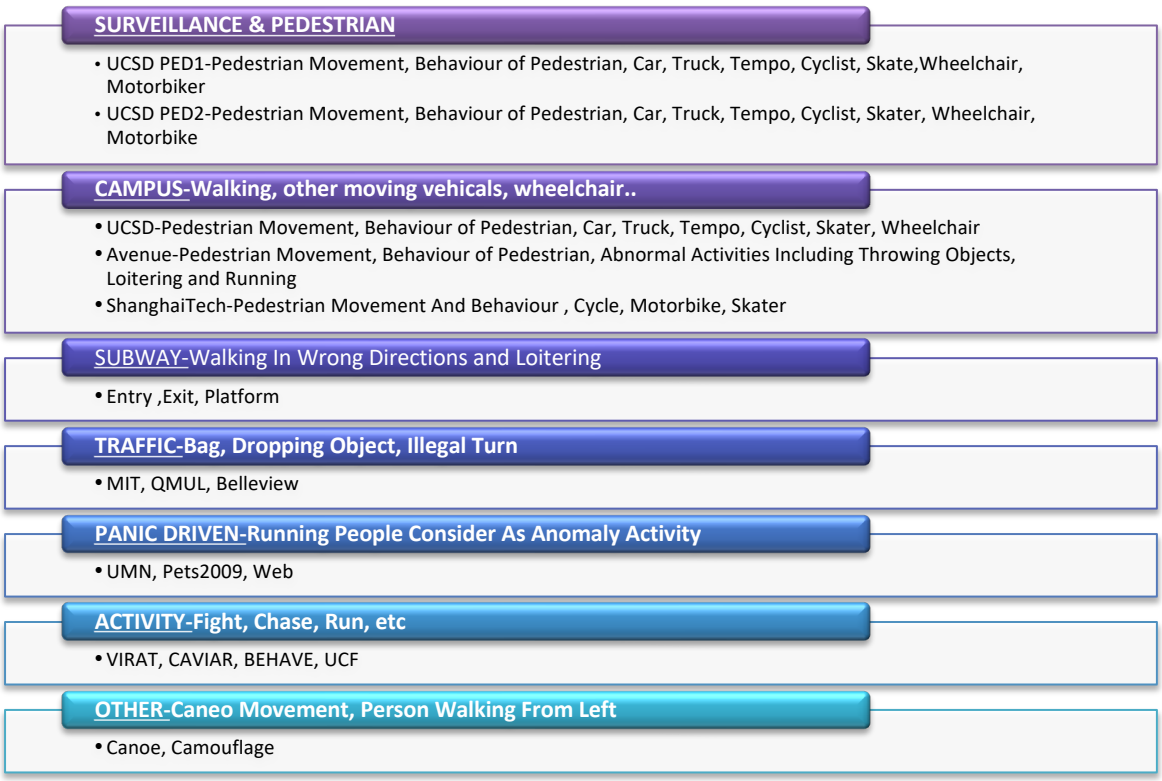

Figure 11: *Datasets available by domain type*

5) Hybrid TimeDistributed ConvLSTM:

The workflow of the existing approach (Figure-12) involves streams (spatial and temporal) that

learn features during the encoding after which decode to generate reconstructed sequences from the video frame sequences. During Training our autoencoder trains on normal records through reconstruction so we are considering this as an unsupervised learning approach. When an abnormal event occurs, the corresponding reconstruction error score is higher than the normal data because the model did not follow the irregular pattern through training. Moreover, Features of the spatial model's convolution layer to identify pathways that could help better understand and represent the learning process of the model at the object level.

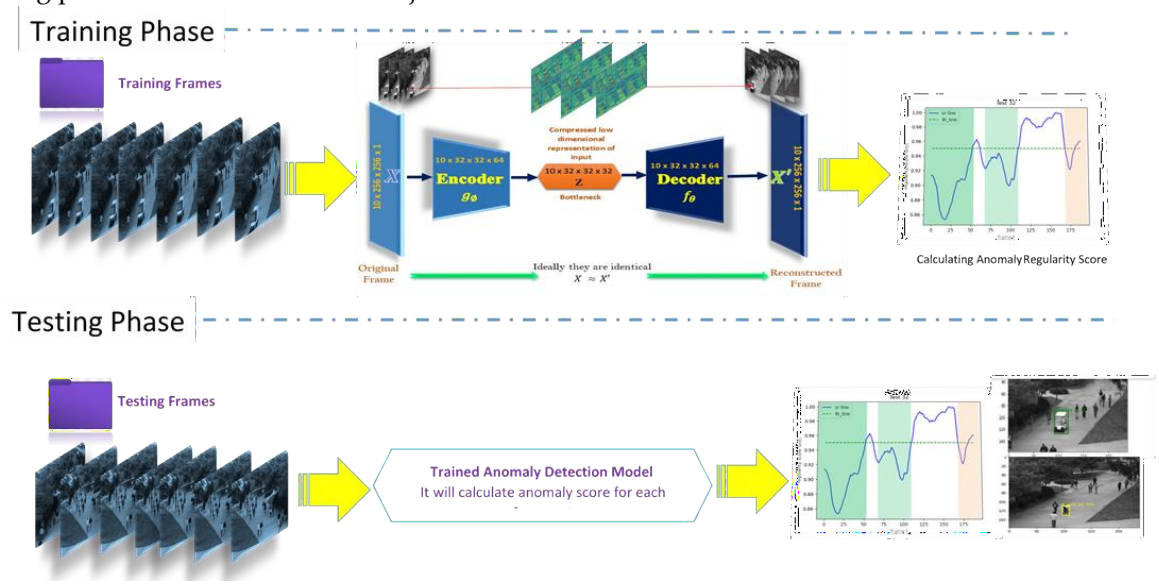

Figure 12: *Pipeline of the Time Distributed spatiotemporal ConvLSTM*

6) Reconstruction based on auto-encoder:

The input to the two-channel network is normal video frames. We trained the model and calculated the reconstruction error between the original frame sequence and the newly reconstructed frame sequence. The reconstruction error is used to calculate the regularity score, which can be further evaluated for the recognition performance. Our approach generates reconstruction errors for the spatial and temporal flows during the testing phase and then merges them accordingly. Our approach has three main steps.

a) Pre-processing: Several video clips were used to build and test the model, which vary in size, recording time and resolution. We decomposed the anomaly detection dataset into a sequence of video frames and normalized the video frame size to 256 x 256 pixels. To ensure that all input video frames are at the same scale, we compute the average pixels of the training image. We then subtract each frame from the global average for normalization. We also convert the image to grayscale to reduce the dimensionality. Due to the large number of training parameters and the limited training dataset, we used the data augmentation method [29] to expand the training dataset in time. frames (for example, in a cube at step 1, all T-frames are sequential, while at step 2 and step 3, the cubes skip one and two video frames, respectively) example of various skipping stride of s1[10]= [1,2,3,4,5,6,7,8,9,10] and s2[10]=[1,3,5,7,9,11,15,17,19,21], s3[10]=[2,4,6,8,10,12,14,16,18,20]. Once data augmentation done, we move for training and building model.

b) Training and testing: The encoder accept a sequence of input frames in chronological order. Two encoders are created here, a spatial encoder and a temporal encoder. The abstract features collected by Spatial Encoder are transmitted to Temporal Encoder to identify motion encoding.

Training and test datasets First, the data set is divided into two parts: train set and test set. The training set only contains videos with regular movements, and we included mixed videos with regular and irregular movements in the test set. The working principle of this model is as follows. Contains only normal motion patterns, no videos with abnormal motions,

$$X_{taining} \in \mathbb{R}^{N training \times R \times C}$$

In given a frame testing sequence from video, which likely to contain anomalies,

$$Y_{testing} \in \mathbb{R}^{N testing \times R \times C}$$

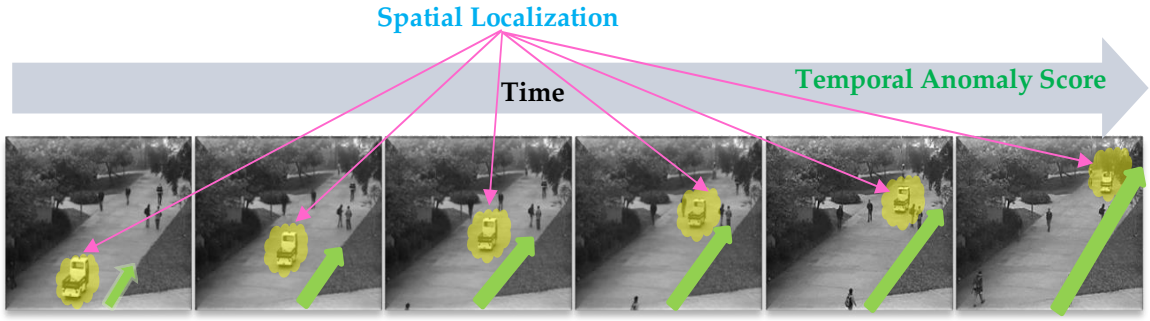

Figure 13: *Imagining anomalous regions and temporal anomaly score*

The problem is to assign an anomaly score to the temporal variation (time change of each frame), and a space score (spatial score) to locate anomalies in space, as shown in the below figure-13. When there is no direct information or guidance available for the positive rare category, the task of detecting anomalies is generally considered to be unsupervised; however, there are no abnormal samples. For,

$$R = \{X_i, Y_i\}, i \in [i, N], where\ Sample\ Y_i = 0$$

In below equations consider "⊛" for convolution operation, and "∘" for Hadamard product. LSTM is the special form of ConvLSTM, so ConvLSTM can be used as the LSTM. Input and state at a timestamp are 3D tensors. Convolution is used for both the input-to-state and state-to-state connection. Hadamard product is used to keep the constant error carousel property of cell.

$$i_t = \sigma(W_i \circledast x_t + U_i \circledast h_{t-1} + V_i \circledast C_{t-1} + b_i) \quad (eq1)$$
$$f_t = \sigma\big(W_f \circledast x_t + U_f \circledast h_{t-1} + V_f \circledast C_{t-1} + b_f\big) \quad (eq2)$$
$$g_t = tanh\big(W_g \circledast x_t + U_g \circledast h_{t-1} + b_g\big) \quad (eq3)$$
$$o_t = \sigma(W_o \circledast x_t + U_o \circledast h_{t-1} + V_o \circledast C_{t-1} + b_o) \quad (eq4)$$
$$C_t = f_t \circ C_{t-1} + i_t \circ g_t\, x \quad (eq5)$$
$$h_t = o_t \tan(C_t) \quad (eq6)$$

As shown in above Figure-13 we have done experimentations on pedestrian dataset so we have used here UCSD Ped1 & Ped2, for Campus Test Avenue and ShanghaiTech are used in experiment. Once we collect the benchmark datasets prepare it for training. So, here preprocess is required to convert video data into frame sequence. So, the whole video is divided into sequence of frames of each size 10fps through Sliding window technique, for example The UCSD Ped1 have Video-1 we have converted into consecutive 200 frames of size 256 x 256 and same way we have generated all frames for all the datasets. Also, we have use scale the frames between pixel value 0 and 1 by dividing each pixel by 256.

c) Learning Features: we use spatial sequence to study the appearance, and we use temporal sequence to find out the temporal consistency in adjacent video frames. The temporal model consists of three parts:

convolutional layers, decoding layers, and the convolution long short-term memory. (ConvLSTM2D). A Convolutional Layer is used to examine the spatial or behavioral characteristics of each frame. The convolution layer is used to learn spatial features, and the Deconvolution layers used to restore the original input size and the ConvLSTM layer outperforms the temporal rules of video. Our spatial model is similar to the temporal model, but the spatial model lacks the Conv LSTM layer, and its input is represented as a single frame rather than sequential frames.

i) Spatial model: Table 3 demonstrations the detailed configuration of the proposed spatial model. It consists of only three layers of folding followed by two layers of deconvolution to improve efficiency. Since anomaly detection focuses more on low-level contours and edge features, only the spatial model is used and uses three layers of convolution for feature extraction. On the other hand, the role of the deconvolution layer is to generate reconstructed video frames and to condense the sparse inputs through operations with multiple filters. Therefore, the spatial size of the output feature maps of a deconvolution layer is larger than the spatial size of its corresponding inputs. Therefore, we extract the appearance of the person in the video through the three-layer convolution layer and restore the initial input dimensions through the two connected deconvolution layers using the layer parameter set through the training process. During the training phase, the learnable parameters were updated in the direction of minimizing the loss function. We use the loss of MSE based on the sigmoid function. By calculating the partial derivatives of the loss function, we were able to update the parameters in an Adam scheme. The process of learning feature is an important step in training a model. At the encoding stage, the model learns the spatial characteristics of the observed object in the video frame and important background information in the observed scene. The inputs and the spatial architecture is relatively simple. The algorithm for visualizing the feature map must make the "black box" of the spatial model transparent, understand the learning process of the model, and trust the final detection result.

ii) Temporal model: The temporal model can have the same formula, but different classes depending on the LSTM requirements. To better examine temporal consistency in adjacent frames, we added three Time Distributed ConvLSTM layers between convolution and deconvolution layers (Figure-14).

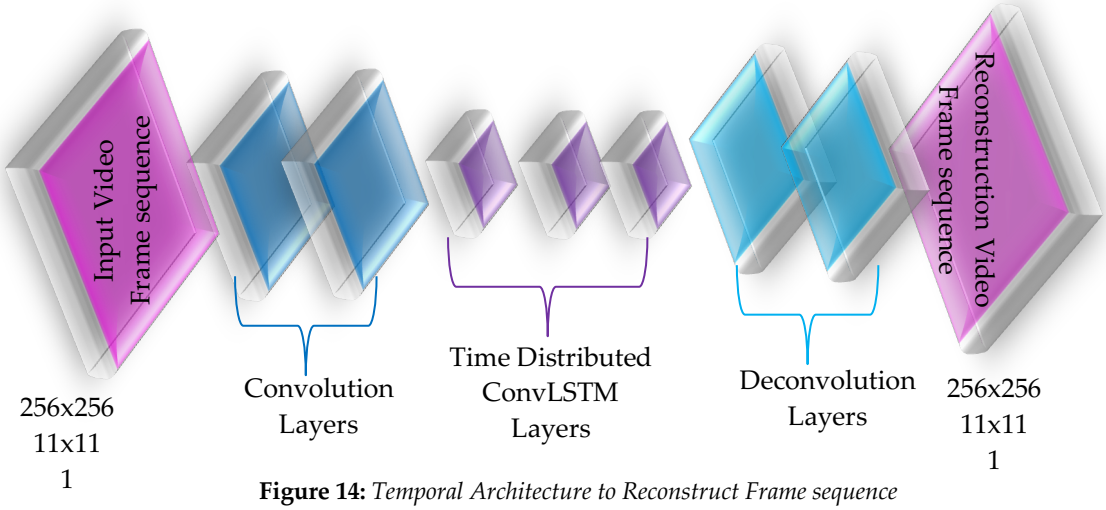

Figure 14: *Temporal Architecture to Reconstruct Frame sequence*

All three layers are equal, and the main difference lies in the number of convolution kernels. ConvLSTM is used to capture the spatiotemporal relationship in the data set. The difference between ConvLSTM and LSTM is that ConvLSTM changes the way LSTM switches from Hadamard product to convolution. The equations 1-5 are re-written as below equations (eq1-eq6). The proposed TSConvLSTM can predict the progress of a video sequence from a large number of input frames. Afterwards, the Regularity Score (RC) estimates come from a set of predicted reconstruction errors (RE). Abnormal video sequences produce lower regularity Scores because they deviate more from the actual sequence over time. The model uses composite structures and examines the influence of

conditions on more meaningful learning. The best model is selected based on the accuracy of reconstruction and prediction. The 2DConvLSTM model performs qualitative and quantitative evaluation and displays the competitive results on the anomaly detection data set. The 2DconvLSTM blocks have proven to be an effective tool for modeling and predicting video sequences.

d) Reconstruction & Regularity Score: After obtaining the reconstructed sequence of the video frame, we calculated its reconstruction error between the original video frame sequences and the reconstructed frame sequences to model the probability distribution of the standard data. In our proposal, the reconstruction is a stochastic process which considers the distance between the reconstruction and the original video frame and the variability of the distribution itself. Here to find the distance between the two pixels of original and reconstructed frame Euclidian Distance is used. To qualitatively analyze whether our model can detect anomalies well, we used the regularity score table to indicate our model's ability to detect anomalies and the smoothness score corresponds to the normal level of each frame of the video sequences.

i) In run-through, we first counted the reconstruction error of the video frame before getting the regularity score $sr(t)$. We calculated the reconstruction error of the pixel intensity value I at the location (x, y) in frame t as follows:

$$E(x,y,t) = \| I(x,y,t) - fw\big(I(x,y,t)\big) \|_2 \qquad (eq7)$$

Where f represents our two-stream model. We calculate the Euclidean distance between the initial pixel of the $t-th$ frame and the pixel of the reconstructed frame as the reconstruction error of the pixel. For each frame, we compute the reconstruction error probability by summing up all the pixel-based probabilities.

ii) Reconstruction error of consecutive frames of unlabeled frame sequence

$$E(t) = \sum_{(x,y)} E(x,y,t) \qquad (eq8)$$

iii) $Sequence\_Reconstruction\_Cost(t)$

$$SrC(t) = \sum_{t'=t}^{t+10} E(t') \qquad (eq9)$$

iv) Abnormality Score $Sa(t)$ is scaling between 0 and 1

$$S_a(t) = \frac{Sequence\ Reconstruction\ Cost(t) - Sequence\ Reconstruction\ Cost(t)_{min}}{Sequence\ Reconstruction\ Cost(t)_{max}}$$

$$S_a(t) = \frac{S_rC(t) - S_rC(t)_{min}}{S_rC(t)_{max}} \qquad (eq10)$$

v) Regularity Score $Sr(t)$-The abnormality score $Sa(t)$ corresponds to the level of abnormality of each frame in the video, which plays a role in indicating the confidence of detection results. On the other hand, the regularity score Sa(t) corresponds to the level of normality can be defined as follows:

$$S_r(t) = 1 - S_a(t) \qquad (eq11)$$

Assume that the regularity score of the current frame is relatively low. If there is no abnormal event in the video frame, the regularity score of the frame should be high. Also, in other-hand, if the regularity score is low then the possibility of abnormality in the video frame is also relatively high.

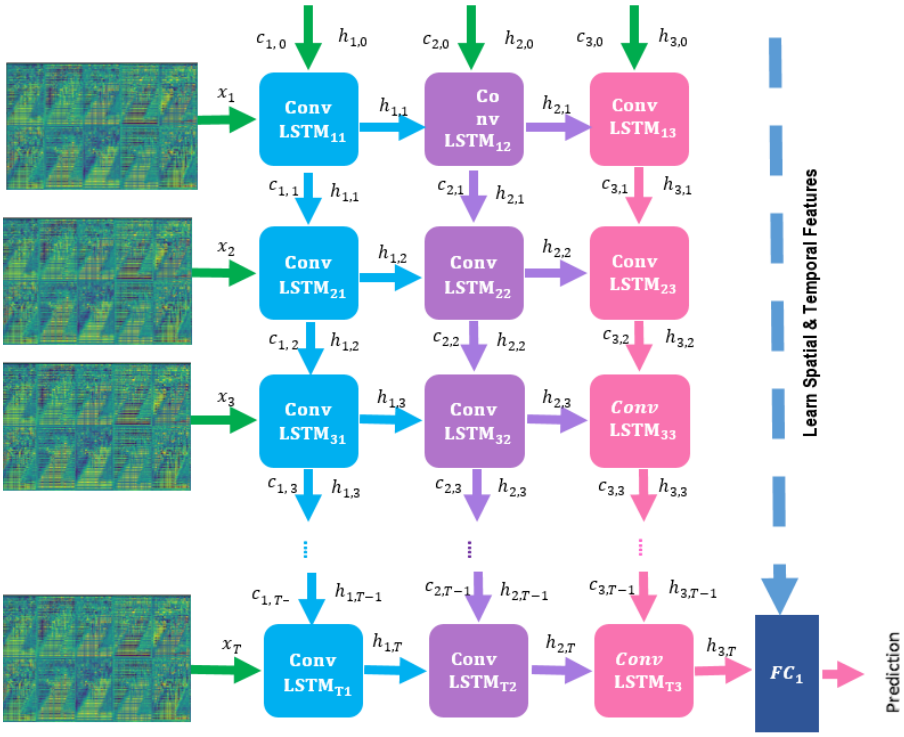

Figure 15: *Layer view of TSConvLSTM Model*

6. Experiment and Results:

1) Data Preprocessing and Model Configuration:

We analyze the overall performance of the proposed approach Time Distributed Spatiotemporal ConvLSTM mainly in relation to a surveillance dataset: UCSD Anomaly Detection Datasets, ShanghaiTech, and CUHK Avenue dataset. The UCSD anomaly detection dataset was collected with a fixed camera mounted on an elevated position overlooking the Campus pedestrian walkway. The density in the broad walkway can vary. Both the UCSD Ped1 and Ped2 datasets contain a train set and a test set. In particular, Ped1 contains 34 train video sequences and 36 test video sequences. The frame resolution is 256 × 256 pixels. In Ped1, people walk to and from the camera to create a foreshortening effect. UCSD Ped2 contains 16 train video sequences and 12 test video sequences with pedestrian traffic parallel to the camera plane. Frame resolution - 256 x 256 pixels. All frames in the train set are normal and contain only pedestrians. In addition to the normal frames, the test set had unusual frames in which cyclists, skaters, minivans, tempo, cars, wheelchairs, or people walking on the lawn were unusual. The second is ShanghaiTech Facility dataset to evaluate Time Distributed Spatiotemporal ConvLSTM method. The ShanghaiTech Campus dataset consists of 13 scenes with 107 items individual sets, each with complex lighting and camera angles. Each color block has a resolution of 856 x 480 pixels. As with the UCSD dataset, all train videos are normal and contain only pedestrians, and the test frames for each scene contain abnormal images All tests are performed on a dedicated server with a GPU with an Intel(R) Processor Core (TM) i7-7700HQ running at 2.80 GHz, 16 GB RAM, Nvidia GeForce GTX 1070 GPU running the Windows 10 operating system also with Ubuntu 16.04 it works well. We use the Python library, which is an open-source machine deep learning library for Python, to implement our anomaly detection architecture. We compared the s Time Distributed Spatiotemporal ConvLSTM with several

advanced video anomaly detection baselines trained with regular videos only and focused on the default unsupervised learning setup. Anomaly detection in all datasets using the AUROC scale is presented in Table 3. Table 3 shows a comparison with other methods using four benchmarks. Our approach delivers competitive or superior results without using a pre-trained network, and Time Distributed Spatiotemporal ConvLSTM improves performance over the well-designed Bansod et.al, 2019 [39], ConvLSTM [14], ITAE [31], ConvLSTMAE [15]. In the CUHK database ConvLSTM [45], MLEPFP [46], ConvLatentAE [44], Wan et.al, 2021 [37] a prediction-based method that stores and updates normal query functions for each memory module.

2) Parameter Selection

Table 3: *Parameter Selection*

Parameter Selection: Input Length, output Length, kernel Size, Type of Normalization, Output Nonlinearity
Conv kernel -(11 x 11 x 1 x 128)
Conv kernel -(5 x 5 x 128 x 64)
Conv kernel -(3 x 3 x 64 x 32)
ConvLSTM-(3 x 3 x 32 x 256) **Recurrent kernel** -(3 x 3 x 64 x 256)-TanH
ConvLSTM-(3 x 3 x 64 x 256) – **Recurrent kernel** -(3 x 3 x 64 x 256)-TanH
ConvLSTM-(3 x 3 x 64 x 256) –**Recurrent kernel** -(3 x 3 x 64 x 256)-TanH
Conv Transpose kernel -(3 x 3 x 32 x 64)
Conv Transpose kernel -(5 x 5 x 64 x 32)
Conv Transpose kernel -(5 x 5 x 128 x 64)
Conv Transpose kernel -(11 x 11 x 128 x 64)
Conv kernel -(11 x 11 x 128 x 1)-Sigmoid

Model Parameters the input videos are converted into sequence of frames and that individual frame converted to grayscale and resized to 256 x 256 pixels. A preliminary Conv-LSTM Encoder-Decoder baseline model was evaluated for use as reference in parameter selection. The baseline model utilizes an input and output length of five, and divides the image into non-overlapping patches. Using the model from [45,48] as reference, but with modification in filter size of 11 x 11, 5x5 and 3 x 3 and three Time Distributed ConvLSTM layers are used, while the total number of filters are 128, 64, 32 respectively to the encoder and transpose decoder to accommodate the larger frame sequence. The Time Distributed ConvLSTM units use recurrent activation sigmoid nonlinearities for the input, output and forget states, and tanH for the hidden and cell states. A sigmoid non-linearity is applied to the final Time Distributed convolutional layer. Due to case insensitivity the "same padding" method means, zeros evenly to the left/right or up/down of the input such that reconstruct frames has the same height/width dimension as the input frames is applied during all convolution operations to retain the frame size.

The baseline model is simpler than the complex Time Distributed ConvLSTM and utilizes only a future decoder. The parameters tested in variations of the TDSTConv LSTM model include the length of both the input and output timestamps, the filter size, and the final output non-linearity function, as shown in Table-1. A filter size of 3x3 was considered for capturing smaller motions, but was not as effective. The commonly used sigmoid nonlinearity function was tested at the final output, but ultimately, the parameters used by the baseline model were found to be the most effective. The parameters were applied to the proposed composite models and evaluated for

accuracy with respect to the baseline model, as shown in Table 3. The composite models have a lower MSE per frame with the unconditioned model performing slightly better.

3) Evaluation parameter of Anomaly Detection Experiments

Quantitative Analysis: Frame-Level AUC. To better compare with other methods, all the experiments are carried out on the same work station with Intel Intel(R) Core (TM) i7-7700HQ CPU @ 2.80GHz 2.80 GHz, NVIDIA GTX 1070, and 16G RAM. If a frame contains at least one abnormal event, it is considered as a correct detection., Detection is compared to the frame-level ground-truth label. The area under the curve (AUC) is the evaluation metrics. Furthermore, some contemporary documents [9, 10] believe that the EER evaluation criteria are a severe sample imbalance between normal and abnormal events. Using EER as an indicator will be misleading in practical applications. We agree with this view and use AUC for evaluation, assuming that the local minimum within 50 frames belongs to the same abnormal event. A temporal window of 50 frames before and after distinct local minima is used to propose anomalous regions, as most anomalous activities are at least one hundred frames long. The proposed local minimum regions within fifty frames of each other are connected to obtain the final abnormal temporal regions. These minima are then considered to be a part of same abnormal event. We consider a detected abnormal region as a correct detection if it has at least fifty percent overlap with the ground truth/ fact table. According to Kozlov et al., 2013 A parameter-sweep at intervals of .05 is performed to determine the threshold parameter for the Persistence1D algorithm.

4) Efficiency Analysis of Model

Table 3 presents the AUC of our method and a series of state-of-the-art methods [5, 6, 8, 11] on the Avenue, the UCSD Ped2, and the Subway Entrance and Exit datasets. As expected, our model performs the best performance on the avenue and subway entrance and exit datasets. In addition, although the version in Avenue and Ped datasets appears to be slightly lower than that in the other complicated architectures, it is still significantly higher than that of lightweight models and that single-level models. These results indicate that a multilevel model [8] or 3D indicator [6] can perform better in crowd scene, such as the UCSD Ped2 dataset. However, the time cost of these methods was also higher. Besides, comparing our spatial model and temporal model and the fusion model, temporal and spatial model have their advantages and disadvantages. Still, the fusion model performs better than the former two on all data sets.

5) Optimization and Initialization

The cost function of equation (eq9) was optimized with Adam optimization. Adam optimization is a stochastic gradient descent method that is based on adaptive estimation of first-order and second-order moments and it was empirically chosen as the most effective. After all the experiments the learning rate of $1e-4$, decay rate of $1e-5$ and epsilon $1e-6$ were finalized. The detailed parameters are shown in table 4. We used a mini-batch of five video sequences and trained the models for up to 25,000 iterations. Early stopping was performed based on the validation loss if necessary. The weights were initialized using the Xavier Weight Initialization. It automatically scales the initialization based on the number of input and output neurons to prevent the weights from starting out too small or large, and vanish or explode in magnitude. The input to-hidden and hidden-to-hidden convolutional filters in the TDSTConvLSTM units all use the same filter size.

Table 4: *The Final Parameter value settings of TDSTConvLSTM*

Parameter Type and value								
Height	Width	Batch size	Learning Rate	Epoch	Optimizer	Stride	Loss	decay
256	256	4	$1e-4$	200	Adam	4	MSE	$1e-5$

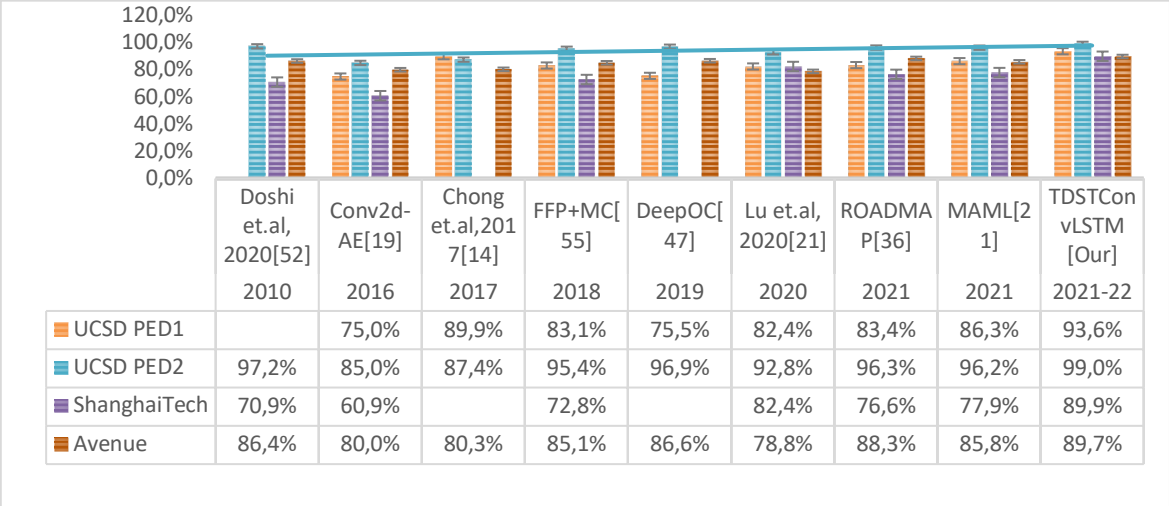

	Doshi et.al, 2020[52]	Conv2d-AE[19]	Chong et.al,2017[14]	FFP+MC[55]	DeepOC[47]	Lu et.al, 2020[21]	ROADMAP[36]	MAML[21]	TDSTConvLSTM [Our]
	2010	2016	2017	2018	2019	2020	2021	2021	2021-22
UCSD PED1		75,0%	89,9%	83,1%	75,5%	82,4%	83,4%	86,3%	93,6%
UCSD PED2	97,2%	85,0%	87,4%	95,4%	96,9%	92,8%	96,3%	96,2%	99,0%
ShanghaiTech	70,9%	60,9%		72,8%		82,4%	76,6%	77,9%	89,9%
Avenue	86,4%	80,0%	80,3%	85,1%	86,6%	78,8%	88,3%	85,8%	89,7%

Figure 16 : *Performance comparison AUC (%) of the anomaly detection result of TDSTCONVLSTM models with state-of-the-art methods on four benchmark datasets*

As shown in Figure-16 the area under the curve AUC of ROC (Receiver Operating Characteristic) curve is extensively used as a measure of the temporal localization of anomaly events. Since the anomaly detection can be taken into consideration as a binary type for each frame, the ROC curve is generated by applying distinct thresholds for the anomaly rating of every frame and calculating the TPR (True Positive Rate) and FPR (False Positive Rate).

6) Proposed Evaluation Criterion

As demonstrated by the experimental results on several video anomaly detection benchmark data sets and we achieve comparable performance contrast with the state-of-the-art unsupervised method with much less running time, indicating the effectiveness, efficiency, and robustness of our proposed approach. According to previous work [10, 12, 13] we evaluated our method by the area under the ROC curve (AUC). The ROC curve is obtained by varying the threshold value of the abnormality evaluation. A higher AUC value. Represents a more precise result of the anomaly detection. To ensure comparability between different methods, we calculated the AUC for the prediction at frame level. The Receiver Operating Characteristic (ROC) of the TimeDistributed Spatiotemporal ConvLSTM with UCSD

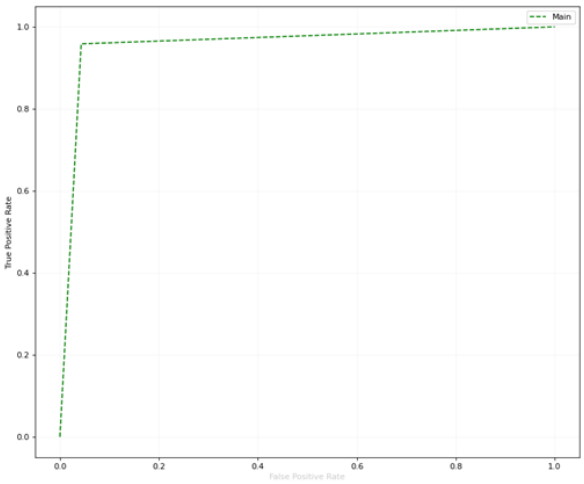

Figure 17: *ROC curve of a TDSTConvLSTM with UCSD Ped1 dataset*

Ped1 and Ped2, Avenue and ShanghaiTech dataset is shown in Figure-17. Figure-18 and 19 shows the Anomaly Regularity Score of Sets.

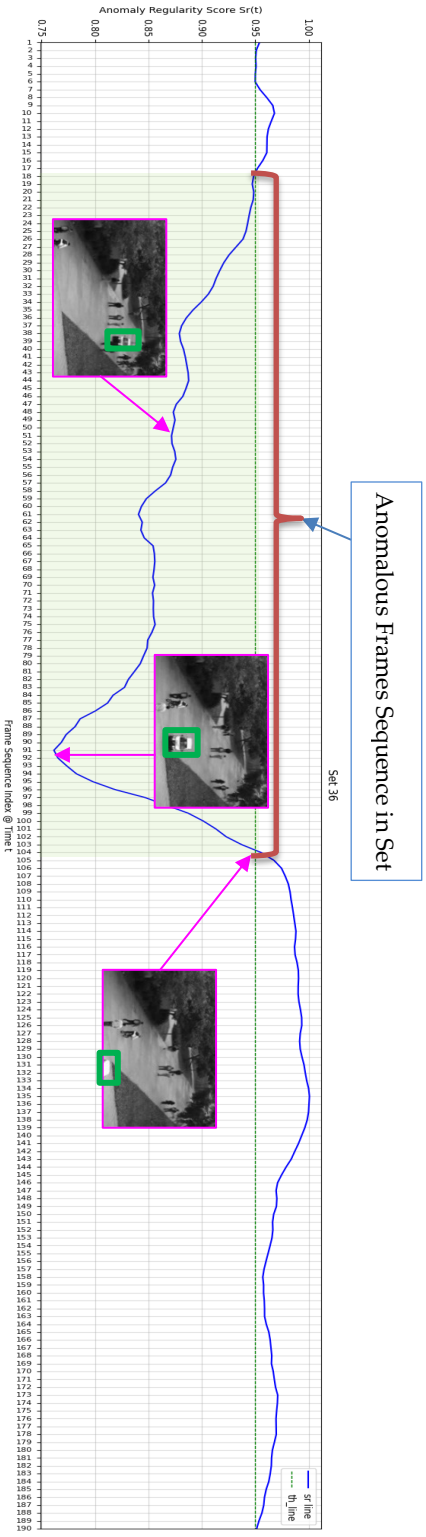

Figure 18: *Performance Analysis of set*

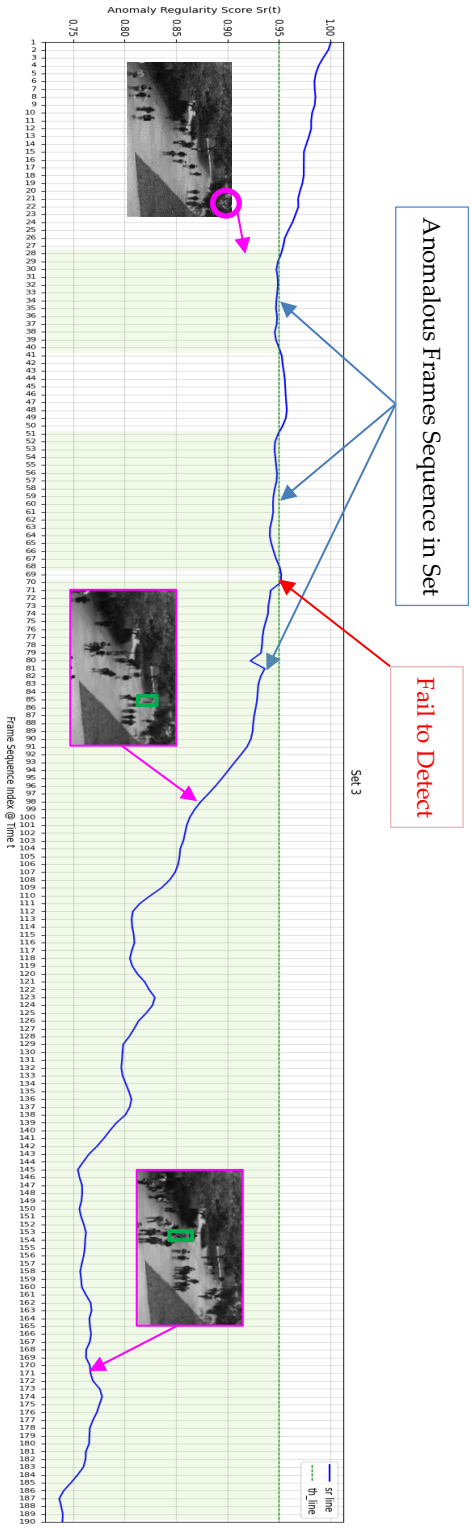

Figure 19: *Performance Analysis of set*

Conclusion

In this paper, we proposed a TDSTConvLSTM modeling of normal features based in a supervised manner for video anomaly detection. We designed the TDSTConvLSTM to implicitly capture representative static and dynamic information of normal scenes without using a pre-trained network. For the complex normality, using the latent features of TDSTConvLSTM, through an experiment on standard benchmarks, TDSTConvLSTM demonstrated high effectiveness in scenes where motion is abnormal by learning dynamic information of normal scenes. Furthermore, the normality modeling of the TDSTConvLSTM feature achieved superior results, especially when the database is extensive and composed of diverse scenes. The proposed method can be expected to model a general distribution and solve practical problems through a vast number of real-world videos with Semi supervised learning. Our results suggest that the proposed method enables fast and reliable detection of abnormal events, with label-free identification of abnormal events. Using only the spatial or temporal stream cannot cause the best result. However, with the information from the two-stream fused, the model has improved efficiency compared with a single stream, while the accuracy is also competitive. It should also be noted that our current model is lightweight and does not consider the complete appearance and motion of the video scenario. Therefore, the training process in our method does not reconstruct all the changes in the properties of appearance and motion, and it may be weak compared with other techniques in a particular dataset for example, GMFC-VAE in Ped2.

References

[1] Chandola V, Banerjee A, Kumar V. Anomaly detection: A survey. ACM computing surveys (CSUR). 2009 Jul 30;41(3):1-58.

[2] Patel P, Thakkar A. "Recent Advancement in Anomaly Detection in Surveillance Videos." International Journal of Recent Technology and Engineering 8, no. 2 (n.d.): 964–70. doi:10.35940/IJRTE.B1759.078219.

[3] Feldstein S. The global expansion of AI surveillance. Washington, DC: Carnegie Endowment for International Peace; 2019 Sep 17.

[4] Chong YS, Tay YH. Abnormal event detection in videos using spatiotemporal autoencoder. InInternational symposium on neural networks 2017 Jun 21 (pp. 189-196). Springer, Cham.

[5] Chong YS, Tay YH. Modeling representation of videos for anomaly detection using deep learning: A review. arXiv preprint arXiv:1505.00523. 2015 May 4.

[6] B. Antic and B. Ommer, "Video parsing for abnormality detection," in Proceedings of the International Conference on Computer Vision, Barcelona, Spain, November 2011.

[7] H. Mobahi, R. Collobert, and J. Weston, "Deep learning from temporal coherence in video," in Proceedings of the 26 th International Conference on Machine Learning, Montreal, Canada, 2009.

[8] W. Li, V. Mahadevan, V. NJIToPA, and M. Intelligence, "Anomaly detection and localization in crowded scenes," IEEE Transactions on Pattern Analysis and Machine Intelligence, vol. 36, pp. 18–32, 2014.

[9] K. Cheng, Y. Chen, and W. Fang, "Video anomaly detection and localization using hierarchical feature representation and Gaussian process regression," in Proceedings of the 2015 IEEE Conference on Computer Vision and Pattern Recognition, Boston, MA, USA, June 2015.

[10] R. Mehran, A. Oyama, and M. Shah, "Abnormal crowd behavior detection using social force model," in Proceedings of the 2009 IEEE Conference on Computer Vision and Pattern Recognition, Miami, FL, USA, June 2009.

[11] T. M. Hospedales, S. Gong, and T. Xiang, "A Markov clustering topic model for mining behaviour in video," in Proceedings of the International Conference on Computer Vision, Kyoto, Japan, October 2009.

[12] Y. Cong, J. Yuan, and J. Liu, "Sparse reconstruction cost for abnormal event detection," in Proceedings

of the 2011 IEEE Conference on Computer Vision and Pattern Recognition, Providence, RI, USA, June 2011.

[13] W. Liu, W. Luo, "Future frame prediction for anomaly detection—a new baseline," 2018

[14] Y. S. Chong "Abnormal event detection in videos using spatiotemporal autoencoder," 2017,

[15] W. Luo, W. Liu, and S. Gao, "Remembering history with convolutional LSTM for anomaly detection," in Proceedings of the International Conference on Multimedia and Expo, Hong Kong, China, July 2017.

[16] K. P. Adhiya, S. R. Kolhe, and S. S. Patil, "Tracking and identification of suspicious and abnormal behaviors using supervised machine learning technique," in Proceedings of the International Conference on Advances in Computing, Communication and Control, Mumbai India, January 2009.

[17] W. Sultani, C. Chen, and M. Shah, "Real-world anomaly detection in surveillance videos," 2018.

[18] BR Kiran, DM Thomas, R. Parakkal An overview of deep learning based methods for unsupervised and semi-supervised anomaly detection in videos. Journal of Imaging.4(2):36, 2018.

[19] M Hasan, Choi J, Neumann J, Roy-Chowdhury AK, Davis LS. Learning temporal regularity in video sequences. InProceedings of the IEEE conference on computer vision and pattern recognition pp. 733-742, 2016.

[20] Wang ZZ, Xie K, Zhang XY, Chen HQ, Wen C, He JB. Small-Object Detection Based on YOLO and Dense Block via Image Super-Resolution. IEEE Access.9:56416-29, Apr 9, 2021

[21] Lu Y, Yu F, Reddy MK, Wang Y. Few-shot scene-adaptive anomaly detection. InEuropean Conference on Computer Vision 2020 Aug 23 (pp. 125-141). Springer, Cham.

[22] M. Mathieu, C. Couprie, and Y. LeCun, "Deep multi-scale video prediction beyond mean square error," arXiv preprint arXiv:1511.05440, 2015

[23] Shrivastava A, Pfister T, Tuzel O, Susskind J, Wang W, Webb R. Learning from simulated and unsupervised images through adversarial training. In Proceedings of the IEEE conference on computer vision and pattern recognition 2017 (pp. 2107-2116).

[24] S. Xingjian, Z. Chen, H. Wang, and D. Yeung, "Convolutional LSTM network: A machine learning approach for precipitation nowcasting," in Advances in Neural Information Processing Systems, pp. 802–810.

[25] Essien A, Giannetti C. A deep learning model for smart manufacturing using convolutional LSTM neural network autoencoders. IEEE Transactions on Industrial Informatics. 2020 Jan 23; 16(9):6069-78.

[26] Chang, Y., Tu, Z., Luo, B., Qin, Q.: Learning spatiotemporal representation based on 3D autoencoder for anomaly detection. In: Cree, M., Huang, F., Yuan, J., Yan, W.Q. (eds.) ACPR 2019. CCIS, vol. 1180, pp. 187–195. Springer, Singapore (2020).

[27] Xu, D., Yan, Y., Ricci, E., Sebe, N.: Detecting anomalous events in videos by learning deep representations of appearance and motion. Comput. Vis. Image Underst. 156, 117–127 (2017)

[28] Yan, M., Meng, J., Zhou, C., Tu, Z., Tan, Y.P., Yuan, J.: Detecting spatiotemporal irregularities in videos via a 3D convolutional autoencoder. J. Vis. Commun. Image Represent. 67, 102747 (2020)

[29] Hinton, G.E., Salakhutdinov, R.R.: Reducing the dimensionality of data with neural networks. Science 313(5786), 504–507 (2006)

[30] Poultney, C., Chopra, S., Cun, Y.L., et al.: Efficient learning of sparse representations with an energy-based model. In: Advances in Neural Information Processing Systems, pp. 1137–1144 (2007)

[31] Rifai, S., Vincent, P., Muller, X., Glorot, X., Bengio, Y.: Contractive autoencoders: explicit invariance during feature extraction. In: International Conference on Machine Learning (ICML), pp. 833–840 (2011)

[32] Vincent, P., Larochelle, H., Bengio, Y., Manzagol, P.A.: Extracting and composing robust features with denoising autoencoders. In: International Conference on Machine Learning (ICML), pp. 1096–1103 (2008)

[33] Blanchard, G., Lee, G.: Semi-supervised novelty detection. J. Mach. Learn. Res. 11, 2973–3009 (2010)

[34] Xie, J., Girshick, R., Farhadi, A.: Unsupervised deep embedding for clustering analysis. In: International Conference on Machine Learning, pp. 478–487 (2016)

[35] A. Sodemann, M. P. Ross, B. J. Borghetti, A review of anomaly detection in automated surveillance, IEEE Transactions on Systems, Man, and Cybernetics, Part C (Applications and Reviews) 42 (6)1257–1272.

[36] Wang X, Che Z, Jiang B, Xiao N, Yang K, Tang J, Ye J, Wang J, Qi Q. Robust Unsupervised Video Anomaly Detection by Multipath Frame Prediction. IEEE Transactions on Neural Networks and Learning Systems. 2021 Jun 4.

[37] Wan B, Jiang W, Fang Y, Luo Z, Ding G. Anomaly detection in video sequences: A benchmark and computational model. arXiv preprint arXiv:2106.08570. 2021 Jun 16.

[38] Basora L, Olive X, Dubot T. Recent advances in anomaly detection methods applied to aviation. Aerospace. 2019 Nov;6(11):117.

[39] Bansod S, Nandedkar A. Transfer learning for video anomaly detection. Journal of Intelligent & Fuzzy Systems. 2019 Jan 1;36(3):1967-75.

[40] R. Chalapathy, S. Chawla, Deep learning for anomaly detection: A survey, arXiv preprint arXiv:1901.03407

[41] Priyanka P. Patel, Dr. Amit R. Thakkar, "Understand Long Short Term Memory for Sequential Data", IJAST, vol. 29, no. 08, pp. 2482 - 2491, Jun. 2020.

[42] X. Chen, B. Li, J. Wang, Y. Zhao and Y. Xiong, "Integrating EMD with Multivariate LSTM for Time Series QoS Prediction," 2020 IEEE International Conference on Web Services (ICWS), 2020, pp. 58-65, doi: 10.1109/ICWS49710.2020.00015.

[43] Patel, Priyanka P., and Amit R. Thakkar. "A Journey From Neural Networks to Deep Networks: Comprehensive Understanding for Deep Learning." Neural Networks for Natural Language Processing. IGI Global, 2020. 31-62.

[44] Ionescu, Radu Tudor, Fahad Shahbaz Khan, Mariana-Iuliana Georgescu, and Ling Shao. "Object-centric auto-encoders and dummy anomalies for abnormal event detection in video." In Proceedings of the IEEE/CVF Conference on Computer Vision and Pattern Recognition, pp. 7842-7851. 2019.

[45] Medel, Jefferson Ryan, and Andreas Savakis. "Anomaly detection in video using predictive convolutional long short-term memory networks." arXiv preprint arXiv:1612.00390 (2016).

[46] Liu, Wen, Weixin Luo, Zhengxin Li, Peilin Zhao, and Shenghua Gao. "Margin Learning Embedded Prediction for Video Anomaly Detection with A Few Anomalies." In IJCAI, pp. 3023-3030. 2019.

[47] P. Wu, J. Liu, and F. Shen, "A deep one-class neural network for anomalous event detection in complex scenes," IEEE transactions on neural networks and learning systems, 2019.

[48] X. Shi, Z. Chen, H. Wang, D. Yeung, W. Wong, W. Woo, Wangchun. "Convolutional LSTM network: A machine learning approach for precipitation nowcasting," in NIPS, pp. 802-810, 2015.

[49] Patel, Priyanka, and Amit Thakkar. "The upsurge of deep learning for computer vision applications." International Journal of Electrical and Computer Engineering 10.1 (2020): 538.

[50] Datta, Leonid. "A survey on activation functions and their relation with xavier and he normal initialization." arXiv preprint arXiv:2004.06632 (2020).

[51] Zhu, Sijie, Chen Chen, and Waqas Sultani. "Video anomaly detection for smart surveillance." arXiv preprint arXiv:2004.00222 (2020).

[52] Doshi, Keval, and Yasin Yilmaz. "Online anomaly detection in surveillance videos with asymptotic bound on false alarm rate." Pattern Recognition 114 (2021): 107865.

[53] Ramachandra, Bharathkumar, Michael Jones, and Ranga Raju Vatsavai. "A survey of single-scene video anomaly detection." IEEE Transactions on Pattern Analysis and Machine Intelligence (2020).

[54] Cho M, Kim T, Kim IJ, Lee S. Unsupervised Video Anomaly Detection via Normalizing Flows with Implicit Latent Features. arXiv preprint arXiv:2010.07524. 2020 Oct 15.

[55] Liu, Wen, Weixin Luo, Dongze Lian, and Shenghua Gao. "Future frame prediction for anomaly detection–a new baseline." In Proceedings of the IEEE conference on computer vision and pattern recognition, pp. 6536-6545. 2018.

[56] Zhu, S., Chen, C., & Sultani, W. (2020). Video anomaly detection for smart surveillance.

A QUASI SUJA DISTRIBUTION

Rama Shanker[1], Reshma Upadhyay[1], Kamlesh Kumar Shukla[2*]

[1]Department of Statistics, Assam University, Silchar, Assam, India, Email: shankerrama2009@gamila.com, resmaupadhaya@gmail.com

[2]Department of Mathematics, Noida International University, Gautam Budh Nagar, India
*Corresponding Author email: kkshukla22@gmail.com

Abstract

A two-parameter quasi Suja distribution which contains Suja distribution as particular case has been proposed for extreme right skewed data. Its statistical properties including moments, skewness, kurtosis, hazard rate function, mean residual life function, stochastic ordering, mean deviations, Bonferroni and Lorenz curves, Renyi entropy measures, and stress-strength reliability have been derived and studied. The estimation of parameters using method of moments and maximum likelihood has been discussed. A simulation study has been presented to know the performance of maximum likelihood estimation. The goodness of fit of the proposed distribution has been presented.

Keywords: Suja distribution, Statistical Properties, parameters estimation, Goodness of fit.

I. Introduction

The search for a suitable distribution for modeling of lifetime data is very challenging because the lifetime data are stochastic in nature. The analysis and modeling of lifetime data are essential in almost every fields of knowledge including engineering, medical science, demography, social sciences, physical sciences finance, insurance, demography, social sciences, physical sciences, literature etc and during recent decades several researchers in statistics and mathematics tried to introduce lifetime distributions. Recently, Sharma *et al* [1] studied comparative study of several one parameter lifetime distributions and observed that there are some datasets which are extreme skewed to the right where these distributions were not giving good fit. In the search for a new lifetime distribution which can be used to model data from various fields of knowledge, Shanker [2] proposed a one parameter distribution Suja distribution which is defined by its probability density function (pdf) and cumulative distribution function (cdf) given by

$$f(x;\theta)=\frac{\theta^5}{\theta^4+24}\left(1+x^4\right)e^{-\theta x};x>0,\theta>0 \tag{1.1}$$

$$F(x;\theta)=1-\left[1+\frac{\theta^4x^4+4\theta^3x^3+12\theta^2x^2+24\theta x}{\theta^4+24}\right]e^{-\theta x};x>0,\theta>0 \tag{1.2}$$

Shanker [2] studied its statistical properties, estimation of parameter using method of moment and method of maximum likelihood and applications to some real lifetime data and observed that Suja distribution gives much closer fit than several one parameter lifetime distributions. Recently, Al-Omari and Alsmairan [3] obtained length-biased Suja distribution and studied its statistical properties and applications. Al-Omari et al [4] proposed power lenth-biased Suja distribution and discussed its properties and applications. Alsmairan and Al-Omari [5] derived weighted Suja distribution and discussed its statistical properties and applications to ball bearings data in safety engineering. Todoka et al [6] have studied on the cdf of various modifications of Suja distribution and discussed their applications in the field of analysis of computer- virus propagation and debugging theory.

The main objective of this paper is to propose a two-parameter quasi Suja distribution which contains Suja distribution as particular case. Its statistical properties including moments, skewness, kurtosis, hazard rate function, mean residual life function, stochastic ordering, mean deviations, Bonferroni and Lorenz curves, Renyi entropy measures, and stress-strength reliability have been derived and studied. The estimation of parameters using method of moments and maximum likelihood methods has been discussed. A simulation study has been presented to know the performance of maximum likelihood estimation. Applications and goodness of fit of the proposed distribution have been discussed.

II. A Quasi Suja Distribution

The pdf and the cdf of quasi Suja distribution QSD are expressed as

$$f(x;\theta,\alpha)=\frac{\theta^4}{\alpha\theta^3+24}\left(\alpha+\theta x^4\right)e^{-\theta x};x>0,\theta>0,\alpha>0 \tag{2.1}$$

$$F(x;\theta,\alpha)=1-\left[1+\frac{\theta^4x^4+4\theta^3x^3+12\theta^2x^2+24\theta x}{\alpha\theta^3+24}\right]e^{-\theta x};x>0,\theta>0,\alpha>0 \tag{2.2}$$

The survival function of QSD is given by

$$S(x;\theta,\alpha)=\left[\frac{\theta^4x^4+4\theta^3x^3+12\theta^2x^2+24\theta x+\left(\alpha\theta^3+24\right)}{\alpha\theta^3+24}\right]e^{-\theta x};x>0,\theta>0,\alpha>0\cdot$$

At $\alpha=\theta$, the pdf and the cdf of QSD reduces to the corresponding pdf and cdf of Suja distribution. Like Suja distribution, QSD is also a convex combination of exponential distribution with parameter θ and gamma distribution with parameters $(5,\theta)$ with mixing proportion $p=\frac{\alpha\theta^3}{\alpha\theta^3+24}\cdot$

The nature of pdf and cdf of QSD for varying values of parameters are shown in the following figures 1 and 2 respectively. From the pdf plots of the QSD, it is clear that it is extreme skewed to the right.

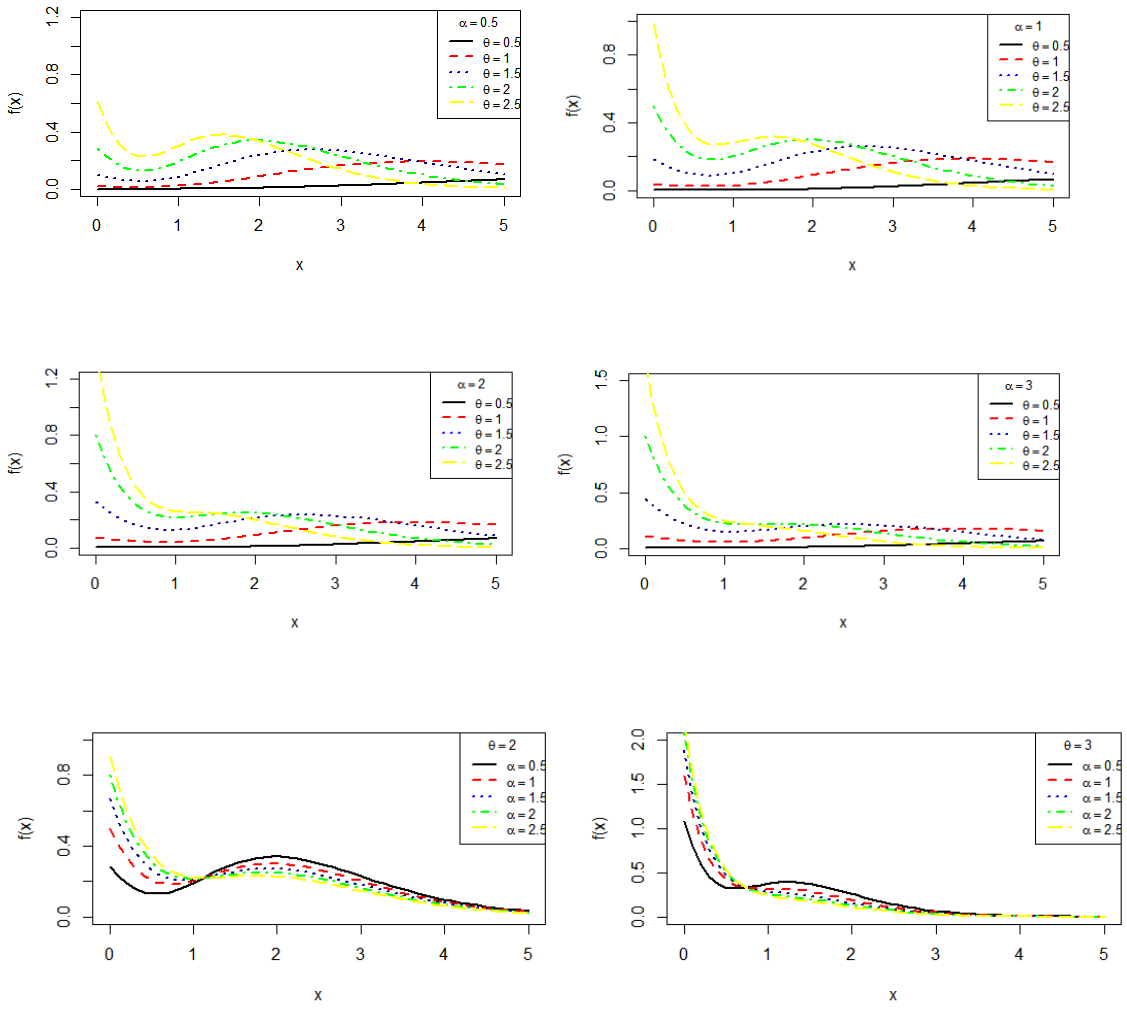

Figure1: *pdf plots of QSD for varying values of parameters*

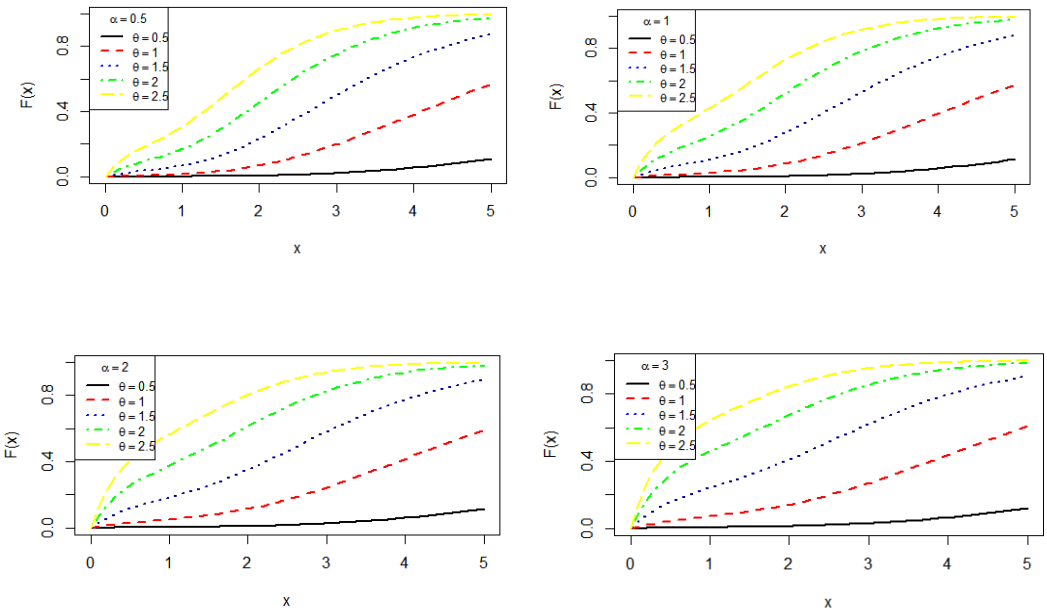

Figure 2: *cdf plots of QSD for varying values of parameters*

III. Measures based on Moments

The r th moment about origin μ_r' of QSD can be obtained as

$$\mu_r' = \frac{r!\left\{\alpha\theta^3 + (r+1)(r+2)(r+3)(r+4)\right\}}{\theta^r\left(\alpha\theta^3+24\right)}; r = 1,2,3,... \tag{3.1}$$

Taking $r = 1,2,3$ and 4, the first four raw moments of QSD can be expressed as

$$\mu_1' = \frac{\alpha\theta^3+120}{\theta\left(\alpha\theta^3+24\right)}, \mu_2' = \frac{2\left(\alpha\theta^3+360\right)}{\theta^2\left(\alpha\theta^3+24\right)}, \mu_3' = \frac{6\left(\alpha\theta^3+840\right)}{\theta^3\left(\alpha\theta^3+24\right)} \text{ and } \mu_4' = \frac{24\left(\alpha\theta^3+1680\right)}{\theta^4\left(\alpha\theta^3+24\right)}$$

Now the relationship between central moments and raw moments gives the central moments as

$$\mu_2 = \frac{\alpha^2\theta^6 + 528\alpha\theta^3 + 2880}{\theta^2\left(\alpha\theta^3+24\right)^2}$$

$$\mu_3 = \frac{2\left(\alpha^3\theta^9 + 1512\alpha^2\theta^6 + 1728\alpha\theta^3 + 69120\right)}{\theta^3\left(\alpha\theta^3+24\right)^3}$$

$$\mu_4 = \frac{9\left(\alpha^4\theta^{12} + 2656\alpha^3\theta^9 + 58752\alpha^2\theta^6 + 1234944\alpha\theta^3 + 3870720\right)}{\theta^4\left(\alpha\theta^3+24\right)^4}$$

The descriptive measures based on moments of QRD such as coefficient of variation (C.V), coefficient of skewness, $\left(\sqrt{\beta_1}\right)$, coefficient of kurtosis $\left(\beta_2\right)$ and index of dispersion $\left(\gamma\right)$ of QSD are obtained as

$$C.V. = \frac{\sqrt{\mu_2}}{\mu_1'} = \frac{\sqrt{\alpha^2\theta^6 + 528\alpha\theta^3 + 2880}}{\alpha\theta^3+120}$$

$$\sqrt{\beta_1} = \frac{\mu_3}{\left(\mu_2\right)^{3/2}} = \frac{2\left(\alpha^3\theta^9 + 1512\alpha^2\theta^6 + 1728\alpha\theta^3 + 69120\right)}{\left(\alpha^2\theta^6 + 528\alpha\theta^3 + 2880\right)^{3/2}}$$

$$\beta_2 = \frac{\mu_4}{\mu_2^2} = \frac{9\left(\alpha^4\theta^{12} + 2656\alpha^3\theta^9 + 58752\alpha^2\theta^6 + 1234944\alpha\theta^3 + 3870720\right)}{\left(\alpha^2\theta^6 + 528\alpha\theta^3 + 2880\right)^2}$$

$$\gamma = \frac{\mu_2}{\mu_1'} = \frac{\alpha^2\theta^6 + 528\alpha\theta^3 + 2880}{\theta\left(\alpha\theta^3+24\right)\left(\alpha\theta^3+120\right)}$$

The coefficient of variation, skweness, kurtosis and index of dispersion for varying values of parameters are shown in the following figures 3, 4, 5, and 6 respectively

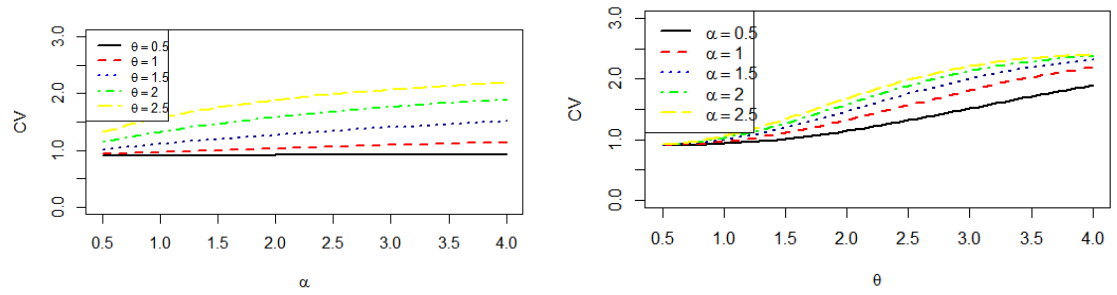

Figure3: *Plots of Coefficient of variation (C.V) of QSD for varying values of parameters*

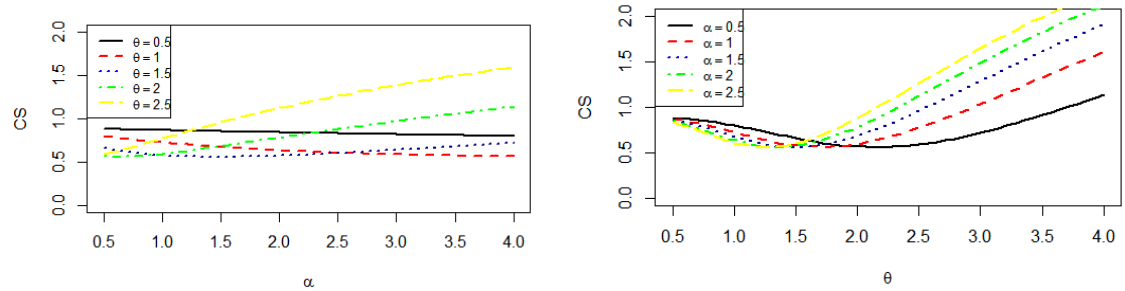

Fig. 4: *Plots of Coefficient of skweness of QSD for varying values of parameters*

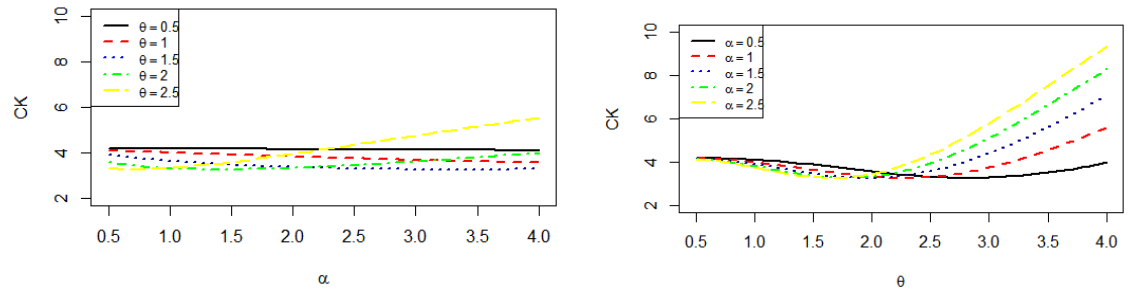

Figure 5: *Plots of Coefficient of kurtosis of QSD for varying values of parameters*

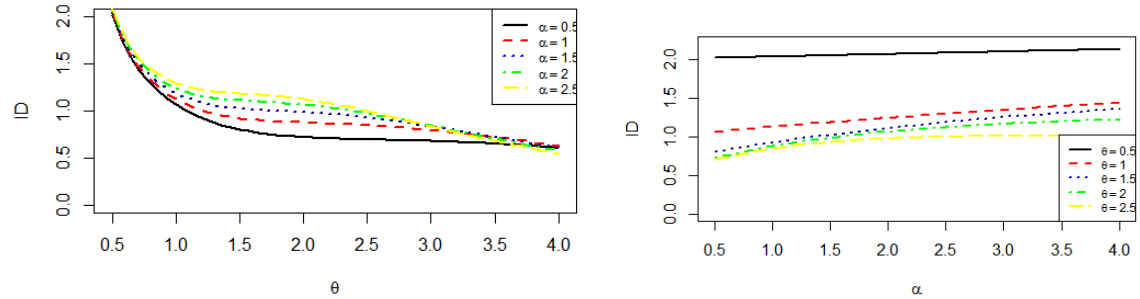

Figure 6:*Plots of Index of dispersion of QSD for varying values of parameters*

IV. Reliability Measures

Let X be a random variable having pdf $f(x)$ and cdf $F(x)$. The hazard rate function $h(x)$ (also known as the failure rate function) and the mean residual life function $m(x)$ of X are respectively defined as

$$h(x)=\lim_{\Delta x\to 0}\frac{P(X<x+\Delta x|X>x)}{\Delta x}=\frac{f(x)}{1-F(x)} \quad \text{and}$$

$$m(x)=E[X-x|X>x]=\frac{1}{1-F(x)}\int_x^\infty [1-F(t)]dt=\frac{1}{S(x)}\int_x^\infty t\,f(t)\,dt-x\,.$$

Now using the pdf and cdf of QSD, the hazard rate function, $h(x)$ and the mean residual life function, $m(x)$ of the QSD are thus obtained as

$$h(x)=\frac{\theta^4(\alpha+\theta x^4)}{\theta^4x^4+4\theta^3x^3+12\theta^2x^2+24\theta x+(\alpha\theta^3+24)}$$

$$\text{and } m(x)=\frac{\theta^4x^4+8\theta^3x^3+36\theta^2x^2+96\theta x+(\alpha\theta^3+120)}{\theta[\theta^4x^4+4\theta^3x^3+12\theta^2x^2+24\theta x+(\alpha\theta^3+24)]}.$$

Obviously, we have $h(0)=\frac{\alpha\theta^4}{\alpha\theta^3+24}=f(0)$ and $m(0)=\frac{\alpha\theta^3+120}{\theta(\alpha\theta^3+24)}=\mu_1'$. The hazard rate function and the mean residual life function of QSD for varying values of parameters are shown in figures 7 and 8 respectively.

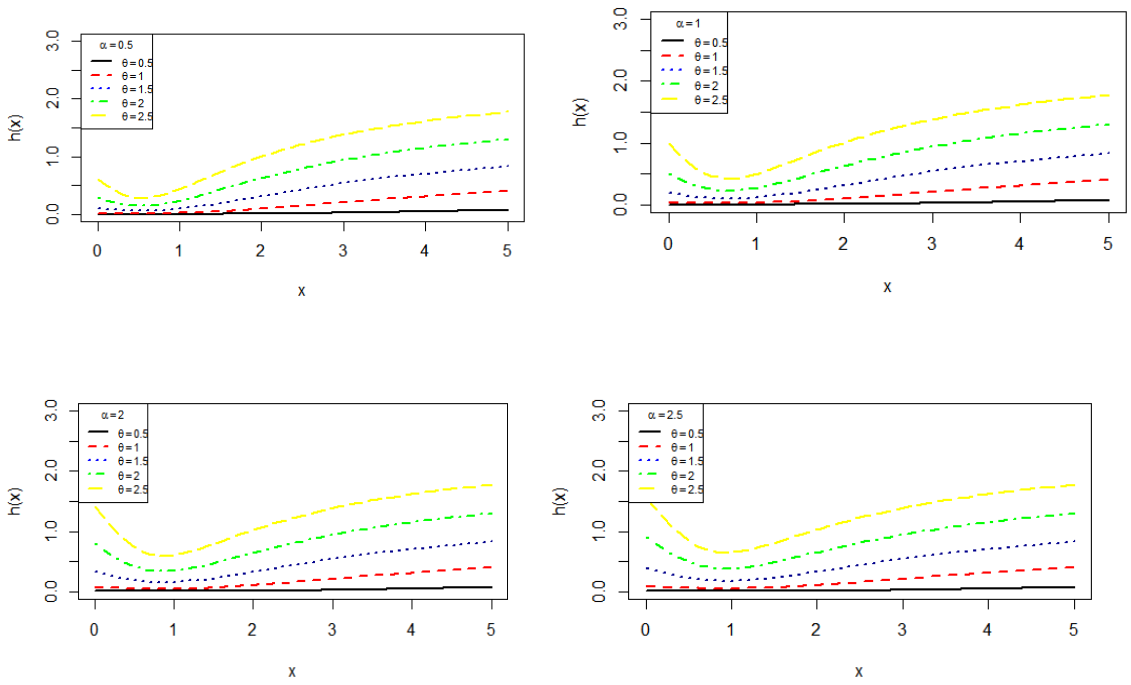

Figure7: *Plots of Hazard function of QSD for varying values of parameters*

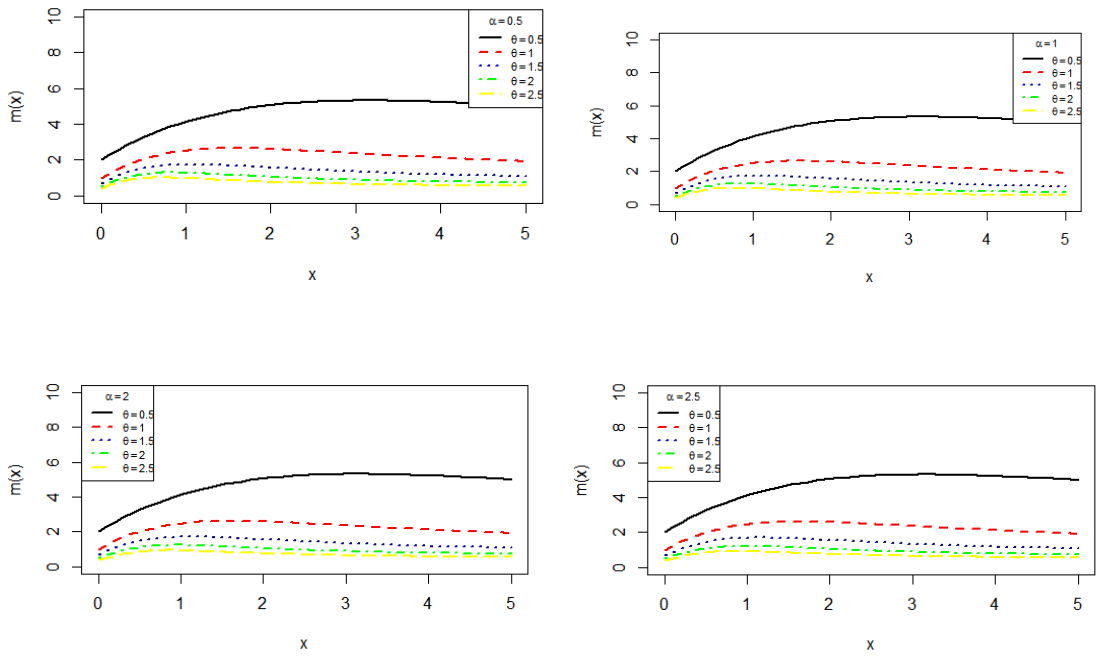

Figure8: *Plots of Mean residual life function of QSD for varying values of parameters*

V. Mean Deviations

The amount of scatter in a population is measured to some extent by the totality of deviations usually from mean and median. These are known as the mean deviation about the mean and the mean deviation about the median and are defined as

$\delta_1(X)=\int_0^\infty |x-\mu| f(x)dx$ and $\delta_2(X)=\int_0^\infty |x-M| f(x)dx$, respectively, where $\mu=E(X)$ and $M=\text{Median}(X)$. The measures $\delta_1(X)$ and $\delta_2(X)$ can be calculated using the relationships

$$\delta_1(X)=\int_0^\mu (\mu-x)f(x)dx+\int_\mu^\infty (x-\mu)f(x)dx$$

$$=\mu F(\mu)-\int_0^\mu x f(x)dx-\mu[1-F(\mu)]+\int_\mu^\infty x f(x)dx$$

$$=2\mu F(\mu)-2\mu+2\int_\mu^\infty x f(x)dx$$

$$=2\mu F(\mu)-2\int_0^\mu x f(x)dx \qquad (5.1)$$

and

$$\delta_2(X)=\int_0^M (M-x)f(x)dx+\int_M^\infty (x-M)f(x)dx$$

$$=M F(M)-\int_0^M x f(x)dx-M[1-F(M)]+\int_M^\infty x f(x)dx$$

$$= -\mu + 2\int_{M}^{\infty} x f(x)\,dx$$

$$= \mu - 2\int_{0}^{M} x f(x)\,dx \tag{5.2}$$

Using the pdf of QSD and the mean of QSD, we get

$$\int_{0}^{\mu} x f(x;\theta,\alpha)\,dx = \mu - \frac{\left\{\theta^5\mu^5 + 5\theta^4\mu^4 + 20\theta^3\mu^3 + 60\theta^2\mu^2 + (\alpha\theta^3 + 120)\theta\mu + (\alpha\theta^3 + 120)\right\}e^{-\theta\mu}}{\theta(\alpha\theta^3 + 24)} \tag{5.3}$$

$$\int_{0}^{M} x f(x;\theta,\alpha)\,dx = \mu - \frac{\left\{\theta^5 M^5 + 5\theta^4 M^4 + 20\theta^3 M^3 + 60\theta^2 M^2 + (\alpha\theta^3 + 120)\theta M + (\alpha\theta^3 + 120)\right\}e^{-\theta M}}{\theta(\alpha\theta^3 + 24)} \tag{5.4}$$

Using expressions from (5.1), (5.2), (5.3), and (5.4), the mean deviation about mean, $\delta_1(X)$ and the mean deviation about median, $\delta_2(X)$ of QSD are obtained as

$$\delta_1(X) = \frac{2\left\{\theta^4\mu^4 + 8\theta^3\mu^3 + 36\theta^2\mu^2 + 96\theta\mu + (\alpha\theta^3 + 120)\right\}e^{-\theta\mu}}{\theta(\alpha\theta^3 + 24)} \tag{5.5}$$

$$\delta_2(X) = \frac{2\left\{\theta^5 M^5 + 5\theta^4 M^4 + 20\theta^3 M^3 + 60\theta^2 M^2 + (\alpha\theta^3 + 120)\theta M + (\alpha\theta^3 + 120)\right\}e^{-\theta M}}{\theta(\alpha\theta^3 + 24)} - \mu \tag{5.6}$$

VI. Bonferroni and Lorenz Curves

The Bonferroni and Lorenz curves (Bonferroni [7]) and Bonferroni and Gini indices have applications not only in economics to study income and poverty, but also in other fields like reliability, demography, insurance and medicine. The Bonferroni and Lorenz curves are defined as

$$B(p) = \frac{1}{p\mu}\int_{0}^{q} x f(x)\,dx = \frac{1}{p\mu}\left[\int_{0}^{\infty} x f(x)\,dx - \int_{q}^{\infty} x f(x)\,dx\right] = \frac{1}{p\mu}\left[\mu - \int_{q}^{\infty} x f(x)\,dx\right] \tag{6.1}$$

and $L(p) = \frac{1}{\mu}\int_{0}^{q} x f(x)\,dx = \frac{1}{\mu}\left[\int_{0}^{\infty} x f(x)\,dx - \int_{q}^{\infty} x f(x)\,dx\right] = \frac{1}{\mu}\left[\mu - \int_{q}^{\infty} x f(x)\,dx\right]$ (6.2)

respectively or equivalently

$$B(p) = \frac{1}{p\mu}\int_{0}^{p} F^{-1}(x)\,dx \tag{6.3}$$

and $$L(p) = \frac{1}{\mu}\int_{0}^{p} F^{-1}(x)\,dx \tag{6.4}$$

respectively, where $\mu = E(X)$ and $q = F^{-1}(p)$.

The Bonferroni and Gini indices are thus defined as

$$B = 1 - \int_{0}^{1} B(p)\,dp \tag{6.5}$$

$$\text{and } G = 1 - 2\int_0^1 L(p)\,dp \tag{6.6}$$

respectively.

Using the pdf of QSD, we have

$$\int_q^\infty x\,f(x;\theta,\alpha)\,dx = \frac{\left\{\theta^5 q^5 + 5\theta^4 q^4 + 20\theta^3 q^3 + 60\theta^2 q^2 + \left(\alpha\theta^3 + 120\right)\theta q + \left(\alpha\theta^3 + 120\right)\right\} e^{-\theta q}}{\theta\left(\alpha\theta^3 + 24\right)} \tag{6.7}$$

Now using equation (6.7) in (6.1) and (6.2), we get

$$B(p) = \frac{1}{p}\left[1 - \frac{\left\{\theta^5 q^5 + 5\theta^4 q^4 + 20\theta^3 q^3 + 60\theta^2 q^2 + \left(\alpha\theta^3 + 120\right)\theta q + \left(\alpha\theta^3 + 120\right)\right\} e^{-\theta q}}{\left(\alpha\theta^3 + 120\right)}\right] \tag{6.8}$$

$$L(p) = 1 - \frac{\left\{\theta^5 q^5 + 5\theta^4 q^4 + 20\theta^3 q^3 + 60\theta^2 q^2 + \left(\alpha\theta^3 + 120\right)\theta q + \left(\alpha\theta^3 + 120\right)\right\} e^{-\theta q}}{\left(\alpha\theta^3 + 120\right)} \tag{6.9}$$

Now using equations (6.8) and (6.9) in (6.5) and (6.6), the Bonferroni and Gini indices are obtained as

$$B = 1 - \frac{\left\{\theta^5 q^5 + 5\theta^4 q^4 + 20\theta^3 q^3 + 60\theta^2 q^2 + \left(\alpha\theta^3 + 120\right)\theta q + \left(\alpha\theta^3 + 120\right)\right\} e^{-\theta q}}{\left(\alpha\theta^3 + 120\right)} \tag{6.10}$$

$$G = \frac{2\left\{\theta^5 q^5 + 5\theta^4 q^4 + 20\theta^3 q^3 + 60\theta^2 q^2 + \left(\alpha\theta^3 + 120\right)\theta q + \left(\alpha\theta^3 + 120\right)\right\} e^{-\theta q}}{\left(\alpha\theta^3 + 120\right)} - 1 \tag{6.11}$$

VII. Order Statistics

Let $X_1, X_2, ..., X_n$ be a random sample of size n from QSD. Let $X_{(1)} < X_{(2)} < ... < X_{(n)}$ denote the corresponding order statistics. The pdf and the cdf of the k th order statistic, say $Y = X_{(k)}$ are given by

$$f_Y(y) = \frac{n!}{(k-1)!(n-k)!} F^{k-1}(y)\left\{1 - F(y)\right\}^{n-k} f(y)$$

$$= \frac{n!}{(k-1)!(n-k)!} \sum_{l=0}^{n-k} \binom{n-k}{l} (-1)^l F^{k+l-1}(y) f(y)$$

and

$$F_Y(y) = \sum_{j=k}^{n} \binom{n}{j} F^j(y)\left\{1 - F(y)\right\}^{n-j} = \sum_{j=k}^{n}\sum_{l=0}^{n-j} \binom{n}{j}\binom{n-j}{l} (-1)^l F^{j+l}(y)$$

respectively, for $k = 1, 2, 3, ..., n$.

Thus, the pdf and the cdf of the k th order statistics of QSD are obtained as

$$f_Y(y)=\frac{n!\theta^4\left(\alpha+\theta x^4\right)e^{-\theta x}}{\left(\alpha\theta^3+24\right)(k-1)!(n-k)!}\sum_{l=0}^{n-k}\binom{n-k}{l}(-1)^l$$

$$\times\left[1-\frac{\theta^4x^4+4\theta^3x^3+12\theta^2x^2+24\theta x+\left(\alpha\theta^3+24\right)}{\alpha\theta^3+24}e^{-\theta x}\right]^{k+l-1}$$

and

$$F_Y(y)=\sum_{j=k}^{n}\sum_{l=0}^{n-j}\binom{n}{j}\binom{n-j}{l}(-1)^l\left[1-\frac{\theta^4x^4+4\theta^3x^3+12\theta^2x^2+24\theta x+\left(\alpha\theta^3+24\right)}{\alpha\theta^3+24}e^{-\theta x}\right]^{j+l}$$

VIII. Stochastic Orderings

Stochastic ordering of positive continuous random variables is an important tool for judging their comparative behavior. A random variable X is said to be smaller than a random variable Y in the

(i) stochastic order $\left(X\le_{st}Y\right)$ if $F_X(x)\ge F_Y(x)$ for all x

(ii) hazard rate order $\left(X\le_{hr}Y\right)$ if $h_X(x)\ge h_Y(x)$ for all x

(iii) mean residual life order $\left(X\le_{mrl}Y\right)$ if $m_X(x)\le m_Y(x)$ for all x

(iv) likelihood ratio order $\left(X\le_{lr}Y\right)$ if $\frac{f_X(x)}{f_Y(x)}$ decreases in x. The following results due to Shaked and Shanthikumar [8] are well known for establishing stochastic ordering of distributions

$$X\le_{lr}Y\Rightarrow X\le_{hr}Y\Rightarrow X\le_{mrl}Y \tag{8.1}$$
$$\Downarrow$$
$$X\le_{st}Y$$

QSD is ordered with respect to the strongest 'likelihood ratio' ordering as shown in the following theorem:

Theorem: Let $X\sim$ QSD$\left(\theta_1,\alpha_1\right)$ and $Y\sim$ QSD$\left(\theta_2,\alpha_1\right)$. If $\theta_1\ge\theta_2$ and $\alpha_1=\alpha_2$, or $\alpha_1\ge\alpha_2$ and $\theta_1=\theta_2$ then $X\le_{lr}Y$ and hence $X\le_{hr}Y$, $X\le_{mrl}Y$ and $X\le_{st}Y$.

Proof: We have

$$\frac{f_X(x)}{f_Y(x)}=\frac{\theta_1^4\left(\alpha_2\theta_2^3+24\right)}{\theta_2^4\left(\alpha_1\theta_1^3+24\right)}\left(\frac{\alpha_1+\theta_1x^4}{\alpha_2+\theta_2x^4}\right)e^{-(\theta_1-\theta_2)x};x>0$$

Now $$\ln\frac{f_X(x)}{f_Y(x)}=\ln\left[\frac{\theta_1^4\left(\alpha_2\theta_2^3+24\right)}{\theta_2^4\left(\alpha_1\theta_1^3+24\right)}\right]+\ln\left(\frac{\alpha_1+\theta_1x^4}{\alpha_2+\theta_2x^4}\right)-\left(\theta_1-\theta_2\right)x$$

. This gives $$\frac{d}{dx}\ln\frac{f_X(x)}{f_Y(x)}=\frac{4\left(\alpha_2\theta_1-\alpha_1\theta_2\right)x^3}{\left(\alpha_1+\theta_1x^4\right)\left(\alpha_2+\theta_2x^4\right)}-\left(\theta_1-\theta_2\right)$$

Thus for $\theta_1\ge\theta_2$ and $\alpha_1=\alpha_2$, or $\alpha_1\ge\alpha_2$ and $\theta_1=\theta_2$, $\frac{d}{dx}\ln\frac{f_X(x)}{f_Y(x)}<0$. This means that $X\le_{lr}Y$ and hence $X\le_{hr}Y$, $X\le_{mrl}Y$ and $X\le_{st}Y$.

IX. Renyi Entropy Measure

An entropy of a random variable X is a measure of variation of uncertainty. A popular

entropy measure is Renyi entropy [9]. If X is a continuous random variable having pdf $f(.)$, then Renyi entropy is defined as

$$T_R(\gamma)=\frac{1}{1-\gamma}\log\left\{\int f^{\gamma}(x)\,dx\right\}, \text{ where } \gamma>0 \text{ and } \gamma\neq 1.$$

Thus, the Renyi entropy of QSD can be obtained as

$$T_R(\gamma)=\frac{1}{1-\gamma}\log\left[\int_0^{\infty}\frac{\theta^{4\gamma}}{\left(\alpha\theta^3+24\right)^{\gamma}}\left(\alpha+\theta x^4\right)^{\gamma}e^{-\theta\gamma x}dx\right]$$

$$=\frac{1}{1-\gamma}\log\left[\int_0^{\infty}\frac{\theta^{4\gamma}\alpha^{\gamma}}{\left(\alpha\theta^3+24\right)^{\gamma}}\left(1+\frac{\theta}{\alpha}x^4\right)^{\gamma}e^{-\theta\gamma x}dx\right]$$

$$=\frac{1}{1-\gamma}\log\left[\int_0^{\infty}\frac{\theta^{4\gamma}\alpha^{\gamma}}{\left(\alpha\theta^3+24\right)^{\gamma}}\sum_{j=0}^{\infty}\binom{\gamma}{j}\left(\frac{\theta}{\alpha}x^4\right)^{j}e^{-\theta\gamma x}dx\right]$$

$$=\frac{1}{1-\gamma}\log\left[\sum_{j=0}^{\infty}\binom{\gamma}{j}\frac{\theta^{4\gamma}\alpha^{\gamma}\theta^{j}}{\left(\alpha\theta^3+24\right)^{\gamma}\alpha^{j}}\int_0^{\infty}e^{-\theta\gamma x}x^{4j}dx\right]$$

$$=\frac{1}{1-\gamma}\log\left[\sum_{j=0}^{\infty}\binom{\gamma}{j}\frac{\theta^{4\gamma+j}\alpha^{\gamma-j}}{\left(\alpha\theta^3+24\right)^{\gamma}}\int_0^{\infty}e^{-\theta\gamma x}x^{4j+1-1}dx\right]$$

$$=\frac{1}{1-\gamma}\log\left[\sum_{j=0}^{\infty}\binom{\gamma}{j}\frac{\theta^{4\gamma+j}\alpha^{\gamma-j}}{\left(\alpha\theta^3+24\right)^{\gamma}}\frac{\Gamma(4j+1)}{(\theta\gamma)^{4j+1}}\right]$$

$$=\frac{1}{1-\gamma}\log\left[\sum_{j=0}^{\infty}\binom{\gamma}{j}\frac{\theta^{4\gamma-3j-1}\alpha^{\gamma-j}}{\left(\alpha\theta^3+24\right)^{\gamma}}\frac{\Gamma(4j+1)}{(\gamma)^{4j+1}}\right]$$

X. Stress-Strength Reliability

The stress- strength reliability describes the life of a component which has random strength X that is subjected to a random stress Y. When the stress applied to it exceeds the strength, the component fails instantly and the component will function satisfactorily till $X>Y$. Therefore, $R=P(Y<X)$ is a measure of component reliability and in statistical literature it is known as stress-strength parameter. It has wide applications in almost all areas of knowledge especially in engineering such as structures, deterioration of rocket motors, static fatigue of ceramic components, aging of concrete pressure vessels etc.

Let X and Y are independent strength and stress random variables having QSD with parameter (θ_1,α_1) and (θ_2,α_2), respectively. Then, the stress-strength reliability R of QSD can be obtained as

$$R=P(Y<X)=\int_0^{\infty}P(Y<X\mid X=x)f_X(x)\,dx=\int_0^{\infty}f(x;\theta_1,\alpha_1)\,F(x;\theta_2,\alpha_2)\,dx$$

$$= 1 - \frac{\theta_1^4 \begin{bmatrix} 40320\theta_1\theta_2^4 + 20160\theta_1\theta_2^3(\theta_1+\theta_2) + 8640\theta_1\theta_2^2(\theta_1+\theta_2)^2 + 2880\theta_1\theta_2(\theta_1+\theta_2)^3 \\ +24\left(\alpha_1\theta_2^4 + \alpha_2\theta_1\theta_2^3 + 24\theta_1\right)(\theta_1+\theta_2)^4 + 24\alpha_1\theta_2^3(\theta_1+\theta_2)^5 + 24\alpha_1\theta_2^2(\theta_1+\theta_2)^6 \\ +24\alpha_1\theta_2(\theta_1+\theta_2)^7 + \left(\alpha_1\alpha_2\theta_2^3 + 24\alpha_1\right)(\theta_1+\theta_2)^8 \end{bmatrix}}{\left(\alpha_1\theta_1^3 + 24\right)\left(\alpha_2\theta_2^3 + 24\right)(\theta_1+\theta_2)^9}.$$

XI. Estimation of Parameters

In this section, the method of moments and the method of maximum likelihood for estimating parameters of QSD have been discussed.

I. Method of Moments

Since QSD has two parameters to be estimated, the first two moments about origin are required to estimate its parameters. We have

$$\frac{\mu_2'}{\left(\mu_1'\right)^2} = \frac{2\left(\alpha\theta^3 + 360\right)\left(\alpha\theta^2 + 24\right)}{\left(\alpha\theta^3 + 120\right)^2} = k \text{ (Say)}$$

Taking $b = \alpha\theta^3$, above equation becomes

$$\frac{2(b+360)(b+24)}{(b+120)^2} = k$$

$$\frac{2\left(b^2 + 384b + 8670\right)}{b^2 + 240b + 14400} = k$$

$$(k-2)b^2 + (240k - 768)b + (14400k - 17340) = 0 \tag{11.1.1}$$

Now, for real root of b, the discriminant of the above equation should be greater than and equal to zero. That is

$$(240k - 768)^2 - 4(k-2)(14400k - 17340) \geq 0 \Rightarrow k \leq 2.45.$$

This means that the method of moments estimate is applicable if $k = \frac{m_2'}{(\bar{x})^2} \leq 2.45$, where m_2' is the second moment about origin of the dataset. Now taking $b = \alpha\theta^3$ and equating the population mean to the sample mean, we get the moment estimate $\tilde{\theta}$ of θ as

$$\frac{\alpha\theta^3 + 120}{\theta\left(\alpha\theta^3 + 24\right)} = \frac{b+120}{\theta(b+24)} = \bar{x} \Rightarrow \tilde{\theta} = \frac{b+120}{(b+24)\bar{x}}.$$

Using the moment estimate of θ in $b = \alpha\theta^3$, we get the moment estimate $\tilde{\alpha}$ of α as

$$\tilde{\alpha} = \frac{b}{\left(\tilde{\theta}\right)^3} = \frac{b(b+124)^3(\bar{x})^3}{(b+120)^3}$$

Thus the method of moment estimates $\left(\tilde{\theta}, \tilde{\alpha}\right)$ of parameters (θ, α) of QSD are given by

$\left(\tilde{\theta},\tilde{\alpha}\right)=\left(\dfrac{b+120}{\left(b+24\right)\bar{x}},\dfrac{b\left(b+124\right)^3\left(\bar{x}\right)^3}{\left(b+120\right)^3}\right)$, where b is the value of the quadratic equation (11.1.1).

II. Method of Maximum likelihood

Let $\left(x_1,x_2,x_3,...,x_n\right)$ be a random sample of size n from QSD$\left(\theta,\alpha\right)$. Then the likelihood function of QSD is given by

$$L=\left(\frac{\theta^4}{\alpha\theta^3+24}\right)^n\prod_{i=1}^{n}\left(\alpha+\theta x_i^{\,4}\right)e^{-n\theta\bar{x}},$$ where $\bar{x}$ is the sample mean.

The log-likelihood function is thus obtained as

$$\log L=n\left[4\log\theta-\log\left(\alpha\theta^3+24\right)\right]+\sum_{i=1}^{n}\log\left(\alpha+\theta x_i^{\,4}\right)-n\theta\bar{x}.$$

The maximum likelihood estimates$\left(\hat{\theta},\hat{\alpha}\right)$ of parameters $\left(\theta,\alpha\right)$are the solution of the following log-likelihood equations

$$\frac{\partial\log L}{\partial\theta}=\frac{4n}{\theta}+\frac{3n\theta\alpha}{\alpha\theta^3+24}+\sum_{i=1}^{n}\frac{x_i^{\,4}}{\alpha+\theta x_i^{\,4}}-n\,\bar{x}=0$$

$$\frac{\partial\log L}{\partial\alpha}=\frac{-n\theta^3}{\alpha\theta^3+24}+\sum_{i=1}^{n}\frac{1}{\alpha+\theta x_i^{\,4}}=0$$

These two log-likelihood equations do not seem to be solved directly. We have to use Fisher's scoring method for solving these two log-likelihood equations. We have

$$\frac{\partial^2\log L}{\partial\theta^2}=\frac{-4n}{\theta^2}+\frac{3n\alpha\left(\alpha\theta^4-48\theta\right)}{\left(\alpha\theta^3+24\right)^2}-\sum_{i=1}^{n}\frac{x_i^{\,8}}{\left(\alpha+\theta x_i^{\,4}\right)^2}$$

$$\frac{\partial^2\log L}{\partial\alpha^2}=\frac{n\theta^6}{\left(\alpha\theta^3+24\right)^2}-\sum_{i=1}^{n}\frac{1}{\left(\alpha+\theta x_i^{\,4}\right)^2}$$

$$\frac{\partial^2\log L}{\partial\theta\,\partial\alpha}=\frac{-72n\theta^2}{\left(\alpha\theta^3+24\right)^2}-\sum_{i=1}^{n}\frac{x_i^{\,4}}{\left(\alpha+\theta x_i^{\,4}\right)^2}=\frac{\partial^2\log L}{\partial\alpha\,\partial\theta}.$$

The following equations can be solved for MLEs $\left(\hat{\theta},\hat{\alpha}\right)$ of $\left(\theta,\alpha\right)$ of QSD

$$\begin{bmatrix}\dfrac{\partial^2\ln L}{\partial\theta^2} & \dfrac{\partial^2\ln L}{\partial\theta\,\partial\alpha}\\ \dfrac{\partial^2\ln L}{\partial\theta\,\partial\alpha} & \dfrac{\partial^2\ln L}{\partial\alpha^2}\end{bmatrix}_{\substack{\hat{\theta}=\theta_0\\ \hat{\alpha}=\alpha_0}}\begin{bmatrix}\hat{\theta}-\theta_0\\ \hat{\alpha}-\alpha_0\end{bmatrix}=\begin{bmatrix}\dfrac{\partial\ln L}{\partial\theta}\\ \dfrac{\partial\ln L}{\partial\alpha}\end{bmatrix}_{\substack{\hat{\theta}=\theta_0\\ \hat{\alpha}=\alpha_0}}$$

where θ_0 and α_0 are the initial values of θ and α, respectively, as given by the method of moments. . These equations are solved iteratively till sufficiently close values of $\hat{\theta}$ and $\hat{\alpha}$ are obtained.

XII. A Simulation Study

In this section, a simulation study has been carried out using R-software. Acceptance and rejection method is used to generate random number, where sample size, $n = 40, 60, 80, 100$, value of $\theta = 0.1, 0.5, 1.0, 1.5 \,\&\, (\alpha = 1, \alpha = 2)$ have been used for calculating Bias error (BE) and MSE (Mean square error) of parameter θ and α which are presented in tables1 &2 respectively.

Table 1. *BE and MSE for* θ *and* α *at* α *=1*

Sample	θ	BE(θ)(MSE(θ))	BE(α) (MSE (α))
40	0.1	0.026829 (0.02879335)	0.051492(0.11741)
	0.5	0.0168297(0.0113295)	0.0291919(0.034087)
	1.0	0.0004329(0.0007498)	0.0041920(0.0007029)
	1.5	-0.0081702(0.0026701)	-0.0208079(0.0173187)
60	0.1	0.01656832(0.0164705)	0.0363314(0.0791985)
	0.5	0.0099016(0.00588256)	0.0196648(0.0232022)
	1.0	0.0015683(0.00014757)	0.00299813(0.000539)
	1.5	-0.0067650(0.0027459)	-0.0136685(0.0112097)
80	0.1	0.01079101(0.00931567)	0.0619808(0.30733037)
	0.5	0.00579101(0.00268286)	0.04948088(0.1958686)
	1.0	-0.00045898(0.00001685)	0.03698088(0.1094068)
	1.5	-0.006708987(0.0036008)	0.02448088(0.0479450)
100	0.1	0.008494785(0.007216137)	0.045858(0.21029559)
	0.5	0.004494785(0.002020309)	0.035858(0.1285795)
	1.0	-0.000505214(0.0002552)	0.025858(0.0668636)
	1.5	-0.005505214(0.00303073)	0.015858(0.0251476)

Table 2. *BE and MSE for* θ *and* α *at* α *=2*

Sample	θ	BE (MSE)	BE (MSE) for alpha
40	0.1	0.01796973(0.0129164485)	0.17092052(1.1685530)
	0.5	0.00796973 (0.0025406641)	0.14592052 (0.8517119)
	1.0	-0.00453027(0.0008209337)	0.12092052 (0.5848709)
	1.5	-0.01703027 (0.0116012033)	0.09592052(0.3680299)
60	0.1	0.016696288(0.0167259624)	0.031357314(0.058996870)
	0.5	0.010029622(0.0060355985)	0.014690648(0.012948908)
	1.0	0.001696288 (0.0001726436)	-0.001976019(0.000234279)
	1.5	-0.006637045 (0.002643022)	-0.018642686(0.020852983)
80	0.1	0.0107846385(0.0093046743)	0.05327416(0.22705089)
	0.5	0.0057846385(0.0026769634)	0.04077416(0.13300257)
	1.0	-0.000465361(0.0000173249)	0.02827416 (0.06395425)
	1.5	-0.006715361(0.0036076864)	0.01577416(0.01990593)
100	0.1	0.0086072384(0.007408455)	0.037134273(0.137895421)
	0.5	0.0046072384(0.002.122665)	0.027134273(0.073626875)
	1.0	-0.000392761(0.0001.542617)	0.017134273(0.029358330)
	1.5	-0.0053927616(0.002908188)	0.007134273(0.005089785)

It is obvious from tables 1 and 2 that as the sample size increases, both the BE and MSE decreases.

XIII. Applications

In this section, the goodness of fit of QSD has been discussed and compared with one parameter life time distributions including exponential distribution, Lindley distribution introduced by Lindley [10], Akash distribution proposed by Shanker [11], Suja distribution and two-parameter lifetime distributions including quasi Lindley distribution (QLD) of Shanker and Mishra [12] and Quasi Akash distribution of Shanker [13]. The pdf and the cdf of these distributions are presented in the table 3.

Table 3: ***pdf and the cdf of one parameter and two-parameter distributions***

Distributions	Pdf	Cdf
QLD	$f(x;\theta,\alpha)=\frac{\theta}{\alpha+1}(\alpha+\theta x)e^{-\theta x}$	$F(x;\theta,\alpha)=1-\left(1+\frac{\theta x}{\alpha+1}\right)e^{-\theta x}$
QAD	$f(x;\theta,\alpha)=\frac{\theta^2}{\alpha\theta+2}(\alpha+\theta x^2)e^{-\theta x}$	$F(x;\theta,\alpha)=1-\left(1+\frac{\theta x(\theta x+2)}{\alpha\theta+2}\right)e^{-\theta x}$
LD	$f(x;\theta)=\frac{\theta^2}{\theta+1}(1+x)e^{-\theta x}$	$F(x;\theta)=1-\left[1+\frac{\theta x}{\theta+1}\right]e^{-\theta x}$
AD	$f(x;\theta)=\frac{\theta^3}{\theta^2+2}(1+x^2)e^{-\theta x}$	$F(x;\theta)=1-\left(1+\frac{\theta x(\theta x+2)}{\theta^2+2}\right)e^{-\theta x}$
Exponential	$f(x;\theta)=\theta e^{-\theta x}$	$F(x;\theta)=1-e^{-\theta x}$

The following dataset table 4 regarding the failure times of 50 electronic components which are extreme skewed to the right available in Murthy et al [14] has been considered to test the goodness of fit of the considered distributions.ML estimates of parameters of the considered distributions along with the values of $-2\log L$, AIC, K-S and p values are presented in table 5. The fitted plots of the considered distributions for dataset in table 4 are shown in figure 9.

Table 4: Failure times data of 50 electronic components

0.036	0.058	0.061	0.074	0.078	0.086	0.102	0.103	0.114	0.116
0.148	0.183	0.192	0.254	0.262	0.379	0.381	0.538	0.570	0.574
0.590	0.618	0.645	0.961	1.228	1.600	2.006	2.054	2.804	3.058
3.076	3.147	3.625	3.704	3.931	4.073	4.393	4.534	4.893	6.274
6.816	7.896	7.904	8.022	9.337	10.940	11.020	13.880	14.730	15.080

Table 5: *ML estimates of the parameters of the considered distributions along with values of* $-2\log L$*, AIC, K-S and p-value*

Distributions	**ML parameters**		$-2\log L$	AIC	**K-S**	**p-value**
	θ	α				
QSD	0.63822	179.0985	182.40	186.40	0.159	0.142
QLD	0.30731	35.0346	220.70	224.70	0.972	0.000
QAD	0.3680	44.9617	218.13	222.13	0.271	0.000
LD	0.59603	--------	197.71	199.71	0.283	0.000
SD	1.12234	--------	317.17	319.17	0.441	0.000
Exponential	0.29913	------	220.68	222.68	0.284	0.000

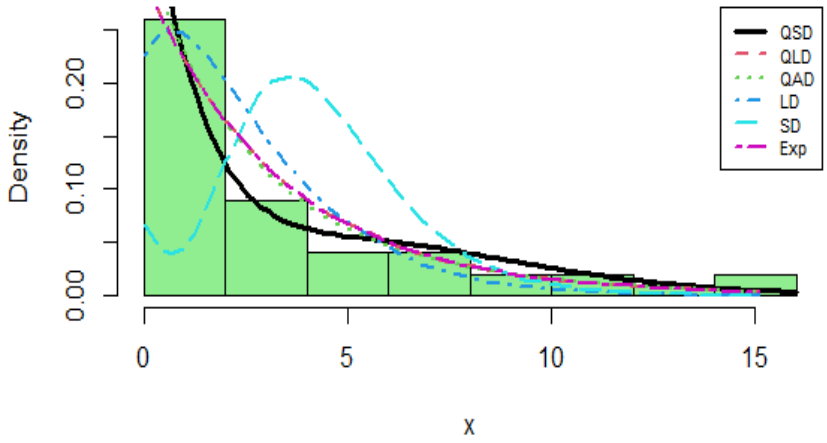

Figure 9 : *Fitted plot of considered distributions on dataset*

It is obvious from the goodness of fit in table 5 and the fitted plots in figure 9 that the QSD gives much closer fit as compared to other considered distributions for the failure time data of electronic components.

XIV. Conclusion

A two-parameter quasi Suja distribution (QSD) of which Suja distribution is a special case has been suggested. The proposed distribution is useful for extreme right skewed data. Its moments, skewness, kurtosis, hazard rate function, mean residual life function, stochastic ordering, mean deviations, Bonferroni and Lorenz curves, Renyi entropy measures, and stress-strength reliability have been derived and studied. Method of moments and maximum likelihood estimation has been studied for estimating parameters. A simulation study has been presented. The goodness of fit of QSD has been presented with failure time data and the fit shows that QSD is the best distribution among the considered distributions.

References

[1] Sharma et al. (2015) Sharma, V., Shanker, R. and Shanker, R. (2019): On someone parameter lifetime distributions and their applications, *Annals of |Biostatistics and Biometric Applications*, 2(5), 1 – 6.

[2] Shanker, R. (2017): Suja distribution and its application, International Journal of Probabiity and Statistics, 6(2), 11 – 19

[3] Al-Omari A. I, Alsmairam, I.K. (2019): Length-biased Suja distribution and Its application, *Journal of Applied Probability and Statistics*, 14(3), 95 – 116

[4] Al-Omari AI, Alhyasat, I.K. and Abu, B.M.A. (2019): Power Length-biased Suja distribution – properties and application, *Electronic Journal of Applied Statistical Analysisl*, 12 (2), 429 – 452.

[5] Alsmairan, I.K. and Al-Omari, A.I. (2020): Weighted Suja distribution with application to ball bearings data, *Life Cycle Reliability and Safety Engineering*, 9, 195 – 211.

[6] Todorka, T., Anton, I., Asen, R. and Nokolay, K. (2020): Comments on some modification of Suja Cumulative Functions with applications to the theory of computer viruses propagation, VIII, *International Journal of Differential Equations and Applications*, 19(1), 83 – 95.

[7] Bonferroni, C.E. (1930): Elementi di Statistca generale, Seeber, Firenze

[8] Shaked, M. and Shanthikumar, J.G.(1994): Stochastic Orders and Their Applications, Academic Press, New York.

[9] Renyi, A. (1961): On measures of entropy and information, in proceedings of the 4th Berkeley symposium on Mathematical Statistics and Probability, 1, 547 – 561, Berkeley, university of California press

[10] Lindley, D.V. (1958): Fiducial distributions and Bayes' theorem, *Journal of the Royal Statistical Society, Series B*, 20, 102- 107.

[11] Shanker, R. (2015): Akash distribution and its Applications, *International Journal of Probability and Statistics*, 4(3), 65 – 75

[12] Shanker, R. and Mishra, A. (2013). A Quasi Lindley Distribution, *African Journal of Mathematics and Computer Science Research* , 6 (4), 64 – 71.

[13] Shanker, R. (2016): A Quasi Akash Distribution, *Assam Statistical Review,* 30(1), 135 -160.

[14] Murthy, D.N.P., Xie, M., Jiang, R. (2004): Weibull Models, John Wiley& sons Inc, Hoboken

Estimation of the Change Point in the Mean Control Chart for Autocorrelated Processes

Rupali Kapase, Vikas Ghute*

•

Department of Statistics
Punyashlok Ahilyadevi Holkar
Solapur University Solapur (MS)-413255, India
rakapase@sus.ac.in, vbghute_stats@rediffmail.com

* Corresponding Author

Abstract

Control charts are the most popular monitoring tools used to monitor changes in a process and distinguish between assignable and chance causes of variations. The time that a control chart gives an out-of-control signal is not the real time of change. The actual time of change is called the change point. Knowing the real time of change will help and simplify finding the assignable causes of the signal which may be the result of the shift in the process parameters. In this paper, we propose a maximum likelihood estimator of the process change point when a Shewhart $\bar{X}$ chart with autocorrelated observations signals a change in the process mean. The performance of the proposed change point estimator when used with $\bar{X}$ chart with AR(1) *process is investigated using simulation study. The results show that the performance of the proposed estimator has good properties in the aspect of expected length and coverage probability. We illustrate the use of proposed change point estimator through an example.*

Keywords: Change point; maximum likelihood estimator; control chart; average run length; autocorrelation; autoregressive process.

1. Introduction

Control chart is an important statistical process tool used to improve the quality of the manufacturing process which is widely used to monitor the process by distinguishing the assignable and chance causes of variations. It also helps us to detect changes in a process with issuing an out-of-control signal. Once control chart gives an out-of-control signal, that is, the assignable cause is present in the process, it is necessary to process practitioner that to identify and remove the sources responsible for the special cause of variability.

For the purpose of process improvement, process practitioner can take corrective action to return the process in the state of statistical control. The time at which the control chart gives an out-of-control signal, is not the real time of change and it shows the change with delay which depends on the size of the shift in process parameter. The actual time of change in the process is called change point. Finding the actual change point has been in great importance for many industries. The change point estimator when used with a control chart monitoring scheme helps

engineers to find actual time of step change. Knowing the actual time of change, leads to easier detection of change cause by limiting the scope of time within which searching for the change cause is done. Change point estimation also reduces the dependency of searching to process engineer's expertise and knowledge which leads to cost reduction. Therefore, change point estimation improves the overall change detection ability of the monitoring system.

Estimating the exact time of a step change in the process parameter of univariate and multivariate control charts has been discussed by various researchers. For univariate processes, Samuel et al. [1, 2] present a technique to estimate the time when a change in the process mean and variance of an independent normal process take place. Samuel et al. [3] estimated the change point in a normal process mean in SPC applications and compared the performance of maximum likelihood estimator with build-in change point estimators of CUSUM and EWMA. Park and Park [4] estimated the change point in the process for mean and variance when $\bar{X}$ and S control chart used simultaneously. Khoo [5] determined the permanent shift in the process mean with CUSUM control chart. Kapase and Ghute [6] estimated the time of a step change in the process mean with Tukey's control chart and individual X control chart and compared the both control charts in detecting the occurrence of the special cause in the process. Kapase and Ghute [7] discussed the maximum likelihood estimator of process change to identify the time of permanent shift in the normal mean with EWMA and MA control charts. Amiri and Allahari [8] presented a literature review on change point estimation methods for a control chart post signal diagnostics. For multivariate processes, Nedumaran et al. [9] have developed a change point MLE for sudden step change in mean of multivariate normal process when the process is monitored by χ^2 control chart. Dogu and Deveci-Kocakoc [10] proposed change point model for generalized variance control chart. Dogu and Deveci-Kocakoc [11] developed a change point estimation procedure for jointly monitoring the mean and covariance of multivariate normal process. Dogu [12] discussed multivariate joint change point estimation procedure for simultaneous monitoring of both location and dispersion under the assumption that the process is being monitored with a multivariate single control chart. Atashgar [13] reviewed the literature on the mean change point of univariate and multivariate processes.

The literature on the use of change point estimation in control charts assumes the independence of observations. In practice, we may come across processes dealing with autocorrelated observations. The processes such as those found in chemical manufacturing, refinery operations, smelting operations, wood product manufacturing, waste water processing and operation of nuclear reactors have been shown to have autocorrelated observations (Timmer et al. [14]). The autocorrelation can have a significant effect on statistical performance of the control charts for monitoring process parameters. In literature, little attention has been given to change point estimation in control charts when the observations are autocorrelated. Timmer and Pignatiello [15] developed three MLE change point estimators for the location, variance and autoregressive parameters for the use when the control charts are applied to autocorrelated data modeled by AR(1) process. Each of these estimators is then applied after a signal from a control chart indicates presence of special cause source of variability. It was shown that for all the three parameters the performance of the MLE change point estimator was superior to that of the other competing control charts.

Shewhart $\bar{X}$ control chart is most commonly used in practice for monitoring the process mean. It is based on the assumption that the sampled process is a normal whose observations are independent and identically distributed. In practice, we may come across processes dealing with autocorrelated observations. The purpose of this paper is to propose a change point estimator based on maximum likelihood approach for estimating the time of step change in the $\bar{X}$ chart when

the observations are autocorrelated. We assume that the process with autocorrelated observations can be modeled by first order autoregressive(AR(1)) model. We derive the maximum likelihood estimator for the time of step change in autocorrelated process mean. The proposed change point estimator is used when $\bar{X}$ chart with AR(1) process to monitor process mean issues a signal. We analyze the performance of our proposed estimator when it applied after $\bar{X}$ chart with AR(1) process signals that a assignable cause is present. An example of the use of proposed estimator is also given.

The paper is organized as follows. In section 2, first order autoregressive AR(1) model is discussed. Section 3 provides the details of $\bar{X}$ chart with AR(1) process. Section 4 gives the details of the change point model. The performance assessment and other performance measurements are provided in section 5. An illustrative example is given in Section 6. In Section 7 conclusions are given.

2. AR (1) Model of Autocorrelation

In this section, the first order autoregressive AR(1) model is presented. The AR(1) process is a time series model that fits many naturally occurring processes with autocorrelated observations. Assume that quality characteristic X follows $N(\mu_0, \sigma_0^2)$ when the process is in-control, where μ_0 and σ_0^2 are known as in-control mean and variance respectively. After each sampling interval i, n observations of quality characteristic X are collected. We also assume that the consecutive observations $\{X_{i,1}, X_{i,2}, \dots, X_{i,n}\}$ of the quality characteristic fit to a first order autoregressive AR(1) model as

$$X_{i,j} - \mu_0 = \phi\left(X_{i,j-1} - \mu_0\right) + \epsilon_j \ , i = 1,2, \dots \ . j = 1,2, \dots, n \tag{1}$$

where $\epsilon_j, j = 1,2, \dots, n$ are independently and identically distributed $N(0, \sigma_\epsilon^2)$ random error variables and ϕ is autocorrelation parameter. It is well known that the mean and variance of $X_{i,j}$ for such a model are $\frac{\mu}{1-\phi}$ and $\frac{\sigma_\epsilon^2}{1-\phi^2}$ respectively.

We consider the situation where the monitoring parameter μ can take one of the two values, either in-control value $\mu_0$or an out-of-control value μ_1. Initially the monitoring parameter has the value μ_0. The change point denoted by τ is the time at which the monitoring parameter changes its in-control value to its out-of-control value. Thus, the AR(1) model for the change point problem with monitoring parameter μ is given by

$$X_t = \mu_t + \phi X_{t-1} + \epsilon_t \ , \tag{2}$$

where $\mu_t = \begin{cases} \mu_0 \ , & if \ t < \tau \\ \mu_1 \ , & if \ t \geq \tau \end{cases}$

3. The $\bar{X}$ Chart for AR(1) Process

In this section, we assume that at time $i = 1,2, \dots$ the consecutive observations $X_{i,1}, X_{i,2}, \dots, X_{i,n}$ of quality characteristic X denote a sequence of samples each of size n taken on quality characteristic X generated by AR(1) model. The plotting statistic of the $\bar{X}$ chart is the sample mean $\bar{X}_i$ given as

$$\bar{X}_i = \frac{X_{i,1} + X_{i,2} + \cdots + X_{i,n}}{n} \tag{3}$$

Alwan and Roberts [16] give the standard deviation of the sample mean $\bar{X}_i$ is for AR(1)

process as

$$\sigma(\bar{X}_i) = \frac{\sigma_0}{\sqrt{n}\psi} \tag{4}$$

where, $\psi^{-1} = \sqrt{1 + \frac{2}{n}\left\{\frac{\phi^{n+1} - n\phi^2 + (n-1)\phi}{(\phi-1)^2}\right\}}$

The control limits *LCL* and *UCL* of two-sided control chart for monitoring the AR(1) quality characteristic are

$$UCL, LCL = \mu_0 \pm k\frac{\sigma_0}{\sqrt{n}\psi} \tag{5}$$

where $k > 0$ is a positive real valued constant defined to satisfy some desired in-control *ARL* denoted as $ARL_{\bar{X}}(0)$. In the $\bar{X}$ chart, if value of the plotting statistic $\bar{X}_i$ falls above the *UCL* or below the *LCL* then there is an indication that the process is out-of-control, that is, the process mean has been changed.

After the occurrence of assignable cause, process mean shifts from μ_0 to $\mu_1 = \mu_0 + \delta\sigma_0$ where δ is the standard shift size expresses as $\delta = \frac{(\mu_1 - \mu_0)}{\sigma_0}$. If $\delta = 0$, process is considered to be in-control otherwise the process is out of control.

The in-control *ARL* values of the $\bar{X}$ chart for the autocorrelated data can be calculated as

$$ARL_{\bar{X}}(0) = \frac{1}{\alpha} \tag{6}$$

$ARL_{\bar{X}}(0)$ is usually specified by the user based on the requirement of the false alarm rate and α is obtained. Using α, the value of the control limits coefficient *k* is obtained by

$$k = -\phi^{-1}(\alpha/2) \tag{7}$$

When the process is out-of-control,

$$ARL_{\bar{X}}(\delta) = \frac{1}{1-\beta} \tag{8}$$

where α and β are type I and type II error probabilities respectively. For $\bar{X}$ chart the probability of type II error is calculated by

$$\beta = \Phi\left(k - \delta\sqrt{n}\,\psi\right) - \Phi\left(-k - \delta\sqrt{n}\,\psi\right) \tag{9}$$

where $\Phi(.)$ is the cumulative distribution function of standard normal $N(0,1)$distribution.

4. Change Point Estimator for Process Mean

We will assume that the parameter μ of the time-series model is initially in-control with a known value of μ_0. However, after an unknown point in time a change in the process parameter occurs from μ_0 to $\mu_1 = \mu_0 + \delta\,\sigma_0/\sqrt{n}$, $\delta \neq 0$, where n is the subgroup size and δ is the unknown magnitude of the change. We also assume that once this step change in the process parameter occurs, the process remains at the new level of μ_1 until assignable cause has been identified and eliminated.

We will consider $\bar{X}$ chart signals at subgroup T that the process is no longer in a state of statistical control. This is the point at which quality engineer must initiate a search for assignable cause of variation. Let τ denote the last subgroup from the in-control process. Thus, $\bar{X}_1, \bar{X}_2, \ldots, \bar{X}_\tau$ are the subgroup averages from the in-control process, while $\bar{X}_{\tau+1}, \bar{X}_{\tau+2}, \ldots, \bar{X}_T$ are the subgroup averages when the process parameter changed.The change point estimator for μ is found by formulating a likelihood function and solving for an estimate of τ, the process change point. The detailed derivation of the change point estimator for μ is derived as follows:

We will assume that the autocorrelated observations are observed from the AR(1) model.

We develop a technique for detecting the change point for the parameter μ.

$$f(\bar{x}) = \frac{\sqrt{n}\,\psi}{\sigma_0\sqrt{2\pi}}\; exp\left\{\frac{-n\,\psi^2}{2\sigma_0^2}(\bar{X}_i - \mu_0/(1-\phi))^2\right\}$$

The likelihood function for the change point problem for μ is defined to be

$$L = \left[\frac{\sqrt{n}\psi}{\sigma_0\sqrt{2\pi}}\right]^T exp\left\{\frac{-n\,\psi^2}{2\sigma_0^2}\sum_{i=1}^{T}(\bar{X}_i - \mu_0/(1-\phi))^2\right\}$$

The log likelihood function (apart from a constant) is

$$\begin{aligned}
\log L &= \frac{-n\,\psi^2}{2\sigma_0^2}\sum_{i=1}^{T}(\bar{X}_i - \mu_0/(1-\phi))^2 \\
&= \frac{-n\,\psi^2}{2\sigma_0^2}\left[(\bar{X}_1 - \mu_0/(1-\phi))^2 + \sum_{i=2}^{T}(\bar{X}_i - \mu_0/(1-\phi))^2\right] \\
&= \frac{-n}{2\sigma_0^2}\left[\psi^2(\bar{X}_1 - \mu_0/(1-\phi))^2 + \psi^2\sum_{i=2}^{T}(\bar{X}_i - \mu_0/(1-\phi))^2\right] \\
&= \frac{-n}{2\sigma_0^2}\left[\psi^2(\bar{X}_1 - \mu_0/(1-\phi))^2 + \sum_{i=2}^{T}(\bar{X}_i - \mu_0 - \phi\bar{X}_{i-1})^2\right] \\
&= \frac{-n}{2\sigma_0^2}\left[\psi^2(\bar{X}_1 - \mu_0/(1-\phi))^2 + \sum_{i=2}^{\tau}(\bar{X}_i - \mu_0 - \phi\bar{X}_{i-1})^2 + \sum_{i=\tau+1}^{T}(\bar{X}_i - \mu_1 - \phi\bar{X}_{i-1})^2\right] \\
\log L &= \frac{-n}{2\sigma_0^2}\left[\psi^2(\bar{X}_1 - \mu_0/(1-\phi))^2 + \sum_{i=2}^{\tau}(\bar{X}_i - \mu_0 - \phi\bar{X}_{i-1})^2\right] + \frac{-n}{2\sigma_0^2}\sum_{i=\tau+1}^{T}(\bar{X}_i - \mu_1 - \phi\bar{X}_{i-1})^2
\end{aligned} \tag{10}$$

We note that Eq. (10) is a function of two unknown parameters τ and μ_1. For a fixed value of τ, it is easy to show that the maximum likelihood estimator of μ_1 is

$$\hat{\mu}_1(\tau) = \tfrac{1}{T-\tau}\textstyle\sum_{i=\tau+1}^{T}(\bar{X}_i - \phi\bar{X}_{i-1}) \tag{11}$$

Substituting this in Eq. (10) we get

$$\begin{aligned}
log\,L(\tau|\bar{x}) &= \frac{-n}{2\sigma_0^2}\left[\psi^2(\bar{X}_1 - \mu_0/(1-\phi))^2 + \sum_{i=2}^{\tau}(\bar{X}_i - \mu_0 - \phi\bar{X}_{i-1})^2\right] + \frac{-n}{2\sigma_0^2}\sum_{i=\tau+1}^{T}(\bar{X}_i - \hat{\mu}_1(\tau) - \phi\bar{X}_{i-1})^2 \\
&= \frac{-n}{2\sigma_0^2}\left[\psi^2(\bar{X}_1 - \mu_0/(1-\phi))^2 + \sum_{i=2}^{\tau}(\bar{X}_i - \mu_0 - \phi\bar{X}_{i-1})^2 + \sum_{i=\tau+1}^{T}(\bar{X}_i - \hat{\mu}_1(\tau) - \phi\bar{X}_{i-1})^2\right] \\
&= \frac{-n}{2\sigma_0^2}\left[\psi^2(\bar{X}_1 - \mu_0/(1-\phi))^2 + \sum_{i=2}^{\tau}\left((\bar{X}_i - \phi\bar{X}_{i-1}) - \mu_0\right)^2 + \sum_{i=\tau+1}^{T}\left((\bar{X}_i - \phi\bar{X}_{i-1}) - \hat{\mu}_1(\tau)\right)^2\right] \\
&= \frac{-n}{2\sigma_0^2}\left[\psi^2(\bar{X}_1 - \mu_0/(1-\phi))^2 + \sum_{i=2}^{\tau}\{(\bar{X}_i - \phi\bar{X}_{i-1})^2 - 2\mu_0(\bar{X}_i - \phi\bar{X}_{i-1}) + \mu_0^2\}\right. \\
&\left. + \sum_{i=\tau+1}^{T}\{(\bar{X}_i - \phi\bar{X}_{i-1})^2 - 2\hat{\mu}_1(\tau)(\bar{X}_i - \phi\bar{X}_{i-1}) + \hat{\mu}_1^2(t)\}\right]
\end{aligned}$$

$$= \frac{-n}{2\sigma_0^2}\left[\psi^2(\bar{X}_1 - \mu_0/(1-\phi))^2 + \left\{\sum_{i=2}^{\tau}(\bar{X}_i - \phi\bar{X}_{i-1})^2 - 2\mu_0\sum_{i=2}^{\tau}(\bar{X}_i - \phi\bar{X}_{i-1}) + (\tau-1)\mu_0^2\right\}\right.$$
$$\left. + \left\{\sum_{i=\tau+1}^{T}(\bar{X}_i - \phi\bar{X}_{i-1})^2 - 2\hat{\mu}_1(\tau)\sum_{i=\tau+1}^{T}(\bar{X}_i - \phi\bar{X}_{i-1}) + (T-\tau)\hat{\mu}_1^2(t)\right\}\right]$$
$$= \frac{-n}{2\sigma_0^2}\left[\psi^2(\bar{X}_1 - \mu_0/(1-\phi))^2 + \left\{\sum_{i=2}^{T}(\bar{X}_i - \phi\bar{X}_{i-1})^2 - 2\mu_0\sum_{i=2}^{\tau}(\bar{X}_i - \phi\bar{X}_{i-1})\right.\right.$$
$$\left.\left. - 2\hat{\mu}_1(\tau)\sum_{i=\tau+1}^{T}(\bar{X}_i - \phi\bar{X}_{i-1}) + (\tau-1)\mu_0^2 + (T-\tau)\hat{\mu}_1^2(t)\right\}\right]$$
$$= \frac{-n}{2\sigma_0^2}\left[\psi^2(\bar{X}_1 - \mu_0/(1-\phi))^2 + \left\{\sum_{i=2}^{T}(\bar{X}_i - \phi\bar{X}_{i-1})^2 - 2\mu_0\sum_{i=2}^{\tau}(\bar{X}_i - \phi\bar{X}_{i-1}) - 2\mu_0\sum_{i=\tau+1}^{T}(\bar{X}_i - \phi\bar{X}_{i-1})\right.\right.$$
$$\left.\left. + 2\mu_0\sum_{i=\tau+1}^{T}(\bar{X}_i - \phi\bar{X}_{i-1}) - 2\hat{\mu}_1(\tau)\sum_{i=\tau+1}^{T}(\bar{X}_i - \phi\bar{X}_{i-1}) + (\tau-1)\mu_0^2 + T\mu_0^2 - T\mu_0^2 + (T-\tau)\hat{\mu}_1^2(t)\right\}\right]$$
$$= \frac{-n}{2\sigma_0^2}\left[\psi^2(\bar{X}_1 - \mu_0/(1-\phi))^2 + \left\{\sum_{i=2}^{T}(\bar{X}_i - \phi\bar{X}_{i-1})^2 - 2\mu_0\sum_{i=2}^{T}(\bar{X}_i - \phi\bar{X}_{i-1}) - 2\mu_0(T-\tau)\hat{\mu}_1(\tau)\right.\right.$$
$$\left.\left. - 2\hat{\mu}_1(\tau)(T-\tau)\hat{\mu}_1(\tau) + \tau\mu_0^2 - \mu_0^2 + T\mu_0^2 - T\mu_0^2 + (T-\tau)\hat{\mu}_1^2(\tau)\right\}\right]$$
$$= \frac{-n}{2\sigma_0^2}\left[\psi^2(\bar{X}_1 - \mu_0/(1-\phi))^2 + \left\{\sum_{i=2}^{T}(\bar{X}_i - \phi\bar{X}_{i-1})^2 - 2\mu_0\sum_{i=2}^{T}(\bar{X}_i - \phi\bar{X}_{i-1}) + 2\mu_0(T-\tau)\hat{\mu}_1(\tau)\right.\right.$$
$$\left.\left. - 2(T-\tau)\hat{\mu}_1^2(\tau) - (T-\tau)\mu_0^2 + (T-1)\mu_0^2 + (T-\tau)\hat{\mu}_1^2(\tau)\right\}\right]$$
$$= \frac{-n}{2\sigma_0^2}\left[\psi^2(\bar{X}_1 - \mu_0/(1-\phi))^2 + \left\{\sum_{i=2}^{T}(\bar{X}_i - \phi\bar{X}_{i-1})^2 - 2\mu_0\sum_{i=2}^{T}(\bar{X}_i - \phi\bar{X}_{i-1})\right.\right.$$
$$\left.\left. + 2\mu_0(T-\tau)\hat{\mu}_1(\tau) - (T-\tau)\mu_0^2 + (T-1)\mu_0^2 - (T-\tau)\hat{\mu}_1^2(\tau)\right\}\right]$$
$$= \frac{-n}{2\sigma_0^2}\left[\psi^2(\bar{X}_1 - \mu_0/(1-\phi))^2 + \left\{\sum_{i=2}^{T}(\bar{X}_i - \phi\bar{X}_{i-1})^2 - 2\mu_0\sum_{i=2}^{T}(\bar{X}_i - \phi\bar{X}_{i-1}) + (T-1)\mu_0^2\right.\right.$$
$$\left.\left. + (T-\tau)[\hat{\mu}_1^2(\tau) - 2\mu_0\hat{\mu}_1(\tau)] + \mu_0^2\right\}\right]$$
$$= \frac{-n}{2\sigma_0^2}\left[\psi^2(\bar{X}_1 - \mu_0/(1-\phi))^2 + \left\{\sum_{i=2}^{T}(\bar{X}_i - \phi\bar{X}_{i-1})^2 - 2\mu_0\sum_{i=2}^{T}(\bar{X}_i - \phi\bar{X}_{i-1}) + (T-1)\mu_0^2\right.\right.$$
$$\left.\left. + (T-\tau)[\hat{\mu}_1(\tau) - \mu_0]^2\right\}\right]$$

The maximum likelihood estimate of τ is the value of t that maximizes the likelihood function. So, $\hat{\tau} = \arg\max_{1<t<T}[(\mathrm{T}-\mathrm{t})(\hat{\mu}_1(\tau) - \mu_0)^2]$.

5. Performance Evaluation

In this section, we study the performance of our proposed estimator using Monte Carlo simulation. The average change point estimate and the precision of the change point estimate are used as the performance measures for the use of proposed estimator. A simulation study is conducted to

examine the performance of proposed change point estimator used to $\bar{X}$ chart when process data are observed from the AR(1) model. In order to assess the performance, the observations are generated from AR(1) process. The in-control average run length (ARL) for the control chart is considered as 370. The change in the process is simulated at the point $\tau = 100$. Assuming that in-control AR(1) process has a $N(\mu_0, \sigma_0^2)$ distribution; the observations from 1 to 100 subgroups of size $n = 4$ with autocorrelation level ϕ are generated from $N(0,1)$ distribution. Starting from the subgroup 101, observations are randomly generated from a $N(\delta, 1)$ distribution until AR(1) $\bar{X}$ chart produces out-of-control signal and this is not a false alarm. At this point $\hat{t}$ is computed. The procedure is repeated 10000 times for each of the magnitude that are studied namely for $\delta =$ 0.5,1.0,1.5,2.0 and 3.0 with different levels of autocorrelation $\phi = -0.8$ to 0.8 in steps of size 0.2.

In Table 1, the expected length of each simulation run for various magnitudes of change in process mean is presented. The expected length $E(T)$ is the expected time at which the $\bar{X}$ chart is expected to issue a signal of a change in the process mean. Since the change had actually occurred following subgroup $\tau = 100$, $E(T) = 100 + ARL$, where ARL is the average run length of control chart for the out-of-control process. The values of $\bar{\hat{t}}$, the average change point estimate from 10000 simulation runs for various sizes of change in process mean for different levels of autocorrelation along with its corresponding standard error estimates are presented in Table 1. As the actual change point for the simulations is $\tau = 100$, the average estimated time of process change $\bar{\hat{t}}$ is expected to be close to 100.

Table 1: *Average change point estimates for* μ *and their standard errors.*

	ϕ								
	-0.8	-0.6	-0.4	-0.2	0.0	0.2	0.4	0.6	0.8
	$\delta = 0.5$								
$E(T)$	352.39	347.40	319.12	290.70	254.64	214.49	172.54	136.42	113.53
$\bar{\hat{t}}$	99.76	100.52	101.64	103.70	104.05	104.58	104.33	103.10	99.81
$s.e.(\bar{\hat{t}})$	0.085	0.1471	0.1947	0.222	0.081	0.229	0.206	0.167	0.127
	$\delta = 1.0$								
$E(T)$	225.05	211.69	187.16	165.51	143.27	127.01	114.78	107.89	104.52
$\bar{\hat{t}}$	100.10	99.99	100.04	100.21	100.30	100.22	100.01	99.34	98.87
$s.e.(\bar{\hat{t}})$	0.0226	0.043	0.056	0.066	0.071	0.077	0.075	0.074	0.078
	$\delta = 1.5$								
$E(T)$	163.70	150.88	134.82	123.75	114.85	109.02	105.50	103.73	102.80
$\bar{\hat{t}}$	100.10	100.00	99.75	99.93	99.82	99.66	99.34	98.99	99.13
$s.e.(\bar{\hat{t}})$	0.0161	0.0256	0.035	0.0388	0.051	0.054	0.0606	0.067	0.064
	$\delta = 2.0$								
$E(T)$	132.99	123.42	115.32	110.09	106.31	104.20	103.05	102.43	102.10
$\bar{\hat{t}}$	100.07	99.98	99.94	99.84	99.73	99.51	99.31	99.27	99.56
$s.e.(\bar{\hat{t}})$	0.015	0.0211	0.0249	0.0371	0.0378	0.0444	0.0504	0.049	0.0391
	$\delta = 3.0$								
$E(T)$	105.67	104.82	103.33	102.46	102.00	101.73	101.58	101.50	101.40
$\bar{\hat{t}}$	99.86	99.93	99.72	99.72	99.60	99.56	99.43	99.59	99.72
$s.e.(\bar{\hat{t}})$	0.0332	0.0216	0.038	0.030	0.0374	0.0344	0.043	0.029	0.026

From Table 1, we observe that for autocorrelation level $\phi = 0.4$ and magnitude of change in mean $\delta = 0.5$, the control chart issue a signal at time 172.54 on average. In this case, the average estimated time of process change is 104.33, which is fairly close to the actual change point 100. Also

for, $\phi = 0.4$ and $\delta = 1.0$, the average estimated time of signal is 100.01. For the cases with $\phi = 0.4$ and $\delta = 1.5$,2.0 and 3.0, the corresponding estimated times of signal are 99.34, 99.31 and 99.43 respectively. Similar pattern of estimated time of signal is observed for all considered levels of autocorrelations and magnitudes of change in process mean. Thus, we conclude that, on average, the proposed maximum likelihood estimator of the time of process change is fairly close to the actual time of change regardless of the magnitude of change in the process mean and the level of autocorrelation.

The precision of the change point estimator for the parameter μ is evaluated by examining the probability that $\hat{\tau}$ is within m observations of the actual change point. The estimated probability that the average change point estimate is within m subgroups of actual change point is shown in Table 2 for several values of m based on 10000 simulations with the autocorrelation levels $\phi =$ 0.2,0.4 and 0.6.

Table 2: *Precision of estimator for* μ *when* $n = 4$ *and* $\tau = 100$.

$\phi = 0.2$					
δ	0.5	1.0	1.5	2.0	3.0
$P(\lvert\hat{\tau} - \tau\rvert = 0)$	0.0894	0.2721	0.4725	0.6226	0.8173
$P(\lvert\hat{\tau} - \tau\rvert \leq 1)$	0.1842	0.4728	0.7058	0.8367	0.9352
$P(\lvert\hat{\tau} - \tau\rvert \leq 2)$	0.2665	0.5697	0.8124	0.9146	0.9631
$P(\lvert\hat{\tau} - \tau\rvert \leq 3)$	0.3192	0.6837	0.8756	0.9469	0.9737
$P(\lvert\hat{\tau} - \tau\rvert \leq 4)$	0.3707	0.7448	0.9134	0.9634	0.9798
$P(\lvert\hat{\tau} - \tau\rvert \leq 5)$	0.4174	0.7925	0.9360	0.9724	0.9834
$P(\lvert\hat{\tau} - \tau\rvert \leq 6)$	0.4599	0.8323	0.9535	0.9773	0.9851
$P(\lvert\hat{\tau} - \tau\rvert \leq 7)$	0.4971	0.8594	0.9639	0.9805	0.9872
$P(\lvert\hat{\tau} - \tau\rvert \leq 8)$	0.5326	0.8838	0.9709	0.9824	0.9888
$P(\lvert\hat{\tau} - \tau\rvert \leq 9)$	0.5619	0.9031	0.9761	0.9844	0.9903
$P(\lvert\hat{\tau} - \tau\rvert \leq 10)$	0.5856	0.9169	0.9781	0.9863	0.9915
$P(\lvert\hat{\tau} - \tau\rvert \leq 11)$	0.6102	0.9276	0.9812	0.9879	0.9920
$\phi = 0.4$					
$P(\lvert\hat{\tau} - \tau\rvert = 0)$	0.1204	0.2302	0.5147	0.6456	0.8239
$P(\lvert\hat{\tau} - \tau\rvert \leq 1)$	0.2095	0.5148	0.7374	0.8504	0.9310
$P(\lvert\hat{\tau} - \tau\rvert \leq 2)$	0.2815	0.6447	0.8380	0.9170	0.9584
$P(\lvert\hat{\tau} - \tau\rvert \leq 3)$	0.3475	0.7250	0.8917	0.9436	0.9692
$P(\lvert\hat{\tau} - \tau\rvert \leq 4)$	0.3968	0.7827	0.9258	0.9585	0.9755
$P(\lvert\hat{\tau} - \tau\rvert \leq 5)$	0.4432	0.8280	0.9443	0.9671	0.9798
$P(\lvert\hat{\tau} - \tau\rvert \leq 6)$	0.4822	0.8596	0.9572	0.9720	0.9827
$P(\lvert\hat{\tau} - \tau\rvert \leq 7)$	0.5192	0.8869	0.9638	0.9753	0.9854
$P(\lvert\hat{\tau} - \tau\rvert \leq 8)$	0.5507	0.9298	0.9679	0.9786	0.9870
$P(\lvert\hat{\tau} - \tau\rvert \leq 9)$	0.5805	0.9240	0.9718	0.9811	0.9885
$P(\lvert\hat{\tau} - \tau\rvert \leq 10)$	0.6038	0.9368	0.9746	0.9832	0.9898
$P(\lvert\hat{\tau} - \tau\rvert \leq 11)$	0.6293	0.9466	0.9778	0.9849	0.9910
$\phi = 0.6$					
$P(\lvert\hat{\tau} - \tau\rvert = 0)$	0.1596	0.3972	0.5823	0.7016	0.8516
$P(\lvert\hat{\tau} - \tau\rvert \leq 1)$	0.2654	0.6030	0.7961	0.8782	0.9411
$P(\lvert\hat{\tau} - \tau\rvert \leq 2)$	0.3411	0.7145	0.8749	0.9269	0.9623
$P(\lvert\hat{\tau} - \tau\rvert \leq 3)$	0.4057	0.7894	0.9141	0.9489	0.9724
$P(\lvert\hat{\tau} - \tau\rvert \leq 4)$	0.4595	0.8379	0.9344	0.9602	0.9800

$P(\|\hat{\tau}-\tau\| \le 5)$	0.5070	0.8719	0.9464	0.9671	0.9838
$P(\|\hat{\tau}-\tau\| \le 6)$	0.5524	0.8986	0.9548	0.9719	0.9857
$P(\|\hat{\tau}-\tau\| \le 7)$	0.5923	0.9149	0.9610	0.9756	0.9877
$P(\|\hat{\tau}-\tau\| \le 8)$	0.6302	0.9301	0.9658	0.9786	0.9893
$P(\|\hat{\tau}-\tau\| \le 9)$	0.6610	0.9422	0.9692	0.9808	0.9911
$P(\|\hat{\tau}-\tau\| \le 10)$	0.6851	0.9505	0.9711	0.9826	0.9919
$P(\|\hat{\tau}-\tau\| \le 11)$	0.7112	0.9555	0.9734	0.9846	0.9926

Consider the case of small level of autocorrelation $\phi = 0.2$ and small change of magnitude $\delta = 0.5$, we observe that the proposed estimator exactly identified the time of change in 8.94% of a total of 10000 simulations carried out. Further there would be 18.42% chance that the estimated change point is within ± 1 subgroup of actual change point and 25.65% chance that the estimated change point is within ± 2 subgroups of the actual change point and 61.02% chance that the estimated change point is within ± 11. As m increases, the value of precision also increases. For the case of large level of autocorrelation $\phi = 0.6$ and large change of magnitude $\delta = 3.0$, we observe that the proposed estimator exactly identified the time of change in 85.16% of a total of 10000 simulations carried out. Further there would be a 94.11 % chance that the estimated change point is within ± 1 subgroup of actual change point and 96.23% chance that the estimated change point is within ± 2 subgroups of the actual change point and 99.26% chance that the estimated change point is within ± 11. Thus, we conclude that the proposed estimator exhibits a good performance in identifying the time of change.

6. An Example

A numerical example is provided to illustrate the use of the proposed change point estimator for $\bar{X}$ chart with AR(1) process. The dataset in this example is generated from normally distributed quality characteristic with $\mu_0 = 1, \sigma_0 = 1$ and $\phi = 0.2$. When the desired type I error is $\alpha = 0.0027$, then the upper and lower control limits for $\bar{X}$ chart using Eq. (5) are *UCL*=1.73891 and *LCL*=-1.73891. Under the assumption that the process is in-control, the first 10 samples each of size $n = 4$ are generated from AR(1) process with $N(\mu_0, \sigma_0^2)$ and the remaining samples each of size $n = 4$ are generated from AR(1)process with $N(\mu_1, \sigma_0^2)$ until $\bar{X}$ chart issued a signal, here μ_1 denotes the changed mean.

The sample observations for each subgroup i, X_{i1}, X_{i2}, X_{i3} and X_{i4} and calculated subgroup averages $\bar{X}_i$ are shown in Table 3.

Table 3: *Observations from normal process with* $\phi = 0.2$ and $n = 4$.

i	X_{i1}	X_{i2}	X_{i3}	X_{i4}	$\bar{X}_i$	t	$\hat{\mu}_1(t)$	C_t
1	-0.7056	-0.3292	-0.7509	-1.0821	-0.7170	0		
2	1.5940	0.5129	-1.5725	-0.1931	0.0853	1	0.4583	7.1425
3	0.5516	1.2266	-0.3674	-0.8348	0.1440	2	0.4653	7.1446
4	-0.1713	1.9423	0.03207	0.2694	0.5181	3	0.4759	7.2465
5	1.5390	-0.9642	-0.3528	-0.8888	-0.1667	4	0.4754	7.0072
6	-0.8516	-0.3973	0.4710	1.7833	0.2514	5	0.5003	7.5089
7	1.0925	0.7734	0.7591	1.9817	1.1517	6	0.5077	7.4759
8	-1.4947	0.4468	-0.4431	-1.0924	-0.6459	7	0.4865	6.6279
9	-0.7333	2.8370	-0.6741	0.6855	0.5288	8	0.5370	7.7860
10	-1.0108	0.2336	2.4691	-1.0286	0.1658	9	0.5323	7.3682
11	1.2306	2.0690	3.2730	-0.0510	1.6304	10	0.5512	7.5966
12	-0.2249	0.8871	1.4378	1.3899	0.8725	11	0.5077	6.1852

13	1.3571	1.4480	-0.8006	0.9300	0.7336	12	0.5060	5.8882
14	-0.9501	-0.9501	-0.2132	0.3868	-0.4317	13	0.5036	5.5785
15	1.5943	1.2325	0.8867	2.3642	1.5194	14	0.5551	6.4703
16	0.9931	-0.4139	2.9077	0.0924	0.8948	15	0.5025	5.0509
17	1.8382	0.5626	1.0340	0.9139	1.0872	16	0.4979	4.7099
18	1.2815	1.5461	-0.4358	1.4192	0.9528	17	0.4751	4.0629
19	2.7691	1.4962	0.1349	0.3950	1.1988	18	0.4598	3.5939
20	1.9336	-0.3313	1.8259	1.7318	1.2900	19	0.4255	2.8969
21	-0.0468	0.9701	0.8853	0.2945	0.5258	20	0.3839	2.2102
22	1.0439	1.1534	0.7997	-0.3568	0.6601	21	0.3922	2.1530
23	1.9355	0.7652	0.8776	-0.0657	0.8782	22	0.3796	1.8736
24	0.7291	-0.9438	1.0241	0.5090	0.3296	23	0.3491	1.4624
25	0.8384	0.8187	-0.2365	0.0117	0.3581	24	0.3668	1.4802
26	1.7822	-0.1980	-1.0260	0.9183	0.3691	25	0.3743	1.4009
27	-0.7695	1.2146	0.2993	0.1080	0.2131	26	0.3828	1.3190
28	-0.4857	0.6726	-0.4337	0.6117	0.0912	27	0.4133	1.3663
29	0.5524	-0.7997	-0.3407	1.6733	0.2713	28	0.4654	1.5159
30	-0.1526	-1.4796	-0.4572	-0.2571	-0.5866	29	0.5007	1.5045
31	0.3958	0.6523	-0.3440	2.0372	0.6853	30	0.7291	2.6578
32	-1.3273	-1.1706	2.2603	1.1004	0.2157	31	0.71069	2.0203
33	-0.6394	-0.2231	2.0017	-0.2361	0.2258	32	0.9214	2.5468
34	-1.9289	1.4110	2.4092	1.3562	0.8119	33	0.8605	2.2213
35	1.5843	2.1275	2.4985	1.6982	1.9771	34	1.8147	3.2933

It can be seen that a total of 35 subgroup averages were obtained before one of them exceeded the upper control limit. Thus, following this first signal from the $\bar{X}$ chart at time $T = 35$, our proposed change point estimator can be applied. The values of C_t statistics are then calculated. The largest value of C_t is 7.7860 which is associated with subgroup 9. Thus, we estimate that subgroup 9 was the first subgroup obtained from the changed process and consequently that subgroup 8 was the last subgroup from the in-control process.

7. Conclusion

In this paper, monitoring the process mean using Shewhart $\bar{X}$ chart in the presence of autocorrelated data under normal process is considered. We have derived the maximum likelihood estimator that is useful for identifying the change point of a step change in the mean of normal process when autocorrelation may exist in the process. We have investigated the performance of our change point estimator when it is used with $\bar{X}$ chart with AR(1) process. The results show that the performance of the proposed estimator has good properties in the aspect of expected length and coverage probability for autocorrelated data.

Acknowledgment

The first author would like to thank the Department of Science and Technology, Government of India, for supporting this research by Inspire Fellowship No. DST/INSPIRE Fellowship / 2016 / IF / 160410.

References

[1] Samuel, T. R., Pignatiello Jr., J. J. and Calvin, J. A. (1998a). Identifying the time of a step-change with $\bar{X}$ control charts. *Quality Engineering,* 10(3): 521-527.

[2] Samuel, T. R., Pignatiello Jr., J. J. and Calvin, J. A. (1998b). Identifying the time of a step-change in a normal process variance. *Quality Engineering,* 10(3): 529-538.

[3] Samuel, T. R., Pignatiello Jr., J. J. and Calvin, J. A. (2001). Estimation of the change point of a normal process mean in SPC applications, *Journal of Quality Technology*, 33: 82-95.

[4] Park, J. and Park, S. (2004). Estimation of the change point in the $\bar{X}$ and S control charts. *Communications in Statistics-Simulation and Computation,* 33(4): 1115-1132.

[5] Khoo, M. B. C. (2004). Determining the time of a permanent shift in the process mean of CUSUM control charts. *Quality Engineering,* 17(1): 87-93.

[6] Kapase, R. A. and Ghute, V.B. (2018). Estimating the period of a step-change in single observation data. *International Journal of Agricultural and Statistical Sciences,* 14: 433-438.

[7] Kapase, R. A. and Ghute, V.B. (2021). Identifying the time of permanent shift in the normal process mean with memory type control charts. *Statistics and Applications*, (Accepted on 09 June 2021).

[8] Amiri, A. and Allahyari, S. (2012). Change point estimation methods for control chart postsignal diagnostics: A literature review. *Quality and Reliability Engineering International*, 28(7): 673-685.

[9] Nedumaran, G., Pignatiello Jr., J. J. and Calvin, J. A. (2000). Identifying the time of a step-change with χ^2control charts. Quality Engineering, 13(2): 153-159.

[10] Dogu, E. and Deveci-Kocakoc, I. (2011). Estimation of change pointin generalized variance control chart. *Communication in Statistics- Simulation and Computation,* 40(3): 345-363.

[11] Dogu, E. and Deveci-Kocakoc, I. (2013). A multivariate change point detection procedure for monitoring mean and covariance simultenously. *Communication in Statistics- Simulation and Computation.* 42: 1235-1255.

[12] Dogu, E. (2015). Identifying the time of step change with multivariate single control charts. *Journal of Statistical Computation and Simulation,* 85(8): 1529-1543.

[13] Atashgar, A. (2013). Identification of change point: an overview. *International Journal of Advanced Manufacturing Technology*, 64: 1663-1683.

[14] Timmer, D. H, Pignatiello Jr., J. J. and Longnecker, M.T. (1998). The development and evaluation of cusum-based control charts for an AR (1) process. *IIE Transaction in Quality and Reliability,* 30: 525-534.

[15] Timmer, D. H. and Pignatiello Jr., J. J. (2003). Change point estimates for the parameters of an AR(1) process. *Quality and Reliability Engineering International* , 19: 355-369.

[16] Alwan, L.C. and Roberts, H.V. (1988). Time-series modeling for statistical process control. *Journal of Business and Economic Statistics,* 6:87-95.

PERFORMABILITY ANALYSIS OF MULTISTATE ASH HANDLING SYSTEM OF THERMAL POWER PLANT WITH HOT REDUNDANCY USING STOCHASTIC PETRINETS

Er. Sudhir Kumar *

•

Research Scholar, Department of Production & Industrial Engg.,
National Institute of Technology, Kurukshetra, Haryana, India
sudhirtamak@gmail.com

Dr. P.C. Tewari

•

Professor & Head, Department of Mechanical Engineering,
National Institute of Technology, Kurukshetra, Haryana, India
pctewari1@gmail.com

Abstract

This work seeks to propose a Petri nets-based technique for evaluating the performability features of ash handling system of a coal-based thermal power plant. The impact of failure and repair parameters on system performance has been determined. For the modelling of the system Stochastic Petri Nets (SPN) an extended version of Petri nets is applied. The recommended methodology used in this study allows for a better understanding of the system's performance behavior under various operating situations. The study provides Decision Support System which will assist managers in making informed decisions about inventory and spare parts for plant operations.

Keywords: Availability, Performability, Petri Nets, Ash Handling System

I. Introduction

In the present era, integrated automation in the industries has evolved a tendency to design and construct the systems with higher flexibility, complexity, and production capacity as a result of rapid technological breakthroughs. Power generation units are also facing a number of obstacles in meeting the rising demand for electricity in both industrial and domestic applications. High productivity, as well as high payback ratios, have become critical for these units' survival. The desire for improved availability has arisen as a result of the dynamic behavior of industrial equipment and systems. As a result, such industrial systems are expected to operate for as long as feasible in order to meet the appropriate level of output requirements. Performability practitioners' jobs have become more difficult as a result of having to investigate, characterize, measure, and analyse system behavior. Industrial systems, on the other hand, are practically impossible to operate without failure. Output losses, on the other hand, could be reduced by using enough redundant parts or expanding the system's production capacity [1].

II. Literature Review

A large number of research papers have sought to use reliability principles to examine the performance of real-world industrial systems. These are largely concerned with the modelling and analysis of multi-component complex systems. Cherry et al. [2] evaluated the plant's long-run availability assuming constant failure rate and repair for its various subsystems in a chemical industry. Dhillon and Rayapati [3] discussed the application of reliability engineering principles to chemical associated industries, as the risk associated with these industries is extremely significant. Singh [4] discussed the use of reliability approaches in a biogas plant was considered. Kumar et al. [5–8] In his research work for studying and evaluating the performance of paper, sugar, and fertilizer industries, Markov approach modelling was applied. Arora and Kumar [9] offered a stochastic study of a thermal power plant's ash handling system to aid plant personnel's in predicting the behavior of running units. Michelson [10] discussed the current state of reliability technology in the process industry and offered recommendations for the future. Singh and Mahajan [11] studied the reliability behavior of a utensil manufacturing plant. Sarkar and Sarkar [12] have addressed strategies for determining the availability and restricting the average availability of a system that is inspected on a regular basis, has a spare unit, and is well-maintained. Dai et al. [13] analyzed the service reliability and availability for a distribution system. Madu [14] in order to achieve competitiveness and customer happiness, the strategic importance of reliability and maintainability management was investigated. Singh and Garg [15] under the premise of constant failure and repair rates did an availability analysis of the core veneer manufacturing system in a plywood manufacturing system. Gupta et al. [16] used exponentially distributed failure rates of various components while evaluating the reliability metrics of a butter producing system in a dairy factory. Singh et al. [17] analyzed the reliability of ash-handling system with ash water pumps in which two units are operational at the same time and the third is a cold standby. More recently, Kumar et al [18, 19, and 20] for modeling and analysis of performability of various complex industrial systems, Petri nets were used.

III. System Description

After coal is burned, ash is continuously produced in the plant, necessitating an efficient ash handling system to dispose of this waste material. Figure 1 depicts the flow diagram of a thermal power plant's coal ash handling system. The following subsystems are arranged in a sequence in this system:

i) Furnace (F): A boiler furnace is used to produce high-temperature heating by combusting coal with the least amount of smoke possible. The outside half of these furnaces is made of cast iron, while the interior is made of a brick shell and glass wool. There is no hot redundancy available for furnace, hence the failure of furnace will shift the whole system into completely down state.

ii) Electrostatic Preceptor (Ei): It is a device that is extensively used to remove fly ash from flowing gas (boiler emissions) with the help of an electric charge. There are two Electrostatic Preceptor provides hot redundancy to the system. Failure of any one of these will brings the system into the state of working in reduced capacity.

iii) Vessel (V): These Vessels are positioned just below the ESP hoppers with the dome valve arrangement. These are supposed to hold the fly ash for a period of time before being transported to the fly ash silos. There is no hot redundancy available for vessel also, hence the failure this will shift the whole system into completely down state.

iv) Compressor Transportation Line (C): In the plant, there is a compressed air station. The

compressed air station supplies air to the pneumatic conveying system and the fabric filter purging system. Similarly, there is no redundant unit available for Compressor Transportation Line. The failure of this will cause complete failure of system.

v) Ash Silo (Ai): It keeps the fly ash generated by the boiler at the highest possible level of continuous operation. There are three number of Ash Silo connected parallelly available in the system.

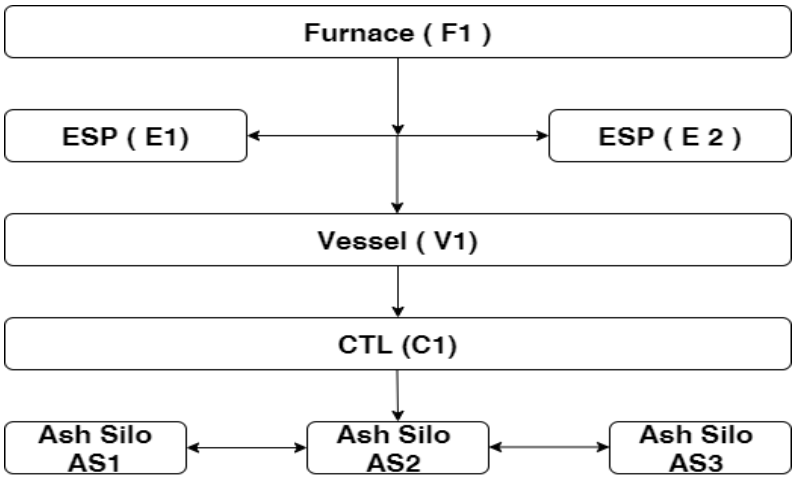

Figure 1: *Flow Diagram of Ash Handling System*

IV. Performance Modeling

The Petri Nets approach was used to create the performance model. It depicts the interactions between the many subsystems of system. When a number of repair facilities aren't up to snuff, all of the failures can't be handled at once, and the failed units have to wait in line to be repaired. In Fig.2, the PN model of the plant's ash handling system is illustrated as follows:

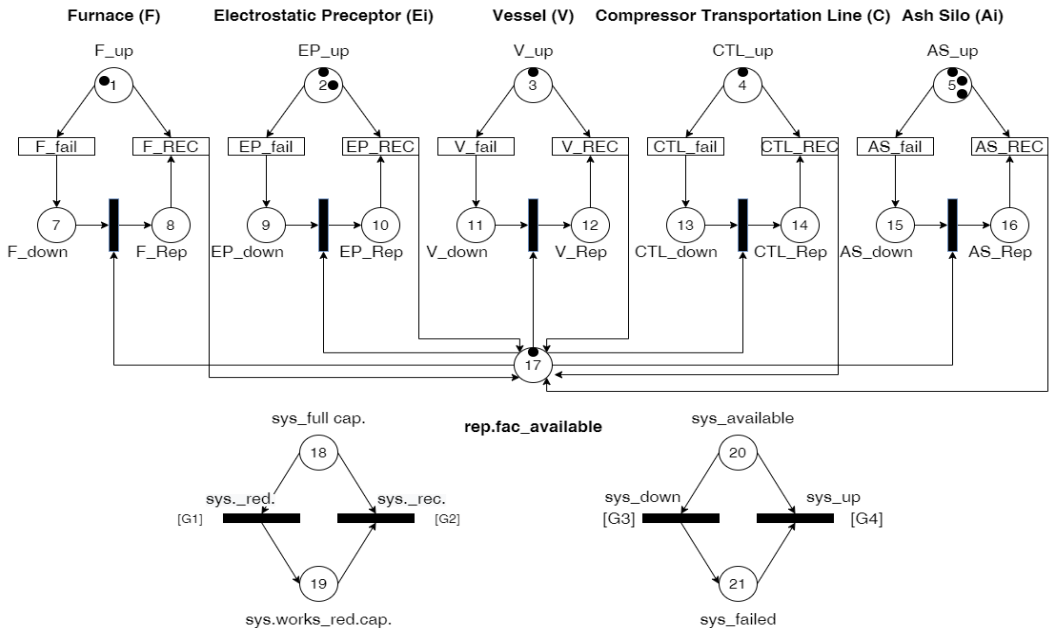

Figure: 2 *Petri Nets Modelling of Ash Handling System*

V. Performance Analysis

The system's dynamic behavior was analyzed utilizing a set of variables to determine the performability parameters. In consultation with the plant's maintenance engineers, the permissible value pair of failure and repair rates for the subsystems (Table 1) was determined. The impact of repairman availability on these factors is also explored. The results are shown in the tables below (Tables 2 to 11) and discussed further below.

Table 1: *Failure and Repair Rated of various subsystems of Ash Handling System*

Name of Subsystem	Failure Rate (per hour)	Repair Rate (per hour)
Furnace	0.0045	0.20
Electrostatic Preceptor	0.014	0.20
Vessel	0.0025	0.125
Compressor Transportation Line	0.014	0.065
Ash Silo	0.00006	0.015

Table 2: *Performability Matrix for Furnace of Ash Handling System in Full Capacity*

	ρ1	0.10	0.15	0.20	0.25	0.30	
μ1							Constant Parameters
0.0025		0.7437	0.7690	0.7710	0.7793	0.7810	
0.0035		0.7389	0.7650	0.7700	0.7714	0.7790	μ2= 0.014 ρ 2= 0.20
0.0045		0.7353	0.7614	0.7680	0.7700	0.7757	μ3= 0.0025 ρ 3=0.125 μ4= 0.014 ρ 4=0.065
0.0055		0.7344	0.7564	0.7610	0.7681	0.7750	μ5= 0.00006 ρ 5=0.015
0.0065		0.7278	0.7530	0.7592	0.7633	0.7677	

Table 3: *Performability Matrix for Furnace of Ash Handling System in Reduced Capacity*

	ρ1	0.10	0.15	0.20	0.25	0.30	
μ1							Constant Parameters
0.0025		8700.42	8731.13	8745.91	8749.65	8757.19	
0.0035		8666.48	8713.40	8732.40	8744.18	8748.26	μ2= 0.014 ρ 2= 0.20
0.0045		8647.71	8702.28	8726.70	8737.67	8746.96	μ3= 0.0025 ρ 3=0.125 μ4= 0.014 ρ 4=0.065
0.0055		8627.91	8689.00	8714.44	8731.01	8740.47	μ5= 0.00006 ρ 5=0.015
0.0065		8599.39	8678.57	8705.44	8720.97	8735.03	

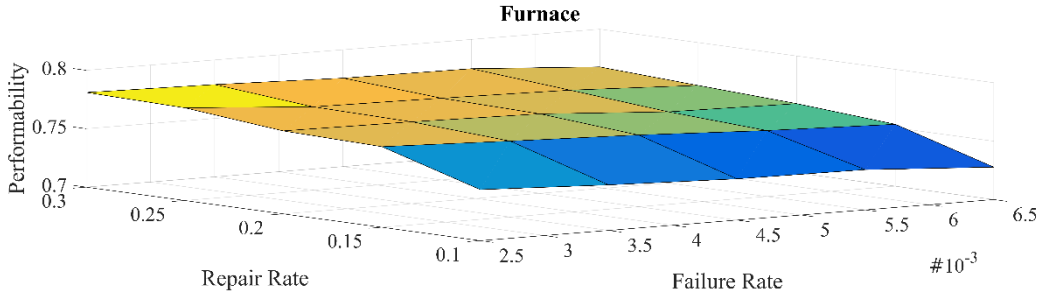

Figure: 3 *Impact of Variation in FRR of Furnace on the Performability of Ash Handling System*

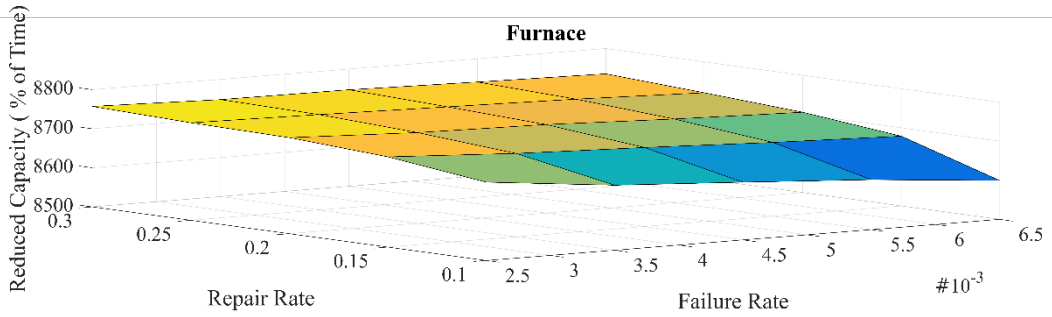

Figure: 4 *Impact of Variation in FRR of Furnace on the Performability of Ash Handling System (Reduced Capacity)*

The change in the failure and repair rates has a moderate impact on the system's availability, as shown in Fig. 3. The system availability is reduced by 5.32 percent due to an increase in furnace failure rates from 0.0025 to 0.0065 and a fall in repair rates from 0.3 to 0.1. However, changes in furnace failure and repair rates have a substantial impact on the system's ability in reduced capacity; variation up to 15.78 percent is observed. Figure 4 depicts the situation.

Table 4: *Performability Matrix for Crusher of ESP Handling System in Full Capacity*

μ2 \ ρ2	0.10	0.15	0.20	0.25	0.30	Constant Parameters
0.012	0.7624	0.7941	0.8043	0.8291	0.8421	
0.013	0.7310	0.7628	0.7871	0.8055	0.8145	μ1=0.0045 ρ 1=0.20
0.014	0.7121	0.7417	0.7680	0.7776	0.8043	μ3= 0.0025 ρ 3=0.125
0.015	0.6790	0.7126	0.7528	0.7660	0.7821	μ4= 0.014 ρ 4=0.065
0.016	0.6541	0.6990	0.7208	0.7504	0.7638	μ5= 0.00006 ρ 5=0.015

Table 5: *Performability Matrix for Crusher of ESP Handling System in Reduced Capacity*

μ2 \ ρ2	0.10	0.15	0.20	0.25	0.30	Constant Parameters
0.012	8621.50	8756.70	8846.73	8909.32	8954.51	
0.013	8520.06	8682.05	8782.05	8856.89	8907.44	μ1=0.0045 ρ 1=0.20
0.014	8434.72	8610.48	8726.70	8810.61	8869.15	μ3= 0.0025 ρ 3=0.125
0.015	8347.87	8544.23	8661.92	8758.54	8829.18	μ4= 0.014 ρ 4=0.065
0.016	8278.33	8477.67	8626.18	8722.35	8789.41	μ5= 0.00006 ρ 5=0.015

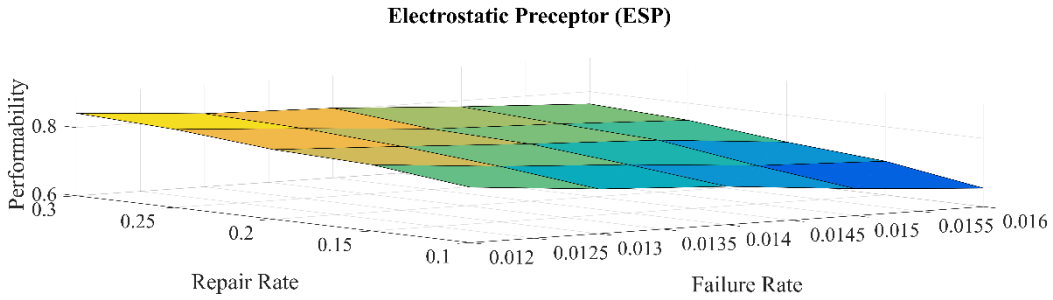

Figure: 5 *Impact of Variation in FRR of ESP on the Performability of Ash Handling System*

The variance in the ESP's failure and repair rates has a major impact on the system's availability, as shown in Figure 5. An increase in ESP failure rate from 0.012 to 0.016, as well as a fall in repair rates from 0.3 to 0.1, reduces system availability by up to 18.80%. The same changes in ESP failure and repair rates, on the other hand, have a moderate impact on the system's performability at reduced capacity varies up to 6.76 percent. Figure 6 depicts the situation.

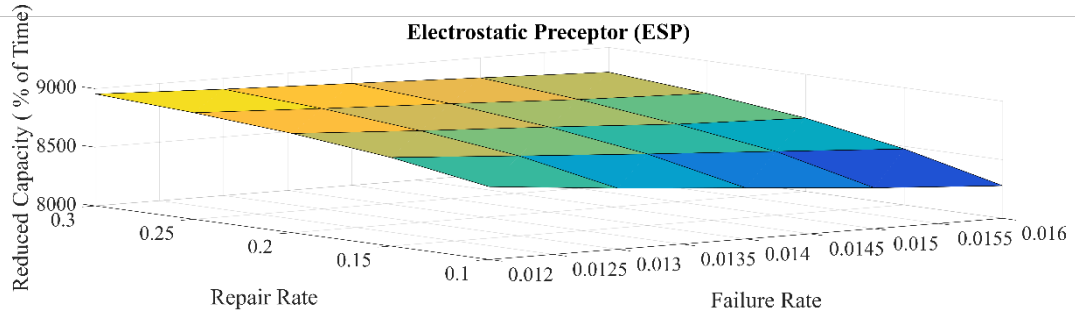

Figure: 6 *Impact of Variation in FRR of ESP on the Performability of Ash Handling System (Reduced Capacity)*

Table 6: *Performability Matrix for Vessel of Ash Handling System in Full Capacity*

μ3 \ ρ3	0.025	0.075	0.125	0.175	0.225	Constant Parameters
0.0021	0.7618	0.7736	0.7742	0.7772	0.7814	μ1=0.0045 ρ 1=0.20
0.0023	0.7550	0.7603	0.7723	0.7760	0.7809	μ2= 0.014 ρ 2= 0.20
0.0025	0.7430	0.7617	0.7680	0.7752	0.7765	μ4= 0.014 ρ 4=0.065
0.0027	0.7354	0.7562	0.7592	0.7616	0.7700	μ5= 0.00006 ρ 5=0.015
0.0029	0.7275	0.7451	0.7544	0.7609	0.7690	

Table 7: *Performability Matrix for Vessel of Ash Handling System in Reduced Capacity*

μ3 \ ρ3	0.025	0.075	0.125	0.175	0.225	Constant Parameters
0.0021	8196.63	8644.88	8877.38	9022.68	9118.56	μ1=0.0045 ρ 1=0.20
0.0023	8061.35	8551.31	8804.98	8962.56	9067.80	μ2= 0.014 ρ 2= 0.20
0.0025	7946.32	8454.31	8726.70	8890.41	9005.73	μ4= 0.014 ρ 4=0.065
0.0027	7796.23	8359.00	8648.22	8824.13	8943.50	μ5= 0.00006 ρ 5=0.015
0.0029	7691.22	8264.24	8566.09	8756.02	8884.35	

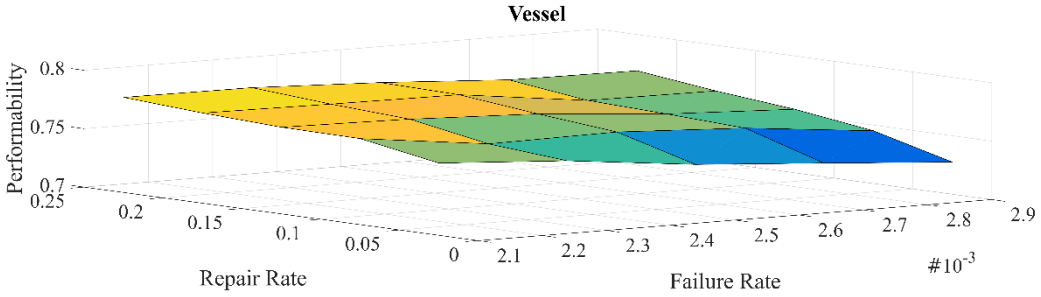

Figure : 7 *Impact of Variation in FRR of Vessel on the Performability of Ash Handling System*

The change in the Vessel's failure and repair rates has a lesser impact on the system's availability, as shown in Fig. 7. The system availability is reduced by 5.39 percent due to an increase in Vessel failure rates from 0.0021 to 0.0029 and a fall in repair rates from 0.225 to 0.025.

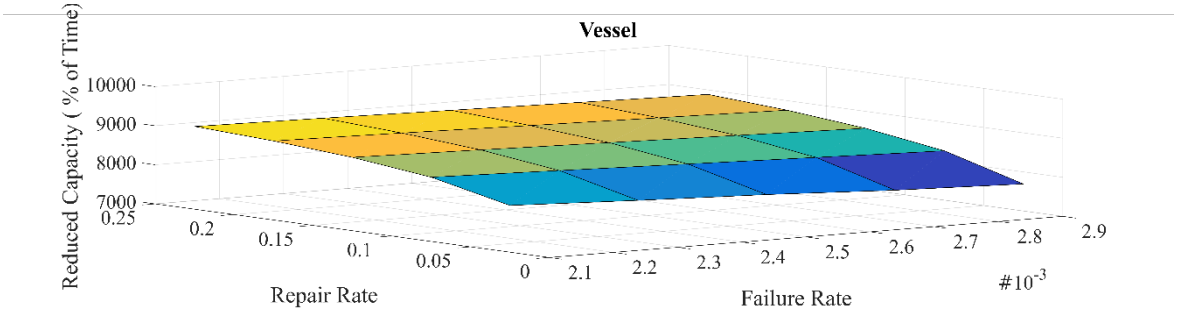

Figure : 8 *Impact of Variation in FRR of Vessel on the Performability of Ash Handling System (Reduced Capacity)*

However, the same fluctuations in the Vessel's failure and repair rates have a significant impact on the system's performability at reduced capacity, up to 14.27 percent change observed. Figure 8 depicts the situation.

Table 8: *Performability Matrix for CTL of Ash Handling System in Full Capacity*

μ4 \ ρ4	0.045	0.055	0.065	0.075	0.085	Constant Parameters	
0.010	0.7166	0.7597	0.7742	0.7781	0.7793		
0.012	0.7012	0.7568	0.7692	0.7713	0.7763	μ1=0.0045	ρ 1=0.20
0.014	0.6930	0.7552	0.7680	0.7687	0.7754	μ2= 0.014	ρ 2= 0.20
0.016	0.6894	0.7483	0.7655	0.7685	0.7733	μ3= 0.0025	ρ 3=0.125
0.018	0.6849	0.7422	0.7586	0.7658	0.7656	μ5= 0.00006	ρ 5=0.015

Table 9: *Performability Matrix for CTL of Ash Handling System in Reduced capacity*

μ4 \ ρ4	0.045	0.055	0.065	0.075	0.085	Constant Parameters	
0.010	8401.68	8690.45	8738.07	8750.19	8762.42		
0.012	8364.56	8682.63	8735.64	8748.93	8756.41	μ1=0.0045	ρ 1=0.20
0.014	8318.63	8671.83	8726.70	8746.05	8751.93	μ2= 0.014	ρ 2= 0.20
0.016	8291.45	8665.80	8719.08	8744.20	8747.90	μ3= 0.0025	ρ 3=0.125
0.018	8271.02	8655.22	8718.37	8735.35	8745.78	μ5= 0.00006	ρ 5=0.015

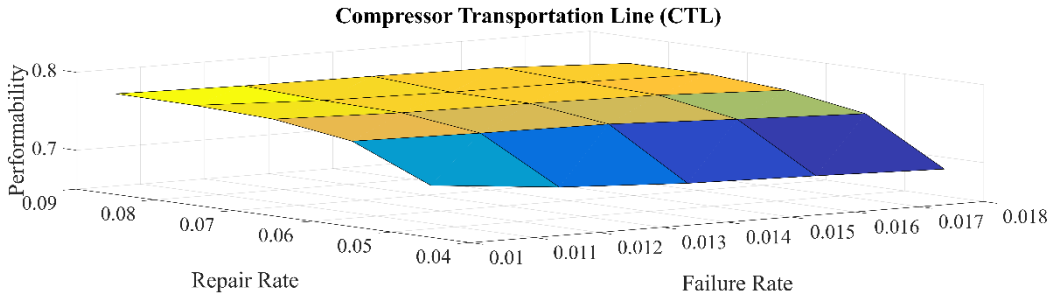

Figure : 9 *Impact of Variation in FRR of CTL on the Performability of Ash Handling System*

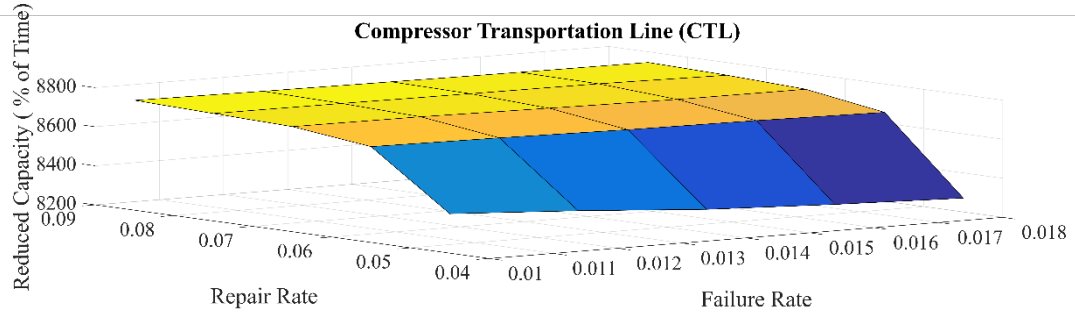

Figure : 10 *Impact of Variation in FRR of CTL on the Performability of Ash Handling System (Reduced Capacity)*

Table 10: *Performability Matrix for Ash Silo of Ash Handling System in Full Capacity*

	ρ5	0.005	0.010	0.015	0.020	0.025	
μ5							Constant Parameters
0.00004		0.7679	0.7674	0.7698	0.7707	0.7740	
0.00005		0.7599	0.7634	0.7685	0.7701	0.7730	μ1=0.0045 ρ 1=0.20
0.00006		0.7576	0.7630	0.7680	0.7661	0.7712	μ2= 0.014 ρ 2= 0.20
0.00007		0.7571	0.7621	0.7646	0.7660	0.7703	μ3= 0.0025 ρ 3=0.125
0.00008		0.7555	0.7576	0.7574	0.7607	0.7616	μ4= 0.014 ρ 4=0.065

Table 11: *Performability Matrix for Ash Silo of Ash Handling System in reduced Capacity*

	ρ5	0.005	0.010	0.015	0.020	0.025	
μ5							Constant Parameters
0.00004		8694.94	8729.57	8742.85	8750.96	8753.96	
0.00005		8674.05	8717.78	8736.01	8743.07	8749.00	μ1=0.0045 ρ1=0.20
0.00006		8653.00	8707.61	8726.70	8736.81	8744.16	μ2= 0.014 ρ 2= 0.20
0.00007		8635.81	8700.05	8721.50	8732.69	8740.76	μ3= 0.0025 ρ 3=0.125
0.00008		8615.26	8687.43	8713.46	8727.31	8736.70	μ4= 0.014 ρ 4=0.065

The change in failure and repair rates of the CTL has a significant impact on the system's availability, as shown in Fig. 9. The system availability is reduced by 9.44 percent due to an increase in CTL failure rates from 0.010 to 0.018 and a fall in repair rates from 0.085 to 0.045. The same changes in CTL failure and repair rates, on the other hand, have the least impact on the system's ability to operate at a reduced capacity of up to 4.91 percent. Figure 10 depicts it.

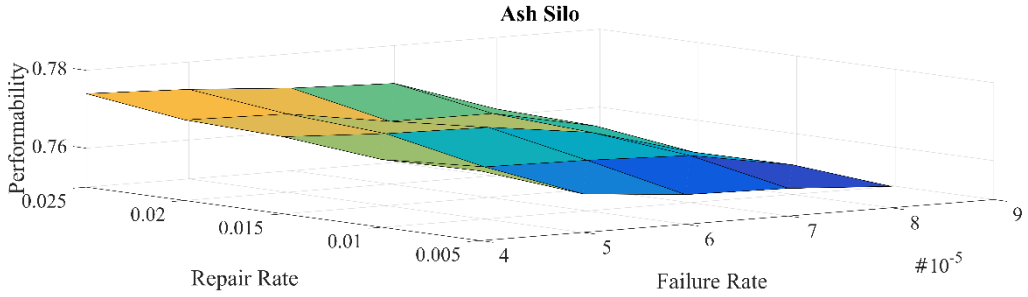

Figure : 11 *Impact of Variation in FRR of Ash Silo on the Performability of Ash Handling System*

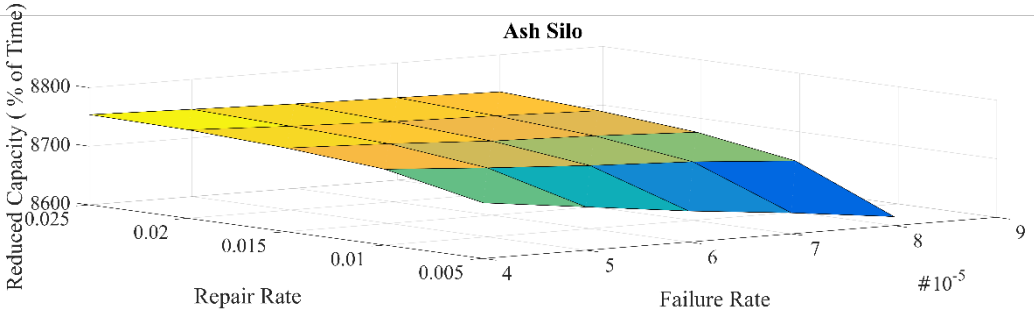

Figure : 12 *Impact of Variation in FRR of Ash Silo on the Performability of Ash Handling System (Reduced Capacity)*

The variance in failure and repair rates of the Ash Silo has a small impact on the system's availability, as shown in Fig. 11. The system availability is reduced by 1.85 percent due to an increase in Ash Silo failure rates from 0.010 to 0.018 and a fall in repair rates from 0.085 to 0.045. However, the same changes in the Ash Silo's failure and repair rates have had the least impact on the system's ability to perform in decreased capacity by up to 1.38 percent. Figure 12 depicts it.

Table 12: *Impact of Variation in the Repair Facilities on Performability of Ash Handling System*

No. of Repair Facilities	1	2	3	4	5
Availability	0.7680	0.7872	0.7877	0.7883	0.7882
Reduced Capacity	8726.70	8918.72	8922.80	8922.86	8922.80

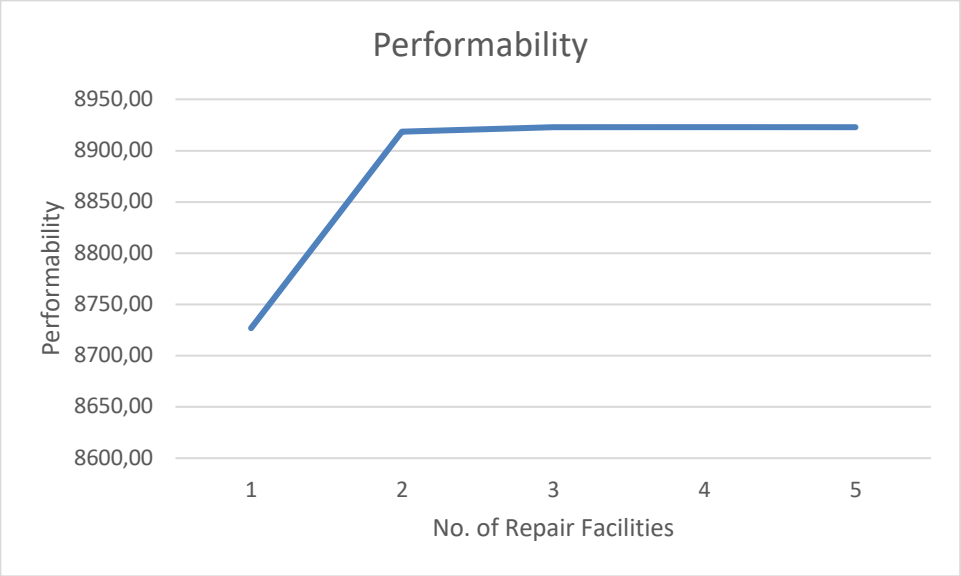

Figure : 13 *Impact of Variation in Repair Facilities on the Performability of Ash Handling System*

The influence of the number of repair facilities on system performance is depicted in Figure 13. When there are two or more repairmen in the system, the performance metrics stabilize. It leads to the conclusion that two separate repair facilities are required to obtain the best system performance.

VI. Conclusions

The Electrostatic Precipitator is the most vital part of the Ash Handling System, and it requires the most meticulous maintenance, according to the results of the current case study. The management will be aided in choosing the product mix by an examination of systems operating at decreased capacity and with degraded quality. The impact of repairmen availability on system performance will aid in resource allocation decisions. This will assist in lowering operation and maintenance expenses while also increasing output volume. It will also assist in raising the product's quality requirements.

Petri Nets can aid in the reduction of the time-consuming computational efforts required by Markov and other similar modelling methods. Choosing an appropriate technique, in fact, has a direct impact on operational and maintenance costs.
Decision Support System was developed based on the analysis as illustrated in Table 13. This will assist managers in making informed decisions about inventory and spare parts for plant operations.

Table 13: *Decision Support System*

Name of Subsystem	Impact of Variations in FRR on Performability at full capacity (percent)	Impact of Variations in FRR on Performability with reduced capacity(%)	Maintenance Priorities Suggestions
Furnace	5.32	15.78	IV
Electrostatic Preceptor	18.80	6.76	I
Vessel	5.39	14.27	III
Compressor Transportation Line	9.44	4.91	II
Ash Silo	1.85	1.38	V

References

[1] Galikowsky C, Sivazlian BD, Chaovalitwongse P (1996) optimal redundancies for reliability and availability of series systems. Microelectron Reliab 36(10):1537–1546.
[2] Cherry, D.H., Grogan, J.C., Holmes, W.A. and Perris, F.A. (1978) 'Availability analysis for chemical plants', Chem. Eng. Prog., Vol. 74, No. 1, pp.55–60.
[3] Dhillon, B. and Rayapati, S. (1988) 'Chemical system reliability: a review', IEEE Trans. Reliab., Vol. 37, No. 2, pp.21–26.
[4] Singh J (1989) Reliability analysis of a biogas plant having two dissimilar units. Microelectron Reliab 29:779–781. doi:10.1016/ 0026-2714(89)90178-9.
[5] Kumar D, Singh IP, Singh J (1988) Reliability analysis of feeding system in the paper industry. Microelectron Reliab 28:213–215. doi:10.1016/0026-2714(88)90353-8.
[6] Kumar D, Singh J, Pandey PC (1989) Maintenance planning for pulping system in the paper industry. Reliab Eng Syst Saf 25 (4):293–302. doi:10.1016/0951-8320(89)90059-8.
[7] Kumar D, Pandey PC, Singh J (1991) Process design for a crystallization system in the urea fertilizer industry. Microelectron Reliab 31:855–859. doi:10.1016/0026-2714(91)90024-2.
[8] Kumar D, Singh J, Pandey PC (1992) Availability analysis of crystallisation system in the sugar industry under common cause failure. IEEE Trans Reliab 41(1):85–91. doi:10.1109/ 24.126677.
[9] Arora N, Kumar D (1997) Availability analysis of steam and power generation systems in the thermal power plant. Microelectron Reliab 37(5):795–799. doi:10.1016/0026-2714(95 001158.
[10] Michelson Q (1998) Use of reliability technology in the process industry. Reliab Eng Syst Saf 60:179–181.
[11] Singh J, Mahajan P (2000) Reliability of utensils manufacturing plant—a case study. Opsearch 36(3):178–185.
[12] Sarkar J, Sarkar S (2001) Availability of a periodically inspected system supported by a spare unit, under perfect repair and perfect upgrade. Stat Probab Lett 53:207–217. doi:10.1016/S0167-7152 (01)00087-6.
[13] Dai YS, Xie M, Poh K, Liu GO (2003) A study of service reliability and availability for distribution system. Reliab Eng Syst Saf 79:103–112. doi:10.1016/S0951-8320(02)00200-4.

[14] Madu CN (2005) Strategic value of reliability and maintainability management. Int J Qual Reliab Manage 22(3):317–328. doi:10.1108/02656710510582516.

[15] Singh J, Garg S (2005) "Availability Analysis of Core Veneer Manufacturing system in Plywood Industry." International Conference on Reliability and Safety Engineering, Indian Institute of Technology, Kharagpur, 497–508.

[16] Gupta P, Lal A, Sharma R, Singh J (2005) Numerical analysis of reliability and availability of the series processes in butter oil processing plant. Int J Qual Reliab Manage 22(3):303–316. doi:10.1108/02656710510582507.

[17] Singh DV, Tuteja R, Taneja G, Minocha A (2005) "Analysis of Reliability Model for an Ash Handling Plant Consisting of Three Pumps." International Conference on Reliability and Safety Engineering, Indian Institute of Technology, Kharagpur, 465–472.

[18] Kumar N, Tewari PC, Sachdeva A (2021), "Stochastic modelling and availability analysis of repairable system of a milk processing plant" Int. J. Simulation and Process Modelling, Vol. 16, No. 4, 2021.

[19] N. Kumar, P.C. Tewari, A. Sachdeva (2020) "Petri Nets Modelling and Analysis of the Veneer Layup System of Plywood Manufacturing Plant" Engineering Modelling 33 (2020) 1-2, 95-107.

[20] Kumar N, Tewari PC, Sachdeva A (2021), "Performance Modeling and Analysis of Refrigeration System of a Milk Processing Plant using Petri Nets" International Journal of Performability Engineering Volume 15, Number 7, July 2019, pp. 1751-1759 DOI: 10.23940/ijpe.19.07. p1.175117.

Analysis of Triple-Unit System with Operational Priority

Jyotishree Ghosh[1], D. Pawar[1*], S.C. Malik[2]

•

[1]Department of Statistics, Amity Institute of Applied Sciences,
Amity University, Noida – 201313, INDIA
[2]Department of Statistics, Maharshi Dayanand University,
Rohtak – 124001, INDIA

[1]jyotishreeg@gmail.com
[1*]dpanwar75@yahoo.com
[2]sc_malik@rediffmail.com

Abstract

Reliability of three non-identical unit system is analyzed for various measures. Initially, main unit is operational, one is warm standby and other is cold standby. Single repair facility is present with the system. Operational priority is given to main unit over standby units. Failure times of all the components are exponentially distributed whereas repair time follows Weibull distribution. All the random variables are statistically independent. Semi-Markov process and regenerative point technique are used to analyze mean time to system failure, availability, busy period and expected number of visits by the server. System model's profit is analyzed for arbitrary values and are shown graphically.

Keywords: Reliability, Non-Identical, Standby, Priority, Semi-Markov, Regenerative Point.

I. Introduction

Unwavering property is the greatest amount of wanted trait of a system. One and all wishes to rehearse exceptionally robust systems in everyday life. Understanding high demand of highly reliable systems, numerous researchers studied various systems under various set of assumptions. Osaki and Asakura [1] discussed two-unit standby redundant system with repair and preventive maintenance, Murari and Goyal [2] studied a system model with three types of repair facilities, Gopalan and Nagarwalla [3] analyzed two-identical-unit cold standby system with repair and preventive maintenance, Dhillon and Yang [4] and Dhillon [5] done reliability and availability analysis of standby systems with common-cause failures and human errors. Goel et al. [6] discussed two-unit cold standby system with preventive maintenance and replacement of the duplicate unit, Kadyan et al. [7] stochastically analyzed non-identical units reliability models with priority and different failure modes, Kishan and Jain [8] studied two non-identical unit standby system with repair, inspection and post-repair under classical and Bayesian viewpoints, Kumar and Saini [9] analyzed single-unit system with preventive maintenance and Weibull distribution for failure and repair activities, Malik and Upma [10] analyzed profit of non-identical units system under preventive maintenance and replacement, Kumar et al. [11][12] analyzed warm standby non-identical units system with single server subject to priority and without priority for operation, Rathee et al. [13] studied two-unit parallel system subject to priority of repair of units over replacement. Kumar et al.

[14][15] analyzed profit of a warm standby non-identical unit system with single server performing in normal/ abnormal environment, also analyzed profit of the system with preventive maintenance, Ashok et al. [16] performed reliability analysis of a redundant system with 'FCFS' repair policy subject to weather conditions, Jain et al. [17] studied the reliability of a 1-out-of-2 system with standby and delayed service. Jain et al. [18] analyzed profit of a 1-out of 2 unit system with a standby unit and arrival time of server.

Every time, it is not feasible to meet the expenses of an identical unit in spare. Therefore, to keep the system operational, non-identical units might be taken as warm/ cold standby. When dealing with highly sensitive server systems in I.T. sector to keep data, we cannot rely on the systems of single unit or single unit in standby. In such cases, there is a need to keep two or more units in standby, therefore, priority is given to non-identical units in standby. Here, we developed and analyzed a reliability model of triple unit system.

II. System Assumptions

- The system comprises of three non-identical units.
- Initially, main unit (M) is operational, one unit (U_1) is warm standby and other unit (U_2) is cold standby.
- Single repair facility is present with the system.
- Operational priority is given to the main unit over the standby units.
- All unit works as new after repair.
- Failure times of the components are exponentially distributed whereas repair time follows Weibull distribution.

III. Method

Expressions for numerous reliability measures including mean time to system failure (MTSF), availability, busy period and expected number of visits by the server are evaluated using semi-Markov process and RPT. Profit of the system is analyzed for arbitrary values and represented graphically.

IV. Notations and Transition Diagram

Mo, U_1o, U_2o	:	Unit M, U_1, U_2 are operative.
U_1ws/U_2cs	:	U_1 is warm standby/ U_2 is cold standby.
Mur/MUR	:	M is under repair/ continuous repair.
U_1ur/U_1UR	:	U_1 is under repair/ continuous repair.
U_1wr/U_1WR	:	U_1 is waiting/ continuously waiting for repair.
U_2ur/U_2UR	:	U_2 is under repair/ continuous repair.
U_2wr/U_2WR	:	U_2 is waiting/ continuously waiting for repair.
$\lambda, \lambda_1, \lambda_2$	:	Failure rate of units M, U_1, U_2 respectively.
$f(t), r(t), r_1(t)$	:	p.d.f. of repair time of units M, U_1, U_2 respectively.
$F(t), R(t), R_1(t)$	:	c.d.f. of repair time of units M, U_1, U_2 respectively.
$q_{ij}(t)/Q_{ij}(t)$	:	p.d.f./ c.d.f. of earliest passing time from regenerative state i to j without passing through any other regenerative state in $(0, t]$.
$M_i(t)$	:	Probability that the system is initially up in regenerative state i at time t.
$W_i(t)$	:	Probability that the server is busy in regenerative state i at time t,.

m_{ij} : Contribution to mean sojourn time (μ_i) in regenerative state i when system transits directly to state j. $\mu_i = \sum_j m_{ij}$ and $m_{ij} = \int t dQ_{ij}(t) = -q_{ij}^*(0)$.

Ⓢ/©/©n : Symbol of Stieltjes/ Laplace/ Laplace 'n' times convolution.

*/** : Symbol of Laplace/ Laplace-Stieltjes transformation.

K_0 : Fixed revenue/ unit operational time of the system.

K_1 : Fixed cost/ unit busy period of the server.

K_2 : Fixed cost/ visit by the server.

P : Profit of the system.

The possible transition states are exhibited in figure 1.

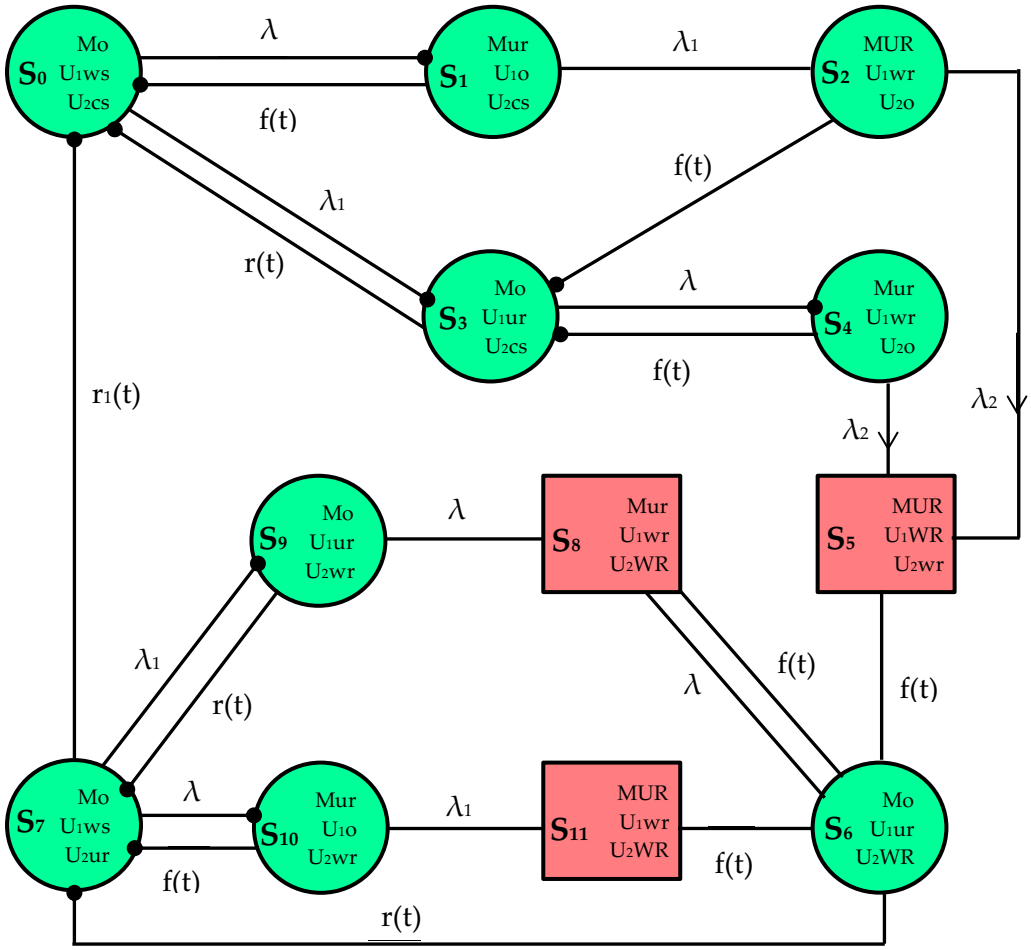

Figure 1: *State Transition Diagram*

V. Analysis of Reliability Measures

a) Transition Probabilities and Mean Sojourn Time

Simple probabilistic considerations for non-zero elements generate the expressions as

$$p_{ij} = Q_{ij}(\infty) = \int_0^\infty q_{ij}(t)dt$$

We have $p_{01} = \frac{\lambda}{\lambda+\lambda_1}$, $p_{03} = \frac{\lambda_1}{\lambda_1+\lambda}$, $p_{10} = f^*(\lambda_1)$, $p_{12} = 1 - f^*(\lambda_1)$, $p_{23} = f^*(\lambda_2)$, $p_{25} = 1 - f^*(\lambda_2)$, $p_{30} =$

$r^*(\lambda),\ p_{34} = 1 - r^*(\lambda),\ p_{43} = f^*(\lambda_2),\ p_{45} = 1 - f^*(\lambda_2),\ p_{56} = p_{86} = p_{11,6} = 1,\ p_{67} = r^*(\lambda),\ p_{68} = 1 - r^*(\lambda),\ p_{70} = r_1^*(\lambda + \lambda_1),\ p_{79} = \frac{\lambda_1}{\lambda+\lambda_1}[1 - r_1^*(\lambda + \lambda_1)],\ p_{7,10} = \frac{\lambda}{\lambda+\lambda_1}[1 - r_1^*(\lambda + \lambda_1),\ p_{97} = r^*(\lambda),\ p_{98} = 1 - r^*(\lambda),\ p_{10,7} = f^*(\lambda_1),\ p_{10,11} = 1 - f^*(\lambda_1)$

It can be easy to verify that

$p_{01} + p_{03} = p_{10} + p_{12} = p_{23} + p_{25} = p_{30} + p_{34} = p_{43} + p_{45} = p_{56} = p_{67} + p_{68} = p_{70} + p_{79} + p_{7,10} = p_{86} = p_{97} + p_{98} = p_{10,7} + p_{10,11} = p_{11,6} = 1$

Now, μ_i in the state S_i are $\mu_i = \sum_j m_{ij}$ and $m_{ij} = \int t dQ_{ij}(t) = -q_{ij}^*(0)$

$\mu_0 = \frac{1}{\lambda+\lambda_1}, \mu_1 = \frac{1}{\lambda_1}[1 - f^*(\lambda_1)], \mu_3 = \frac{1}{\lambda}[1 - r^*(\lambda)], \mu_4 = \frac{1}{\lambda_2}[1 - f^*(\lambda_2)], \mu_7 = \frac{1}{\lambda+\lambda_1}[1 - r_1^*(\lambda + \lambda_1)], \mu_9 = \frac{1}{\lambda}[1 - r^*(\lambda)], \mu_{10} = \frac{1}{\lambda_1}[1 - f^*(\lambda_1)]$

b) Reliability and MTSF

Let cdf of earliest passage time from regenerative state i to a failed state is $\phi_i(t)$. The recursive relations for $\phi_i(t)$ are

$\phi_0(t) = Q_{01}(t)\ \textcircled{s}\ \phi_1(t) + Q_{03}(t)\ \textcircled{s}\ \phi_3(t)$

$\phi_1(t) = Q_{10}(t)\ \textcircled{s}\ \phi_0(t) + Q_{13.2}(t)\ \textcircled{s}\ \phi_3(t) + Q_{15.2}(t)$

$\phi_3(t) = Q_{30}(t)\ \textcircled{s}\ \phi_0(t) + Q_{34}(t)\ \textcircled{s}\ \phi_4(t)$

$\phi_4(t) = Q_{43}(t)\ \textcircled{s}\ \phi_3(t) + Q_{45}(t)$ … (1)

Taking LST of (1) and solving for $\phi^{**}(s)$, we have

$$R^*(s) = \frac{1-\phi^{**}(s)}{s} \quad \text{… (2)}$$

The reliability of the system can be obtained by taking inverse LT of (2).

The MTSF is given by $\lim_{s\to 0} R^*(s)$. Thus,

$$MTSF = \frac{N_0}{D_0}, \text{ where}$$

$N_0 = (\mu_0 + \mu_1 p_{01})(1 - p_{43}p_{34}) + (\mu_3 + \mu_4 p_{34})(p_{01}p_{13.2} + p_{03})$ and $D_0 = (1 - p_{34}p_{43})(1 - p_{01}p_{10}) - p_{30}(p_{01}p_{13.2} + p_{03})$

c) Steady State Availability

Let $A_i(t)$ be the probability of the system to be operational at time 't' provided that the system arrived at regenerative state i at $t = 0$. The recursive relations for $A_i(t)$ are

$A_0(t) = M_0(t) + q_{01}(t) \copyright A_1(t) + q_{03}(t) \copyright A_3(t)$

$A_1(t) = M_1(t) + q_{10}(t) \copyright A_0(t) + q_{13.2}(t) \copyright A_3(t) + [q_{17.2,5,6}(t) + q_{17.2,5(6,8)^n}(t)] \copyright A_7(t)$

$A_3(t) = M_3(t) + q_{30}(t) \copyright A_0(t) + q_{34}(t) \copyright A_4(t)$

$A_4(t) = M_4(t) + q_{43}(t) \copyright A_3(t) + [q_{47.5,6}(t) + q_{47.5(6,8)^n}(t)] \copyright A_7(t)$

$A_7(t) = M_7(t) + q_{70}(t) \copyright A_0(t) + q_{79}(t) \copyright A_9(t) + q_{7,10}(t) \copyright A_{10}(t)$

$A_9(t) = M_9(t) + [q_{97}(t) + q_{97.(6,8)^n}(t)] \copyright A_7(t)$

$A_{10}(t) = M_{10}(t) + [q_{10,7}(t) + q_{10,7.11,6}(t) + q_{10,7.11,(6,8)^n}(t)] \copyright A_7(t)$ … (3)

where, $M_0(t) = e^{-(\lambda+\lambda_1)t}$, $M_1(t) = e^{-\lambda_1 t}\overline{F(t)}$, $M_3(t) = e^{-\lambda t}\overline{F(t)}$, $M_4(t) = e^{-\lambda_2 t}\overline{F(t)}$, $M_7(t) = e^{-(\lambda+\lambda_1)t}\overline{R_1(t)}$, $M_9(t) = e^{-\lambda t}\overline{R(t)}$, $M_{10}(t) = e^{-\lambda_1 t}\overline{F(t)}$

Taking LT of (3) and solving for $A^*(s)$. The steady state availability is given by

$$A(\infty) = \lim_{s\to 0} sA^*(t) = A = \frac{N_1}{D_1}, \text{ where}$$

$N_1 = [p_{70}\{(M_0 + M_1 p_{01})(1 - p_{34}p_{43}) + (M_3 + M_4 p_{34})(p_{03} + p_{01}p_{13.2})\} + D_0(M_7 + M_9 p_{79} + M_{10}p_{7,10})]$,

$D_1 = [p_{70}\{(\mu_0 + \mu_1 p_{01})(1 - p_{34}p_{43}) + (\mu_3 + \mu_4 p_{34})(p_{03} + p_{01}p_{13.2})\} + D_0(\mu_7 + \mu_9 p_{79} + \mu_{10}p_{7,10})]$ and D_0 is already specified.

d) Busy Period Analysis

Let $B_i(t)$ be the probability that the server is employed in restoring the unit at time 't' given that the system arrived at regenerative state i at $t = 0$. The recursive relations for $B_i(t)$ are

$B_0(t) = q_{01}(t)©B_1(t) + q_{03}(t)©B_3(t)$

$B_1(t) = W_1(t) + q_{10}(t)©B_0(t) + q_{13.2}(t)©B_3(t) + [q_{17.2,5,6}(t) + q_{17.2,5(6,8)^n}(t)]©B_7(t)$

$B_3(t) = W_3(t) + q_{30}(t)©B_0(t) + q_{34}(t)©B_4(t)$

$B_4(t) = W_4(t) + q_{43}(t)©B_3(t) + [q_{47.5,6}(t) + q_{47.5(6,8)^n}(t)]©B_7(t)$

$B_7(t) = W_7(t) + q_{70}(t)©B_0(t) + q_{79}(t)©B_9(t) + q_{7,10}(t)©B_{10}(t)$

$B_9(t) = W_9(t) + [q_{97}(t) + q_{97.(6,8)^n}(t)]©B_6(t)$

$B_{10}(t) = W_{10}(t) + [q_{10,7}(t) + q_{10,7.11,6}(t) + q_{10,7.11,(6,8)^n}(t)]©B_6(t)$ … (4)

where, $W_1(t) = e^{-\lambda_1 t}\overline{F(t)}$, $W_3(t) = e^{-\lambda t}\overline{F(t)}$, $W_4(t) = e^{-\lambda_2 t}\overline{F(t)}$, $W_7(t) = e^{-(\lambda+\lambda_1)t}\overline{R_1(t)}$, $W_9(t) = e^{-\lambda t}\overline{R(t)}$, $W_{10}(t) = e^{-\lambda_1 t}\overline{F(t)}$

Taking LT of (4) and solving for $B^*(s)$. The busy period of the server can be obtained as

$$B(\infty) = \lim_{s\to 0} s\,B^*(s) = B = \frac{N_2}{D_1}, \text{ where}$$

$N_2 = [p_{70}\{(W_1 p_{01})(1 - p_{34}p_{43}) + (W_3 + W_4 p_{34})(p_{03} + p_{01}p_{13.2})\} + D_0(W_7 + W_9 p_{79} + W_{10}p_{7,10})]$ and D_0, D_1 are previously specified.

e) Expected Number of Visits by the Server

Let expected number of visits by the server in *(0, t]* is $N_i(t)$, given that the system arrived at the regenerative state i at $t = 0$. The recursive relations for $N_i(t)$ are

$N_0(t) = Q_{01}(t)\,ⓢ\,\{1 + N_1(t)\} + Q_{03}(t)\,ⓢ\,\{1 + N_3(t)\}$

$N_1(t) = Q_{10}(t)\,ⓢ\,N_0(t) + Q_{13.2}(t)\,ⓢ\,N_3(t) + \left[Q_{17.2,5,6}(t) + Q_{17.2,5(6,8)^n}(t)\right]ⓢ\,N_7(t)$

$N_3(t) = Q_{30}(t)\,ⓢ\,N_0(t) + Q_{34}(t)\,ⓢ\,N_4(t)$

$N_4(t) = Q_{43}(t)\,ⓢ\,N_3(t) + \left[Q_{47.5,6}(t) + Q_{47.5(6,8)^n}(t)\right]ⓢ\,N_7(t)$

$N_7(t) = Q_{70}(t)\,ⓢ\,N_0(t) + Q_{79}(t)\,ⓢ\,N_9(t) + Q_{7,10}(t)\,ⓢ\,N_{10}(t)$

$N_9(t) = \left[Q_{97}(t) + Q_{97.(6,8)^n}(t)\right]ⓢ\,N_6(t)$

$N_{10}(t) = \left[Q_{10,7}(t) + Q_{10,7.11,6}(t) + Q_{10,7.11,(6,8)^n}(t)\right]ⓢ\,N_6(t)$ … (5)

Taking LT of (5) and solving for $N^{**}(s)$. The expected number of visits by the server can be obtained as

$$N(\infty) = \lim_{s\to 0} s\,N^{**}(s) = N = \frac{N_3}{D_1}, \text{ where}$$

$N_3 = p_{70}(1 - p_{34}p_{43})$ and D_1 is already specified.

VI. Profit Analysis

In steady state, system model's profit can be evaluated as $P = K_0 A - K_1 B - K_2 N$

VII. Particular Case

Let $f(t) = \alpha\eta t^{\eta-1}e^{-\alpha t^\eta}$, $r(t) = \alpha_1\eta t^{\eta-1}e^{-\alpha_1 t^\eta}$, $r_1(t) = \alpha_2\eta t^{\eta-1}e^{-\alpha_2 t^\eta}$ … (6)

are pdfs of Weibull distribution for repair time of units M, U_1 and U_2 respectively. Where α, α_1 and α_2 are different scale parameters and η is shape parameter.

On taking $\eta = 1$ in (6), Weibull distribution becomes exponential distribution. The transition probabilities $p_{01}$and p_{03} remains same whereas the remaining are

$p_{10} = \frac{\alpha}{\alpha+\lambda_1}, p_{12} = \frac{\lambda_1}{\alpha+\lambda_1}, p_{23} = \frac{\alpha}{\alpha+\lambda_2}, p_{25} = \frac{\lambda_2}{\alpha+\lambda_2}, p_{30} = \frac{\alpha_1}{\alpha_1+\lambda_2}, p_{34} = \frac{\lambda_2}{\alpha_1+\lambda_2}, p_{43} = \frac{\alpha}{\alpha+\lambda_2}, p_{45} = \frac{\lambda_2}{\alpha+\lambda_2}, p_{56} = p_{86} = p_{11,6} = 1, p_{67} = \frac{\alpha_1}{\lambda+\alpha_1}, p_{68} = \frac{\lambda}{\lambda+\alpha_1}, p_{70} = \frac{\alpha_2}{\alpha_2+\lambda+\lambda_1}, p_{79} = \frac{\lambda_2}{\alpha_2+\lambda+\lambda_1}, p_{70} = \frac{\lambda}{\alpha_2+\lambda+\lambda_1}, p_{97} = \frac{\alpha_1}{\alpha_1+\lambda}, p_{98} = \frac{\lambda}{\lambda+\alpha_1}, p_{10,7} = \frac{\alpha}{\alpha+\lambda_1}, p_{10,11} = \frac{\lambda_1}{\alpha+\lambda_1}$

Then μ_i are $\mu_0 = \frac{1}{\lambda+\lambda_1}$, $\mu_1 = \frac{\Gamma(1+\frac{1}{\eta})}{(\alpha+\lambda_1)^{\frac{1}{\eta}}}$, $\mu_3 = \frac{\Gamma(1+\frac{1}{\eta})}{(\alpha_1+\lambda_1)^{\frac{1}{\eta}}}$, $\mu_4 = \frac{\Gamma(1+\frac{1}{\eta})}{(\alpha+\lambda_2)^{\frac{1}{\eta}}}$, $\mu_7 = \frac{\Gamma(1+\frac{1}{\eta})}{(\lambda+\lambda_1+\alpha_2)^{\frac{1}{\eta}}}$, $\mu_9 = \frac{\Gamma(1+\frac{1}{\eta})}{(\lambda+\alpha_1)^{\frac{1}{\eta}}}$, $\mu_{10} = \frac{\Gamma(1+\frac{1}{\eta})}{(\alpha+\lambda_1)^{\frac{1}{\eta}}}$

Similarly, $W_1 = \frac{\Gamma(1+\frac{1}{\eta})}{(\alpha+\lambda_1)^{\frac{1}{\eta}}}$, $W_3 = \frac{\Gamma(1+\frac{1}{\eta})}{(\alpha_1+\lambda_1)^{\frac{1}{\eta}}}$, $W_4 = \frac{\Gamma(1+\frac{1}{\eta})}{(\alpha+\lambda_2)^{\frac{1}{\eta}}}$, $W_7 = \frac{\Gamma(1+\frac{1}{\eta})}{(\lambda+\lambda_1+\alpha_2)^{\frac{1}{\eta}}}$, $W_9 = \frac{\Gamma(1+\frac{1}{\eta})}{(\lambda+\alpha_1)^{\frac{1}{\eta}}}$, $W_{10} = \frac{\Gamma(1+\frac{1}{\eta})}{(\alpha+\lambda_1)^{\frac{1}{\eta}}}$

and $M_0 = \frac{1}{\lambda+\lambda_1}$, $M_1 = \frac{\Gamma(1+\frac{1}{\eta})}{(\alpha+\lambda_1)^{\frac{1}{\eta}}}$, $M_3 = \frac{\Gamma(1+\frac{1}{\eta})}{(\alpha_1+\lambda_1)^{\frac{1}{\eta}}}$, $M_4 = \frac{\Gamma(1+\frac{1}{\eta})}{(\alpha+\lambda_2)^{\frac{1}{\eta}}}$, $M_7 = \frac{\Gamma(1+\frac{1}{\eta})}{(\lambda+\lambda_1+\alpha_2)^{\frac{1}{\eta}}}$, $M_9 = \frac{\Gamma(1+\frac{1}{\eta})}{(\lambda+\alpha_1)^{\frac{1}{\eta}}}$, $M_{10} = \frac{\Gamma(1+\frac{1}{\eta})}{(\alpha+\lambda_1)^{\frac{1}{\eta}}}$

i) For $\eta = 0.5$, the repair time distribution reduces to $f(t) = \frac{\alpha}{2\sqrt{t}}e^{-\alpha\sqrt{t}}$, $r(t) = \frac{\alpha_1}{2\sqrt{t}}e^{-\alpha_1\sqrt{t}}$, $r_1(t) = \frac{\alpha_2}{2\sqrt{t}}e^{-\alpha_2\sqrt{t}}$

As a result μ_i changes to $\mu_0 = \frac{1}{\lambda+\lambda_1}$, $\mu_1 = \frac{2}{(\alpha+\lambda_1)^2}$, $\mu_3 = \frac{2}{(\alpha_1+\lambda_1)^2}$, $\mu_4 = \frac{2}{(\alpha+\lambda_2)^2}$, $\mu_7 = \frac{2}{(\lambda+\lambda_1+\alpha_2)^2}$, $\mu_9 = \frac{2}{(\lambda+\alpha_1)^2}$, $\mu_{10} = \frac{2}{(\alpha+\lambda_1)^2}$

Similarly, $M_0 = \frac{1}{\lambda+\lambda_1}$, $M_1 = \frac{2}{(\alpha+\lambda_1)^2}$, $M_3 = \frac{2}{(\alpha_1+\lambda_1)^2}$, $M_4 = \frac{2}{(\alpha+\lambda_2)^2}$, $M_7 = \frac{2}{(\lambda+\lambda_1+\alpha_2)^2}$, $M_9 = \frac{2}{(\lambda+\alpha_1)^2}$, $M_{10} = \frac{2}{(\alpha+\lambda_1)^2}$

and $W_1 = \frac{2}{(\alpha+\lambda_1)^2}$, $W_3 = \frac{2}{(\alpha_1+\lambda_1)^2}$, $W_4 = \frac{2}{(\alpha+\lambda_2)^2}$, $W_7 = \frac{2}{(\lambda+\lambda_1+\alpha_2)^2}$, $W_9 = \frac{2}{(\lambda+\alpha_1)^2}$, $W_{10} = \frac{2}{(\alpha+\lambda_1)^2}$

ii) For $\eta = 1$, the repair time distribution reduces to exponentials having pdf $f(t) = \alpha e^{-\alpha t}$, $r(t) = \alpha_1 e^{-\alpha_1 t}$, $r_1(t) = \alpha_2 e^{-\alpha_2 t}$

As a result μ_i changes to $\mu_0 = \frac{1}{\lambda+\lambda_1}$, $\mu_1 = \frac{1}{\alpha+\lambda_1}$, $\mu_3 = \frac{1}{\alpha_1+\lambda_1}$, $\mu_4 = \frac{1}{\alpha+\lambda_2}$, $\mu_7 = \frac{1}{\lambda+\lambda_1+\alpha_2}$, $\mu_9 = \frac{1}{\lambda+\alpha_1}$, $\mu_{10} = \frac{1}{\alpha+\lambda_1}$

Similarly, $M_0 = \frac{1}{\lambda+\lambda_1}$, $M_1 = \frac{1}{\alpha+\lambda_1}$, $M_3 = \frac{1}{\alpha_1+\lambda_1}$, $M_4 = \frac{1}{\alpha+\lambda_2}$, $M_7 = \frac{1}{\lambda+\lambda_1+\alpha_2}$, $M_9 = \frac{1}{\lambda+\alpha_1}$, $M_{10} = \frac{1}{\alpha+\lambda_1}$

and $W_1 = \frac{1}{\alpha+\lambda_1}$, $W_3 = \frac{1}{\alpha_1+\lambda_1}$, $W_4 = \frac{1}{\alpha+\lambda_2}$, $W_7 = \frac{1}{\lambda+\lambda_1+\alpha_2}$, $W_9 = \frac{1}{\lambda+\alpha_1}$, $W_{10} = \frac{1}{\alpha+\lambda_1}$

VIII. Graphical Presentation

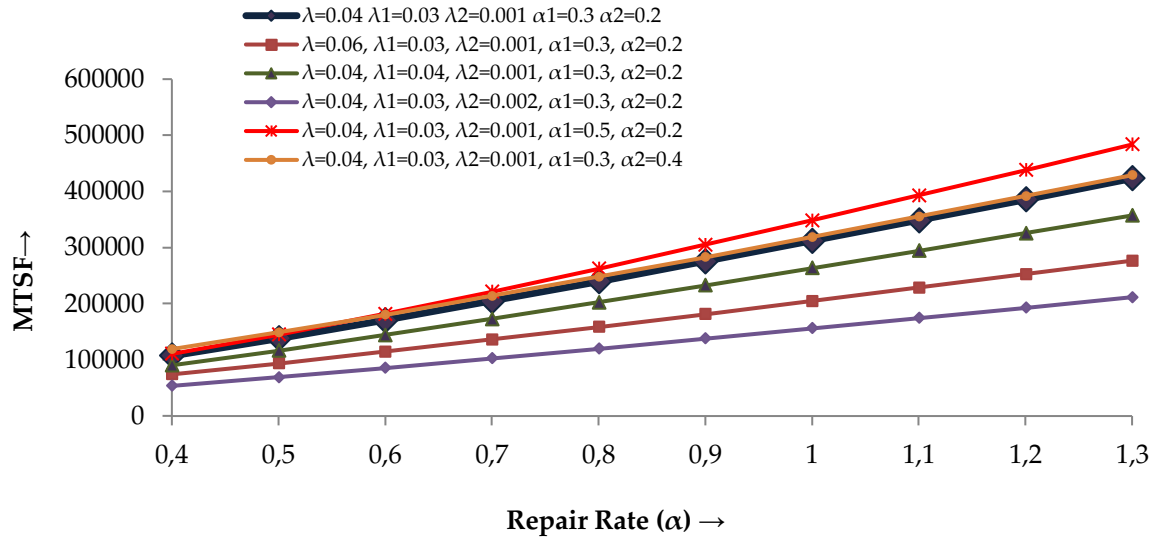

Figure 2: *MTSF vs Repair rate (η = 0.5)*

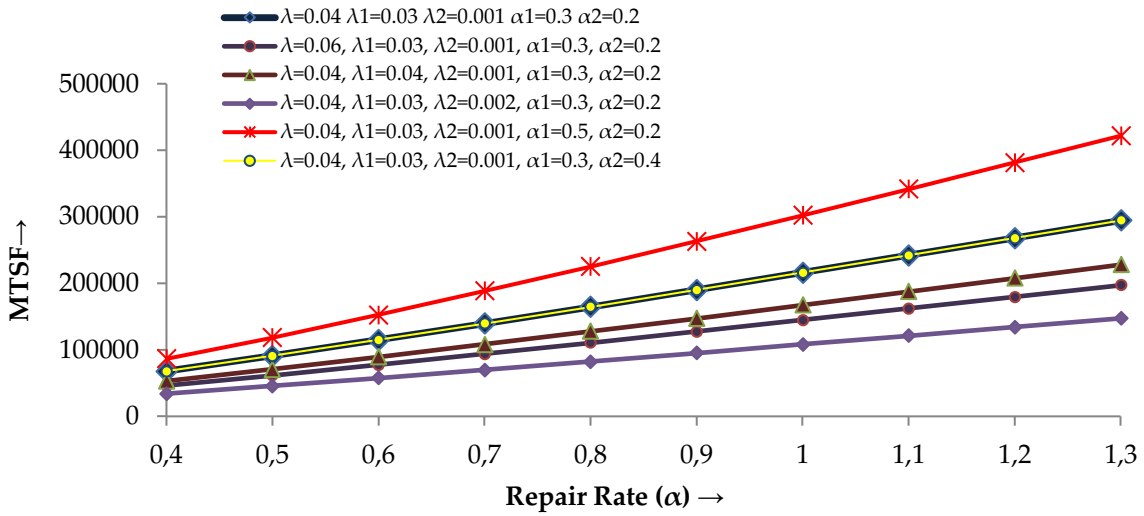

Figure 3: *MTSF vs Repair rate (η = 1)*

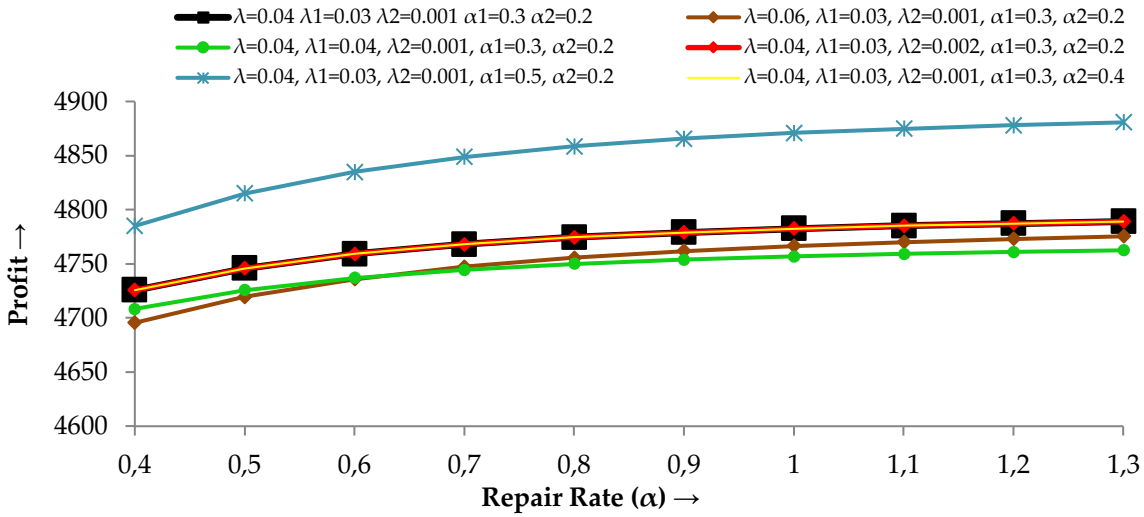

Figure 4: *Profit vs Repair rate (η = 0.5)*

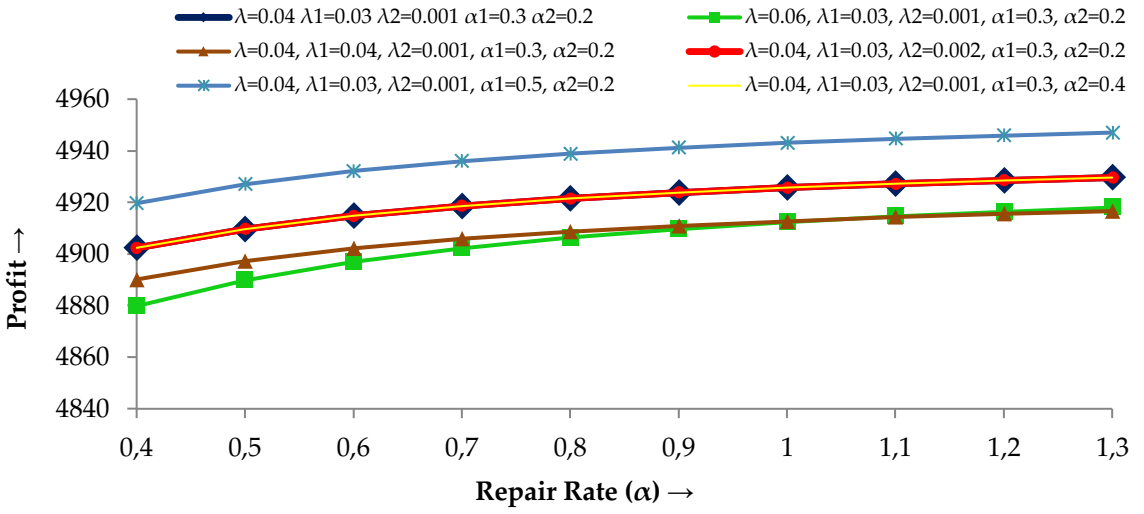

Figure 5: *Profit Vs Repair Rate (η = 1)*

IX. Conclusion

Figure 2 clearly indicate that for $\eta = 0.5$, MTSF is increasing with increasing repair rate of main unit (α) while figure 3 indicate comparatively less increment in MTSF for increasing α when $\eta = 1$. Therefore, we conclude that MTSF increases with increasing α. Figure 4 shows that for $\eta = 0.5$, system model's profit is increasing with increasing α whereas figure 5 shows relatively higher increase in profit for increasing α and α_1 (restoration rate of warm standby unit) when $\eta = 1$. Hence, profit of the system increases with increasing α and α_1 for constant η.

Present study concludes that the increasing restoration rate of the main unit increases MTSF whereas to make the system more profitable we should increase repair rate of both main as well as warm standby units.

References

[1] Osaki, Shunji and Asakura, Tatsuyuki (1970). A two-unit standby redundant system with repair and preventive maintenance. Journal of Applied Probability, 7(3):641-648.

[2] Murari, K. and Goyal, V. (1984). Comparison of two-unit cold standby reliability models with three types of repair facilities. Microelectronics Reliability, 24(1):35-49.

[3] Gopalan, M. N. and Nagarwalla, H. E. (1985). Cost-benefit analysis of a one-server two-unit cold standby system with repair and preventive maintenance. Microelectronics Reliability, 25(2):267-269.

[4] Dhillon, B.S. and Yang, N. (1992). Reliability and availability analysis of warm standby systems with common-cause failures and human errors. Microelectronics Reliability, 32(4):561-575.

[5] Dhillon, B.S. (1993). Reliability and availability analysis of a system with standby and common cause failures. Microelectronics Reliability, 33(9):1343-1349.

[6] Goel, L.R.; Mumtaz, S.Z. and Gupta, Rakesh (1996). A two-unit duplicating standby system with correlated failure-repair/ replacement times. Microelectronics Reliability, 36(4):517-523.

[7] Kadyan, M.S.; Chander, S. and Grewal, A.S. (2004). Stochastic analysis of non-identical units reliability models with priority and different modes of failure. Journal of Decision and Mathematical Sciences, 9(1-3):59-82.

[8] Kishan, Ram and Jain, Divya (2012). A two non-identical unit standby system model with repair, inspection and post-repair under classical and Bayesian viewpoints. Journal of Reliability and Statistical Studies, 5(2):85-103.

[9] Kumar, A. and Saini, M. (2014). Cost-benefit analysis of a single-unit system with preventive maintenance and Weibull distribution for failure and repair activities. Journal of Applied Mathematics, Statistics and Informatics, 10(2):5-19.

[10] Malik, S.C. and Upma (2016). Cost-benefit analysis of a system of non-identical units under preventive maintenance and replacement. Journal of Reliability and Statistical Studies, 9(2):17-27.

[11] Kumar, Ashok; Pawar, Dheeraj and Malik, S.C. (2018a). Profit analysis of a warm standby non-identical units system with single server subject to priority. International Journal on Future Revolution in Computer Sciences & Communication Engineering, 4(10):108-112.

[12] Kumar, Ashok; Pawar, Dheeraj and Malik, S.C. (2018b). Economic analysis of a warm standby system with single server. International Journal of Mathematics and Statistics Invention, 6(5):1-6.

[13] Rathee, Reetu; Pawar, D. and Malik, S.C. (2018). Reliability modelling and analysis of a parallel unit system with priority to repair over replacement subject to maximum operation and repair times. International Journal of Trend in Scientific Research and Development, 2(5):350-358.

[14] Kumar, Ashok; Pawar, Dheeraj and Malik, S.C. (2019a). Profit analysis of a warm standby non-identical unit system with single server performing in normal/abnormal environment. Life Cycle Reliability and Safety Engineering, 8(3):219-226.

[15] Kumar, Ashok; Pawar, Dheeraj and Malik, S.C. (2019b). Profit analysis of a warm standby non-identical unit system with single server subject to preventive maintenance. International Journal of Agriculture and Statistical Sciences, 15(1):261-269.

[16] Kumar, Ashok; Pawar, D. and Malik, S.C. (2020). Reliability analysis of a redundant system with 'FCFS' repair policy subject to weather conditions. International Journal of Advanced Science and Technology, 29(3):7568-7578.

[17] Jain, Pooja; Pawar, D. and Malik, S.C. (2020). Reliability measures of a 1-out-of-2 system with standby and delayed service. International Journal of Mechanical and Production Engineering Research and Development, 10(3):12725-12732.

[18] Jain, Pooja; Pawar, D. and Malik, S.C. (2022). Profit analysis of a 1-out of 2 unit system with a standby unit and arrival time of server. International Journal of Agricultural and Statistical Sciences, 18(1):29-33.

Reliability Estimation of a Serial System Subject to General and Gumbel-Hougaard Family Copula Repair Policies

Ibrahim Yusuf
•
Department of Mathematical Sciences,
Bayero University Kano, Nigeria
iyusuf.mth@buk.edu.ng

Nafisatu Muhammad Usman
•
Department of Arts and Humanity, School of General Studies,
Kano State Polytechnic, Kano, Nigeria
mamankhairat2015@gmail.com

Abdulkareem Lado Ismail
•
Department of Mathematics, Kano State College of Education, Kano, Nigeria
ladgetso@gmail.com

Abstract

Abstract: The dependability analysis of a hybrid series-parallel system with five subsystems A, B, C, D, and E is the subject of this research. Subsystem A has two active parallel units, whereas subsystem B has two out of four active units. Both units have a failure and repair time that is exponential. There are two states in the system under consideration: partial failure and complete failure. To assess the system's dependability, the system's first-order partial differential equations are constructed from the system transition diagram, resolved using the supplementary variables technique, and the reliability models are Laplace transformed. Failure times are assumed to follow an exponential distribution, whereas repair times are expected to follow a general distribution and a Gumbel-Hougaard family copula distribution. Reliability measurements of testing system effectiveness are derived and investigated, including reliability, availability, MTTF, sensitivity MTTF, and cost function. Tables and graphs show some of the most relevant findings.

Keywords: Reliability, estimation, availability, MTTF, Series system, Gumbel-Hougaard family copula

1. Introduction

Series-parallel systems are made up of multiple subsystems that are connected in a series. Each subsystem is made up of units or components that are connected in a parallel fashion. When all of the subsystems of a series-parallel system are operational, the system operates. Partially or completely failing such systems is possible. When any of the parallel units or components of the subsystem failed, it resulted in a partial failure of the system. This failure will not stop the system from working; rather, depending on the configuration of the components, the system will continue to operate at full or decreased capacity (see Ram and Manglik [29] and Ram et al. [30]). When any of the subsystems fails, the system's operation comes to a halt, resulting in total failure.

The majority of industrial and manufacturing systems are set up in a series-parallel fashion. Because of their widespread use in industrial and manufacturing settings, determining the reliability, availability, and profitability of series-parallel systems as industrial and manufacturing systems has become a more pressing concern. A good example can be found in a computer network (see Yusuf et al. [42], Rawal et al. [31] and Rawal et al. [32]). Feeding, crushing, refining, steam generation, evaporation, crystallization, fertilizer plant, sugar plant crystallization unit, and piston manufacturing factory are all instances of these systems.

Some studies consider reliability block diagrams to identify the role of cascading failures on the reliability of series–parallel systems (see Xie et al [35]) or consider optimal component grouping in series–parallel and parallel–series systems composed of k subsystems to improve reliability and availability of series–parallel systems (see Xie et. al.[36]). The reliability of such a system can be improved by determining the best time for performing PM and also finding the number of spare parts and facilities in single-item replacement and parallel systems to minimize the expected average cost per unit time (see Fallahnezhad and Najafian [7]), or by performing maintenance to the system components (see Chauhan and Malik [5]), or by performing maintenance to the system components (see Fallahnezhad and Najafian [7]). (see Khatab et al.[18]).

The importance of ensuring the survival of industrial and manufacturing systems, as well as their accompanying economies, through dependability, availability, and profit optimization has become critical to their expansion. The percentage of time that the system is available to users is known as system availability. When the system's dependability and availability are improved (increased), the accompanying income is improved as well. Crystallization system of a sugar plant, uncaser system of a brewing plant, thermal plant, two-wheeler automobile, cattle feed, and ice cream making unit of a milk plant are examples of such industrial and manufacturing systems (see Aggarwal et al. [2], Garg et al. [11] and Kumar and Mudgil [21]).

Studies on reliability and availability modeling, as well as performance evaluation of industrial and manufacturing systems, have been conducted, as indicated above. To determine the reliability and availability models of such systems, the governing differential difference equations are obtained and solved with Runge–Kutta fourth-order and using genetic algorithm method to analyze the system's reliability (see Aggarwal et al. [3], Garg et al. [12], Kadiyan et al. [17]) and making decisions using the developed model (see Aggarwal et al. [3], Garg et al (see Gupta and Tewari [14] and Fadi and Sibai [6])

Maintaining a high level of system reliability, availability, manufacturing output, and revenue generating requires proper maintenance planning. As a result, it's critical that the equipment is always available. Several approaches for studying behavioral studies (see Arvind et al. [4]) and maintenance planning and problem identification (see Khanduja et al. [16] and Xu et al. [37]) have been abandoned. Reliability, availability, mean time to failure, mean time between failures, and mean time to repair are all indicators of such performance.

The degree of identification of the most critical subsystem that results in low reliability, availability, and profit between the subsystems is critical in analyzing the performance of the system (see Kumar et al. [23] and Kumar and Lata [24]) / subsystems through reliability, availability, and generated profit, as well as the degree of identification of the most critical subsystem that results in low reliability, availability, and profit between the subsystems (see Freiheit et al. [8]). The ideal profit level, at which the profit is highest, can be identified using this mathematical approach (see Kumar and Tewari [22]).

Reliability, availability, and revenue enhancement literature Consider the options by categorizing the configurations' dependability and choosing the optimum structure that maximizes system reliability (see Peng et al. [28]). Particle swarm optimization (see Garg and Sharma [13]) and the concept of inherent availability (see Kaur et al. [19]) are two further ways for increasing reliability.

Few studies consider the application of redundancy application problem as a means of a maximizing the system reliability, availability and profit (see Mohammed et al. [27] and Zhu et al. [41]), identification and elimination of the most critical component with low reliability (see Yusuf et al. [39] and Yusuf [40]), by considering general repair as a way regaining the system to its former position before complete failure (see Yusuf et al. [38]), by employing human operator to avoid catastrophic breakdown (see Gahlot et al.[9],Gulati et al. [10],Lado and Singh [25], Lado et al. [26] and Singh and Ayagi [33]) or through the study of optimization allocation problem for a repairable series-parallel system having failure dependencies among the units of the system so as to reduce the number of repair teams are available for each subsystem (see Hu et al. [15]).

Existing literatures above either ignores the importance of repair policies on reliability, availability, mean time to failure and profit on both industrial growth, employment, increase in volume of business, etc. Most literatures laid emphasis of availability and performance evaluation of the systems alone without paying much attention to the impact of copula and general repair policies on reliability, availability, mean time to failure and generated revenue.

More sophisticated models of repairable series parallel systems should be developed to assist in reducing risk of a complete breakdown, operating costs, prolonging the overall reliability, availability, mean time to failure as well as generated revenue (profit). For this reason, this paper considered a series-parallel system consisting of five subsystem A, B, C, D and E. The performance of the system is studied using the supplementary variable technique and Laplace transforms. The various measures of reliability such as availability, reliability, mean time to system failure (MTTF), sensitivity for MTTF and cost analysis have been computed for various values of failure and repair rates.

The paper is organized as follows: Section 2 captures the description of the system, assumption and notations used for the study. Section 3 deals with the formulation and solution of mathematical model. Section 4 focuses on the analytical part of the study in which some particular cases are taken for discussion. The paper is concluded in section 5.

2. Notations, Assumptions, and Description of the System

2.1. Notations

t: Time variable on a time scale.

s: Laplace transform variable for all expressions

$\beta_1 / \beta_2 / \beta_3 / \beta_4 / \beta_5$: Failure rate of subsystem 1/ subsystem 2/ subsystem 3/ subsystem 4 and / subsystem 5 respectively.

$\phi(y) / \phi(z)$: Repair rate of subsystem 2 / subsystem 3.

$\mu_0(x) / \mu_0(y) / \mu_0(z) / \mu_0(m) / \mu_0(n)$: Repair rate for complete failed states of subsystem 1 / subsystem 2/ subsystem 3/ subsystem 4 and / subsystem 5 respectively.

$p_i(t)$: The probability that the system is in S_i state at instants for i =0 to 11

$\overline{P}(s)$: Laplace transformation of state transition probability $p(t)$

$P_i(x, t)$: The probability that a system is in state S_i for i=1..., the system under repair and elapse repair time is (x, t) with repair variable x and time variable t

$P_i(y, t)$: The probability that a system is in state S_i for i=1..., the system under repair and elapse repair time is (y, t) with repair variable y and time variable t

$P_i(z, t)$: The probability that a system is in state S_i for i=1…, the system under repair and elapse repair time is (z, t) with repair variable z and time variable t

$P_i(m, t)$: The probability that a system is in state S_i for i=1…, the system under repair and elapse repair time is (m, t) with repair variable m and time variable t

$P_i(n, t)$: The probability that a system is in state S_i for i=1…, the system under repair and elapse repair time is (n, t) with repair variable n and time variable t

$E_p(t)$: Expected profit during the time interval [0, t)

K_1, K_2: Revenue and service cost per unit time, respectively.

$\mu_0(x)$: The expression of joint probability according to Gumbel-Hougaard family copula definition

$$c_\theta\left(u_1(x), u_2(x)\right) = \exp\left(x^\theta + \left\{\log\phi(x)^\theta\right\}^{\frac{1}{\theta}} \right), \quad (1)$$

$1 \le \theta \le \infty$.

Where

$$\mu_1 = \phi(x) \quad (2)$$

and

$$u_2 = e^x \quad (3)$$

2.2 Assumptions

i. Firstly, it is assumed that all subsystems are in perfect operational state.

ii. Failure of any unit leads to insufficient performance of the system.

iii. Secondly, subsystem 1, subsystem 4, subsystem 5, one unit from subsystem 2 and at least three units from subsystem3 are compulsory for the system to operate.

iv. Thirdly, the system will not operate if any of the subsystems completely fail.

v. If a unit of the system failed, it can be tackled when it is in operation or failed state.

vi. All failure rates are constant and assumed to follow exponential distribution.

vii. General distribution is employed to repair partially failed states while Gumbel-Hougaard family copula distribution takes care of complete failed state.

viii. The repaired unit of the system is assumed to operate like new and no harm shows in the repair process.

ix. However, as soon as the failed unit gets repaired, it is ready to take the load for successful perform of the system.

2.3 Descriptions of the System

This system consists of five different subsystems. Subsystem 1/ Subsystem 4/ Subsystem 5: One unit whose failure led to complete failure of the system. Subsystem 2: Consists of two homogeneous units working under 1-out-of-2 policy in parallel configuration. If one unit fails, the system is partially operative and failed unit is assigned for repair. The failure of the second unit will automatically result in complete failure of the system. Subsystem 3: Consisting of four homogeneous units that work under 3-out-of-4 policy in parallel configuration. System experience partial failure if one unit fails and failed unit is assigned for repair system is operative while complete failure occurred if additional unit fails. General repair method is assigned for partially failed state and completely failed state is carried out by copula repair method.

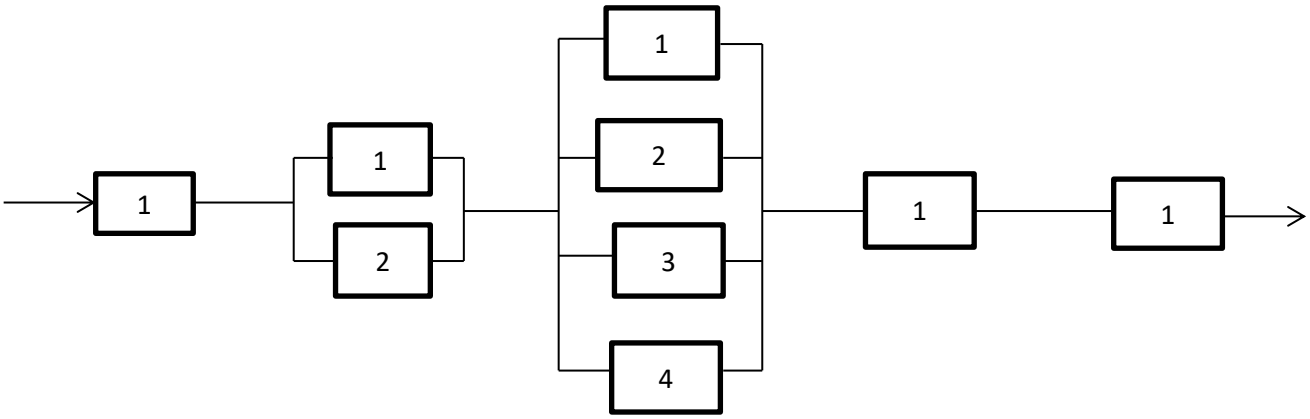

Figure 1: *System reliability block diagram*

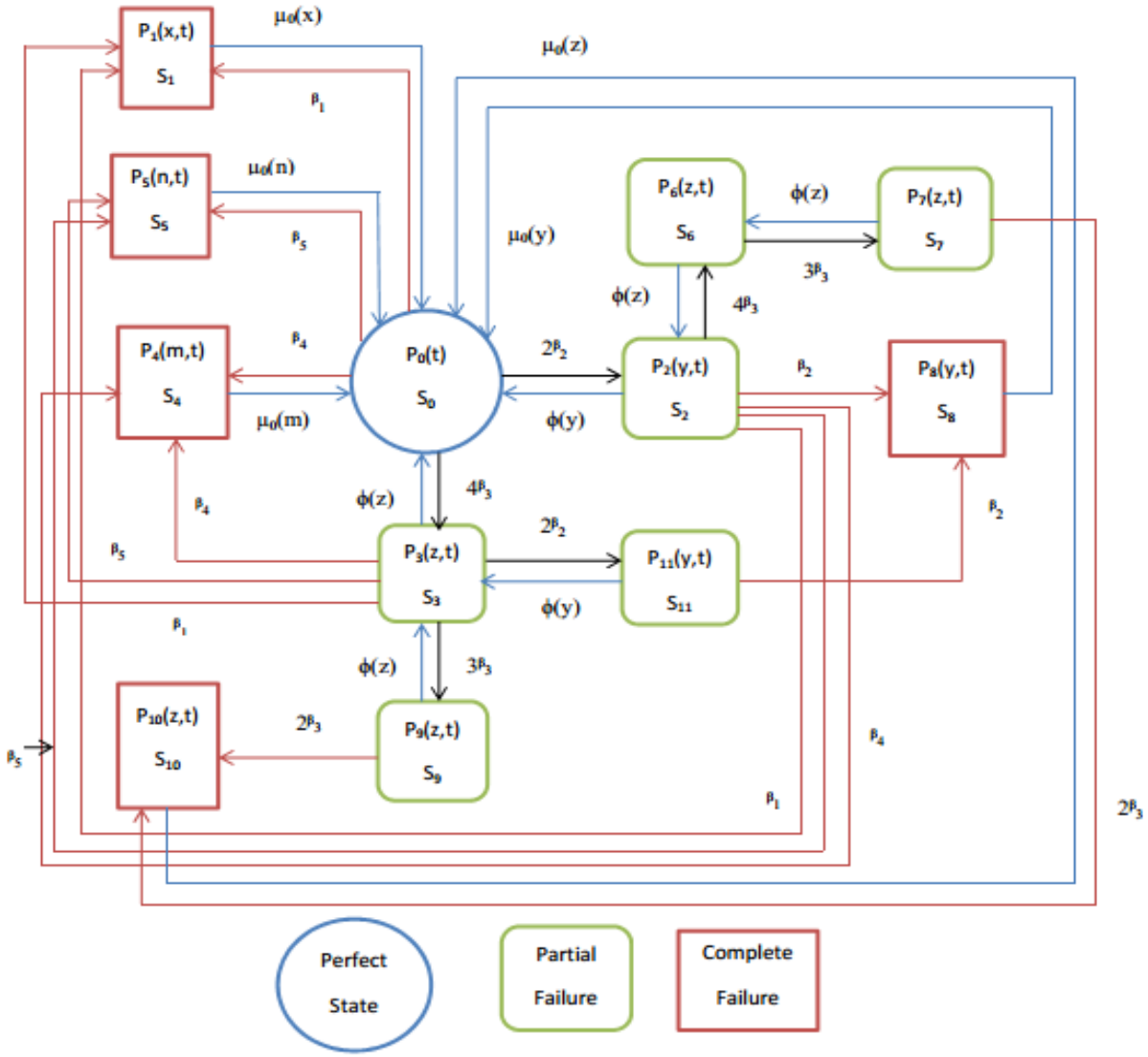

Figure 2: *Transition diagram of the System*

States Description

S_o: Good working state, all subsystems are adequate.

$S_1 / S_4 / S_5$: Completely failed states as such the system stopped working.

S_2 / S_{11}: One unit is operating and the second is on standby mode, system work in full capacity.

S_3 / S_6: Three units are operating while the remaining unit is on standby mode, system work in full capacity.

S_7 / S_9: One unit from subsystem 3 failed and is assigned for repair, system work partially.

S_8: Complete failed state due to the failure of second unit from subsystem 2.

S_{10}: Complete failed state due to the failure of second unit from subsystem 3.

3. Reliability Model Formulation

The resulting sets of partial differential equations are obtained through the transition diagram of the Mathematical model, by observing at probability of deliberations and connection of impacts.

$$\left(\frac{\partial}{\partial t}+2\beta_1+2\beta_2+4\beta_3+\beta_4+\beta_5\right)p_0(t)=\int_0^\infty \phi(y)\,p_2(y,t)dy+\int_0^\infty \phi(z)\,p_3(z,t)dz+\int_0^\infty \mu_0(x)\,p_1(x,t)dx+$$

$$\int_0^\infty \mu_0(y)\,p_8(y,t)dy+\int_0^\infty \mu_0(z)\,p_{10}(z,t)dz+\int_0^\infty \mu_0(m)\,p_4(m,t)dm+\int_0^\infty \mu_0(n)\,p_5(n,t)dn \quad (4)$$

$$\left(\frac{\partial}{\partial t}+\frac{\partial}{\partial x}+\mu_0(x)\right)p_1(x,t)=0 \quad (5)$$

$$\left(\frac{\partial}{\partial t}+\frac{\partial}{\partial y}+\beta_1+\beta_2+4\beta_3+\beta_4+\beta_5+\phi(y)\right)p_2(y,t)=0 \quad (6)$$

$$\left(\frac{\partial}{\partial t}+\frac{\partial}{\partial z}+\beta_1+2\beta_2+3\beta_3+\beta_4+\beta_5+\phi(z)\right)p_3(z,t)=0 \quad (7)$$

$$\left(\frac{\partial}{\partial t}+\frac{\partial}{\partial m}+\mu_0(m)\right)p_4(m,t)=0 \quad (8)$$

$$\left(\frac{\partial}{\partial t}+\frac{\partial}{\partial n}+\mu_0(n)\right)p_5(n,t)=0 \quad (9)$$

$$\left(\frac{\partial}{\partial t}+\frac{\partial}{\partial z}+3\beta_3+\phi(z)\right)p_6(z,t)=0 \quad (10)$$

$$\left(\frac{\partial}{\partial t}+\frac{\partial}{\partial z}+2\beta_3+\phi(z)\right)p_7(z,t)=0 \quad (11)$$

$$\left(\frac{\partial}{\partial t}+\frac{\partial}{\partial y}+\mu_0(y)\right)p_8(y,t)=0 \quad (12)$$

$$\left(\frac{\partial}{\partial t}+\frac{\partial}{\partial z}+2\beta_3+\phi(z)\right)p_9(z,t)=0 \tag{13}$$

$$\left(\frac{\partial}{\partial t}+\frac{\partial}{\partial z}+\mu_0(z)\right)p_{10}(z,t)=0 \tag{14}$$

$$\left(\frac{\partial}{\partial t}+\frac{\partial}{\partial y}+\beta_2+\phi(y)\right)p_{11}(y,t)=0 \tag{15}$$

3.1 Boundary and Initial Conditions

$$p_1(0,t)=\beta_1 p_0(t) \tag{14}$$

$$p_2(0,t)=2\beta_2 p_0(t) \tag{15}$$

$$p_3(0,t)=4\beta_3 p_0(0,t) \tag{16}$$

$$p_4(0,t)=\beta_4\left(p_0(t)+p_2(0,t)+p_3(0,t)\right) \tag{17}$$

$$p_5(0,t)=\beta_5\left(p_0(t)+p_2(0,t)+p_3(0,t)\right) \tag{18}$$

$$p_6(0,t)=4\beta_3 p_2(0,t) \tag{20}$$

$$p_7(0,t)=3\beta_3 p_6(0,t) \tag{21}$$

$$p_8(0,t)=\beta_2\left(p_2(0,t)+p_{11}(0,t)\right) \tag{22}$$

$$p_9(0,t)=3\beta_3 p_3(0,t) \tag{23}$$

$$p_{11}(0,t)=2\beta_3\left(p_7(0,t)+p_9(0,t)\right) \tag{24}$$

$$p_{11}(0,t)=2\beta_2 p_3(0,t) \tag{25}$$

All state transition probabilities are zero whenever t = 0 except $p_0(0)=1$.

3.2 Solution of Reliability Model

Captivating Laplace transformation of the equations (1) to (25) with the support of boundary conditions the following equations are obtained.

$$\left(s+\beta_1+2\beta_2+4\beta_3+\beta_4+\beta_5\right)\overline{p}_0(\mathrm{s})=1+\int_0^\infty\phi(y)\overline{p}_2(y,\mathrm{s})dy+\int_0^\infty\phi(z)\overline{p}_3(z,s)dz+\int_0^\infty\mu_0(x)\overline{p}_1(x,s)dx+$$

$$\int_0^\infty\mu_0(y)\overline{p}_8(y,s)dy+\int_0^\infty\mu_0(z)\overline{p}_{10}(z,s)dz+\int_0^\infty\mu_0(m)\overline{p}_4(m,s)dm+\int_0^\infty\mu_0(n)\overline{p}_5(n,s)dn \tag{26}$$

$$\left(s+\frac{\partial}{\partial x}+\mu_0(x)\right)\overline{p}_1(x,s)=0 \tag{27}$$

$$\left(s+\frac{\partial}{\partial y}+\beta_1+\beta_2+4\beta_3+\beta_4+\beta_5+\phi(y)\right)\overline{p}_2(y,\mathrm{s})=0 \tag{28}$$

$$\left(s+\frac{\partial}{\partial z}+\beta_1+2\beta_2+3\beta_3+\beta_4+\beta_5+\phi(z)\right)\overline{p}_3(z,\mathrm{s})=0 \quad (29)$$

$$\left(s+\frac{\partial}{\partial m}+\mu_0(m)\right)\overline{p}_4(m,s)=0 \quad (30)$$

$$\left(s+\frac{\partial}{\partial n}+\mu_0(n)\right)\overline{p}_5(n,s)=0 \quad (31)$$

$$\left(s+\frac{\partial}{\partial z}+3\beta_3+\phi(z)\right)\overline{p}_6(z,\mathrm{s})=0 \quad (32)$$

$$\left(s+\frac{\partial}{\partial z}+2\beta_3+\phi(z)\right)\overline{p}_7(z,\mathrm{s})=0 \quad (33)$$

$$\left(s+\frac{\partial}{\partial y}+\mu_0(y)\right)\overline{p}_8(y,s)=0 \quad (34)$$

$$\left(s+\frac{\partial}{\partial z}+2\beta_3+\phi(z)\right)\overline{p}_9(z,\mathrm{s})=0 \quad (35)$$

$$\left(s+\frac{\partial}{\partial z}+\mu_0(z)\right)\overline{p}_{10}(z,s)=0 \quad (36)$$

$$\left(s+\frac{\partial}{\partial y}+\beta_2+\phi(y)\right)\overline{p}_{11}(y,\mathrm{s})=0 \quad (37)$$

Boundary conditions

$$\overline{p}_1(0,s)=\beta_1\overline{p}_0(s) \quad (38)$$

$$\overline{p}_2(0,s)=2\beta_2\overline{p}_0(s) \quad (39)$$

$$\overline{p}_3(0,s)=4\beta_3\overline{p}_0(s) \quad (40)$$

$$\overline{p}_4(0,s)=\beta_4\left(\overline{p}_0(0)+\overline{p}_2(0,s)+\overline{p}_3(0,s)\right) \quad (41)$$

$$\overline{p}_5(0,s)=\beta_5\left(\overline{p}_0(0)+\overline{p}_2(0,s)+\overline{p}_3(0,s)\right) \quad (42)$$

$$\overline{p}_6(0,s)=4\beta_3\overline{p}_2(0,s) \quad (43)$$

$$\overline{p}_7(0,s)=3\beta_3\overline{p}_6(0,s) \quad (44)$$

$$\overline{p}_8(0,s)=\beta_2\left(\overline{p}_2(0,s)+\overline{p}_{11}(0,s)\right) \quad (45)$$

$$\overline{p}_9(0,s)=3\beta_3\overline{p}_3(0,s) \quad (46)$$

$$\overline{p}_{10}(0,s)=2\beta_3\left(\overline{p}_7(0,s)+\overline{p}_9(0,s)\right) \quad (47)$$

$$\bar{p}_{11}(0,s) = 2\beta_2 \bar{p}_3(0,s) \tag{49}$$

Outlining of equation (3.24) - (3.35) with the support of equation (3.36) to (3.46) the following result is obtained.

$$\bar{p}_0(s) = \frac{1}{D(s)} \tag{50}$$

$$\bar{p}_1(s) = \frac{\beta_1}{D(s)}\left\{\frac{1-\bar{s}_{\mu_0}(s)}{s}\right\} \tag{51}$$

$$\bar{p}_2(s) = \frac{2\beta_2}{D(s)}\left\{\frac{1-\bar{s}_{\phi}(s+\beta_1+\beta_2+4\beta_3+\beta_4+\beta_5)}{s+\beta_1+\beta_2+4\beta_3+\beta_4+\beta_5}\right\} \tag{52}$$

$$\bar{p}_3(s) = \frac{4\beta_3}{D(s)}\left\{\frac{1-\bar{s}_{\phi}(s+\beta_1+2\beta_2+3\beta_3+\beta_4+\beta_5)}{s+\beta_1+2\beta_2+3\beta_3+\beta_4+\beta_5}\right\} \tag{53}$$

$$\bar{p}_4(s) = \left(\frac{\beta_4+2\beta_2\beta_4+4\beta_3\beta_4}{D(s)}\right)\left\{\frac{1-\bar{s}_{\mu_0}(s)}{s}\right\} \tag{54}$$

$$\bar{p}_5(s) = \left(\frac{\beta_5+2\beta_2\beta_5+4\beta_4\beta_5}{D(s)}\right)\left\{\frac{1-\bar{s}_{\mu_0}(s)}{s}\right\} \tag{55}$$

$$\bar{p}_6(s) = \frac{8\beta_2\beta_3}{D(s)}\left\{\frac{1-\bar{s}_{\phi}(s+3\beta_3)}{s+3\beta_3}\right\} \tag{56}$$

$$\bar{p}_7(s) = \frac{24\beta_2\beta_3^2}{D(s)}\left\{\frac{1-\bar{s}_{\phi}(s+2\beta_3)}{s+2\beta_3}\right\} \tag{57}$$

$$\bar{p}_8(s) = \left(\frac{2\beta_2^2+8\beta_2^2\beta_3}{D(s)}\right)\left\{\frac{1-\bar{s}_{\mu_0}(s)}{s}\right\} \tag{58}$$

$$\bar{p}_9(s) = \frac{12\beta_3^2}{D(s)}\left\{\frac{1-\bar{s}_{\phi}(s+2\beta_3)}{s+2\beta_3}\right\} \tag{59}$$

$$\bar{p}_{10}(s) = \left(\frac{48\beta_2\beta_3^3+24\beta_3^3}{D(s)}\right)\left\{\frac{1-\bar{s}_{\mu_0}(s)}{s}\right\} \tag{60}$$

$$\bar{p}_{11}(s) = \frac{8\beta_2\beta_3}{D(s)}\left\{\frac{1-\bar{s}_{\phi}(s+\beta_2)}{s+\beta_2}\right\} \tag{61}$$

Where D(s) is well-defined as

$$D(s)=\left\{s+\beta_1+2\beta_2+4\beta_3+\beta_4+\beta_5-\left(\begin{array}{l}2\beta_2\bar{s}_{\phi}\left(s+\beta_1+\beta_2+4\beta_3+\beta_4+\beta_5\right)+\\4\beta_3\bar{s}_{\phi}\left(s+2\beta_1+2\beta_2+3\beta_3+\beta_4+\beta_5\right)+\\\left[\beta_1+\left(2\beta_2^2+8\beta_2^2\beta_3\right)+\left(48\beta_2\beta_3^3+24\beta_3^3\right)+\right.\\\left.\left(\beta_4+2\beta_2\beta_4+4\beta_3\beta_4\right)+\left(\beta_5+2\beta_2\beta_5+4\beta_4\beta_5\right)\right]\bar{s}_{\mu_0}(s)\end{array}\right)\right\} \quad (62)$$

(60)

If all Laplace transformations of the state transition probabilities that the system is operating is added together the result is obtained as:

$$\bar{p}_{up}(s)=\left[\bar{p}_0(s)+\bar{p}_2(s)+\bar{p}_3(s)+\bar{p}_6(s)+\bar{p}_7(s)+\bar{p}_9(s)+\bar{p}_{11}(s)\right] \quad (63)$$

Therefore,

$$\bar{p}_{up}(s)=\frac{1}{D(s)}\left\{\begin{array}{l}1+2\beta_2\left(\frac{1-\bar{s}_{\phi}\left(s+\beta_1+\beta_2+4\beta_3+\beta_4+\beta_5\right)}{s+\beta_1+\beta_2+4\beta_3+\beta_4+\beta_5}\right)+\\4\beta_3\left(\frac{1-\bar{s}_{\phi}\left(s+\beta_1+2\beta_2+3\beta_3+\beta_4+\beta_5\right)}{s+\beta_1+2\beta_2+3\beta_3+\beta_4+\beta_5}\right)+\\8\beta_2\beta_3\left(\frac{1-\bar{s}_{\phi}\left(s+3\beta_3\right)}{s+3\beta_3}\right)+24\beta_2\beta_3^2\left(\frac{1-\bar{s}_{\phi}\left(s+2\beta_3\right)}{s+2\beta_3}\right)\\+12\beta_3^2\left(\frac{1-\bar{s}_{\phi}\left(s+2\beta_3\right)}{s+2\beta_3}\right)+8\beta_2\beta_3\left(\frac{1-\bar{s}_{\phi}\left(s+\beta_2\right)}{s+\beta_2}\right)\end{array}\right\} \quad (64)$$

On the other hand, the sum of all Laplace transformations of the state probabilities that the system fails can be summarized in the equation below;

$$\bar{p}_{down}(s)=1-\bar{p}_{up}(s)) \quad (65)$$

4. Analytical study of the model for particular cases

4.1 Availability analysis of the model for copula repair method

Supposing

$$S_{\mu_0}(s)=\bar{S}_{\exp[x^{\theta}+\{\log\phi(x)\}^{\theta}]^{1/\theta}}(s)=\frac{\exp[x^{\theta}+\{\log\phi(x)\}^{\theta}]^{1/\theta}}{s+\exp[x^{\theta}+\{\log\phi(x)\}^{\theta}]^{1/\theta}} \quad (66)$$

$$\bar{S}_{\phi}(s)=\frac{\phi}{s+\phi}, \quad (67)$$

and considering the same values of failure rates as $\beta_1=\beta_2=\beta_3=\beta_4=\beta_5=0.02$, $\phi=\mu=x=y=z=m=n=1$ and repair rates as $\phi(y)=\phi(z)=1$ in equation (62), and carrying inverse Laplace transform, the expression obtained is availability function.

$$\bar{p}_{up}(s)=\left\{\begin{array}{l}-0.002531e^{-1.04000t}+0.025983e^{-2.79218t}\\-0.019633e^{-1.25934t}+0.999411e^{-0.00677t}\\-0.001770e^{-1.02000t}-0.001459e^{-0.06000t}\end{array}\right\} \quad (68)$$

Supposing different values of time variable t = 0, 1…10, units of time in equation (68), availability is computed (Table 1).

Table 1: *Availability computation using copula repair method*

Time	0	1	2	3	4	5	6	7	8	9	10
Availability	1.0000	0.9866	0.9837	0.9761	0.9724	0.9660	0.9595	0.9531	0.9467	0.9403	0.9339

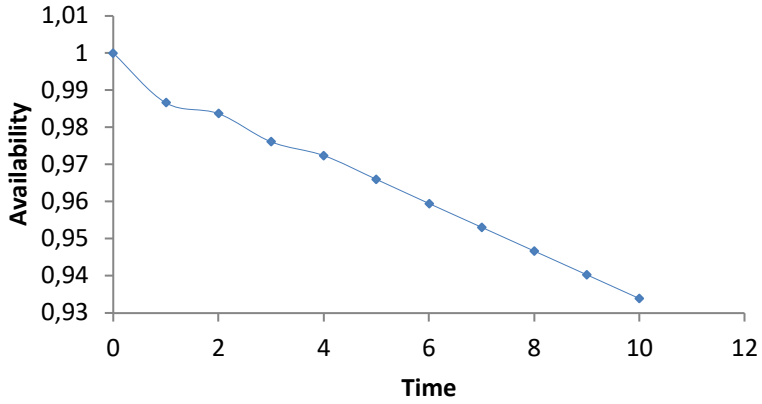

Figure 3: *Availability against time when copula repair method is used*

4.2 Availability analysis of the model for general repair method

Supposing, $\bar{S}_{\phi}(s)=\frac{\phi}{s+\phi}$, and considering the same values of failure rates as $\beta_1=\beta_2=\beta_3=\beta_4=\beta_5=0.02$, $\phi=\mu=x=y=z=m=n=1$ and repair rates as $\phi(y)=\phi(z)=1$ in equation (62), and carrying inverse Laplace transform, the expression obtained is availability function.

$$\bar{p}_{up}(s)=\left\{\begin{array}{l}-0.036975e^{-1.04000t}+0.001825e^{-1.02000t}\\+0.008761e^{-1.29593t}+0.068653e^{-1.03754t}\\+0.961175e^{-0.00651t}-0.003440e^{-0.06000t}\end{array}\right\} \quad (69)$$

Allowing different values of time variable t = 0, 1…10, units of time in equation (69), availability is computed (Table 2).

Table 2: *Availability computation using general repair method*

Time	0	1	2	3	4	5	6	7	8	9	10
Availability	1.0000	0.9680	0.9532	0.9441	0.9369	0.9305	0.9243	0.9183	0.9123	0.9064	0.9005

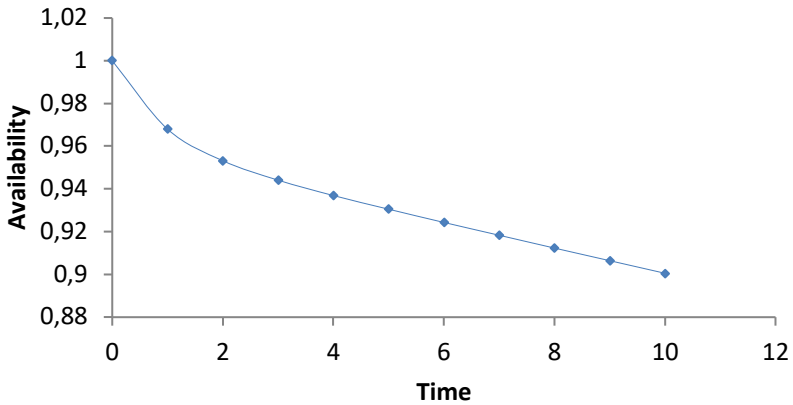

Figure 4: *Availability against time when general repair method is used*

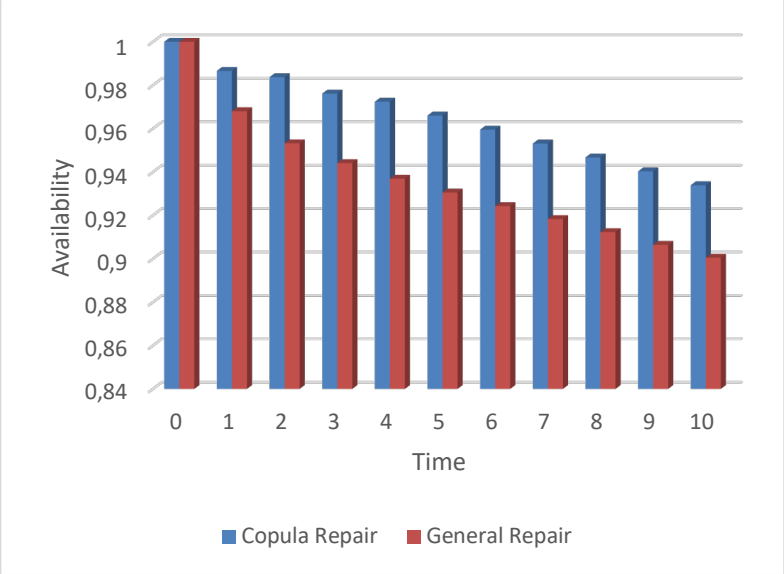

Figure 5: *Variation of Availability with to time under different repair policies*

4.3 Reliability Analysis of the model

Allowing all repair rates $\phi(y), \phi(z) and \mu_0$ in equation (62) to zero, considering the values of failure rates as $\beta_1 = \beta_2 = \beta_3 = \beta_4 = \beta_5 = 0.02$ and captivating inverse Laplace transformation, the expression follows is reliability function.

$$R(t) = \begin{Bmatrix} -5.082323e^{-0.18000t} + 6e^{-0.16000t} + 0.026666e^{-0.06000t} \\ +0.035657e^{-0.04000t} + 0.020000e^{-0.02000t} \end{Bmatrix} \quad (70)$$

Taking different values of time variable t = 0, 1…10, units of time in equation (70), reliability is computed (Table 3).

Table 3: *Computation of reliability with respect to time*

Time	0	1	2	3	4	5	6	7	8	9	10
Reliability	1.0000	0.9467	0.8868	0.8237	0.7597	0.6967	0.6358	0.5779	0.5235	0.4729	0.4261

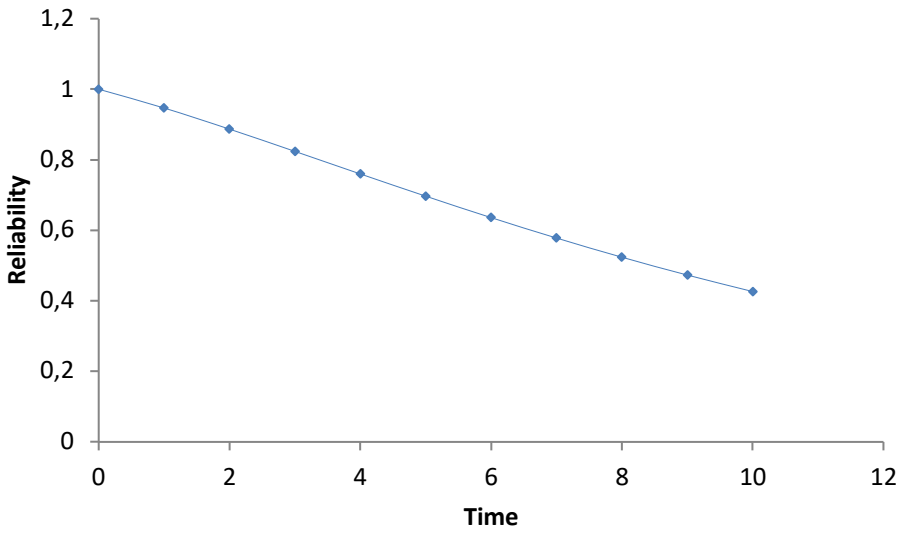

Figure 6: *Reliability function against time variable*

4.4 MTTF Analysis of the model

Letting all repairs to zero in equation (62) and the limit as s becoming close to zero, MTTF expression is obtained as:

$$MTTF = \lim_{s\to 0} \overline{p}_{up}(s) = \frac{1}{\beta_1 + 2\beta_2 + 4\beta_3 + \beta_4 + \beta_5} \left\{ \begin{array}{l} 1 + \dfrac{2\beta_2}{\beta_1 + \beta_2 + 4\beta_3 + \beta_4 + \beta_5} + \\ \dfrac{4\beta_3}{\beta_1 + 2\beta_2 + 3\beta_3 + \beta_4 + \beta_5} + \\ \dfrac{8\beta_2}{3} + 12\beta_2\beta_3 + 14\beta_3 \end{array} \right\} \quad (71)$$

Assuming $\beta_1 = \beta_2 = \beta_3 = \beta_4 = \beta_5 = 0.02$ and varying $\beta_1, \beta_2, \beta_3, \beta_4, \beta_5$ one by one respectively as 0.01, 0.02...0.09 in equation (67), MTTF of the model is calculated with respect to failure rate (Table 4).

Table 4: *Computation of MTTF with respect to failure rate*

Failure rates	$MTTF\ \beta_1$	$MTTF\ \beta_2$	$MTTF\ \beta_3$	$MTTF\ \beta_4$	$MTTF\ \beta_5$
0.01	12.5772	12.5864	13.1197	12.5772	12.5772
0.02	11.6007	11.6007	11.6007	11.6007	11.6007
0.03	10.7579	10.8229	10.5096	10.7579	10.7579
0.04	10.0240	10.1850	9.6802	10.0240	10.0240
0.05	9.3795	9.6470	9.0273	9.3795	9.3795
0.06	8.8096	9.1835	8.4996	8.8096	8.8096
0.07	8.3024	8.7779	8.0643	8.3024	8.3024
0.08	7.8482	8.4184	7.6993	7.8482	7.8482
0.09	7.4394	8.0964	7.3887	7.4394	7.4394

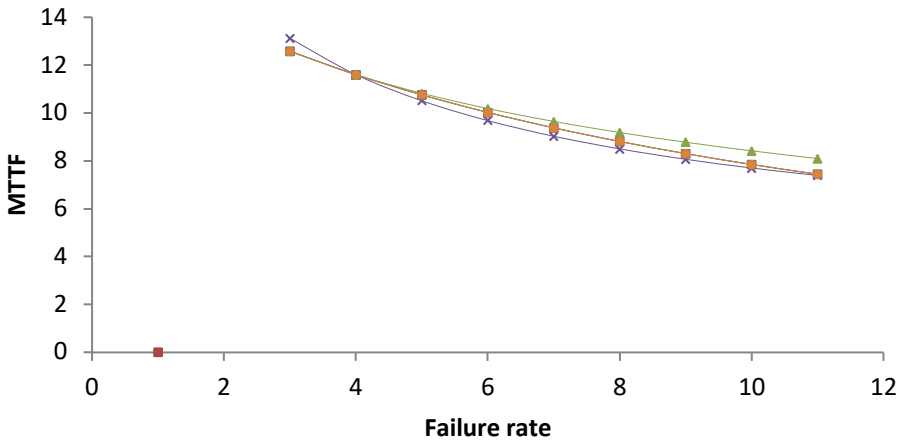

Figure 7: *MTTF against Failure rates*

4.5 Sensitivity Analysis of the model

Taking partial differential of the MTTF with respect to failure rates yield sensitivity of the model, there and then considering the failure rates as, $\beta_1 = \beta_2 = \beta_3 = \beta_4 = \beta_5 = 0.02$ in the partial differential function of the MTTF gives result as presented in Table 5.

Table 5: *Computation of sensitivity with respect to failure rate*

Failure rate	$\frac{\partial(MTTF)}{\beta_1}$	$\frac{\partial(MTTF)}{\beta_2}$	$\frac{\partial(MTTF)}{\beta_3}$	$\frac{\partial(MTTF)}{\beta_4}$	$\frac{\partial(MTTF)}{\beta_5}$
0.01	-105.3564	-112.4063	-183.4378	-105.3564	-105.3564
0.02	-90.4902	-86.7073	-126.5997	-90.4902	-90.4902
0.03	-78.4748	-69.9443	-94.1730	-78.4748	-78.4748
0.04	-68.6385	-58.2793	-73.0555	-68.6385	-68.6385
0.05	-60.4937	-49.7372	-58.3667	-60.4937	-60.4937
0.06	-53.6804	-43.2241	-47.7029	-53.6804	-53.6804
0.07	-47.9283	-38.0960	-39.7100	-47.9283	-47.9283
0.08	-43.0317	-33.9527	-33.5643	-43.0317	-43.0317
0.09	-38.8316	-30.5346	-28.7380	-38.8316	-38.8316

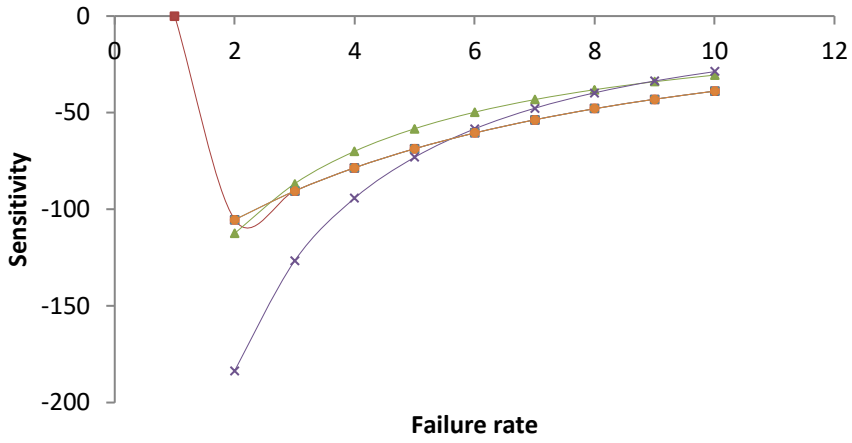

Figure 8: *Sensitivity against failure rates*

4.6 Profit Analysis of the model

4.6.1 Profit analysis using copula repair method:

Cost or profit investigation which is known as expected profit is done by integrating the $p_{up}(t)$ of the system, then multiplying the result by revenue per unit time (k_1) and eventually subtracting service cost per unit time (k_2) the relation that follows summaries the saying.

$$E_p(t) = K_1 \int_0^t P_{up}(t)dt - K_2 t \tag{72}$$

Captivating fixed values of parameters of equation (62), equation (69) just arrive as

$$E_p(t) = k_1 \left\{ \begin{matrix} 0.002434e^{-1.04000t} - 0.009305e^{-2.79218t} + 0.015590e^{-1.25934t} - \\ 147.5751111e^{-0.00677t} + 0.001735e^{-1.02000t} + 0.001376e^{-1.06000t} + \\ 147.5632 \end{matrix} \right\} - k_2(t) \tag{73}$$

Assuming K_1= 1and K_2= 0.1, 0.2..., 0.5, respectively and changing t = 0, 1, 2...10, units of time, the expected profit computations are done in the subsequent (Table 6).

Table 6: *Computation of profit within the limit (0, t], when copula repair is used*

Time	$E_p(t)$ K_2=0.1	$E_p(t)$ K_2=0.2	$E_p(t)$ K_2=0.3	$E_p(t)$ K_2=0.4	$E_p(t)$ K_2=0.5
0	0	0	0	0	0
1	0.8899	0.7899	0.6899	0.5899	0.4899
2	1.7753	1.5753	1.3753	1.1753	0.9753
3	2.6566	2.3566	2.0566	1.7566	1.4566
4	3.5322	3.1322	2.7322	2.3322	1.9322
5	4.4015	3.9015	3.4015	2.9015	2.4015
6	5.2643	4.6643	4.0643	3.4643	2.8643
7	6.1207	5.4207	4.7207	4.0207	3.3207
8	6.9706	6.1706	5.3706	4.5706	3.7706
9	7.8141	6.9141	6.0141	5.1141	4.2141
10	8.6513	7.6513	6.6513	5.6513	4.6513

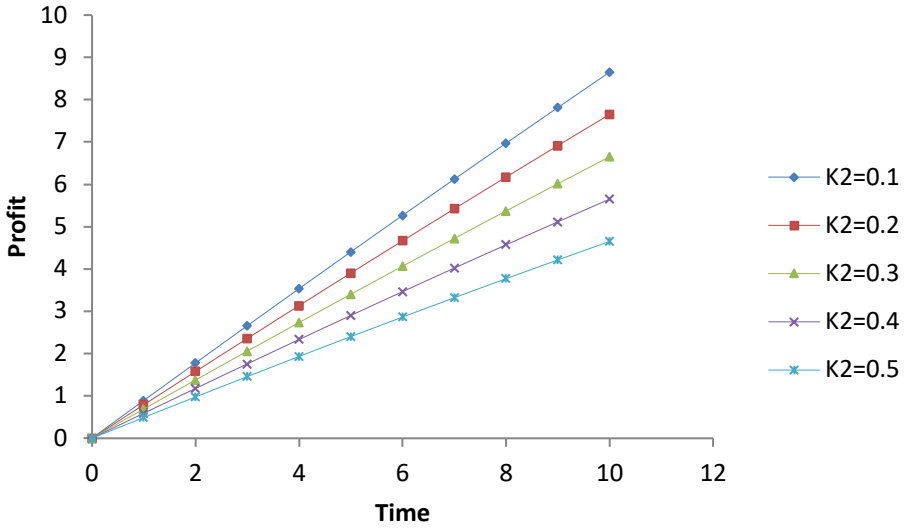

Figure 9: *Profit against time when copula repair method is used*

4.6.2 Profit inquiry using general repair method:

$$E_p(t) = K_1 \int_0^t P_{up}(t)dt - K_2 t \tag{74}$$

Captivating fixed values of parameters of equation (62), equation (71) just arrive as

$$E_p(t) = k_1 \left\{ \begin{matrix} 0.035553e^{-1.04000t} - 0.001789e^{-1.02000t} - 0.006760e^{-1.29593t} - \\ 0.066169e^{-1.03754t} - 147.527359e^{-0.00651t} + 0.003246e^{-1.06000t} + \\ 147.5632 \end{matrix} \right\} - k_2(t) \tag{75}$$

Assuming K_1= 1and K_2= 0.1, 0.2..., 0.5, respectively and changing t = 0, 1, 2...10. Units of time, the expected profit computations are done in Table 7.

Table 7: *Computation of profit within the limit (0, t], when general repair is used*

Time	$E_p(t)$ K_2=0.1	$E_p(t)$ K_2=0.2	$E_p(t)$ K_2=0.3	$E_p(t)$ K_2=0.4	$E_p(t)$ K_2=0.5
0	0	0	0	0	0
1	0.8816	0.7816	0.6816	0.5816	0.4816
2	1.7415	1.5415	1.3415	1.1415	0.9415
3	2.5899	2.2899	1.9899	1.6999	1.3899
4	3.4303	3.0303	2.6303	2.2303	1.8303
5	4.2641	3.7641	3.2641	2.7641	2.2641
6	5.0915	4.4915	3.8915	3.2915	2.6915
7	5.9129	5.2129	4.5129	3.8129	3.1129
8	6.7282	5.9282	5.1282	4.3282	3.5282
9	7.5376	6.6376	5.7376	4.8376	3.9376
10	8.3411	7.3411	6.3411	5.3411	4.3411

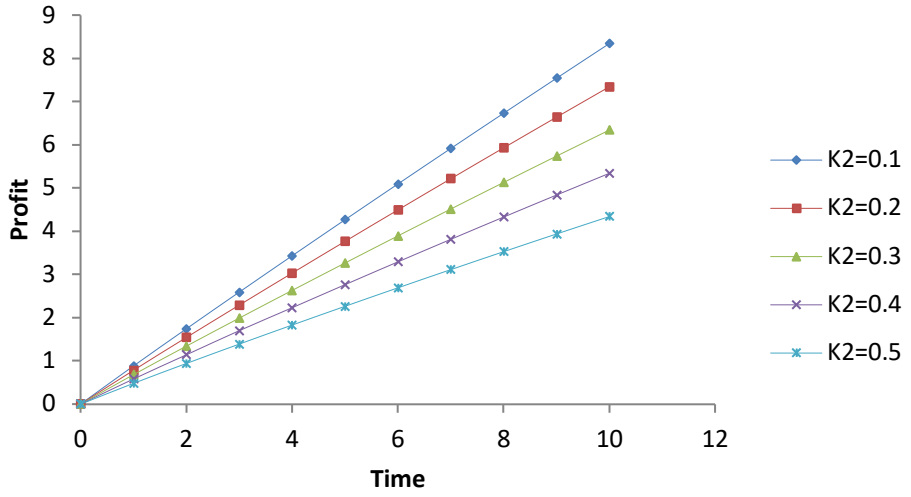

Figure 10: *Profit against time when general repair method is used*

5. Discussion and Concluding Remark

Table 1 and Figure 3 depicted the availability variation with respect of time. From Figure 3 it is clear that as failure rates increases than availability deceases when copula repair policy is employed. Similar observation can be Table 2 and Figure 4 presents the availability of system when the repair follows general distribution.

Table 3 and Figure 6 presents variation of reliability with respect to time. The reliability of system decreases with time when the failure rates increases. From Table 3 and Figure 6, it is enough to conclude that reliability has lower values in comparison with availability values in Tables 1 and 2.

Table 4 and Figure 7 depicts the mean-time-to-failure (MTTF) of the system with respect to variation in failure rates β_1, β_2, β_3, β_4 and β_5 respectively when other parameters are kept constant. The variation in MTTF corresponding to β_1, β_2, β_3, β_4 and β_5 are slightly closer. This analysis suggests that the failure rates β_1, β_2, β_3, β_4 and β_5 are more responsible for successful operation of the system. Table 6 and Figure 8 gives the information of the sensitivity analysis studied in this

work. Table 5 and Figure 8 gives the information of the sensitivity analysis studied in section 6.5 of this work.

Table 6 and Figure 9 and Table 7 and Figure 10 depicted the profit variation with respect of time via two types of repair employing copula repair approach and general repair. From Table 6 and Figure 9 it is clear that as failure rates increases than profit deceases when copula repair policy is employed. Similarly, Table 7 and Figure 10 presents the profit of system when the repair follows general distribution. It is clear that as failure rates increases than profit deceases when general repair policy is employed.

Comparative analysis of copula and general repair in Table 1 and Table 2 are presented in Figure 5 which compare the two results of availability with respect to time under copula and general repair. It is evident from Table 1 and Table 2 and Figure 5 that availability of the system is better when the repair follows copula distribution.

Comparative analysis of copula and general repair in Table 6 and Table 7 which compare the results of profit with respect to time under copula and general repair when K_2= 0.5,04,0.3,0.2,0.1. It is evident from Table 6 and Table 7 when comparing the two procedures, repair policy of general and copula distributions, it appears that the predicted profit is larger when the repair policy is follows by copula distribution and lower when the repair follows general distribution. In both circumstances, the predicted profit is highest when the service cost is lowest and lowest when the service cost is highest. In conclusion, copula repair method yields better result, compared to general repair method; therefore, copula repair method is recommended for effective performance of the system.

References

[1] Abdelfattah Mustafa, A. (2017). Improving the Reliability of a Series-Parallel System Using Modified Weibull Distribution, International Mathematical Forum,12(6), 257 269 https://doi.org/10.12988/imf.2017.611155

[2] Aggarwal A. K, Kumar S, Singh V, Garg TK, 2014. Markov modelling and reliability analysis of urea synthesis system of a fertilizer plant. Journal of Industrial Engineering International, 11, 1-14, DOI 10. 1007/s40092-014-0091-5.

[3] Aggarwal, A. K.,Kumar, S. and Singh, V, 2017. Mathematical modeling and fuzzy availability analysis for serial processes in the crystallization system of a sugar plant, Journal of Industrial Engineering International, 13:47–58, DOI 10.1007/s40092-016-0166-6.

[4] Arvind K Lal, A. K., Manwinder Kaur M and Lata, S. (2013). Behavioral study of piston manufacturing plant through stochastic models, Journal of Industrial Engineering International, 9(24), 1-10. http://www.jiei-tsb.com/content/9/1/24

[5] Chauhan, S.K and S.C. Malik. (2016). Reliability Evaluation of Series-Parallel and Parallel-Series Systems for Arbitrary Values of the Parameters, International Journal of Statistics and Reliability Engineering Vol. 3(1), pp. 10-19.

[6] Fadi N. Sibai, F.N. (2014). Modelling and output power evaluation of series parallel photovoltaic modules, International Journal of Advanced Computer Science and Applications,5(1),129-136.

[7] Fallahnezhad, M. S. and Najafian, E. (2016): A model of preventive maintenance for parallel, series, and single-item replacement systems based on statistical analysis, Communications in Statistics - Simulation and Computation, DOI: 10.1080/03610918.2016.1183781

[8] Freiheit, T., Shpitalni, M and Hu, S.J, 2004. Productivity of paced parallel-serial manufacturing lines with and without crossover, Journal of Manufacturing Science and Engineering, 126, 361-367.

[9] Gahlot, M., Singh, V.V., Ayagi, H.I. and Goel, C.K. (2018) 'Performance assessment of repairable system in series configuration under different types of failure and repair policies using copula linguistics', International Journal of Reliability and Safety, Vol. 12, No. 4, pp.348–374.

[10] Gulati, J., Singh, V.V., Rawal, D.K. and Goel, C.K. (2016) 'Performance analysis of complex system in series configuration under different failure and repair discipline using copula', International Journal of Reliability, Quality and Safety Engineering, Vol. 23, No. 2, pp.812–832.

[11] Garg D, Kumar K, and Singh J., 2010a. Availability analysis of a cattle feed plant using matrix method. Int J Eng 3(2):201–219

[12] Garg S, Singh J and Singh D. V., 2010b. Availability analysis of crankcase manufacturing in a two-wheeler automobile industry. Appl Math Model 34:1672–1683

[13] Garg, H and Sharma S.P., 2011. Multi-objective optimization of crystallization unit in a fertilizer plant using particle swarm optimization. Int J Appl Sci Eng 9(4):261–276

[14] Gupta S, and Tewari P.C., 2011. Simulation modeling in a availability thermal power plant. J Eng Sci Technol Rev 4(2):110–117.

[15] Hu, L., Yue, D and Li, J., 2012. Availability analysis and design optimization for repairable series-parallel system with failure dependencies, International Journal of Innovative Computing, Information and Control, 8(10A), 6693-6705.

[16] Khanduja R, Tewari PC, Kumar D., 2012. Steady state behaviour and maintenance planning of bleaching system in a paper plant. Int J Ind Eng 7(12):39–44

[17] Kadiyan S, Garg RK, Gautam R., 2012. Reliability and availability analysis of uncaser system in a brewery plant. Int J Res Mech Eng Technol 2(2):7–11.

[18] Khatab, A, Aghezzaf, E, Diallo, C and Djelloul, I. (2017). Selective maintenance optimization for series-parallel systems alternating missions and scheduled breaks with stochastic durations, International Journal of Production Research, 55:10, 3008-3024. DOI: 10.1080/00207543.2017.1290295

[19] Kaur, M., Lal, A.K., Bhatia, S.S and Reddy, A.S., 2013c. On use of corrective maintenance data for performance analysis of preventively maintained textile industry, Journal of Reliability and Statistical Studies, 6(2), 51-63.

[20] Kumar, A., Saini, M. and Malik, S. C., 2014. Stochastic modelling of a concrete mixture plant with preventive maintenance, Application and Applied Mathematics, 9(1): 13-27.

[21] Kumar V and Mudgil V., 2014. Availability optimization of ice cream making unit of milk plant using genetic algorithm, IntManag Bus Stu, 4(3), 17-19.

[22] Kumar S, and Tewari PC., 2011. Mathematical modelling and performance optimization of CO2 cooling system of a fertilizer plant. Int J IndustEng Comp, 2, 689-698

[23] Kumar R, Sharma AK, Tewari PC., 2011. Performance modelling of furnace draft air cycle in a thermal plant. Int J EngSci Tech, 3(8), 6792-6798.

[24] Kumar, A and Lata, S., 2012. Reliability evaluation of condensate system using fuzzy Markov Model, Annals of Fuzzy Mathematics and Informatics, 4(2), 281-291.

[25] Lado, A.K. and Singh, V.V. (2019) 'Cost assessment of complex repairable system consisting of two subsystems in the series configuration using Gumbel Hougaard family copula'. International Journal of Quality Reliability and Management, Vol. 36, No. 10, pp.1683–1698.

[26] Lado, A.K., Singh, V.V., Kabiru, H.I. and Yusuf, I. (2018) 'Performance and cost assessment of repairable complex system with two subsystems connected in series configuration', International Journal Reliability and Applications, Vol. 19, No. 1, pp.27–42.

[27] Mohammadi, M, Mortazavi, S.M and Karbasian, M.(2018). Developing a Method for Reliability Allocation of Series-Parallel Systems by Considering Common Cause Failure, International Journal of Industrial Engineering & Production Research, 29(2),213 - 230

[28] Peng, R, Zhai,Q, Xing, L and Yang,J. (2016) Reliability analysis and optimal structure of series-parallel phased-mission systems subject to fault-level coverage, IIE Transactions, 48:8, 736-746, DOI: 10.1080/0740817X.2016.1146424

[29] Ram, M and Manglik, M., 2016. An analysis to multi-state manufacturing system with common cause failure and waiting repair strategy, Cogent Engineering 3: 1266185, 1-20, http://dx.doi.org/10.1080/23311916.2016.1266185

[30] Ram, M., Singh, S.B. and Singh, V.V. (2013) 'Stochastic analysis of a standby system with waiting repair strategy', IEEE Transactions on System, Man, and Cybernetics System, Vol. 43, No. 3, pp.698–707.

[31] Rawal, D.K., Ram, M. and Singh, V.V. (2014) 'Modeling and availability analysis of internet data center with various maintenance policies', International Journal of Engineering, IJE Transactions A: Basics, Vol. 27, No. 4, pp.599–608.

[32] Rawal, D.K., Ram, M. and Singh, VV. (2015) 'Study of reliability measures of a local area network via copula linguistics approach', International J. of Quality Reliability and Management, Vol. 32, No. 1, pp.97–111.

[33] Singh, V.V. and Ayagi, H.I. (2018) 'Stochastic analysis of a complex system under preemptive resume repair policy using Gumbel-Hougaard family copula', International Journal of Mathematics in Operation Research, Vol. 12, No. 2, pp.273–291.

[34] Tewari PC, Khaduja R, and Gupta, M., 2012 Performance enhancement for crystallization unit of a sugar plant using genetic algorithm technique. J Ind Eng Int 8(1):1–6

[35] Joachims J. Learning to Classify Text Using Support Vector Machines: Methods, Theory and Algorithms, Kluwer, 2002.

[36] Xie,L., Lundteigen, M.A and Liu, Y. (2020).Reliability and barrier assessment of series–parallel systems subject to cascading failures, https://doi.org/10.1177/1748006X19899235

[37] Xie, L., Wei, Y and Li, P. (2019) .On optimal heterogeneous components grouping in series-parallel and parallel-series systems, Probability in the Engineering and Informational Sciences, Volume 33, Issue 4, 564-578. https://doi.org/10.1017/S0269964818000499

[38] Xu,Q,-Z, Guo,L, -M, Shi,H,-P and Wang, N. (2016). Selective maintenance problem for series–parallel system under economic dependence, Defence Technology, 12(5), 388-400. https://doi.org/10.1016/j.dt.2016.04.004

[39] Yusuf, I., Lado, A.K. and Ali, U.A. (2020) 'Reliability analysis of communication network system with redundant relay station under partial and complete failure', J. Math. Comput. Sci., Vol. 10, No. 4, pp.863–880

[40] Yusuf, I., Sani, B and Yusuf, B. (2019). Profit analysis of a series-parallel system under partial and complete failures, Journal of Applied Sciences, 19(6),565-574.

[41] Yusuf, I., 2014. Comparative analysis of profit between three dissimilar repairable redundant systems using supporting external device for operation, Journal of Industrial Engineering International,10:77, 1-9, DOI 10.1007/s40092-014-0077-3

[42] Yusuf, I., Maihulla, A. S and Bala, S. I. (2021). Reliability and Performance Analysis of a Series-Parallel System using Gumbel–Hougaard Family Copula. *Journal of Computational and Cognitive Engineering*, 01–10. https://doi.org/10.47852/bonviewJCCE2022010101

[43] Zhu, S, Xiang, Y and Coit, D. (2018).Redundancy Allocation for Serial-Parallel System Considering Heterogeneity of Components, ASME 2018 13th International Manufacturing Science and Engineering Conference, https://doi.org/10.1115/MSEC2018-6481

Optimization of Reliability under Different flow state of Multistate Flow Network

Nalini Kanta Barpanda[1]
Ranjan Kumar Dash[2]
•
Sambalpur University[1]
Odisha University of Technology and Research[2]
nkbarpanda@suniv.ac.in[1]
rkdash@outr.ac.in[2]

Abstract

This paper focuses on maximizing the reliability of multistate flow network(MFN) by meeting the demand to flow from source to destination. The reliability maximization problem is formulated considering the different flow state of the edges and their corresponding existence probabilities. A method based on genetic algorithm is proposed to maximize the reliability of MFN searching through the state space. Each step of the proposed method is illustrated by taking a suitable example network. The values of computed reliability by the proposed method is exactly same as computed by the deterministic approach. The reliability of some benchmark networks are evaluated under different demand levels. The reliability of a practical example network is evaluated and compared against the reliability value computed by some deterministic approaches of similar interest. The computational time of the proposed method is also compared with these methods. The comparison findings reveal that the proposed method surpasses existing methods on the basis of computed reliability values and computational time.

Keywords: reliability, minimal cutset, state space, genetic algorithm

1. Introduction

The reliability is a critical performance parameter to assess the operationality of many real-time networks like interconnection networks used in high-performance computing, computer networks, transportation system, mobile ad-hoc networks, wireless sensor networks, telecommunication networks to name a few. When it comes to determining how networks work, the binary network model has performed well in conventional reliability assessment. Even though, the binary network model has flaws because it assumes that network components can only be in one of two states: fully operational or completely failed [1-7]. In the last few years, researchers have expanded the binary network model to a multi-state network model for more practical applications where network components have more than two levels of performance. The success of such networks is mostly assessed by the amount of data or unit of products that can be successfully flowed across them. In other words, it's natural to assume that these networks have certain designated origins and destinations and that the links that connect them have a variety of flow states. Because the flows are stochastic, each one has a set of intrinsic probabilities. The success probability of transferring d units

of product or d quantity of data from a specific pair of source nodes to a specific pair of destination nodes can be described as the reliability of such a multistate flow network at a given demand level d.

In the past, reliability evaluation of multistate networks drew a lot of attention, and it's still a matter of contention, especially when it comes to big networks that are explored in real-time. Multi-valued Decision Diagram (MDD)[8, 9], Monte-Carlo Simulation method (MCS)[10], State Space Decomposition method (SSD)[11- 13], Universal Generating Function (UGF) method[14], and d-MPs/d-MCs method[15-23] are the most commonly used approaches for evaluating MFN reliability. Chen et al.[15] presented an approach for fast enumeration of d-MPs. The work carried out in [16] searched for all d-MCs of multistate flow network and then the duplicate d-MCs were detected and discarded. The work presented in [17] evaluated the reliability of the stochastic flow network under budget and time constraints by using intersecting MPs. The work in [18] followed state-space decomposition method and recursively generated unique d-MPs. The problem of evaluating the reliability of an MFN with a cost constraint in terms of minimal cuts is addressed in the work[19]. Similar work can be found in [20].

Xu et al. [21] integrated a flow-max algorithm and enumeration algorithm to solve the d-MP problem of a multistate flow network. Niu et al. [22] introduced an approach to generate d-MCs more accurately after removing the redundant MCs. The authors in [23] combined the max-flow algorithm with the partition technique to generate the d-MPs. Rushdi et al. [24] evaluated the reliability of a multistate flow network using the map method.

The research [25] considers the cost and spoilage limitations when evaluating the reliability of a multi-state distribution network (MSDN). Under delivery spoilage and budget constraints, reliability is defined as the likelihood that the MSDN will be able to distribute a sufficient quantity of items to meet market demand.

The reliability of a multi-state delivery network with different suppliers, transfer stations, and marketplaces connected by branches of multi-state capacities, delivering a specific commodity or service between their end vertices is the focus of the work [26].

The network reliability of a multistate network is calculated using an efficient technique based on the sum of disjoint products (SDP) principle in [27]. In addition, to improve the efficiency of reliability evaluation, a recursive function with simplified methods is presented.

The above-mentioned studies demonstrated that numerous methodologies for evaluating MFN reliability were used to simplify the reliability evaluation process. In some circumstances, the reliability of small to medium-sized networks, and even large networks, is evaluated deterministically with a huge amount of computational time. Using various heuristic methods, this computational time can be reduced significantly, unless the estimated reliability values are compromised. The works [28-29] used a genetic algorithm to evaluate the reliability of the binary state networks. However, the application of heuristic techniques to multistate flow networks for their reliability evaluation is very limited[30-31]. The work carried out in this paper is an attempt to reduce the computational time for evaluating the reliability of a multistate flow network using a genetic algorithm. The rest of the paper is organized as follows:

In Section-2, the reliability maximization problem is formulated and GA based method is proposed to maximize the reliability of MFN. Secion-3 illustrates the proposed method by taking a suitable example. Simulated results are presented in Section-4. The reliability of a practical distribution network is computed and compared against some existing method in Section-5. Section-6 concludes the paper with future scope.

2. Methods

2.1 Formulation of Reliability maximization problem under different flow states

2.1.1 Flow model of Multistate network

The multistate flow network (MFN) can be represented as a directed graph(G) with N vertices and E edges. The edges exhibit multiple states in terms of the different flow capacity states. The flow capacity state f_i for an edge $e_i \in E$ can be defined as a non-negative inter randomly selected from 0 to F_i. Since, f_i is the capacity state of e_i, the capacity vector f can be defined as follows:

$$f = (f_1,\ f_2,\ \cdots f_m)\ \text{ where, } f_i \in F_i \tag{1}$$

If (s, t) are the source and destination nodes respectively, the maximum amount of flow from s to t can be represented as $F(f: s \to t)$. For a capacity level (d), the following condition must hold:

$$F(f: s \to t) = d \tag{2}$$

2.1.2 Capacity vector space

The capacity vector space can be directly defined by using Eq(1) as

$$S(f) = \{(f_1, f_2, \cdots f_m) |\ 0 \le f_i \le F_i\ for\ 1 \le i \le m\} \tag{3}$$

The capacity state of an edge f_i occurs with a probability, say $p(f_i)$ or in other words, it can be stated that the edge e_i has the probability p to have the capacity state f_i.

2.1.3 Success state

As per the max-flow min-cut theorem [24], the capacity level (d) is attainable only when

$$\min\ [F(C_j)] \ge d \tag{4}$$

where, C_j is the jth minimal cut set with $j = 1, 2, \cdots K$ and K is the maximum number of cut sets between s and t. Since, each minimal cut set may contain one or more number of edges, sum of their capacity states must be greater than or equal to d and in turns the MC is termed as d-MC.

The state of a network in terms of different flows along the edges is said to be success if it satisfies Eq.(4) for each generated MCs. Mathematically,

$$s(f) = \begin{cases} if\ \min\ [F(C_j)] \ge d, & Success \\ else & No \end{cases} \tag{5}$$

The probability of the success state is calculated as:

$$p\big(s(f)\big) = \prod_{i=1}^{m} p(f_i) \tag{6}$$

Let, *Succ* be the set of all the successful state.

The reliability of the network permitting capacity level (d) is calculated from Eq. (4) and (5) as:

$$R(d) = \sum_{s \in Succ} p(s(f)) \tag{7}$$

2.1.4 Formulation of Reliability maximization problem

For a given multistate flow network with a set of edges whose flow distribution is governed by some probability measures, the Reliability maximization problem can be stated as finding the optimal flow state of each edge so that the overall reliability is maximized while meeting the capacity level d. Mathematically, this multi-objective problem can be formulated as:

$$\max \{R(d)\} \tag{8}$$

such that

$$(f: s \to t) = d \tag{9}$$

$$\min [F(C_j)] \geq d, j = 1, 2, \cdots K \tag{10}$$

$$f = (f_1, f_2, \cdots f_m) \text{ where, } f_i \in F_i \tag{11}$$

$$0 \leq f_i \leq F_i \; for \; 1 \leq i \leq m \tag{12}$$

2.2 Proposed GA based method to maximize the reliability of MFN under different flow states

2.2.1 Encoding scheme

The capacity of each edge $e_i \in E$ is represented by f_i and its occurrence is defined by the probability, $p(f_i)$. The following encoding scheme is adopted in this work to encode each edge:

$$e_i(f_i) = \begin{cases} f_i & if \; e_i \in C_j \\ 0 & otherwise \end{cases} \tag{13}$$

2.2.2 Initial population

The initial population can be defined directly from the capacity vector space by using Eq(3) as

$$Pop = \left\{e_1(f_1), e_2(f_2) \cdots e_m(f_m)\right) \tag{14}$$

Where,

$$0 \leq e_i(f_i) \leq F_i \; for \; 1 \leq i \leq m\}$$

2.2.3 Generation of MCs

The minimal cutsets (C) are generated by using the method [32] such that

$$C = \cup_j \{C_j\}, j = 1, 2, \cdots K \tag{15}$$

2.2.4 Refinement of initial population

The initial population is checked for each MC, C_j and the chromosomes that satisfies condition (4) are kept in this list while discarding the rest.

2.2.5 Fitness function

The fitness function evaluates the reliability of the network by using the Eq. (7).

2.2.6 Selection

The reliability of each chromosome belonging to the population is evaluated and the parents are selected from them having the best two values of reliability.

2.2.7 Crossover

The crossover is a single-point random operation performed on the parents (P1, P2).
Let CP be if the randomly selected crossover point. The algorithm for crossover operation is presented below:

Algorithm I:

Cross_over (CP)
for i = 1 to CP-1
C1[i]=P1[i]
C2[i]=P2[i]
for j= CP to m
C1[j]=P2[i]
C1[j]=P1[i]
return (P1, P2, C1, C2)

The steps of the proposed GA based method are presented in the flowchart

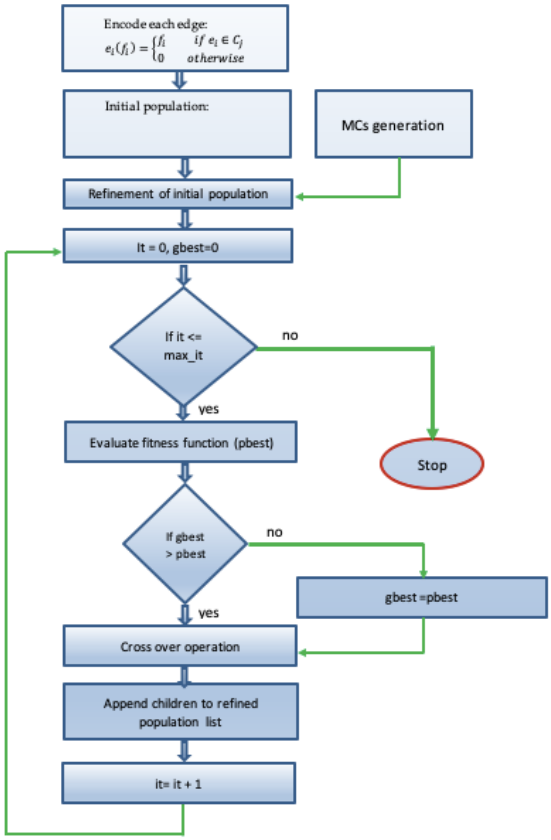

Figure 1: Flowchart of the proposed GA based method

3. Illustration

To illustrate the proposed GA-based approach, the following sample network is considered as an example.

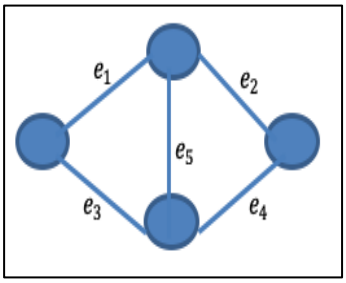

Figure 2: Example network [24]

The states and their corresponding state probabilities are presented in Table 1.

Table 1: *States and state probability of edges of Fig.2 (as per [24])*

Edge	Capacity state	Probability state
e_1	0	0.2
	2	0.8
e_2	0	0.1
	2	0.9
e_3	0	0.2
	3	0.4
	4	0.4
e_4	0	0.3
	2	0.7
	0	0.1
e_5	2	0.9

The size of the initial population is 48 and the flow for each edge satisfies Eq(13) and (14).
The MCs are generated by using method [32] and are enlisted below:

$C_1 = \{e_1,\ e_3\}$
$C_2 = \{e_2,\ e_4\}$
$C_3 = \{e_1,\ e_4, e_5\}$
$C_4 = \{e_2,\ e_3, e_5\}$

The chromosome must satisfy Eq.(4) for each the above mentioned MCs.
For example:
Chromosome =[2, 0, 4, 2, 0] does not satisfy (4), since

$e_1 = 2, e_2 = 0, e_3 = 4\ , e_4 = 2, e_5 = 0$
$F(C_1) = f_1 + f_3 = 6\ > 4$
$F(C_2) = f_2 + f_4 = 2\ \not> 4$
$F(C_3) = f_1 + f_4 + f_5 = 4$
$F(C_4) = f_2 + f_3 + f_5 = 4$

Such chromosomes must be discarded from the population.

The fitness of the chromosome is evaluated using Eq. (6) in the following manner:

Let's assume that chromosome contains the capacity vector i.e. [2, 2, 4, 2, 0]. The probability vector associated with the flow for each edge is [0.8, 0.9, 0.4, 0.7, 0.1].

The reliability of this chromosome can be computed as:

$R(c) = p(f_i) \times p(f_2) \times p(f_3) \times p(f_4) \times p(f_4)$

= 0.02016

Thus, the overall reliability of the network is calculated by summing over the feasible states (chromosome). The selection function extracts two chromosomes of having best and next to best reliability values.

The working cross over function is exemplified below:

Let P1 ([2, 2, 4, 2, 4]) and P2 ([2, 2, 3, 2, 0])be the parents and the cross over point be 2. The two children are generated as follows:

c1=[2, 2, 4, 2, 0] and c2=[2, 2, 3, 2, 4]

Since, both c1 and c2 satisfy condition (5). Both are added to the population. After performing all these steps, the computed reliability is 0.44856 (which is the same to the value of computed reliability in the work [24]).

The resultant capacity vectors are presented below:

[2, 2, 3, 2, 4], [2, 2, 3, 2, 0], [2, 2, 4, 2, 4], [2, 2, 4, 2, 0], [0, 2, 4, 2, 4]

4. Results

The simulation is carried out by using Python in Google colab environment. The generated MCs are stored in a matrix format with one MC per row. The refinement step of the proposed method is performed by element-wise multiplication of each chromosome of the population with each row of the matrix containing the MCs. The reliability of some benchmark networks are evaluated by the proposed method.

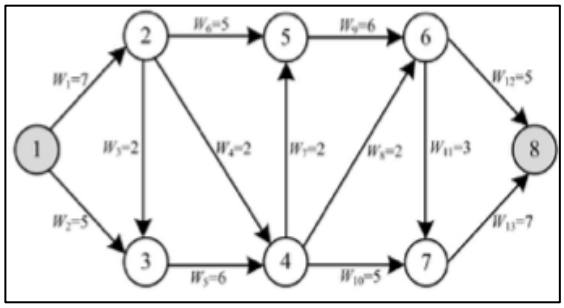

Network- 1

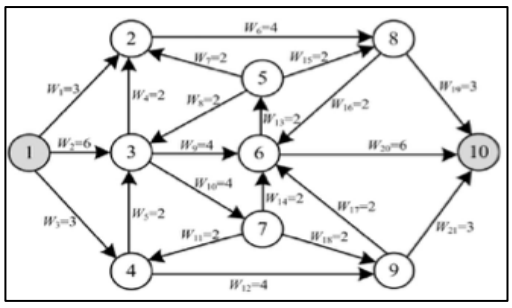

Network-2

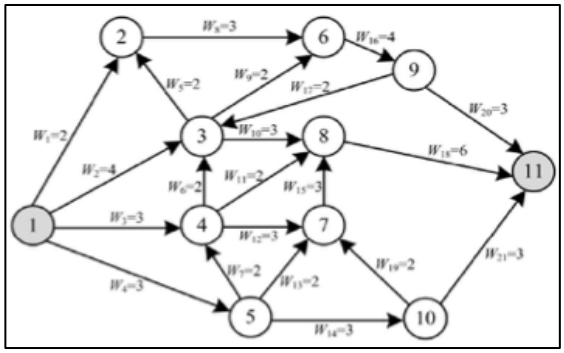

Network-3

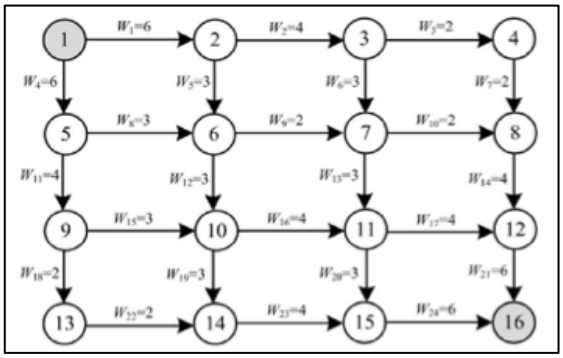

Network-4

Figure 3: The networks of [16]

The maximum flow for each edge is shown in the respective networks (Fig. 3). The probabilities of the occurrence of corresponding capacities are presented in Table 2.

Table 2: *State probability of different flow state*

pl	0	1	2	3	4	5	6	7
[0,2]	0.3	0.3	0.4	-	-	-	-	-
[0,3]	0.25	0.25	0.25	0.25	-	-	-	-
[0,4]	0.2	0.2	0.2	0.2	0.2	-	-	-
[0,5]	0.16	0.16	0.16	0.16	0.16	0.2	-	-
[0,6]	0.14	0.14	0.14	0.14	0.14	0.14	0.16	-
[0,7]	0.12	0.12	0.12	0.12	0.12	0.12	0.12	0.14

The reliability of networks (Fig. 3) are calculated under different capacity levels like 2, 3, 5, 7, 9, and 11 and are presented in Table 3. Table 3 also contains the number of d-MC generated for each capacity level.

Table 3: *Evaluation of reliability*

Network	#MC	d-MC	#d-MC	Reliability
1	16	2-MC	8202	0.9999
		3-MC	6491	0.7913
		5-MC	2652	0.4533
		7-MC	401	0.1488
		9-MC	192	0.0324
		11-MC	30	0.0036
2	58	2-MC	35355	0.9933
		3-MC	21522	0.6046
		5-MC	15433	0.4335
		7-MC	10231	0.2874
		9-MC	5600	0.1573
		11-MC	616	0.0173
3	110	2-MC	97223	0.9999
		3-MC	83435	0.8097
		5-MC	75340	0.7345
		7-MC	64457	0.6509
		9-MC	29531	0.5099
		11-MC	260	0.0002
4	330	2-MC	132910	0.9999
		3-MC	121023	0.6902
		5-MC	110334	0.3429
		7-MC	105049	0.1908
		9-MC	12834	0.0988
		11-MC	6904	0.0189

The following observations can be drawn from Table 3:

1. All the networks are robust in terms of reliability to accommodate the capacity level of 2 and 3.

2. A demand 5 can be reached to the destination through Network 3 with a high reliability value of 0.73 while this possibility falls to less than 50% for networks 1 and 2 respectively. Network 4 is the least competent network to cope with this demand.
3. Network 3 has a reliability value of 0.5 to meet the demand 9 which is satisfactory. However, other networks fall far away from meeting this demand.
4. None of the networks show satisfactory values of reliability for demand 11. Hence, the demand 11 cannot be achieved by any of these networks.

5. Discussion

The network depicted in Fig 4 is a practical distribution network [16] (or [23]). The details of the network can be found in [16] (or [23]). The capacity states and the probability states of each edge are as per [16] (or [23]) and are presented in Table 4. Both methods have evaluated the reliability of this network using the minimal cutset methods.

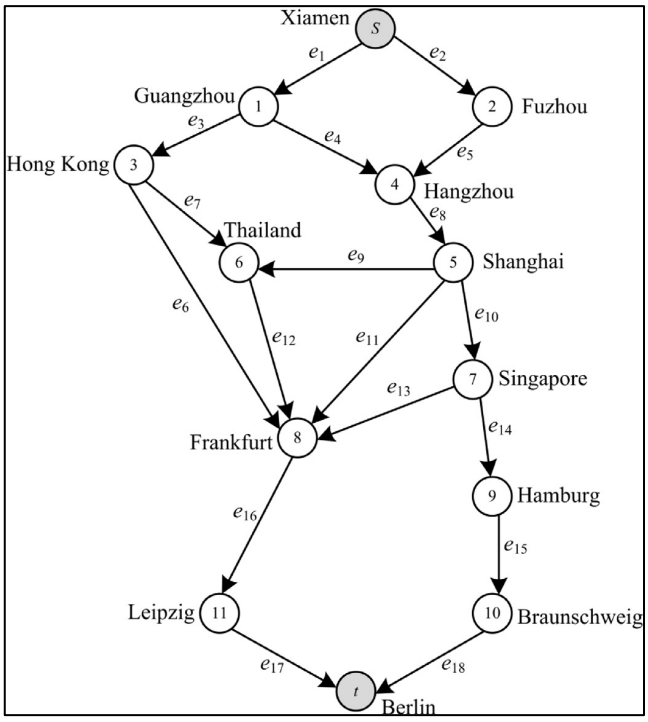

Figure 4: The networks of [16]

The method presented in [16] claimed of generating the exact number of d-MC by discarding duplicate d-MC while the work carried out in [23] also found the correct d-MC after removing the duplicate d-MCs. However, the number of 5-MCs (with d=5) generated for the practical network by methods [16] and [23] is different, and hence their estimated reliability values are likewise different. Both the methods use the state enumeration technique to evaluate the reliability of searching over the entire search space. In contrast to their methods, the proposed method uses a genetic algorithm to maximize the reliability by performing a heuristic search over the state space. The proposed method also results in distinct d-MCs by validating all the generated MCs. The number of d-MCs and the computed reliability values are presented in Table 5 for d=5. It can be observed from this table that the computed reliability value by the proposed method is 5% more than methods [16] and [23].

Table 4: *Capacity of edges and their corresponding probability (Fig. 4)*

Edges	Capacity of edges					State probability of different flow state				
e_1	0	1	2	3	4	0.002	0.003	0.008	0.05	0.937
e_2	0	1	2	3	-	0.002	0.002	0.05	0.946	-
e_3	0	1	2	3	-	0.015	0.022	0.023	0.94	-
e_4	0	1	2	3	-	0.001	0.022	0.03	0.947	-
e_5	0	1	2	3	-	0.002	0.22	0.04	0.936	-
e_6	0	1	2	3	-	0.001	0.026	0.05	0.923	-
e_7	0	1	2	3	-	0.002	0.003	0.05	0.945	
e_8	0	1	2	3	4	0.002	0.0050	0.008	0.017	0.968
e_9	0	1	2	3	-	0.012	0.023	0.03	0.935	-
e_{10}	0	1	2	3	-	0.011	0.024	0.03	0.935	-
e_{11}	0	1	2	3	-	0.005	0.008	0.016	0.971	-
e_{12}	0	1	2	3	4	0.001	0.001	0.005	0.005	0.943
e_{13}	0	1	2	3	4	0.001	0.001	0.005	0.005	0.988
e_{14}	0	1	2	3	-	0.012	0.012	0.04	0.936	-
e_{15}	0	1	2	3	-	0.003	0.011	0.011	0.975	-
e_{16}	0	1	2	3	4	0.003	0.007	0.01	0.02	0.96
e_{17}	0	1	2	3	4	0.001	0.006	0.01	0.014	0.969
e_{18}	0	1	2	3	-	0.002	0.004	0.01	0.984	-

Table 5: *Comparison of computed reliability*

Method	Number of d-MCs	Reliability
Method [22]	104	0.716992
Method [23]	135	0.802607
Proposed method	167	0.850135

In order to compare the computational time, the computational time to evaluate the reliability of the said network using SDP approach is considered for method[16] and [23](the time to generate the d-MCs is excluded). The computational time required by [16], [23] and the proposed method are shown in Fig. 5. Fig. 5 displays the proposed method, which saves approximately 82% of the computing time compared to methods [16] and [23].

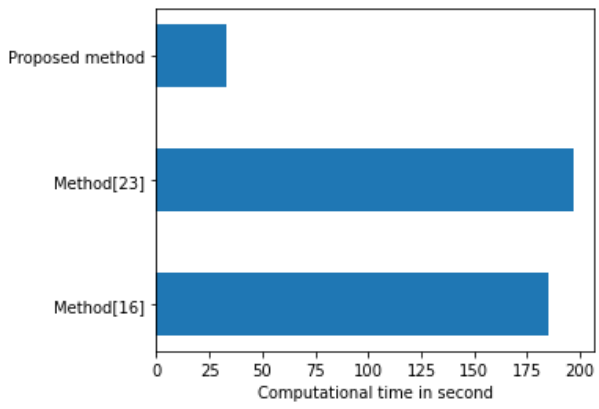

Figure 5: Comparison of computational time

6. Conclusion

In this paper, the reliability maximization problem is formulated under different flow states of a multistate flow network. A genetic algorithm-based method is proposed to maximize the reliability of the multistate flow network. The proposed method is well illustrated by taking a suitable example. The reliability of four different benchmark networks are evaluated under different demand levels. The reliability of a practical distribution network is evaluated and compared against some existing methods. The comparison ensures the robustness of the proposed method in terms of computed reliability values as well as the required computational time. Further, the work carried out in this paper may be extended to include cost and time constraints.

References

[1] Panda, D. K., & Dash, R. K. (2013, December). A New and Efficient Approach Based on Binary Decision Diagram to Evaluate the K-terminal Reliability of Distributed Networks. In 2013 International Conference on Machine Intelligence and Research Advancement (pp. 574-578). IEEE.

[2] Panda, D. K., & Dash, R. K. (2019). Network reliability evaluation and analysis of multistage interconnection networks. Int. J. Eng. Adv. Technol.(IJEAT), 8(3), 1729-1737.

[3] Dash, R. K., & Tripathy, C. R. (2010). Polynomial algorithms for evaluation of reliability of parallel computer interconnection systems.

[4] Barpanda, N. K., Jena, S., & Dash, R. K. (2014). Network Reliability Evaluation of Fault Tolerant Varietal Hypercube Network. International Journal of Advanced Research in Computer Science, 5(4), 132-135.

[5] Tripathy, P. K., Dash, R. K., & Tripathy, C. R. (2010, July). A self generating disjoint minimal cut-set method for evaluating the reliability of interconnection networks. In 2010 International Conference on Signal Processing and Communications (SPCOM) (pp. 1-5). IEEE.

[6] Panda, D. K., & Dash, R. K. (2017). Reliability evaluation and analysis of mobile ad hoc networks. International Journal of Electrical and Computer Engineering, 7(1), 479.

[7] Mishra, P., & Dash, R. K. (2020, December). A Novel Method for Evaluation of Reliability of WSN Under Different Failure Models. In 2020 IEEE International Symposium on Sustainable Energy, Signal Processing and Cyber Security (iSSSC) (pp. 1-6). IEEE.

[8] Ramirez-Marquez, J. E., & Coit, D. W. (2005). A Monte-Carlo simulation approach for approximating multi-state two-terminal reliability. Reliability Engineering & System Safety, 87(2), 253-264.

[9] Shrestha, A., Xing, L., & Coit, D. W. (2010). An efficient multistate multivalued decision diagram-based approach for multistate system sensitivity analysis. IEEE Transactions on Reliability, 59(3), 581-592.

[10] Jane, C. C., & Laih, Y. W. (2010). Computing multi-state two-terminal reliability through critical arc states that interrupt demand. IEEE Transactions on Reliability, 59(2), 338-345.

[11] Zhao, X., Wang, S., Wang, X., & Cai, K. (2018). A multi-state shock model with mutative failure patterns. Reliability Engineering & System Safety, 178, 1-11.

[12] Bai, G., Zuo, M. J., & Tian, Z. (2015). Search for all d-MPs for all d levels in multistate two-terminal networks. Reliability Engineering & System Safety, 142, 300-309.

[13] Bai, G., Tian, Z., & Zuo, M. J. (2016). An improved algorithm for finding all minimal paths in a network. Reliability Engineering & System Safety, 150, 1-10.

[14] Levitin, G. (2005). The universal generating function in reliability analysis and optimization (Vol. 6). London: Springer.

[15] Chen, S. G., & Lin, Y. K. (2016). Searching for d-MPs with fast enumeration. Journal of Computational Science, 17, 139-147.

[16] Niu, Y. F., Gao, Z. Y., & Lam, W. H. (2017). A new efficient algorithm for finding all d-minimal cuts in multi-state networks. Reliability Engineering & System Safety, 166, 151-163.
[17] Panda, D. K., Dash, R. K., & Mohapatra, S. K. (2017). Reliability Evaluation of Stochastic-Flow Network Through Two Minimal Intersecting Paths Under Budget and Time Constraints. International Journal of Pure and Applied Mathematics, 117(19), 457-467.
[18] Bai, G., Tian, Z., & Zuo, M. J. (2018). Reliability evaluation of multistate networks: An improved algorithm using state-space decomposition and experimental comparison. IISE Transactions, 50(5), 407-418. (25)
[19] Forghani-elahabad, M., & Kagan, N. (2019). Assessing reliability of multistate flow networks under cost constraint in terms of minimal cuts. International Journal of Reliability, Quality and Safety Engineering, 26(05), 1950025.
[20] Forghani-elahabad, M., & Kagan, N. (2019). Reliability evaluation of a stochastic-flow network in terms of minimal paths with budget constraint. IISE Transactions, 51(5), 547-558.
[21] Xu, X. Z., Niu, Y. F., & Li, Q. (2019). Efficient enumeration of-minimal paths in reliability evaluation of multistate networks. Complexity, 2019.
[22] Niu, Y. F., & Xu, X. Z. (2019). A new solution algorithm for the multistate minimal cut problem. IEEE Transactions on Reliability, 69(3), 1064-1076.
[23] Niu, Y. F., Wan, X. Y., Xu, X. Z., & Ding, D. (2020). Finding all multi-state minimal paths of a multi-state flow network via feasible circulations. Reliability Engineering & System Safety, 204, 107188.
[24] Rushdi, A. M., & Alsalami, O. M. (2020). Reliability evaluation of multi-state flow networks via map methods. Journal of Engineering Research and Reports, 13(3), 45-59.
[25] Niu, Y. F., He, C., & Fu, D. Q. (2022). Reliability assessment of a multi-state distribution network under cost and spoilage considerations. Annals of Operations Research, 309(1), 189-208.
[26] Rushdi, A. M. A., & Amashah, M. H. (2021, March). Symbolic reliability analysis of a multi-state network. In 2021 National Computing Colleges Conference (NCCC) (pp. 1-4). IEEE.
[27] Huang, D. H., Chang, P. C., & Lin, Y. K. (2022). A multi-state network to evaluate network reliability with maximal and minimal capacity vectors by using recursive sum of disjoint products. Expert Systems with Applications, 193, 116421.
[28] Tripathy, P. K., Dash, R. K., & Tripathy, C. R. (2012). A genetic algorithm based approach for topological optimization of interconnection networks. Procedia Technology, 6, 196-205.
[29] Tripathy, P. K., Dash, R. K., & Tripathy, C. R. (2013). A new genetic algorithm based method for topological optimization of interconnection networks. International Journal of Computer Applications, 63(3).
[30] Yeh, C. T., Lin, Y. K., & Yang, J. Y. (2018). Network reliability maximization for stochastic-flow network subject to correlated failures using genetic algorithm and tabu search. Engineering Optimization, 50(7), 1212-1231.
[31] Lin, Y. K., & Yeh, C. T. (2011). Maximal network reliability with optimal transmission line assignment for stochastic electric power networks via genetic algorithms. Applied Soft Computing, 11(2), 2714-2724.
[32] Tripathy, P. K., Swain, S., Dash, R. K., & Tripathy, C. R.(2017). A minimal cut-set based enumerative approach for two-terminal reliability estimation. Int. J. Control Theory Appl, 10(13), 11-18.

Inversion Method of Consistency Measure Estimation Expert Opinions

A. Bochkov[1*], N. Zhigirev[2], A. Kuzminova[3]

•

[1*]Deputy Head of Integrated R&D Unit,
JSC NIIAS, 107078 Moscow, Russia
e-mail: a.bochkov@gmail.com
[2]KALABI IT, 107045 Moscow, Russia,
e-mail: nnzhigirev@mail.ru
[3] Associate Professor, Department of Computer Systems and Technologies, Institute of Intelligent Cybernetic Systems National Research Nuclear University, MEPhI, 115409 Moscow, Russia
e-mail: avkuzminova@mephi.ru

Abstract

The problem of collective choice is the problem of combining several individual experts' opinions about the order of preference of objects (alternatives) being compared into a single "group" preference. The complexity of collective choice consists in the necessity of processing the ratings of the compared alternatives set by different experts in their own private scales. This article presents the author's original algorithm for processing expert preferences in the problem of collective choice, based on the notion of the total "error" of the experts and measuring their contribution to the collective measure of their consistency. The presentation of the material includes the necessary theoretical part consisting of basic definitions and rules, the statement of the problem and the method itself based on the majority rule, but in the group order of objects.

Keywords: collective choice, permutation, group, inconsistency, inversion, graph, rating, Schulze method, skating method, Pareto-optimal solutions.

1. Introduction

In practice, the efficiency of decision-making requires the development and application of specialized algorithmic and methodological support. If a group of experts participates in the decision support process, the so-called collective (group) choice problem arises. The existing algorithms for solving collective choice problems [1-3] can be divided into three classes.

A representative of the first class is the Schulze method [4] (based on the proof of the Arrow theorem) with the selection of Pareto-optimal solutions (Schwartz exception) from the first ranking to the last, with the selection recalculating the criteria for the next step. The disadvantage of the method is a rather complicated algorithm of constant recalculation, which significantly complicates the practical use of the method.

A typical representative of the second class is the skating-system well-proven in ballroom dance competitions [5]. It is simple in computational calculations and is based on the so called

understandable majority principle. Unfortunately, in many ways, this simplicity can lead to unstable decisions, and therefore, the impossibility to distribute the final places among the competitors in one round, or recognize a draw between competitors [6, 7].

The third class consists of regression models, type nonlinear factor analysis and other methods of information compression [8, 9], in which the desired solution is constructed in the form of the problem of minimization of accumulated errors. The difference between the methods of the third class is that they are not focused on the choice of the leader in the ratings, but are determined by the optimum, which is influenced by the entire volume of data.

The mentioned methods of solving the problems of collective choice in general are inherent to the problem of coordinating the experts' evaluations when comparing the evaluated objects.

In 1951 C. Arrow formulated [10] the theorem "On the impossibility of collective choice within the framework of the ordinality method", mathematically generalizing the Condorcet paradox [11]. The theorem states that within the framework of this approach there is no method for combining individual preferences for three or more alternatives, which would satisfy some quite fair conditions (the axioms of choice) and would always give a logically consistent result.

When ambiguous expert opinions are superimposed on the uncertainty of the objects themselves, some hierarchy is assumed in solving the choice problem. This is the case, for example, in the method of hierarchy analysis [12], when each of M of experts has his/her own, different from the others, opinion concerning the weights of the objects under consideration N objects through the coefficients of the preference matrix ($S_{ij}^m = \frac{w_j^m}{w_i^m}$ $(i = 1, \dots, N;\ j = 1, \dots, N\ ; i \neq j; m = 1, \dots, M)$).

Usually, weights are averaged and work with a generalized matrix S_{ij} this usually leads, as a rule, to a violation of the basic axioms of the "right" choice (universality, completeness, monotone, lack of a dictator, independence) proposed by W. Pareto [13, 14], R. Koch [15], C. Plott [16] and others. The rejection of one or another averaging procedure complicates the choice problem and leads, for example, to the need to solve the problem of "merging multidimensional scales" [17].

Earlier [18], the authors argued that to obtain consistent decisions, experts need to reach consensus, at least within the accuracy of determining private ratings in the full order of objects, and then seek agreement in the weighting coefficients between the neighboring nearest objects, setting a single scale. In this article we consider a method belonging to the third class of algorithms in decision theory, aimed at finding the optimum of the consistency measure, the restoration of the full collective order in preferences based on private ratings of experts.

2. Basic definitions and rules

Let us introduce several basic definitions.

Definition 1. Arbitrary mutually one-valued mapping $g: X \leftrightarrow g(X)$ of multiple first N natural numbers $X = \langle 1, 2, 3, \dots, N \rangle$ is called a permutation $N$of row (permutation):

$$\begin{array}{lccccccc} X= & \{ & x_1 = 1 & & x_2 = 2 & \dots & x_N = N & \} \\ g: & \updownarrow & & \updownarrow & & \updownarrow & \updownarrow & \\ g(X)= & \{ & g_1 = g(x_1) & & g_2 = g(x_2) & \dots & g_N = g(x_N) & \} \end{array}$$

The set $G = \{g\}$ forms a group of dimensionalities $N!$.

Definition 2. An inverse permutation to g is defined as $(g^{-1}(j) = k) \Leftrightarrow (g(k) = j)\ \forall j, k$.

An example of all permutations for $N = 4$ is given in Table 1. In principle, for any N each permutation can be assigned an index in the lexicographic order (LG-order) of values $g(X)$ (columns 1, 2 in Table 1).

Definition 3. The first permutation by index which is equal to the unit permutation in the group $^1g = \langle 1234 \rangle = E$ we will call "true" or natural order. The last permutation with ordinates in reverse

order: ${}^{24}g = \langle 4321 \rangle = \bar{E}$- the complete inversion, which is at the last determinable level $N(N-1)/2$.

Definition 4. For a permutation of $g = \langle g_1\ g_2\ g_{3\ldots}g_N \rangle$ a pair of indices $(g_i,\ g_j)$ is called an inversion [19] if $(i < j)\&\big(g_j > g_i\big)$.

Definition 5: A table of permutation inversions g is a sequence of numbers $\{b_1\ b_2\ \ldots\ b_N\}$ where b_j - is the number of elements greater than j and to the left of j. In other words, b_j - is the number of inversions with the second term equal to j.

Table 1. *Full table of permutations for* $N = 4$

Index g	Numeric code g in the LG order	Root synonym g	Synonym g, based on in versions, [other synonyms of minimum word length]	Error level, word length	Reverse re-installation	Inversion Tables, their sum, Σ				
1	*2*	*3*	*4*	*5*	*6*	*7*	*8*	*9*	*10*	*11*
1	< 1234>	E	E, [-]	**0**	< 1234>	0	0	0	0	**0**
2	< 1243>	c	c, [-]	**1**	< 1243>	0	0	1	0	**1**
3	< 1324>	b	b, [-]	**1**	< 1324>	0	1	0	0	**1**
4	< 1342>	cb	cb, [-]	**2**	< 1423>	0	2	0	0	**2**
5	< 1423>	bc	bc, [-].	**2**	< 1342>	0	1	1	0	**2**
6	< 1432>	bcb	cbc, [-]	**3**	< 1432>	0	2	1	0	**3**
7	< 2134>	a	a, [-]	**1**	< 2134>	1	0	0	0	**1**
8	< 2143>	ac	ac, [ca]	**2**	< 2143>	1	0	1	0	**2**
9	< 2314>	ba	ba, [-].	**2**	< 3124>	2	0	0	0	**2**
10	< 2341>	cba	cba, [-]	**3**	< 4123>	3	0	0	0	**3**
11	< 2413>	bac	bac, [bca].	**3**	< 3142>	2	0	1	0	**3**
12	< 2431>	bcba	cbac, [cbca]	**4**	< 4132>	3	0	1	0	**4**
13	< 3124>	ab	ab, [-]	**2**	< 2314>	1	1	0	0	**2**
14	< 3142>	acb	acb, [cab].	**3**	< 2413>	1	2	0	0	**3**
15	< 3214>	aba	bab, [-]	**3**	< 3214>	2	1	0	0	**3**
16	< 3241>	acba	cbab, [caba].	**4**	< 2413>	3	1	0	0	**4**
17	< 3412>	bacb	bacb, [bcab]	**4**	< 3412>	2	2	0	0	**4**
18	< 3421>	bacba	cbacb, [cbcab, bcbab, bcaba]	**5**	< 4312>	3	2	0	0	**5**
19	< 4123>	abc	abc, [-]	**3**	< 2341>	1	1	1	0	**3**
20	< 4132>	abcb	acbc, [cabc].	**4**	< 2431>	1	2	1	0	**4**
21	< 4213>	abac	babc, [abca].	**4**	< 3241>	2	1	1	0	**4**
22	< 4231>	abcba	cbabc, [acbca, cabca, cabac]	**5**	< 4231>	3	1	1	0	**5**
23	< 4312>	abacb	bacbc, [babcb, bcabc, abcab]	**5**	< 3421>	2	2	1	0	**5**
24	< 4321>	abacba	cbacbc, [cbcabc, bcbabc, bcabac, bcabca, bacbac, bac bca, babcba, abcaba, abcbab, acbcab, acbacb, cabcab, cabacb]	**6**	< 4321>	3	2	1	0	**6**

Definition 6. For any g there exists a set of $AT(g)$ (English, Adjacent Trans position) - "adjacent, neighboring" permutations, the number of which is exactly $(N-1)$. All the edges $E \times AT(E)$ consist of the forming elements of the group G. The elements of the multiplicity of formants $E \times AT(E)$ can be regarded as symbols s of some alphabet A (Table 2).

Table 2. *Nodes of the 1st error level consist of one symbol of the alphabet A*

In order, adjacent to the "truth" E	Error level	Alphabet A	The node of the 1st error level is a word of one symbol A
	0		$E = E \times E$
1	1	a	$a = E \times a = \langle 2, 1, 3, 4, \ldots, N-1, N \rangle$
2	1	b	$b = E \times b = \langle 1, 3, 2, 4, \ldots, N-1, N \rangle$
3	1	c	$c = E \times c = \langle 1, 2, 4, 3, \ldots, N-1, N \rangle$
…	1	…	…
$N-1$	1	z	$z = E \times z = \langle 1, 2, 4, 3, \ldots, N, N-1 \rangle$

z - conditional symbol $(N-1)$ of the formant. For $N = 4$, $E \times AT(E) = \{a, b, c\}$, consequently: $z = c$.

Definition 7. A weighted graph of a group $V(G, G \times G)$ consists of nodes G and the weight of an edge $(g_1 \times g_2)$ is equal to s, when $\left(g_2 \in AT(g_1)\right)\&(g_2 = g_1 s)$.

The structure of the graph $V(G, G \times G)$ is determined dynamically by the error levels. At the upper (zero) level there is only a single permutation E. At the second and further levels there are only nodes formed by joining only one symbol of the alphabet A.

The parity property of permutations is noteworthy: $aa = bb = cc = \cdots = zz = E$, because of which the graph of the group can be treated as an undirected graph.

Definition 8. Each g can be interpreted as a path, or some sequence of directed segments of the graph $V$and vice versa.

The way from $v \in G$ в $v' \in G$ passes through the edges connecting neighboring permutations and is equal to $v' = vs_1 \cdot \ldots \cdot s_T$ where $s_1 \ldots s_T$ - symbols of the alphabet A, T - is the length of the word.

Definition 9. The set of all finite words S over a finite alphabet A is countable. Hence, each nonzero word can be assigned an index q.

$$S = \bigcup_{q=1}^{\infty} S^q,\ S^q = \prod_{t=1}^{T^q} s_t^q,$$

where T^q - is the number of symbols in the word S^q.

For each word $S^q = \left\{S_1^q \cdot \ldots \cdot S_{T^q}^q\right\}$ there is one inverse word S^{q^*}: $S^{q^*} = \left\{s_1^{q^*} = s_{T^q}^{q^*}; \ldots; s_{T^q}^{q^*} = s_1^q\right\}$.

Definition 10. The words S^q и S^k - are synonymous if $s_1^q \cdot \ldots \cdot s_{T^q}^q \cdot s_1^{k^*} \cdot \ldots \cdot s_{T^{k^*}}^{k^*} = E$.

Definition 11. Among identical synonyms we can distinguish a finite set of minimal words in length T_{min} from the node $g = v'$ in "truth" E $(v^{-1} = E)$: $g = v^{-1}v' = s_1 \ldots s_T$ - (**synonym**(g)).

Definition 12. Among the words from (**synonym**(g)) there is a "root synonym" with a minimal form of LG-order based on the order of elements in A.

A root synonym is a word derived from a numerical code by the "bubble" sort algorithm [20] when moving toward the "truth" E. A different way of obtaining root synonyms is presented in Table 3. It proceeds from the method of sequentially destroying inversions followed by transforming a sequence of synonyms from the current synonym to the root synonym using group-forming equations (see Definition 13).

Each permutation g has exactly one root synonym of length $T(g)$, coinciding with dynamically determined error rate and total number of inversions in the table of inversions - Σ (Table 3). In our case for <4321> it is a word of 6 symbols "**abacba**".

Table 3: *Algorithms of building synonyms by different methods*

Method of sequential inversion reduction ("first" optimal in word length synonym)									Bubble sort algorithm (optimal word-length "root" synonym)								
Error level	Code	1	2	3	4		Σ		Error level	Code	1	2	3	4		Σ	
6	4321	**3**	2	1	0	**c**	***6***		6	4321	3	2	**1**	0	**a**	***6***	
5	4312	**2**	2	1	0	**b**	***5***		5	3421	3	**2**	0	0	**b**	***5***	
4	4132	**1**	2	1	0	**a**	***4***		4	3241	**3**	1	0	0	**a**	***4***	
3	1432	0	**2**	1	0	**c**	***3***		3	2341	**3**	0	0	0	**c**	***3***	
2	1423	0	**1**	1	0	**b**	***2***		2	2314	**2**	0	0	0	**b**	***2***	
1	1243	0	0	**1**	0	**c**	***1***		1	2134	**1**	0	0	0	**a**	***1***	
0	1234	0	0	0	0		***0***	**cbacbc**	0	1234	0	0	0	0		***0***	**abacba**

When the numerical code coincides, a network structure of the graph V is formed when the neighboring nodes are at a distance of one on the inversion level.

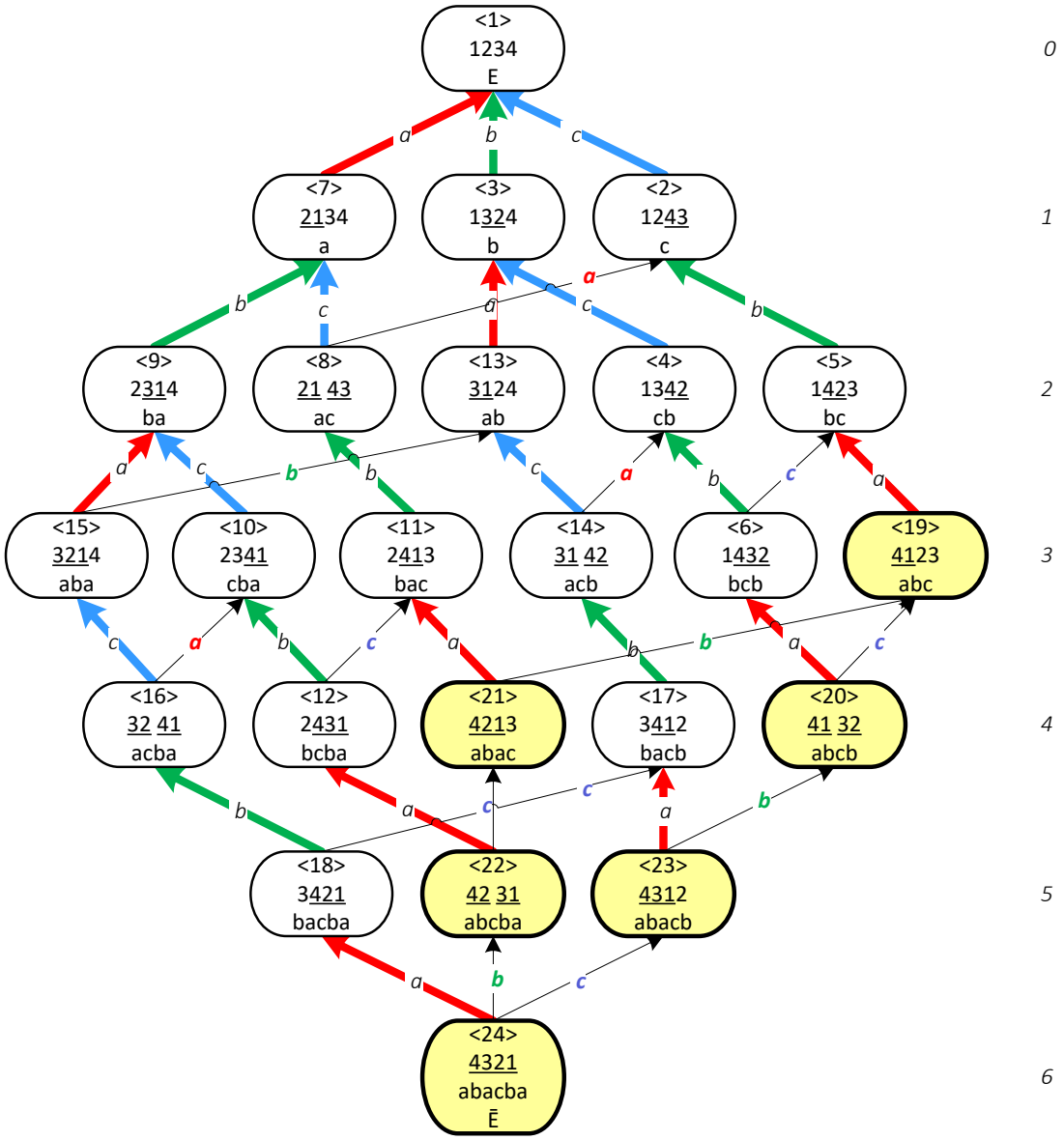

Figure 1: *Structure of the graph for* $N = 4$

Fig. 1 shows the structure of such a graph V for $N = 4$. The thick and thin edges represent the symbols s, in layers participating in generation of new neighboring nodes. The content of filling nodes is a representation of the permutation index g (column 1 in Table 1), its numerical code (column 2) and the content of the root word symbol for permutation g (column 3). The thick lines of the graph V in Fig. 1 correspond to its representation as a dictionary of root synonyms of permutation in the form of a spanning tree graph V. Their direction coincides with whether there is an inversion (up) or not (down) at the specified place. The six end nodes of the tree are represented by elements with yellow filling, such as {<19>; < 4123>; abc}. The underlined inversion, for <19> only (a) brings the next node closer to the "truth" E, reducing the number of errors by exactly one.

The dictionary of root synonyms is built according to the following principle: only those relations between permutations that are older in LG-order remain in cycles. For example, the cycle $< 1 >< 7 >< 8 >< 2 >< 1 >$ (a) we break by the connection $< 2 >< 8 >$ since the connection $< 1 > < 7 >$ (Fig. 2a) is smaller than connection $< 1 >< 2 >$ (c).

A similar operation must be repeated for the lower sections of cycles <6>, <14>, <15>, <12>, <16>,

<20>, <21>, <18>, <22>, <23> and twice on <24> to break 12 more cycles and form the tree. For $N = 4$ analyzing the equalities describing the right and left branches of the cycles, we come to the necessity and sufficiency of six equalities: $= E$, $bb = E$, $cc = E$, $ac = ca$ $(Fig. 2a)$, $aba = bab$, $bcb = cbc$, (Fig. 2b), which are necessary to construct synonyms of words in permutations (Table 1, columns 3, 4).

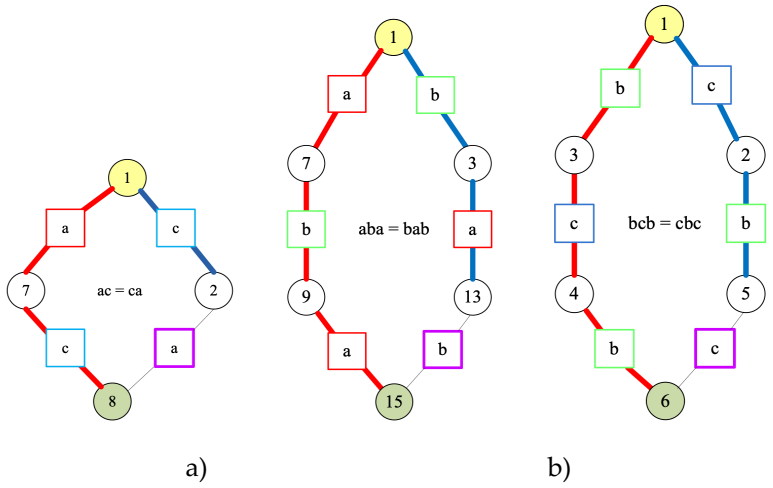

Figure 2: *Illustration of breaking network cycles*

For $N \geq 5$ such enumeration of relations is difficult, so it is reasonable to introduce the notion of canonical formative equations (CFE).

Definition 13. The canonical formative equations are a necessary and sufficient list of equations that fully specify the rules for constructing root and other synonyms through the alphabet A.

Thus, in Table 3 it is possible to perform conversions with the help of CFE: "cbacbc" = "cbabcb" = "cabacb" = "acbcab" = "abcbab" = "abcaba" = "abacba".

Table 4 shows regularities that take into account the parity laws of permutations and lozenge closures at the 2 error level.

The sign "*" in Table 4 marks the necessary inverse permutations of the 2nd level of inversions. For example, if the left-hand side of the equations "ac" sets the equivalent right-hand side of "ca" then you must replace "ca" with "ac", etc. By adding third-level inversion relations versions: $aba = bab; bcb = cbc;\ cdc = dcd;\ ded = ede;\ \ldots;\ xyx = yxy;\ yzy = zyz$, we define a complete set of CFE.

Table 4: *Automatic construction of CFE at 1-2 error levels*

		The second argument								
		a	b	c	d	e	…	x	y	z
The first argument	a	*E*		**ac***	ad*	ae*	…	ax*	ay*	az*
	b		*E*		bd*	be*	…	bx*	by*	bz*
	c	**ca**		*E*		ce*	…	cx*	cy*	cz*
	d	da	db		*E*		…	dx*	dy*	dz*
	e	ea	eb	ec		*E*	…	ex*	ey*	ez*
	…	…	…	…	…	…	…	…	…	…
	x	xa	xb	xc	xd	xe	…	*E*		xz*
	y	ya	yb	yc	yd	ye	…		*E*	
	z	za	zb	zc	zd	ze	…	zx		*E*

3. Problem statement

Let us consider N comparison objects $O_1, \dots, O_k, \dots, O_N$ which indices are the first N members of the natural series $E_{POI} = \langle 1, \dots, k, \dots, N \rangle$ - correspond to the order of presentation of the objects for the expertise. In the examination of objects participate M experts $E_1, \dots, E_m, \dots, E_M$. Each of the experts E_m has his own idea of the order of objects $g_m = \langle g_{m,1}, \dots, g_{m,n}, \dots, g_{m,N} \rangle$ which indexes increase with decreasing of some quality of objects from the expert's point of view. The value $g_{m,1}$ corresponds to the index of object O_{k_1}, taking part in examination with maximal quality according to expert's opinion E_m, a $g_{m,N}$ - the worst-quality object with the index O_{k_N}:

$$\mathrm{G} = \left(g_{m,n}\right)_{\substack{m=\overline{1,M} \\ n=\overline{1,N}}} = \begin{pmatrix} g_{1,1} & \cdots & g_{1,N} \\ \cdots & \ddots & \cdots \\ g_{M,1} & \cdots & g_{M,N} \end{pmatrix}.$$

Thereby g_m - it is a permutation of object ratings (POR), the argument of which is the order of $E_{POR} = \langle 1, \dots, n, \dots, N \rangle$.

Places $p_m = \langle p_{m,1}, \dots, p_{m,k}, \dots, p_{m,N} \rangle$ by values inverse to POR g_m $(p_m = g_m^{-1})$ are permutations of object indices (POI) with argument E_{POI}:

$$\mathrm{P} = \left(p_{m,n}\right)_{\substack{m=\overline{1,M} \\ n=\overline{1,N}}} = \begin{pmatrix} p_{1,1} = g_{1,1}^{-1} & \cdots & p_{1,N} = g_{1,N}^{-1} \\ \cdots & \ddots & \cdots \\ p_{M,1} = g_{M,N}^{-1} & \cdots & p_{M,N} = g_{M,N}^{-1} \end{pmatrix}.$$

It is necessary to find the compression of all private POR rankings g_m $(m = 1, \dots, M)$ in the form of a POR $g_m^* = \langle g_1^*, \dots, g_N^* \rangle$ which would reduce the total inconsistency of expert evaluations $g_{m,n} \to g_m^*$ (based on the equality of all participants in the examination), measured in the inversions of the transitions from $g_{m,n}$ к g_m^*, that is

$$K^* = \min K(g) = \min_{g_m} \left(\sum_{m=1}^{M} K_m\left(\langle g_1, \dots, g_N \rangle\right) \right),$$

where $K_m\left(\langle g_1, \dots, g_N \rangle\right)$ - is the sum of inversions in the evaluations of the m expert, K^*- is the limiting measure of inconsistency of experts' opinions chapter.

Finding an optimum in permutations of object rankings is equivalent to finding an object index over p^*: $p^* = \langle p_1^*, \dots, p_N^* \rangle$, since $K(g_m^*) = K(p_m^*)$where $p^* = (g^*)^{-1}$ (the lengths of the reciprocal paths $(E \to g)$ are the same as the forward paths $(p = g^{-1} \to E)$ at any g) (Table 5).

Table 5: *Solution search table $P(g)$ with table of inversions $B(g, P)$*

POR	Arg E	1	…	n	…	N	POI	Arg E	1	…	k	…	N	Criterion inconsistencies
POR	Func g	g_1	…	g_n	…	g_N	POI	Func p	g_1^{-1}	…	g_k^{-1}	…	g_N^{-1}	
POI	Arg E	1	…	k	…	N	POI	Arg E	1	…	k	…	N	
1	$p_1(g)$	p_{1,g_1}	…	p_{1,g_k}	…	p_{1,g_N}		$B_1(p_1(g))$	$B_{1,1}$	…	$B_{1,k}$	…	$B_{1,N}$	$K_1(g) = \sum_{k=1}^{N} B_{1,k}$
…	…	…	…	…	…	…			…	…	…	…	…	…
m	$p_m(g)$	p_{m,g_1}	…	p_{m,g_k}	…	p_{m,g_N}		$B_m(p_m(g))$	$B_{1,1}$	…	$B_{m,k}$	…	$B_{m,N}$	$K_m(g) = \sum_{k=1}^{N} B_{m,k}$
…	…	…	…	…	…	…			…	…	…	…	…	…
M	$p_M(g)$	p_{M,g_1}	…	p_{M,g_k}	…	p_{M,g_N}		$B_M(p_M(g))$	$B_{M,1}$	…	$B_{M,k}$	…	$B_{M,N}$	$K_M(g) = \sum_{k=1}^{N} B_{M,k}$
														$K(g) = \sum_{m=1}^{M} K_m(g)$

4. Method description

This problem belongs to the class of integer programming problems (on the structure as a graph - $V(G, G \times G)$ POR graph, arranged by error levels). Methods for solving such problems are well developed [21, 22], but none of them guarantees that, starting with some permutation, we will

certainly get into a global minimum, which may not be the only one. At the very least, what can be guaranteed is a complete search of all POR. This option is possible for $N \leq 10$. For each g counts $K(P_m, g)$ and the sum of $K(g)$, and the current state of the set of global minima is "memorized".

A subset of $g \in G$ for which $K(g) = K^*$, we call the set of global minima - G^K. Since M is odd, it, like the set of local minima, consists of isolated solutions (permutations).

Let us consider a pair of $(l,\ l+1)$ columns in $P(g)$. $l = 1, \dots, N-1$ corresponds to the symbol s_l of the alphabet A (Table 6).

Table 6: *Neighboring Pair Table* $P(g)$

Expert	POR g	g_l	g_{l+1}
		l	$l+1$
1	$P_1(g)$	$P_{1,g_l}(E)$	$P_{1,g_{l+1}}(E)$
…		…	…
m	$P_m(g)$	$P_{m,g_l}(E)$	$P_{m,g_{l+1}}(E)$
…		…	…
M	$P_M(g)$	$P_{M,g_l}(E)$	$P_{M,g_{l+1}}(E)$

Rule 1. If $P_m\ g_l(E) < P_m\ g_{l+1}(E)$, then the sum of inversions $K(g_m)$ is increased by 1, and if $P_m\ g_l(E) > P_m\ g_{l+1}(E)$, the sum of inversions decreases by 1.

Rule 2. The decrease and increase of the sum depend on the number of rows in which the second condition M^2 (Rule1) dominates the first condition M^1. The ratio is $M^1 + M^2 = M$. Then the sum $K(g)$ from the influence of s_l will decrease by exactly $M^2 - M^1$ units $(if\ M^2 > M/2)$ or increase by $M^1 - M^2$ units $(if\ M^2 < M/2)$.

Rule 3. "Cutoff condition." The POR g belongs to the set of local minima G^P if for all $j = 1, \dots, N-1$ the sum of errors only increases with rotation of neighboring columns by the symbol s_j. That is $g \in G^P$ has neighboring nodes of the graph V, exceeding by sum the found local optimum g by at least one.

The search G^P makes sense with large N, but with small N it is also effective, since the decrease (increase) of some selected pair does not depend on the place where the pair is located, but only on the contents of the resulting inversions.

Depending on the number of compared objects (N) two variants of the range are possible.

Variant 1. "Direct calculation". At small N $(N \leq 6)$ it is possible to create a "directory" in LG-order. Then to build G^P and G^K it is necessary to exclude from it the POR where the "cut-off condition" is not satisfied. Calculate for all $g \in G^P$ value $K(g)$ and choose the optimal one.

Let us explain the above on the example for $N = 4$ (Table 7).

Table 7: *Initial data* $P(E)$ *and optimality criterion calculation* $K(E)$

	POI E	1	2	3	4	Inversion Tables				$K_m(E)$
		O_1	O_2	O_3	O_4	1→1	2→2	3→3	4→4	
E_1	P_1	1	4	2	3	0	1	1	0	2
E_2	P_2	2	3	1	4	2	0	0	0	2
E_3	P_3	3	2	1	4	2	1	0	0	3
E_4	P_4	4	2	3	1	3	1	1	0	4
E_5	P_5	1	4	3	2	0	2	1	0	3
E_6	P_6	2	4	1	3	2	0	1	0	3
E_7	P_7	2	1	4	3	1	0	1	0	2
									Optimality criterion $K(E)$:	20

Let us create a matrix of full pairwise comparisons of columns for the POI $P(E)$ for $(i = 1, N;\ j = 1, N;\ i \neq j)$ (Table 8).

Table 8: *Results of counting inversions on a pair of columns*

i \ j	1	2	3	4
1	x	3	**4**	1
2	**4**	x	**5**	**4**
3	3	2	x	3
4	**6**	3	**4**	x

A fragment of the calculation for $(i = 1;\ j = 2, 3, 4)$ is given in Table 9.

Table 9: *Checking the "cutoff condition" (sum of column inversions* $(i = 1)$

1	→	**2**		**1**	→	**3**		**1**	→	**4**
1		4		1		2		1		3
2		3		2	1	1		2		4
3	1	2		3	1	1		3		4
4	1	2		4	1	3		4	1	1
1		4		1		3		1		2
2		4		2	1	1		2		3
2	1	1		2		4		2		3
	3				**4**				1	

Table 8 shows that the "cutoff condition" is not satisfied by 6 pairs of columns: 1→3, 2→1, 2→3, 2→4, 4→1, 4→3. As you can see, for the $N = 4$ directory g (Table 1) will contain 24 POIs. At the level of inversions (a) from 24 indexes values 12 elements with indexes (3-4, 7-12, 19-20, 23-24) will be discarded (due to "wrong pairs"), at the level (b) - 7 POI with indexes (1, 6, 15-17, 21-22), at the level (c) - 4 POI with indexes (2, 5, 13, 18). As a result, G^P and G^K consist of one POI with the index ${}^{14}g = g^* = \langle 3\ 1\ 4\ 2 \rangle$ for which we will further calculate the value of the optimal criterion (Table 10).

Table 10. *POR optimum* g^* *and calculation of the optimality criterion* $K(g^*)$

	POR g^*	**3**	**1**	**4**	**2**	Inversion Tables				$K_m(g^*)$
		O_3	O_1	O_4	O_2	1→1	2→2	3→3	4→4	
E_1	P_1	2	1	3	4	1	0	0	0	1
E_2	P_2	1	2	4	3	0	0	1	0	1
E_3	P_3	1	3	4	2	0	2	0	0	2
E_4	P_4	3	4	1	2	2	2	0	0	4
E_5	P_5	3	1	2	4	1	1	0	0	2
E_6	P_6	**1**	**2**	**3**	**4**	0	0	0	0	**0**
E_7	P_7	4	2	3	1	3	1	1	0	5
									Optimality criterion $K(g^*)$:	**15**

As can be seen from Table 10, expert E6 "guessed" the optimal solution $K_6(g^*) = 0$. Experts E1 and E2 made only one error each, E3 and E5 made two errors each, and E4 and E7 made too many errors. The next step is to use the POR g^* to reconstruct the optimal POI $p^* = (g^*)^{-1}$. Consequently, the required places $p^*(E) = \langle 2, 4, 1, 3 \rangle$.

Variant 2. "Iterations." In general, you can use a cutoff rule directly starting with some starting POI, e.g. from ${}^{0}\boldsymbol{g} = E_{POI}$. The complete absence of cutoff guarantees that the local minimum is found in the ${}^{3}\boldsymbol{g} = \boldsymbol{bac}$ (Table 11).

Table 11.

1	2	3	4	5	6	7	8	9	10
	g	${}^0\boldsymbol{g}$ =E	$K_m({}^0\boldsymbol{g})$	${}^1\boldsymbol{g}=\boldsymbol{b}$	$K_m({}^1\boldsymbol{g})$	${}^2\boldsymbol{g}=\boldsymbol{ba}$	$K_m({}^2\boldsymbol{g})$	${}^3\boldsymbol{g}=\boldsymbol{bac}$	$K_m({}^3\boldsymbol{g})$
		⟨1234⟩		⟨1324⟩		⟨3124⟩		**⟨3142⟩**	
E_1	P_1	1423	2	1243	1	2143	2	2134	1
E_2	P_2	2314	2	2134	1	1234	0	1243	1
E_3	P_3	3214	3	3124	2	1324	1	1342	2
E_4	P_4	4231	5	4321	6	3421	5	3412	4
E_5	P_5	1432	3	1342	2	3142	3	3124	2
E_6	P_6	2413	3	2143	2	1243	1	1234	0
E_7	P_7	2143	2	2413	3	4213	4	4231	5
		a=3; **b=5**; c=3	20	**a=4**; b=2; **c=4**	17	a=3; b=3; **c=4**	16	a=3; b=1; c=3	15

The presence at the end of iteration (a=4; b=2; c=4) of ambiguity of choice makes us return to the beginning of this stage and consider another alternative ${}^{2+}\boldsymbol{g}=\boldsymbol{bc}$ c $K({}^{2+}\boldsymbol{g})$=16 and conclude that the search is terminated because ${}^{3+}\boldsymbol{g}=\boldsymbol{bca}$ c $K({}^{3+}\boldsymbol{g})$=15 is a copy of ⟨3142⟩ by CFE.

5. Concluding remarks

It is beyond the scope of this article to compare the proposed method with other methods of information compression (e.g., factor analysis, the averaging method, or the Schulze method), which will be discussed later.

The further development of this method implies its application in ranking determinations that allow equality of evaluations of compared objects when determining the weights of compared objects (similar to pairwise comparisons in the method of hierarchy analysis [12] and solving problems of heterogeneous scales merging [17, 18]).

References

[1] Kemeny J., Snell J. Cybernetic modeling. Some Applications. Moscow: Soviet Radio, 1972. - 192 p.

[2] Larichev O.I. Theory and Methods of Decision-Making, and Chronicle of Events in the Enchanted Lands. 2nd edition, revised and enlarged. Moscow: Logos Publisher, 2002. - 382 p. - ISBN 5-94010-180-1.

[3] Kaplinsky A.I., Russman I.B., Umyvakin V.M. Modeling and algorithmization of weakly formalized problems of choosing the best choice of systems. Voronezh: Publishing house of the All-Russian State University of Civil Engineering, 1991. - 168 p.

[4] Markus Schulze, The Schulze Method of Voting. Computer Science and Game Theory. - Cornell University, 2018. URL: https://doi.org/10.48550/arXiv.1804.02973.

[5] Ralf Pickelmann,1999. Das Skating system. URL: http://www.tbw.de/rpcs/skating.

[6] Ferran Rovira,1997. ¿Porqu´e ganamos, porqu´e perdemos? TopDance, 15, 16. URL: http://inicia.es/de/ballrun/skating.htm.

[7] Xavier Mora, The Skating System. 2nd edition. July 2001. URL: https://mat.uab.cat/~xmora /escrutini/skating2en.pdf

[8] Lisitsin D.V. Methods of Regression Models Construction. Novosibirsk: NSTU, 2011. 77 p.

[9] Kim O. J., Mueller C.W., Klecka W.R., et al. Factor, discriminant, and cluster analysis. Ed. by I. S. Enyukov. - Moscow: Finances and Statistics, 1989. - 215 p.

[10] Kenneth J. Arrow, 1951, 2nd ed. Social Choice and Individual Values, Yale University Press.

ISBN 0-300-01364-7

[11] Condorcet J. Esquisse d'un tableau historique des progres de l'esprit humain. - Librocom, 2011. – 280 p. - (From the Heritage of World Philosophical Thought. Social Philosophy). ISBN 978-5-397-01568-4.

[12] Saaty T. Decision Making. Method of hierarchy analysis. M. Radio and Communications. 1993. – 278 p. URL: http://rosculturexpertiza. ru/files/valuation/saati. pdf.

[13] Nogin V. D. The Set and the Pareto Principle. - St. Petersburg: Publishing and Printing Association of Higher Education Institutions, 2022, 2nd ed. Revised and supplemented - 111 p.

[14] Pareto V. Textbook of Political Economy. RIOR, 2018. 592 p.

[15] Koch R. The 80/20 Principle. Eksmo, 2012. 443 p.

[16] Ross M. Miller, Charles R. Plott, and Vernon L. Smith. Intertemporal Competitive Equilibrium: An Empirical Study of Speculation. Economics. Quarterly Journal of Economics. - Volume 91. Issue 4, November 1977. pp. 599-624. URL: https://doi.org/10.2307/1885884

[17] Bochkov, A.V., Lesnykh, V.V., Zhigirev, N.N., Lavrukhin, Yu.N. Some methodical aspects of critical infrastructure protection // Safety Science, V. 79, Nov. 2015. Pp. 229-242. URL: https://doi.org/10.1016/ j.ssci.2015.06.008.

[18] Zhigirev, N.; Bochkov, A.; Kuzmina, N.; Ridley, A. Introducing a Novel Method for Smart Expansive Systems' Operation Risk Synthesis. Mathematics 2022, 10, 427. URL: https://doi. org/10.3390/math10030427.

[19] Knuth D. E. The Art of Programming. Volume 3. Sorting and Searching. The Art of - Computer Programming. Volume 3. Sorting and Searching / ed. by V. T. Tertyshny (Ch. 5) and I.V. Krasikov (Ch. 6). - Moscow: Williams, 2007. T. 3. 832 p. - ISBN 5-8459-0082-1.

[20] Levitin A. V. Chapter 3. Brute Force Method: Bubble Sorting // Algorithms. Introduction to development and analysis. Moscow: Williams, 2006. pp. 144-146. 576 p. ISBN 978-5-8459-0987-9

[21] Coffman A., Henri-Laborder A. Methods and Models of Operations Research. Integer - programming. Textbook. - Moscow: Mir, 1977. 432 p.

[22] Schraever A. The theory of linear and integer programming. Monograph in two volumes. Translated from English: World, 1991. (360 p.) 344 p.

ANALYSIS OF THE CONTROLLED SECURITY MODEL WITH UNCOUNTABLE NUMBER OF LINEAR LIMITATIONS ON MANAGEMENT STRATEGIES

O. B. Zaitseva
•
Assistant Professor, Moscow Aviation Institute
(National Research University),
Moscow, 125993 Russia
E-mail: o_zaiceva@mail.ru

Abstract

The work analyzes the security model described by the controlled semi-Markov process with catastrophes. Management optimization is associated with determining the frequency of restoration work of the subsystem (security subsystem) which acts up attempts of malicious persons to disrupt the normal operation of the main system. The optimization criterion is the mathematical expectation of the time before the catastrophe (the moment of the first successful attempt to disrupt the normal operation of the main system). In the context of new linear limitations on management strategies, the structure of the optimal strategy was examined.

Keywords: controlled semi-Markov process, safety, management, strategy, randomization, optimization problem.

1. Introduction. Description Of Structural Elements Of Security Model Under Examination

Before we set a mathematical problem, let us describe a real physical (practical) situation, the mathematical model of which will be the object of examination of the present work.

Let us suppose that some system S is operating, performing important, responsible and necessary work. Let us suppose that there is another system S_0 (opponent, malicious person) which tries to disrupt the high-quality performance of the work of the original system S. Finally, there is a security system S_1 which must act up attempts to disrupt the uninterrupted operation of the original system and ensure its safe operation.

Regarding the "functioning" of the system S_0 we assume that the moments of attempts (attacks) to disrupt the operation of the main system S form a discrete set on the time axis. Regarding the operation of the system S_1 we assume that it can break and restore (the exact description of this process will be given below). Therefore, periods of good operation interchange with periods when the security system cannot perform its protection functions. For this reason one of the main hypothesis is formulated as follows: *if the moment of the attempt to disrupt the operation of the system S falls during the period of good operation, then this attempt is acted up, if this moment falls during the period of broken operation and restoration, then an undesired event (catastrophe) occurs*. If it is possible to reduce the periods of broken operation and restoration of the security system, that is, to manage the operation process, then by linking the moment of catastrophe with this control process, it is possible to set a mathematical task of finding the optimal management strategy. This will be done below.

2. Mathematical Hypotheses

1. With regard to system S, there is no need to introduce any mathematical hypotheses, since management is related only to the security system S_0, and the moment of catastrophe depends on the state of the system S_1 and the characteristics of the system S_0.
2. Regarding the system S_0, we assume that the flow of attempts (attacks) in time is described by the stationary Poisson process with the parameter λ. In the Poisson process the intervals η between adjoined attacks are independent collectively and distributed according to exponential law with the parameter λ

$$P\{\eta < x\} = \begin{cases} 0, & x \le 0, \\ 1 - e^{-\lambda x}, & x > 0. \end{cases} \quad (1)$$

The Poisson process is the Markov process. For the arbitrary moment t, the waiting time until the next attempt (attack) is also distributed according to the exponential law (1) with the same parameter. This property will be used when deriving basic relations.

3. The system S_1 breaks and the uptime ξ is distributed according to the law

$$F(x) = P\{\xi < x\} = \begin{cases} 0, & x \le 0, \\ 1 - e^{-\mu x}, & x > 0, \end{cases} \quad \bar{F}(x) = 1 - F(x) = P\{\xi \ge x\} = e^{-\mu x}, \quad x > 0.$$

4. Let us suppose that the breakdown that appeared during the operation of the system is not detected (does not appear) by itself, and if we mark random time of the independent manifestation of the breakdown as ζ, then its distribution is equal to $(x) = P\{\zeta < x\} = 0, x < \infty$, that is, the random time of the independent manifestation of the breakdown with the probability of one is equal to infinity.

Further, we will describe the maintenance process (control process). At the beginning moment $t_0 = 0$, the operation of the security system begins and a planned preventive update (prevention) of the system is assigned through the time $\upsilon \ge 0$ distributed according to the law $G(u) = P\{\upsilon < u\}, \quad G(0) = 0.$

If the security system is not broken by the appointed moment $\upsilon \ge 0$, that is the event $\{\upsilon < \xi\}$ occurred, then at the moment of $\upsilon \ge 0$ a planned preventive update of the system will begin which according to the hypothesis updates the system completely. Let us mark the duration of this planned preventive (prevention) update γ_1, and the distribution function of this time length we mark $\bar{F}_1(x) = P\{\gamma_1 \ge x\}$.

If the system breaks by the assigned moment $\upsilon \ge 0$ (the event $\{\upsilon \ge \xi\}$ occurred), but its breakdown was not detected by itself (the event $\{\upsilon < \xi + \zeta\}$ occurred), then the planned emergency system update will begin at the assigned moment $\upsilon \ge 0$. The duration of this restoration work we will mark γ_2, and the distribution law we will mark $F_2(x) = P\{\gamma_2 < x\}, \bar{F}_2(x) = P\{\gamma_2 \ge x\}$.

In the future for mathematical expectations entered above the restoration times $\gamma_i, \quad i = 1,2$ we will use the symbols

$$T_i = \int_0^\infty \bar{F}_i(x)dx, \quad i = 1,2. \quad (2)$$

After the possible restoration works, when the security system is fully updated according to the hypothesis, the moment of the next preventive restoration work is rescheduled regardless of the past run of the process and the entire maintenance process is repeated again.

It is easy to see that the evolution of the security system S_1 is described with the semi-Markov process $\xi(t)$, in which Markov moments are the moments of the beginning and end of restoration work. When determining a set of states let us note that at the start of restoration work it is known which restoration work begins. The duration of restoration work depends only on its type. Therefore, at this moment, the past run of the process and the future behavior of the process are independent if it is known which restoration work begins.

At the end of restoration work, the system by definition is a new one and the moment of eventual preventive prevention is rescheduled regardless of the past. Therefore, even at this moment of the end of restoration, the past run of the process and the future behavior of the process are independent.

Let us consider $\xi(t) = 1$, if at the nearest Markov moment, preceding moment t, the planned preventive prevention of the system begins. Let us consider $\xi(t) = 2$, if at the nearest Markov moment, preceding t, the planned emergency restoration of the system begins. Finally, we assume $\xi(t) = 0$ if the closest Markov moment, preceding t, is the moment the security system is updated. It should be noted here that part of the time in this state the security system spends in a broken state (hidden breakdown), and the breakdown does not appear itself, and that is why the model provides for periodic determination of the state of the security system.

5. In accordance with the basic hypothesis of the occurrence of catastrophes, formulated above, it is now possible to describe the effect of this process on the evolution of the security system S_1.

Let us enter into consideration the absorption state, in which the process $\xi(t)$ passes at the moment of the first unreflected attack. Such an event will occur when the attack appears on the restoration period (states 1 or 2) or on the latent breakdown period (state 0). At this moment t we consider that $\xi(t) = 3$.

Therefore, the process $\xi(t)$ characterizing the evolution of the security system and taking values from the finite set $E = \{0,1,2,3\}$ is described. Figure 1 shows the transition graph of the process $\xi(t)$.

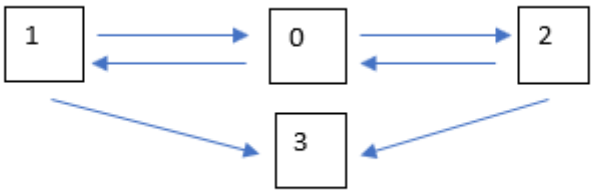

Figure 1: *Transition graph of the process* $\xi(t)$

3. Determination Of Process Characteristics. Setting The Mathematical Task

The random process $\xi(t)$ described above is a homogeneous controlled semi-Markov process with a finite set of states $E = \{0,1,2,3\}$, management is realized only in state 0 and is contained in choosing the period through which the restoration work should begin. Therefore, trajectories are step functions and equality $U = 0, +\infty)$ is true for the management (decision) space U in state 0. The management strategy is determined by the distribution of $G(u) = P\{v < u\}$, $G(0) = 0$, that is, it belongs to a set of Markov homogeneous randomize strategies.

More details on the construction, characteristics and properties of homogeneous controlled semi-Markov processes with a finite set of states can be found in [1].

A homogeneous controlled semi-Markov process $X(t) = \big(\xi(t), u(t)\big)$ is defined as a two-dimensional step process, the first component of which $\xi(t)$ describes the evolution of the controlled component, and the second one $u(t)$ describes the control process. One of the main characteristics of the homogeneous controlled semi-Markov process is the semi-Markov kernel $Q_{ij}(t,u)$, $i,j \in E$, $t \in 0, +\infty)$, $u \in U$ which is defined as the conditional probability that the following condition of the first component will be the condition j and transition to this state will happen until moment t under as long as the previous condition is i and the decision u is made.

Construction of a semi-Markov kernel.

From the description of the system functioning it follows that if $i = 1,2$, the following equalities are true

$$Q_{i0}(t) = Q_{i0}(t,u) = P\{\gamma_i < t, \eta > \gamma_i\} = \int_0^t e^{-\lambda x} dF_i(x),$$
$$Q_{ij}(t,u) = 0, \quad j = 1,2,$$
$$Q_{i3}(t) = Q_{i3}(t,u) = P\{\eta < t, \eta < \gamma_i\} = \int_0^t \lambda e^{-\lambda x} \bar{F}_i(x) dx \quad (3)$$

The last equalities in (3) are true, since the Markov moments of the beginning and end of restoration work interchange. In addition, to go to zero state, it is necessary and enough that the carried out restoration work ends before moment t and there are no attacks during the restoration work. To go to state 3, it is necessary and enough that the attack takes place before t, and the carried out restoration work before that moment does not end.

It should be noted that these functions are independent of management, since in states $i = 1,2$, management is not realized.

If $i = 0$, the following equalities are true:

$$Q_{00}(t,u) = 0, \quad Q_{01}(t,u) = \begin{cases} 0, & u > t, \\ e^{-\mu u}, & u < t, \end{cases}$$
$$Q_{02}(t,u) = \begin{cases} 0, & u > t, \\ \frac{\mu}{\mu-\lambda}\left(e^{-\lambda u} - e^{-\mu u}\right), & u < t, \end{cases} \quad Q_{03}(t,u) = \begin{cases} 1 - \frac{\mu}{\mu-\lambda} e^{-\lambda t} + \frac{\lambda}{\mu-\lambda} e^{-\mu t}, & u > t, \\ 1 - \frac{\mu}{\mu-\lambda} e^{-\lambda u} + \frac{\lambda}{\mu-\lambda} e^{-\mu u}, & u < t, \end{cases} \quad (4)$$

With the limit transition if $t \to \infty$, we get the transition probabilities of the states of the imbedded Markov chain $p_{ij} = lim_{t\to\infty} \int_0^\infty Q_{ij}(t,u) dG(u)$, $\quad i,j \in E = \{0,1,2,3\}$.

For the model under examination, we have from equalities (3) and (4)

$$p_{00} = 0, \quad p_{01} = \int_0^\infty e^{-\mu u} dG(u), \quad p_{02} = \int_0^\infty \frac{\mu}{\mu-\lambda}\left(e^{-\lambda u} - e^{-\mu u}\right) dG(u)$$
$$p_{03} = \int_0^\infty \left(1 - \frac{\mu}{\mu-\lambda} e^{-\lambda u} + \frac{\lambda}{\mu-\lambda} e^{-\mu u}\right) dG(u)$$
$$p_{i0} = \int_0^\infty e^{-\lambda x} dF_i(x), p_{ij} = 0, \quad j = 1,2, p_{i3} = \int_0^\infty \lambda e^{-\lambda x} \bar{F}_i(x) dx, i = 1,2. \quad (5)$$

It is not difficult to test the obvious equality if *i=0,1,2*

$$lim_{t\to\infty} \sum_{j\in E} Q_{ij}(t) = \sum_{j\in E} p_{ij} = 1.$$

Now we will formulate a mathematical task. When describing the security model, it was noted that attacks are reflected, when the moments of attacks fall on the periods of good operation of the security system, and the moment of the first unreflected attack is determined as a catastrophe moment. The security system will not be able to defeat the attack if it is in restoration states $i = 1,2$. In addition, and in the state $i = 0$ part of the period, the security system can be in the state of latent breakdown and skip the attack. Therefore, the increase in the safety of operation of the main system S or the increase in the efficiency of operation of the security system S_1 will be associated with the numerical characteristic of a random moment of catastrophe - the mathematical expectation of the time before the catastrophe. This expectation depends on the initial characteristics, in particular, on the distribution function $G(u)$, which determines the periodicity of planned restoration work. In the future, we will say that the distribution $G(u)$ determines the management strategy. It should be noted here that in the model under examination, the management is realized only in state $i = 0$ and depends only on the state at the moment of decision-making. Therefore, in this case, the strategy has the property of Markov, homogeneity (there is no dependence on calendar time). In addition, the model considers a class of randomize strategies, since a random experiment is used when choosing a solution (the implementation of a random coefficient having a distribution $G(u)$ determines the solution). The set of distribution definition $G(u)$ we will call the management space $R^+ = (0, \infty)$.

Thus, we come to the following mathematical tasks:

- to calculate the dependence of the mathematical expectation of the time before the catastrophe $M(\tau/\xi(0) = 0) = M_0(G)$ from the distribution $G(u)$ determining the

management strategies (here τ is the time before the catastrophe and it is assumed that the security system is good at zero moment);

- to find the maximum functional $M_0(G)$ by the set of *permissible* management strategies and determine the strategy on which this extremum is achieved.

Further, let us be clear the concept of permissible strategies (distributions) introduced above.

Let us mark the functional $M(\tau/\xi(0)=i)=M_i(G)=M_i$ and Ω_1, $G\in\Omega_1$, the set of distributions for which these functionals exist. Next, we will introduce two distribution functions.

$$0\le G_1(t)\le G_2(t)\le 1, t\ge 0, G_1(t)=G_2(t)=0, t\le 0,$$

and define a set of distributions

$$\Omega_2=\{0\le G_1(t)\le G(t)\le G_2(t)\le 1\} \quad (6)$$

Then the set of permissible distributions by the equality

$$\Omega=\Omega_1\cap\Omega_2 \quad (7)$$

Let us note that limitations (6) can be represented as limitations of the type of inequalities on linear functionals

$$G_1(t)\le\int_0^{+\infty}u(x,t)\,dG(x)\le G_2(t), u(x,t)=\begin{cases}1, x<t,\\0, x\ge t;\end{cases} t\in[0,+\infty).$$

Now, in the accepted notations, it is possible to formulate a mathematical task: *to determine the maximum* $M(\tau/\xi(0)=i)=M_i(G)=M_i$ *by the set of permissible distributions (7) and the distribution* $G^{(0)}$ *- the strategy on which this maximum is achieved,* $\max\limits_{G\in\Omega}M_0(G)=M_0\left(G^{(0)}\right)$.

4. Definition Of Target Functional Structure

Let us calculate the dependency of mathematical expectations of the time before the catastrophe. For conditional mathematical expectations $M_i=M(\tau/\xi(0)=i)$, $i=0,1,2$, we write out a system of algebraic equations using the formula of full mathematical expectation

$$M_0=\sum_{i=1}^{3}M_{0i}p_{0i}$$

$$M_i=M_{i0}p_{i0}+M_{i3}p_{i3},\quad i=1,2, \quad (8)$$

where M_{ij} means a conditional mathematical expectation of the time before the catastrophe if $\xi(0)=i$ and this component made the first transition to the state j. From the above description, there are the following equalities

$$M_{0i}=\frac{\int_0^\infty\int_0^\infty td_tQ_{i1}(t,u)dG(u)}{p_{0i}}+M_i, i=1,2,$$

$$M_{i3}=\frac{\int_0^\infty td_tQ_{i3}(t)}{p_{i3}},\quad i=0,1,2,\quad M_{i0}=\frac{\int_0^\infty td_tQ_{i0}(t)}{p_{i0}}+M_0, i=1,2. \quad (9)$$

Substituting (9) into equations (8), we obtain a system of algebraic equations

$$M_0=\int_0^\infty\int_0^\infty td_t\left(\sum_{i=1}^{3}Q_{0i}(t,u)\right)dG(u)+M_1p_{01}+M_2p_{02}$$

$$M_i=\int_0^\infty td_tQ_{i0}(t)+\int_0^\infty td_tQ_{i3}(t)+M_0p_{i0},\ i=1,2.$$

Solution of this system

$$M_0=\frac{\int_0^\infty\int_0^\infty td_t(\sum_{i=1}^{3}Q_{0i}(t,u))dG(u)+\sum_{i=1,2}p_{0i}\sum_{j=0,3}\int^\infty td_tQ_{ij}(t)}{1-p_{10}p_{01}-p_{20}p_{02}}$$

determines the functional under examination - the mathematical expectation of the time before the catastrophe. If we take into account the equations (2) and (4), we get

$$\sum_{i=1}^{3}Q_{0i}(t,u)=\begin{cases}1-\dfrac{\mu}{\mu-\lambda}e^{-\lambda t}+\dfrac{\lambda}{\mu-\lambda}e^{-\mu t}, & u>t,\\1, & u<t,\end{cases}$$

$$\sum_{j=0,3} Q_{ij}(t) = 1 - \bar{F}_i(t)e^{-\lambda t}, i = 1,2.$$

Thus, taking into account (5), we finally obtain that $M_0 = M_0(G)$ is bilinear functional

$$M_0(G) = \frac{\int_0^{+\infty} A(u)dG(u)}{\int_0^{+\infty} B(u)dG(u)}, \quad (10)$$

in which the subintegral functions are determined by the equalities

$$A(u) = \frac{(\mu+\lambda)}{\lambda\mu} - \frac{1}{(\mu-\lambda)\lambda\mu}\left(\mu^2 e^{-\lambda u} - \lambda^2 e^{-\mu u}\right) +$$
$$+e^{-\mu u}\int_0^{\infty} \bar{F}_1(t)e^{-\lambda t}dt + \frac{\mu}{\mu-\lambda}\left(e^{-\lambda u} - e^{-\mu u}\right)\int_0^{\infty} \bar{F}_2(t)e^{-\lambda t}dt$$
$$B(u) = 1 - e^{-\mu u}\int_0^{\infty} e^{-\lambda x}dF_1(x) - \frac{\mu}{\mu-\lambda}\left(e^{-\lambda u} - e^{-\mu u}\right)\int_0^{\infty} e^{-\lambda x}dF_2(x) \quad (11)$$

5. Solution Of Optimization Task. Optimal Management Strategy Construction

The above research proves that the task of constructing the optimal management strategy is now formulated as follows: *to determine the maximum of the bilinear functional (10), in which the subintegral functions are determined by equalities (11), by the set of distribution functions satisfying conditions (6) and (7), and the distribution* $G^{(0)}$ *where this maximum is reached*

$$M_0\left(G^{(0)}\right) = max_{G\in\Omega} M_0(G).$$

The basis for solving the task will be two statements:

- A theorem on distribution structure where the maximum linear functional over the set of distributions (7) is achieved, the proof of which is given in [2];
- A theorem on coincidence of sets of distributions where the maximum of bilinear functional is reached and the maximum of specially selected linear functional is reached, the proof of which is given in [3].

Further we will give the definitions of these statements.

THEOREM [2]. If there is the maximum of the linear functional $\mathrm{L(G)} = \int_0^{+\infty} \mathrm{C(u)dG(u)}$ with respect to the set (7) and the subintegral function C(u) has the maximum at point $0 \le t_1 \le +\infty$ and in the area $0 < t < t_1$ the subintegral function is non-decreasing, and in the area $t_1 < t < +\infty$ the subintegral function is non-increasing, then the maximum of the functional is achieved on the distribution

$$G^{(0)}(u) = \begin{cases} G_1(u), & 0 \le u \le u_1, \\ G_2(u), & u_1 < u \le +\infty, \end{cases} \quad (12)$$

that is

$$\max_{G\in\Omega} L(G) = L(G^{(0)}) =$$
$$= \int_0^{tu} \mathrm{C}(u)dG_1(u) + \mathrm{C}(u_1)\left[\lim_{u\to u_1+0} G_2(u) - G_1(u_1)\right] + \int_{u_1+0}^{+\infty} \mathrm{C}(u)dG_2(u) = C. \quad (13)$$

and the following equality is correct

$$\max_{u\in[0,\infty)} \left\{\int_0^u \mathrm{C}(x)dG_1(x) + \mathrm{C}(t)\left[\lim_{x\to t+0} G_2(x) - G_1(u)\right] + \int_{u+0}^{+\infty} \mathrm{C}(x)dG_2(x)\right\} = C. \quad (14)$$

LEMMA [3]. If there is the maximum of bilinear functional $\mathrm{M_0(G_0)} = \max_{\mathrm{G}\in\Omega} \mathrm{M_0\,(G)} = \mathrm{C}$ (10) in some set distributions Ω then

$$\{\Phi: M_0(\Phi) = C = max_{G\in\Omega} M_0(G)\} = \{\Phi: max_{G\in\Omega} L(G) = L(\Phi)\},$$

where the subintegral function of the linear functional $L(G) = \int_0^{+\infty} C(u)dG(u)$ is defined by the equality $C(u) = \mathrm{A}(u) - C\mathrm{B}(u)$.

The lemma condition about existence of the maximum of functional (10) means that the set $\{\Phi: M_0(\Phi) = C = max_{G\in\Omega} M_0(G)\}$ is not empty.

The converse statement is also true.

STATEMENT. If there is such a constant C for which

$$\left\{\Phi: max_{G\in\Omega} \int_0^{\infty}\left(A(u) - CB(u)\right)dG(u) = \int_0^{\infty}\left(A(u) - CB(u)\right)d\Phi(u)\right\} \neq \emptyset,$$

then there is the maximum of bilinear functional (10) and this maximum is C.

From the above statements follows

COROLLARY [2]. If there is the maximum of bilinear functional $\mathrm{M_0(G_0) = \max_{G\in\Omega} M_0\,(G) = C}$ (10) in set distributions Ω, determined by correlations (6) and (7), and function $\mathrm{C(u) = A(u) - CB(u)}$ has the maximum in the point $0 \le t_1 \le +\infty$ and in the area $0 < t < t_1$ subintegral function is non-decreasing, and in the area $t_1 < t < +\infty$ the subintegral function is non-increasing, then the maximum of this bilinear functional is reached on distribution (12) and

$$\max_{G\in\Omega} M_0(G) = M_0(G^{(0)}) =$$

$$= \max_{u\in[0,\infty)} \frac{\int_0^u A(x)dG_1(x) + A(u)\left[\lim_{t\to u+0} G_2(t) - G_1(u)\right] + \int_{u+0}^{+\infty} A(x)dG_2(u)}{\int_0^u B(x)dG_1(x) + B(u)\left[\lim_{t\to u+0} G_2(t) - G_1(u)\right] + \int_{u+0}^{+\infty} B(x)dG_2(x)} = C. \quad (15)$$

If you use these statements to find the maximum of the bilinear functional $M_0(G)$ *(10)*, in which the subintegral functions are determined by equations (11), then the task will result in examining the function $C(u) = \mathrm{A}(u) - C\mathrm{B}(u)$.

To simplify transformations let us enter symbols

$$\beta_i = \int_0^\infty \bar{F}_i(t)e^{-\lambda t}dt\,, \alpha_i = \int_0^\infty e^{-\lambda t}dF_i(t)\,, i = 1,2,$$

$$\alpha_i = -\int_0^\infty e^{-\lambda t}d\bar{F}_i(t) = 1 - \lambda\beta_i \ge 0.$$

Then, taking into account the equalities (11) and the accepted symbols for the function $C(u)$, we have

$$C(u) = \mathrm{A}(u) - C\mathrm{B}(u) =$$

$$= \frac{(\mu+\lambda)}{\lambda\mu} - \frac{1}{\mu\lambda(\mu-\lambda)}\left(\mu^2e^{-\lambda u} - \lambda^2e^{-\mu u}\right) + e^{-\mu u}\beta_1 + \frac{\mu}{\mu-\lambda}\left(e^{-\lambda u} - e^{-\mu u}\right)\beta_2 -$$

$$-\mathrm{C}\left(1 - e^{-\mu u}(1-\lambda\beta_1) - \frac{\mu}{\mu-\lambda}\left(e^{-\lambda u} - e^{-\mu u}\right)(1-\lambda\beta_2)\right),$$

$C(0) = \beta_1(1 - \mathrm{C}\lambda) \le 0, C(\infty) = \frac{(\mu+\lambda)}{\lambda\mu} - \mathrm{C}$ (16)

The latter inequality follows from the obvious correlations

$$\beta_1 > 0, C \ge \tfrac{1}{\lambda}.$$

For the derivative of the function $C(u)$ after transformations, we have the equality

$$\frac{dC(u)}{du} == \frac{1}{(\mu-\lambda)}\left(\mu e^{-\lambda u} - \lambda e^{-\mu u}\right) - \mu e^{-\mu u}\beta_1 - \frac{\mu}{\mu-\lambda}\left(\lambda e^{-\lambda u} - \mu e^{-\mu u}\right)\beta_2 -$$

$$-\mathrm{C}\left(\frac{\mu^2}{\mu-\lambda}(\beta_2-\beta_1)(1-\lambda C)(1-\lambda\beta_1) + \frac{\mu}{\mu-\lambda}\left(\lambda e^{-\lambda u} - \mu e^{-\mu u}\right)(1-\lambda\beta_2)\right) =$$

$$= e^{-\mu u}\left[\frac{1}{(\mu-\lambda)}(C\mu\lambda - 1) + \frac{\lambda}{\mu-\lambda}\beta_1(1-\lambda C) + \frac{\mu^2}{\mu-\lambda}(\beta_2-\beta_1)(1-\lambda C)\right] +$$

$$+e^{-\lambda u}\left[\frac{\mu}{(\mu-\lambda)}(1-\lambda\beta_2)(1-\lambda\mathrm{C})\right].$$

Now the derivative under examination can be represented as the product of two functions

$$\frac{dC(u)}{du} = \Psi_1(u)\Psi_2(u)$$

$$\Psi_1(u) = e^{-\mu u}, \Psi_2(u) = C_0 + C_1,$$

$$C_0 = \left[\frac{1}{(\mu-\lambda)}(C\mu\lambda - 1) + \frac{\lambda}{\mu-\lambda}\beta_1(1-\lambda C) + \frac{\mu^2}{\mu-\lambda}(\beta_2-\beta_1)(1-\lambda C)\right]$$

$$C_1 = \frac{\mu}{(\mu-\lambda)}(1-\lambda\beta_2)(1-\lambda\mathrm{C})$$

The first function $\Psi_1(u)$ is positive and the second function $\Psi_2(u)$ is decreasing since

$$\frac{d\Psi_2(u)}{du} = e^{(\mu-\lambda)u}\mu(1-\lambda\beta_2)(1-\lambda\mathrm{C}) \le 0.$$

Thus, it has been proved that the derivative of the function (16) changes the sign from plus to minus up to one time, that is, the function (16) is either monotonic in the area $R^+ = 0, \infty)$ or has the maximum on area boundaries and fully satisfies the conditions of the above statements.

Therefore, the maximum of the functional (10), in which the subintegral functions are determined by the equalities (11), over the set distributions satisfying the inequalities $\{G: 0 \le G_1(u) \le G(u) \le G_2(u) \le 1, 0 \le u \le +\infty\}$ (6), is achieved on the distribution

$$G^{(0)}(u) = \begin{cases} G_1(u), & 0 \le u \le u_1, \\ G_2(u), & u_1 < u \le +\infty, \end{cases}$$

moreover, the parameter u_1 is defined as maximum point of function 15. We remind that functions A(u) and B(u) are defined by equalities (11).

6. Conclusion

The conducted researches allowed to bring the task of functional analysis - the search for the extremum of bilinear functional by the set distribution functions to the task of mathematical analysis - the search for the maximum of some function by the set of real numbers. This essentially simplifies the practical use of the results set forth.

References

[1] Kashtanov, V.A. The Structure of the Functional of Accumulation Defined on a Trajectory of Semi-Markov Process with a Finite Set of States. Theory of Probability and its Appllications. Vol. 60, No. 2 (2016), pp. 281-294.

[2] Kashtanov, V.A., Zaitseva, O.B. & Efremov, A.A. Controlled Semi-Markov Processes with Constraints on Control Strategies and Construction of Optimal Strategies in Reliability and Safety Models. *Math Notes* 109, 585–592 (2021).

[3] Kashtanov, V.A. Discrete distributions in control problems, in Probabilistic Methods in Discrete mathematics, Proceeding of the Fourth International Petrozavodsk Conference (Petrozavodsk, Russia, June 3-7, 1996), VSP, Utrecht, 1997, pp. 267-274.

A new continuous probability model based on a trigonometric function: Theory and applications

Anwar hassan

•

University of Kashmir
Anwar.hassan5@gmail.com

Murtiza Ali Lone

•

University of Kashmir
murtazastat@gmail.com

Ishfaq Hassain Dar*

•

University of Kashmir
ishfaqqh@gmail.com*

Peer Bilal Ahmad

•

Department of Mathematical Science, IUST
peer.bilal@islamicuniversity.edu.in

Abstract

In this manuscript, we highlight a new probability distribution based on a trigonometric function, obtained by specializing the Sine-G family of distributions with exponentiated exponential distribution. The proposed distribution is quite flexible in terms of density and hazard rate functions. Several mathematical properties of the proposed distribution are also explored. For applicability of proposed distribution, two real data sets are scrutinized and it is sensed that proposed distribution leads to a better fit than all other models taken under consideration.

Keywords: Sine-G; Exopentiated exponential distribution; Hazard rate function; Order statistic; Simulation study; Maximum likelihood estimation.

1. Introduction

In distribution theory proposing new family of distributions by incorporating an extra parameter is most common among researchers. The purpose of incorporating a new parameter is to increasing the data fitting strength of the proposed probability models. Although researchers are quite successful in doing so, however they are little concerned about the over parameterization

and complexities that arise due to addition of new parameters. To know more about such families one can go through [11],[9],[6],[3],[8], [18], [17] and [1]. So keeping in view the limitations of having extra parameters, some researchers have come up with family of distributions that not only can be used to model the complex data structures, but also are void of extra parameters. Among them lets recall [10],[12],[13],[15] and [16]. After getting motivated by aforementioned work on probability models having parsimony in parameters we have introduced a new model based on Sine-G (SG) family of distribution proposed by [15]. The introduced model, namely Sine-G exponentiated exponential (SGEE) distribution has been obtained by taking the baseline distribution as exponentiated exponential distribution. The SGEE distribution has same number of parameters as baseline distribution and has greater flexibility than some well-known two parameteric probability distributions including the baseline distribution.
The rest of the manuscript is presented as, In Section 2 a brief introduction about Sine-G family of distributions is given. In Section 3, a member of the SG family namely, SGEE distribution is examined in detail and its general properties are studied including, quantile, moments, moment generating functon, order statistic etc. The maximum likelihood estimation and simulation study are discussed in Section 4. In Section 5, to check the applicability of SGEE two data sets have been scrutinized. Finally, the paper ends in Section 6 with concluding remarks.

2. Sine-G (SG) Family Of Disrtibutions

Let $G(y)$ be the baseline commulative distribution function (CDF) of any random variable Y. Then the CDF, $F(y)$ of the sine-G family of distributions proposed by [15] is given by

$$F(y) = \sin\left(\frac{\pi}{2}G(y)\right) \quad ; y \in \mathbb{R},$$

The corresponding probability density function(PDF) is given by

$$f(y) = \frac{\pi}{2}g(y)\cos\left(\frac{\pi}{2}G(y)\right) \quad ; y \in \mathbb{R},$$

The survival function $S(y)$ for SG is given by

$$\begin{aligned} S(y) =& 1 - \sin\left(\frac{\pi}{2}G(y)\right) \quad ; y \in \mathbb{R} \\ =& \left(\sin\left(\frac{\pi}{4}G(y)\right) - \cos\left(\frac{\pi}{4}G(y)\right)\right)^2 \end{aligned}$$

The hazard rate function $\lambda(y)$ is given by

$$\lambda(y) = \frac{\frac{\pi}{2}g(y)\cos\left(\frac{\pi}{2}G(y)\right)}{\left(\sin\left(\frac{\pi}{4}G(y)\right) - \cos\left(\frac{\pi}{4}G(y)\right)\right)^2} \tag{1}$$

3. Sine-G Exponentiated Exponential (SGEE) Distribution And Its Properties

Suppose the random variable Y has exponentiated exponential distribution with CDF $G(y) = (1 - e^{-\theta y})^{\alpha}$; $y, \alpha, \theta > 0$ then the CDF of the SGEE distribution is given by

$$F(y) = \sin\left(\frac{\pi}{2}(1 - e^{-\theta y})^{\alpha}\right) \quad ; \quad \alpha, \theta, y > 0$$

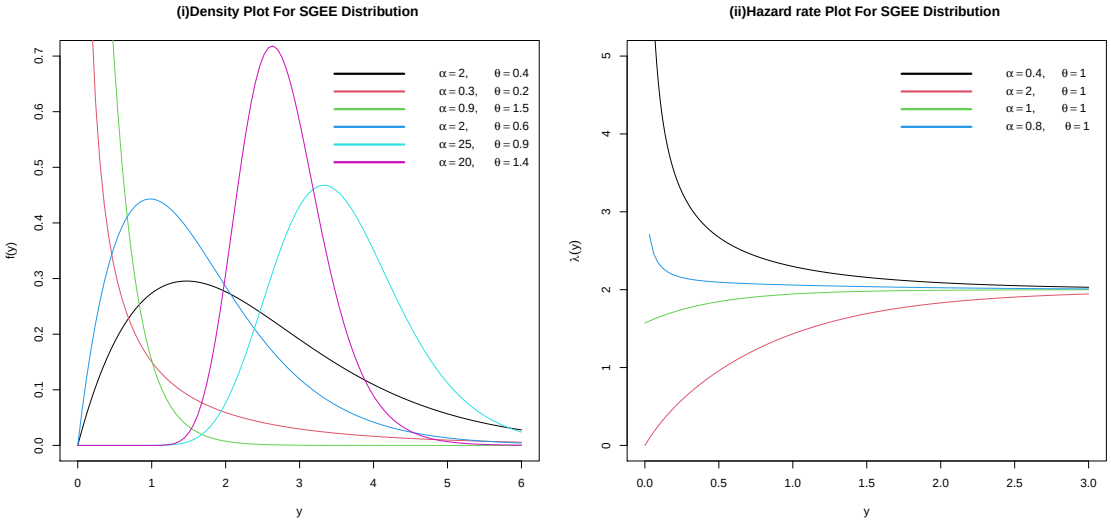

Figure 1: *Plots of the SGEE density and hazard function for different values of α and θ.*

The corresponding PDF is

$$f(y) = \alpha\frac{\pi}{2}\theta e^{-\theta y}(1-e^{-\theta y})^{\alpha-1}\cos\left(\frac{\pi}{2}(1-e^{-\theta y})^{\alpha}\right) \quad ;\alpha,\theta,y>0. \tag{2}$$

The survival and hazard rate functions are, respectively, given by

$$S(y) = 1-\sin\left(\frac{\pi}{2}(1-e^{-\theta y})^{\alpha}\right) \quad ;\alpha,\theta,y>0 \tag{3}$$

and

$$\lambda(y) = \frac{f(y)}{S(y)}$$

$$\lambda(y) = \frac{\alpha\frac{\pi}{2}\theta e^{-\theta y}(1-e^{-\theta y})^{\alpha-1}\cos\left(\frac{\pi}{2}(1-e^{-\theta y})^{\alpha}\right)}{\left(\sin\left(\frac{\pi}{4}(1-e^{-\theta y})^{\alpha}\right)-\cos\left(\frac{\pi}{4}(1-e^{-\theta y})^{\alpha}\right)\right)^2}; \quad \alpha,\theta,y>0$$

Some important series expansions:

$$e^{x} = \sum_{j=0}^{\infty}\frac{x^{j}}{j!} \tag{4}$$

$$\cos x = \sum_{j=0}^{\infty}(-1)^{j}\frac{x^{2j}}{2j!} \tag{5}$$

$$\sin x = \sum_{j=0}^{\infty}(-1)^{j}\frac{x^{2j+1}}{2j+1!} \tag{6}$$

$$(1-x)^{n} = \sum_{j=0}^{n}(-1)^{j}\binom{n}{j}x^{j} \tag{7}$$

3.1. Quantile Function

The quantile function of SGEE is given by

$$Y = -\frac{1}{\theta}log\left[1-\left(\frac{2}{\pi}\sin^{-1}(1-U)\right)^{\frac{1}{\alpha}}\right]$$

where U $\sim (0,1)$ distribution. The q^{th} quantile of SGEE distribution is given by

$$y_q = -\frac{1}{\theta} log\left[1 - \left(\frac{2}{\pi}\sin^{-1}(1-q)\right)^{\frac{1}{\alpha}}\right]$$

The median is obtained as

$$y_{0.5} = -\frac{1}{\theta} log\left[1 - \left(\frac{2}{\pi}\sin^{-1}(\frac{1}{2})\right)^{\frac{1}{\alpha}}\right]$$

3.2. Moments

The r^{th} moment of the SGEE distribution is given by

$$\begin{aligned} E(Y^r) &= \int_0^\infty y^r f(y)dy \\ &= \int_0^\infty y^r \alpha \frac{\pi}{2}\theta e^{-\theta y}(1-e^{-\theta y})^{\alpha-1} cos\left(\frac{\pi}{2}(1-e^{-\theta y})^\alpha\right) dy \end{aligned}$$

by putting $e^{-\theta y} = z$ and using the series expansions (7) and (5), we get

$$E(Y^r) = \frac{\alpha}{\theta^r}\sum_{j=0}^{\infty}\sum_{k=0}^{\alpha(2j+1)-1}\frac{(-1)^{j+k}}{2j!}(\frac{\pi}{2})^{2j+1}\binom{\alpha(2j+1)-1}{k}\int_0^1(-logz)^r z^k dz \tag{8}$$

again putting $-logz = u$ in (8), we get r^{th} moment as

$$E(Y^r) = \frac{\alpha}{\theta^r}\sum_{j=0}^{\infty}\sum_{k=0}^{\alpha(2j+1)-1}\frac{(-1)^{j+k}}{2j!}(\frac{\pi}{2})^{2j+1}\binom{\alpha(2j+1)-1}{k}\frac{\Gamma(r+1)}{(k+1)^{r+1}} \tag{9}$$

3.3. Moment Generating Function

The moment generating function of SGEE distribution is defined by

$$M_Y(t) = \int_0^\infty e^{ty} f(y)dy,$$

again using (4), (5) and (7) we have the final expression of MGF as

$$M_Y(t) = \alpha\sum_{r=0}^{\infty}\sum_{j=0}^{\infty}\sum_{k=0}^{\alpha(2j+1)-1}\frac{(-1)^{j+k}(\frac{\pi}{2})^{2j+1}}{2j!(k+1)^{r+1}}\left(\frac{t}{\theta}\right)^r\binom{\alpha(j+1)-1}{k} \;; t<\theta$$

3.4. Mean Residual Life And Mean Waiting Time

The mean residual life function, say $\mu(t)$, is defined by

$$\mu(t) = \frac{1}{S(t)}\left(E(t) - \int_0^t yf(y)dy\right) - t \tag{10}$$

Table 1: *Average values of MLEs their corresponding MSEs and Bias.*

Sample size	Parameter		MLEs		MSE		Bias	
n	α	θ	$\hat{\alpha}$	$\hat{\theta}$	$\hat{\alpha}$	$\hat{\theta}$	$\hat{\alpha}$	$\hat{\theta}$
30	0.8	0.5	0.86876	0.55268	0.04713	0.02634	0.06876	0.05268
		1	0.88261	1.12988	0.04109	0.11373	0.08261	0.12988
		1.5	0.88609	1.72108	0.04381	0.32292	0.08609	0.22108
		2	0.88888	2.31489	0.05774	0.58598	0.08888	0.31489
	1	0.5	1.06555	0.53199	0.05840	0.03184	0.06555	0.03199
		1	1.08661	1.13391	0.07117	0.08813	0.08661	0.13391
		1.5	1.08243	1.68584	0.08902	0.28176	0.08243	0.18584
		2	1.06703	2.15094	0.11414	0.50617	0.06702	0.15094
	1.5	0.5	1.65896	0.54400	0.23140	0.01787	0.15896	0.04400
		1	1.56549	1.04447	0.14145	0.04484	0.06549	0.04447
		1.5	1.65654	1.61426	0.30000	0.16226	0.15654	0.11426
		2	1.72030	2.25512	0.27791	0.36792	0.22030	0.25512
	2	0.5	2.22021	0.53030	0.40033	0.01187	0.22021	0.03030
		1	2.22111	1.06212	0.46756	0.05600	0.22111	0.06211
		1.5	2.31075	1.69956	0.61034	0.18055	0.31075	0.19956
		2	2.22600	2.17031	0.57051	0.26500	0.22600	0.17031
50	0.8	0.5	0.84206	0.54269	0.02796	0.02565	0.04206	0.04269
		1	0.79948	1.00343	0.02079	0.06482	-0.00051	0.00343
		1.5	0.83571	1.61962	0.01981	0.13657	0.03571	0.11962
		2	0.81309	2.05569	0.02020	0.24927	0.01309	0.05569
	1	0.5	1.03527	0.52180	0.03822	0.01277	0.03527	0.02180
		1	1.08685	1.08659	0.04641	0.05628	0.08685	0.08659
		1.5	1.06537	1.68051	0.05138	0.19718	0.06537	0.18051
		2	1.01739	2.02631	0.02842	0.14193	0.01739	0.02630
	1.5	0.5	1.63833	0.53194	0.14694	0.00855	0.13833	0.03194
		1	1.60152	1.07540	0.15908	0.04964	0.10152	0.07540
		1.5	1.53020	1.53325	0.10391	0.06558	0.03020	0.03325
		2	1.56678	2.08532	0.07309	0.14002	0.06678	0.08532
	2	0.5	2.15774	0.52840	0.24240	0.00829	0.15774	0.02840
		1	2.09796	1.02776	0.16712	0.02854	0.09796	0.02776
		1.5	2.11604	1.56729	0.21126	0.09217	0.11604	0.06729
		2	2.19453	2.08430	0.35438	0.11187	0.19453	0.08430

where

$$E(t) = \frac{\alpha}{\theta}\sum_{j=0}^{\infty}\sum_{k=0}^{\alpha(2j+1)-1}\frac{(-1)^{j+k}}{(k+1)^2 2j!}\left(\frac{\pi}{2}\right)^{2j+1}\binom{\alpha(2j+1)-1}{k} \tag{11}$$

and

$$\int_0^t xf(x)dx = \frac{\alpha}{\theta}\sum_{j=0}^{\infty}\sum_{k=0}^{\alpha(2j+1)-1}\frac{(-1)^{j+k}}{(k+1)^2 2j!}\left(\frac{\pi}{2}\right)^{2j+1}\binom{\alpha(2j+1)-1}{k}\gamma\left(\theta t(k+1),2\right) \tag{12}$$

Substituting (3), (11) and (12) in (10), we get $\mu(t)$ as

$$\begin{aligned}\mu(t) =& \frac{1}{1-\sin\left(\frac{\pi}{2}(1-e^{-\theta t})^{\alpha}\right)}\frac{\alpha}{\theta}\sum_{j=0}^{\infty}\sum_{k=0}^{\alpha(2j+1)-1}\frac{(-1)^{j+k}}{(k+1)^2 2j!}\left(\frac{\pi}{2}\right)^{2j+1}\binom{\alpha(2j+1)-1}{k}\\ &\times\left[1-\gamma(\theta t(k+1))\right]-t\end{aligned}$$

where $\gamma(a,b) = \int_0^a y^{b-1}e^{-y}dy$ is the lower incomplete gamma function.

Table 2: *Average values of MLEs their corresponding MSEs and Bias.*

Sample size	Parameter		MLEs		MSE		Bias	
n	α	θ	$\hat{\alpha}$	$\hat{\theta}$	$\hat{\alpha}$	$\hat{\theta}$	$\hat{\alpha}$	$\hat{\theta}$
100	0.8	0.5	0.82267	0.52370	0.01321	0.01083	0.02267	0.02370
		1	0.79728	0.99739	0.00716	0.02731	-0.00271	-0.00260
		1.5	0.82011	1.54754	0.01276	0.06654	0.02011	0.04754
		2	0.79681	1.99112	0.01290	0.12323	-0.00318	-0.00887
	1	0.5	1.03990	0.51737	0.01768	0.00528	0.03990	0.01737
		1	1.01765	1.03115	0.01432	0.02452	0.01765	0.03115
		1.5	1.02663	1.55358	0.01549	0.04853	0.02663	0.05358
		2	1.03361	2.07698	0.02073	0.10262	0.03360	0.07698
	1.5	0.5	1.54919	0.51586	0.04621	0.00518	0.04919	0.01586
		1	1.55740	1.02647	0.04768	0.01628	0.05740	0.02646
		1.5	1.56732	1.56766	0.03581	0.03419	0.06731	0.06766
		2	1.57208	2.10929	0.04142	0.08105	0.07208	0.10929
	2	0.5	2.04186	0.50132	0.07637	0.00288	0.04186	0.00132
		1	2.04210	1.02675	0.08509	0.01862	0.04210	0.02675
		1.5	2.10625	1.54551	0.13007	0.03257	0.10625	0.04551
		2	2.06746	2.04980	0.08307	0.06683	0.06746	0.04980
200	0.8	0.5	0.79883	0.50439	0.00455	0.00428	-0.00116	0.00439
		1	0.80354	1.01873	0.00364	0.01240	0.00354	0.01873
		1.5	0.79510	1.48724	0.00360	0.02438	-0.00489	-0.01275
		2	0.79160	2.01861	0.00621	0.06748	-0.00839	0.01861
	1	0.5	0.99809	1.50664	0.00558	0.01866	-0.00190	0.00664
		1	1.00884	2.03002	0.00997	0.05265	0.00884	0.03002
		1.5	1.00041	1.51007	0.00670	0.02119	0.00041	0.01007
		2	1.00884	2.03002	0.00997	0.05265	0.00884	0.03002
	1.5	0.5	1.56024	0.51511	0.02153	0.00224	0.06024	0.01511
		1	1.51925	1.01414	0.01833	0.00859	0.01925	0.01414
		1.5	1.53288	1.52218	0.02876	0.02280	0.03288	0.02218
		2	1.52145	2.01055	0.02441	0.03646	0.02145	0.01055
	2	0.5	2.03758	0.50909	0.03859	0.00208	0.03758	0.00909
		1	2.07367	1.03099	0.05998	0.00920	0.07367	0.03099
		1.5	2.01058	1.50662	0.04448	0.01675	0.01054	0.00662
		2	2.02562	2.01343	0.03551	0.02001	0.02562	0.01343

The mean waiting time of Y, say $\bar{\mu}(t)$, is given by

$$\bar{\mu}(t) = t - \frac{1}{F(t)} \int_0^t y f(y) dy$$

$$\bar{\mu}(t) = t - \frac{1}{\sin\left(\frac{\pi}{2}(1-e^{-\theta t})^{\alpha}\right)} \frac{\alpha}{\theta} \sum_{j=0}^{\infty} \sum_{k=0}^{\alpha(2j+1)-1} \frac{(-1)^{j+k}}{(k+1)^2 2j!} \left(\frac{\pi}{2}\right)^{2j+1} \binom{\alpha(2j+1)-1}{k} \times \gamma\left(\theta t(k+1), 2\right)$$

3.5. Order Statistics

Let $Y_1, Y_2, ..., Y_n$ be a random sample of size n, and if $Y_{i:n}$ denote the i^{th} order statistic, then the PDF of $Y_{i:n}$, say $f_{i:n}(y)$ is given by

$$f_{i:n}(y) = \frac{n!}{(i-1)!(n-i)!} F(y)^{i-1} f(y) (1 - G(y))^{n-i}.$$

We can write the PDF $f_{i:n}(y)$ of i^{th} order statistic of SGEE distribution as

$$f_{i:n}(y) = \frac{\alpha \pi \theta e^{-\theta y} (1 - e^{-\theta y})^{\alpha - 1}}{2B(i, n-i+1)} \frac{sin^n\left(\frac{\pi}{2}(1-e^{-\theta y})^{\alpha}\right)}{tan\left(\frac{\pi}{2}(1-e^{-\theta y})^{\alpha}\right)} cosec^{n-i}\left(\frac{\pi}{2}(1-e^{-\theta y})^{\alpha} - 1\right)$$

Where $B(a, b)$ is the beta function.

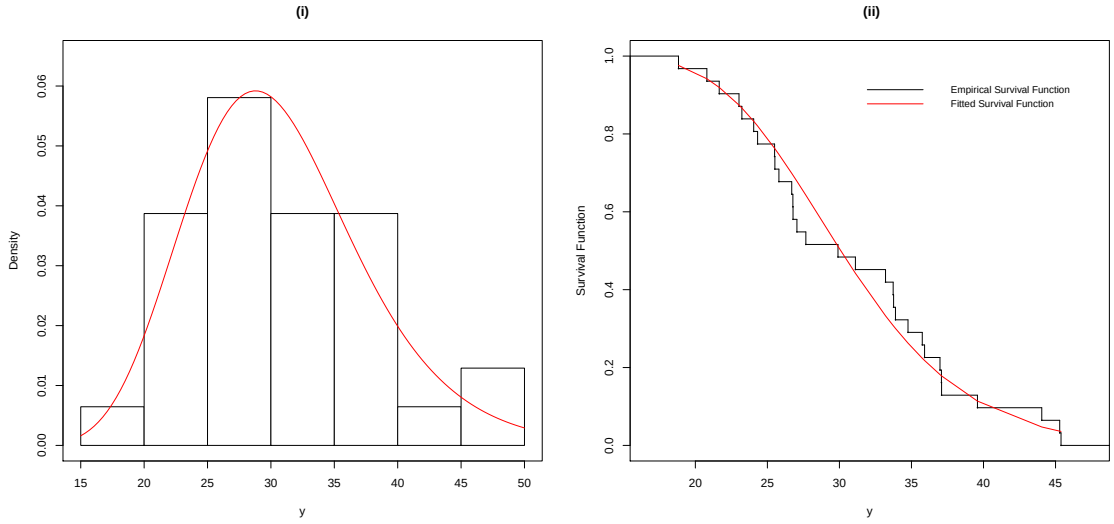

Figure 2: *(i) The relative histogram and the fitted SGEE distribution. (ii) The empirical survival function and fitted SGEE survival function for data set I.*

4. Statistical Inference

4.1. Maximum Likelihood Estimation

Let $y_1, y_2, ..., y_n$ be a random sample from SGEE distribution, then the logarithm of the likelihood function is given by

$$l = nlog(\frac{\alpha\pi}{2}) + nlog\theta - \theta\sum_{i=1}^{n} y_i + \sum_{i=1}^{n} log(1-e^{-\theta y_i})^{\alpha-1} + \sum_{i=1}^{n} log\left[cos\left(\frac{\pi}{2}(1-e^{-\theta y_i})^{\alpha}\right)\right], \quad (13)$$

by differentiating partially (13) with respect to the parameters α and θ and equating the derivatives to zero, we get

$$\frac{\partial l}{\partial \alpha} = \frac{n}{\alpha} + \sum_{i=1}^{n} log(1-e^{-\theta y_i})\left[1 - \frac{\pi}{2}(1-e^{-\theta y_i})^{\alpha} tan\left(\frac{\pi}{2}(1-e^{-\theta y_i})^{\alpha}\right)\right] = 0$$

$$\frac{\partial l}{\partial \theta} = \frac{n}{\theta} - \sum_{i=1}^{n} y_i + \sum_{i=1}^{n}\left(\frac{y_i e^{-\theta y_i}}{1-e^{-\theta y_i}}\right)\left[(\alpha-1) - \frac{\alpha\pi}{2}(1-e^{-\theta y_i})^{\alpha} tan\left(\frac{\pi}{2}(1-e^{-\theta y_i})^{\alpha}\right)\right] = 0$$

It is clear that these equations cannot be solved analytically, so the MLEs of parameters are obtained through R software.

Theorem 1: *If the parameter θ is known, then the MLE of α exists and is unique.*

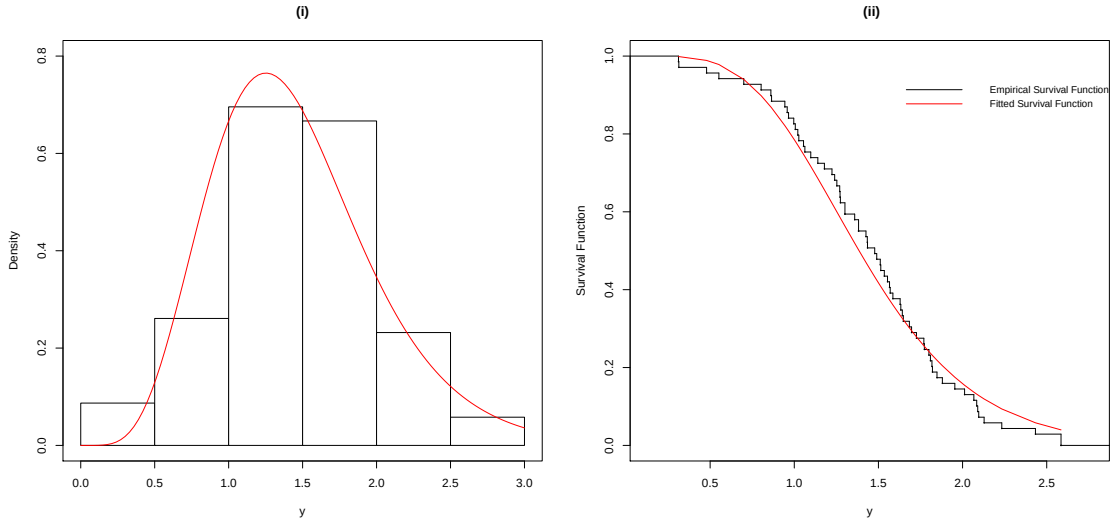

Figure 3: *(i) The relative histogram and the fitted SGEE distribution. (ii) The empirical survival function and fitted SGEE survival function for data set II.*

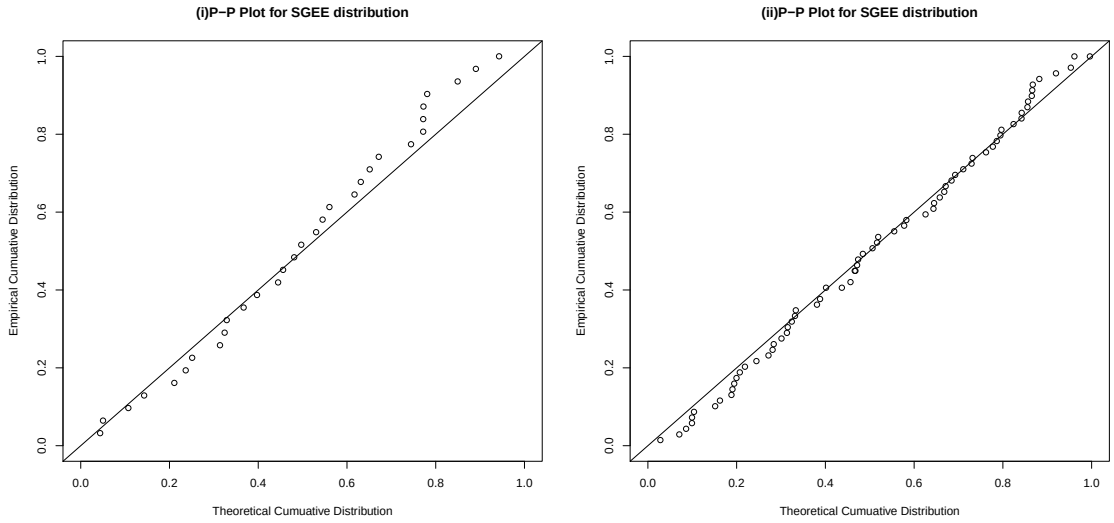

Figure 4: *P-P plot for the SGEE distribution for data set I and data set II*

Proof: Since,

$$\frac{\partial l}{\partial \alpha} = \frac{n}{\alpha} + \sum_{i=1}^{n} log(1 - e^{-\theta y_i}) \left[1 - \frac{\pi}{2}(1 - e^{-\theta y_i})^{\alpha} tan\left(\frac{\pi}{2}(1 - e^{-\theta y_i})^{\alpha}\right)\right]$$

$$\lim_{\alpha \to 0} \frac{\partial l}{\partial \alpha} = \infty + \sum_{i=1}^{n} log(1 - e^{-\theta y_i}) \left[1 - \frac{\pi}{2} tan \frac{\pi}{2}\right] = \infty$$

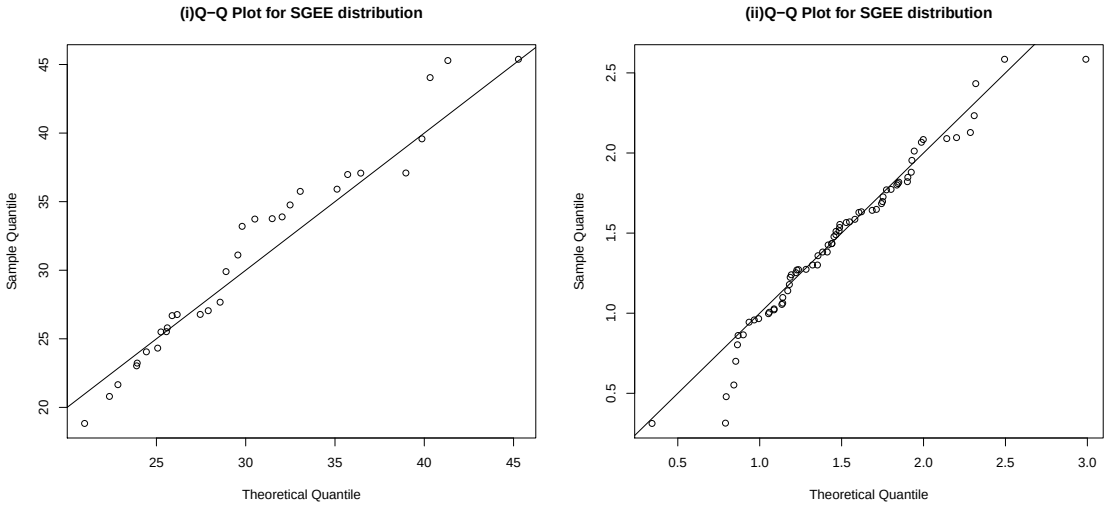

Figure 5: *Q-Q plot for the SGEE distribution for data set I and data set II*

Also

$$\lim_{\alpha\to\infty}\frac{\partial l}{\partial\alpha}=0+\sum_{i=1}^{n}log(1-e^{-\theta y_i})<0,$$

therefore, there exists atleast one root say $\hat{\alpha}(0,\infty)$, such that $\frac{\partial l}{\partial\alpha}=0$
For uniqueness of root, we have

$$\frac{\partial^2 l}{\partial\alpha^2}=-\frac{n}{\alpha^2}-\frac{\pi}{2}(1-e^{-\theta y_i})^{\alpha}\sum_{i=1}^{n}\left(log(1-e^{-\theta y_i})\right)^2\left[\frac{\pi}{2}sec^2\left(\frac{\pi}{2}(1-e^{-\theta y_i})^{\alpha}\right)+tan\left(\frac{\pi}{2}(1-e^{-\theta y_i})^{\alpha}\right)\right]<0$$

Hence the proof.

■

Theorem 2: *If the parameter α is known, then the MLE of θ exists and is unique.*
Proof: Since,

$$\frac{\partial l}{\partial\theta}=\frac{n}{\theta}-\sum_{i=1}^{n}y_i+\sum_{i=1}^{n}\left(\frac{y_i e^{-\theta y_i}}{1-e^{-\theta y_i}}\right)\left[(\alpha-1)-\alpha\frac{\pi}{2}(1-e^{-\theta y})^{\alpha}tan\left(\frac{\pi}{2}(1-e^{-\theta y})^{\alpha}\right)\right]$$

$$\lim_{\theta\to 0}\frac{\partial l}{\partial\theta}=\infty$$

Also

$$\lim_{\theta\to\infty}\frac{\partial l}{\partial\theta}=0-\sum_{i=1}^{n}y_i<0$$

Therefore, there exists atleast one root say $\hat{\theta}(0,\infty)$, such that $\frac{\partial l}{\partial\theta}=0$
For uniqueness of root, we have

$$\frac{\partial^2 l}{\partial \theta^2} = -\frac{n}{\theta^2} - \sum_{i=1}^{n} y_i + \sum_{i=1}^{n} \left(\frac{y_i e^{-\theta y_i}}{1 - e^{-\theta y_i}} \right)^2 \left[\alpha \; x \left\{ \alpha \; x \sec^2(x) + (\alpha - 1) \tan(x) \right\} + (\alpha - 1) e^{-\theta y_i} \right] < 0$$

where,

$$x = \frac{\pi}{2}(1 - e^{-\theta y})^{\alpha}$$

Hence proved.

■

Table 3: *MLEs and -2l, AIC, AICC, BIC , K-S statistic and P-value for data set I.*

Model	$\hat{\alpha}$	$\hat{\theta}$	-2l	AIC	AICC	BIC	K-S statistic	p-value
SGEE	0.07832 (1.29403)	0.11465 (0.01650)	208.3183	212.3183	212.7468	215.1862	0.13013	0.6235
G	0.93208 (1.76667)	0.61445 (0.15676)	208.3212	212.3212	212.7691	215.2292	0.13189	0.6232
APE	1.26948 (1.18703)	9.55912 (0.89405)	222.5222	226.5222	226.9508	229.3902	0.1757	0.2619
NAPTE	1.91332 (1.67776)	9.99821 (0.70944)	218.8185	222.8185	223.2470	225.6864	0.15716	0.3877
EE	1.47335 (0.95528)	0.14956 (0.01917)	208.8087	212.8087	213.2372	215.6766	0.13588	0.5697
R	2.36356 (0.00830)	-	236.4447	238.4447	238.5826	239.8787	0.31888	0.0026
E	0.032455 (0.00582)	-	250.5289	252.5289	252.6668	253.9629	0.39128	0.0012

4.2. Simulation Study

To acertain the consistency and stability of the estimates, the simulation study was performed by taking samples of size (n=30, 50, 100 and 200) each replicated 100 times for different parameter vectors $\alpha = (0.8, 1, 1.5, 2)$, $\theta = (0.5, 1, 1.5, 2)$, were obtained from SGEE distribution. In each case, the average values of MLEs (estimates) and the corresponding empirical mean squared errors (MSEs) and bias were considered. The simulation results are displayed in table 1 and table 2. From tables 1 and 2, it is obvious that as the sample size increases the MSE and bais decreases in all the cases.

5. Applications

To justify the validity and applicability of the SGEE distribution two real data sets have been used. The data set I is the strength of glass of the aircraft window taken from [4] and was also recently

Table 4: *MLEs and -2l, AIC, AICC, BIC , K-S statistic and P-value for data set II.*

Model	$\hat{\alpha}$	$\hat{\theta}$	-2l	AIC	AICC	BIC	K-S statistic	p-value
SGEE	1.75535 (1.39591)	1.36922 (0.14288)	106.0445	110.0445	110.2263	114.5127	0.08801	0.6590
G	0.99694 (1.68238)	4.82104 (1.02421)	106.1653	110.1653	110.2250	114.6335	0.08977	0.6275
APE	1.29960 (1.68238)	2.04747 (1.02421)	108.8658	112.8658	113.0476	117.3340	0.09277	0.5925
NAPTE	0.82534 (1.15467)	1.89659 (1.66053)	113.3371	117.3371	117.5190	121.8054	0.11192	0.3531
EE	0.82839 (2.03418)	1.89659 (0.18852)	112.5386	116.5386	116.5983	120.7727	0.10192	0.4031
R	1.08350 (0.06521)	-	118.8298	120.8298	120.8895	123.0639	0.31888	0.0026
E	0.68902 (0.08294)	-	189.4026	191.4026	191.4623	193.6367	0.36224	0.0001

reported by [2] The data set II finds its source in [14] and was also reported by [7] It is about the tensile strength (with unit in GPa) for single carbon fibers.

For comparision purpose, we compared the proposed SGEE distribution with several other models namely, gamma (G), alpha power exponential (APE) [9], noval alpha power transformed exponential (NAPTE) [6], exponentiated exponential (EE) [5], Rayleigh (R) and Exponential (E) distributions. From table (3) and (4) it is ostensive that SGEE distribution has the smallest values of the criteria -2l, AIC, AICC, BIC, K-S statistic and maximum p-value among all other distributions. Hence, we can say that the proposed model fits better for these data sets. Figure 2(i) and 3(i) display relative histograms for data set I and II respectively. Also, the Figure 2(ii) and 3(ii) shows the plots of the fitted SGEE survival function and empirical survival function of the data set I and II, respectively.

6. Concluding Remarks

A new continuous probability model based on a trigonometric function was introduced having symmetric, decreasing and positively skewed density function. Some of the well-known mathematical properties of the introduced model were also discussed. The authenticity and applicability of the introduced model was examined by considering two real data sets, it was perceived that the SGEE distribution is more appropriate for the given data sets than all other competitive models.

References

[1] Hassan, Anwar and Dar, IH and Lone, MA. A novel family of generating distributions based on trigonometric function with an application to exponential distribution. *Journal of Scientific Research*, 65(5):172-179, 2021.

[2] Ahmad Aijaz, Afaq Ahmad, and Rajnee Tripathi. Inverse analogue of ailamujia distribution with statistical properties and applications. *Asian Research Journal of Mathematics*, pages 36–46, 2020.

[3] Gauss M Cordeiro, Edwin MM Ortega, and Daniel CC da Cunha. The exponentiated generalized class of distributions. *Journal of data science*, 11(1):1–27, 2013.

[4] Edwin R Fuller Jr, Stephen W Freiman, Janet B Quinn, George D Quinn, and W Craig Carter. Fracture mechanics approach to the design of glass aircraft windows: A case study. In *Window and dome technologies and materials IV*, volume 2286, pages 419–430. International Society for Optics and Photonics, 1994.

[5] Rameshwar D Gupta and Debasis Kundu. Exponentiated exponential family: an alternative to gamma and weibull distributions. *Biometrical Journal: Journal of Mathematical Methods in Biosciences*, 43(1):117–130, 2001.

[6] Muhammad Ijaz, Wali Khan Mashwani, Atilla Göktaş, and Yuksel Akay Unvan. A novel alpha power transformed exponential distribution with real-life applications. *Journal of Applied Statistics*, pages 1–16, 2021.

[7] Farrukh Jamal, Christophe Chesneau, Dalal Lala Bouali, and Mahmood Ul Hassan. Beyond the sin-g family: The transformed sin-g family. *Plos one*, 16(5):e0250790, 2021.

[8] Ponnambalam Kumaraswamy. A generalized probability density function for double-bounded random processes. *Journal of hydrology*, 46(1-2):79–88, 1980.

[9] Abbas Mahdavi and Debasis Kundu. A new method for generating distributions with an application to exponential distribution. *Communications in Statistics-Theory and Methods*, 46(13):6543–6557, 2017.

[10] Zafar Mahmood and Christophe Chesneau. A new sine-g family of distributions: properties and applications. 2019.

[11] Albert W Marshall and Ingram Olkin. A new method for adding a parameter to a family of distributions with application to the exponential and weibull families. *Biometrika*, 84(3):641–652, 1997.

[12] SK Maurya, A Kaushik, SK Singh, and U Singh. A new class of distribution having decreasing, increasing, and bathtub-shaped failure rate. *Communications in Statistics-Theory and Methods*, 46(20):10359–10372, 2017.

[13] SK Maurya, D Kumar, SK Singh, and U Singh. One parameter decreasing failure rate distribution. *International Journal of Statistics & Economics*, 19(1):120–138, 2018.

[14] Mohammad Z Raqab, Mohamed T Madi, and Debasis Kundu. Estimation of p (y< x) for the three-parameter generalized exponential distribution. *Communications in Statistics—Theory and Methods*, 37(18):2854–2864, 2008.

[15] Luciano Souza, Wilson Junior, Cicero De Brito, Christophe Chesneau, Tiago Ferreira, and Lucas Soares. On the sin-g class of distributions: theory, model and application. *Journal of Mathematical Modeling*, 7(3):357–379, 2019.

[16] Luciano Souza, Wilson Rosa de O Júnior, Cícero Carlos R de Brito, Christophe Chesneau, Renan L Fernandes, and Tiago AE Ferreira. Tan-g class of trigonometric distributions and its applications. *CUBO, A Mathematical Journal*, 23(1):01–20, 2021.

[17] Ahmad, Aijaz and Jallal, Muzamil and Ahmad, Afaq. A novel approach for constructing distributions with an example of the Rayleigh distribution. *Reliability: Theory & Applications*, 67(1):52-64, 2022.

[18] Lone, MA and Dar, IH and Jan, TR. A new method for generating distributions with an application to Weibull distribution. *Reliability: Theory & Applications*, 67(1):223–239, 2022.

On Markov–up processes and their recurrence properties

A.Yu. Veretennikov[1)], M.A. Veretennikova[2)]

•

[1)]Institute for Information Transmission Problems, Moscow, Russia;
e-mail: ayv@iitp.ru
[2)]University of Warwick, UK;
e-mail: maveretenn@gmail.com

Abstract

A simple model of the new notion of "Markov up" processes is proposed; its positive recurrence and ergodic properties are shown under the appropriate conditions. A one-dimensional process in discrete time moves upwards as if it were Markov, and goes down in a more complicated way, remembering all its past from the moment of its "u-turn" down. Also, it is assumed that in some sense its move downwards becomes more and more probable after each step in this direction.

Keywords: Markov-up process; recurrence

MSC: 60K15

1. Introduction

The idea of integer valued processes which behave like markovian on the periods of growing and in a more complicated non-markovian way on the periods of decreasing was suggested by Alexander Dmitrievich Solovyev in a private communication in the late 90's [2]. In this phase of his research activity he only worked on applied projects. Hence, there is no doubt that this idea was also an applied one, most likely related to the theory of reliability, which was one of his main interests. To the best of the authors knowledge he did not leave any published notes on this theme. Also, the authors are not aware of any other publications devoted to this idea, although certain close models do exist in the literature. In this paper a toy model of this idea is proposed.

Consider a process $X_n, n \geq 0$ on $\mathbb{Z}_+ = \{0, 1, \ldots\}$, or on $\mathbb{Z}_{0,\bar{N}} = \{0, \ldots \bar{N}\}$ with some $0 < \bar{N} < \infty$, possessing the following property: for any $n \geq 1$ where the last jump was up (including staying), it is assumed that for some function $\phi(i,j), i, j \in \mathbb{Z}_+$,

$$\mathbb{P}(X_{n+1} = j | \mathcal{F}_n^X; X_n \geq X_{n-1}) = \phi(X_n, j), \tag{1}$$

that is, the "movement upwards remains markovian"; the "decision" to turn downwards is also markovian in the first instant; however, where the last jump was down, the next probability distribution may depend on some part of the past trajectory: namely for some function $\psi(X_n, \ldots X_{\zeta_n})$

$$\mathbb{P}(X_{n+1} = j | \mathcal{F}_n^X; X_n < X_{n-1}) = \psi(X_n, \ldots X_{\zeta_n}), \tag{2}$$

where ζ_n is the last turning time from "up" to "down" before n; it is formally defined in (3) in what follows. Hence, the "memory" of the process while moving down is limited by the last time of turning down; the latter moment may not be bounded. These assumptions reflect the property that while the process "goes up" its transition probabilities for any jump up obey the Markov property (1); as soon as it goes down, its transition probabilities "must" remember some past values of the trajectory, namely, from the last jump up moment. The case of equality $X_n = X_{n-1}$

– or staying at its place – is included in the movement up; probably it *may* be shifted to the movement down, but apparently it would change the calculus and we do not pursue studying all possibilities here at once. Also, some more complicated rules could be introduced instead of those described above; however, our goal is just to show a simplest version of the idea of a "Markov up" process and to discuss some recurrence and ergodic properties which this model may possess.

As a rationale, the model may be applied to a situation of the evolution of some involved many-component device which may have several states and which "goes up" while it is working, or it "goes down" if one or several of the critical components in this device break down, after which the evolution does not stop but becomes more and more chaotic with a likely further disbalance or even, or, at least, dependent on all the states after their break down: the device "remembers" the event of the faults in the critical components all the time until they are repaired (in the simplest example fixing is just reloading the system), after which the transmission may resume again and the behaviour becomes "markovian" again, satisfying the condition (1). There is also some evidence that certain disastrous processes related to complicated devices may expose similar features: once some critical failure occurs, the process of destruction may accelerate and be unpredictably chaotic until some rescue arrives.

Note that the probability of such a model to be at some subset in the state space could be viewed as a characteristic of the reliability of this device. Suppose that the movement "up" of the process X is treated as approaching to some goal which is a high enough level above zero, and that at any moment of time the position of X above the minimal level N brings some profit, while falling down below the level N is regarded as a failure with no dividends or even with some loss due to the expenses for repairing with the necessity to recover and to start raising up again. Then the dynamical, or instantaneous reliability of the system may be defined as the probability $r(t) := \mathbb{P}(X_t > N)$. Naturally, we are interested in computing this function $r(t)$, or, at least, its limit $r(\infty) := \lim_{t\to\infty} r(t)$, or its stationary value if the latter exists. Indeed, traditionally all features of a model are evaluated and described in a stationary regime. It is well known that very often in probability models such a limit coincides with the stationary value of $r(t)$. In such a setting the property of a positive recurrence may help to show that this invariant or limiting probability $r(\infty)$ exists. The next important question would be to find the rate of this convergence; it is not pursued in this paper. The issue of the bounds for the rate of this convergence is left until further research and publications. Here we just recall that positive recurrence is naturally linked to the existence of a stationary regime (see the corollary 6 in what follows).

The paper [3] proposes a Markov model for the daily dynamics of the Fire Weather Index (FWI), which estimates the risk of wildfire. The authors do indicate that in fact the probability of wildfire escaping will grow as the duration of a several-day intensive fire onset increases. Statistical analysis in the paper concerns the suitable order of the Markov chain. It shows that for the data analyzed mostly a Markov chain of order 1 is suitable, however sometimes order 2 is preferable. Data is limited to the province of Ontario, and the appropriate order may be different elsewhere. In our model the length of memory is not fixed, which allows greater flexibility. It also takes into account duration of the last fire onset, which may be beneficial. For example, the paper [4] supports the idea that the total area burnt by a fire is an exponential function of time after ignition. Such amplification of chaos and further imbalance is discussed in the previous paragraph about functionality of a multi-component device. Evidence of local memory dependence suggests that possibly a Markov-up process should be a reasonable model for evolution of an index which quantifies realistic damage from fire. For the process to be called Markov-up the worse the prognosis of the total damage the lower the index should be. In case of working with a variable such as FWI ranging from 0 (low danger) to 100 (extreme danger), perhaps, we could just as well introduce the notion of a "Markov-down" process, reversing the directions of jumps with the specified transition probability characteristics. For fire damage index dynamics it would be appropriate to consider a variation of the Markov-down process, in which return to Markov behaviour happens after the index reaches a 'low' danger threshold level in several sequential steps. Note that this index may also be regarded as a reliability type

characteristic where the reliability value could be defined as a probability that this index does not exceed some level. What is more, actually, the probability of each possible value of this index could be a more accurate and informative characteristic of an "extended reliability" type. The theory in this paper concerns the simplest version of a Markov-up process.

Note that according to (2) the "transition probabilities" $\mathbb{P}(X_{n+1}=j|X_n,\dots X_{\zeta_n})$ after jumps down do not depend on n, that is,

$$\mathbb{P}(X_{n+1}=j|X_n,\dots,X_{\zeta_n})|_{\zeta_n=m,X_n=a_0,\dots,X_{\zeta_n}=a_m}$$

$$=\mathbb{P}(X_{n+k+1}=j|X_{n+k},\dots,X_{\zeta_{n+k}})|_{\zeta_{n+k}=m,X_{n+k}=a_0,\dots,X_{\zeta_{n+k}}=a_m},$$

for any $m\geq 0$ and $k\geq 0$ in the case of

$$a_0>\dots>a_m,$$

where it is assumed that $X_{\zeta_n-1}\leq a_m$. Similar assumption is made about the probabilities $\mathbb{P}(X_{n+1}=j|X_n)$ after jumps up, see (1). This corresponds to the "homogeneous" situation, in which it makes sense to pose a question about ergodic properties. For the conditional probabilities after the "jumps down" the memory could be, in principle, unlimited, in the sense that it is not described by, say, m-Markov chains (i.e., with the memory of length m) except for the case of a finite $\bar{N}$. However, the process "does not remember anything which is older than the last turn down", that is, there is no dependence of future probabilities on the past earlier than time ζ_n for each n. The moment ζ_n itself is interpreted as the last jump up before the fault occurs, and all the time before the faulty component is fixed, the device keeps record of what has happened from that moment to the present time, and the transition probabilities depend on this memory. The first jump up after a series of jumps down signifies that the faulty component is fixed and, hence, movement up resumes. The movement in both directions can have several options, that is, it is not assumed that any jump up is by +1 and any jump down is with -1. Naturally, from zero there are only jumps up, or the process may stay at its place. The model with a finite $\bar{N}$ does not differ too much from the infinite version: since we are interested in bounds which would not depend on $\bar{N}$, the calculus would be very similar: the only point is that at $\bar{N}$ it should be specified what kind of jumps are possible; we do not pursue this version here assuming $\bar{N}=\infty$.

Models with more involved dependencies are possible: for example, instead of the immediate switching to "Markov" probabilities after one jump up, it could be assumed that such a switch occurs after several steps up, or after the average in time of consequent jumps up or down exceeds some level, etc. Probably, some other adjustments of the model may be performed in order to include some specific features of forest fires mentioned earlier.

We are interested in establishing ergodic properties for the model (1)–(2) under certain "recurrence" and "non-singularity" assumptions. So, recurrence is one of the key points addressed here.

There are some ideological similarities of the proposed model with renewal processes, and with a (more general) notion of Hawkes processes, and also with semi-Markov processes. Actually, this is a special case of semi-Markov type, as well as a special case of a regeneration process. Moreover, as we shall see in what follows, some transformation of the model based on the enlarged state space turns out to be a particular Markov process, which is not really surprising since, as is well-known, any process may be regarded as Markov after a certain change of the state space. Yet, this is not always useful. In any case, ergodic properties of the model are to be established from scratch, and markovian features will only be used in what concerns the invariant measure via the Harris – Khasminskii principle.

An extended abstract preceding this publication was presented at the ICMS5 conference in November 2020, see [5]. Because of many new objects, quite a few definitions will be repeatedly reminded to the reader during the text. The paper consists of five section: Introduction, The model and assumptions, Auxiliary lemmata, Main results (theorem 5 and corollary 6), Proof of theorem 5, and Proof of corollary 6.

2. The model and the assumptions

We use standard notation $a \wedge b = \min(a, b)$, $a \vee b = \max(a, b)$.

Further notations: Let us define for each $n \geq 0$ the random variables

$$\zeta_n := \inf(k \leq n : \Delta X_i := X_{i+1} - X_i < 0, \forall i = k, \dots n), \ (\inf(\emptyset) = +\infty), \tag{3}$$

$$\xi_n := \sup(k \geq n : \text{all increments } \Delta X_i \geq 0, \forall\, n \leq i \leq k) \vee n. \tag{4}$$

$$\chi_n := \sup(k \geq n : \text{all increments } \Delta X_i < 0, \forall\, n \leq i \leq k) \vee n. \tag{5}$$

Also, let

$$\hat{X}_{i,n} := X_i 1(\zeta_n \wedge n \leq i \leq n), \quad \tilde{\mathcal{F}}_n = \sigma(\zeta_n; \hat{X}_{i,n} : 0 \leq i \leq n). \tag{6}$$

Note that the family $(\tilde{\mathcal{F}}_n)$ is not a filtration, and this is not required. We have, $\tilde{\mathcal{F}}_n \subset \mathcal{F}_n$ and $1(\zeta_n \wedge n = n)\mathbb{E}(\xi|\tilde{\mathcal{F}}_n) = 1(\zeta_n \wedge n = n)\mathbb{E}(\xi|X_n)$ $\forall \xi$. Also, note that $\hat{X}_{n,n} = X_n$ for any n.

Now let us state the **assumptions** which rewrite from scratch the formulae (1) and (2).

A1. Random memory depth: *For any n,*

$$\mathbb{P}(X_{n+1} = j|\mathcal{F}_n) = \mathbb{P}(X_{n+1} = j|\tilde{\mathcal{F}}_n) \quad a.s., \tag{7}$$

and the latter conditional probability does not depend on n given the past $X_n, \dots X_{\zeta_n \wedge n}$, which serves as the analogue of the homogeneity.
The random memory depth is what clearly distinguishes the proposed model from Markov chains with a fixed memory length also known as complex Markov chains.
A2. Irreducibility (local mixing): *For any $x \leq N$ and for two states $y = x$ and $y = x + 1$*

$$\mathbb{P}(X_{n+1} = y|\tilde{\mathcal{F}}_n, X_n = x) \geq \rho > 0.$$

Note that $2\rho \leq 1$. Along with the recurrence condition, the assumption A2 will guarantee the irreducibility of the process in the extended state space where the process becomes Markov, see (15) below.
A3. Recurrence-1: *There exists $N \geq 0$ such that*

$$(\textit{jump down} \equiv (X_{n+1} < X_n)|\tilde{\mathcal{F}}_n, N < X_n) \geq \kappa_0 > 0; \tag{8}$$

$$\mathbb{P}(X_{n+1} < X_n|\tilde{\mathcal{F}}_n, N < X_n < X_{n-1}) \geq \kappa_1 > 0,$$

etc., and for any $n \geq m$

$$\mathbb{P}(X_{n+1} < X_n|\tilde{\mathcal{F}}_n, N < X_n < \ldots < X_{n-m+1}) \geq \kappa_{m-1} > 0, \ \forall\, 1 \leq m, \tag{9}$$

Note that $\kappa_0 \leq \kappa_1 \leq \dots$ Denote

$$q = 1 - \kappa_0; \quad q < 1.$$

Then

$$\mathbb{P}(\text{jump up} \equiv (X_{n+1} \geq X_n)|\tilde{\mathcal{F}}_n, N < X_n) \leq 1 - \kappa_0 = q < 1.$$

A4. Recurrence-2: *It is assumed that the following infinite product converges*

$$\bar{\kappa}_\infty := \prod_{i=0}^{\infty} \kappa_i > 0; \tag{10}$$

and

$$\sum_{i\geq 1} i(1-\kappa_i) < \infty. \tag{11}$$

Let

$$\bar{q} := 1 - \bar{\kappa}_\infty (< 1) \quad \& \quad q := 1 - \kappa_0 \quad (< 1).$$

Note that

$$\mathbb{P}(\text{jump up} \equiv (X_{n+1} \geq X_n) | \tilde{\mathcal{F}}_n, N < X_n) \leq 1 - \kappa_0 = \bar{\kappa}_0 = q < 1.$$

A5. Jump up moment bound:

$$M_1 := \operatorname*{ess\,sup}_{\mathbb{P}} \sup_{\omega} \sup_{n} \mathbb{E}((X_{n+1} - X_n)_+ | \tilde{\mathcal{F}}_n) < \infty. \tag{12}$$

Let

$$\bar{q} = 1 - \bar{\kappa}_\infty \ (< 1).$$

This is the upper bound for the probability that the fall down is not successful, i.e., that the "floor" $[0, N]$ is not reached in one go.

Denote

$$\bar{\kappa}_m := \prod_{i=0}^{m} \kappa_i \quad (\geq \bar{\kappa}_\infty > 0).$$

Let us emphasize that the index i in κ_i is not the state where the process X is, but the value for how long the process is falling down. The process remembers for how long it has been going down so far, and the longer it goes down the more probable is to continue in this direction, at least, until the process reaches $[0, N]$. Equivalently,

$$\sum \ln \kappa_i < \infty.$$

Of course, this implies that $\kappa_i \to 1$ as $i \to \infty$, which is, clearly, a weaker condition than (10). Convergence of the sequence κ_i to 1, if it is monotonic, may be interpreted in a way that the longer the decreasing trajectory, the more faulty components in the device: each jump down makes some additional disorder in the system, which further increases the probability to continue falling down.

Example 1. *The assumption (11) is satisfied, for example, under the condition* $1 - \kappa_m \leq \frac{C}{m^3}$, *or, equivalently,*

$$\kappa_m \geq 1 - \frac{C}{m^3}.$$

An exponential rate of the approach of the sequence κ_m *to* 1 *accepted in some applied models of a fire evolution could be interpreted as the inequality*

$$\kappa_m \geq 1 - \exp(-\lambda m)$$

with some $\lambda > 0$.

The assumption (12) is valid, for example, if there exists a nonrandom constant $C \geq 0$ *such that with probability one*

$$X_{n+1} - X_n \leq C < \infty.$$

Denote

$$\tau = \tau^1 := \inf(t \geq 0 : X_t \leq N); \ \gamma := \inf(t \geq \tau : X_{t-1} \leq X_t = N).$$

The regeneration occurs not at moment τ, but at moment γ. However, the expectation of γ may be evaluated via $\mathbb{E}_x\tau$. Hence, it will be useful to introduce the following two sequences of stopping times with respect to the filtration $\mathcal{F}_n^X$ by induction:

$$T^n := \inf(t > \tau^n : X_t > N), \quad \tau^{n+1} := \inf(t > T^n : X_t \le N).$$

The convention. With the initial position $X_0 = x$ we assume that any artificial "admissible past" is allowed, that is, we accept that there is some fictitious past which could have preceded this state; we include in this past nothing if the artificial state X_{-1} does not exceed X_0, or we add the fictitious past trajectory from the last starting moment of the fall ζ_0: $X_{\zeta_0}, \dots, X_{-1}$. From the assumption (A1) it follows that the process $(Y_n, \mathcal{F}_n^Y)$ is Markov; of course, $\mathcal{F}_n^Y = \mathcal{F}_n^X$.

Let us recall the definitions of Greeks:

$$\zeta_n := \inf(k \le n : \Delta X_i := X_{i+1} - X_i < 0, \forall i = k, \dots n) \qquad (\inf(\emptyset) = \infty);$$

$$\hat{X}_{i,n} := X_i 1(\zeta_n \wedge n) \le i \le n), \quad \tilde{\mathcal{F}}_n = \sigma(\zeta_n; \hat{X}_{i,n} : 0 \le i \le n);$$
$$\xi_n := \sup(k \ge n : \text{all increments } \Delta X_i \ge 0, \forall\, n \le i \le k) \vee n;$$
$$\chi_n := \sup(k \ge n : \text{all increments } \Delta X_i < 0, \forall\, n \le i \le k) \vee n.$$

3. Auxiliary lemmata

Lemma 2. *Under the assumption (A3) for any $x > N$,*

$$\mathbb{E}_x(\xi_0 - 0) \le M_2 = \frac{q}{(1-q)^2}.$$

Proof. Recall that the random variable ξ_n was defined by the formula

$$\xi_n := \sup(k \ge n : \text{all increments } \Delta X_i \ge 0, \forall\, n \le i \le k) \vee n.$$

We use the notations from the proof of lemma 4 (below): for $i \ge n$ let

$$e_i = 1(X_{i+1} \ge X_i),\ \bar{e}_i = 1(X_{i+1} < X_i),\ \Delta X_i = X_{i+1} - X_i,\ \ell_n^i = \bar{e}_i \prod_{k=n}^{i-1} e_k \ (\text{assume } \prod_{n}^{n-1} = 1).$$

The bounds in this lemma and in the other lemmata will not depend on the initial state x, so we drop this index in $\mathbb{E}_x$ and $\mathbb{P}_x$ in this section (but not in the proof of the main result). We have, for $i \ge n$

$$\mathbb{E}_x(e_i | X_i > N) = \mathbb{P}(X_{i+1} \ge X_i | X_i > N)$$

$$= \mathbb{E}_x(\mathbb{P}_x(X_{i+1} \ge X_i | \tilde{\mathcal{F}}_i, X_i > N) | X_i > N) \le 1 - \kappa_0 = q.$$

Then almost surely

$$\xi_n - n = \sum_{k=0}^{\infty} k\bar{e}_{n+k} \prod_{i=n}^{n+k-1} e_i = \sum_{k=1}^{\infty} k\bar{e}_{n+k} \prod_{i=n}^{n+k-1} e_i = \sum_{k=1}^{\infty} k\ell_n^{n+k}.$$

So, we estimate,

$$\mathbb{E}_x(\xi_n - n) = \mathbb{E} \sum_{k=1}^{\infty} k\bar{e}_{n+k} \prod_{i=n}^{n+k-1} e_i \le \sum_{k=1}^{\infty} k\mathbb{E}_x \prod_{i=n}^{n+k-1} e_i$$

$$\le \sum_{k=1}^{\infty} kq^k = q \sum_{k=1}^{\infty} kq^{k-1} = \frac{q}{(1-q)^2} := M_2 < \infty. \qquad \text{QED}$$

Let us recall,

$$\tau := \inf(t \geq 0 : X_t \leq N), \quad \chi_n := \sup(k \geq n : \text{all increments } \Delta X_i < 0, \forall\, n \leq i \leq k) \vee n,$$

and

$$\mathbb{P}_x(X_{n+1} < X_n | \tilde{\mathcal{F}}_n, N < X_n < \ldots < X_{n-m+1}) \geq \kappa_{m-1} > 0, \quad \forall\, 1 \leq m,$$

and also

$$\chi_n := \sup(k \geq n : \text{all increments } \Delta X_i < 0, \forall\, n \leq i \leq k) \vee n.$$

Lemma 3. *Under the assumptions (A3)-(A4), for any $x > N$, ($n = 0$)*

$$\mathbb{E}_x(\chi_n - n)1(\chi_n < \tau) \leq \sum_{i \geq 1} i(1 - \kappa_i) := M_3 < \infty.$$

Proof. Similarly to the calculus of the previous lemma but with the replacement of e_i by $\bar{e}_i$ and vice versa, we have

$$(\chi_n - n)1(\chi_n < \tau) \leq \sum_{k=1}^{\infty} k e_{n+k} 1(n + k - 1 < \tau) \prod_{i=n}^{n+k-1} \bar{e}_i,$$

so,

$$\mathbb{E}_x(\chi_n - n)1(\chi_n < \tau) \leq \mathbb{E}_x \sum_{k=1}^{\infty} k e_{n+k} 1(n + k - 1 < \tau) \prod_{i=n}^{n+k-1} \bar{e}_i$$

$$\leq \sum_{k=1}^{\infty} k \mathbb{E}_x 1(n + k - 1 < \tau)(\prod_{i=n}^{n+k-1} \bar{e}_i) \mathbb{E}_x(e_{n+k} | \Delta X_i < 0, 0 \leq i \leq n + k - 1)$$

$$\overset{A3}{\leq} \sum_{k=1}^{\infty} k \mathbb{E}_x 1(n + k - 1 < \tau)(\prod_{i=n}^{n+k-1} \bar{e}_i)(1 - \kappa_k) \leq \sum_{k=1}^{\infty} k(1 - \kappa_k) =: M_3 \overset{A4}{<} \infty. \quad \text{QED}$$

Let us recall once more,

$$\xi_n := \sup(k \geq n : \text{all increments } \Delta X_i \geq 0, \forall\, n \leq i \leq k) \vee n.$$

Lemma 4. *Under the assumptions (A3) and (A5) the expected value of the maximum positive increment over any single period of running up (non-strictly) until the first jump down is finite:*

$$\sup_{n,x} \mathbb{E}_x(X_{\xi_n} - X_n)_+ \leq M_4 < \infty.$$

Proof. First of all, it suffices to show that

$$\sup_{n,x} \mathbb{E}_x(X_{\xi_n} - X_n)_+ | \tilde{\mathcal{F}}_n) \leq M_4 < \infty.$$

Further, we have

$$\sup_{n,x} \mathbb{E}_x((X_{\xi_n} - X_n)_+ | \tilde{\mathcal{F}}_n, X_n \leq N) \leq N + \sup_{n,x} \mathbb{E}_x((X_{\xi_n} - X_n)_+ | \tilde{\mathcal{F}}_n, X_n > N).$$

Hence, it suffices to show only

$$\sup_{n,x} \mathbb{E}_x((X_{\xi_n} - X_n)_+ | \tilde{\mathcal{F}}_n, X_n > N) \leq M < \infty \qquad (a.s.)$$

In other words, it is sufficient to establish for $n = 0$ that

$$\sup_{x>N} \mathbb{E}_x (X_{\xi_0} - x)_+ \le M < \infty.$$

With the same notations $e_i = 1(X_{i+1} \ge X_i)$, $\bar{e}_i = 1(X_{i+1} < X_i)$, $\Delta X_i = X_{i+1} - X_i$, $\ell_n^i = \bar{e}_i \times \prod_{k=n}^{i-1} e_k$ we have,

$$\mathbb{E}_x (X_{\xi_n} - X_n)_+ = \mathbb{E}_x \sum_{i=n+1}^{\infty} \ell_n^i (X_i - X_n) = \sum_{i=n+1}^{\infty} \mathbb{E}_x \ell_n^i (X_i - X_n)$$

(assuming that the latter sum converges; note that all its terms are non-negative). Further,

$$\mathbb{E}_x \ell_n^i (X_i - X_n) = \mathbb{E}_x (\ell_n^i \sum_{j=n}^{i-1} \Delta X_j) = \sum_{j=n}^{i-1} \mathbb{E}_x \ell_n^i \Delta X_j$$

For each single term in this sum we have ($n \le j \le i-1$)

$$\mathbb{E}_x \ell_n^i \Delta X_j = \mathbb{E}_x \mathbb{E}_{\mathcal{F}_{j+1}} (\prod_{k=n}^{j} e_k) \Delta X_j (\prod_{k'=j+1}^{i-1} e_{k'}) = \mathbb{E} (\prod_{k=n}^{j} e_k) \Delta X_j \mathbb{E}_{\mathcal{F}_{j+1}} (\prod_{k'=j+1}^{i-1} e_{k'})$$

$$= \mathbb{E}_x (\prod_{k=n}^{j} e_k) \Delta X_j \mathbb{E}_{\tilde{\mathcal{F}}_{j+1}} (\prod_{k'=j+1}^{i-1} e_{k'}) \overset{(A3)}{\le} \mathbb{E}_x (\prod_{k=n}^{j} e_k) \Delta X_j \times q^{i-j-1}$$

$$= q^{i-j-1} \mathbb{E}_x (\prod_{k=n}^{j-1} e_k) \mathbb{E}_{\mathcal{F}_j} e_j \Delta X_j = q^{i-j-1} \mathbb{E}_x (\prod_{k=n}^{j-1} e_k) \mathbb{E}_{\tilde{\mathcal{F}}_j} e_j \Delta X_j$$

$$\overset{(A5)}{\le} M_1 q^{i-j-1} \mathbb{E}_x (\prod_{k=n}^{j-1} e_k) \le M_1 q^{i-j-1} q^{j-n} = M_1 q^{i-n-1}.$$

Hence,

$$\mathbb{E}_x \ell_n^i (X_i - X_n) = \sum_{j=n}^{i-1} \mathbb{E}_x \ell_n^i \Delta X_j \le \sum_{j=n}^{i-1} M_1 q^{i-n-1} = (i-n) M_1 q^{i-n-1}$$

and so

$$\mathbb{E}_x (X_{\xi_n} - X_n)_+ \le M_1 \sum_{i=n+1}^{\infty} (i-n) q^{i-n-1} =: M_4 < \infty,$$

as required. Lemma 4 is proved. QED

4. Main results

Theorem 5. *Under the assumptions (A1) – (A5) there exist constants $C_1, C_2 > 0$ such that*

$$\mathbb{E}_x \tau \le x + C_1. \tag{13}$$

and there exist constants $C_2, C_3 > 0$ such that

$$\mathbb{E}_x \gamma \le C_2 x + C_3. \tag{14}$$

Here $C_1 \le \frac{M_4 \bar{q}}{1-\bar{q}}$.

Corollary 6. *Under the assumptions of the theorem 5 the process X_n has a stationary measure.*

5. Proof of theorem 5

0. First of all let us state the idea of the proof. We will establish the property of recurrence towards the interval $[0, N]$ due to the recurrence assumptions, which property holds true despite the non-markovian behaviour. Further, inside $[0, N]$ coupling holds true on each step with a positive probability bounded away from zero on the jump up (or stay); after such a coupling, the process does not remember its past given the present before it started falling down. Hence, de-coupling is not possible.

Formally, let us make the process (strong) Markov by extending its state space. For this aim it suffices to define

$$Y_n := X_n 1(X_n \geq X_{n-1}) + (X_n, \dots X_{\zeta_n})^T 1(X_n < X_{n-1}) \equiv (X_n, \dots X_{\zeta_n \wedge n})^T \tag{15}$$

(here T stands for the transposition; recall that $\zeta_n < n$ in case of $X_n < X_{n-1}$; in any case, the vector Y_n is of a finite, but variable dimension which is random).

1. Recurrence. Due to (10), from *any* state $y > N$ there is a positive probability to attain the set $[0, N]$ in a single monotonic fall down with no stopovers with a probability no less than $\bar{\kappa}_\infty$. The time required for such a monotonic trajectory from y to $[0, N]$ is no more than $y - N - 1$. However, other scenarios are possible with stopovers and temporary runs up. Hence, to evaluate the expected value of τ some calculus is needed.

Let us establish the bound (13).

$$\mathbb{E}_x \tau \leq x + C. \tag{16}$$

If $x \leq N$, then $\tau = 0$ and the bound is trivial. Let $x > N$. Recall that slightly abusing notations we only write down the initial position x, while in fact there might be some non-trivial prehistory $\tilde{\mathcal{F}}_0$. The process may start descending straight away, or after several steps up (or after staying at state x for some time). In the latter case the position X_{ξ_0} from which the descent starts admits the bound

$$(\mathbb{E}_x X_{\xi_0} - x)_+ \leq M_4$$

(see lemma 4).

Case I: at $t = 0$ the process is falling down.
Let us define stopping times

$$t_0 = T_0 = 0,\ T_1 = \chi_{t_0},\ t_1 = \xi_{T_1},\ T_2 = \chi_{t_1},\ t_2 = \xi_{T_2},\ T_3 = \chi_{t_2}, \dots$$

In words, T_i is the end of the next partial fall after t_{i-1}; t_i is the end of the next run up after T_i. There might be a.s. finitely many excursions down and up, and the last fall down will finish at $[0, N]$.

Let us recall that

$$\xi_n := \max(k \geq n : \text{all increments } \Delta X_i \geq 0,\ \forall\, n \leq i \leq k) \vee n,$$

and

$$\chi_n := \max(k \geq n : \text{all increments } \Delta X_i < 0,\ \forall\, n \leq i \leq k) \vee n.$$

We have $\forall x > N$

$$\mathbb{E}_x(\xi_0 - 0) \leq \sum_i i q^i =: M_2.$$

and $\forall x > N$

$$\mathbb{E}_x(\chi_0 - 0) \leq M_3.$$

Note that

$$T_i - t_{i-1} \leq X_{t_{i-1}}.$$

Denote by A_i ($i \geq 1$) the event of precisely $i-1$ unsuccessful attempts to descend to the floor $[0, N]$, after which on the ith attempt it does attain the floor; by B_j let us denote jth unsuccessful attempt to fall down until reaching the floor $[0, N]$ (probability that it is unsuccessful is less that $\bar{q} < 1$); B_j^c is the event where the jth fall down is successful. Then we have $\tau = T_i$ on $A_i = (\bigcap_{1\leq j\leq i-1} B_j) \bigcap B_i^c$. The probability of A_i does not exceed $\bar{q}^{i-1}$. (Recall, $\bar{q} = 1 - \bar{\kappa}_\infty$.) So, we estimate,

$$\mathbb{E}_x\tau = \sum_{i\geq 1}\mathbb{E}_x\tau 1(A_i) \leq \sum_{i\geq 1}\mathbb{E}_x 1(A_i)T_i = \sum_{i\geq 1}\mathbb{E}_x 1(\bigcap_{1\leq j\leq i-1} B_j)\bigcap B_i^c)T_i$$

$$\stackrel{2}{=} \sum_{i\geq 1}\mathbb{E}_x\left(\prod_{1\leq j\leq i-1} 1(B_j)\right)1(B_i^c)T_i \stackrel{3}{=} \sum_{i\geq 1}\mathbb{E}_x\mathbb{E}_{\mathcal{F}_{t_{i-1}}}\left(\prod_{1\leq j\leq i-1} 1(B_j)\right)1(B_i^c)T_i$$

$$\stackrel{4}{=} \sum_{i\geq 1}\mathbb{E}_x\left(\prod_{1\leq j\leq i-1} 1(B_j)\right)\mathbb{E}_{\mathcal{F}_{t_{i-1}}}1(B_i^c)T_i$$

$$\stackrel{5}{=} \sum_{i\geq 1}\mathbb{E}_x\left(\prod_{1\leq j\leq i-1} 1(B_j)\right)\mathbb{E}_{\mathcal{F}_{t_{i-1}}}1(B_i^c)(T_i - t_{i-1} + t_{i-1})$$

$$\stackrel{6}{=} \sum_{i\geq 1}\mathbb{E}_x\left(\prod_{1\leq j\leq i-1} 1(B_j)\right)1(B_i^c)t_{i-1} + \sum_{i\geq 1}\mathbb{E}_x\left(1\prod_{1\leq j\leq i-1}(B_j)\right)\mathbb{E}_{\mathcal{F}_{t_{i-1}}}1(B_i^c)(T_i - t_{i-1})$$

$$\stackrel{7}{\leq} \sum_{i\geq 1}\mathbb{E}_x\left(\prod_{1\leq j\leq i-1} 1(B_j)\right)1(B_i^c)t_{i-1} + \sum_{i\geq 1}\mathbb{E}_x\left(1\prod_{1\leq j\leq i-1}(B_j)\right)\mathbb{E}_{\mathcal{F}_{t_{i-1}}}1(B_i^c)X_{t_{i-1}}$$

$$\stackrel{8}{\leq} \sum_{i\geq 1}\mathbb{E}_x\left(\prod_{1\leq j\leq i-1} 1(B_j)\right)1(B_i^c)t_{i-1} + \sum_{i}\mathbb{E}_x\left(\prod_{1\leq j\leq i-1} 1(B_j)\right)1(B_i^c)X_{t_{i-1}}.$$

Note that $B_j \in \mathcal{F}_{T_j}$. We are going to show that

$$\sum_{i\geq 1}\mathbb{E}_x\left(\prod_{1\leq j\leq i-1} 1(B_j)\right)t_{i-1} \leq C \tag{17}$$

and

$$\sum_{i\geq 1}\mathbb{E}_x\left(\prod_{1\leq j\leq i-1} 1(B_j)\right)1(B_i^c)X_{t_{i-1}} \leq x + C. \tag{18}$$

Step 1.

$$t_{i-1} = (t_{i-1} - T_{i-1}) + (T_{i-1} - t_{i-2}) + ... + (T_1 - t_0) + (t_0 - T_0).$$

We have

$$\mathbb{E}_x\left(\prod_{1\leq j\leq i-1} 1(B_j)\right)(t_{i-1} - T_{i-1}) = \mathbb{E}_x\mathbb{E}_{\mathcal{F}_{T_{i-1}}}\left(\prod_{1\leq j\leq i-1} 1(B_j)\right)(t_{i-1} - T_{i-1})$$

$$= \mathbb{E}_x\left(\prod_{1\leq j\leq i-1} 1(B_j)\right)\mathbb{E}_{\mathcal{F}_{T_{i-1}}}(t_{i-1} - T_{i-1}) \stackrel{lemma\,1}{\leq} M_2\mathbb{E}_x\left(\prod_{1\leq j\leq i-1} 1(B_j)\right) \leq M_2\bar{q}^{i-1};$$

also,

$$\mathbb{E}_x\left(\prod_{1\le j\le i-1}1(B_j)\right)(T_{i-1}-t_{i-2})=\mathbb{E}_x\mathbb{E}_{\mathcal{F}_{t_{i-2}}}\left(\prod_{1\le j\le i-1}1(B_j)\right)(T_{i-1}-t_{i-2})$$

$$=\mathbb{E}_x\left(\prod_{1\le j\le i-2}1(B_j)\right)\mathbb{E}_{\mathcal{F}_{t_{i-2}}}1(B_{i-1})(T_{i-1}-t_{i-2})\overset{lemma\,2}{\le}M_3\mathbb{E}_x\left(\prod_{1\le j\le i-2}1(B_j)\right)\le M_3\bar{q}^{i-2};$$

further,

$$\mathbb{E}_x\left(\prod_{1\le j\le i-1}1(B_j)\right)(t_{i-2}-T_{i-2})=\mathbb{E}_x\left(\prod_{1\le j\le i-2}1(B_j)\right)(t_{i-2}-T_{i-2})\mathbb{E}_{\mathcal{F}_{t_{i-1}}}1(B_{i-1})$$

$$\le\bar{q}\,\mathbb{E}_x\left(\prod_{1\le j\le i-2}1(B_j)\right)(t_{i-2}-T_{i-2})\le\bar{q}M_2\bar{q}^{i-2}=M_2\bar{q}^{i-1},$$

and

$$\mathbb{E}_x\left(\prod_{1\le j\le i-1}1(B_j)\right)(T_{i-2}-t_{i-3})=\mathbb{E}_x\mathbb{E}_{\mathcal{F}_{T_{i-2}}}\left(\prod_{1\le j\le i-1}1(B_j)\right)(T_{i-2}-t_{i-3})$$

$$=\mathbb{E}_x\left(\prod_{1\le j\le i-2}1(B_j)\right)(T_{i-2}-t_{i-3})\mathbb{E}_{\mathcal{F}_{T_{i-2}}}1(B_{i-1})$$

$$\le\bar{q}\mathbb{E}_x\left(\prod_{1\le j\le i-2}1(B_j)\right)(T_{i-2}-t_{i-3})\le\bar{q}M_3\bar{q}^{i-3}=M_3\bar{q}^{i-2};$$

etc. By induction we obtain

$$\mathbb{E}_x\left(\prod_{1\le j\le i-1}1(B_j)\right)t_{i-1}\le iM_2\bar{q}^{i-1}+(i-1)M_3\bar{q}^{i-2}.$$

Hence, the first desired inequality (17) is true,

$$\sum_i\mathbb{E}_x\left(\prod_{1\le j\le i-1}1(B_j)\right)t_{i-1}\le M_2\sum_{i\ge1}(i-1)\bar{q}^{i-1}+M_3\sum_{i\ge2}(i-2)\bar{q}^{i-1}=:C<\infty.$$

Step 2. Note that $X_{t_j}\ge X_{T_j}$, so that $X_{t_j}-X_{t_{j-1}}\le X_{t_j}-X_{T_j}$. Also, in the case under the consideration $X_{t_0}=x$. Hence, we have,

$$X_{t_{i-1}}=(X_{t_{i-1}}-X_{t_{i-2}})+\ldots+(X_{t_1}-X_{t_0})+(X_{t_0}-x)+x.$$

So,

$$\mathbb{E}_x \left(\prod_{1\le j\le i-1} 1(B_j) \right) 1(B_i^c) X_{t_{i-1}}$$

$$= \mathbb{E}_x \left(\prod_{1\le j\le i-1} 1(B_j) \right) 1(B_i^c) \left(x + (X_{t_0} - x) + \sum_{k=1}^{i-1} (X_{t_k} - X_{t_{k-1}}) \right)$$

$$\le \mathbb{E}_x \left(\prod_{1\le j\le i-1} 1(B_j) \right) 1(B_i^c) \left(x + \sum_{k=1}^{i-1} (X_{t_k} - X_{T_k}) \right)$$

$$= x \times \mathbb{E}_x \prod_{1\le j\le i-1} 1(B_j) 1(B_i^c) + \mathbb{E}_x \left(\prod_{1\le j\le i-1} 1(B_j) \right) 1(B_i^c) \sum_{k=1}^{i-1} (X_{t_k} - X_{T_k})$$

$$\le x \times \mathbb{E}_x \prod_{1\le j\le i-1} 1(B_j) 1(B_i^c) + \mathbb{E}_x \left(\prod_{1\le j\le i-1} 1(B_j) \right) \sum_{k=1}^{i-1} (X_{t_k} - X_{T_k}).$$

For any $1 \le k \le i-1$ we estimate

$$\mathbb{E}_x \left(\prod_{1\le j\le i-1} 1(B_j) \right) (X_{t_k} - X_{T_k}) = \mathbb{E}_x \mathbb{E}_{\mathcal{F}_{t_k}} \left(\prod_{1\le j\le i-1} 1(B_j) \right) (X_{t_k} - X_{T_k})$$

$$= \mathbb{E}_x \left(\prod_{1\le j\le k} 1(B_j) \right) (X_{t_k} - X_{T_k}) \mathbb{E}_{\mathcal{F}_{t_k}} \left(\prod_{k+1\le j\le i-1} 1(B_j) \right)$$

$$\le \mathbb{E}_x \left(\prod_{1\le j\le k} 1(B_j) \right) (X_{t_k} - X_{T_k}) \bar{q}^{i-k-1} = \bar{q}^{i-k-1} \mathbb{E}_x \left(\prod_{1\le j\le k} 1(B_j) \right) \mathbb{E}_{\mathcal{F}_{T_k}} (X_{t_k} - X_{T_k})$$

$$\overset{lemma\,3}{\le} M_4 \bar{q}^{i-k-1} \mathbb{E}_x \left(\prod_{1\le j\le k} 1(B_j) \right) \le M_4 \bar{q}^{i-k-1+k} = M_4 \bar{q}^{i-1}.$$

Therefore, since $1 = \sum_i \left(\prod_{1\le j\le i-1} 1(B_j) \right) 1(B_i^c)$ a.s., we get

$$\sum_i \mathbb{E}_x \left(\prod_{1\le j\le i-1} 1(B_j) \right) 1(B_i^c) X_{t_{i-1}}$$

$$\le x \mathbb{E}_x \sum_i \prod_{1\le j\le i-1} 1(B_j) 1(B_i^c) + M_4 \sum_i i \bar{q}^{i-1} \le x + \frac{M_4}{1-\bar{q}}.$$

This shows (18), as required.

Case II: at $t = 0$ the process is going up. Let us define stopping times

$$T_0 = 0,\ t_0 = \xi_0,\ T_1 = \chi_{t_0},\ t_1 = T_1 + \xi_{T_1},\ T_2 = t_1 + \chi_{t_1},\ \dots$$

(T_i is the end of the next partial fall after t_{i-1}; t_i is the end of the next run up after T_i. There might be a.s. finitely many excursions down and up, and the last fall down will finish at $[0, N]$.) We have,

$$t_{i-1} = (t_{i-1} - T_{i-1}) + (T_{i-1} - t_{i-2}) + ... + (T_1 - t_0) + (t_0 - T_0).$$

So, we estimate

$$\mathbb{E}_x \tau = \sum_{i\ge 1} \mathbb{E}_x \tau 1(A_i) = \sum_{i\ge 1} \mathbb{E}_x 1(A_i) T_i = \sum_{i\ge 1} \mathbb{E}_x 1(\bigcap_{1\le j\le i-1} B_j) \bigcap B_i^c) T_i$$

$$\stackrel{2}{=} \sum_{i\ge 1} \mathbb{E}_x \left(\prod_{1\le j\le i-1} 1(B_j) \right) 1(B_i^c) T_i \stackrel{3}{=} \sum_{i\ge 1} \mathbb{E}_x \mathbb{E}_{\mathcal{F}_{t_{i-1}}} \left(\prod_{1\le j\le i-1} 1(B_j) \right) 1(B_i^c) T_i$$

$$\stackrel{4}{=} \sum_{i\ge 1} \mathbb{E}_x \left(\prod_{1\le j\le i-1} 1(B_j) \right) \mathbb{E}_{\mathcal{F}_{t_{i-1}}} 1(B_i^c) T_i$$

$$\stackrel{5}{=} \sum_{i\ge 1} \mathbb{E}_x \left(\prod_{1\le j\le i-1} 1(B_j) \right) \mathbb{E}_{\mathcal{F}_{t_{i-1}}} 1(B_i^c)(T_i - t_{i-1} + t_{i-1})$$

$$\stackrel{6}{=} \sum_{i\ge 1} \mathbb{E}_x \left(\prod_{1\le j\le i-1} 1(B_j) \right) 1(B_i^c) t_{i-1} + \sum_{i\ge 1} \mathbb{E}_x \left(1 \prod_{1\le j\le i-1} (B_j) \right) \mathbb{E}_{\mathcal{F}_{t_{i-1}}} 1(B_i^c)(T_i - t_{i-1})$$

$$\stackrel{7}{\le} \sum_{i\ge 1} \mathbb{E}_x \left(\prod_{1\le j\le i-1} 1(B_j) \right) 1(B_i^c) t_{i-1} + \sum_{i\ge 1} \mathbb{E}_x \left(1 \prod_{1\le j\le i-1} (B_j) \right) \mathbb{E}_{\mathcal{F}_{t_{i-1}}} 1(B_i^c) X_{t_{i-1}}$$

$$\stackrel{8}{\le} \sum_{i\ge 1} \mathbb{E}_x \left(\prod_{1\le j\le i-1} 1(B_j) \right) 1(B_i^c) t_{i-1} + \sum_{i\ge 1} \mathbb{E}_x \left(\prod_{1\le j\le i-1} 1(B_j) \right) 1(B_i^c) X_{t_{i-1}}$$

Note that $B_j \in \mathcal{F}_{T_j}$. We are going to show that

$$\sum_{i\ge 1} \mathbb{E}_x \left(\prod_{1\le j\le i-1} 1(B_j) \right) t_{i-1} \le C \tag{19}$$

and

$$\sum_{i\ge 1} \mathbb{E}_x \left(\prod_{1\le j\le i-1} 1(B_j) \right) 1(B_i^c) X_{t_{i-1}} \le x + C. \tag{20}$$

Step 3. We have

$$\mathbb{E}_x \left(\prod_{1\le j\le i-1} 1(B_j) \right) (t_{i-1} - T_{i-1}) = \mathbb{E}_x \mathbb{E}_{\mathcal{F}_{T_{i-1}}} \left(\prod_{1\le j\le i-1} 1(B_j) \right) (t_{i-1} - T_{i-1})$$

$$= \mathbb{E}_x \left(\prod_{1\le j\le i-1} 1(B_j) \right) \mathbb{E}_{\mathcal{F}_{T_{i-1}}} (t_{i-1} - T_{i-1}) \stackrel{lemma\,1}{\le} M_2 \mathbb{E}_x \left(\prod_{1\le j\le i-1} 1(B_j) \right) \le M_2 \bar{q}^{i-1},$$

and

$$\mathbb{E}_x\left(\prod_{1\le j\le i-1}1(B_j)\right)(T_{i-1}-t_{i-2})=\mathbb{E}_x\mathbb{E}_{\mathcal{F}_{t_{i-2}}}\left(\prod_{1\le j\le i-1}1(B_j)\right)(T_{i-1}-t_{i-2})$$

$$=\mathbb{E}_x\left(\prod_{1\le j\le i-2}1(B_j)\right)\mathbb{E}_{\mathcal{F}_{t_{i-2}}}1(B_{i-1})(T_{i-1}-t_{i-2})\overset{lemma\,2}{\le}M_3\mathbb{E}_x\left(\prod_{1\le j\le i-2}1(B_j)\right)\le M_3\bar{q}^{i-2};$$

further,

$$\mathbb{E}_x\left(\prod_{1\le j\le i-1}1(B_j)\right)(t_{i-2}-T_{i-2})=\mathbb{E}_x\left(\prod_{1\le j\le i-2}1(B_j)\right)(t_{i-2}-T_{i-2})\mathbb{E}_{\mathcal{F}_{t_{i-1}}}1(B_{i-1})$$

$$\le\bar{q}\,\mathbb{E}_x\left(\prod_{1\le j\le i-2}1(B_j)\right)(t_{i-2}-T_{i-2})\le\bar{q}M_2\bar{q}^{i-2}=M_2\bar{q}^{i-1};$$

$$\mathbb{E}_x\left(\prod_{1\le j\le i-1}1(B_j)\right)(T_{i-2}-t_{i-3})=\mathbb{E}_x\mathbb{E}_{\mathcal{F}_{T_{i-2}}}\left(\prod_{1\le j\le i-1}1(B_j)\right)(T_{i-2}-t_{i-3})$$

$$=\mathbb{E}_x\left(\prod_{1\le j\le i-2}1(B_j)\right)(T_{i-2}-t_{i-3})\mathbb{E}_{\mathcal{F}_{T_{i-2}}}1(B_{i-1})$$

$$\le\bar{q}\mathbb{E}_x\left(\prod_{1\le j\le i-2}1(B_j)\right)(T_{i-2}-t_{i-3})\le\bar{q}M_3\bar{q}^{i-3}=M_3\bar{q}^{i-2};$$

etc. By induction we obtain

$$\mathbb{E}_x\left(\prod_{1\le j\le i-1}1(B_j)\right)t_{i-1}\le iM_2\bar{q}^{i-1}+(i-1)M_3\bar{q}^{i-2}.$$

Hence, the first desired inequality (19) is true,

$$\sum_{i\ge1}\mathbb{E}_x\left(\prod_{1\le j\le i-1}1(B_j)\right)t_{i-1}\le M_2\sum_{i\ge1}i\bar{q}^{i-1}+M_3\sum_{i\ge2}(i-1)\bar{q}^{i-1}=:C<\infty.$$

Step 4. Note that $X_{T_0}=x$, and

$$X_{t_{i-1}}\le x+\sum_{j=1}^{i-1}(X_{t_j}-X_{T_j}).$$

So, we have,

$$\mathbb{E}_x\left(\prod_{1\le j\le i-1}1(B_j)\right)1(B_i^c)X_{t_{i-1}}\le\mathbb{E}_x\left(\prod_{1\le j\le i-1}1(B_j)\right)1(B_i^c)\left(x+\sum_{j=1}^{i-1}(X_{t_j}-X_{T_j})\right)$$

$$=x\mathbb{E}_x\prod_{1\le j\le i-1}1(B_j)1(B_i^c)+\mathbb{E}_x\left(\prod_{1\le j\le i-1}1(B_j)\right)1(B_i^c)\sum_{j=1}^{i-1}(X_{t_j}-X_{T_j})$$

$$\le x\mathbb{E}_x\prod_{1\le j\le i-1}1(B_j)1(B_i^c)+\mathbb{E}_x\left(\prod_{1\le j\le i-1}1(B_j)\right)\sum_{k=1}^{i-1}(X_{t_k}-X_{T_k}).$$

For any $1 \le k \le i-1$ we estimate

$$\mathbb{E}_x \left(\prod_{1\le j\le i-1} 1(B_j) \right) (X_{t_k} - X_{T_k}) = \mathbb{E}_x \mathbb{E}_{\mathcal{F}_{t_k}} \left(\prod_{1\le j\le i-1} 1(B_j) \right) (X_{t_k} - X_{T_k})$$

$$= \mathbb{E}_x \left(\prod_{1\le j\le k} 1(B_j) \right) (X_{t_k} - X_{T_k}) \mathbb{E}_{\mathcal{F}_{t_k}} \left(\prod_{k+1\le j\le i-1} 1(B_j) \right)$$

$$\le \mathbb{E}_x \left(\prod_{1\le j\le k} 1(B_j) \right) (X_{t_k} - X_{T_k}) \bar{q}^{i-k-1} = \bar{q}^{i-k-1} \mathbb{E}_x \left(\prod_{1\le j\le k} 1(B_j) \right) \mathbb{E}_{\mathcal{F}_{T_k}} (X_{t_k} - X_{T_k})$$

$$\overset{lemma\,3}{\le} M_4 \bar{q}^{i-k-1} \mathbb{E}_x \left(\prod_{1\le j\le k} 1(B_j) \right) \le M_4 \bar{q}^{i-k-1+k} = M_4 \bar{q}^{i-1}.$$

Therefore, since $1 = \sum_{i\ge 1} \left(\prod_{1\le j\le i-1} 1(B_j) \right) 1(B_i^c)$ a.s., we get

$$\sum_{i\ge 1} \mathbb{E}_x \left(\prod_{1\le j\le i-1} 1(B_j) \right) 1(B_i^c) X_{t_{i-1}}$$

$$\le x \mathbb{E}_x \sum_{i\ge 1} \prod_{1\le j\le i-1} 1(B_j) 1(B_i^c) + M_4 \sum_i \bar{q}^{i-1} \le x + \frac{M_4}{1-\bar{q}}.$$

This shows (20), as required. In both cases I and II the bound (13) is proved.

Step 5. Let us establish the bound (14). Recall the notations introduced earlier after the assumptions:

$$\tau = \tau^1 := \inf(t \ge 0 : X_t \le N); \quad \gamma = \gamma^1 := \inf(t \ge \tau : X_{t-1} \le X_t = N),$$

and

$$T^n := \inf(t > \tau^n : X_t > N), \quad \tau^{n+1} := \inf(t > T^n : X_t \le N), \quad n \ge 1,$$

and $T^0 := 0$. Also, let

$$\gamma^{n+1} := \inf(t > \gamma^n : X_{t-1} \le X_t = N).$$

We have due to the assumption (A5)

$$\mathbb{E}_x X_{T^n} \le C, \quad n \ge 1; \quad \text{also,} \quad \mathbb{E}_x X_{T^0} = x.$$

Therefore, by virtue of the bound (13) we have,

$$\mathbb{E}_x(\tau^{n+1} - T^n) = \mathbb{E}_x \mathbb{E}_x(\tau^{n+1} - T^n | \tilde{\mathcal{F}}_{T^n}) \le \mathbb{E}_x X_{T^n} + C \le C, \quad n \ge 1,$$

and

$$\mathbb{E}_x(\tau^1 - T^0) \le x + C, \quad n = 0.$$

Also, due to the assumptions there exists $p \in (0,1)$ such that

$$\mathbb{P}_x(\gamma > T^n) \le p^n \quad \Longleftrightarrow \quad \mathbb{P}_x(\gamma \le T^n) \ge 1 - p^n, \quad n \ge 1.$$

Also,

$$\mathbb{E}_x(T^n - \tau^n) \le C, \quad n \ge 1.$$

Thus, also

$$\mathbb{E}(T^{n+1} - T^n) = \mathbb{E}(T^{n+1} - \tau^{n+1} + \tau^{n+1} - T^n) \le C.$$

Moreover,

$$\mathbb{E}(T^{n+1} - T^n | \mathcal{F}^X_{T^n}) \le C.$$

It follows by induction that

$$\mathbb{E}T^n \le Cn + x.$$

So, we estimate

$$\mathbb{E}_x\gamma = \sum_{n\ge 0} \mathbb{E}_x\gamma 1(T^n < \gamma \le T^{n+1}) \le \sum_{n\ge 0} \mathbb{E}_x T^{n+1} 1(T^n < \gamma \le T^{n+1})$$

$$= \sum_{n\ge 0} \mathbb{E}_x \mathbb{E}_x(T^{n+1} 1(T^n < \gamma \le T^{n+1}) | \mathcal{F}^X_{T^n})$$

$$= \sum_{n\ge 0} \mathbb{E}_x \mathbb{E}_x((T^n + T^{n+1} - T^n) 1(T^n < \gamma \le T^{n+1}) | \mathcal{F}^X_{T^n})$$

$$\le \sum_{n\ge 0} \mathbb{E}_x \mathbb{E}_x((T^n + T^{n+1} - T^n) 1(T^n < \gamma) | \mathcal{F}^X_{T^n})$$

$$= \sum_{n\ge 0} \mathbb{E}_x T^n 1(T^n < \gamma) + \sum_{n\ge 0} \mathbb{E}_x 1(T^n < \gamma) \underbrace{\mathbb{E}_x((T^{n+1} - T^n) | \mathcal{F}^X_{T^n})}_{\le C + x1(n=0)}.$$

Further, with any integer $M > 0$, denoting $\mathbb{E}_x T^n 1(T^n < \gamma) =: d_n$, we have (note that $d_0 = 0$),

$$\sum_{n=0}^{M} \underbrace{\mathbb{E}_x T^n 1(T^n < \gamma)}_{=:d_n} = \sum_{n=0}^{M} \mathbb{E}_x (T^{n-1} + T^n - T^{n-1}) 1(T^n < \gamma) 1(T^{n-1} < \gamma)$$

$$= d_0 + \sum_{n=1}^{M} \mathbb{E}_x T^{n-1} 1(T^n < \gamma) 1(T^{n-1} < \gamma) + \sum_{n=1}^{M} \mathbb{E}_x (T^n - T^{n-1}) 1(T^n < \gamma) 1(T^{n-1} < \gamma)$$

$$= d_0 + \sum_{n=1}^{M} \mathbb{E}_x T^{n-1} 1(T^{n-1} < \gamma) \underbrace{\mathbb{E}_x (1(T^n < \gamma) | \mathcal{F}^X_{T^{n-1}})}_{\le p}$$

$$+ \sum_{n=1}^{M} \mathbb{E}_x 1(T^{n-1} < \gamma) \mathbb{E}_x ((T^n - T^{n-1}) 1(T^n < \gamma) | \mathcal{F}^X_{T^{n-1}})$$

$$\le d_0 + \sum_{n=1}^{M} p d_{n-1} + \sum_{n=1}^{M} \mathbb{E}_x 1(T^{n-1} < \gamma) \mathbb{E}_x ((T^n - \tau^n + \tau^n - T^{n-1}) 1(T^n < \gamma) | \mathcal{F}^X_{T^{n-1}})$$

$$= \sum_{n=1}^{M} p d_{n-1} + \sum_{n=1}^{M} \mathbb{E}_x 1(T^{n-1} < \gamma) [\mathbb{E}_x ((T^n - \tau^n) 1(T^n < \gamma) | \mathcal{F}^X_{T^{n-1}})$$

$$+ \underbrace{\mathbb{E}_x ((\tau^n - T^{n-1}) 1(T^n < \gamma) | \mathcal{F}^X_{T^{n-1}}))}_{\le Cp + x1(n=1)}].$$

We have,

$$\sum_{n=1}^{M} \mathbb{E}_x 1(T^{n-1} < \gamma) \underbrace{\mathbb{E}_x ((\tau^n - T^{n-1}) 1(T^n < \gamma) | \mathcal{F}^X_{T^{n-1}}))}_{\le Cp + x1(n=1)}$$

$$\le C + x + Cp \sum_{n=1}^{M} \mathbb{E}_x 1(T^{n-1} < \gamma) \le C + x + C \sum_{n=0}^{M-2} p^n \le C + x.$$

Further,

$$\sum_{n=1}^{M} \mathbb{E}_x 1(T^{n-1} < \gamma)[\mathbb{E}_x((T^n - \tau^n)1(T^n < \gamma)|\mathcal{F}^X_{T^{n-1}})]$$

$$= \sum_{n=1}^{M} \mathbb{E}_x 1(T^{n-1} < \gamma)\mathbb{E}_x[\mathbb{E}_x\{(T^n - \tau^n)1(T^n < \gamma)|\mathcal{F}^X_{\tau^n}\}|\mathcal{F}^X_{T^{n-1}}]$$

$$\le \sum_{n=1}^{M} \mathbb{E}_x 1(T^{n-1} < \gamma)\mathbb{E}_x[\underbrace{\mathbb{E}_x\{(T^n - \tau^n)|\mathcal{F}^X_{\tau^n}\}}_{\le C}|\mathcal{F}^X_{T^{n-1}}]$$

$$\le C\sum_{n=1}^{M} \mathbb{E}_x 1(T^{n-1} < \gamma) \le C\sum_{n\ge 0} p^{n-1} \le C.$$

Thus,

$$\sum_{n=0}^{M} d_n \le p(C + \sum_{n=0}^{M-1} d_n) + C + x,$$

which by the monotone convergence theorem implies that

$$\sum_{n=0}^{\infty} d_n \le C(1 + x)$$

and

$$\mathbb{E}_x\gamma \le \sum_{n\ge 0} d_n + C \le C + Cx.$$

The bound (14) is justified and the proof of the theorem is completed. QED

6. Proof of Corollary 6

The existence of an invariant measure for the process Y follows from the Harris – Khasminskii principle via the formula

$$\mu^Y(A) := c\,\mathbb{E}_{N-}\sum_{n=1}^{\gamma} 1(Y_n \in A),$$

where c is the normalising constant, A is any measurable set in the state space of the process Y, and by $\mathbb{E}_{N-}$ we understand the initial condition $X_0 = N$ with any preceding fictitious state $X_{-1} \le N$. By the assumptions, the distribution of X_1 only depends on X_0 given this condition. So, this state – with the convention of the preceding state in $[0, N]$ – is, indeed, a regeneration point.

To apply it to the process X let us take any bounded measurable function $f(y)$ ($y = (y^1, \ldots)$), which only depends on the first variable $y^1 = x$:

$$\int f(y)\mu^Y(dy) := c\mathbb{E}_{N-}\sum_{n=1}^{\gamma} f(Y_n).$$

The latter expression in the right hand side determines an invariant measure for the process X with a notation $g(y^1) := f(y)$:

$$\int g(y^1)\mu^Y(dy) := c\mathbb{E}_{N-}\sum_1^\gamma g(Y_n^1),$$

where $X_n = Y_n^1$. So, the invariant measure for X reads

$$\mu^X(A^1) := c\mathbb{E}_{N-}\sum_{n=1}^\gamma 1(Y_n^1 \in A^1).$$

The corollary is proved. QED

Acknowledgements

For the first author the part consisting of theorem 5 and lemma 4 was supported by Russian Foundation for Basic Research grant 20-01-00575_a.

References

[1] K.B. Athreya and P. Ney, A new approach to the limit theory of recurrent Markov chains, Trans. Amer. Math. Soc. 245, pp. 493-501, 1978.
[2] A.D. Solovyev, private communication, 1999.
[3] D. L. Martell, A Markov Chain Model of Day to Day Changes in the Canadian Forest Fire Weather Index. International Journal of Wildland Fire, 9(4), pp. 265-273, 1999.
[4] G. Ramachandran, Exponential Model of Fire Growth. In Fire Safety Science: Proceedings of The First International Symposium, Editors Cecile E. Grant and Patrick J. Pagni, Hemisphere Publishing Corporation, Washington, 1986, pp. 657-666.
[5] A. Veretennikov, M. Veretennikova, On the notion of Markov-up processes, In book: Ed. by D.V. Kozyrev. The 5th International Conference on Stochastic Methods (ICSM5). 23-27 November 2020, Russia, Moscow. M.: RUDN, 2020, pp. 219-223; http://www.mathnet.ru/php/presentation.phtml?option_lang=eng&presentid=29154.

DISCRETE-TIME WORKING VACATIONS QUEUE WITH IMPATIENT CLIENTS AND CONGESTION DEPENDENT SERVICE RATES

K. Jyothsna[1,*], P. Vijaya Kumar[2], Ch. Gopala Rao[3],

•

[1,*]Department of Basic Sciences and Humanities, Vignan's Institute of Engineering for Women, Visakhapatnam, Andhra Pradesh, India.
mail2jyothsnak@yahoo.co.in, drjyothsnak1984@gmail.com
[2]Department of Mathematics, GITAM (Deemed to be University), Visakhapatnam, Andhra Pradesh, India.
vprathi@gitam.edu
[3]Department of Mathematics, MVGR College of Engineering, Vizianagaram, Andhra Pradesh, India.
gopalchalumuri83@gmail.com

Abstract

The current research article explores a finite capacity discrete-time multiple working vacations queue with impatient clients and congestion dependent service rates. An arriving client can choose either to enter the queue or balk with a certain probability. Due to impatience, he may renege after joining the queue as per geometric distribution. Rather than totally shutting down the service throughout the vacation period, the server functions with a different service rate. The times of services during regular service and during working vacation periods are considered to be geometrically distributed. The vacation periods are also presumed to be geometrically distributed. In addition, the service rates are considered to be dependent on the number of clients in the system during regular service period and during working vacation period. The model's steady-state probabilities are calculated using matrix approach and a recursive solution is also provided. The recursive solution is used for obtaining the corresponding continuous-time results. Various system performance metrics are presented. Finally, the numerical representation of the consequences of the model parameters on the performance metrics is furnished.

Keywords: Queue, discrete-time, working vacations, balking, reneging, congestion dependent service rates

1. Introduction

A discrete-time queueing model is one in which the time between two arrivals and the service times are discrete random variables. Such queueing models are more relevant than the continuous-time queuing models for designing and monitoring the efficacy of computer systems, communications network systems, industrial and production systems, traffic systems and healthcare systems. Furthermore, discrete-time analysis can be used to approximate a continuous-time system but this is not the case in reverse. Shizhong Zhou et al. [13] investigated a discrete-time queue with preferred customers and partial buffer sharing. Michiel De Muynck et al. [9] analysed a discrete-time queue with general service demands and phase-type service capacities. A discrete-time queue with three different strategies has been studied by Ivan Atencia et al. [7].

Individuals are always concerned while waiting for service, hence dissatisfaction is a most noteworthy characteristic in queueing systems. In reality, queues with impatient clients frequently occur where clients become irritated owing to lengthy waiting lines. Due to which, clients either balk (i.e., refuse to join the queue) or renege (i.e., abandon the queue without being served). In real-world congestion situations, performance examination of queueing systems with balking and reneging is advantageous since fresh managerial insights are gained. The importance of the aforementioned queueing systems can be seen in telecom companies, networking and telecommunication systems, production system, machinery operating systems, health emergency rooms, inventory management systems, etc. The amount of lost revenues can be estimated using the balking and reneging probabilities when deciding on the service rate of servers required in the service system to satisfy the needs that change over time. The concept of balking and reneging has been introduced by Haight [5] and Haight [6], respectively. Customers' balking and reneging behaviour in queueing theory were compared by Amit and Sonja [1]. Rakesh Kumar [10] conducted an economic analysis of a finite buffer multi server queuing model including balking, reneging and customer retention. The busy period study of a queuing model with balking and reneging was presented by Wang and Zhang [17]. G. S. Kuaban et al. [8] investigated a multi-server queuing model with balking and correlated reneging.

Working vacation (WV) models are the ones in which the server stays available and serves clients at a lower rate throughout the vacation period. If the queue is not empty at the vacation termination epoch, the server enters a regular service period with regular service rates; otherwise, the server returns to WV. Such type of working vacation policy is termed as multiple working vacations (MWV). This type of working vacation policy was introduced by Servi and Finn [12]. The discrete-time multiple working vacation queue with balking has been studied by Vijaya Laxmi et al. [14]. Vijaya Laxmi and Jyothsna [15] analyzed a finite buffer discrete-time batch service queue with multiple working vacations. A survey on working vacation queueing models has been presented by Chandrsekaran et al. [2]. Rama Devi et al. [11] analyzed an $M/M/1$ queue with working vacation, server failure and customer's impatience.

Queues with single server whose service rates are proportional to the queue size are accurate models for systems where the server's performance must be adjusted in accordance to the quantity of clients in the queue. In congestion dependent queueing systems, the server's service rate may be influenced by the availability of work in the system. The service rate for each client can be dynamically updated as a function of the number of clients in the system using congestion dependent services. Furthermore, queueing networks get benefited from queueing models with finite capacity and congestion dependent services, which often add to the complexity of these systems' solutions. For literature on congestion dependent queues, see [4, 16, 3] and the references therein.

The current paper considers a finite buffer discrete-time MWV queue with impatient clients and congestion dependent service rates. Service times are supposed to be geometrically distributed and congestion dependent throughout regular service and during working vacations. The inter-arrival times of clients and vacation times are both presumed to be geometrically distributed. The queue is analyzed under the late arrival system with delayed access (LAS-DA) and the steady-state system length distributions are obtained using matrix approach and a recursive solution is also provided. The results of the corresponding continuous-time queue are obatined from the recursive solution of the discrete-time queue. A few model performance metrics are developed using the steady-state probabilities. Finally, the parameter effect on the performance indices of the system is exhibited through some numerical results.

The remaining part of the paper is laid out in the following manner. In Section 2, the description of the model and steady-state probabilities are presented. The performance metrics of the model are displayed in Section 3. Section 4 depicts the impact of the model parameters on the performance metrics in the form of a table and graphs. The paper is concluded in Section 5.

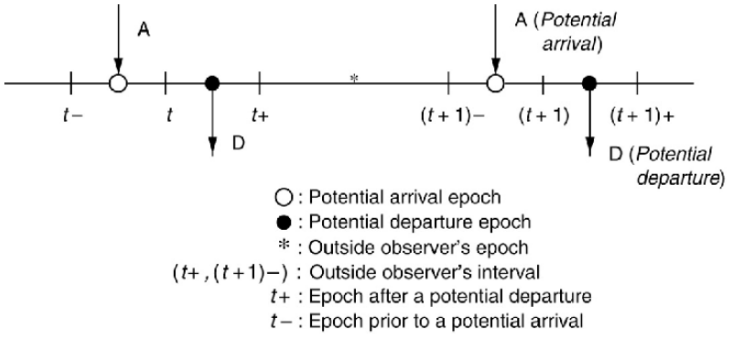

Figure 1: *Different time instants in late arrival system with delayed access (LAS-DA)*

2. Description of the model and steady-state probabilities

Under the late arrival system with delayed access (LAS-DA), we study a finite buffer discrete-time balking and reneging single server queue with multiple working vacations and congestion dependent service rates. Suppose that the time axis is divided into equal-length intervals with the duration of a slot being equal to one and are labeled as $0, 1, 2, \ldots, t, \ldots$. A possible arrival of a client occurs in $(t-, t)$ while a potential departure of the client occurs in $(t, t+)$. The different time instants in LAS-DA are displayed in Figure 1.

The system is presumed to have a finite capacity N. The inter-arrival times A of clients are independent and geometrically distributed with probability mass function (p.m.f.) $P(A = i) = \bar{\lambda}^{i-1}\lambda, i \geq 1, 0 < \lambda < 1$ where for $x \epsilon [0, 1]$, we denote $\bar{x} = 1 - x$. If a client arrives and discovers the system is busy, the client can choose to join the queue or balk. When the system size is n, let b_n indicate the probability that a client will join the queue for service or will balk with probability $\bar{b}_n$. Furthermore, we assume that $b_0 = 1, 0 < b_n < b_{n+1} \leq 1, 1 \leq n \leq N-1, b_N = 0$.

Each client will wait a specified amount of time T for service to commence after joining the queue. If it hasn't started by then, he'll become frustrated and exits the queue without being served. The impatient time T is geometrically distributed and independent with common p.m.f. $P(T = i) = \bar{\alpha}^{i-1}\alpha, i \geq 0, 0 < \alpha < 1$. As an impatient client's arrival and departure without service are unrelated, $r(n) = (n-1)\alpha, 1 \leq n \leq N$ can be used as the function of the average reneging rate of the client.

The clients are served on a first-come first-served (FCFS) discipline. The service times of clients S are geometrically distributed and independent with p.m.f. $P(S = i) = \bar{\mu}_n^{i-1}\mu_n, i \geq 1, 0 < \mu_n < 1$ when there are n clients in the system. The durations of service during a working vacation period S_v are geometrically distributed and independent with p.m.f. $P(S_v = i) = \bar{\eta}_n^{i-1}\eta_n, i \geq 1, 0 < \eta_n < 1$. When the server detects that the system is vacant, it follows multiple working vacation policy. Upon return of the server after a working vacation discovers that the system is vacant, another working vacation commences. Or else, the server initiates a regular service period. The vacation times V are geometrically distributed and independent with p.m.f. $P(V = i) = \bar{\phi}^{i-1}\phi, i \geq 0, 0 < \phi < 1$.

Let $P_n, 0 \leq n \leq N$ be the probability that the system has n clients when the server is on WV at steady-state and when the server is in regular service period $Q_n, 1 \leq n \leq N$ represents the probability that there are n clients in the system. The steady-state equations can be expressed as

follows based on the one-step transition analysis.

$$
\begin{aligned}
P_0 &= \bar{\lambda}P_0 + h_1(\eta_1)P_1 + t_2(\eta_2)P_2 + h_1(\mu_1)Q_1 + t_2(\mu_2)Q_2, && (1)\\
P_n &= \bar{\phi}\left(g_n(\eta_n)P_n + f_{n-1}(\eta_{n-1})P_{n-1} + h_{n+1}(\eta_{n+1})P_{n+1} + t_{n+2}(\eta_{n+2})P_{n+2}\right), \\
&\quad 1 \le n \le N-2, && (2)\\
P_{N-1} &= \bar{\phi}\left(g_{N-1}(\eta_{N-1})P_{N-1} + f_{N-2}(\eta_{N-2})P_{N-2} + h_N(\eta_N)P_N\right), && (3)\\
P_N &= \bar{\phi}\left(g_N(\eta_N)P_N + f_{N-1}(\eta_{N-1})P_{N-1}\right), && (4)\\
Q_1 &= g_1(\mu_1)Q_1 + h_2(\mu_2)Q_2 + t_3(\mu_3)Q_3 + \phi\big(g_1(\eta_1)P_1 + \lambda P_0 + h_2(\eta_2)P_2 + t_3(\eta_3)P_3)\big), && (5)\\
Q_n &= g_n(\mu_n)Q_n + h_{n+1}(\mu_{n+1})Q_{n+1} + t_{n+2}(\mu_{n+2})Q_{n+2} + f_{n-1}(\mu_{n-1})Q_{n-1} + \phi\big(g_n(\eta_n)P_n \\
&\quad + f_{n-1}(\eta_{n-1})P_{n-1} + h_{n+1}(\eta_{n+1})P_{n+1} + t_{n+2}(\eta_{n+2})P_{n+2}\big),\ 2 \le n \le N-2, && (6)
\end{aligned}
$$

$$
\begin{aligned}
Q_{N-1} &= g_{N-1}(\mu_{N-1})Q_{N-1} + h_N(\mu_N)Q_N + f_{N-2}(\mu_{N-2})Q_{N-2} + \phi\big(g_{N-1}(\eta_{N-1})P_{N-1} \\
&\quad + f_{N-2}(\eta_{N-2})P_{N-2} + h_N(\eta_N)P_N\big), && (7)\\
Q_N &= g_N(\mu_N)Q_N + f_{N-1}(\mu_{N-1})Q_{N-1} + \phi\big(g_N(\eta_N)P_N + f_{N-1}(\eta_{N-1})P_{N-1}\big), && (8)
\end{aligned}
$$

where

$$
\begin{aligned}
f_n(x) &= \begin{cases} \lambda, n = 0, \\ \lambda b_n \bar{x}\left(1 - (n-1)\alpha\right),\ 1 \le n \le N-1, \end{cases} \\
g_n(x) &= \begin{cases} (1-\lambda b_1)\bar{x} + \lambda b_1 x\ :\ n = 1, \\ (1-\lambda b_n)\bar{x}(1-(n-1)\alpha) + \lambda b_n\left(x(1-(n-1)\alpha) + \bar{x}(n-1)\alpha\right),\ 2 \le n \le N, \end{cases} \\
h_n(x) &= \begin{cases} (1-\lambda b_1)x,\ n = 1, \\ (1-\lambda b_n)\left(x(1-(n-1)\alpha) + \bar{x}(n-1)\alpha\right) + \lambda b_n x(n-1)\alpha,\ 2 \le n \le N, \end{cases} \\
t_n(x) &= (1-\lambda b_n)x(n-1)\alpha,\ 2 \le n \le N.
\end{aligned}
$$

Matrix Solution

To determine the steady-state probabilities, we propose a matrix solution. The infinitesimal generator of the Markov process can be represented as below using the lexicographical sequence for the states.

$$
\mathbf{Q} = \begin{pmatrix}
\mathbf{A}_0 & \mathbf{D}_0 & & & & & & & \\
\mathbf{B}_1 & \mathbf{A}_1 & \mathbf{D}_1 & & & & & & \\
\mathbf{C}_2 & \mathbf{B}_2 & \mathbf{A}_2 & \mathbf{D}_2 & & & & & \\
 & \mathbf{C}_3 & \mathbf{B}_3 & \mathbf{A}_3 & \mathbf{D}_3 & & & & \\
 & & \ddots & \ddots & \ddots & & & & \\
 & & & & \mathbf{C}_{N-2} & \mathbf{B}_{N-2} & \mathbf{A}_{N-2} & \mathbf{D}_{N-2} & \\
 & & & & & \mathbf{C}_{N-1} & \mathbf{B}_{N-1} & \mathbf{A}_{N-1} & \mathbf{D}_{N-1} \\
 & & & & & & \mathbf{C}_N & \mathbf{B}_N & \mathbf{A}_N
\end{pmatrix},
$$

where

$$
\begin{aligned}
\mathbf{A}_0 &= \begin{pmatrix} -\lambda \end{pmatrix};\quad \mathbf{D}_0 = \begin{pmatrix} \bar{\phi}f_0(\eta_0) & \lambda\phi \end{pmatrix}; \\
\mathbf{B}_1 &= \begin{pmatrix} h_1(\eta_1) \\ h_1(\mu_1) \end{pmatrix};\quad \mathbf{C}_2 = \begin{pmatrix} t_1(\eta_2) \\ t_1(\mu_2) \end{pmatrix}; \\
\mathbf{A}_n &= \begin{pmatrix} \bar{\phi}g_n(\eta_n) - 1 & \phi g_n(\eta_n) \\ 0 & g_n(\mu_n) \end{pmatrix}, 1 \le n \le N; \\
\mathbf{B}_n &= \begin{pmatrix} \bar{\phi}h_n(\eta_n) & \phi h_n(\eta_n) \\ 0 & h_n(\mu_n) \end{pmatrix},\ 2 \le n \le N; \\
\mathbf{C}_n &= \begin{pmatrix} \bar{\phi}t_n(\eta_n) & \phi t_n(\eta_n) \\ 0 & t_n(\mu_n) \end{pmatrix},\ 3 \le n \le N.
\end{aligned}
$$

Let $\mathbf{\Pi} = (\mathbf{\Pi}_0, \mathbf{\Pi}_1, \ldots, \mathbf{\Pi}_{N-1}, \mathbf{\Pi}_N)$ be the vector of steady-state probabilities, where $\mathbf{\Pi}_0 = (P_0)$, $\mathbf{\Pi}_n = (P_n, Q_n)$, for $1 \leq n \leq N$. The equations at steady-state $\mathbf{\Pi Q} = \mathbf{0}$ can be expressed as

$$\begin{aligned}
\mathbf{\Pi}_0\mathbf{A}_0 + \mathbf{\Pi}_1\mathbf{B}_1 + \mathbf{\Pi}_2\mathbf{C}_2 &= \mathbf{0}, && (9)\\
\mathbf{\Pi}_0\mathbf{D}_0 + \mathbf{\Pi}_1\mathbf{A}_1 + \mathbf{\Pi}_2\mathbf{B}_2 + \mathbf{\Pi}_3\mathbf{C}_3 &= \mathbf{0}, && (10)\\
\mathbf{\Pi}_{n-1}\mathbf{D}_{n-1} + \mathbf{\Pi}_n\mathbf{A}_n + \mathbf{\Pi}_{n+1}\mathbf{B}_{n+1} + \mathbf{\Pi}_{n+2}\mathbf{C}_{n+2} &= \mathbf{0},\ 2 \leq n \leq N-2, && (11)\\
\mathbf{\Pi}_{N-2}\mathbf{D}_{N-2} + \mathbf{\Pi}_{N-1}\mathbf{A}_{N-1} + \mathbf{\Pi}_N\mathbf{B}_N &= \mathbf{0}, && (12)\\
\mathbf{\Pi}_{N-1}\mathbf{D}_{N-1} + \mathbf{\Pi}_N\mathbf{A}_N &= \mathbf{0}. && (13)
\end{aligned}$$

After recursive substitutions, equations (11) to (13) yields

$$\mathbf{\Pi}_n = \mathbf{\Pi}_N\mathbf{M}_n\mathbf{D}_n^{-1}, 1 \leq n \leq N-1, \quad (14)$$

where

$$\begin{aligned}
\mathbf{M}_{N-1} &= -\mathbf{A}_N,\\
\mathbf{M}_{N-2} &= -\mathbf{M}_{N-1}\mathbf{D}_{N-1}^{-1} - \mathbf{B}_N,\\
\mathbf{M}_{N-3} &= -\mathbf{M}_{N-2}\mathbf{D}_{N-2}^{-1}\mathbf{A}_{N-2} - \mathbf{M}_{N-1}\mathbf{D}_{N-1}^{-1}\mathbf{B}_{N-1} - \mathbf{C}_N,\\
\mathbf{M}_n &= -\mathbf{M}_{n+1}\mathbf{D}_{n+1}^{-1}\mathbf{A}_{n+1} - \mathbf{M}_{n+2}\mathbf{D}_{n+2}^{-1}\mathbf{B}_{n+2} - \mathbf{M}_{n+3}\mathbf{D}_{n+3}^{-1}\mathbf{C}_{n+3}, 1 \leq n \leq N-4.
\end{aligned}$$

Assuming P_N to be known, equation (10) and(14) yields Q_N in P_N. From equations (14), $P_n (0 \leq n \leq N-1)$ and $Q_n, (1 \leq n \leq N-1)$ can be evaluated in terms of P_N. Finally, P_N is computed from the normalization condition $P_0 + \sum_{n=1}^{N} \mathbf{\Pi}_n\mathbf{e} = 1$, where $\mathbf{e}$ is a column vector with each component equal to one. The steady-state probabilities are calculated using a computer code.

Recursive Solution

In order to approximate the corresponding continuous-time results we have obtained the expressions of the steady-state probabilities using recursive method though the matrix method is easy to program and implement. Solving the equations (2) to (8) recursively and utilizing the normalization condition $\sum_{n=0}^{N} P_n + \sum_{n=1}^{N} Q_n = 1$, the explicit expressions of the steady-state probabilities are obtained as

$$P_n = \psi_n \left(\sum_{n=0}^{N} \psi_n + \sum_{n=1}^{N} (\omega_n + k\varphi_n) \right)^{-1},\ 0 \leq n \leq N,$$

$$Q_n = (\omega_n + k\varphi_n) \left(\sum_{n=0}^{N} \psi_n + \sum_{n=1}^{N} (\omega_n + k\varphi_n) \right)^{-1},\ 1 \leq n \leq N,$$

where

$$
\begin{aligned}
\psi_N &= 1,\\
\psi_{N-1} &= (1-\bar{\phi}g_N(\eta_N))/\bar{\phi}f_{N-1}(\eta_{N-1}),\\
\psi_{N-2} &= \left((1-\bar{\phi}g_{N-1}(\eta_{N-1}))\,\psi_{N-1}-\bar{\phi}h_N(\eta_N)\right)/\bar{\phi}f_{N-2}(\eta_{N-2}),\\
\psi_n &= \left((1-\bar{\phi}g_{n+1}(\eta_{n+1}))\,\psi_{n+1}-\bar{\phi}h_{n+2}(\eta_{n+2})\psi_{n+2}-\bar{\phi}t_{n+3}(\eta_{n+3})\psi_{n+3}\right)/\bar{\phi}f_n(\eta_n),\\
&\quad n=N-3,\ldots,0,\\
\varphi_N &= 1,\ \omega_N=0,\\
\varphi_{N-1} &= (1-g_N(\mu_N))/f_{N-1}(\mu_{N-1}),\\
\omega_{N-1} &= -\phi\left(g_N(\eta_N)+f_{N-1}(\eta_{N-1})\psi_{N-1}\right)/f_{N-1}(\mu_{N-1}),\\
\varphi_{N-2} &= \left((1-g_{N-1}(\mu_{N-1}))\varphi_{N-1}-h_N(\mu_N)\right)/f_{N-2}(\mu_{N-2}),\\
\varphi_n &= (1-g_{n+1}(\mu_{n+1}))\varphi_{n+1}-h_{n+2}(\mu_{n+2})\varphi_{n+2}-t_{n+3}(\mu_{n+3})\varphi_{n+3})/f_n(\mu_n),\\
&\quad n=N-3,\ldots,1,\\
\omega_{N-2} &= \big(((1-g_{N-1}(\mu_{N-1}))\omega_{N-1}-h_N(\mu_N)\omega_N)-\phi\big(g_{N-1}(\eta_{N-1})\psi_{N-1}\\
&\quad +f_{N-2}(\eta_{N-2})\psi_{N-2}+h_N(\eta_N)\psi_N\big)\big)/f_{N-2}(\mu_{N-2}),\\
\omega_n &= \big(((1-g_{n+1}(\mu_{n+1}))\omega_{n+1}-h_{n+2}(\mu_{n+2})\omega_{n+2}-t_{n+3}(\mu_{n+3})\omega_{n+3})-\phi\big(g_{n+1}(\eta_{n+1})\psi_{n+1}\\
&\quad +f_n(\eta_n)\psi_n+h_{n+2}(\eta_{n+2})\psi_{n+2}+t_{n+3}(\eta_{n+3})\psi_{n+3}\big)\big)/f_n(\mu_n), n=N-3,\ldots,1,\\
k &= \big(\phi\big(g_1(\eta_1)\psi_1+\lambda\psi_0+h_2(\eta_2)\psi_2+t_3(\eta_3)\psi_3\big)-\big((1-g_1(\mu_1))\omega_1-h_2(\mu_2)\omega_2\\
&\quad -t_3(\mu_3)\omega_3\big)\big)/\big((1-g_1(\mu_1))\varphi_1-h_2(\mu_2)\varphi_2-t_3(\mu_3)\varphi_3\big).
\end{aligned}
$$

Remark: In continuous-time context, let β, ν_n, ϱ_n and ς represent the arrival rate, service rates during regular busy period, during WV period and vacation rate, respectively. Further, let the time axis be divided into equal length slots of length $\Delta > 0$, so that $\lambda = \beta\Delta$, $\mu_n = \nu_n\Delta$, $\eta_n = \varrho_n\Delta$ and $\phi = \varsigma\Delta$ where Δ is small enough. Now, the results of the corresponding continuous-time $M/M(n)/1/N/MWV$ queue with balking and reneging are obtained by substituting λ, μ_n, η_n and ϕ in the recursive solution.

3. Performance metrics

Let L_s denote the mean of the number of clients in the system and is expressed as

$$L_s = \sum_{n=1}^{N} n(P_n + Q_n).$$

During regular service and during WV, the busy probability of the server are denoted as p_b and p_v, respectively. The probabilities p_b and p_v are given by

$$p_b = \sum_{n=1}^{N} Q_n,\ p_v = \sum_{n=0}^{N} P_n.$$

The average balking rate (br), average reneging rate (rr) and the average rate of client loss due to impatience (lr) are given as

$$
\begin{aligned}
br &= \sum_{n=1}^{N} \lambda(1-b_n)(P_n+Q_n),\\
rr &= \sum_{n=1}^{N} (n-1)\alpha(P_n+Q_n),\\
lr &= br + rr.
\end{aligned}
$$

Table 1: *Performance metrics for different* η_m

η_m	0.054167	0.216667	0.4874999	0.866667	1.35417
L_s	2.075441	2.074633	2.073842	2.073065	2.072303
lr	0.545119	0.544945	0.544773	0.544603	0.544436
p_b	0.965786	0.965623	0.965460	0.965297	0.965134
p_v	0.034214	0.034376	0.034539	0.034702	0.034866

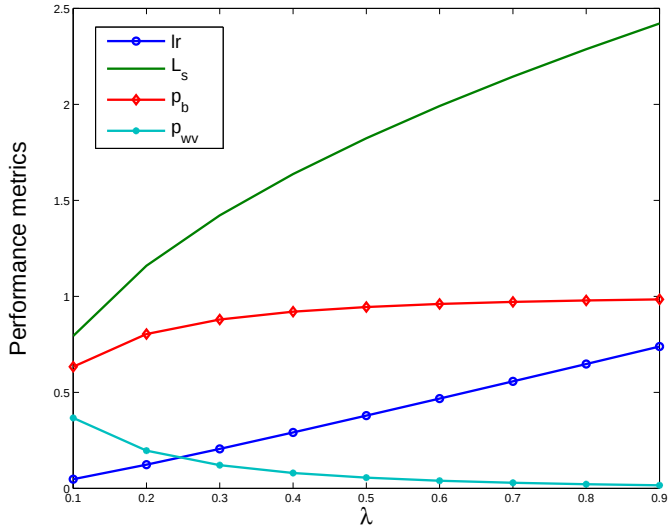

Figure 2: *λ versus performance metrics*

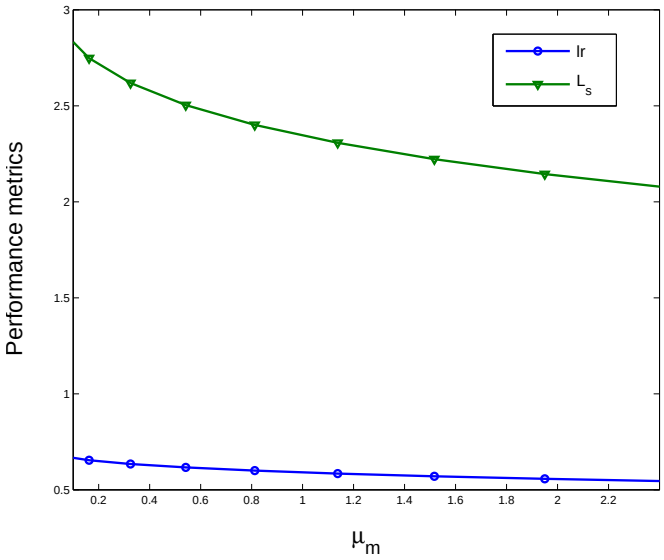

Figure 3: *Impact of μ_m on lr and L_s*

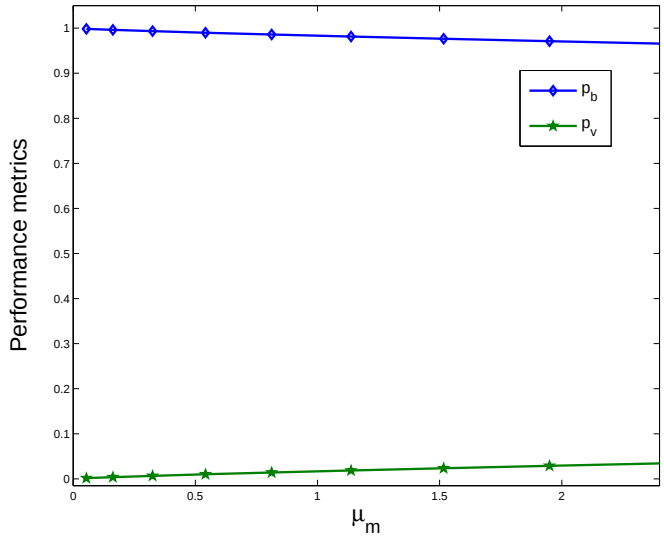

Figure 4: *μ_m versus p_b and p_v*

4. Numerical results

The influence of the system parameters on the model's various performance metrics is presented in this section. The capacity of the system is assumed as $N = 12$. The balking function is taken as $b_n = 1/(n+1)$, $1 \leq n \leq N-1$ with the assumption that $b_0 = 1$ and $b_N = 0$. The model parameters are arbitrarily chosen to be $\lambda = 0.7, \phi = 0.6, \alpha = 0.09$. The congestion-dependent service rates of the system are taken to be $\mu_n = 0.8n/N, \eta_n = 0.6n/N$ with means $\mu_m = 0.433333$ and $\eta_m = 0.325$, respectively.

The values of the performance metrics for various mean service rates during WV are presented in Table 1. The average number of clients in the system (L_s), average rate of losing a client (lr) and the probability of the server in regular service (p_b) - all show a diminishing trend as the mean service rate during WV grows. With an increase in η_m, the probability of the server being in WV (p_v) increases.

The arrival rate's impact on the different performance metrics of the model is displayed in Figure 2. From the figure it is evident that the performance metrics lr, L_s and p_b increase with the increase of λ while the performance metric p_v decreases with the increase of λ.

The influence of mean service rate during regular busy period μ_m on the performance measures L_s and lr is depicted in Figure 3. It is clearly apparent from the graph that both L_s and lr decrease with the increase of μ_m as intuitively expected.

Figure 4 presents the changes in p_b and p_v with the the increase of μ_m. With the increase of μ_m, the probability of the service being busy with regular service (p_b) falls but the probability of the server being busy in WV (p_v) increases.

5. Conclusions

The study of a finite buffer discrete-time congestion dependent queue with balking, reneging and multiple working vacations is presented in this paper. The stationary probabilities of the model are obtained using matrix method as well as recursive method. Different performance characteristics of the model such as average number of clients in the system, busy probability of the server during regular service, busy probability of the server during working vacations, average balking rate, average reneging rate and average rate of loosing a client are presented. A variety of numerical findings in the form of tables and graphs are used to demonstrate com-

putational experiences. Future research can be focussed on the extension our findings to a $GI/Geo(n)/1/N$ queue with WV and impatient clients.

References

[1] Amit I. Pazgal and Sonja Rasdas (2008). Comparison of customer balking and reneging behavior to queueing theory predictions: An experimental study. *Computers & Operations Research*, 35(8):2537-2548.

[2] Chandrasekaran, V. M., Indhira, K., Saravanarajan, M. C. and Rajadurai, P. (2016). A survey on working vacation queueing models. *International Journal of Pure and Applied Mathematics*, 106(6): 33-41.

[3] Doo Il Choi and Dae-Eun Lim (2020). Analysis of the state-dependent queueing model and its application to battery swapping and charging stations. *Sustainability*, 12(6) issue.2343:1-15.

[4] Goswami, V., Vijaya Laxmi, P. and Jyothsna, K. (2013). Analysis of $GI/M(n)/1/N$ queue with state-dependent multiple working vacations. *OPSEARCH*, 50(1):106-124.

[5] Haight, F. A. (1957). Queueing with balking. *Biometrika*, 44:360-369.

[6] Haight, F. A. (1959). Queueing with reneging. *Metrika*, 2:86-197.

[7] Ivan Atencia, Garcia, J. L. G., Venegas, G. A. B, Cielos, P. R., Garcia, M. A. G. and Dominguez Y. P. (2021). A discrete-time queueing system with three different strategies. *Journal of Computational and Applied Mathematics*, 393(113486):1-9.

[8] Kuaban, G. S., Rakesh Kumar, Bhavneet Singh Soodan and Piotr Czekalski (2020). A multi-server queuing model with balking and correlated reneging with application in health care management. *IEEE Access*, 8:169623-169639.

[9] Michiel De Muynck, Herwig Bruneel and Sabine Wittevrongel (2017). Analysis of a discrete-time queue with general service demands and phase-type service capacities. *Journal of Industrial and Management Optimization*, 13(4):1901-1926.

[10] Rakesh Kumar (2013). Economic analysis of an $M/M/c/N$ queuing model with balking, reneging and retention of reneged customers. *OPSEARCH*, 50:383-403.

[11] Rama Devi, V. N., Ankamma Rao, A. and Chandan K. (2019). $M/M/1$ queue with working vacation, server failure and customer's impatience, *International Journal of Scientific & Technology Research*, 8(9):2262-2268.

[12] Servi, L. D. and Finn, S. G. (2002). $M/M/1$ queue with working vacations ($M/M/1/WV$). *Performance Evaluation*, 50:41-52.

[13] Shizhong Zhou, Liwei Liu, Jianjun Li (2015). A discrete-time queue with preferred customers and partial buffer sharing, *Mathematical Problems in Engineering*, Volume 2015, Article ID 173938, 12 pages, http://dx.doi.org/10.1155/2015/173938

[14] Vijaya Laxmi. P., Goswami, V. and Jyothsna, K. (2013). Analysis of discrete-time single server queue with balking and multiple working vacations. *Quality Technology & Qualitatitive Management*, 10(4):443-456.

[15] Vijaya Laxmi, P. and Jyothsna, K. (2014). Finite buffer $GI/Geo/1$ batch servicing queue with multiple working vacations. *RAIRO Operations Research*, 48:521–543.

[16] Vijaya Laxmi, P. and Jyothsna, K. (2015). On renewal input state dependent working vacations queue with impatient customers. *International Journal of Mathematics in Operational Research*, 7(6):661–680.

[17] Wang Qiangqiang, Zhang Bin (2018). Analysis of a busy period queuing system with balking, reneging and motivating. *Applied Mathematical Modelling*. 64:480-488.

QUEUING SYSTEM WITHOUT QUEUE AND DETERMINISTIC SERVICE TIME

Gurami Tsitsiashvili, Tatiana Radchenkova

•

Russia, 690041, Vladivostok, Radio street 7
Institute for Applied Mathematics
Far Eastern Branch of Russian Academy Sciences
guram@iam.dvo.ru, tarad@yandex.ru

Abstract

There is a model of fault-counting data collected in the testing process of software development. In this model it is performed simulation based on the infinite server queueing model using the generated sample data of the fault detection time to visualize the efficiency of fault correction activities. In this model the thinning method using intensity functions of the delayed S-shaped and inflection S-shaped software reliability growth models [2], [3] to generate sample data of the fault detection time from the fault-counting data.

But this model does not allow to analyse such systems without dependence of input and service intensities. In this paper, we consider a queuing system model with an infinite number of servers and a deterministic service time. The input flow to the system is non-stationary Poisson. It is investigated analytically how the parameter of the Poisson distribution characterizing the number of customers in the system depends on the service time in the presence of a peak load determined by the variable intensity of the input flow. In numerical simulations it is shown how graphs of the Poisson distribution parameter depends on deterministic service time.

Keywords: Poisson flow, deterministic service time, queuing system with infinite servers.

Introduction

In [1] fault-counting data are collected in the testing process of software development. The authors perform simulation based on the infinite server queueing model using the generated sample data of the fault detection time to visualize the efficiency of fault correction activities. They apply the thinning method using intensity functions of the delayed S-shaped and inflection S-shaped software reliability growth models [2], [3] to generate sample data of the fault detection time from the fault-counting data. As a result the simulation based on the infinite server queueing model using the generated sample data of the fault detection time to visualize the efficiency of fault correction activities is performed in conditions of non-stationary intensity of the input flow. This approach makes it possible to raise the question of the behaviour of the queuing system in peak load mode.

However, the inclusion in the queuing model of the dependence between the intensities of the input flow and the service may be too restrictive. Indeed, if we assume that the customers service times are deterministic, then such a restriction no longer works. At the same time, a similar queuing system based on the infinite server queuing model is also found in other applications, for example, in the system of admission of visitors to services (for example, to a sports facility)

[4]. Moreover, the deterministic distribution of service time in combination with the admission of visitors at arbitrary times turns out to be a very convenient tool for attracting them to service. For this model, the question arises in what ways it is possible to reduce the number of customers in the system in peak load mode.In this paper, it is shown that the variation of the deterministic service time is a factor that can significantly affect the behaviour of the system in peak load mode.

I. Nonstationary Poisson model of a continuously functioning service system

The calculation of non-stationary queuing models is usually much more complicated than the calculation of stationary models. However, in many systems of everyday public services, it is usually necessary to deal with non-stationary systems. Therefore, it is necessary to build a non-stationary queuing model in such a way that its calculation would be quite simple and convenient.

In this paper, this can be achieved by assuming the determinism of the service time and the Poisson nature of the input non-stationary flow of customers. Consider the Poisson model of a queuing system in which customers form the following Poisson flow model. Each customer is in the system for the time α, then leaves the system. The moments of arrival of applications into the system form a Poisson flow with an intensity of $\lambda(t)$, $-\infty < t < \infty$. The peculiarity of this model is its non-stationarity and the possibility of including in it a group receipt of customers with different parameters of the Poisson distribution of their numbers.

Thus, this model adapts to the conditions of functioning of real service systems: continuously operating swimming pools, outdoor skating rinks, gyms, aerobics and fitness halls, ski bases. In the language of queuing theory, such a system can be interpreted as a system with a Poisson flow of customers having varying intensity, an infinite number of servers and a deterministic service time.

Here the function $\lambda(t)$ is assumed to be continuous at $0 \le t \le T - \alpha$,

$$\lambda(t) = 0,\ t < 0 \text{ or } T - \alpha \le t.$$

As an example of such a flow of moments when users come to the system, we can assume that these are visitors of a continuously working pool coming to free swimming. Then for a fixed time t, $0 \le t \le T$, the number of users who came to the pool has a Poisson distribution with the parameter

$$\Lambda(t) = \int_{t-\alpha}^{t} \lambda(\tau)d\tau,\ 0 \le t \le T. \tag{1}$$

This non-stationary queuing model can have numerous generalizations: multiphase systems and acyclic service networks, systems with multiple flows having different deterministic service times, etc. It can also be applied to the calculation of conveyor systems for processing parts.

II. Basic properties of the non-stationary model with deterministic service times

Let the function $\lambda(t)$ has a single extremum (maximum) at the point $t_* > a$. Consequently $\lambda(t)$ is non-decreasing in interval $0 \le t < t_*$ and non-increasing in interval $t_* < t \le T - a$. It follows from the formula (1) that the function $\Lambda(t)$ has maximum at point t^*, if the following equality takes place

$$\Lambda'(t) = \lambda(t^*) - \lambda(t^* - a) = 0. \tag{2}$$

Property 1. From the properties of the function $\lambda(t)$ follows the inequalities

$$t_* < t^* < t_* + a. \tag{3}$$

Thus, the maximum of the function $\Lambda(t)$ is shifted to the right relative to the maximum of the function $\lambda(t)$.

Property 2. From the formula (1) we have

$$\Lambda(t^*) \le a\lambda(t_*). \tag{4}$$

Therefore, reducing the parameter a allows smoothing the peak of the function $\Lambda(t)$.

Property 3. If the following condition is true

$$2a = T,\ \int_0^{T-a} \lambda(\tau)d\tau \ge \lambda(t_*), \tag{5}$$

then the peak of the function $\Lambda(t)$ may be higher than the peak of the function $\lambda(t)$:

$$\Lambda(t^*) \ge \lambda(t_*). \tag{6}$$

Another condition of the formula (6) is

$$\lambda(t) \ge \lambda_*,\ 0 < t \le T - a,\ a\lambda_* \ge \lambda(t_*). \tag{7}$$

III. Numerical experiments

All experiments will be made for the function

$$\lambda(t) = \frac{\exp\left(-(t-b)^2/\left(2c\right)\right)}{\sqrt{2\pi c}},\ 0 < t < T - a,\ \lambda(t) = 0,\ t \le 0 \text{ or } T - a \le t$$

with different meanings of parameter a.

Figure 1 shows that an increase in parameter a causes the maximum of the function $\Lambda(t)$ to grow and shift to the right relative to the maximum of the function $\lambda(t)$.

IV. Conclusion

The results of an analytical study of the $\Lambda(t)$ function showed that parameter a, which characterizes the deterministic time of servicing customers in this system without a queue, is a convenient tool for smoothing the peak load characterized by the intensity of the input flow. The properties of the queuing model with the infinite number of servers and deterministic service time established in the work and computational experiments allow us to discover how service time affects the parameter of the Poisson distribution of the number of customers in the system. A decrease in this parameter leads to a smoothing of the peak in the intensity of the input flow, and an increase leads to an increase in this peak. Therefore, this study allows us to determine how to choose the service time in order to avoid peak loads in the system.

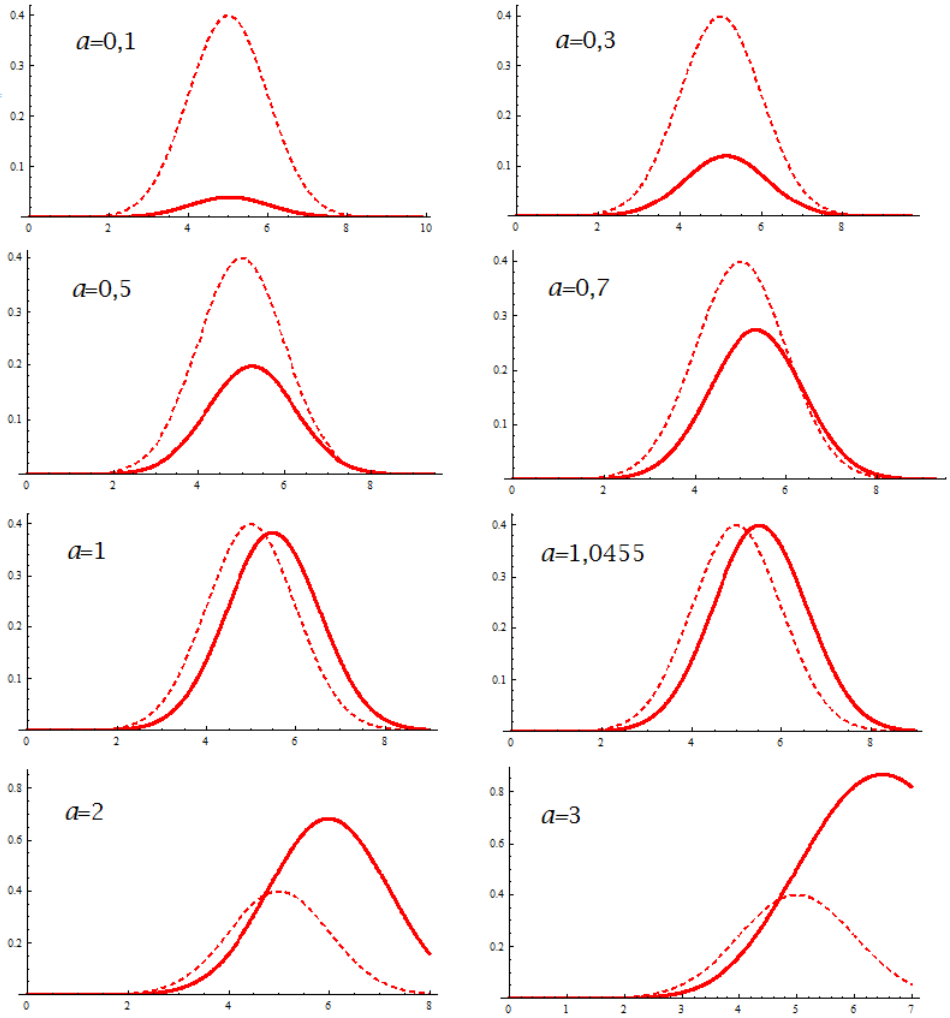

Fig. 1. Graphs of functions $\lambda(t)$ (dotted line), $\Lambda(t)$ (solid line) for $T = 10$, $b = 5$, $c = 1$.

V. Conclusion

The properties of the queuing model with the infinite number of servers and deterministic service time established in the work and computational experiments allow us to discover how service time affects the parameter of the Poisson distribution of the number of customers in the system. A decrease in this parameter leads to a smoothing of the peak in the intensity of the input flow, and an increase leads to an increase in this peak. Therefore, this study allows us to determine how to choose the service time in order to avoid peak loads in the system.

References

[1] Y. Minamino, Y., Makita, Y., Inoue, Sh., Yamada, Sh. (2022) Efficiency Evaluation of Software Faults Correction Based on Queuing Simulation. Mathematics, 10 (9), 1438.

[2] Pham, H. Software Reliability . Springer -Verlag, Singapor e, 2000.

[3] Yamada, S. Software Reliability Modelling, Fundamentals and Applications, Springer -Verlag, 132, Tokyo/Heidelber g, 2014.

[4] Tsitsiashvili, G. Sh. (2020) Non-stationar y Poisson model of a continuously functioning queuing system. Jour nal of Physics: Confer ence Series. The XIII Inter national Confer ence Computer -Aided Technologies in Applied Mathematics (ICAM 2020), 1680 (1): 01205013.

The Log-Hamza distribution with statistical properties and application

An alternative for distributions having domain (0,1).

Aijaz Ahmad*

•

Department of Mathematics, Bhagwant University, Ajmer, India
aijazahmad4488@gmail.com

Afaq Ahmad

•

Department of Mathematical Science, IUST
baderaafaq@gmail.com

I. H. Dar

•

Department of Statistics, University of Kashmir, Srinagar, India
ishfaqqh@gmail.com

Rajnee Tripathi

•

Department of Mathematics, Bhagwant University, Ajmer, India
rajneetripathi@hotmail,com

Abstract

This work suggests a novel two-parameter distribution known as the log-Hamza distribution, in short (LHD). The significant property of the investigated distribution is that it belongs to the family of distributions that have support (0,1). Several statistical features of the investigated distribution were studied, including moments, moment generating functions, order statistics, and reliability measures. For different parameter values, a graphical representation of the probability density function (pdf) and the cumulative distribution function (CDF) is provided. The distribution's parameters are determined using the well-known maximum likelihood estimation approach. Finally, an application is used to evaluate the effectiveness of the distribution.

Keywords: Log transformation, Hamza distribution, moments, maximum likelihood estimation.

1. Introduction

Statistical distribution is important in modelling many sorts of data from various disciplines of resear ch. Statisticsians have focused their efforts on developing new distributions or generalising current distributions by introducing additional parameters. The major reason for these extensions is to improve the efficiency of these distributions while analysing increasingly complicated data.

The Beta distribution, Kumarasw amy distribution, and Topp-Leone distribution are the most commonly used bound support distributions. Among these distributions, the Beta distribution is the most common and has applications in many fields of study , including bio-science, engineer - ing, economics, and finance. The fundamental disadv antage of the beta distribution is that its cumulativ e distribution function (c.d.f) comprises a beta function that cannot be written in closed for m.The aim of this paper is to intr oduce a new distribution which is consider ed an alter nativ e to the family of distributions having support (0,1). To achie ve this goal, the Hamza distribution is used to generate a new distribution which is defined on an open inter val (0,1) . In this regar d, a note w orthy effort has been attempted to limit many continuous distributions in unit inter vals, including: Topp-Leone [12], Nadarajah and kotz [10], Cor deir o and castr o [3], Gomez-Deniz et al. [4], Mazucheli et al. [7], Ghitany et al.[5], Haq et al.[6], Menezes et al.[8], Rodrigues et al.[11], Aijaz et al.[1].

2. The Log-Hamza Distribution

Suppose a random variable X follo w Hamza distribution with probability density function (p.d.f)

$$f(x;\alpha,\beta) = \frac{\beta^6}{\alpha\beta^5+120}\left(\alpha+\frac{\beta}{6}x^6\right)e^{-\beta x} \quad ; \quad x>0,\alpha,\beta>0 \tag{1}$$

The corr esponding cumulativ e distribution function (c.d.f) is giv en as

$$F(x;\alpha,\beta) = 1-\left[1+\frac{\beta x((\beta x)^5+6(\beta x)^4+30(\beta x)^3+120(\beta x)^2+360(\beta x)+720)}{6(\alpha\beta^5+120)}\right]e^{-\beta x} \quad ; \quad x>0,\alpha,\beta>0 \tag{2}$$

Suppose a random variable $Y = e^{-X} \implies X = -ln(Y)$, then the probability density function (pdf) of Y is giv en as

$$f(y;\alpha,\beta) = \frac{\beta^6}{\alpha\beta^5+120}\left(\alpha+\frac{\beta}{6}(ln(y))^6\right)y^{\beta-1} \quad ; \quad 0<y<1,\alpha,\beta>0 \tag{3}$$

Figur e (1.1) and (1.2) repr esents som e possible shapes of pdf of LHD for diff er ent values of parameters

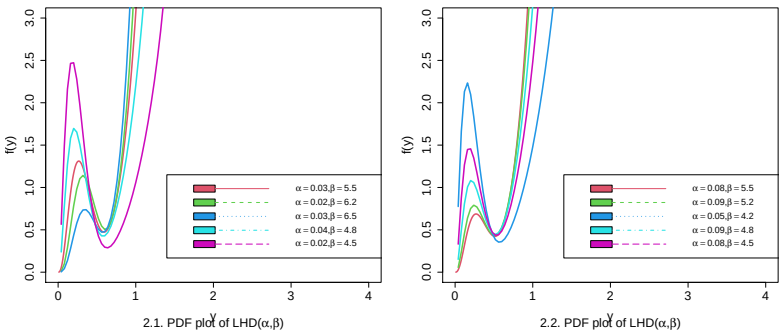

Figure 1

The corr esponding cumulativ e distribution function (cdf) is giv en by

$$F(y;\alpha,\beta) = \left[1 + \frac{((\beta ln(y))^6 - 6(\beta ln(y))^5 + 30(\beta ln(y))^4 - 120(\beta ln(y))^3}{6(\alpha\beta^5 + 120)} + \frac{360(\beta ln(y))^2 - 720(\beta ln(y)))}{6(\alpha\beta^5 + 120)}\right] y^\beta \quad ; \quad 0 \le y \le 1, \alpha, \beta > 0 \tag{4}$$

3. Reliability Measures of Log-Hamza Distribution

This section is focused on researching and developing distinct ageing indicators for the formulated distribution.

3.1. Survival function

Suppose Y be a continuous random variable with cdf $F(y)$.Then its Survival function which is also called reliability function is defined as

$$S(y) = p_r(Y > y) = \int_y^\infty f(y)dy = 1 - F(y)$$

Therefore, the survival function for log-Hamza distribution is given as

$$\begin{aligned} S(y;\alpha,\beta) =& 1 - F(y,\alpha,\beta) \\ S(y) =& 1 - \left[1 + \frac{((\beta ln(y))^6 - 6(\beta ln(y))^5 + 30(\beta ln(y))^4 - 120(\beta ln(y))^3}{6(\alpha\beta^5 + 120)} + \frac{360(\beta ln(y))^2 - 720(\beta ln(y)))}{6(\alpha\beta^5 + 120)}\right] y^\beta \quad ; \quad 0 \le y \le 1, \alpha, \beta > 0 \end{aligned} \tag{5}$$

3.2. Hazard rate function

The hazard rate function of a random variable y is denoted as

$$h(y;\alpha,\beta) = \frac{f(y,\alpha,\beta)}{S(y,\alpha,\beta)} \tag{6}$$

using equation (3) and (4) in equation (6), then the hazard rate function of log-Hamza distribution is given as

$$h(y) = \frac{\beta^6\left(\alpha + \frac{\beta}{6}(ln(y))^6\right) y^{\beta-1}}{6(\alpha\beta^5 + 120) - [6(\alpha\beta^5 + 120) + (A)]\, y^\beta} \quad ; \quad 0 < y < 1, \alpha, \beta > 0$$

where

$$A = (\beta ln(y))^6 - 6(\beta ln(y))^5 + 30(\beta ln(y))^4 - 120(\beta ln(y))^3 + 360(\beta ln(y))^2 - 720(\beta ln(y))$$

Figure (3.1) and (3.2) represents some possible shapes of hrf of LHD for different values of parameters

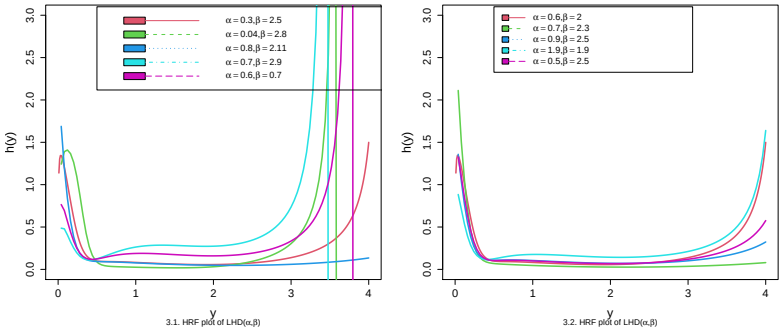

Figure 2

3.3. Cumulativ e hazar d rate function

The cumulativ e hazar d rate function of a random variable y is giv en as

$$H(y,\alpha,\beta) = -ln[\bar{F}(y,\alpha,\beta)] \tag{7}$$

using equation (12) in equation (17), then we obtain cumulativ e hazar d rate function of IWB-III distribution

$$H(y,\alpha,\beta) = -ln\left[1-\left(1+\frac{((\beta ln(y))^6-6(\beta ln(y))^5+30(\beta ln(y))^4-120(\beta ln(y))^3}{6(\alpha\beta^5+120)} + \frac{360(\beta ln(y))^2-720(\beta ln(y)))}{6(\alpha\beta^5+120)}\right)y^{\beta}\right] \tag{8}$$

3.4. Mean residual function

The mean residual lifetime is the predicted residual life or the average completion period of the constituent after it has exceeded a certain duration y. It is extremely significant in reliability investigations.
Mean residual function of random y variable can be obtained as

$$\begin{aligned} m(y;\alpha,\beta) &= \frac{1}{S(y,\alpha,\beta)}\int_y^1 tf(t,\alpha,\beta)dt - y \\ &= \frac{1}{S(y,\alpha,\beta)}\frac{\beta^6}{(\alpha\beta^5+120)}\int_y^1\left(\alpha+\frac{\beta}{6}(ln(t))^6\right)t^{\beta-1}dt - y \end{aligned}$$

Making substitution $ln(t) = -z$, sothat $0 \le z \le -ln(y)$, we have

$$m(y;\alpha,\beta) = \frac{1}{S(y,\alpha,\beta)}\frac{\beta^6}{(\alpha\beta^5+120)}\int_0^{-ln(y)}\left(\alpha+\frac{\beta}{6}z^6\right)e^{-\beta z}dz - y$$

After solving the integral, we get

$$m(y;\alpha,\beta) = \frac{1}{S(y,\alpha,\beta)}\frac{\beta^5}{(\alpha\beta^5+120)}\left\{\alpha(1-y^{\beta})+\frac{1}{6\beta^5}\gamma\left(5,ln(y^{-\beta})\right)\right\} - y$$

Where $\gamma(a,x) = \int_0^x u^{a-1}e^{-u}du$ denotes lower incomplete gamma function

4. Statistical Properties Of log-Hamza Distribution

This section is devoted to deriv e and examine disttinct properties of log-Hamza

4.1. Moments

Let y denotes a random variable, then the r^{th} moment of log-Hamza is denoted as $\mu_r^{'}$ and is given by

$$\begin{aligned}\mu_r^{'} =& E(y^r) = \int_0^1 y^r f(y,\alpha,\beta)dy \\ =& \frac{\beta^6}{\alpha\beta^5+120}\int_0^1 y^{r+\beta-1}\left(\alpha+\frac{\beta}{6}(ln(y))^6\right)dy\end{aligned}$$

Making substitution $ln(y) = -z$, so that $0 < z < \infty$, we have

$$\mu_r^{'} = \frac{\beta^6}{\alpha\beta^5+120}\int_0^\infty \left(\alpha+\frac{\beta}{6}z^6\right)e^{-(\beta+r)z}dz$$

After solving the integral, we have

$$\mu_r^{'} = \frac{\beta^6[(\beta+r)^6+120\beta]}{(\alpha\beta^5+120)(\beta+r)^7}$$

The first four raw moments of log-Hamza distribution are given as.

$$\mu_1^{'} = \frac{\beta^6[(\beta+1)^6+120\beta]}{(\alpha\beta^5+120)(\beta+1)^7} \qquad \mu_2^{'} = \frac{\beta^6[(\beta+2)^6+120\beta]}{(\alpha\beta^5+120)(\beta+2)^7}$$

$$\mu_3^{'} = \frac{\beta^6[(\beta+3)^6+120\beta]}{(\alpha\beta^5+120)(\beta+3)^7} \qquad \mu_4^{'} = \frac{\beta^6[(\beta+4)^6+120\beta]}{(\alpha\beta^5+120)(\beta+4)^7}$$

4.2. Moment generating function

suppose Y denotes a random variable follows log-Hamza distribution. Then the moment generating function of the distribution denoted by $M_Y(t)$is given

$$\begin{aligned}M_Y(t) = E(e^{ty}) &= \int_0^1 e^{ty} f(y;\alpha,\beta)dy \\ &= \int_0^1 \left(1+ty+\frac{(ty)^2}{2!}+\frac{(ty)^3}{3!}+....\right)f(y;\alpha,\beta)dy \\ &= \sum_{r=0}^{\infty}\frac{t^r}{r!}\int_0^\infty y^r f(y;\alpha,\beta)dy \\ &= \sum_{r=0}^{\infty}\frac{t^r}{r!}E(y^r) \\ &= \sum_{r=0}^{\infty}\frac{t^r}{r!}\frac{\beta^6[(\beta+r)^6+120\beta]}{(\alpha\beta^5+120)(\beta+r)^7}\end{aligned}$$

The characteristics function of the log-Hamza distribution denoted as $\phi_Y(t)$ can be yeild by replacing $t = it$ where $i = \sqrt{-1}$

$$\phi_Y(t) = \sum_{r=0}^{\infty}\frac{(it)^r}{r!}\frac{\beta^6[(\beta+r)^6+120\beta]}{(\alpha\beta^5+120)(\beta+r)^7}$$

4.3. Incomplete moments

The general expression for incomplete moments is given as

$$\begin{aligned}T(t) =& \int_0^t y^r f(y;\alpha,\beta)dy \\ =& \frac{\beta^6}{\alpha\beta^5+120}\int_0^t y^{r+\beta-1}\left(\alpha+\frac{\beta}{6}(ln(y))^6\right)dy\end{aligned}$$

Making substitution $ln(y) = -z$, so that $-lnt(t) \leq z \leq \infty$, we have

$$= \frac{\beta^6}{\alpha\beta^5 + 120} \int_{-ln(t)}^{\infty} \left(\alpha + \frac{\beta}{6} z^6\right) e^{-(r+\beta)z} dz$$

After solving the integral, we get

$$T(t) = \frac{\beta^6}{\alpha\beta^5 + 120} \left(\frac{t^{\beta+r}}{\beta + r} + \frac{\beta}{6(\beta + r)} \Gamma\left(5, ln(t^{-(\beta+r)}\right)\right)$$

wher e $\Gamma(a, x) = \int_x^{\infty} u^{a-1} e^{-u} du$ denotes the upper incomplete gamma function.

5. Order Statistics of Log-Hamza Distribution

Let us suppose $Y_1, Y_2, ..., Y_n$ be random samples of size n from log-Hamza distribution with pdf $f(y)$ and cdf F(y). Then the probability density function of the k^{th} order statistics is given as

$$f_Y(k) = \frac{n!}{(k-1)!(n-1)!} f(y) \left[F(y)\right]^{k-1} \left[1 - F(y)\right]^{n-1} \tag{9}$$

Using equation (3) and (4) in equation (10), we have

$$\begin{aligned} f_Y(k) =& \frac{n!}{(k-1)!(n-1)!} \frac{\beta^6}{\alpha\beta^5 + 120} \left(\alpha + \frac{\beta}{6}(ln(y))^6\right) y^{\beta-1} \\ & \times \left[\left[1 + \frac{((\beta ln(y))^6 - 6(\beta ln(y))^5 + 30(\beta ln(y))^4 - 120(\beta ln(y))^3 + 360(\beta ln(y))^2 - 720(\beta ln(y)))}{6(\alpha\beta^5 + 120)}\right] y^{\beta}\right]^{k-1} \\ & \times \left[1 - \left[1 + \frac{((\beta ln(y))^6 - 6(\beta ln(y))^5 + 30(\beta ln(y))^4 - 120(\beta ln(y))^3 + 360(\beta ln(y))^2 - 720(\beta ln(y)))}{6(\alpha\beta^5 + 120)}\right] y^{\beta}\right]^{n-k} \end{aligned}$$

The pdf of the first order statistics Y_1 of log-Hamza distribution is given by

$$\begin{aligned} f_Y(1) =& n \frac{\beta^6}{\alpha\beta^5 + 120} \left(\alpha + \frac{\beta}{6}(ln(y))^6\right) y^{\beta-1} \\ & \times \left[1 - \left[1 + \frac{((\beta ln(y))^6 - 6(\beta ln(y))^5 + 30(\beta ln(y))^4 - 120(\beta ln(y))^3 + 360(\beta ln(y))^2 - 720(\beta ln(y)))}{6(\alpha\beta^5 + 120)}\right] y^{\beta}\right]^{n-1} \end{aligned}$$

The pdf of the n^{th} order statistics Y_n of log-Hamza distribution is given by

$$\begin{aligned} f_Y(1) =& n \frac{\beta^6}{\alpha\beta^5 + 120} \left(\alpha + \frac{\beta}{6}(ln(y))^6\right) y^{\beta-1} \\ & \times \left[\left[1 + \frac{((\beta ln(y))^6 - 6(\beta ln(y))^5 + 30(\beta ln(y))^4 - 120(\beta ln(y))^3 + 360(\beta ln(y))^2 - 720(\beta ln(y)))}{6(\alpha\beta^5 + 120)}\right] y^{\beta}\right]^{n-1} \end{aligned}$$

6. Maximum Likelihood Estimation of log-Hamza Distribution

Let the random samples $y_1, y_2, y_3, ..., y_n$ are drawn from log-Hamza distribution. The likelihood function of n observations is given as

$$L = \prod_{i=1}^{n} \frac{\beta^6}{\alpha\beta^5 + 120} \left(\alpha + \frac{\beta}{6}(ln(y))^6\right) y^{\beta-1}$$

The log-likelihood function is given as

$$l = 6nlog(\beta) - nlog(\alpha\beta^6 + 120) + \sum_{i=1}^{n} log(\alpha + \frac{\beta}{6}(log(y_i))^6) + (\beta - 1) \sum_{i=1}^{n} logy_i \tag{10}$$

The partial derivatives of the log-likelihood function with respect to α and β are given as

$$\frac{\partial l}{\partial \alpha} = \frac{-n\beta^5}{(\alpha\beta^5+120)} + \sum_{i=1}^{n} \frac{6}{(6\alpha+\beta(ln(y_i))^6)} \tag{11}$$

$$\frac{\partial l}{\partial \beta} = \frac{6n}{\beta} - \frac{5n\alpha\beta^4}{(\alpha\beta^5+120)} + \sum_{i=1}^{n} \frac{(ln(y_i))^6}{6\alpha+\beta(ln(y_i))^6} + \sum_{i=1}^{n} log(y_i) \tag{12}$$

For interval estimation and hypothesis tests on the model parameters, an information matrix is required. The 2 by 2 observed matrix is

$$I(\xi) = \frac{-1}{n}\begin{bmatrix} E\left(\frac{\partial^2 logl}{\partial\alpha^2}\right) & E\left(\frac{\partial^2 logl}{\partial\alpha\partial\beta}\right) \\ E\left(\frac{\partial^2 logl}{\partial\beta\partial\alpha}\right) & E\left(\frac{\partial^2 logl}{\partial\beta^2}\right) \end{bmatrix}$$

The elements of above information matrix can be obtain by differentiating equations (12) and (13) again partially. Under standard regularity conditions when $n \to \infty$ the distribution of $\hat{\xi}$ can be approximated by a multivariate normal $N(0, I(\hat{\xi})^{-1})$ distribution to construct approximate confidence interval for the parameters. Hence the approximate $100(1-\psi)\%$ confidence interval for α and β are respectively given by

$$\hat{\alpha} \pm Z_{\frac{\psi}{2}}\sqrt{I^{-1}_{\alpha\alpha}(\hat{\xi})} and \quad \hat{\beta} \pm Z_{\frac{\psi}{2}}\sqrt{I^{-1}_{\beta\beta}(\hat{\xi})}$$

where

$$\frac{\partial^2 l}{\partial\alpha^2} = -\sum_{i=1}^{n} \frac{36}{(6\alpha+\beta(ln(y_i))^6)^2}$$

$$\frac{\partial^2 l}{\partial\beta^2} = \frac{-6n}{\beta^2} - \frac{5n\alpha\beta^3(120-\alpha\beta^5)}{(\alpha\beta^5+120)^2} - \sum_{i=1}^{n} \frac{(ln(y_i))^6}{(6\alpha+\beta(ln(y_i))^6)^2}$$

$$\frac{\partial^2 l}{\partial\alpha\partial\beta} = \frac{\partial^2 l}{\partial\beta\partial\alpha} = \frac{600n\beta^4}{(\alpha\beta^5+120)^2} + \sum_{i=1}^{n} \frac{6(ln(y_i))^6}{(6\alpha+\beta(ln(y_i))^6)^2}$$

7. Data Aanalysis

This subsection evaluates a real-world data set to demonstrate the log-Hamza distribution's applicability and effectiveness. The log-Hamza distribution (LHD) adaptability is determined by comparing its efficacy to that of other analogous distributions such as beta distribution (BD), Kumaraswamy distribution (KSD) and Topp-Leone distribution (TLD).

To compare the versatility of the explored distribution, we consider the criteria like AIC (Akaike information criterion), CAIC (Consistent Akaike information criterion), BIC (Bayesian information criterion) and HQIC (Hannan-Quinn information criterion). Distribution having lesser AIC, CAIC, BIC and HQIC values is considered better.

$$AIC = -2l + 2p, \qquad AICC = -2l + 2pm/\,(m-p-1), \qquad BIC = -2l + p(log(m))$$

$$HQIC = -2l + 2plog(log(m)) \qquad K.S = max_{1\le j\le m}\left(F(x_j) - \frac{j-1}{m}, \frac{j}{m} - F(x_j)\right)$$

Where $'l'$ denotes the log-likelihood function,'p'is the number of parameters and'm'is the sample size.

Data set: The following observation are due to Caramanis et al [2] and Mazmumdar and Gaver [9], where they compare the two distinct algorithms called SC16 and P3 for estimating unit capacity factors. The values resulted from the algorith SC16 are

0.853, 0.759, 0.866, 0.809, 0.717, 0.544, 0.492, 0.403, 0.344, 0.213, 0.116, 0.116, 0.092,
0.070, 0.059, 0.048, 0.036, 0.029, 0.021, 0.014, 0.011, 0.008, 0.006.

The ML estimates with corresponding standard errors in parenthesis of the unknown parameters

Table 1: *Descriptive statistics for data set*

Min.	Max.	Ist Qu.	Med.	Mean	3rd Qu.	kurt.	Ske w.
0.0060	0.8660	0.0325	0.1160	0.2881	0.5180	1.9741	0.7676

Table 2: *The ML Estimates (standard error in parenthesis) for data set*

Model	$\hat{\alpha}$	$\hat{\beta}$
LHD	1.9503	2.0969
	(1.5513)	(0.2355)
BD	0.4869	1.1679
	(0.1208)	(0.3577)
KSD	0.5043	0.0242
	(1.1862)	(0.3264)
TLD	0.5943	....
	(0.1239)	....

Table 3: *Comparison criterion and goodness-of-fit statistics for data set*

Model	-2l	AIC	AICC	BIC	HQIC	K.S statistic	p-value
LHD	-25.551	-21.551	-20.951	-19.280	-20.980	0.1034	0.9663
BD	-19.214	-15.214	-14.614	-12.943	-14.643	0.183	0.4202
KSD	-19.341	-15.341	-14.741	-13.070	-14.770	0.178	0.4526
TLD	-16.230	-14.230	-14.039	-13.094	-13.944	0.168	0.5273

are presented in Table 2 and the comp arison statistics, AIC, BIC, CAIC, HQIC and the goodness-of-fit statistic for the data set are displa yed in Table 3.

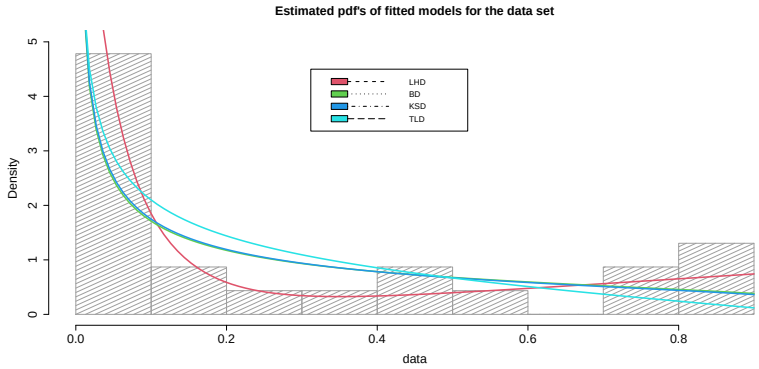

Figure 3

It is obser ved from table 3 that LHD provides best fit than other competativ e models based on the measur es of statistics, AIC, BIC, AICC, HQIC and K-S statistic. Along with p-value s of each model.

8. Conclusion

This study proposed a new two parameters distribution known as Log-Hamza distribution which is defined on unit inter val and is used for modelling the real life data. Several structural properties

of the proposed distribution including moments, moment generating function, order statistics and reliability measures has been discussed. The parameters of the distribution are estimated by famous method of maximum likelihood estimation. Finally the efficiency of the distribution is examined through an application when compared with Beta distribution, Kumaraswamy distribution and Topp-Leone distribution.

References

[1] A. Aijaz, M.Jallal, S.Q. Ain Ul and R.Tripathi. The Hamza distribution with statistical properties and applications. *Asian journal of probability and statistics*, *8 (2020)*, 28-42.

[2] M. Caramanis,J.Stremel, W. Fleck and S. Daneil. Probabilistic production costing: an investigation of alternative algorithms. *Internation journal of electrical power and energy system,5(2),(1983)*, 75-86.

[3] G.M. Corderio and M. de Castro. A new family of generalized distribution. *Journal of statistical computation and simulation,81(7)* (2011),75-86.

[4] Gomez-Deniz, M.A.Sordo, E. Calderin-Ojeda. The Log-Lindley distribution as an alternative to beta regression model with applications in insurance.. *Insurance: Mathematics and Economics*,*54 (2014)*, 49-57.

[5] M.E. Ghitnay, J. Mazucheli. A.F.B. Menezes and F. Alqallaf. The unit-Inverse Gaussian distribution: A new alternative to two-parameter distribution on the unit interval. *Commum. Stat. theory methods*, *48 (2019)*, 3423-3438.

[6] M.A Haq,S. Hashmi, K. Aidi, P.L. Ramos and F. Louzada. Unit modified Burr-III distribution: Estimation, characterization and validation test. *Ann. data sci.*, *87(15) (2020)*.

[7] J. Mazucheli, A.F.B. Menezes, L.B Fernandes, R.P. de Oliveria and M.E. Ghitney. The unit-Weibull distribution and associated inference. *J.Appl. probab. Stat*, *13 (2018)*,1-22.

[8] A.F.B. Menezes, J. Mazucheli and S. Dey. The unit-Gompertz distribution with applications. *Statistica*, *79 (2019)*,25-43.

[9] M. Mazumdar and D.P. Gaver. On the computation of power-generating system reliability indexes. *Tecnometrics*, *26(2) (2019)*,173-185.

[10] S. Nadarajah and S. Kotz. Moments of some J-shaped distribution. *journal of applied statistics*, *30(3) (2003)*,311-317.

[11] J. Rodrigues, J.L. Bazan and A.K. Aflexible procedure for formulating probability distribution on the unit-interval with applications. *Commun. stat. Theory methods*, *49 (2020)*, 738-754.

[12] C.W. Topp and F.C. Leone. A family of J-Shaped frequency function. *journal of the American statistical association*, *50(269) (1955)*, 209-219.

RT&A, No 3 (69)
Volume 17, September 2022

Sensitivity and Economic Analysis of an Insured System with Extended Conditional Warranty

Kajal Sachdeva

•

Department of Mathematics, Maharshi Dayanand University, Rohtak, Haryana, India
kajal.rs.maths@mdurohtak.ac.in

Gulshan Taneja

•

Department of Mathematics, Maharshi Dayanand University, Rohtak, Haryana, India
drgtaneja@gmail.com

Amit Manocha*

•

Department of Applied Sciences, TITS Bhiwani, Haryana, India
amitmanocha80@yahoo.com

*Corresponding Author

Abstract

Warranty and insurance are equally essential for a technological system to cover repair/replacement costs of all types of losses, i.e., natural wear/tear or unexpected external force/accidents. This paper examines the sensitivity and profitability of a stochastic model whose defects may cover under conditional warranty/insurance. The system user may extend the warranty period by paying an additional price. As a result, the system functions in normal warranty, extended warranty, and during non-warranty periods. If a system fault occurred is covered under warranty conditions, the manufacturer is responsible for all repair/replacement costs during normal/extended warranty which otherwise are paid by the insurance provider if covered under an insurance claim, or else, the user is responsible for the entire cost when coverage of fault neither falls in warranty conditions nor under the insurance policy. Using Markov and the regenerative process, various measures of system effectiveness associated with the profit of the user and the manufacturer are examined. Relative sensitivity analysis of the profit function and availability has been performed for all periods.

Keywords: Extended Conditional Warranty; Sensitivity Analysis; Profit; Insurance Cover

1. Introduction

Competitors add and offer new features to advertise their products in today's continuously expanding technological landscape. Offering a warranty on a system can be very beneficial to a company's growth. It relieves buyers' concerns, demonstrates the system's reliability, and is promotional. A warranty is a formal promise issued to the user for the free repair or system replacement if it fails. Researchers have focused their attention on warranty systems, policies, and warranty expense management in the past few decades [1–3, 6]. Generally, warranties cover the cost of failures that are defined in the contract at the time of purchased. Taneja [12] described the reliability analysis of a system with predetermined warranty conditions. Further, this work has extended to warranty period and non-warranty period [9–11]. Many systems have enormous

maintenance costs and are operated for long periods. Manufacturers are offering the option of extending the warranty period with an additional charge to avoid the cost of repair/replacement for an extensive period. Jack and Murthy [4] proposed the idea of employing a game-theoretic technique to determine the length and duration of an extended warranty based on the consumer's risk attitude. Padmanabhan and Rao [7] estimated the basic warranty time to be three years, a smart option for the increasing demand for long-term service contracts. Rinsaka and Sandoh [8] discussed an extended warranty in which the manufacturer replaces the system after the first failure and only performs minor repairs on subsequent failures. They also examined the optimal pricing for such an extended warranty.
However, financial protection is provided by insurance and warranty both against unpredictable damage or loss. There is a thin strip between them. While insurance protects against unintentional damage or loss, warranty protects against defective parts. Purchasing both at the same time is likely advantageous since it provides peace of mind in knowing that including insurance covers accidental damages, the warranty will cover faulty parts, effectively including the majority of faults/accidents that emerge in a technical system. Lutz and Padmanabhan [5] investigated the impact of impartial and independent insurance providers on manufacturer price strategy.
The cost analysis of an insured system with an extended conditional warranty is yet to be investigated. This paper proposes a model for a system with a conditional normal/extended warranty and long-term insurance which is structured as follows. Section 2 discusses the system's assumptions and description of the model. Section 3 describes the notations used in the analysis. Section 4 covers the system's stochastic modelling. The profitability measures and profit functions for the user, manufacturer, and insurance provider are drafted in Sections 5, 6, 7. Section 8 describes the sensitivity and relative sensitivity functions of availabilities and profit functions. Section 9 illustrates the above measurements using fixed parameter values that follow an exponential distribution. Section 10 concludes the study with interpretations.

2. Assumptions and System Characterizations

Following are the characterizations and suppositions used in the analysis of considered system:

1. The system consists of a single insured unit dividing its whole lifetime into three periods, i.e. normal warranty, extended warranty, and non-warranty periods.
2. The manufacturer or insurance provider inspects the failed system to assure
   (a) Whether system's flaws are covered by a warranty, an insurance claim, or neither.
   (b) Whether the system can be repaired or needs to be replaced.
3. In the case of normal and extended warranty periods, if an inspection indicates that
   (a) the defects are within the warranty domain, then the manufacturer bears the repair/replacement costs
   (b) the fault is covered by insurance, the repair/replacement costs are covered by the insurance company.
   (c) the defects are not covered by warranty or insurance, the user is responsible for all costs.
4. During the non-warranty period, the insurance provider or the user is solely responsible for repair/replacement costs as the case may be.
5. Transition time distributions have been taken as arbitrarily and the random variables that are involved are independent.

The system is depicted in Figure 1. The number of replacements, the availability, and the expected busy period are all calculated. The profit functions are assessed. The sensitivity analysis is also

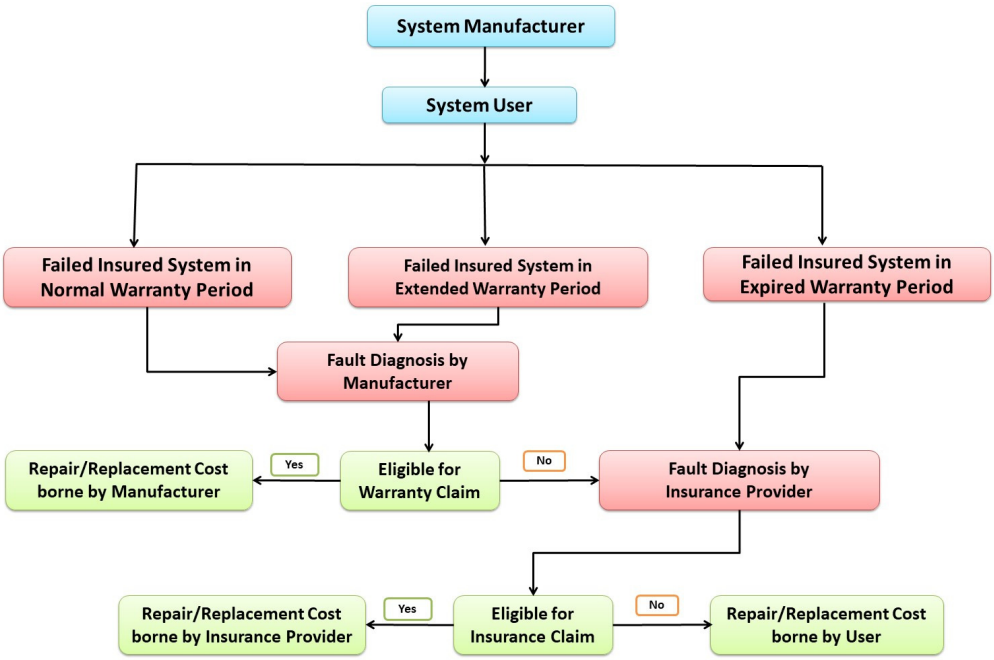

Figure 1: *System description*

performed for availability in three different time zones, as well as the manufacturer's and user's profit functions. Numerical estimates are based on exponential distributions. Various results are drawn about profitability and sensitivity.

3. Nomenclature

The following is the nomenclature for different probabilities/transition densities:

E_0	system state at time t=0
$p_w / \overline{p_w}$	probability that a fault is approved/ not approved under warranty conditions.
$r / \overline{r}$	probability that the fault is repairable or incurable, and that the system should be replaced.
$p_n / p_{et} / p_{ex}$	probability of a system failure within the normal/extended/non-warranty period.
$p_s / \overline{p_s}$	probability that the fault is covered or not covered under the provisions of the insurance policy.
$f_w(t)$	p.d.f. of failure time.
$i^m(t) / i^s(t)$	p.d.f. of the repairman's inspection time as contracted by the manufacturer/insurance provider.
$g^n(t) / g^{et}(t) / g^{ex}(t)$	p.d.f. of the repair time during normal/ extended/ expired warranty period
$h^n(t) / h^{et}(t) / h^{ex}(t)$	p.d.f. of the replacement time during normal/ extended/ expired warranty period
$Ak_i(t)$	probability that the system is operational at time t it is given that $E_0 = i$ during warranty period 'k=N/T/X'.

$IK_i(t)$	probability that the repairman of manufacturer or insurance company is busy in inspection at time t it is given that $E_0 = i$ during warranty period 'k'.
$Bk_i^m(t)(Bk_i^u(t))$	probability that the repairman of manufacturer is busy for repair/replacement when charges are borne by manufacturer or insurance provider (user) itself at time t it is given that $E_0 = i$ during warranty period 'k'.
$Rk_i^m(t)(Rk_i^u(t))$	expected number of replacement upto time t, when expenses are borne by manufacturer or insurance provider (user), given that $E_0 = i$ during warranty period 'k'.

The states of the system are specified by the following notations:

O_k	operational unit in warranty period 'k'.
Fk_I	failure unit under inspection by manufacturer in warranty period 'k'.
Fk_{IS}	failure unit under inspection by insurance provider in warranty period 'k'.
$FM_{RN}(FM_{RPN})/FM_{RT}(FM_{RPT})$	failure unit under repair(replacement) in normal/extended warranty period, for which charges are to be paid by manufacturer.
FS_{Rk}/FS_{RPk}	failure unit under repair/replacement in warranty period 'k', for which charges are to be paid by insurance provider.
FU_{Rk}/FU_{RPk}	failed system under repair/replacement in warranty period 'k', for which expenses are to be borne by user itself.

where k stands for normal(N), extended(T), expired(X).

4. Stochastic Model

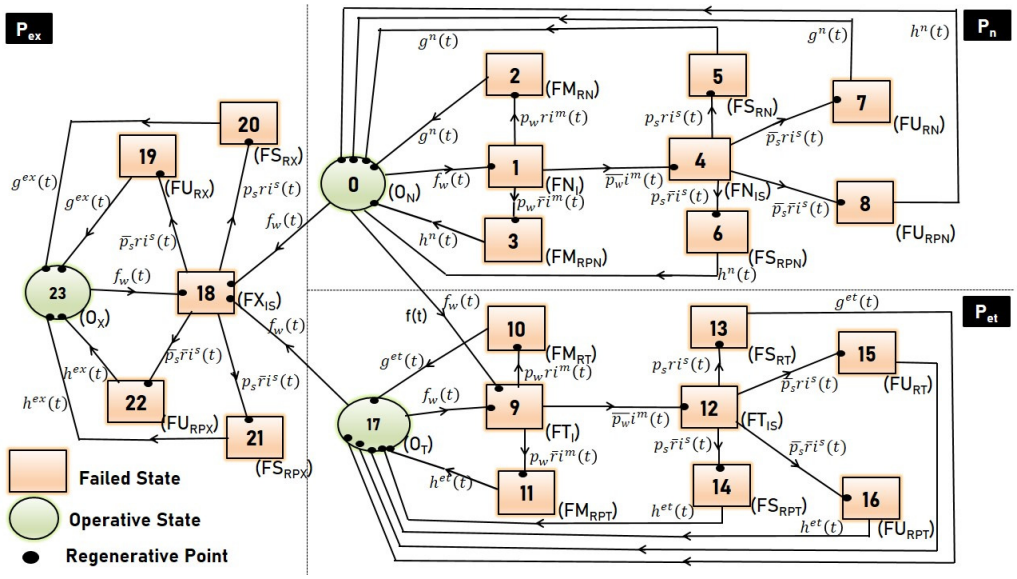

Figure 2: *State transition diagram*

Figure 2 illustrates the transition between several stages of the system. The state space is made up of the regenerative states, S={0, 1, 2, ..., 23}, where O={0, 17, 23} is operative state spaces

and F={1, 2, 3, 4, 5, 6, 7, 8, 9, 10, 11, 12, 13, 14, 15, 16, 18, 19, 20, 21, 22} is failed state space respectively. From figure 2, it may be observed that when system enters into a new state there is no continuation of inspection, repair and replacement from the previous state and hence at each time point, the process restarts probabilistically and thus the corresponding state where the system enters becomes the regenerative state. Further, it may also be observed that future state is independent of past and it depends only on present, thereby satisfying the Markov property. Therefore, the state transitions satisfy the Markov process and form the regenerative points. Thus, regenerative point technique is used to find various characteristics of the system.
The transition densities $q_{ij}(t)$ are:

$q_{01}(t) = f_w(t)$, $q_{12}(t) = p_w r i^m(t)$, $q_{13}(t) = p_w \bar{r} i^m(t)$ $q_{14}(t) = \overline{p_w} i^m(t)$,
$q_{45}(t) = p_s r i^s(t)$, $q_{46}(t) = p_s \bar{r} i^s(t)$, $q_{47}(t) = \overline{p_s} r i^s(t)$, $q_{48}(t) = \overline{p_s} \bar{r} i^s(t)$,
$q_{20}(t) = g^n(t)$ $q_{30}(t) = h^n(t)$, $q_{50}(t) = g^n(t)$, $q_{60}(t) = h^n(t)$
$q_{70}(t) = g^n(t)$, $q_{80}(t) = h^n(t)$ $q_{09}(t) = f_w(t)$, $q_{9,10}(t) = p_w r i^m(t)$,
$q_{9,11}(t) = p_w \bar{r} i^m(t)$ $q_{9,12}(t) = \overline{p_w} i^m(t)$, $q_{12,13}(t) = p_s r i^s(t)$, $q_{12,14}(t) = p_s \bar{r} i^s(t)$,
$q_{12,15}(t) = \overline{p_s} r i^s(t)$, $q_{12,16}(t) = \overline{p_s} \bar{r} i^s(t)$, $q_{10,17}(t) = g^{et}(t)$ $q_{11,17}(t) = h^{et}(t)$,
$q_{13,17}(t) = g^{et}(t)$, $q_{14,17}(t) = h^{et}(t)$ $q_{15,17}(t) = g^{et}(t)$, $q_{16,17}(t) = h^{et}(t)$
$q_{0,18}(t) = f_w(t)$, $q_{17,18}(t) = f_w(t)$, $q_{17,9}(t) = f_w(t)$ $q_{18,19}(t) = \overline{p_s} r i^s(t)$,
$q_{18,20}(t) = p_s r i^s(t)$, $q_{18,21}(t) = p_s \bar{r} i^s(t)$, $q_{18,22}(t) = \overline{p_s} \bar{r} i^s(t)$, $q_{19,23}(t) = g^{ex}(t)$
$q_{20,23}(t) = g^{ex}(t)$, $q_{21,23}(t) = h^{ex}(t)$ $q_{22,23}(t) = h^{ex}(t)$, $q_{23,18}(t) = f_w(t)$,

Mean sojourn time (μ_i) in state i, i $\in$ S is given as
μ_i=$\int_0^\infty t$ (corresponding p.d.f. of time for moving from i^{th} state) dt
Defining m_{ij}= $\int_0^\infty t q_{ij}(t)dt$, contribution to mean sourjoun time, we have

$$m_{01} = \int_0^\infty t q_{01}(t)dt = \int_0^\infty t f(t)dt = \mu_0$$

$$\begin{aligned} m_{12} + m_{13} + m_{14} &= \int_0^\infty t q_{12}(t)dt + \int_0^\infty t q_{13}(t)dt + \int_0^\infty t q_{14}(t)dt \\ &= \int_0^\infty t p_w r i^m(t)dt + \int_0^\infty t p_w \bar{r} i^m(t)dt + \int_0^\infty t \overline{p_w} i^m(t)dt \\ &= \int_0^\infty t i^m(t)dt \\ &= \mu_1 \end{aligned}$$

Similarly,

$m_{09} = m_{0,18} = \mu_0$; $m_{20} = \mu_2$
$m_{30} = \mu_3$ $m_{45} + m_{46} + m_{47} + m_{48} = \mu_4$;
$m_{50} = \mu_5$; $m_{60} = \mu_6$
$m_{70} = \mu_7$; $m_{80} = \mu_8$
$m_{9,10} + m_{9,11} + m_{9,12} = \mu_9$; $m_{10,17} = \mu_{10}$
$m_{11,17} = \mu_{11}$; $m_{12,13} + m_{12,14} + m_{12,15} + m_{12,16} = \mu_{12}$;
$m_{13,17} = \mu_{13}$ $m_{14,17} = \mu_{14}$;
$m_{15,17} = \mu_{15}$ $m_{16,17} = \mu_{16}$;
$m_{17,9} = m_{17,18} = \mu_{17}$ $m_{18,19} + m_{18,20} + m_{18,21} + m_{18,22} = \mu_{18}$;
$m_{19,23} = \mu_{19}$ $m_{20,23} = \mu_{20}$;
$m_{21,23} = \mu_{21}$ $m_{22,23} = \mu_{22}$;
$m_{23,18} = \mu_{23}$

In the following sections, several system profitability measures are achieved.

5. System Availability

1. **During Extended Warranty Period**

By definition of $AT_i(t)$, i=0, 9, 10, 11, 12, 13, 14, 15, 16, 17 (defined in Section 3) and the transitions that occurs during the extended warranty period, we have

$$\begin{aligned} AT_0(t) &= \overline{f_w(t)} + \int_0^t q_{09}(u) AT_9(t-u)du \\ &= M_0(t) + q_{09}(t) \odot AT_9(t) \end{aligned} \tag{1}$$

The term on L.H.S. of eq^n (1) denotes that the system is operational at time t given that $E_0 = 0$. The first term on R.H.S. indicates that the system will remain in state 0 rather than transitioning to another state.The second term denotes that the system transitions from state 0 to state 9 in time u<t and and then continues operational for t-u time from state 9 onwards.
Similarly the other recurrence relations are:

$$\begin{cases} AT_9(t) = q_{9,10}(t) \odot AT_{10}(t) + q_{9,11}(t) \odot AT_{11}(t) + q_{9,12}(t) \odot AT_{12}(t) \\ AT_{10}(t) = q_{10,17}(t) \odot AT_{17}(t) \\ AT_{11}(t) = q_{11,17}(t) \odot AT_{17}(t) \\ AT_{12}(t) = q_{12,13}(t) \odot AT_{13}(t) + q_{12,14}(t) \odot AT_{14}(t) + q_{12,15}(t) \odot AT_{15}(t) + q_{12,16}(t) \odot AT_{16}(t) \\ AT_{13}(t) = q_{13,17}(t) \odot AT_{17}(t) \\ AT_{14}(t) = q_{14,17}(t) \odot AT_{17}(t) \\ AT_{15}(t) = q_{15,17}(t) \odot AT_{17}(t) \\ AT_{16}(t) = q_{16,17}(t) \odot AT_{17}(t) \\ AT_{17}(t) = M_{17}(t) + q_{17,9}(t) \odot AT_9(t) \end{cases} \tag{2}$$

Solving eq^n(1)-(2) for $AT_0^*(s)$, where $AT_0^*(s)$ = L$[AT_0(t)]$, we have

$$AT_0^*(s) = \frac{K_1(s)}{T_1(s)}$$

$$\begin{aligned} K_1(s) &= M_0^*(s) + q_{09}^*(s)q_{9,10}^*(s)q_{10,17}^*(s)M_{17}^*(s) + q_{09}^*(s)q_{9,11}^*(s)q_{11,17}^*(s)M_{17}^*(s) \\ &- q_{17,9}^*(s)q_{9,10}^*(s)q_{10,17}^*(s)M_0^*(s) - q_{17,9}^*(s)q_{9,11}^*(s)q_{11,17}^*(s)M_0^*(s) \\ &+ q_{09}^*(s)q_{9,12}^*(s)q_{12,13}^*(s)q_{13,17}^*(s)M_{17}^*(s) + q_{09}^*(s)q_{9,12}^*(s)q_{12,14}^*(s)q_{14,17}^*(s)M_{17}^*(s) \\ &- q_{17,9}^*(s)q_{9,12}^*(s)q_{12,13}^*(s)q_{13,17}^*(s)M_0^*(s) + q_{09}^*(s)q_{9,12}^*(s)q_{12,15}^*(s)q_{15,17}^*(s)M_{17}^*(s) \\ &- q_{17,9}^*(s)q_{9,12}^*(s)q_{12,14}^*(s)q_{14,17}^*(s)M_0^*(s) + q_{09}^*(s)q_{9,12}^*(s)q_{12,16}^*(s)q_{16,17}^*(s)M_{17}^*(s) \\ &- q_{17,9}^*(s)q_{9,12}^*(s)q_{12,15}^*(s)q_{15,17}^*(s)M_0^*(s) - q_{17,9}^*(s)q_{9,12}^*(s)q_{12,16}^*(s)q_{16,17}^*(s)M_0^*(s) \\ &= NT_1^*(s)(say) \end{aligned} \tag{3}$$

$$\begin{aligned} T_1(s) &= 1 - q_{17,9}^*(s)q_{9,11}^*(s)q_{11,17}^*(s) - q_{17,9}^*(s)q_{9,12}^*(s)q_{12,13}^*(s)q_{13,17}^*(s) \\ &- q_{17,9}^*(s)q_{9,12}^*(s)q_{12,14}^*(s)q_{14,17}^*(s) - q_{17,9}^*(s)q_{9,12}^*(s)q_{12,15}^*(s)q_{15,17}^*(s) \\ &- q_{17,9}^*(s)q_{9,12}^*(s)q_{12,16}^*(s)q_{16,17}^*(s) - q_{17,9}^*(s)q_{9,10}^*(s)q_{10,17}^*(s) \\ &= DT_1^*(s)(say) \end{aligned} \tag{4}$$

The system's steady state availability is evaluated using Abel's lemma as:

$$AT_0 = \lim_{s \to 0} sAT_0^*(s) = \frac{NT_1^*(0)}{DT_1^{*'}(0)} = \frac{NT_1}{DT_1} \tag{5}$$

Differentiating eq^n (4) w.r.t. s,

$$\begin{aligned} DT_1^{*'}(s) = {} & q_{11,6}^{*}{}'(s)(-q_{67}^{*}(s)q_{7,11}^{*}(s) - q_{68}^{*}(s)q_{8,11}^{*}(s) - q_{69}^{*}(s)q_{9,11}^{*}(s) \\ & - q_{6,10}^{*}(s)q_{10,11}^{*}(s)) - q_{67}^{*}{}'(s)q_{7,11}^{*}(s)q_{11,6}^{*}(s) - q_{68}^{*}{}'(s)q_{8,11}^{*}(s)q_{11,6}^{*}(s) \\ & - q_{69}^{*}{}'(s)q_{9,11}^{*}(s)q_{11,6}^{*}(s) - q_{6,10}^{*}{}'(s)q_{10,11}^{*}(s)q_{11,6}^{*}(s) \\ & - q_{7,11}^{*}{}'(s)q_{11,6}^{*}(s)q_{67}^{*}(s) - q_{8,11}^{*}{}'(s)q_{11,6}^{*}(s)q_{68}^{*}(s) \\ & - q_{9,11}^{*}{}'(s)q_{11,6}^{*}(s)q_{69}^{*}(s) - q_{10,11}^{*}{}'(s)q_{11,6}^{*}(s)q_{6,11}^{*}(s) \end{aligned} \tag{6}$$

Taking lim s $\to$ 0 in eq^n (3) and (6), we get

$$\begin{aligned} NT_1 = {} & \mu_{17}(p_w r + p_w\bar{r} + \overline{p_w}p_s r + \overline{p_w}p_s\bar{r} + \overline{p_w p_s}r + \overline{p_w p_s r}) - \mu_0(p_w r \\ & + p_w\bar{r} + \overline{p_w}p_s r + \overline{p_w}p_s\bar{r} + \overline{p_w p_s}r + \overline{p_w p_s r} - 1) \\ = {} & \mu_{17} \end{aligned} \tag{7}$$

$$\begin{aligned} DT_1 = {} & m_{9,12}(p_s r + p_s\bar{r} + \overline{p_s}r + \overline{p_s r}) + m_{9,10} + m_{9,11} + \overline{p_w}\mu_{12} + p_w r m_{10,17} \\ & + p_w\bar{r}m_{11,17} + \overline{p_w}p_s r m_{13,17} + \overline{p_w}p_s\bar{r}m_{14,17} + \overline{p_w p_s}r m_{15,17} + \overline{p_w p_s}\bar{r}m_{16,17} \\ = {} & \mu_{17} + \mu_9 + \mu_{10}p_w r + \mu_{11}p_w\bar{r} + \mu_{12}\overline{p_w} + \mu_{13}\overline{p_w}p_s r + \mu_{14}\overline{p_w}p_s\bar{r} + \mu_{15}\overline{p_w p_s}r \\ & + \mu_{16}\overline{p_w p_s}\bar{r} \end{aligned} \tag{8}$$

2. **During Normal Warranty Period**
Similarly, steady-state availabilities during normal warranty period are given as

$$AN_0 = \frac{NN_1}{DN_1}; \tag{9}$$

where

$$NN_1 = \mu_0,$$
$$DN_1 = \mu_0 + \mu_1 + p_w r\mu_2 + p_w\bar{r}\mu_3 + \overline{p_w}\mu_4 + \overline{p_w}p_s r\mu_5 + \overline{p_w}p_s\bar{r}\mu_6 + \overline{p_w p_s}r\mu_7 + \overline{p_w p_s}\bar{r}\mu_8$$

3. **During Non Warranty Period**
Proceeding as above case, the steady-state availability during expired warranty period is:

$$AX_0 = \frac{NX_1}{DX_1} \tag{10}$$

where

$$NX_1 = \mu_{23}, \qquad DX_1 = \mu_{18} + \overline{p_s}r\mu_{19} + p_s r\mu_{20} + p_s\bar{r}\mu_{21} + \overline{p_s\bar{r}}\mu_{22}$$

6. Expected Busy Period and number of replacements

Using the definitions of Ik_i, Bk_i^m and Bk_i^u,i $\in$ S (defined in section 3) and the identical steps outlined in the preceding section, the expected time a repairman spends inspecting, repairing, or replacing a failed system in different warranty periods is given as:

$Ik_0 = \frac{Nk_2}{Dk_1}$; $\quad Bk_0^m = \frac{Nk_3}{Dk_1}$; $\quad Bk_0^u = \frac{Nk_4}{Dk_1}$; $\quad$ k=N, T, X.

where

$NN_2 = \mu_1 + \overline{p_w}\mu_4$; $\quad NT_2 = \mu_9 + \overline{p_w}\mu_{12}$; $\quad NX_2 = \mu_{18}$;
$NN_3 = p_w r\mu_2 + p_w\bar{r}\mu_3 + \overline{p_w}p_s r\mu_5 + \overline{p_w}p_s\bar{r}\mu_6$;
$NT_3 = p_w r\mu_{10} + p_w\bar{r}\mu_{11} + \overline{p_w}p_s r\mu_{13} + \overline{p_w}p_s\bar{r}\mu_{14}$; $\quad NX_3 = p_s r\mu_{20} + p_s\bar{r}\mu_{21}$;
$NN_4 = \overline{p_w p_s}r\mu_7 + \overline{p_w p_s}\bar{r}\mu_8$; $\quad NT_4 = \overline{p_w p_s}r\mu_{15} + \overline{p_w p_s}\bar{r}\mu_{16}$; $\quad NX_4 = \overline{p_s}r\mu_{19} + \overline{p_s\bar{r}}\mu_{22}$;

Furthermore, the expected number of replacements for three warranty periods in steady-state, according to the definitions of Rk_i^m and Rk_i^u,i ∈ S (specified in section 3), are:

$Rk_0^m = \frac{Nk_5}{Dk_1}$; $Rk_0^u = \frac{Nk_6}{Dk_1}$; k=N, T , X

where,

$NN_5 = p_w\bar{r} + \overline{p_w}p_s\bar{r}$; $NT_5 = p_w\bar{r} + \overline{p_w}p_s\bar{r}$; $NX_5 = p_s\bar{r}$;

$NN_6 = \overline{p_w}p_s\bar{r}$; $NT_6 = \overline{p_w}p_s\bar{r}$; $NX_6 = \overline{p_s}\bar{r}$;

7. Cost-Benefit Analysis

The financial analysis aids both the maker and the consumer in identifying the variables that may result in long-term loss. In this section, we created profit functions to do a cost estimate. A profit function is a mathematical relationship between a system's total output and total expenditure. Thus, profit functions in steady-state are:

Profit to System and Insurance Provider

$$\begin{aligned} PM = {} & CP + EP - MP + SP - CM_1(p_nIN_0 + p_{et}IT_0) - CS_1(p_nIN_0 + p_{et}IT_0 + p_{ex}IX_0) \\ & - CM_2(p_nBN_0^m + p_{et}BT_0^m + p_{ex}BX_0^m) - CM_3(p_nRN_0^m + p_{et}RT_0^m + p_{ex}RX_0^m) \end{aligned} \tag{11}$$

Profit to System User

$$\begin{aligned} PU = {} & R_0(p_nAN_0 + p_{et}AT_0 + p_{ex}AX_0) - CU_2(p_nBN_0^u + p_{et}BT_0^u + p_{ex}BX_0^u) \\ & - CU_3(p_nRN_0^u + p_{et}RT_0^u + p_{ex}RX_0^u) - CP - EP - SP \end{aligned} \tag{12}$$

where,

CP= Expenses of purchasing the system
MP= Manufacturing cost of the system
EP= Expenses of extending the warranty period
SP= Expenses associated with insuring the system
R_0= Revenue generated by the system.
CM_1/CS_1= Expenses incurred by the manufacturer/insurance provider in hiring a repairman for inspection.
$CM_2(CU_2)$= Expenses incurred by the manufacturer or insurance company (user) in engaging a repairman for repair/replacement.
$CM_3(CU_3)$= Expenses incurred when a system is replaced, which are covered by the manufacturer or the insurance company (user).

All of the costs listed above are per unit time.

8. Sensitivity Analysis

Sensitivity analysis is an approach that examines whether a parameter has a high or low influence on the derived measures. Due to the wide range of numerical values for various parameters, relative sensitivity analysis is performed to compare the effects of various parameters. A relative sensitivity function is a standardized version of a sensitivity function.The sensitivity (Δ_{rk}, δ_{rs}) and relative sensitivity functions (z_{rk}, z_{rs}) for availabilities (AN_0, AT_0, AX_0) and profit functions (PM,PU) are defined using the eq^ns (5), (9), (10), (11) and (12) and stated as follows:

$$\Delta_{rk} = \frac{\partial(Ak_0)}{\partial r}; \qquad z_{rk} = \frac{\Delta_{rk}r}{Ak_0} \qquad k = N, T, X \tag{13}$$

and

$$\delta_{rs} = \frac{\partial(Ps)}{\partial r}; \qquad z_{rs} = \frac{\delta_{rs}r}{Ps}; \qquad s = U, M \tag{14}$$

where r is the parameter

9. Results and Discussions

The system characteristics determined in the preceding sections 5-8 are illustrated numerically in this section. Assume that all of the distributions are exponentially distributed and their probability density functions are as follows:

$$\begin{cases} f_w(t) = \lambda_w e^{-\lambda_w t}, & i^m(t) = \gamma_m e^{-\gamma_m t}, & i^s(t) = \gamma_s e^{-\gamma_s t} \\ h^n(t) = \beta_n e^{-\beta_n t}, & h^{et}(t) = \beta_t e^{-\beta_t t}, & g^n(t) = \alpha_n e^{-\alpha_t t} \\ g^{et}(t) = \alpha_t e^{-\alpha_t t}, & g^{ex}(t) = \alpha_x e^{-\alpha_x t}, & h^{ex}(t) = \beta_x e^{-\beta_x t} \end{cases} \tag{15}$$

Consider the fixed value of parameters as

$$\begin{aligned} &p_w = 0.7, \overline{p_w} = 0.3, p_n = 0.2, p_{et} = 0.3, p_{ex} = 0.5, r = 0.7, \bar{r} = 0.3, p_s = 0.8, \overline{p_s} = 0.2, \\ &\lambda_w = 0.0005, \gamma_m = 1.5, \gamma_s = 1.2, \alpha_n = 0.5, \alpha_t = 0.4, \beta_n = 0.02, \beta_t = 0.02, \alpha_x = 0.25, \\ &\beta_x = 0.01, CP = 150, EP = 15, SP = 20, MP = 120, R_0 = 500, CM_1 = 80, CM_2 = 100, \\ &CM_3 = 15,000, CS_1 = 90, CU_2 = 120, CU_3 = 15,000. \end{aligned} \tag{16}$$

9.1. Variation in Profit Functions

The profit function has been graphically represented as a function of various parameters in this section. Figure 3 shows the change in manufacturer's profit (PM) versus p_s and λ_w. Profit falls

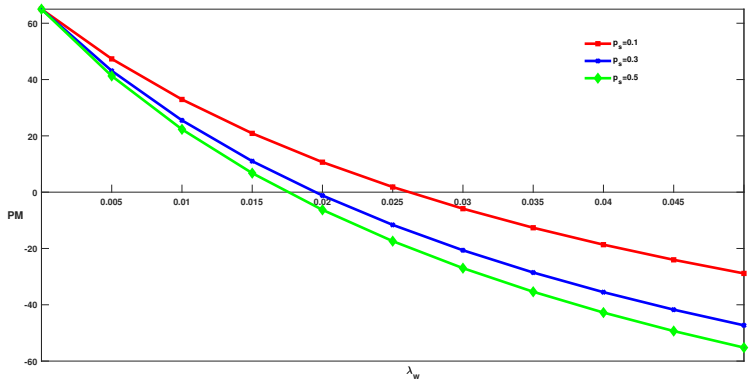

Figure 3: *Manufacturer's Profit (PM) for varied λ_w and p_s*

rapidly as λ_w and p_s rises.
The variation occured in user's profit (PU) due to changes in R_0 and $\bar{r}$ is depicted in Figure 4. Profit begins to rise as R_0 rises, and as $\bar{r}$ rises, profit declines. Figure 5 shows the decrease in profit differential (PU-PM) versus SP and MP. As SP rises, the profit margin narrows, whereas as MP rises, the profit margin widens. Lower/upper bounds for a system's profitability can also be determined, few of them mentioned are:

1. PM ≥ 0 if $\lambda_w \leq 0.018$ for $p_s = 0.5$.
2. PU ≥ 0 if $R_0 \geq 150$ for $\bar{r} = 0.1$.
3. PU $\geq$ PM if SP ≤ 132 for MP=100.

Lower/upper limits for other parameters can be interpreted in the same way.

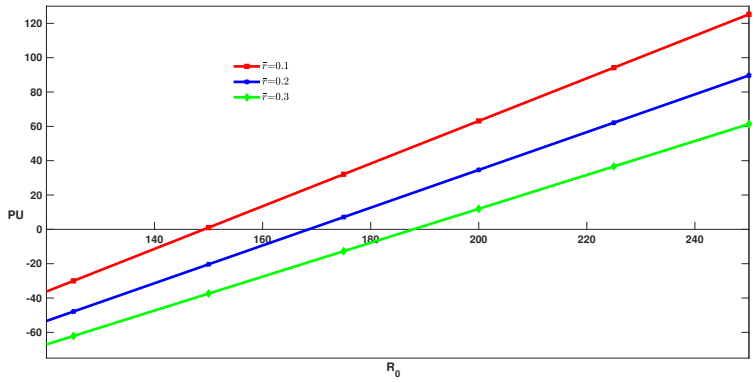

Figure 4: *User's Profit (PU) for varied R_0 and $\bar{r}$*

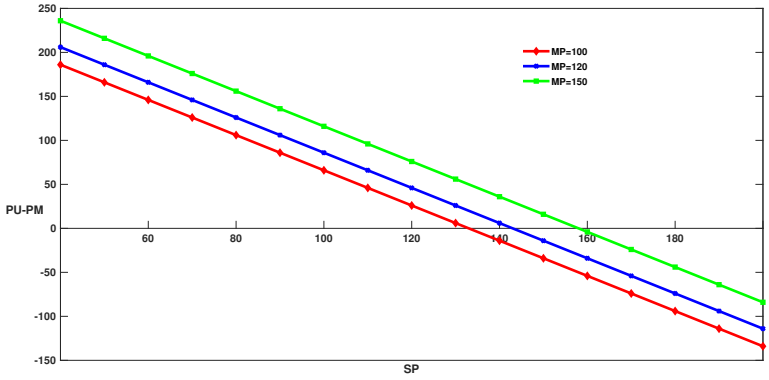

Figure 5: *Difference of Profit (PU-PM) for varied SP and MP*

9.2. Numerical Calculations for Sensitivity Analysis

We compute the sensitivity analysis for profit functions and availabilities in this section by treating all transition densities as exponential and having fixed parameter values as stated in eq^n (15) and eq^n (16) respectively.
The results for sensitivity and relative sensitivity functions for availabilities and profit functions (specified in section 8) are shown in Tables 1, 2 and 3 respectively. The absolute value of both the functions is considered for various conclusions.
It has been confirmed that

1. The availability of three alternative warranty times (AN_0,AT_0,AX_0) is substantially influenced by λ_w. Variation in γ_s and γ_m, on the other hand, appears to have the slightest effect.

2. The profit functions PM and PU are both quite sensitive to CP and R_0.

3. A relative change in PU and PM is caused by variations in CU_3 and CM_3.

Table 1: *Relative Sensitivity Analysis of Availabilities w.r.t. different rates*

Parameter (r)	Sensitivity Analysis $\Delta_r = \frac{\partial(A_0)}{\partial r}$	Relative Sensitivity Analysis $z_r = \frac{\Delta_r * r}{A_0}$
	Normal Warranty Period	
λ_w	-1982.8	-1
γ_m	$2.1842 * 10^{-4}$	$3.3047 * 10^{-4}$
γ_s	$1.0239 * 10^{-4}$	$1.2393 * 10^{-4}$
α_n	0.0014	$7.0606 * 10^{-4}$
β_n	0.3686	0.0074
	Extended Warranty Period	
λ_w	-17.3586	-0.0088
γ_m	$2.1835 * 10^{-4}$	$3.3042 * 10^{-4}$
γ_s	$1.0235 * 10^{-4}$	$1.2390 * 10^{-4}$
α_t	0.0021	$8.4742 * 10^{-4}$
β_t	0.3685	0.0074
	Expired Warranty Period	
λ_w	-32.53	-0.0165
α_x	0.0054	0.0014
β_x	1.4508	0.0148
γ_s	$3.3583 * 10^{-4}$	$4.0977 * 10^{-4}$

Table 2: *Relative Sensitivity of Manufacturer's Profit w.r.t. different rates/costs*

	Profit for System Manufacturer	
Parameter (r)	Sensitivity Analysis $\delta_r^m = \frac{\partial(P^m)}{\partial r}$	Relative Sensitivity Analysis $z_r^m = \frac{\delta_r^m * r}{P^m}$
λ_w	$-5.5312 * 10^3$	-0.0445
γ_m	0.0251	$6.0533 * 10^{-4}$
γ_s	0.0266	$5.1320 * 10^{-4}$
α_n	0.0253	$2.0338 * 10^{-4}$
β_n	6.7710	0.0022
α_t	-0.0014	$-9.0035 * 10^{-6}$
β_t	-0.2475	$-7.9585 * 10^{-5}$
α_x	0.2118	$8.5131 * 10^{-4}$
β_x	56.7230	0.0091
CM_1	$-2.2718 * 10-4$	$-2.9220 * 10^{-4}$
CS_1	$-4.3206 * 10-4$	$-6.2519 * 10^{-4}$
CM_2	-0.0081	-0.0130
CM_3	$-1.2890 * 10^{-4}$	-0.0311
CP	1	2.4117
EP	1	0.2412
MP	-1	-1.9293
SP	1	0.3216

Furthermore, the order in which input variables effect availabilities (A_0^n, A_0^{et}, A_0^{ex}) and profit functions (P^m,P^u) are

- Availability(AN_0): $\lambda_w > \beta_n > \alpha_n > \gamma_m > \gamma_s$.
- Availability(AT_0): $\lambda_w > \beta_t > \alpha_t > \gamma_m > \gamma_s$.
- Availability(AX_0): $\lambda_w > \beta_x > \alpha_x > \gamma_s$.
- Profit Function(P^m):$CP > MP > SP > EP > \lambda_w > CM_3 > CM_2 > \beta_x > \beta_n > \alpha_x > CS_1 > \gamma_m > \gamma_S > CM_1 > \alpha_n > \beta_t > \alpha_t$.
- Profit Function(P^u): $R_0 > CP > SP > EP > \lambda_w > \beta_x > \beta_t > \beta_n > \alpha_x > CU_3 > \gamma_s > \alpha_t > \gamma_m > \alpha_n > CU_2$.

Table 3: *Sensitivity and Relative Sensitivity of User's Profit w.r.t. different rates/costs*

	Profit for System User	
Parameter (r)	Sensitivity Analysis $\delta_r^u = \frac{\partial(P^u)}{\partial r}$	Relative Sensitivity Analysis $z_r^u = \frac{\delta_r^u * r}{P^u}$
λ_w	$-1.3446 * 10^5$	-0.0218
α_x	1.4179	0.0012
β_x	379.7890	0.0123
γ_s	0.1094	$4.2598 * 10^{-4}$
γ_m	0.0546	$2.6575 * 10^{-4}$
α_n	0.1396	$2.2649 * 10^{-4}$
β_n	37.3800	0.0024
α_t	0.3270	$4.2442 * 10^{-4}$
β_t	56.0506	0.0036
R_0	0.9874	1.6020
CU_2	-0.0019	$-7.3982 * 10^{-5}$
CU_3	$-1.9213 * 10^{-5}$	$-9.3514 * 10^{-4}$
CP	-1	-0.4867
EP	-1	-0.0487
SP	-1	-0.0649

10. Conclusion

The sensitivity and economic analysis of the insured system operating under normal warranty, extended warranty, and no warranty conditions were explored in this study. Various profitability indicators and profit functions for the user, manufacturer, and insurance provider have been drafted using Markov and regenerative techniques. After that, the measures are assessed using numerical calculation in which the transition density follows an exponential distribution. For system profitability, lower/upper bounds of the measures involved have been identified. The failure rate has significant influence on availability and profit, whereas the inspection rate has the least. Revenue and cost pricing also significantly impacts the system's profit. This research gives optimum analysis regarding benefits for the user, the manufacturer as well as the insurance provider.

Funding

The first author delightedly acknowledges the University Grants Commission (UGC), New Delhi, India for providing financial support.

Disclosure statement

The authors declare that they have no conflict of interest.

References

[1] Blischke, W. R. (1990). Mathematical models for analysis of warranty policies. *Mathematical and computer modelling*, 13(7): 1–16.

[2] Blischke, W. R., and Murthy, D. N. P. (1992). Product warranty management - I: A taxonomy for warranty policies. *European journal of operational research*, 62(2): 127–148.

[3] Diaz, V. G., Gomez, J. F., Lopez, M., Crespo, A., and de Leon, P. M. (2009). Warranty cost models State-of-Art: A practical review to the framework of warranty cost management. *ESREL*, 2051–2059.

[4] Jack, N., and Murthy, D. P. (2007). A flexible extended warranty and related optimal strategies. *Journal of the Operational Research Society*, 58(12): 1612–1620.

[5] Lutz, N. A., and Padmanabhan, V. (1998). Warranties, extended warranties, and product quality. *International Journal of Industrial Organization*, 16(4): 463–493.

[6] Murthy, D. N. P., and Blischke, W. R. (2000). Strategic warranty management: A life-cycle approach. *IEEE Transactions on Engineering Management*, 47(1): 40–54.

[7] Padmanabhan, V., and Rao, R. C. (1993). Warranty policy and extended service contracts: Theory and an application to automobiles. *Marketing Science*, 12(3): 230–247.

[8] Rinsaka, K., and Sandoh, H. (2006). A stochastic model on an additional warranty service contract. *Computers & Mathematics with Applications*, 51(2): 179–188.

[9] Solkhe, M.,and Taneja, G. (2019). Reliability and Availability Analysis of a system with Periods Before and After Expiry of Conditional Warranty. *International Journal of Agricultural and Statistical Sciences* 15: 281–288.

[10] Solkhe, M.,and Taneja, G. (2018). A Reliability Model on a System with Conditional Warranty and Intervention of Higher Authority on denial of Valid Claim. *International Journal of Applied Engineering Research*, 13(24): 16762–16769.

[11] Solkhe, M.,and Taneja, G. (2019). A Reliability Model on a System with Conditional Warranty and Possibility of Denial of Valid Claim. *Journal of Advance Research in Dynamical & Control Systems*, 11(1): 1282–1292.

[12] Taneja, G. (2010). Reliability Model for a System with Conditional Warranty and various types of Repair/Replacement. *Advances in Information Theory and Operations Research*, 214–220.

ESTIMATION AND TESTING PROCEDURES OF $P(Y < X)$ FOR THE INVERSE DISTRIBUTIONS FAMILY UNDER TYPE-II CENSORING

Kuldeep Singh Chauhan

•

Ram Lal Anand College, University of Delhi, New Delhi-110021
Kuldeepsinghchauhan.stat@rla.du.ac.in

Abstract

We recommended an inverse distributions family. The challenge of estimating $R(t)$ and P in type-II censoring was measured to produce Uniformly Minimum Variance Unbiased Estimator (UMVUE) and Maximum Likelihood Estimator (MLE). The estimators have been created for $R(t)$ and P.Testing approaches for $R(t)$ and P under type-II censoring have been constructed for hypotheses associated with various parametric functions. The author provides an alternate method for generating these estimators.A comparative assessment of two estimating techniques has been conducted. The simulation technique has been used to assess the performance of estimators.

Keywords: Inverse distributions family; testing procedures; bootstrap sampling

1. Introduction

The reliability function describes the probability of a failur e-free procedur e until time t. The estimation of the stress-str ength $[P(Y < X)]$ parameter , aimed at displa ying system efficienc is one of the most important challenges in statistical infer ence, which can be applied to a wide variety of fields such as longe vity mechanical system dependability , statistics, and bio-statistics. In reliab ility, the $P = P(Y < X)$ parameter , which define the lifetime for a specifi system, places the strength X against the stress Y. Several scholars have measur ed the problems of estimation of reliability functions under censoring.Lin et al. [13] illustrated the inverse gamma model's role in lifetime distribution.The inverse Weibull distribution produced a good fit discussed by Erto [11]. The infer ence reliability and $P(Y < X)$ of a scaled Burr distribution were calculated by Surles and Padgett [16].Yadav et al. [18] estimated the P (Y< X) of the inverse Weibull distribution With a progr essiv e type-II censoring technique.Chatur vedi and Kumari [7] conducted a reliable Bayesian study of the generalized inverted family of distributions. Enis and Geisser [10] acquir e an estimate of the likelihood that Y< X. Weerahandi and Johnson [17] investigated testing reliability in $P(Y < X)$ while X and Y are repeatedly distributed. Estimators of $P(Y < X)$ in the gamma model are explor ed by Constatine et al. [9].A comparativ e study for Burr distribution is presented in $R(t)$ and P estimated by Awad and Gharraf [1].Nigm and Amboeleneen [14] use progr essiv e censoring to evaluate the parameters of the Inverse Weibull distribution. Chaudhar y and Chauhan [6] perfor med estimation and test appr oaches for $P(Y < X)$ of the Weibull distribution with type- I and type-II censoring.Chatur vedi and Kumari [3] developed estimate and analysis processes for the reliability of a broad range of distributions.

We consider a family of inverse distributions, which is reflecte in this paper .The UMVUES and MLES of $R(t)$ and P are calculated using type-II censoring. A new appr oach for estimating the UMVUES and MLES of $R(t)$ was invented, in which the expr ession of $R(t)$ and P is not requir ed. Initially , the estimators for $R(t)$ are generated using this method.The $R(t)$ deriv ativ e estimators are used to construct the p.d.f. at a certain point, and then de termine P estimators.W e calculated P by considering instances in which X and Y are similar distributions but have dissimilar values. We

now have extended the findin to any distribution from the projected inverse distributions family wher e X and Y are members. The testing procedur es are also being planned.A perfor mance comparison perfor mance of two estimating appr oaches was conducted. The simulation technique was used to examine the perfor mance of estimators.

2. Inverse Distributions Family

Suppose a random variable $(r.v.)Y$ having pdf

$$f(y;\gamma,\beta,\mu) = \frac{\gamma^{\beta} G^{\beta-1}\left(y^{-1};\mu\right) G'\left(y^{-1};\mu\right)}{y^2\Gamma(\beta)} \exp\left(-\gamma G\left(y^{-1};\mu\right)\right) \quad y>0,\gamma>0,\beta>0 \tag{1}$$

Where, $G\left(y^{-1};\mu\right)$, is depend on μ and a function of y. Further more, $G\left(y^{-1};\mu\right)$ real-v alued, rigor ously reducing function of y with $G(\infty;\mu)=\infty$ and $G'\left(y^{-1};\mu\right)$ stances for the deriv ative of $G\left(y^{-1};\mu\right)$ by y^{-1}.Let β and μ are know n and γ is unkno wn during this whole section.
The (1) demonstrates that the inv erse distributions family can be transfor med into the inv erse distributions listed belo w as special cases:

1. If $G(y;\mu)=y^p, p>0, \beta>0$, we obtained the inv erse generalized gamma distribution.
2. If $G(y;\mu)=y^2, \beta=k+1$, (k $=0$), we achie ved the inv erse Rayleigh distribution.
3. If $G(y;\mu)=\log\left(1+\frac{y^b}{v^b}\right), b>0, v=1, \beta>1$, we achie ved the inv erse Burr distribution.
4. If $G(y;\mu)=\log\left(1+\frac{y^b}{v^b}\right), b=1, v>1, \beta>1$,we obtained the inv erse Lomax distribution.
5. If $G(y;\mu)=\log\left(\frac{y}{a}\right)$ and $\beta=1$, we achie ved the inv erse Par eto distribution.
6. If $G(y;\mu)=y^r\exp(ay), r>0, a>0, \beta=1$, we obtained the inv erse modifie Weibull distribution.
7. If $G(y;\mu)=\mu y+\frac{vy^2}{2}, \alpha=\beta=1$,we obtained the inv erse linear exponential distribution.
8. If $G(y;\mu)=\log y$, we achie ved the inv erse log-gamma distribution.

3. UMVUES of γ and Reliability Functions

We inv estigate estimation with censor ed type-II data. Suppose $Y_{(1)} \le Y_{(2)} \le \ldots\ldots\ldots\ldots\ldots Y_{(n)}$. Assume n objects are subjected to a test, when the firs r obser vations are noted, the test is stopped. Supposing, $0<r<n$, be the lifespans of leading r values. Noticeably , $(n-r)$ objects stay aliv e awaiting $Y_{(r)}$.

Lemma 1. Suppose $S_r=\sum_{i=1}^{r} G\left(y_{(i)}^{-1},\mu\right)+(n-r)G\left(y_{(r)}^{-1},\mu\right)$. Then, for the inv erse distributions family , S_r is complete and sufficien indicated as (1). Additionally , the pdf of S_r is

$$k\left(s_r;\mu\right)=\frac{\gamma^{r\beta}s_r^{r\beta-1}}{\Gamma(r\beta)}\exp\left(-\gamma s_r\right) \tag{2}$$

Proof. From (1), the joint pdf is

$$f^*\left(\underline{y}_{(i)}, i=1,2,\ldots n;\gamma,\beta,\mu\right)=n!\prod_{i=1}^{n}G'\left(y_{(i)}^{-1};\mu\right)\exp\left\{-\gamma\sum_{i=1}^{n}G\left(y_{(i)}^{-1};\mu\right)\right\} \tag{3}$$

When we integrate $y_{(r+1)}, y_{(r+2)}, \ldots\ldots\ldots, y_{(n)}$ throughout the region $y_{(r)} \leq y_{(r+1)} \leq \ldots \leq y_{(n)}$, we get the likelihood as

$$h\left(\underline{y}_{(i)}, (i = 1, 2, \ldots\ldots r); \gamma, \mu\right) = n(n-1)\ldots\ldots\ldots\ldots(n-r+1)\gamma^r \prod_{i=1}^{r} G'\left(y_{(i)}^{-1}, \mu\right) \exp\left(-\gamma s_r\right) \tag{4}$$

S_r is sufficien by Fisher -Neyman factorization theorem [15]. In (1), put $A = G\left(y^{-1}; \mu\right)$, the pdf is

$$k(a; \gamma, \beta, \underline{\theta}) = \frac{\gamma^{\beta} a^{\beta-1}}{\Gamma(\beta)} \exp(-\gamma a); a > 0$$

S_r go by Johnson and Kotz [12] discovered the additiv e property of gamma distribution. Meanwhile, S_r is associated with the exponential distributions family, and it is still complete. ■

Theorem 1. The UMVUE of γ^{-p} is, for $p \in (-\infty, \infty)$,

$$\hat{\gamma}^{-p} = \begin{cases} \frac{\Gamma(r\beta)}{\Gamma(r\beta+p)} s_r^p, & n\beta + p > 0 \\ 0, & \text{other wise} \end{cases}$$

Proof. From Lemma 1,

$$E\left(s_r^p\right) = \frac{\gamma^{n\beta}}{\Gamma(n\beta)} \int_0^{\infty} s_r^{n\beta+p-1} \exp\left(-\gamma s_r\right) ds_r = \left\{\frac{\Gamma(n\beta+p)}{\Gamma(n\beta)}\right\} \gamma^{-p}$$

and the theorem obser ves from Lehmann-S cheffe theorem [15]. ■

Remark 1. We can write (1) as

$$f(y; \gamma, \beta, \mu) = \frac{G^{\beta-1}\left(y^{-1}; \mu\right) G'\left(y^{-1}; \mu\right)}{y^2 \Gamma(\beta)} \sum_{i=0}^{\infty} \frac{(-1)^i}{i!} G'\left(y^{-1}; \mu\right) \cdot \gamma^{i+\beta}$$

From Chatur vedi and Tomar [5] (Lemma 1) and theorem 1, for integer -yalued β, the UMVUE of $f(y; \alpha, \beta, \mu)$ for stipulated point y

$$\begin{aligned} \hat{f}(y; \gamma, \beta, \mu) &= \frac{G^{\beta-1}\left(y^{-1}; \mu\right) G'\left(y^{-1}; \mu\right)}{y^2 \Gamma(\beta)} \sum_{i=0}^{\infty} \frac{(-1)^i}{i!} G'\left(y^{-1}; \mu\right) \hat{\gamma}^{i+\beta} \\ &= \frac{G^{\beta-1}\left(y^{-1}; \mu\right) G^2\left(y^{-1}; \mu\right)}{y^2 \Gamma(\beta)} \sum_{i=0}^{\infty} \frac{(-1)^i}{i!} G^i\left(y^{-1}; \mu\right) \frac{\Gamma(r\beta)}{\Gamma(r\beta+i)} s_r^{i+\beta}, \end{aligned}$$

Theorem 2. The UMVUE of $f(y; \alpha, \beta, \mu)$ for a stipulated point y

$$\hat{f}_{II}(y, \gamma, \beta, \mu) = \left\{ \begin{array}{l} \frac{G^{\beta-1}\left(y^{-1};\mu\right) G^t\left(y^{-1};\mu\right)}{y^2 S_r^{\beta} B((r-1)\beta, \beta)} \left[1 - \frac{G\left(y^{-1};\mu\right)}{S_r}\right]^{r-1)\beta-1}, \quad G\left(y^{-1}; \mu\right) < S_r \end{array} \right.$$

Proof. Using remark 1 and theorem 1, we acquir e the requir ed solution ■

Theorem 3. The UMVUE of $R(t)$
Where

$$I_z(s, q) = \frac{1}{\beta(s, q)} \int_0^z x^{s-1}(1-x)^{q-1} dx$$

The incomplete beta function

Proof. Now, let us suppose the expectation

$$\int_t^{\infty} \hat{f}_{II}(y; \gamma, \beta, \mu) dy$$

The integration to S_r

$$= \int_t^\infty \left\{ \int_t^\infty \hat{f}(y;\gamma,\beta,\mu)dy \right\} k(s_r;\gamma,\beta,\mu)\, ds_r$$
$$= \int_t^\infty \left[E_{S_r}\{\hat{f}(y;\gamma,\beta,\mu)\} \right] dy$$
$$= \int_t^\infty f_{II}(y;\gamma,\beta,\mu)dy$$
$$= R_{II}(t)$$

■

Suppose two independent rv's X and Y follow the inverse distributions families $f_1(x_9,\gamma_1,\beta_1,\mu_1)$ and $f_2(y;\gamma_2,\beta_2,\mu_2)$, sequentially ,

$$f_{1II}(x;\gamma_1,\beta_1,\mu_1) = \frac{\gamma_1^\beta G^{\beta-1}\left(x^{-1};\mu_1\right) G'\left(x^{-1};\mu_1\right)}{x^2\Gamma(\beta_1)} \exp\left(-\gamma_1 G\left(x^{-1};\mu_1\right)\right)$$
$$x>0, \gamma_1>0, \beta_1>0$$
$$f_{2II}(y;\gamma_2,\beta_2,\mu_2) = \frac{\gamma_2^{\beta_2} H^{\beta_2-1}\left(y^{-1};\mu_2\right) H'\left(y^{-1};\mu_2\right)}{y^2\Gamma(\beta_2)} \exp\left(-\gamma_2 H\left(y^{-1};\mu_2\right)\right)$$
$$y>0, \gamma_2>0, \beta_2>0$$

Where β_1,β_2,μ_1 and μ_2 are well-known, however γ_1 and γ_2 are unknown. Suppose n objects arranged X and m objects arranged Y are subjected to a lifespan test, and that the expiry quantities for X and Y are r and r', separately . As well as notation by $S=\sum_{i=1}^r G\left(x_i^{-1};\mu_1\right)$ and $T=\sum_{i=1}^{r'} H\left(y_i^{-1};\mu_2\right)$

Theorem 4. The UMUVE of P is The summations range from 0 to $(r-1)\beta_1-1$ in case $(r-1)\beta_1$ is an integer .

Proof. From theorem 3

$$\hat{f}_{1II}(x;\gamma_1,\beta_1,\mu_1) = \begin{cases} \frac{G^{\beta_1-1}\left(x^{-1};\mu_1\right)G'\left(y^{-1};\mu_1\right)}{x^1 T^{\hat{\beta}}\beta((r^-1)\beta_1,\beta_1)} \left[1-\frac{G\left(y^{-1};\mu_1\right)}{S}\right. & \left., \mathrm{G}\left(x^{-1};\mu_1\right)<S\right]^{(r-1)\beta_-1} \\ 0, & \text{other wise} \end{cases} \quad (5)$$

$$\hat{f}_{2II}(y;\gamma_2,\beta_2,\mu_2) = \begin{cases} \frac{H^{\beta_2-1}\left(y^{-1};\mu_2\right)H'\left(y^{-1};\mu_2\right)}{y^2 T^{\hat{\beta}_2}\beta((r'-1)\beta_2,\beta_2)} \left[1-\frac{H\left(y^{-1};\mu_2\right)}{T}\right. & \left., \mathrm{H}\left(y^{-1};\mu_2\right)<T\right]^{(r'-1)\beta_2-1} \\ 0, & \text{other wise} \end{cases} \quad (6)$$

The UMVUES of $f_1(x;\gamma_1,\beta_1,\mu_1)$ and $f_2(y;\gamma_2,\beta_2,\mu_2)$ for specifie pints $'x'$ and $'y'$ separately , similarly , from theorem 4, we get the UMVUE of P

$$\hat{P}_{II} = \int_{y=0}^\infty \int_{x=y}^\infty \hat{f}_{1I}(x;\gamma_1,\beta_1,\mu_1)\,\hat{f}_{2I}(y;\gamma_2,\beta_2,\mu_2)\,dxdy$$

Using (5) and (6) we get

$$\hat{P}_{II} = \frac{1}{B((r-1)\beta_1,\beta_1)B((r'-1)\beta_2,\beta_2)S^{\beta_1}T^{\beta_2}}$$
$$\int_{y=[H^*(T)]^{-1}}^\infty \int_{x=y}^\infty \left\{ \frac{G^{\beta-1}\left(x^{-1};\mu_1\right)G'\left(x^{-1};\mu_1\right)}{x^2} \right\} \left[1-\frac{G\left(x^{-1};\mu_1\right)}{S}\right]^{(r-1)\beta_1-1}$$
$$\left\{ \frac{H^{\beta_2-1}\left(y^{-1};\mu_2\right)H'\left(y^{-1};\mu_2\right)}{y^2} \right\} \left[1-\frac{H\left(y^{-1};\mu_2\right)}{T}\right]\Bigg]^{(r'-1)\beta_2-1} dxdy$$

■

Corollary 1. If $\mu_1 = \mu_2 = \mu$, and $G\left(x^{-1};\mu\right) = H\left(x^{-1};\mu\right)$

$$\hat{P}_{II} = \begin{cases} \dfrac{1}{B\left((n-1)\beta_1,\beta_1\right)B\left((m-1)\beta_2,\beta_2\right)}\left(\dfrac{S}{T}\right)^{\beta_2}\displaystyle\sum_{i=0}^{\infty}\frac{(-1)^i}{(\beta_1+i)}\begin{pmatrix}\{(n-1)\beta_1\}-1\\ i\end{pmatrix} \\ \qquad\displaystyle\sum_{j=0}^{\infty}\frac{(-1)^j}{(\beta_1+\beta_2+i+j)}\begin{pmatrix}(m-1)\beta_2-1)\left(\frac{S}{T}\right)^j,\\ j\end{pmatrix} \text{ if } S<T \\ \dfrac{1}{B\left((n-1)\beta_1,\beta_1\right)B\left((m-1)\beta_2,\beta_2\right)}\left(\dfrac{T}{S}\right)^{\beta}\displaystyle\sum_{i=0}^{\infty}\frac{(-1)^i}{(\beta_1+i)}\begin{pmatrix}\{(n-1)\beta_1\}-1\\ i\end{pmatrix} \\ \qquad\left(\frac{T}{S}\right)^i B\left(\beta_1+\beta_2+i,(m-1)\beta_2\right), \quad \text{if } S>T \end{cases}$$

The summatio n over i, from 0 to $\{(n-1)^*\beta_1\}-1$, if $(n-1)\beta_1$ is an integer and the summation over j, from 0 to $(m-1)\beta_2$, if $(m-1)\beta_2$ is an integer.

Proof. we get From Theorem 4 for $S \leqslant T$,

$$\hat{P}_{II} = \left\{\frac{1}{B\left((n-1)\beta_1,\beta_1\right)B\left((m-1)\beta_2,\beta_2\right)}\right\}\sum_{i=0}^{\infty}\frac{(-1)^i}{(\beta_1+i)}\begin{pmatrix}\{n-1\}\beta_1-1\\ i\end{pmatrix}$$
$$\cdot\int_0^{\frac{s}{T}} w^{\beta_2-1}(1-w)^{(m-1)\beta_2-1}\left(\frac{Tw}{S}\right)^{\beta+i}dw$$

and for $S > T$, from Theorem 2,

$$\hat{P}_{II} = \frac{1}{\beta\left((n-1)\beta_1,\beta_1\right)\beta\left((m-1)\beta_2,\beta_2\right)}\left(\frac{T}{S}\right)^{\beta}\sum_{i=0}^{\infty}\frac{(-1)^i}{(\beta_1+i)}$$
$$\cdot\begin{pmatrix}\{n-1\}\beta_1-1\\ i\end{pmatrix}\left(\frac{T}{S}\right)^i\int_0^1 w^{\beta_1+\beta_2+i-1}(1-w)^{(m-1)\beta_2-1}dw$$

and the second contention proved. ■

Remark 2. (i) UMVUES of $R(t)$ and P are calculated independently using sampling pdf under type II censoring of UMVUES $R(t)$ and P, as proved in theorems 3 and 4. As a result, we identifie two estimation concerns that indicated interdependence.
(ii) The UMVUES of P was achieved using type-II censoring, whereas X and Y followed a similar distribution, possibly with dissimilar parameters or possibly with similar parameters, also while X and Y followed distinct distributions under all three conditions.
(iii) In theorem 4, if $n \to \infty$ then $\mathrm{Var}(\hat{\gamma}) \to 0$. We know that, $\hat{f}(y;\gamma,\beta,\mu)_2\hat{R}(t)$ and $\hat{P}$ are consistent estimators of $f(y;\gamma,\beta,\mu), R(t)$ and P, respectiv ely because these are continuous functions. So, $\hat{\gamma}$ is a consistent estimator of γ.

4. MLES of γ and Reliability Functions

Using the lemma 1

$$\tilde{\gamma}^{-p} = \left(\frac{r}{S_r}\right)^{-p} \tag{7}$$

Theorem 5. The MLE for a specifie point y

$$\tilde{f}_{II}(y;\gamma,\beta,\mu) = \frac{(\tilde{\gamma})^{\beta}G^{\beta-1}\left(y^{-1};\mu\right)G'\left(y^{-1};\mu\right)}{y^2\Gamma(\beta)}\exp\left(-\tilde{\gamma}G\left(y^{-1};\mu\right)\right)$$

Proof. We can obtain from (7) and use the MLE's one-to-one property. ■

Theorem 6. $\tilde{R}(t)$ is the MLE of R(t)

$$\tilde{R}(t) = J_{\frac{r}{S_r}G\left(t^{-1};\mu\right)}(\beta), \text{ and } J_y(p) = \frac{1}{\Gamma(p)}\int_0^{\infty} x^{p-1}e^{-x}dx$$

This is an incomplete gamma function.

Proof. Using MLE's invariance property and theorem 5

$$\tilde{R}(t) = \int_t^{\infty} \tilde{f}_{II}(y;\gamma,\beta,\mu)dy$$

$$= \frac{\left(\frac{r}{S_r}\right)^{\beta}}{\Gamma(\beta)}\int_t^{\infty} \frac{G^{\beta-1}\left(y^{-1};\mu\right)G'\left(y^{-1};\mu\right)}{y^2}\exp\left(-\frac{r}{S_r}G\left(y^{-1};\mu\right)\right)dy$$

$$= \frac{1}{\Gamma(\beta)}\int_{\frac{r}{S_r}G\left(t^{-1};\mu\right)}^{\infty} x^{\beta-1}e^{-x}dx$$

■

Corollary 2. When $\beta = 1$,

$$\tilde{R}(t) = \exp\left(-\frac{r}{S_r}G\left(t^{-1};\mu\right)\right)$$

Theorem 7. $\tilde{P}$ is the MLE of P

$$\tilde{P} = \frac{(\tilde{\gamma}_2)^{\beta_2}}{\Gamma(\beta_1)\Gamma(\beta_2)}\int_{y=0}^{Y_{(v)}}\left[\int_{z-\left(\tilde{\gamma}g\left(\tilde{x}_{(\tau)}^{-1};\mu 4\right)\right)}^{\gamma_1 g\left(y^{-1};\mu_4\right)} e^{-z}z^{\beta-1}dz\right]$$

$$\frac{H^{\beta_2-1}\left(y^{-1};\mu_2\right)H'\left(y^{-1};\mu_2\right)}{y^2}\exp\left(-\tilde{\gamma}_2 H\left(y^{-1};\mu_2\right)\right)dy$$

Proof. Using the MLE's one-to-one condition and theorem 5,

$$= \frac{(\tilde{\gamma}_1)^{\beta_1}(\tilde{\gamma}_2)^{\beta_2}}{\Gamma(\beta_1)\Gamma(\beta_2)}\int_{y=0}^{y_{(m)}}\int_{x=y}^{X_{(n)}}\left\{\frac{G^{\tilde{\beta}-1}\left(x^{-1};\mu_1\right)G'\left(x^{-1};\mu_1\right)}{x^2}\right\}$$

$$\exp\left(-\tilde{\gamma}_1 G\left(x^{-1};\mu_1\right)\right)\left\{\frac{H^{\beta_2-1}\left(y^{-1};\mu_2\right)H'\left(y^{-1};\mu_2\right)}{y^2}\right\}\exp\left(-\tilde{\gamma}_2 H\left(y^{-1};\mu_2\right)\right)dxdy$$

$$= \frac{(\tilde{\gamma}_1)^{\beta_1}(\tilde{\gamma}_2)^{\beta_2}}{\Gamma(\beta_1)\Gamma(\beta_2)}\int_{y=0}^{y_r'}\frac{H^{\tilde{\beta}_2-1}\left(y^{-1};\mu_2\right)H'\left(y^{-1};\mu_2\right)}{y^2}\exp\left(-\tilde{\gamma}_2 H\left(y^{-1};\mu_2\right)\right)$$

$$\left\{\int_{z=\tilde{\gamma}_1 G\left(X_{(r)}^{-1};\mu_1\right)}^{\tilde{\gamma}_1 G\left(y^{-1};\mu_1\right)} e^{-z}\left(\frac{z}{\tilde{\gamma}_1}\right)^{\beta_1-1}\frac{dz}{\tilde{\gamma}_1}\right\}dy$$

■

Remark 3. (i) UMVUES are acceptable for the MLES under remarks 2.
(ii) There is no need to use reliability function expressions to obtain UMVUES and MLES.

5. Hypotheses Testing

Putting the hypothesis to the test $H_0 : \gamma = \gamma_0$ versus $H_1 : \gamma \neq \gamma_0$, from *eq.*(1), The likelihood function for γ

$$L(\gamma/\underline{y}) = n\cdot(n-1).---(n-r-1)\cdot\gamma^{r\beta}\prod_{i=1}^{r}\left\{\frac{G^{\beta-1}\left(y^{-1};\mu\right)G\left(y^{-1};\mu\right)}{x^2}\right\}\exp\left(-\gamma S_r\right) \quad (8)$$

For H_0

$$\text{Sup } L(\gamma/\underline{y}) = n\cdot(n-1)\cdot----.(n-r-1)\cdot\gamma_0^{r\beta}\prod_{i=1}^{r}\left\{\frac{G^{\beta-1}\left(y^{-1};\mu\right)G\left(y^{-1};\mu\right)}{x^2}\right\}\exp\ (-\gamma_0 S_r)$$

$$\Theta_0 = \{\gamma : \gamma = \gamma_0\}$$

$$SupL(\gamma/\underline{y}) = n.(n-1).----.(n-r-1).\left(\frac{r}{S_r}\right)^r\prod_{i=1}^{r}\left\{\frac{G^{\beta-1}\left(y^{-1};\mu\right)G'\left(y^{-1};\mu\right)}{x^2}\right\}\exp(-r)$$

$$\Theta = \{\gamma : \gamma = \gamma_0\}$$

Likelihood ratio

$$\Phi(\underline{x}) = \left\{\frac{\text{Sup . L}(\gamma/\underline{x})}{\text{SupL }(\gamma/\underline{x})}\right\} = \left(\frac{\gamma_0^{\beta}S_r}{r}\right)\exp\ (-(r+\gamma_0 S_r)) \tag{9}$$

And if $\beta = 1$

$$\Phi(\underline{x}) = \left(\frac{\gamma_0 S_r}{r}\right)\exp\ (-(r+\gamma_0 S_r)) \tag{10}$$

We note from (10) we get $2\gamma_0 S_r \sim \chi^2_{2r}$, the rejection region is given by

$$\{0 < S_r < m_0\}\cup\{m_0' < S_r < \infty\}$$

Where m_0 and m' obtained from

$$P\left[\chi^2_{2r} < 2\gamma_0^{\beta}m_0 \text{ or } 2\gamma_0^{\beta}m_0' < \chi^2_{2r}\right] = \alpha$$

Thus

$$m_0 = 2\gamma_0^{\beta}\chi^2_{2r}\left(1-\frac{\alpha}{2}\right) \text{ and } m_0' = 2\gamma_0^{\beta}\chi^2_{2r}\left(\frac{\alpha}{2}\right)$$

For $H_0 : \gamma \le \gamma_0$ against $H_1 : \gamma > \gamma_0$, It follows from (8) that, for $\gamma_1 < \gamma_2$

$$\frac{k\left(y_{(1)}, y_{(2)}, \ldots\ldots\ldots\ldots\ldots y_{(r)};\gamma_2,\mu\right)}{k\left(y_{(1)}, y_{(2)}, \ldots\ldots\ldots\ldots\ldots y_{(r)};\gamma_1,\mu\right)} = \left(\frac{\gamma_2}{\gamma_1}\right)^r\exp\ (-(\gamma_2-\gamma_2)\,S_r) \tag{11}$$

It follows that from (11) that $\left(y_{(1)}, y_{(2)}, \ldots\ldots\ldots\ldots\ldots y_{(r)};\gamma_2,\mu\right)$ has a maximum likelihood ratio in S_r. Thus, the UMPCR for analysis $H_0 : \gamma \le \gamma_0$ against $H_1 : \gamma > \gamma_0$ is given by

$$\Phi\left(y_{(1)}, y_{(2)}, \ldots\ldots\ldots\ldots\ldots..y_{(r)}\right) = \begin{bmatrix} 1, & s, \le m_0' \\ 0, & \text{otherrise}\end{bmatrix}$$

Where m' obtained from

$$P\left[\chi^2_{2r} < 2\gamma_0^{\beta}m_0\right] = \alpha$$

Therefore

$$m_0' = 2\gamma_0^{\beta}\chi^2_{2r}\left(1-\frac{\alpha}{2}\right)$$

Now for $H_0 : P = P_0$ against $H_1 : P \ne P_0$ under type II censoring. Then H_0 is equivalent to $\gamma_1 = m\gamma_0$, under H_0

$$\hat{\gamma}_1 = \frac{m\,(r+r')}{mS+T} \quad \hat{\gamma}_2 = \frac{(r+r')}{mS+T}$$

For m the likelihood of γ_1 and γ_2 for, $\underline{x}_{(i)}; i = 1, 2, \ldots\ldots..r$ and $\underline{y}_{(j)}; j = 1, 2, \ldots\ldots..r$ is given by Then

$$L\left(\gamma_1,\gamma_1/\underline{x}_{(i)},\underline{y}_{(j)}\right) = m\gamma_1^r\gamma_2^{r'}\exp\ (-(\gamma_1 S-\gamma_2 T))$$

$$\text{Sup } L\left(\gamma_1,\gamma_1/\underline{x}_{(i)},\underline{y}_{(j)}\right) = \frac{mm'\exp\ (-(r+r')}{(mS+T)^{r+r'}}$$

$$\text{Sup } L\left(\ \gamma_1,\gamma_1/\underline{x}_{(i)},\underline{y}_{(j)}\right) = \frac{m\exp\ (-(r+r')}{S^rT^{r'}}$$

Then likelihood ratio

$$\lambda\left(\gamma_1, \gamma_1 / \underline{x}_{(i)}, \underline{y}_{(j)}\right) = m\frac{\left(\frac{mS}{T}\right)^r}{\left[1+\frac{mS}{T}\right]^{r+r'}}$$

The F-statistic and using the statistic that

$$\frac{S}{T} \sim \frac{r_1\gamma_1}{r'\gamma_2}F_{(2r,2r)}(.) \quad \left\{\frac{S}{T} < m_2 \text{ and } \frac{S}{T} > m_2\right\}$$

m_2 and m_2 obtained from the giv en condition

$$P\left[\frac{r'mS}{rT} < F_{2r,2r'} \cup \frac{r'mS}{rT} > F_{2r',2r'}\right] = \alpha$$

$$m_2 = \frac{r}{r'm}F_{(2r,2r)}\left(1-\frac{\alpha}{2}\right) \text{ and } m_2' = \frac{r}{r'm}F_{(2r,2r')}\left(\frac{\alpha}{2}\right)$$

6. Result

We can see in remarks 2(iii) wher e $\hat{\gamma}, f(x;\gamma,\beta,\mu), R(t)$ and P are consistent estimators.

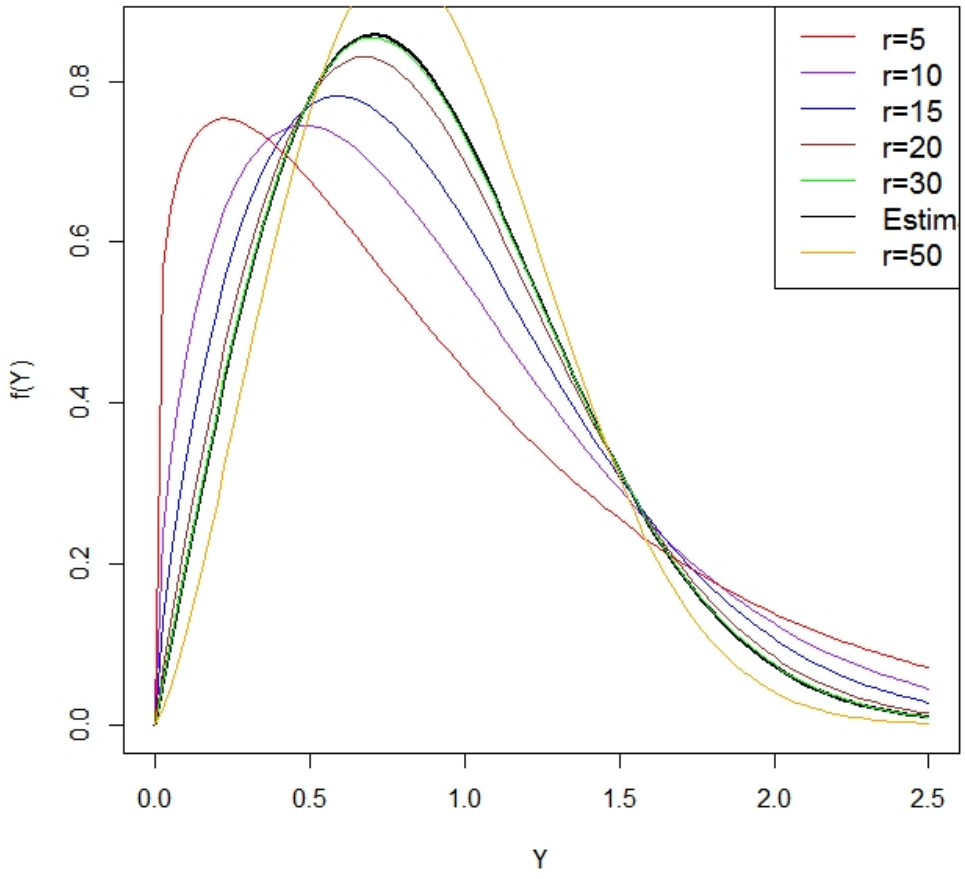

Figure 1: *Uniformly Minimum Variance Unbiased Estimator*

Table 1: *Estimate of R(t) Using Simulation Approach*

r		**10**		**15**		**50**	
t	$R(t)$	$\tilde{R}(t)$	$\hat{R}(t)$	$\tilde{R}(t)$	$\hat{R}(t)$	$\tilde{R}(t)$	$\hat{R}(t)$
15	0.988256	0.982199	0.987858	0.985162	0.989151	0.987757	0.988996
		- 0.006058	- 0.000399	- 0.003095	0.000894	- 0.000500	0.000740
		0.000342	0.000271	0.000167	0.000134	0.00004	0.000038
		0.050549	0.042173	0.039335	0.034016	0.020675	0.019854
		79.2216	73.58140	83.6338	80.0726	87.3715	86.9576
20	0.917915	0.910388	0.914626	0.915237	0.918637	0.918618	0.919682
		- 0.007528	- 0.003289	- 0.002678	0.000722	0.000703	0.001767
		0.003464	0.003984	0.002017	0.002234	0.000565	0.000585
		0.178809	0.188914	0.145604	0.152525	0.079166	0.080517
		86.77420	85.8389	89.1520	88.8500	89.8782	89.8563
25	0.798104	0.79897	0.793371	0.801307	0.797564	0.80119	0.799987
		0.000866	- 0.004733	0.003204	- 0.000540	0.003086	0.001883
		0.008834	0.010559	0.005178	0.005855	0.001404	0.001456
		0.295848	0.323471	0.237045	0.252153	0.125086	0.127418
		88.3448	88.3294	90.0189	90.0201	90.3765	90.3809
30	0.670807	0.680869	0.666155	0.679482	0.669284	0.675551	0.672371
		0.010061	- 0.004652	0.008675	- 0.001523	0.004743	0.001564
		0.012591	0.014486	0.007144	0.007823	0.001827	0.001874
		0.356619	0.38318	0.278715	0.291637	0.14255	0.144326
		88.0549	87.9343	89.7265	89.6547	90.4366	90.4364
45	0.389714	0.409555	0.387121	0.402778	0.387598	0.394959	0.390400
		0.019841	- 0.002593	0.013064	- 0.002116	0.005245	0.000686
		0.011188	0.011276	0.005701	0.005672	0.001285	0.001279
		0.331236	0.331191	0.245934	0.244903	0.118951	0.118657
		85.906	85.5138	88.3818	88.2268	90.2805	90.2736
50	0.32968	0.349176	0.32759	0.342179	0.327687	0.334531	0.330208
		0.019486	- 0.002090	0.012499	- 0.001993	0.004851	0.000528
		0.009403	0.009186	0.004661	0.004541	0.001024	0.001013
		0.301375	0.296388	0.221558	0.218317	0.106079	0.105504
		85.3279	84.9272	88.0684	87.9203	90.2329	90.2261
55	0.281492	0.300028	0.279791	0.293153	0.279655	0.285911	0.281906
		0.018536	- 0.001701	0.011661	- 0.001837	0.004419	0.000414
		0.007747	0.007379	0.003752	0.003595	0.000808	0.000795
		0.27164	0.263625	0.198166	0.193649	0.094143	0.093416
		84.8402	84.4478	87.8163	87.6789	90.1936	90.1871
60	0.242535	0.25984	0.241133	0.253268	0.24086	0.246532	0.242865
		0.017305	- 0.001402	0.010733	- 0.001675	0.003997	0.00033
		0.006327	0.005901	0.003004	0.00284	0.000636	0.000625
		0.243921	0.23421	0.176869	0.171694	0.083515	0.082718
		84.4303	84.0555	87.6127	87.4872	90.1612	90.1552
70	0.184604	0.199307	0.183617	0.193547	0.183228	0.187856	0.184825
		0.014703	- 0.000987	0.008943	- 0.001377	0.003252	0.000221
		0.004203	0.003797	0.001936	0.001794	0.000401	0.000391
		0.196726	0.185941	0.141401	0.135939	0.066187	0.065382
		83.7942	83.4651	87.3111	87.2079	90.1126	90.1076

Table 2: *Estimation of P Using Simulation Approach*

r, r'	**(10, 10)**		**(10, 15)**		**(15, 15)**		**(25, 25)**	
(m, n)	$\tilde{P}$	$\hat{P}$	$\tilde{P}$	$\hat{P}$	$\tilde{P}$	$\hat{P}$	$\tilde{P}$	$\hat{P}$
(5, 5)	0.66625	0.55623	0.79245	0.4739	0.85131	0.38238	0.88938	0.30929
	-0.00042	-0.11044	-0.00755	-0.32610	-0.00583	-0.47476	0.0005	-0.57960
	0.0131	0.00542	0.00825	0.0149	0.00521	0.01713	0.00226	0.01262
	0.37465	0.22246	0.29287	0.37771	0.21917	0.42422	0.15231	0.36142
	89.4513	80.3704	88.3766	85.7414	85.8522	89.4548	87.8912	88.9059
(5, 10)	0.66939	0.536	0.80224	0.46939	0.853	0.3872	0.88923	0.3223
	0.00272	-0.13067	0.00224	-0.33061	-0.00415	-0.46995	0.00034	-0.56659
	0.01343	0.00452	0.00617	0.01127	0.00525	0.01481	0.00244	0.0124
	0.38062	0.1954	0.25112	0.31962	0.23214	0.40524	0.15582	0.35937
	89.8872	78.3713	88.461	84.4431	87.5116	90.3086	87.722	89.3048
(10, 10)	0.66096	0.65675	0.79749	0.70795	0.84474	0.65375	0.88476	0.5824
	-0.00591	-0.00991	-0.00251	-0.09205	-0.01241	-0.20340	-0.00413	-0.30649
	0.00709	0.0055	0.0032	0.00192	0.00329	0.00603	0.00155	0.00975
	0.26423	0.21508	0.17838	0.119	0.18275	0.24016	0.12176	0.32224
	88.238	82.9781	87.8595	74.2657	86.8354	84.0915	87.1155	89.1193
(15, 15)	0.66441	0.66743	0.80245	0.77868	0.85492	0.76714	0.88795	0.71988
	-0.00226	0.00076	0.00245	-0.02132	-0.00223	-0.09000	-0.00094	-0.16901
	0.00604	0.00588	0.00166	0.0005	0.00127	0.00126	0.00092	0.00398
	0.26138	0.25845	0.13777	0.06267	0.11497	0.10138	0.09689	0.19464
	89.9864	89.6238	90.897	75.9468	88.7437	77.2489	88.1403	85.3064
(15, 25)	0.66978	0.66943	0.79561	0.76784	0.85674	0.76313	0.88892	0.72191
	0.00311	0.00277	-0.00439	-0.03216	-0.00040	-0.09401	0.00003	-0.16698
	0.00324	0.00312	0.00234	0.00088	0.00111	0.00131	0.00065	0.00287
	0.18845	0.18624	0.15194	0.08226	0.10749	0.10513	0.08171	0.16528
	90.1082	90.2303	87.77	75.2671	89.2306	75.7539	88.6398	85.857
(25, 25)	0.66432	0.66728	0.79942	0.79972	0.85627	0.84052	0.88749	0.84112
	-0.00234	0.00061	-0.00058	-0.00028	-0.00088	-0.01662	-0.00140	-0.04777
	0.00296	0.00304	0.00182	0.00149	0.00084	0.00032	0.00054	0.00027
	0.17797	0.18026	0.14352	0.12584	0.09115	0.04498	0.0799	0.05119
	89.8014	89.7715	90.4715	88.2366	88.2113	73.121	90.712	76.8041
(25, 30)	0.66545	0.66744	0.79985	0.7996	0.85393	0.83576	0.88492	0.84001
	-0.00122	0.00077	-0.00015	-0.00040	-0.00322	-0.02138	-0.00397	-0.04888
	0.00278	0.00285	0.00145	0.0012	0.0013	0.00054	0.00062	0.00031
	0.17136	0.1736	0.1295	0.11518	0.11215	0.05916	0.07973	0.04987
	89.5562	89.6143	90.8001	89.2747	87.3483	72.9983	88.8342	74.4235
(30, 30)	0.66466	0.67086	0.79943	0.80168	0.85183	0.84563	0.88852	0.86285
	-0.00201	0.00419	-0.00057	0.00168	-0.00531	-0.01151	-0.00037	-0.02604
	0.00223	0.0019	0.00127	0.00117	0.00115	0.00067	0.00048	0.00014
	0.16182	0.14227	0.11788	0.11381	0.10656	0.07456	0.0739	0.02872
	91.3111	89.3985	89.6646	89.5152	87.8413	80.5097	90.0725	71.648

Figure 1 is plotted $\hat{f}(y, \gamma, \beta, \mu)$ under type II censoring for various values of r $= 5(5), 10, 15, 20,$ 30 and 50 and concludes that the curves of $\hat{f}(y, \gamma, \beta, \mu)$ getting closer to the curve of $f(y; \gamma, \beta, \mu)$ as r increases.For $r = 30$, validates the consistency property of the estimators, because the curves overlap.We have presented a simulation study when γ is unknown with the bootstrap re-sampling procedure for r $= 10(5)15$ and 50 while other parameters are known. If $G\left(y^{-1}; \mu\right) = y^2, \beta = 1,$ and $\gamma = 1$. Table 1 shows computation using 500 bootstrap replications with a 95% confidenc coefficien to obtain the estimated value of UMVUES and MLES for $R(t)$, bias, variance, and MSES, for different values of t.Also displa y simulation trials using the bootstrap re-sampling procedure for $(\mathrm{n}, \mathrm{m}) = (5, 10),(10, 10), (15, 15), (15, 25), (25, 25), (25, 30), (30, 30))$ across different $(r', r') = (10, 10), (10, 15), (15, 15)$ and $(25, 25)$, while γ_1 and γ_2 are unidentifie but the other parameters are identifie to estimate P. The free sample is produced as of (1), if $G\left(x^{-1}; \mu\right) = \log(x),$ $\beta_1 = \beta_2 = 1$, $G\left(y^{-1}, \mu\right) = \log(y), \gamma_1 = 1$ and $\gamma_2 = \frac{1}{2}, \frac{1}{4}, \frac{1}{6}$ and $\frac{1}{8}$. Table 2 shows computations using 500 bootstrap replications with a 95% confidenc coefficien to obtain the estimated value of UMVUES and MLES P, bias, variance, and mean sum of squares (MSES).

7. Discussion

We established estimation algorithms for the inverse distributions family based on type-II censoring in this paper .The point estimates are taken into consideration. Hypotheses were generated for many parametric functions, and UMPCR was achieved. Simulation techniques are used to study the efficiency of the UMVUES and MLES of reliability functions, as well as other parameters. For type-II censorship, the UMVUE of $R(t)$ is superior to the MLE of $R(t)$ for different t. Further more, for all values of (r, r'), the MLE of P outperfor ms the UMVUE of P. On the other hand for large t, UMVUE comes to be more effective than MLE of $R(t)$. From the study of P it has been determined that for $m < n$, UMVUE is superior to MLE for P. Alternatively, for $n < m$, it is concluded that MLE is superior to UMVUE for P. As n and m rise both estimators yield equally effective. Using Figure 1, we validated the consistency property of the estimators under censoring approaches.

8. References

[1] Awad, A. M and Gharraf, M.K. (1986). Estimation of $P(Y < X)$ in the Burr case: comparative study *Commun.statist. B- Simul. Comp.*, 15(2), 389-403.

[2] Chaturvedi, A. ,Kang SB and Pathak T. (2016). Estimation and testing procedures for the reliability functions of generalized half logistic distribution *J. Korean Stat Soc.*, 45, 314-328.

[3] Chaturvedi, A. ,Kumari T. (2017). Estimation and testing procedures for the reliability functions of a general class of distributions *Commun. Stat-Theor. Meth.*, 46(22), 70-82.

[4] Chaturvedi, A. ,Kumari T. (2019). Robust Bayesian Analysis of a generalized inverted family of distributions *Comm. Stat. Simul. Comput.*, 48(8), 2244-2268.

[5] Chaturvedi, A. and Tomer, S.K. (2002). Classical and Bayesian reliability estimation of the negative binomial distribution *Jour. Applied Statist. Sci.*, 11 (1), 33-43.

[6] Chaudhary, A. and Chauhan, K. (2009). Estimation and testing procedures for the reliability function of Weibull distribution under type I and type II censoring, Journal of statistics sciences *Jour. Applied Statist. Sci.*, 1(2), 121-136.

[7] Chaturvedi, A. ,Pathak, A. and Kumar, N. (2019). Statistical inferences for the reliability functions in the proportional hazard rate models based on progressive type-II right censoring *Journal of Statistical Computation and Simulation*, 89 (1), 1-31.

[8] Chaturvedi, A. and Malhotra, A. (2018) Estimation of $P(X > Y)$ for the positive exponential family of distributions *Statistica*, 78(2), 149-167.

[9] Constantine, K. , Karson, M. and Tse, S. K. (1986). Estimators of P (Y<X) in the gamma case *Commun. Statist. - Simul. Comp.*, 15, 365-388.

[10] Enis, P. and Geisser, S. (1971). Estimation of the probability that $Y < X$ *Jour. Amer. Statist. Assoc.*, 66, 162-168.

[11] Erto, P. (1989). Genesis, properties, and identificatio of the inverse Weibull lifetime model. Statistica Applicata *Jour. Applied Statist. Sci.*, 1, 117-128.

[12] Johnson, N. L. and Kotz, S. (1970). Continuous Univariate Distributions-I *John Wiley and Sons, New York*.

[13] Lin, C.T., Duran, B. S. and Lewis, T. O. (1989). Inverted gamma as a life distribution *Microelectron Reliab.*, 29, 613-626.

[14] Nigm, El. S.M., Aboeleneen, Z. (2007). Estimation of the parameters of Inverse Weibull distribution with progressive censoring data *Journal of Applied Statistical Science*, 15,39-47.

[15] Rohatgi, V. K., and Saleh, A. K. Md. E. (2012). An introduction to probability and statistics, . *John Wiley and Sons, New York*.

[16] Surles, J. G. and Padgett, W. J. (2001). Inference for reliability and stress-strength for a scaled Burr type X distribution. *Lifetime Data Analysis*, , 7, 187-200.

[17] Weerahandi, S. and Johnson, R. A. (1992). Testing reliability in a stress-strength model when x and y are normally distributed. *Technometrics*, 34(1), 83-91

[18] Yadav, A.S., Singh, S.K. and Singh U. (2018). Estimation of stress-strength reliability for inverse Weibull distribution under progressive type-II censoring scheme. , *Journal of Industrial and Production Engineering*, 35(1), 48-55.

RT&A, No 3 (69)
Volume 17, September 2022

A NOVEL, RELIABLE, ASPECT-BASED SENTIMENT CLASSIFICATION [NRABSC] FOR DIFFERENT INDUSTRY DOMAINS USING HYBRID DEEP LEARNING MODELS

Dhaval Bhoi[1*], Amit Thakkar[2]

•

[1*]U & P U. Patel Department of Computer Engineering,
Chandubhai S. Patel Institute of Technology, Faculty of Technology & Engineering,
Charotar University of Science and Technology (CHARUSAT),
Changa - 388421, Gujarat, India
dhavalbhoi.ce@charusat.ac.in

[2]Department of Computer Science & Engineering,
Chandubhai S. Patel Institute of Technology, Faculty of Technology & Engineering,
Charotar University of Science and Technology (CHARUSAT),
Changa - 388421, Gujarat, India
amitthakkar.it@charusat.ac.in

Abstract

Customers nowadays are more opinionated than they have ever been. They appreciate interacting with industries or businesses and providing feedback like positive, neutral and negative. Customers leave a plethora of information every time they connect with a company, whether it is through a mention or a review, letting businesses know what they are doing well and wrong. However, wading through all of this data by hand may be laborious task. Aspect-based sentiment analysis, on the other hand, can assist you in overcoming this issue. Because of their inherent competency in the semantic synchronization among aspects with associated contextual terms, attention mechanisms and Convolutional Neural Networks (CNNs) are often utilized for aspect-based sentiment categorization. However, because these models lack a mechanism for accounting for important syntactical restrictions and long-range word dependencies, they may incorrectly identify syntactically irrelevant contextual terms as hints for determining aspect emotion. To solve this problem, we suggest establishing a Graph Convolutional Network (GCN) over a sentence's dependency tree, which is generated using bidirectional Long Short Term Memory (Bi-LSTM). A new aspect-specific sentiment categorization system is proposed as a result of it. Studies on several testing sets show how our suggested approach is on par with a number of state-of-the-art deep learning models in terms of reliable performance efficacy, and that the graph convolution structure appropriately captures both syntactic and semantic data and lengthy-term associations to perform reliable sentiment classification based on the aspects present in the review sentences.

Keywords: Aspect Based Sentiment Classification, Performance Reliability Analysis, Deep Learning

1. Introduction

Our lives have become increasingly reliant on social media. People nowadays are not only limited to using such platforms to communicate with others, but they are also active in expressing their opinions on any event they feel worthy of discussion. This shows the need for analysing such vast

amount of multimedia data [1]. Sentiment analysis can be undertaken at several levels, including document, phrase, and feature/aspect levels. [2]. Statement level sentiment analysis is used to categorise a sentence into one of three categories: negative, positive, or neutral. To categorise a document, sentiment analysis at the document level is used. While sentiment analysis at the aspect level is used to categorise each element of an aspects and entity mentioned in a review. As a consequence, decision makers in any sector, business, or institution may classify their clients' likes and dislikes in more detail. They may then make better decisions about various marketing tactics based on this information. It is possible to boost the potential of a rising industry growth performance. Different granularity level of sentiment classification is shown in Figure 1 below.

Sentiment classification relying on aspects (often referred to as aspect-level classification) seeks to find out the appropriate sentiment polarity of aspects expressly stated in sentences. For instance, the sentiment polarities for a couple of features of the pizzas and staff are positive and negative, correspondingly, in a review regarding a restaurant claiming "The pizzas were delicious, but the staff took very long to serve." This task is usually stated as guessing the polarity of a given (sentence, aspect) pair combination. It includes to identify aspect in a given sentence and to classify the statement according to the aspect into positive, negative or neutral category.

From idea through disposal, all facets of the asset lifetime are crucial to a company's or any specific industry success [3]. When using aspect-based sentiment categorization to tackle problems in diverse industries, such as the computer business and the restaurant industry, there are numerous hurdles needed to be faced. Aspect Term Extraction (ATE), Aspect Category Detection (ACD), and Aspect Based Sentiment Classification (ABSC) are among the issues. ABSC also aims to find reliable and scalable solutions to the problem automatically. To accomplish aspect-based sentiment classification in this study, we employed a novel and hybrid dependable approach named Bidirectional Long Short Term Memory (Bi-LSTM) and Graph Convolutional Network (GCN). This proposed technique has the potential to improve ABSC's performance, and in turn, it will aid several industrial domains in understanding client feedback. The proposed approach aids in the identification of emotion expressed by industry stakeholders. We have currently limited our research to perform aspect level sentiment classification on laptop domain reviews and restaurant reviews expressed by people who have used their services.

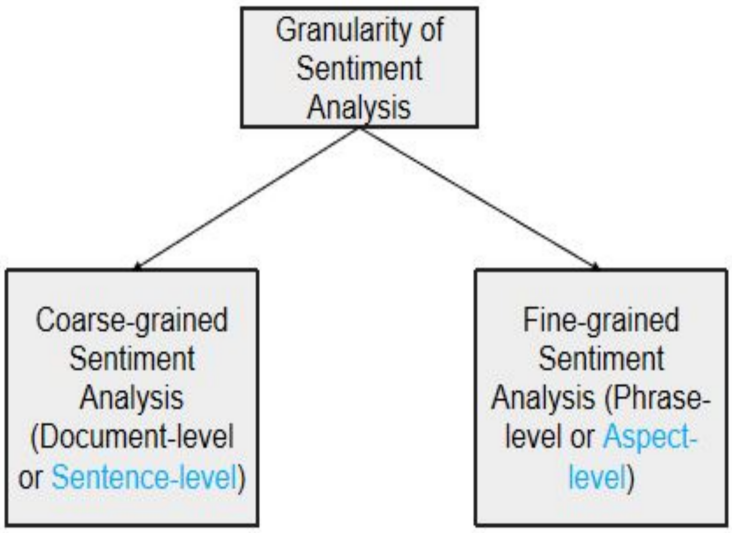

Figure 1: *Sentiment Analysis: Granularity*

2. Related Work

A variety of ways for dealing with ABSC challenges have been proposed in recent years, including traditional machine learning and neural network methods. This section will cover the related study of aspect-based sentiment classification.

2.1. Machine Learning Methods

Existing machine learning techniques for the ABSC problem are largely focused on feature engineering. This also indicates that a large amount of work is spent gathering and assessing data, defining features based on the dataset's attributes, and obtaining sufficient language resources for lexicon creation. The Support Vector Machine (SVM) [4] is a well-known machine learning algorithm that gets decent results when dealing with aspect-level sentiment classification when incorporated implicit aspects into account, their aspect extraction accuracy improved significantly. However, like with other classic machine learning approaches, manually designing features is time consuming and inefficient [5]. Furthermore, the method's performance suffers significantly when the dataset changes. As a result, traditional machine learning algorithms are limited in their applicability and difficult to adapt to a variety of datasets. As a result, it is the primary rationale for opting for deep learning over machine learning.

2.2. Deep Learning Methods

Recent work is increasingly integrating with Neural Networks (NN) because NN-based techniques may extract original features and transfer them into continuous and low-dimensional vectors without the requirement for feature engineering.

Recursive Neural Network (RecNN) is a form of neural network used to learn a directed acyclic graph structure from data. Tree based RecNN was introduced by [6] and [7]. To accomplish aspect based sentiment categorization, the authors of [8] employed LSTM, Target Dependent LSTM (TD-LSTM), and Target Connection (TC-LSTM). In addition, the end-to-end training of the LSTM model for ABSC included commonsense knowledge of sentiment-related topics [9]. Bi-RNN was utilised by the authors of 1 to simulate the syntax and semantics in sentences, as well as the relationship between the aspects and their surrounds words. Authors of [10] proposes employing a hierarchical bidirectional LSTM model for ABSC that can learn both intra and inter sentence connections, which uses Hierarchical bi-directional attention-based RNNs (HRNN). These models, on the other hand, are unable to capture aspect level sentiment classification with improved performance. We presented a hybrid deep learning model to overcome the limitations of existing techniques. The next part talks at length about it.

3. Proposed System

For a given (sentence-review, aspect) pair (s, a), where aspect a= $\{a_1, a_2, ..a_n\}$ is a sub-sequence of the sentence of sentence for a given sentence-review s=$\{w_1, w_2, w_3, .., w_n\}$. Sentence s is classified into positive, negative or neutral according to the content of the aspect. To minimise the distance between aspect and opinion words and capture long-term dependencies, a Dependency Tree is employed to express syntactic dependencies paths between review sentence words. Bi-LSTM Model learns hidden state representation $H_c = \{h_1, h_2, h_3, .., h_n\}$, where h_i represents the hidden state vector at different time step $t_1, t_2, ..t_n$ in the forward and backward direction for an arbitrary review sentence to be contextualized.

For document-word relationships, tree topologies, link prediction, and relation extraction, GCNs have been applied. For training, GCNs can employ both node features and structure. Each GCN layer uses features from near neighbours to encode and update representations of nodes in the graph. The GCN's primary principle is to take the weighted average of all node attributes of

all neighbours (including itself): The weights of lower-degree nodes are increased. The feature vectors are then fed into a neural network for training.

AX adds up the characteristics of neighbouring nodes but ignores the characteristics of the node itself. The Adjacency Matrix is A, and the feature vector is X. Although Adjacency Matrix A with self loop has been included, they are still not normalised. To avoid numerical instability and vanishing gradient, normalisation is essential. Normalized features are calculated using value CAX, where C is the inverse of D. Our Proposed Approach is presented in the below Figure 2.

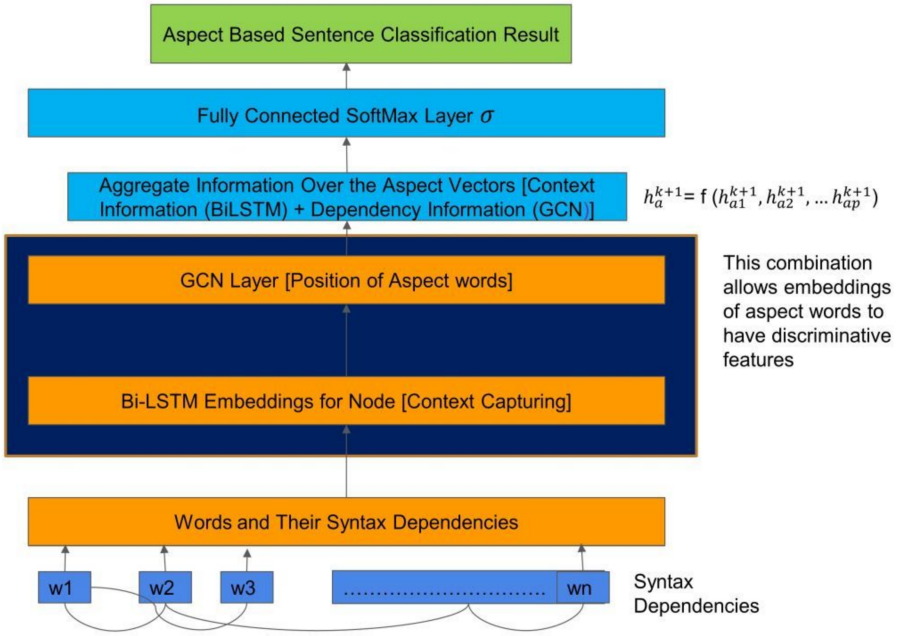

Figure 2: *Our Proposed Approach*

The sentence's features will be learned using Bi-LSTM, which will then be enhanced by using GCN.As GCN is capable of effectively capturing and encoding syntactical information as well as long-range dependencies. Only aspect vectors encoded with information from opinion words are aggregated in the final representation for the ABSC task. BiLSTM and GCN provide for discriminating features in aspect word embeddings, resulting in improved supervisory signals for the classification process.

$$h_i{}^{k+1} = \phi(\sum_{j=1}^{n} c^i A_{ij}(W^{(k)} h_j^{(k)} + b^{(k)}) \tag{1}$$

Where, $h_j{}^k$ is the hidden state representation for given node j at the k^{th} layer of GCN, $b^{(k)}$ is the bias term considered, $W^{(k)}$ is the weight parameter matrix, $c^i = 1/d^i$ (d^i denotes degree of node i in the constructed graph), $\phi(.)$ is the relu elementwise non-linear activation function, $h_i^{(0)}$ represents the initial embeddings modeled by BiLSTM and $h_i^{(k+1)}$ is the final output at layer k for node i .

$$J(\theta 1, \theta 2) = -\sum_{(a,s)\epsilon D} \sum_{c \epsilon C} y_c((a,s)) log \hat{y_c}((a,s)) \tag{2}$$

Where, D is the collection of aspect-sentence pairs datasets, C is the collection of distinct sentiment classes such as Positive, Negative and Neutral, $y_C((a,s))$ is the actual ground truth for (a,s) while $\hat{y_c}((a,s))$ is the model prediction for givne (a,s), while $(\theta 1, \theta 2)$ are the trainable parameters for BiLSTM and GCN.

3.1. Dataset

To asses the effectiveness and reliability of our proposed approach We have used two different kinds of datasets of computer industry and restaurant industries. Laptop14 data belongs to computer industry contains review related to laptops while Restaurant14, Restaurant15 and Restaurant16 belong to restaurant industry.

Table 1: *Dataset Details*

Dataset	Size of the Dataset		
	Positive	**Negative**	**Neutral**
Restaurant2014-training Dataset	2164	807	637
Restaurant2014-testing Dataset	728	196	196
Laptop2014-training Dataset	994	870	464
Laptop2014-testing Dataset	341	128	169
Restaurant2015-training Dataset	1178	382	50
Restaurant2015-testing Dataset	439	328	35
Restaurant2016-training Dataset	1620	709	88
Restaurant2016-testing Dataset	597	190	38

In our study, we have included review sentences containing positive, negative and neutral sentiment classification. Dataset detail and dataset preview are shown in Table 1 and Table 2 respectively. Aspect term is denoted between two $ symbols while type of sentiment is denoted using 1, 0 and -1 for positive, neutral and negative respectively.

Table 2: *Dataset Preview*

Sentence	Aspect Term	Sentiment Type
T was easy	Set up	1 (Positive)
No T is included	Installation disk	0 (Neutral)
Did not enjoy the new arrival windows 10 and T	Touchscreen Functionality	-1 (Negative)

3.2. Performance Evaluation Measures

To test the effectiveness of our suggested strategy NRABSC, we employed accuracy (A) and F1 score (F1) as performance assessment measures to evaluate the actual prediction performance of our proposed hybrid deep learning approach with existing deep learning models LSTM and CNN. A true positive sample is one in which the selected model predicts the positive class correctly. A true negative sample, on the other hand, is an outcome in which the model makes correct prediction regarding the negative class. A false positive sample is one in which the model estimates the positive class incorrectly. A false negative sample is one in which the model predicts the negative class incorrectly.True Positive samples are represented by TPS, True Negative samples by TNS, False Positive samples by FPS, and False Negative samples by FNS. Calculations for Accuracy, Precision, Recall and F1-Score are done using the formulas as shown in Equations 3, 4, 5 and 6.

$$A = \frac{TPS + FNS}{TPS + FPS + TNS + FNS} \tag{3}$$

$$P = \frac{TPS}{TPS + FPS} \tag{4}$$

$$R = \frac{TPS}{TPS + FNS} \tag{5}$$

$$F1 = \frac{2 * P * R}{P + R} \tag{6}$$

4. Results and Discussion

Proposed reliable hybrid deep learning approach NRABSC is compared with baseline models LSTM and CNN to prove its effectiveness. Experiments are performed on various standard benchmark dataset Laptop14, Restaurant14, Restaurant15 and Restaurant16. Our proposed approach gives highly reliable results for restaurant laptop and restaurant domain as shown in the below Table 3, 4 ,5, 6 and Figure 3, 4, 5 and 6 for both the performance measures Accuracy and F1-Score.

Table 3: *Performance Result for Laptop14 Dataset*

Model	Accuracy	F1-Score
LSTM	69.80	63.64
CNN	74.97	70.80
Our Proposed Model [NRABSC]	75.60	71.87

Table 4: *Performance Result for Restaurant14 Dataset*

Model	Accuracy	F1-Score
LSTM	77.98	67.35
CNN	81.04	72.52
Our Proposed Model [NRABSC]	81.37	72.44

Table 5: *Performance Result for Restaurant15 Dataset*

Model	Accuracy	F1-Score
LSTM	77.12	55.90
CNN	79.46	59.19
Our Proposed Model [NRABSC]	79.64	62.82

Table 6: *Performance Result for Restaurant16 Dataset*

Model	Accuracy	F1-Score
LSTM	86.69	65.33
CNN	87.88	64.88
Our Proposed Model [NRABSC]	88.85	72.10

5. Conclusion and Future Work

In order to increase the performance of the computer and hotel industries, the proposed approach generates extremely trustworthy outcomes. It can then be used to other industrial sectors to produce domain-independent outcomes. We looked at the problems that current systems have with aspect-specific sentiment categorization and found that GCN is well suited to solving them. As a result, we have suggested a new structure that uses GCN to classify sentiment depending on aspects. GCN improves total efficiency by exploiting both syntactical knowledge and long-range phrase relationships, according to testing data. The following components of this study should be

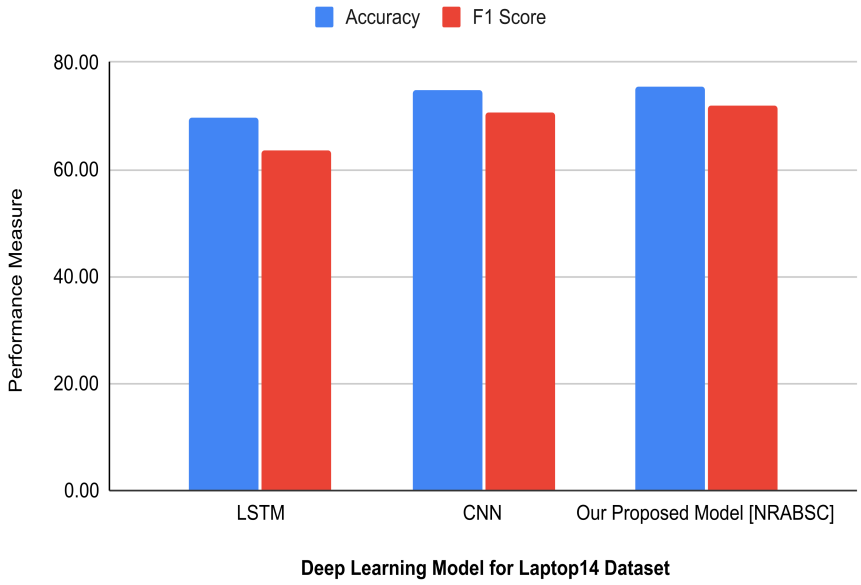

Figure 3: *Performance Result on Laptop14 Dataset*

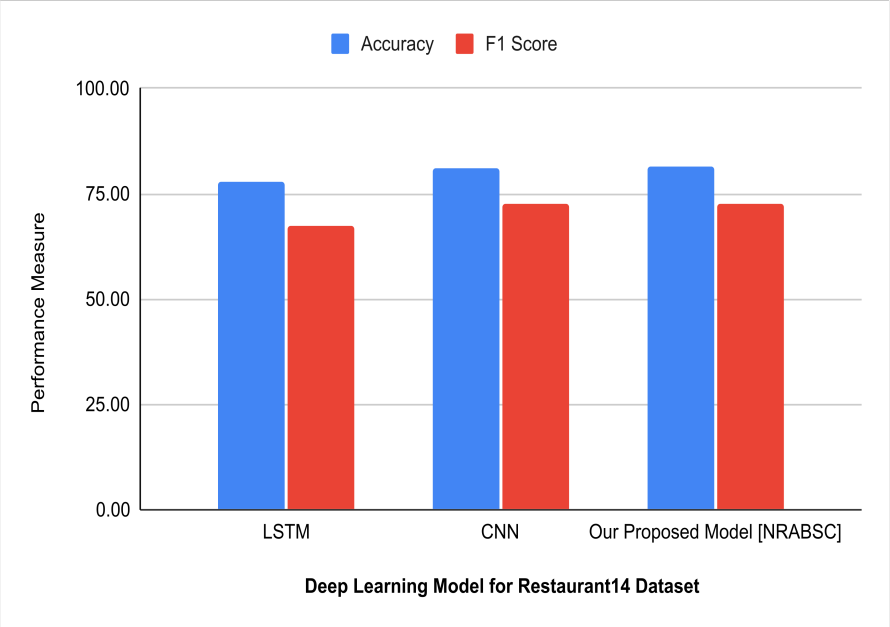

Figure 4: *Performance Result on Restaurant14 Dataset*

enhanced. To begin with, the border knowledge syntactical dependence trees, i.e. the name of each border, is not used in this study. We intend to create a graph neural network that takes the edge labels into account. Existing understanding, on the other hand, could be included. Finally, by incorporating relationships among both the aspects words, the RHABSC model can be expanded to concurrently judge emotions of various features. In the future, we will highlight significant concerns and suggest possible solutions, including new models like as the BERT language model and GANs.

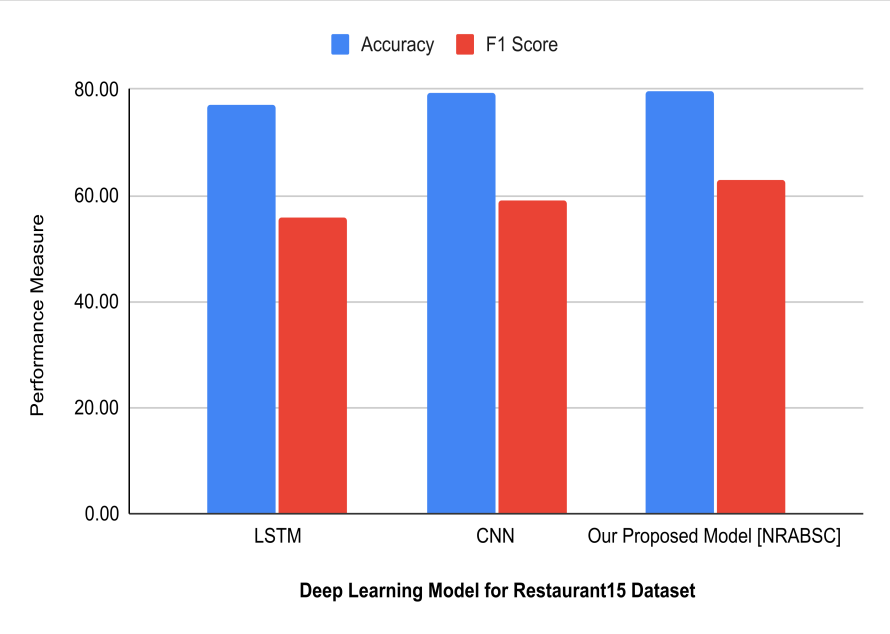

Figure 5: *Performance Result on Restaurant15 Dataset*

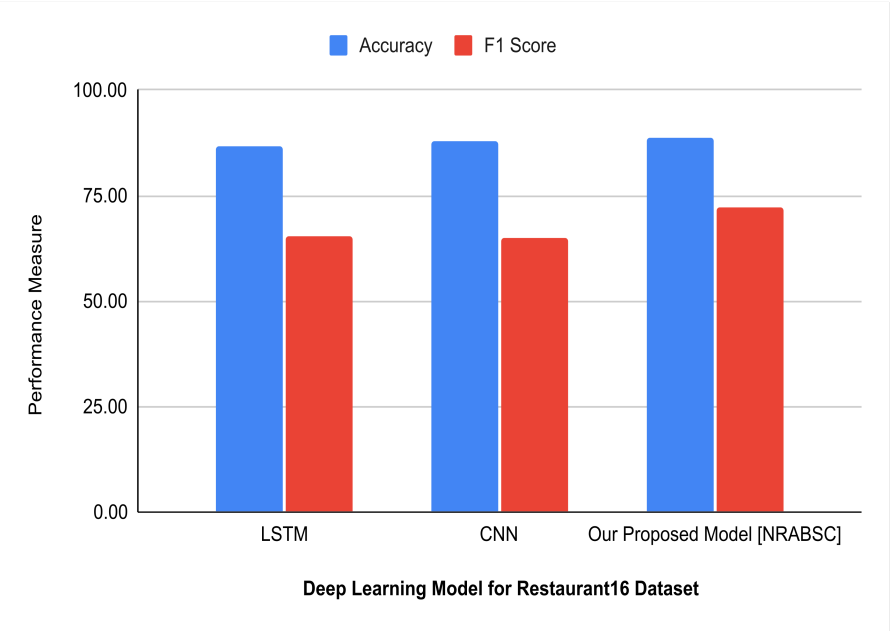

Figure 6: *Performance Result on Restaurant16 Dataset*

Acknowledgement

The authors would like to express special thanks of gratitude to the Principal (CSPIT) and Dean of the Faculty of Technology and Engineering (FTE). Authors would like to acknowledge the Head of the U & P U. Patel Department of Computer Engineering at CSPIT, Faculty of Technology and Engineering, Charotar University of Science and Technology, Changa, for their continuous suggestions, encouragement, guidance, and support throughout the research. We would like to thank Management for their unwavering moral support and encouragement throughout the years.

Declaration of Conflicting Interests

The Author(s) declare(s) that there is no conflict of interest.

References

[1] Wankhade, M., Rao, A.C.S. Kulkarni, C. A survey on sentiment analysis methods, applications, and challenges. Artif Intell Rev (2022). https://doi.org/10.1007/s10462-022-10144-1.

[2] Suhariyanto, R. Abdullah, R. Sarno, and C. Fatichah, Aspect-Based Sentiment Analysis for Sentence Types with Implicit Aspect and Explicit Opinion in Restaurant Review Using Grammatical Rules, Hybrid Approach, and SentiCircle,´ Int. J. Intell. Eng. Syst., vol. 14, no. 5, pp. 177-187, 2021, doi: 10.22266/ijies2021.1031.17.

[3] Igor Shubinsky , Alexei Zamyshlaev , Alexander Bochkov (2022). APPLICATION OF ARTIFICIAL INTELLIGENCE IN RUSSIA'S RAILWAY NETWORK ASSET MANAGEMENT. Reliability: Theory Applications, 17 (SI 3 (66)), 42-48. doi: 10.24412/1932-2321-2022-366-42-48.

[4] Alqaryouti, O., Siyam, N., Abdel Monem, A. and Shaalan, K. (2020), "Aspect-based sentiment analysis using smart government review data", Applied Computing and Informatics, Vol. ahead-of-print No. ahead-of-print. https://doi.org/10.1016/j.aci.2019.11.003.

[5] Anadkat, K., Diwanji, H., Modasiya, S. (2022). Effect of Preprocessing in Human Emotion Analysis Using Social Media Status Dataset. Reliability: Theory Applications, 17(1), 104-112. Retrieved from http://www.gnedenko.net/RTA/index.php/rta/article/view/847.

[6] Li Dong, Furu Wei, Chuanqi Tan, Duyu Tang, Ming Zhou, and Ke Xu. 2014. Adaptive Recursive Neural Network for Target-dependent Twitter Sentiment Classification. In Proceedings of the 52nd Annual Meeting of the Association for Computational Linguistics (Volume 2: Short Papers), pages 49-54, Baltimore, Maryland. Association for Computational Linguistics.

[7] Thien Hai Nguyen and Kiyoaki Shirai. 2015. PhraseRNN: Phrase Recursive Neural Network for Aspect-based Sentiment Analysis. In Proceedings of the 2015 Conference on Empirical Methods in Natural Language Processing, pages 2509"2514, Lisbon, Portugal. Association for Computational Linguistics.

[8] Duyu Tang, Bing Qin, Xiaocheng Feng, Ting Liu. 2016. Effective LSTMs for Target-Dependent Sentiment Classification. In Proceedings of COLING 2016, the 26th International Conference on Computational Linguistics: Technical Papers, pages 3298-3307, Osaka, Japan, December 11-17 2016.

[9] Ma, Y., Peng, H., Cambria, E. (2018). Targeted Aspect-Based Sentiment Analysis via Embedding Commonsense Knowledge into an Attentive LSTM. Proceedings of the AAAI Conference on Artificial Intelligence, 32(1).

[10] Meishan Zhang, Yue Zhang, and Duy-Tin Vo. 2016. Gated neural networks for targeted sentiment analysis. In Proceedings of the Thirtieth AAAI Conference on Artificial Intelligence (AAAI'16). AAAI Press, 3087-3093.

RT&A, No 3 (69)
Volume 17, September 2022

MEASURES TO ENSURE THE RELIABILITY OF WATER SUPPLY IN THE MLDB SYSTEM USING REFRIGERATION

Ramanpreet Kaur *[1], Upasana Sharma [2]

*[1,2] Department of Statistics, Punjabi University ,Patiala
*[1]rkgill9192@gmail.com
[2]usharma@pbi.ac.in

Abstract

Various components work together to form a system's overall structure. Last but not least, how well each component functions affects how the system functions. Both a functioning and failing state are possible for a system built from components. Failure has a big effect on the way systems work in industry. So, in order to enhance system performance, it is essential to get rid of these errors. The aim of this research is to assess the scope of water supply concerns in the MLDB (Multi-Level Die Block) system at the Piston Foundry Plant.The MLDB system, which consists of a robotic key unit that works with the water supply, is the subject of this research. Robotic failure and a lack of water supply cause the system to fail.A reliability model is created in order to calculate MTSF (mean time to system failure), availability, busy times for repair, and profit evaluation. The abovementioned measurements were computed numerically and graphically using semi-Markov processes and the regenerating point technique. The results of this study are novel since no previous research has concentrated on the critical function of water delivery in the MLDB system in piston foundries. According to the discussion, the findings are both highly exciting and beneficial for piston manufacturing businesses who use the MLDB system. For companies that make pistons and use the MLDB system, the conclusions, according to the debate, are particularly beneficial.

Keywords: MLDB, MTSF, availability , semi-Markov process, regenerating point technique.

1. Introduction

Many study articles on reliability exist in the literatur e and many estimations such as reliability , availability , engagement length and other factors for standb y system have been taken. Reliability principles have been utilised in different manufacturing and technological areas throught the last 45 years. Previously , resear chers examined the various ways to standb y systems such as: Sriniv asan [10] gave an examination of warm standb y system dependability for a repair facility . The stochastic standb y system beha viour with repair time was handled by Kumar et al. [4]. Shar ma and Kaur [8] conducted a cost-benefi analysis of a compr essor standb y system. A power plant system's cold standb y unit was stochastically modelled by Shar ma and Shar ma[9].

Some authors provided an overview of the different reliability modelling methodologies used in die casting systems such as: High Pressur e Grain structur e and segr egation in die casting of magnesium and aluminium alloys Characteristics mentioned by Laukli [5]. High pressur e die cast AlSi9Cu3 (Fe) alloys are provided by Timelli [11] using constitutiv e and stochastic models to anticipate the impact of casting fl ws on the mechanical properties. Die Casting Process Modeling and Optimization for ZAMAK Alloy giv en by Shar ma [7]. Existing epistemic uncertainty in die-casting is modelled for reliability and optimised by Yourui et al.[12]. Sensitivity study for the casting method provided by Kumar [3]. An Early Investigation of a Lightw eight provided by Muller et al. [6] Die Casting Die Using a Modular Design Appr oach. High pressur e die casting machine reliability analysis of two unit standb y system offered by Bhatia and Shar ma

[1]. The Casting Process Optimization Case Study: A Review of the Reliability Techniques used by Chaudhari and Vasudevan [2]. According to the discussion above, every researcher has addressed reliability analysis of the die casting method used in piston foundries. Research finding pertaining to the MLDB system in piston foundries have not been discovered. A few of them, though, have gathered and analysed real data. There are a variety of systems in piston foundry operations that must be analysed using real data at various rates and costs. Our efforts are closing this gap by gathering genuine data from a company called Federal-Mogul Powertrain, India Limited, which is based in Bahadurgarh, Punjab, near Patiala. Federal-Mogul is the world's leading maker of world-class pistons, piston rings and cylinder linears, with products for two-and three-wheelers, vehicles and tractors, among other applications.

The purpose of this research is to assess the MLDB system's water supply problems. For the MLDB system in the piston plant, a reliability model has been established. The MLDB system is an enhanced version of the die casting technology that was introduced to raise the piston foundry's output rate. For the operation of the MLDB system in the piston plant, there is one main unit, which is robotic and two sub-units. Water is supplied to the system via a fan (WSF). The system fails due to a lack of water supply. We create a novel reliability model to overcome the failure in water supply, which differ from the present approach in the piston plant. A main robotic unit that works with the water supply through a refrigeration(WSR) is required for the operation of this new model, the MLDB system. To run the entire system, both the robotic and the WSR units must be operational. Water supply from fan(WSF) is utillised as a cold standby unit for better working conditions. System failure occurs due to robotic failure and a lack of water supply.

For the model, there are a few assumptions that need to be made:

- S0 is the starting state of the system.
- The main unit, i.e. robotic, receives priority for repair.
- All failure and repair times were calculated using an exponential distribution.
- After each repair in the states, the system performs a new function.
- A repair man is dispatched as soon as a unit fails.

2. Methods

The following are the materials and methods that were used to complete this research:

Semi-Markov processes and regenerating point techniques are employed in order to tackle the challenges. Many system effectiveness metrics have been acquired, including mean time to system breakdown, system availability, busy period for repair and predicted number of repairs. The profit are also made. Using C++, Python and MS Excel programming, graphical analyses are created for a specifi situation.

3. Notations and States for the Model

$Rb \rightarrow$ Main unit of the MLDB system i.e. Robotic.

$O(Rb) \rightarrow$ Main unit of the MLDB system is in operating state.

$WSR \rightarrow$ Water supply refrigerator for the system.

$WSF \rightarrow$ Water supply fan for the system.

$O(WSR) \rightarrow$ Water supply refrigerator is in operating state.

$O(WSF) \rightarrow$ Water supply fan is in operating state.

$CS(WSF) \rightarrow$ WSF is in cold standby state.

$\lambda, \lambda_1, \lambda_2 \rightarrow$ Failure rates of the main unit i.e. Robotic, WSF and WSR respectively.

$Fr(Rb) \rightarrow$ Failures of the main unit i.e. Robotic under repair.

$Fr(WSR), Fr(WSF) \rightarrow$ Failur es of the WSR and WSF are under repair respectiv ely.

$FR(WSF), FR(WSR) \rightarrow$ Repair is continuing from previous state for WSF and WSR respectiv ely.

$Fwr(WSF), Fwr(WSR) \rightarrow$ Failed WSF and WSR are waiting for repair respectiv ely.

$G(t), g(t) \rightarrow$ c.d.f. and p.d.f of repair time for Robotic.

$G_1(t), g_1(t) \rightarrow$ c.d.f. and p.d.f of repair time for WSR.

$G_2(t), g_2(t) \rightarrow$ c.d.f. and p.d.f of repair time for WSF.

4. The System's Reliability Measur es

4.1. Transition Probabilities

The various phases of the system are depicted in a transition diagram (see in **Fig.1**).

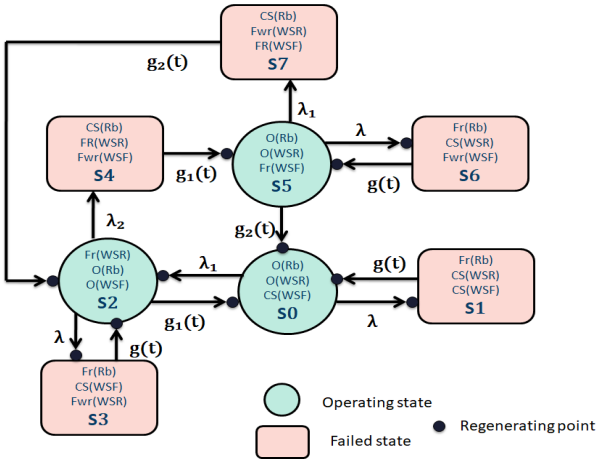

Figure 1: *State Transition Diagram*

The epochs of entry into states S0, S1, S2, S3, S5 and S6 are regenerativ e states, while the rest are non-regenerativ e stages. The operational states are S0, S2 and S5, while the failing states are S1, S3, S4, S6 and S7. The transition probabilities are:

$$
\begin{aligned}
dQ_{01}(t) &= \lambda e^{-(\lambda+\lambda_1)t}dt & dQ_{02}(t) &= \lambda_1 e^{-(\lambda+\lambda_1)t}dt \\
dQ_{10}(t) &= g_1(t)dt & dQ_{20}(t) &= g_1(t)e^{-(\lambda+\lambda_2)t}dt \\
dQ_{23}(t) &= \lambda e^{-(\lambda+\lambda_2)t}\bar{G_1}(t)dt & dQ_{24}(t) &= \lambda_2 e^{-(\lambda+\lambda_2)t}\bar{G_1}(t)dt \\
dQ_{25}^{(4)}(t) &= [\lambda_2 e^{-(\lambda+\lambda_2)t}\copyright 1]g_1(t)dt & dQ_{50}(t) &= g_2(t)e^{-(\lambda+\lambda_1)t}dt \\
dQ_{56}(t) &= \lambda e^{-(\lambda+\lambda_1)t}\bar{G_2}(t)dt & dQ_{57}(t) &= \lambda_1 e^{-(\lambda+\lambda_1)t}\bar{G_2}(t)dt \\
dQ_{52}^{(7)}(t) &= [\lambda_1 e^{-(\lambda+\lambda_1)t}\copyright 1]g_2(t)dt & dQ_{72}(t) &= g_2(t)dt \\
dQ_{45}(t) &= g_1(t)dt & dQ_{65}(t) &= g(t)dt \\
dQ_{32}(t) &= g(t)dt
\end{aligned}
\tag{1}
$$

The non-zer o elements p_{ij} can be repr esented as belo w:

$$p_{01} = \frac{\lambda}{\lambda+\lambda_1} \qquad p_{02} = \frac{\lambda_1}{\lambda+\lambda_1}$$

$$p_{20} = g_1^*(\lambda+\lambda_2) \qquad p_{23} = \frac{\lambda[1-g_1^*(\lambda+\lambda_2)]}{(\lambda+\lambda_2)}$$
$$p_{24} = p_{25}^{(4)} = \frac{\lambda_2[1-g_1^*(\lambda+\lambda_2)]}{(\lambda+\lambda_2)} \qquad p_{50} = g_2^*(\lambda+\lambda_1)$$
$$p_{56} = \frac{\lambda[1-g_2^*(\lambda+\lambda_1)]}{(\lambda+\lambda_1)} \qquad p_{57} = p_{52}^{(7)} = \frac{\lambda_1[1-g_2^*(\lambda+\lambda_1)]}{(\lambda+\lambda_1)}$$
$$p_{10} = p_{32} = p_{65} = g^*(0) = 1 \qquad p_{45} = g_1^*(0) = 1$$
$$p_{72} = g_2^*(0) = 1 \tag{2}$$

It is also verifie that:

$$p_{01} + p_{02} = 1 \qquad p_{20} + p_{23} + p_{24} = 1$$
$$p_{20} + p_{23} + p_{25}^{(4)} = 1 \qquad p_{50} + p_{56} + p_{57} = 1$$
$$p_{50} + p_{56} + p_{52}^{(7)} = 1 \qquad p_{10} = p_{32} = p_{45} = p_{65} = p_{72} = 1 \tag{3}$$

When it (time) is calculated from the epoch of arriv al into state 'j', the unconditional mean time taken by the system to transit for each regeneration state 'i'is mathematically define as:

$$m_{ij} = \int_0^\infty t dQ_{ij}(t) = -q_{ij}^*(0) \tag{4}$$

it is also verifie that

$$m_{01} + m_{02} = \mu_0 \qquad m_{20} + m_{23} + m_{24} = \mu_2$$
$$m_{20} + m_{23} + m_{25}^{(4)} = K_1 \qquad m_{50} + m_{56} + m_{57} = \mu_5$$
$$m_{50} + m_{56} + m_{52}^{(7)} = K_2 \qquad m_{10} = \mu_1$$
$$m_{32} = \mu_3 \qquad m_{45} = \mu_4$$
$$m_{65} = \mu_6 \qquad m_{72} = \mu_7 \tag{5}$$

wher e

$$m_{01} = \int_0^\infty t\lambda e^{-(\lambda+\lambda_1)t}dt \qquad m_{02} = \int_0^\infty t\lambda_1 e^{-(\lambda+\lambda_1)t}dt$$
$$m_{20} = \int_0^\infty g_1(t)te^{-(\lambda+\lambda_2)t}dt \qquad m_{23} = \int_0^\infty \lambda te^{-(\lambda+\lambda_2)t}\bar{G_1}(t)dt$$
$$m_{24} = \int_0^\infty \lambda_2 te^{-(\lambda+\lambda_2)t}\bar{G_1}(t)dt \qquad m_{25}^{(4)} = \int_0^\infty t[\lambda_2 e^{-(\lambda+\lambda_2)t}\copyright 1]g_1(t)dt$$
$$m_{50} = \int_0^\infty g_2(t)te^{-(\lambda+\lambda_1)t}dt \qquad m_{56} = \int_0^\infty \lambda te^{-(\lambda+\lambda_1)t}\bar{G_2}(t)dt$$
$$m_{57} = \int_0^\infty \lambda_1 te^{-(\lambda+\lambda_1)t}\bar{G_2}(t)dt \qquad m_{52}^{(7)} = \int_0^\infty t[\lambda_1 e^{-(\lambda+\lambda_1)t}\copyright 1]g_2(t)dt$$
$$m_{10} = m_{32} = m_{65} = \int_0^\infty tg(t)tdt \qquad m_{45} = \int_0^\infty tg_1(t)tdt$$
$$m_{72} = \int_0^\infty tg_2(t)tdt \qquad K_1 = \int_0^\infty \bar{G_1}(t)dt$$
$$K_2 = \int_0^\infty \bar{G_2}(t)dt \tag{6}$$

The mean sojour n time (μ_i) in the regenerativ e state 'i'is define as the period of time spent in that state befor e transitioning to any other state:

$$\mu_i = E(T_i) = \int_0^\infty P(T_i > t) \tag{7}$$

As we get

$$\mu_0 = \frac{1}{\lambda+\lambda_1} \qquad \mu_2 = \frac{1-g_1^*(\lambda+\lambda_2)}{\lambda+\lambda_2}$$
$$\mu_5 = \frac{1-g_2^*(\lambda+\lambda_1)}{\lambda+\lambda_1} \qquad \mu_1 = \mu_3 = \mu_6 = -g^*(0)$$
$$\mu_4 = -g_1^*(0) \qquad \mu_7 = -g_2^*(0) \tag{8}$$

4.2. Mean Time To System Failure

The failed states of the system are considered absorbing to determine the mean time to system failure (MTSF) of the system. The following recursive relation for $\phi_i(t)$ is obtained with probabilities arguments:

$$\phi_0(t) = Q_{01}(t) + Q_{02}(t)Ⓢ\phi_2(t)$$
$$\phi_2(t) = Q_{20}(t)Ⓢ\phi_0(t) + Q_{23}(t) + Q_{24}(t) \tag{9}$$

Taking Laplace Stieltje Transforms(L.S.T) of these relations in equations(9) and solving for $\phi_o^{**}(s)$ we obtain

$$\phi_o^{**}(s) = \frac{N(s)}{D(s)} \tag{10}$$

where

$$N(s) = Q_{01}^{**}(s) + Q_{02}^{**}(s)[Q_{23}^{**}(s) + Q_{24}^{**}(s)] \tag{11}$$
$$D(s) = [1 - Q_{02}^{**}(s)Q_{20}^{**}] \tag{12}$$

Now the mean time to system failure (MTSF) , when the system started at the beginning of state S0 is

$$T = \lim_{s\longrightarrow 0} \frac{1-\phi_o^{**}(s)}{s} \tag{13}$$

Using L' Hospital rule and putting the value of $\phi_o^{**}(s)$ from equation(13), we have

$$T_0 = \frac{N}{D} \tag{14}$$

where

$$N = \mu_0 + \mu_2[p_{02}] \tag{15}$$
$$D = 1 - p_{02}p_{20} \tag{16}$$

4.3. Availability Analysis

Let $A_i(t)$ be the probability that the system is in the up state at instant t, given that the system entered the regenerative state i at t=0. The following recursive relations are satisfie by the availability $A_i(t)$:

$$A_0(t) = M_0(t) + q_{01}(t)©A_1(t) + q_{02}(t)©A_2(t)$$
$$A_1(t) = q_{10}(t)©A_0(t)$$
$$A_2(t) = M_2(t) + q_{20}(t)©A_0(t) + q_{23}(t)©A_3(t) + q_{25}^{(4)}(t)©A_5(t)$$
$$A_3(t) = q_{32}(t)©A_2(t)$$
$$A_5(t) = M_5(t) + q_{50}(t)©A_0(t) + q_{56}(t)©A_6(t) + q_{52}^{(7)}(t)©A_2(t)$$
$$A_6(t) = q_{65}(t)©A_5(t) \tag{17}$$

where

$$M_0(t) = e^{-(\lambda+\lambda_1)t} \qquad M_2(t) = e^{-(\lambda+\lambda_2)t}\bar{G_1}(t)$$
$$M_5(t) = e^{-(\lambda+\lambda_1)t}\bar{G_2}(t) \tag{18}$$

Taking Laplace Transfor mation of the abo ve equation(18) and letting s$\longrightarrow$ 0, we get

$$M_0^*(0) = \mu_0 \qquad M_2^*(0) = \mu_2$$
$$M_5^*(0) = \mu_5 \tag{19}$$

Taking Laplace transfor m of the abo ve equations(17) and solving them for

$$A_0^*(s) = \frac{N_1(s)}{D_1(s)} \tag{20}$$

wher e

$$N_1(s) = M_0^*(s)[1 - q_{23}^*(s)q_{32}^*(s) - q_{56}^*(s)q_{65}^*(s) - q_{25}^{(4)*}(s)q_{52}^{(7)*}(s) + q_{23}^*(s)q_{32}^*(s) - q_{56}^*(s)q_{65}^*(s)] + M_2^*(s)q_{02}^*(s)[1 - q_{56}^*(s)q_{65}^*(s)] + M_5^*(s)q_{02}^*(s)q_{25}^{(4)*}(s) \tag{21}$$

$$D_1(s) = [1 - q_{56}^*(s)q_{65}^*(s) - q_{23}^*(s)q_{32}^*(s) + q_{23}^*(s)q_{32}^*(s)q_{56}^*(s)q_{65}^*(s) - q_{25}^{(4)*}(s)q_{52}^{(7)*}(s)] - q_{01}^*(s)q_{10}^*(s)[1 - q_{56}^*(s)q_{65}^*(s) - q_{23}^*(s)q_{32}^*(s) + q_{23}^*(s)q_{32}^*(s)q_{56}^*(s)q_{65}^*(s) - q_{25}^{(4)*}(s)q_{52}^{(7)*}(s)] - q_{02}^*(s)q_{20}^*(s) + q_{02}^*(s)q_{20}^*(s)q_{56}^*(s)q_{65}^*(s) - q_{02}^*(s)q_{50}^*(s)q_{25}^{(4)*}(s) \tag{22}$$

In steady state, system availability is giv en as

$$A_0 = \lim_{s\longrightarrow 0} sA_0^*(s) = \frac{N_1}{D_1} \tag{23}$$

wher e

$$N_1 = \mu_0[1 - p_{23} - p_{56} + p_{23}p_{56} - p_{25}^{(4)}p_{52}^{(7)}] + \mu_2[p_{02}(1 - p_{56})] + \mu_5[p_{02}p_{25}^{(4)}] \tag{24}$$

$$D_1 = \mu_0[1 - p_{23} - p_{56} + p_{23}p_{56} - p_{25}^{(4)}p_{52}^{(7)}] + \mu_1 p_{01}[1 - p_{23} - p_{56} + p_{23}p_{56} - p_{25}^{(4)}p_{52}^{(7)}] + K_1 p_{02}[1 - p_{56}] + K_2 p_{02}p_{25}^{(4)} + \mu_6[p_{02}p_{23}p_{56}] \tag{25}$$

4.4. Busy Period Analysis of the Repair man

Let $BR_i(t)$ be the pr obability that the repair man is busy at time t giv en that the system enter ed regenerativ e state i at i=0. The recursiv e relation for $BR_i(t)$ ar e as follo ws:

$$BR_0(t) = q_{01}(t)\copyright BR_1(t) + q_{02}(t)\copyright BR_2(t)$$
$$BR_1(t) = W_1(t) + q_{10}(t)\copyright BR_0(t)$$
$$BR_2(t) = W_2(t) + q_{20}(t)\copyright BR_0(t) + q_{23}(t)\copyright BR_3(t) + q_{25}^{(4)}(t)\copyright BR_5(t)$$
$$BR_3(t) = W_3(t) + q_{32}(t)\copyright BR_2(t)$$
$$BR_5(t) = W_5(t) + q_{50}(t)\copyright BR_0(t) + q_{56}(t)\copyright BR_6(t) + q_{52}^{(7)}(t)\copyright BR_2(t)$$
$$BR_6(t) = W_6(t) + q_{65}(t)\copyright BR_5(t) \tag{26}$$

wher e

$$W_1(t) = \bar{G}(t) \qquad W_2(t) = e^{-(\lambda+\lambda_2)t}\bar{G_1}(t) \qquad W_3(t) = \bar{G}(t)$$
$$W_5(t) = e^{-(\lambda+\lambda_1)}\bar{G_2}(t)dt \qquad W_6(t) = \bar{G}(t) \tag{27}$$

Taking Laplace Transfor mation of the abo ve equation(27) and letting s$\longrightarrow$ 0, we get

$$W_1^*(0)=\mu_1 \qquad W_2^*(0)=\mu_2 \qquad W_3^*(0)=\mu_3$$
$$W_5^*(0)=\mu_5 \qquad W_6^*(0)=\mu_6 \tag{28}$$

Taking Laplace transfor m of the abo ve equations(26) and solving them for

$$BR_0^*(s)=\frac{N_2(s)}{D_1(s)} \tag{29}$$

wher e

$$\begin{aligned}N_2(s)=&W_1^*(s)q_{01}^*(s)[1-q_{23}^*(s)q_{32}^*(s)-q_{56}^*(s)q_{65}^*(s)+q_{23}^*(s)q_{32}^*(s)q_{56}^*(s)q_{65}^*(s)]+\\&W_2^*(s)q_{02}^*(s)[1-q_{56}^*(s)q_{65}^*(s)]+W_3^*(s)q_{02}^*(s)[q_{23}^*(s)-q_{56}^*(s)q_{65}^*(s)]+\\&W_5^*(s)q_{02}^*(s)q_{25}^{(4)*}(s)+W_6^*(s)q_{02}^*(s)q_{25}^{(4)*}(s)q_{56}^*(s)\end{aligned} \tag{30}$$

The value of $D_1(s)$ is alr eady define in equation(22).

System total fraction of the time when it is under repair in steady state is giv en by

$$BR_0=\lim_{s\longrightarrow 0} sBR_0^*(s)=\frac{N_2}{D_1} \tag{31}$$

wher e

$$\begin{aligned}N_2=&\mu_1[p_{01}(1-p_{23}-p_{56}+p_{23}p_{56}-p_{25}^{(4)}p_{52}^{(7)})]+\mu_2[p_{02}(1-p_{56})]\\&+\mu_3[p_{02}(p_{23}-p_{56})]+\mu_5[p_{02}p_{25}^{(4)}]+\mu_6[p_{02}p_{56}p_{25}^{(4)}]\end{aligned} \tag{32}$$

The value of D_1 is alr eady define in equation(25).

4.5. Expected Number of Repairs

Let $ER_i(t)$ be the expected no. of repairs in (0,t] giv en that the system enter ed regenerativ e state i at i=0. The recursiv e relations for $ER_i(t)$ ar e as follo ws:

$$\begin{aligned}ER_0(t)&=Q_{01}(t)\textcircled{S}[1+ER_1(t)]+Q_{02}(t)\textcircled{S}[1+ER_2(t)]\\ER_1(t)&=Q_{10}(t)\textcircled{S}ER_0(t)\\ER_2(t)&=Q_{20}(t)\textcircled{S}ER_0(t)+Q_{23}(t)\textcircled{S}[1+ER_3(t)]+Q_{25}^{(4)}(t)\textcircled{S}[1+ER_5(t)]\\ER_3(t)&=Q_{32}(t)\textcircled{S}ER_2(t)\\ER_5(t)&=Q_{50}(t)\textcircled{S}ER_0(t)+Q_{56}(t)\textcircled{S}[1+ER_6(t)]+Q_{52}^{(7)}(t)\textcircled{S}ER_2(t)\\ER_6(t)&=Q_{65}(t)\textcircled{S}ER_5(t)\end{aligned} \tag{33}$$

Taking L.S.T.of abo ve relations and obtain the value of $VR_0^{**}(s)$, we get

$$ER_0^{**}(s)=\frac{N_3(s)}{D_1(s)} \tag{34}$$

wher e

$$\begin{aligned}N_3(s)=&(Q_{01}^{**}(s)+Q_{02}^{**}(s))[1-Q_{23}^{**}(s)Q_{32}^{**}(s)-Q_{56}^{**}(s)Q_{65}^{**}(s)-Q_{25}^{(4)**}(s)Q_{52}^{(7)**}(s)\\&+Q_{23}^{**}(s)Q_{32}^{**}(s)-Q_{23}^{**}(s)Q_{32}^{**}(s)-Q_{56}^{**}(s)Q_{65}^{**}(s)]+(Q_{23}^{**}(s)+Q_{25}^{(4)**}(s))\\&[1-Q_{56}^{**}(s)Q_{65}^{**}(s)+Q_{56}^{**}(s)Q_{25}^{(4)**}(s)]\end{aligned} \tag{35}$$

The value of $D_1(s)$ is alr eady define in equation(22).

For system steady state, the number of repairs per unit time is given by

$$ER_0 = \lim_{s \longrightarrow 0} sER_0^{**}(s) = \frac{N_3}{D_1} \tag{36}$$

where

$$N_3 = [1 - p_{23} - p_{56} + p_{23}p_{56} - p_{25}^{(4)}p_{52}^{(7)}] + p_{02}(1 - p_{20})[1 - p_{56} + p_{56}p_{25}^{(4)}] \tag{37}$$

The value of D_1 is already define in equation(25).

5. Profi Analysis

The profi incurred by the system model in steady state is calculated as follows:

$$P = Z_0A_0 - Z_1BR_0 - Z_2ER_0 - Z_3 \tag{38}$$

where

P = Profit
Z_0 = Revenue per unit up time.
Z_1 = Cost per unit up time for which the repair man is busy for repair.
Z_2 = Cost per repair.
Z_3 = Installation Cost.

6. Particular Cases

For the particular case, the failure rates and repair rates are exponentially distributed as follows:

$$g(t) = \alpha e^{-\alpha t} \qquad g_1(t) = \alpha_1 e^{-\alpha_1 t}$$
$$g_2(t) = \alpha_2 e^{-\alpha_2 t}$$

As we get,

$$p_{01} = \frac{\lambda}{\lambda + \lambda_1}$$
$$p_{02} = \frac{\lambda_1}{\lambda + \lambda_1} \qquad p_{20} = \frac{\alpha_1}{\lambda + \lambda_2\alpha_1}$$
$$p_{23} = \frac{\lambda}{(\lambda + \lambda_2 + \alpha_1)} \qquad p_{24} = p_{25}^{(4)} = \frac{\lambda_2}{(\lambda + \lambda_2 + \alpha_1)}$$
$$p_{50} = \frac{\alpha_2}{\lambda + \lambda_1 + \alpha_2} \qquad p_{56} = \frac{\lambda}{(\lambda + \lambda_1 + \alpha_2)}$$
$$p_{57} = p_{52}^{(7)} = \frac{\lambda_1}{(\lambda + \lambda_1 + \alpha_2)} \qquad p_{10} = p_{32} = p_{65} = p_{45} = p_{72} = 1$$
$$\mu_0 = \frac{1}{\lambda + \lambda_1} \qquad \mu_2 = \frac{1}{(\lambda + \lambda_2 + \alpha_1)}$$
$$\mu_5 = \frac{1}{\lambda + \lambda_1 + \alpha_2} \qquad \mu_1 = \mu_3 = \mu_6 = \frac{1}{\alpha}$$
$$\mu_4 = K_1 = \frac{1}{\alpha_1} \qquad \mu_7 = K_2 = \frac{1}{\alpha_2} \tag{39}$$

Based on the facts received i.e.,

Table 1: *Information Gathered*

Description	Notation	Rate(/hr)
Failur e Rate of robotic	λ	0.001378336 / hr
Failur e Rate of WSF	λ_2	0.000117273 / hr
Repair Rate of robotic	α	0.20271061 / hr
Repair Rate of WSF	α_2	0.005767389 / hr

The remaining values are assumed and are listed in Table 2:

Table 2: *Assumed Values*

Description	Notation	Rate(/hr)
Failur e Rate of WSR	λ_1	0.000018325 / hr
Repair Rate of WSR	α_1	0.003728205 / hr
Revenue per unit uptime(per month)	Z_0	Rs.10, 80, 000
Cost per unit uptime, when repair man is busy for repair(per month)	Z_1	Rs.12, 466
Cost per reapir(per month)	Z_2	Rs.18, 350

Various measur es of system effectiv eness are sho wn in Table 3:

Table 3: *Results*

Description	Notation	Rate(/hr)
Mean Time to System Failur e	T_0	714.866577 / hrs
Availability of the system	A_0	0.909847
Busy period of Repair man	BR_0	0.21322
Expected no. of Repairs	ER_0	0.002053
Profi	P	Rs.14, 21, 955

7. Graphical Repr esentation

This study has prepar ed graphs for the MTSF (as sho wn in Figur e.2), Profi as a result of failur e rate of main unit(λ)(Figur e 3.) and revenue (uptime of the system per unit) (Z_0) for various estimates of repair man cost for busy work in (Z_1) is sho wn in Figur e 4.

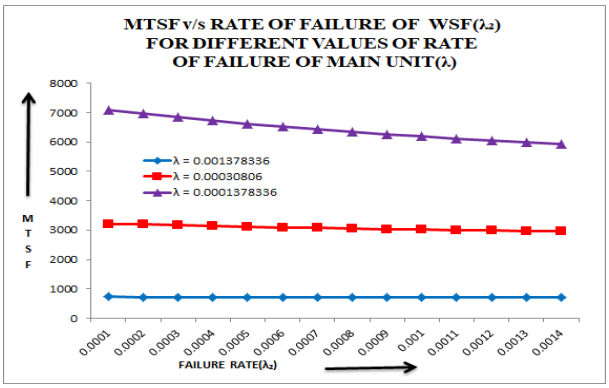

Figure 2: *MTSF v/s Failure Rate*

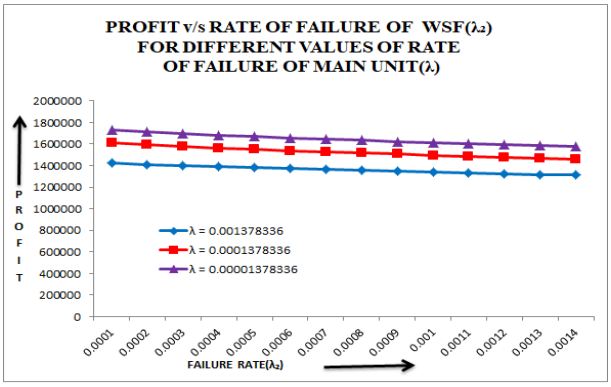

Figure 3: *Profit v/s Failure Rate*

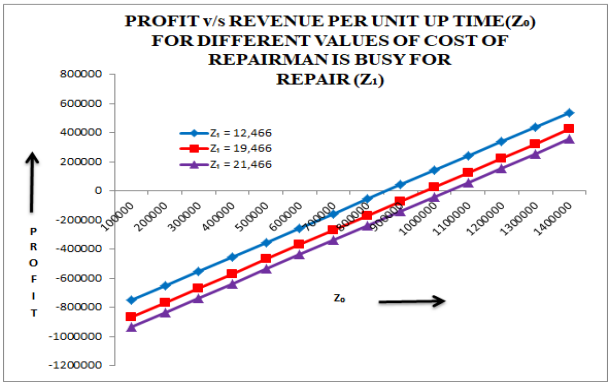

Figure 4: *Profit v/s Revenue*

8. Discussion

Discussion for the FAILURE RATE v/s MTSF and PROFIT v/s FAILURE RATE in the **Table 4.**

Table 4: *Results*

Variation	Effect
$\lambda/\ \lambda_1$ increasing $(\uparrow)$	MTSF decreases $(\downarrow)$
$\lambda/\ \lambda_1$ increasing $(\uparrow)$	Profi decreases $(\downarrow)$

As shown in above table, the behaviour of MTSF and Profi w.r.t. rate of failure of Main unit for the different values of the rate of failure of WSF. It clear from the table that MTSF and Profi gets decreased with increase in values of rate of failure of Main unit i.e. λ. Also MTSF and Profi decreases as failure rate of WSF i.e. λ_1 increases.

Discussion for the PROFIT v/s REVENUE in the **Table 5.** as below:

Table 5: *Results*

Variation	Effect
Z_0 increasing $(\uparrow)$	Profi increases $(\uparrow)$
$Z_1 = 12,466$; Profi $>=<$ according as z_0	when Z_0 is $>=<$ 8, 00, 000
$Z_1 = 19,466$; Profi $>=<$ according as z_0	when it $Z_0 >=<$ 9, 25, 525
$Z_1 = 21,466$; Profi $>=<$ according as z_0	when it $Z_0 >=<$ 9, 98, 980

Above table depicts the behaviour of the profi w.r.t. revenue per unit uptime of the system (Z_0) for different values of cost of repair man is busy under repair (Z_1). The graph exhibits that there is inclination in the trend of profi increases with increases in the values of Z_0. Also, following conclusion can be drawn from the discussion for Profi v/s Revenue :

For $Z_1 = 12,466$, the profi is positive or zero or negative according as Z_0 is $>=<$ 8,00,000. Hence, for this case the revenue per unit up time should be fixed equal or greater than 8,00,000.

Similarly, discussion for other values of Z_1.

9. Conclusion

The conclusion is based on data from Federal-Mogul Powertrain. By using various parameters in the existing model at piston plant, the numerical value of profi is calculated as Rs. 10,45,838 and profi for current research is Rs. 14,21,955. From numerical values it has been shown that profi for new model is greater as compare to existing model, when referigerator facility is used. The finding of this study are novel since no previous research has highlighted the critical function of water supply for the MLDB system in piston foundries. The discussion reveal that the results analysed are quite interesting and beneficia for piston manufacturing businesses who use the MLDB system. In the same way, system designers might apply the escommended strategy to their own sectors. The generated equations can be used to figure out how practical different mechanism-type systems are.

References

[1] Bhatia Pooja and Sharma Shweta(2019) Reliability analysis of two unit standby system for high pressure die casting machine. *Arya Bhatta Journal of Mathematics and Informatics*, 11(1):19-28.

[2] Chaudhari Amit and Vasudevan Hari(2020) A Review of the Reliability Techniques Used in the Case of Casting Process Optimization. *Arya Bhatta Journal of Mathematics and Informatics*, 6(4):309-316.

[3] Kumar Amit, Varshney A and Ram Mangey(2015) Sensitivity analysis for casting process under stochastic modelling. *International Journal of Industrial Engineering Computations*, 6(3):419-432.

[4] Kumar Ashish, Baweja Sonali and Barak M(2015) Stochastic behavior of a cold standby system with maximum repair time. *Decision Science Letters*, 4(4):569-578.

[5] Laukli, Hans Ivar(2004) High Pressure Die Casting of Aluminium and Magnesium Alloys: Grain Structure and Segregation Characteristics. *Fakultet for naturvitenskap og teknologi*, 19(4):150-164.

[6] Müller Sebastian, Müller Anke,Rothe Felix, Dilger Klaus and Dröder Klaus(2018) An Initial Study of a Lightweight Die Casting Die Using a Modular Design Approach. *International Journal of Metalcasting*, 12(4):870-883.

[7] Sharma Satpal(2014) Modeling and Optimization of Die Casting Process for ZAMAK Alloy. *Journal of Engineering & Technology*, 4(2):217-229.

[8] Sharma Upasana and Kaur Jaswinder (2016). Cost benefi analysis of a compressor standby system with preference of service, repair and replacement is given to recently failed unit. *International Journal of Mathematics Trends and Technology*, 30(2):104-108.

[9] Sharma Upasana and Sharma Gunjan(2018) Stochastic modelling of a cold standby unit working in a power plant system. *International Journal of Innovative Knowledge Concepts*, 6(8):49-54.

[10] Srinivasan(2006) Reliability analysis of a three unit warm standby redundant system with repair. *Annals of Operations Research*, 143(1):227-239.

[11] Timelli Giulio(2010) Constitutive and stochastic models to predict the effect of casting defects on the mechanical properties of High Pressure Die Cast AlSi9Cu3 (Fe) alloys. *Metallurgical Science and Tecnology*, 28(2):117-129.

[12] Yourui Tao, Shuyong Duan and Xujing Yang (2016). Reliability modeling and optimization of die-casting existing epistemic uncertainty. *International Journal on Interactive Design and Manufacturing (IJIDeM)*, 10(2):51-57.

RT&A, No 3 (69)
Volume 17, September 2022

Type 1 Topp-Leone $q-$Exponential Distribution and its Applications

Nicy Sebastian[1], Jeena Joseph[1] and Princy T[2]

•

[1]Department of Statistics, St Thomas College, Thrissur, Kerala, India-680 001
nicycms@gmail.com, sony.jeena@gmail.com
[2]Department of Statistics, Cochin University of Science and Technology
Cochin, Kerala, India 682 022
princyt.t@gmail.com

Abstract

The main purpose of this paper is to discuss a new lifetime distribution, called the type 1 Topp-Leone generated q-exponential distribution(Type 1 TLqE). Using the quantile approach various distributional properties, L−moments, order statistics, and reliability properties were established. We suggested a new reliability test plan, which is more advantageous and helps in making optimal decisions when the lifetimes follow this distribution. The new test plan is applied to illustrate its use in industrial contexts. Finally, we proved empirically the importance and the flexibility of the new model in model building by using a real data set.

Keywords: Type 1 Topp-Leone generated q-exponential distribution, Quantile density function, Quantile function, Hazard quantile function, $L-$moments, Reliability Test Plan.

1. Introduction

There are many statistical distributions which plays an important role in modeling survival and life time data such as exponential, weibull, logistic etc. Almost all these distributions with unbounded support. But there are situations in real life, in which observations can take values only in a limited range such as percentages, proportions or fractions. Papke and Wooldridge [12] claims that in many economic settings, such as fraction of total weekly hours spent working, pension plan participation rates, industry market shares, fraction of land area allocated to agriculture etc., the variable bounded between zero and one. Thus it is important to have models defined on the unit interval in order to have reasonable results.

A new distribution was introduced in 1955, called Topp Leone (TL) distribution, defined on finite support, proposed Topp and Leone [20] and used it as a model for failure data. A random variable X is distributed as the TL with parameter α denoted by $x \sim TL_{(\alpha)}$, with a cumulative distribution function

$$F_{TL}(x) = x^{\alpha}(2-x)^{\alpha}, 0 < x < 1, \alpha > 0. \tag{1}$$

The corresponding probability function is

$$f_{TL}(x) = 2\alpha x^{\alpha-1}(1-x)(2-x)^{\alpha-1}. \tag{2}$$

Topp Leone distribution provides closed forms of cumulative density function (cdf) and the probability density function (pdf) and describes empirical data with J-shaped histogram such as powered tool band failures, automatic calculating machine failure. The Topp Leone distribution

had been received little attention until Nadarajah and Kotz [10] discovered it. Further information and application of TL distribution can be obtained from Ghitany et al. [2], Kotz and Seier [7].

Lifetime data plays an important role in a wide range of applications such as medical, engineering an social sciences. When there is a need for more flexible distributions, almost all researchers are about to use the new one with more generalization. An excellent review of Lee et al. [9] has provided through knowledge of several methods for generating families of continuous univariate distributions. They discussed some noticeable developments after 1980, are method of generating skew distributions, beta generated method, method of adding parameters, transformed-transformer method, and composite method. The beta generated (BG) family of distributions belongs to a parameter adding method (Lee et al. [9], Kumaraswamy [8]). In a similar manner the relation of a random variable X having the TLG distribution and a random variable T having TL distribution is $X = G^{-1}(T)$, with $T \sim TL(\alpha)$. This relation demonstrates that the pdf of TL distribution, (2), is transformed into a new pdf through the function $G(\cdot)$ The cdf of TL generated random variable X is defined as

$$F_{TLG}(x) = \int_0^{G(x)} h(t)dt$$

where $h(t)$ is the pdf of TL variable and $G(x)$ is the cdf of any arbitrary random variable. Thus the cdf of TL generated random variable is

$$F_{TLG}(x) = 2\alpha \int_0^{G(x)} t^{\alpha-1}(1-t)(2-t)^{\alpha-1}dt = G(x)^{\alpha}(2-G(x))^{\alpha}. \tag{3}$$

By differentiating, we get the corresponding pdf,

$$f_{TLG}(x) = 2\alpha g(x)(1-G(x))G(x)^{\alpha-1}(2-G(x))^{\alpha-1}, \alpha > 0. \tag{4}$$

In reliability analysis, a frequently used distribution is exponential distribution having the characterizing property of constant hazard function. Due to this, exponential distribution is sometimes not suitable for analyzing data. This implies the need for more generalization. In such situations we use distribution called Topp-Leone Exponential distribution (TLE). TLE distribution comes as the combination of TL distribution and exponential distribution. Here TL distribution is the generator and exponential is the parent distribution. Sangsanit and Bodhisuwan [16] presented the Topp-Leone generated exponential (TLE) distribution as an example of the Topp-Leone generated distribution. A random variable X possessing TLE distribution having cdf and probability function defined respectively as

$$F_{TLE}(x) = (1-exp(-\lambda x))^{\alpha}(2-(1-exp(-\lambda x)))^{\alpha} = (1-exp(-2\lambda x))^{\alpha}$$

and

$$f_{TLE}(x) = 2\alpha\lambda exp(-2\lambda x)(1-exp(-2\lambda x))^{\alpha-1},$$

where α is the shape parameter and λ is the scale parameter .

Various entropy measures have been developed by mathematicians and physicists to describe several phenomena, depending on the field and the context in which it is being used. Tsallis [19], introduced a generalization of the Boltzmann-Gibbs entropy. Tsallis statistics have found applications in many areas such as physics, chemistry, biology, medicine, economics, geophysics, etc. By maximizing Tsallis entropy, subject to certain constraints, leads to the Tsallis distribution, also known as q-exponential distribution, which has the form $f(x) = c[1-(1-q)x]^{\frac{1}{(1-q)}}$ where c is the normalizing constant. Various applications and generalizations of the q-exponential distribution are given in Picoli et al. [13]. In the limit $q \to 1$, q-entropy converges to Boltzmann-Gibbs entropy.

An important characteristic of q-exponential distribution is that it has two parameters q and λ providing more flexibility with regard to its decay, differently from exponential distribution. The q exponential distribution is defined by its cdf and pdf as,

$$F_{1qE}(x) = 1-[1-(1-q)\lambda x]^{\frac{(2-q)}{1-q}}. \tag{5}$$

$$f_{1qE}(x) = (2-q)\lambda[1-(1-q)\lambda x]^{\frac{1}{1-q}}, 1-\lambda(1-q)x > 0, \lambda > 0, q < 2, q \neq 0 \tag{6}$$

The parameter q is known as entropy index. As $q \to 1$, the q-exponential distribution becomes exponential distribution. In that sense q-exponential distribution is a generalization of exponential distribution. The parameters q and λ determine how quickly the pdf decays. In the reliability context, an important characteristic of the q-exponential distribution is its hazard rate, which is not necessarily constant as in exponential distribution.

The rest of the paper is organized as follows. In section 2 we will discuss the Type 1 Topp-Leone q-Exponential Distribution. In section 3 consists of the quantile properties of Type 1 TLqE distribution. Section 4, we described a new reliability test plan for type 1 TLqE distribution and its applications are also discussed. In Section 5, we apply the Type 1 TLqE distribution to a real data sets to show that it can be used quite effectively in analyzing lifetime data. Finally, concluding remarks and future work are addressed in Section 6.

2. Type 1 Topp-Leone q-Exponential Distribution

In this section we discuss the type 1 Topp-Leone generated $q-$ exponential (TLqE) distribution introduced by combining the TL distribution with $q-$ exponential distribution, for more details see Sebastian et al. [17]. Substituting (5) and (6) in (3) and (4) respectively we will get the distribution function and density function of TLqE distribution as follows:

$$F_{1TLqE}(x) = \{1-[1-(1-q)\lambda x]^{2(\frac{2-q}{1-q})}\}^{\alpha}, x > 0, \lambda, \alpha > 0, q < 2, q \neq 0.$$

and

$$f_{1TLqE}(x) = 2\alpha\lambda(2-q)[1-(1-q)\lambda x]^{\frac{3-q}{1-q}}\{1-[1-(1-q)\lambda x]^{2(\frac{2-q}{1-q})}\}^{\alpha-1},$$

where $1-[1-(1-q)\lambda x]^{2(\frac{2-q}{1-q})} > 0, \lambda, \alpha > 0, q < 2.$

Figure 1: *Plots of F(x) of TLqE distribution for $\alpha = 1.1, \lambda = 0.1$ (left) and for $\lambda = 0.3, q = 1.1$ (right).*

Figure 2: *Plots of f(x) of TLqE distribution for* $\alpha = 1.1, \lambda = 0.1$ *(left) and for* $\lambda = 0.3, q = 1.1$ *(right).*

In Figure 1 and Figure 2, we can see the plots of cdf and pdf of TLqE for different values of the shape parameters α and q. The survival function, the probability density function and the Hazard function are the three important functions that characterize the distribution of the survival times. Here

$$S(x) = 1 - \{1 - [1 - (1-q)\lambda x]^{2(\frac{2-q}{1-q})}\}^{\alpha},$$

and

$$h(x) = \frac{2\alpha\lambda(2-q)[1-(1-q)\lambda x]^{\frac{3-q}{1-q}}\{1-[1-(1-q)\lambda x]^{2(\frac{2-q}{1-q})}\}^{\alpha-1}}{1-\{1-[1-(1-q)\lambda x]^{2(\frac{2-q}{1-q})}\}^{\alpha}}$$

respectively are the survival and the hazard function of TLqE distribution. Figure 3, gives the plots of $h(x)$ of TLqE distribution for different values of the shape parameters α and q.

Figure 3: *Plots of h(x) of TLqE distribution for* $\alpha = 1.1, \lambda = 0.1$ *(left) and for* $\lambda = 0.3, q = 1.1$ *(right).*

As $q \to 1$ then $f_{1TLqE}(x)$ goes to

$$f_{3TLqE}(x) = 2\alpha\lambda e^{-2\lambda x}\left(1 - e^{-2\lambda x}\right)^{\alpha-1}, \lambda, \alpha > 0, x > 0, \tag{7}$$

and the correspond cdf is

$$F_{3TLqE}(x) = \left(1 - e^{-2\lambda x}\right)^{\alpha}, x > 0, \lambda, \alpha > 0.$$

3. Quantile properties of type 1 Topp-Leone $q-$Exponential Distribution

3.1. Distributional characteristics

In modelling and analysis of statistical data, probability distribution can be specified either in terms of distribution function or by the quantile function. Quantile functions have several

interesting properties that are not shared by distributions, which makes it more convenient for analysis. For example, the sum of two quantile functions is again a quantile function. For a nonnegative random variable X with distribution function F(x), the quantile function $Q(u)$ is defined by (see Nair et al. [11])

$$Q(u) = F^{-1}(u) = inf\{x : F(x) \geq u\}, \quad 0 \leq u \leq 1 \tag{8}$$

For every -$\infty < x < \infty$ and $0 < u < 1$, we have

$$F(x) \geq u \text{ if and only if } Q(u) \leq x.$$

Thus, if there exists an x such that $F(x) = u$, then $F(Q(u)) = u$ and $Q(u)$ is the smallest value of x satisfying $F(x) = u$. Further, if $F(x)$ is continuous and strictly increasing, $Q(u)$ is the unique value x such that $F(x) = u$, and so by solving the equation $F(x) = u$, we can find x in terms of u which is the quantile function of X.

By using inversion method, we can generate a randon variate from TLqE distribution. We have already seen that the relationship between a random variable X, having TLqE distribution, and a random variable T, having the TL distribution, is

$$\begin{aligned} X &= G^{-1}(t) \\ &= \frac{1-(1-t)^{\frac{1-q}{2-q}}}{(1-q)\lambda} \end{aligned} \tag{9}$$

where $G^{-1}(\cdot)$ is related to inversion of the q-exponential cdf. The quantile function of the TL distribution is

$$t = 1 - \sqrt{1-u^{\frac{1}{\alpha}}}, \tag{10}$$

where u is picked from the uniform distribution over $(0, 1)$. Then the quantile function of type 1 TLqE distribution is obtained by using equation (9) and (10),

$$Q(u) = \frac{1-\left(\sqrt{1-u^{\frac{1}{\alpha}}}\right)^{(\frac{1-q}{2-q})}}{(1-q)\lambda}, q < 2. \tag{11}$$

The quantile-based measures of the distributional characteristics like location, dispersion, skewness, and kurtosis are useful for estimating parameters of the model by matching population characteristics with corresponding sample characteristics. We can obtain the median as Median $= Q(\frac{1}{2})$. Dispersion is measured by the interquartile range, $IQR = Q(\frac{3}{4}) - Q(\frac{1}{4})$. Skewness is measured by Galton's coefficient, $S = \frac{Q(\frac{3}{4})+Q(\frac{1}{4})-2M}{IQR}$. Moors proposed a measure of kurtosis as, $T = \frac{Q(\frac{7}{8})-Q(\frac{5}{8})+Q(\frac{3}{8})-Q(\frac{1}{8})}{IQR}$.

If $f(x)$ is the probability function of X, then $f(Q(u))$ is called the density quantile function. The derivative of $Q(u)$,

$$q(u) = Q^{'}(u),$$

is known as the quantile density function of X. If $F(x)$ is right continuous and strictly increasing, we have

$$F(Q(u)) = u \tag{12}$$

so that F(x) = u implies x = Q(u). When f(x) is the probability density function (PDF) of X; we have from (12)

$$q(u)f(Q(u)) = 1 \tag{13}$$

Quantile function has several properties that are not shared by distribution function. See Nair et al. [11] for details. Now the qunatile density of type 1 TLqE distribution is obtained as

$$q(u) = \frac{1}{2\alpha\lambda(2-q)} u^{\frac{1}{\alpha}-1} \left(1-u^{\frac{1}{\alpha}}\right)^{\frac{q-3}{2(2-q)}}. \tag{14}$$

For the proposed family of distribution, the density function $f(x)$ can be written in terms of the distribution function as

$$f(x) = 2\alpha\lambda(2-q) \frac{F(x)^{1-\frac{1}{\alpha}}}{\left(1-(F(x))^{\frac{1}{\alpha}}\right)^{\frac{q-3}{2(2-q)}}}. \tag{15}$$

For all values of the parameters, the density is strictly decreasing in x and it tends to zero as $x \to \infty$.

3.2. $L-$moments

The L-moments are often found to be more desirable than the conventional moments in describing the characteristics of the distributions as well as for inference. A unified theory and a systematic study on $L-$ moments have been presented by Hosking [3].
The r^{th} $L-$ moment is given by

$$L_r = \int_0^1 \sum_{k=0}^{r-1} (-1)^{r-1-k} \binom{r-1}{k} \binom{r-1+k}{k} u^k Q(u) du. \tag{16}$$

Theorem 1. For the type 1 TLqE distribution, the r^{th} $L-$ moment can be obtained by using the following recurrence relation,

$$L_r = \sum_{k=0}^{r-1} (-1)^{r-1-k} \binom{r-1}{k} \binom{r-1+k}{k} \frac{\alpha}{\lambda(1-q)} \left[B(1,k\alpha) - B(\frac{(1-q)}{2(2-q)}+1, k\alpha)\right]. \tag{17}$$

So we can evaluate the $L-$coefficient of variation (τ_2), analogous to the coefficient of variation based on ordinary moments is given by, $\tau_2 = \frac{L_2}{L_1}$. Similarly the $L-$coefficient of skewness, (τ_3) and kurtosis, (τ_4) of type 1 Topp-Leone generated q-exponential quantile function respectively can be obtained as $\tau_3 = \frac{L_3}{L_2}$ and $\tau_4 = \frac{L_4}{L_3}$.

3.3. Order statistics of type 1 Topp-Leone q-Exponential Distribution

If $X_{r:n}$ is the rth order statistic in a random sample of size n, then the density function of $X_{r:n}$ can be written as

$$f_r(x) = \frac{1}{B(r, n-r+1)} f(x) F(x)^{r-1} (1-F(x))^{n-r} \tag{18}$$

From Eq.(15), we have

$$f_r(x) = \frac{2\alpha\lambda(2-q)}{B(r,n-r+1)} \frac{F(x)^{r-\frac{1}{\alpha}} (1-F(x))^{n-r}}{\left(1-(F(x))^{\frac{1}{\alpha}}\right)^{\frac{q-3}{2(2-q)}}}. \tag{19}$$

Hence,

$$\begin{aligned} \mu_{r:n} = E(X_{r:n}) &= \int x f_r(x) dx \\ &= \frac{2\alpha\lambda(2-q)}{B(r,n-r+1)} \int_0^\infty x \frac{F(x)^{r-\frac{1}{\alpha}} (1-F(x))^{n-r}}{\left(1-(F(x))^{\frac{1}{\alpha}}\right)^{\frac{q-3}{2(2-q)}}} dx. \end{aligned} \tag{20}$$

In quantile terms, we have

$$E(X_{r:n}) = \frac{2\alpha\lambda(2-q)}{B(r,n-r+1)} \int_0^1 Q(u) \frac{u^{r-\frac{1}{\alpha}}(1-u)^{n-r}}{\left(1-(u)^{\frac{1}{\alpha}}\right)^{\frac{q-3}{2(2-q)}}} du. \tag{21}$$

For the type 1 TLqE distribution, the first-order statistic $X_{1:n}$ has the quantile function

$$Q_1(u) = Q(1-(1-u)^{\frac{1}{n}}) = \frac{1}{\lambda(1-q)} \left[1-\left(1-(1-u)^{\frac{1}{n}}\right)^{\frac{1}{\alpha}}\right]^{\frac{(1-q)}{2(2-q)}}, \tag{22}$$

and the nth order statistic $X_{n:n}$ has the quantile function

$$Q_n(u) = Q(u^{\frac{1}{n}}) = \frac{1}{\lambda(1-q)} \left[1-(1-u^{\frac{1}{n\alpha}})\right]^{\frac{(1-q)}{2(2-q)}}. \tag{23}$$

3.4. Hazard quantile function

One of the basic concepts employed for modeling and analysis of lifetime data is the hazard rate. In a quantile setup, Nair et al. [11] defined the hazard quantile function, which is equivalent to the hazard rate. The hazard quantile function $H(u)$ is defined as

$$H(u) = h(Q(u))) = (1-u)^{-1} fQ(u) = [(1-u)q(u)]^{-1}. \tag{24}$$

Thus $H(u)$ can be interpreted as the conditional probability of failure of a unit in the next small interval of time given the survival of the unit until $100(1-u)\%$ point of the distribution. Note that $H(u)$ uniquely determines the distribution using the identity,

$$Q(u) = \int_0^u \frac{dp}{(1-p)H(p)}. \tag{25}$$

The hazard quantile functions of type 1 TLqE distribution is

$$H(u) = \left((1-u)\frac{1}{2\alpha\lambda(2-q)} u^{\frac{1}{\alpha}-1}\left(1-u^{\frac{1}{\alpha}}\right)^{\frac{q-3}{2(2-q)}}\right)^{-1} \tag{26}$$

with $H(0) = \infty$ and $H(1) = 0$. Plots of hazard quantile function for different values of parameters are given in figure 4.

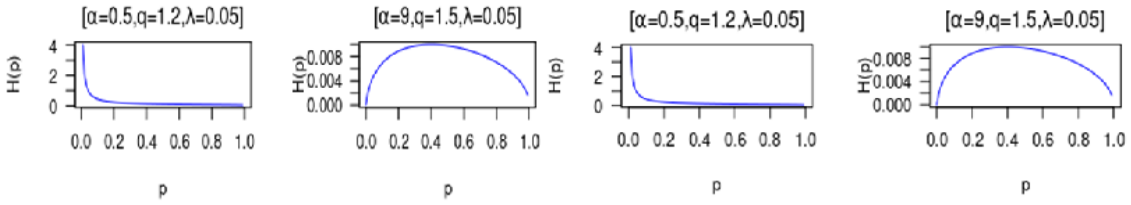

Figure 4: *Plots of hazard quantile function*

No.	Parameter region	Shape of hazard quantile function
1	$0 < \alpha < 1$ and $q < 2$	Decreasing hazard rate (DHR)
2	$\alpha > 0$ and $q < 2$	Upside-down Bathtub
3	$\alpha = 1$, $q < 2$ and $\lambda = 0$	Constant
4	$\alpha = 1$ and $q < 2$	DHR

Table 1: *Behavior of the hazard quantile function for different regions of parameter space.*

3.5. Mean residual quantile function

Another concept used in reliability is that of residual life $X_t = (X - t|X > t)$ with survival function

$$\bar{F}_t(x) = \bar{F}(t+x)/\bar{F}(t), \quad x \geq 0, 0 < t < T.$$

The mean residual life function is then

$$m(t) = E(X_t) = [\bar{F}(t)]^{-1} \int_t^\infty \bar{F}(x)dx.$$

Accordingly, the mean residual quantile function is defined by Nair et al. [11] as

$$M(u) = mQ(u) = (1-u)^{-1} \int_u^1 (Q(t) - Q(u))dt \tag{27}$$

which is the average remaining life beyond the $100(1-u)\%$ point of the distribution. For the type 1 TLqE distribution, $M(u)$ has the form

$$M(u) = \frac{1}{\lambda(1-q)} \left[\frac{\alpha}{1-u} B_{(1-u^{1/\alpha})} \left(\frac{(1-q)}{2(2-q)} + 1, \alpha \right) + (1-u^{1/\alpha})^{\frac{(1-q)}{2(2-q)}} \right]. \tag{28}$$

where $B_u(a,b) = \int_0^u x^{a-1}(1-x)^{b-1}dx$ is the incomplete beta function.

3.6. Reversed hazard quantile function

The reversed hazard quantile function is (Nair et al. [11]) defined by

$$A(u) = \frac{1}{uq(u)} \tag{29}$$

and it determines the distribution through the formula

$$Q(u) = \int_0^u \frac{1}{pA(p)}dp. \tag{30}$$

For type 1 TLqE distribution,

$$A(u) = q(u) = \frac{1}{2\alpha\lambda(2-q)} u^{\frac{1}{\alpha}-2} \left(1 - u^{\frac{1}{\alpha}}\right)^{\frac{q-3}{2(2-q)}}. \tag{31}$$

4. Reliability Test Plan

Acceptance sampling plan is an inspection procedure used to determine whether to accept or reject a specific quantity of material. (See Kantam et al. [6], Rao et al. [15], Jose and Joseph [4], Joseph and Jose [5] etc.) If it is applied to a series of lots, it prescribes a procedure that will give a specified probability of accepting lots of given quality.

In statistical quality control, acceptance sampling plan is concerned with the inspection of a sample of products taken from a lot and the decision whether to accept or reject the lot based on the quality of the product. Here we discuss the reliability test, with its operating characteristic function plan for accepting or rejecting a lot where the lifetime of the product follows type 1 Topp - Leone $q-$ exponential distribution. In a life testing experiment, the procedure is to terminate the test by a predetermined time 't' and note the number of failures. If the number of failures at the end of time 't' does not exceed a given number 'c', called acceptance number then we accept the lot with a given probability of at least 'p'. But if the number of failures exceeds 'c' before

time 't', we reject the lot. For such truncated life test and the associated decision rule, we are interested to obtain the smallest sample size to make at a decision. Even though a large number of distributions belonging to Topp-Leone generated family have been developed with wide range of applications, none of these have been applied in acceptance sampling to develop reliability test plans.This motivated the present study.
Assume that the lifetime of a product T follows the type 1 Topp-Leone $q-$ exponential distribution with cumulative distribution function (cdf)

$$F(t) = \{1 - [1 - (1-q)\frac{t}{\lambda}]^{2(\frac{2-q}{1-q})}\}^{\alpha}, t > 0, \lambda, \alpha > 0, q < 2. \tag{32}$$

Let λ_0 be the required minimum average life time and the shape parameters α and q are known. Then

$$F_{TLqE}(t; \alpha, q, \lambda) \leq G_{TLqE}(t; \alpha, q, \lambda_0) \Leftrightarrow \lambda \geq \lambda_0. \tag{33}$$

A sampling plan is specified by the number of units n on test, the acceptance number c, the maximum test duration t and the minimum average lifetime represented by λ_0.

The probability of accepting a bad lot (consumer 's risk) should not exceed the value $1 - p^*$, where p^* is a lower bound for the probability that a lot of true value λ below λ_0 is rejected by the sampling plan. For fixed p^* the sampling plan is characterized by $(n, c, t/\lambda_0)$. Binomial distribution can be used to find the acceptance probability for sufficiently large lots. The aim is to determine the smallest positive integer n for given values of c and t/ λ_0 such that

$$L(p_0) = \sum_{i=0}^{c} \binom{n}{i} {p_0}^i (1-p_0)^{n-i} \leq 1 - p^* \tag{34}$$

where $p_0 = F_{TLqE}(t; \alpha, q, \lambda_0)$ given by (32) which indicates failure probability before time 't' which depends only on the ratio t/ λ_0. The operating characteristic function $L(p)$ is the acceptance probability of the lot as a function of the failure probability $p(\lambda) = F_{TLqE}(t; \alpha, q, \lambda)$

The average life time of the product is increasing with λ and the failure probability $p(\lambda)$ decreases implying that the operating characteristic function is increasing in λ. The minimum values of n satisfying (34) are obtained for $\alpha = 2, q = 1.1$ and p^*=0.75, 0.95, 0.99 and t/λ_0 = 0.248, 0.361, 0.482, 0.602, 0.903, 1.204, 1.505 and 1.806. The results are displayed in Table 2.

If $p_0 = F_{TLqE}(t; \alpha, q, \lambda_0)$ is small and n is very large, the binomial probability may be approximated by Poisson probability with parameter $\theta = np_0$ so that (34) becomes

$$L_1(p_0) = \sum_{i=0}^{c} \frac{\theta^i}{i!} e^{-\theta} \leq 1 - p^* \tag{35}$$

The minimum values of n satisfying (35) are obtained for the same combination of values of α, q, p^* and t/λ_0 and are displayed in Table 3.

The operating characteristic function of the sampling plan (n,c,t/ λ_0) gives the probability L(p) of accepting the lot with

$$L(p) = \sum_{i=0}^{c} \binom{n}{i} {p_0}^i (1-p_0)^{n-i} \tag{36}$$

where $p = F(t, \lambda)$ is considered as a function of λ.

Table 2: *Minimum sample size using binomial approximation*

p^*	c	t/ λ_0							
		0.248	0.361	0.482	0.602	0.903	1.204	1.505	1.806
	0	11	6	4	3	2	1	1	1
	1	22	12	8	6	4	3	3	2
	2	32	17	11	9	6	4	4	4
	3	41	22	15	11	7	6	5	5
	4	51	27	18	14	9	7	6	6
0.75	5	60	33	22	17	11	9	8	7
	6	70	38	25	19	13	10	9	8
	7	79	43	29	22	14	12	10	9
	8	88	48	32	24	16	13	11	11
	9	97	52	35	27	18	14	13	12
	10	106	57	39	30	20	16	14	13
	0	24	12	8	6	4	3	2	2
	1	38	20	13	10	6	4	4	3
	2	50	27	17	13	8	6	5	5
	3	62	33	22	16	10	8	7	6
	4	73	39	26	19	12	9	8	7
0.95	5	84	45	30	22	14	11	9	8
	6	95	51	34	25	16	12	11	10
	7	106	56	37	28	18	14	12	11
	8	116	62	41	31	20	15	13	12
	9	126	68	45	34	22	17	15	13
	10	136	73	49	37	24	18	16	14
	0	36	19	12	9	5	4	3	2
	1	52	27	18	13	13	6	5	4
	2	66	35	23	17	17	8	6	5
	3	80	42	27	20	20	9	8	7
	4	92	49	32	24	24	11	9	8
0.99	5	104	55	36	27	27	13	11	9
	6	116	61	41	30	30	14	12	11
	7	128	68	45	33	33	16	13	12
	8	139	74	49	36	36	17	15	13
	9	150	80	53	39	39	19	16	14
	10	162	86	57	42	42	21	17	16

Table 3: *Minimum sample size using poisson approximation*

p^*	c	t/ λ_0							
		0.248	0.361	0.482	0.602	0.903	1.204	1.505	1.806
	0	12	7	5	4	3	2	2	2
	1	23	13	9	7	5	4	4	3
	2	33	18	13	10	7	6	5	5
	3	43	23	16	13	9	7	7	6
	4	52	29	20	15	11	9	8	7
0.75	5	62	34	23	18	12	10	9	9
	6	71	39	27	21	14	12	11	10
	7	80	44	30	23	16	13	12	11
	8	89	49	34	26	18	15	13	12
	9	99	54	37	29	20	16	15	14
	10	108	59	40	31	21	18	16	15
	0	25	14	10	8	5	4	4	4
	1	40	22	15	12	8	7	6	6
	2	52	29	20	15	11	9	8	7
	3	64	36	24	19	13	11	10	9
	4	76	42	29	22	15	13	11	11
0.95	5	87	48	33	25	17	14	13	12
	6	98	54	37	28	20	16	14	14
	7	109	60	41	32	22	18	16	15
	8	119	65	45	35	24	20	18	17
	9	130	71	49	38	26	21	19	18
	10	140	77	52	41	28	23	21	19
	0	38	21	15	11	8	7	9	6
	1	55	30	21	16	11	9	12	8
	2	70	38	26	20	14	12	15	10
	3	83	46	31	24	17	14	18	12
	4	96	53	36	28	19	16	21	13
0.99	5	109	59	41	31	22	18	24	15
	6	120	66	45	35	24	20	26	17
	7	132	72	49	38	26	22	29	18
	8	144	79	54	42	28	23	31	20
	9	156	85	58	45	31	25	34	21
	10	167	91	62	48	33	27	36	23

Table 4: *Values of the Operating Characteristic function for the sampling plan (n,c,t/λ_0)*

				λ/λ_0						
p^*	n	c	t/ λ_0	2	2.5	3	3.5	4	4.5	5
0.75	32	2	0.241	0.8821	0.9541	0.9804	0.9909	0.9954	0.9975	0.9986
	17	2	0.361	0.8665	0.9453	0.9758	0.9884	0.9940	0.9967	0.9981
	11	2	0.482	0.8594	0.9403	0.9728	0.9866	0.9930	0.9961	0.9977
	9	2	0.602	0.8113	0.9144	0.9591	0.9792	0.9888	0.9937	0.9962
	6	2	0.903	0.7429	0.8711	0.9334	0.9640	0.9797	0.9880	0.9927
	4	2	1.204	0.7926	0.8952	0.9449	0.9696	0.9825	0.9895	0.9935
	4	2	1.505	0.6387	0.7926	0.8801	0.9291	0.9568	0.9729	0.9825
	4	2	1.806	0.4854	0.6703	0.7926	0.8688	0.9158	0.9449	0.9632
0.95	50	2	0.241	0.7096	0.8689	0.9389	0.9699	0.9843	0.9913	0.9949
	27	2	0.361	0.6638	0.8383	0.9208	0.9595	0.9782	0.9877	0.9928
	17	2	0.482	0.6579	0.8306	0.9149	0.9555	0.9756	0.9861	0.9917
	13	2	0.602	0.6111	0.7968	0.8936	0.9425	0.9677	0.9812	0.9886
	8	2	0.903	0.5499	0.7448	0.8567	0.9181	0.9518	0.9708	0.9817
	6	2	1.204	0.4955	0.6944	0.8184	0.8911	0.9334	0.9582	0.9731
	5	2	1.505	0.4409	0.6410	0.7756	0.8595	0.9109	0.9423	0.9619
	5	2	1.806	0.2792	0.4788	0.6410	0.7572	0.8359	0.8883	0.9231
0.99	66	2	0.241	0.5459	0.7689	0.8838	0.9398	0.9675	0.9817	0.9892
	35	2	0.361	0.4989	0.7292	0.8572	0.9232	0.9573	0.9753	0.9852
	23	2	0.482	0.4582	0.6921	0.8307	0.9059	0.9462	0.9683	0.9806
	17	2	0.602	0.4242	0.6588	0.8055	0.8887	0.9349	0.9608	0.9757
	17	2	0.903	0.3109	0.5421	0.7126	0.8221	0.8892	0.9298	0.9546
	8	2	1.204	0.2681	0.4858	0.6596	0.7792	0.8567	0.9061	0.9374
	6	2	1.505	0.2866	0.4955	0.6612	0.7764	0.8523	0.9015	0.9334
	5	2	1.806	0.2792	0.4788	0.6410	0.7572	0.8359	0.8883	0.9231

The values of n and c are determined by means of operating characteristics (OC) function for given value of p^* and t/ λ_0 are displayed in Table 4 by considering the fact that $p = F(\frac{t}{\lambda_0}/\frac{\lambda}{\lambda_0})$.

The producer 's risk is the probability of rejecting a lot when $\lambda > \lambda_0$.We can compute the producer 's risk by first finding $p = F(t;\lambda)$ and then using the binomial distributi on function. For the given value of producer 's risk say 0.05 we obtain p from the sampling plan given in Table 1 subject to the condition that

$$\sum_{i=0}^{c} \binom{n}{i} {p_0}^i (1-p_0)^{n-i} \geq 0.95 \tag{37}$$

The minimum value of λ/λ_0 satisfying (37) for the sampling plan (n,c,t/ λ_0) and for the given p^* are listed in Table 5.

4.1. Explanation of the tables

Assume that the lifetime follows type 1 TLqE distribution with α=2 and q=1.1. Suppose that the experimenter is interested in establishing that the true unknown average life is at least 1000 hours with confidence p^* = 0.75. It is desired to stop the experiment at t = 602 hours. Then, for an acceptance number c = 2, the required n is 9 (Table 2) . If during 602 hours, no more than 2 failures out of 9 are observed, then the experimenter can assert that the average life is at least 1000 hours with a confidence level of 0.75. If the Poisson approximation to binomial probability is used, the value of n is 10 (Table 3) . For this sampling plan (n = 9, c = 2, t/ λ_0=0.602) under the type 1 TLqE distribution, the operating characteristic values from Table 3 are given below.
Comparing with Reliability Test Plans for Marshall- Olkin Extended Exponential distribution (see Rao et al. [15]), for α=2, acceptance number c=9, for the specified ratio t/ λ_0=0.482 and confidence level p^*=0.75, the minimum sample size is 49 using binomial approximation, whereas for type 1 TLqE distribution it is 35. Similarly , if we are considering each value of c and each vale of t/ λ_0, the scaled termination time is uniformly smaller than those for the present reliability test plans.This improvement makes the new test plan more advantageous and helps in making optimal decisions.

Table 5: *Minimum ratio of true λ and required λ_0 for the acceptability of a lot with producer's risk of 0.05 for $\alpha = 2, q = 1.1$*

p^*	c	t/ λ_0							
		0.241	0.361	0.482	0.602	0.903	1.204	1.505	1.806
0.75	0	6.6277	6.9167	7.4538	8.5749	10.0789	9.02959	10.8794	12.9175
	1	3.3083	3.3984	3.6148	3.8266	4.5121	4.9581	6.1036	5.0452
	2	2.5084	2.6096	2.6871	2.9107	3.3462	3.1597	3.8907	4.6549
	3	2.1518	2.7074	2.3305	2.3933	2.5223	2.9791	3.0960	3.6261
	4	1.9886	2.0125	2.0707	2.2308	2.3344	2.4468	2.5469	3.0898
	5	1.8547	1.9365	1.9647	2.0913	2.2343	2.4174	2.6911	2.7487
	6	1.7632	1.8542	1.8795	1.9327	2.0847	2.1529	2.3735	2.4319
	7	1.7019	1.7454	1.8105	1.8628	1.9042	2.1529	2.1756	2.2671
	8	1.6283	1.6914	1.7471	1.7379	1.8576	2.0156	2.0471	2.4124
	9	1.5945	1.6413	1.6744	1.7379	1.8576	1.8908	2.1317	2.3129
	10	1.5624	1.5946	1.6406	1.7093	1.8130	1.8908	2.0063	2.1783
0.95	0	9.2357	10.6374	11.5682	12.5609	13.9643	16.5278	16.0189	19.2227
	1	4.3401	4.7867	4.9101	5.1202	5.8541	6.0161	7.2767	7.3615
	2	3.1957	3.3984	3.5699	3.7542	4.1055	4.3640	4.8318	5.6912
	3	2.6899	2.8940	3.0059	3.1139	3.2874	3.8654	4.2043	4.4687
	4	2.4550	2.5494	2.6871	2.7369	2.9548	3.0668	3.5219	3.7152
	5	2.2687	2.3403	2.4084	2.5180	2.6971	2.8961	3.0217	3.2294
	6	2.1163	2.1899	2.2584	2.3362	2.4825	2.5905	3.0217	3.2294
	7	2.0186	2.0965	2.1290	2.1820	2.3698	2.5389	2.7524	2.9591
	8	1.9320	2.0125	2.0707	2.0913	2.3001	2.3603	2.5195	2.7204
	9	1.8547	1.9365	1.9647	2.0490	2.1721	2.3055	2.5195	2.5581
	10	1.8074	1.8806	1.9163	2.0086	2.1721	2.2019	2.3635	2.4565
0.99	0	12.2925	13.5082	13.2554	14.7459	17.3020	20.5092	20.6597	21.2298
	1	5.3685	5.5826	5.9984	6.0065	9.0097	7.6532	8.7403	9.0242
	2	3.7269	3.9328	4.1647	4.3518	6.5277	5.3182	5.4550	5.7982
	3	3.1957	3.2789	3.4039	3.4961	5.2442	4.1826	4.8318	5.0452
	4	2.7589	2.8940	3.0059	3.1819	4.6708	3.7256	3.8335	4.2262
	5	2.5084	2.6096	2.7086	2.8206	4.2051	3.3635	3.7239	3.6261
	6	2.3569	2.4134	2.5856	2.6591	3.9886	2.9791	3.2546	3.6261
	7	2.2279	2.3172	2.4084	2.4538	3.6622	2.8961	2.9504	3.3029
	8	2.1163	2.2099	2.2865	2.3251	3.4877	2.6037	2.9504	3.0234
	9	2.0498	2.1326	2.1914	2.2308	3.3462	2.5389	2.7524	2.8362
	10	1.9886	2.0619	2.1290	2.1820	3.2308	2.5389	2.5748	2.8362

Table 6: *Values of the operating characteristic function L(p) for values of $\lambda/\ \lambda_0$.*

$\lambda/\ \lambda_0$	2	2.5	3	3.5	4	4.5	5
L(p)	0.8113	0.9144	0.9591	0.9792	0.9888	0.9937	0.9962

4.2. Application

Consider the following ordered failure times of the release of a software given in terms of hours from starting of the execution of the software up to the time at which a failure of the software is occurred (see Wood [21]). This data can be regarded as an ordered sample of size n = 9 consisting of the observations $\{254, 788, 1054, 1393, 2216, 2880, 3593, 4281, 5180\}$. Let the required average lifetime be 1000 hours and the testing time be t = 602 hours, which leads to ratio of t/ λ_0 = 0.602 with a corresponding sample size n = 9 and an acceptance number c = 2, which are obtained from Table 1 for p^* = 0.75. Therefore, the sampling plan for the above sample data is (n =9, c = 2, t/ λ_0 = 0.602). Based on the observations, we have to decide whether to accept the product or reject it. We accept the product only if the number of failures before 602 hours is less than or equal to 2. However, the confidence level is assured by the sampling plan only if the given life times follow type 1 TLqE distribution. In order to confirm that the given sample is generated by lifetimes following the type 1 TLqE distribution, we have compared the sample quantiles and the corresponding population quantiles and found a satisfactory agreement. Thus, the adoption of the decision rule of the sampling plan seems to be justified. In the sample of 9 units, there is only one failure at 254 hours before t = 602 hours. Therefore we accept the product.

5. Numerical Illustration

The data consists of the number of successive failure for the air conditioning system reported of each member in a fleet of thirteen Boeing 720 jet air planes. The pooled data with 214 observations was considered by Proschan [14]. 50, 130, 487, 57, 102, 15, 14, 10, 57, 320, 261, 51, 44, 9, 254, 493, 33, 18, 209, 41, 58, 60, 48, 56, 87, 11, 102, 12, 5, 14, 14, 29, 37, 186, 29, 104, 7, 4, 72, 270, 283, 7, 61, 100, 61, 502, 220, 120, 141, 22, 603, 35, 98, 54, 100, 11, 181, 65, 49, 12, 239, 14, 18, 39, 3, 12, 5, 32, 9, 438, 43, 134, 184, 20, 386, 182, 71, 80, 188, 230, 152, 5, 36, 79, 59, 33, 246, 1, 79, 3, 27, 201, 84, 27, 156, 21, 16, 88, 130, 14, 118, 44, 15, 42, 106, 46, 230, 26, 59, 153, 104, 20, 206, 5, 66, 34, 29, 26, 35, 5, 82, 31, 118, 326, 12, 54, 36, 34, 18, 25, 120, 31, 22, 18, 216, 139, 67, 310, 3, 46, 210, 57, 76, 14, 111, 97, 62, 39, 30, 7, 44, 11, 63, 23, 22, 23, 14, 18, 13, 34, 16, 18, 130, 90, 163, 208, 1, 24, 70, 16, 101, 52, 208, 95, 62, 11, 191, 14, 71.

Table 7: *The values of estimated parameters of Dataset 1*

The model	Estimate and Standard Error (in paranthesis) of Dataset 1
Type 1 TLqE	α=1.2150 (0.2422), λ=0.0149 (0.0079), q=1.3883(0.1279)
TLE	α=0.9036 (0.0884), λ=0.0052 (0.0005)
E	λ =0.0112 (0.0008)

Table 8: *Goodness of fit of collection of different distributions for the data set.*

	AIC	CAIC	BIC	HQIC	A^*	w^*	K-S	p value	-log L
Type 1 TLqE	1964.01	1964.18	1973.60	1967.92	0.46	0.06	0.04	0.78	979.02
TLE	1968.37	1968.44	1974.74	1970.95	1.37	0.25	0.07	0.28	982.18
E	1967.47	1967.49	1970.65	1968.76	2.08	0.40	0.08	0.13	982.73

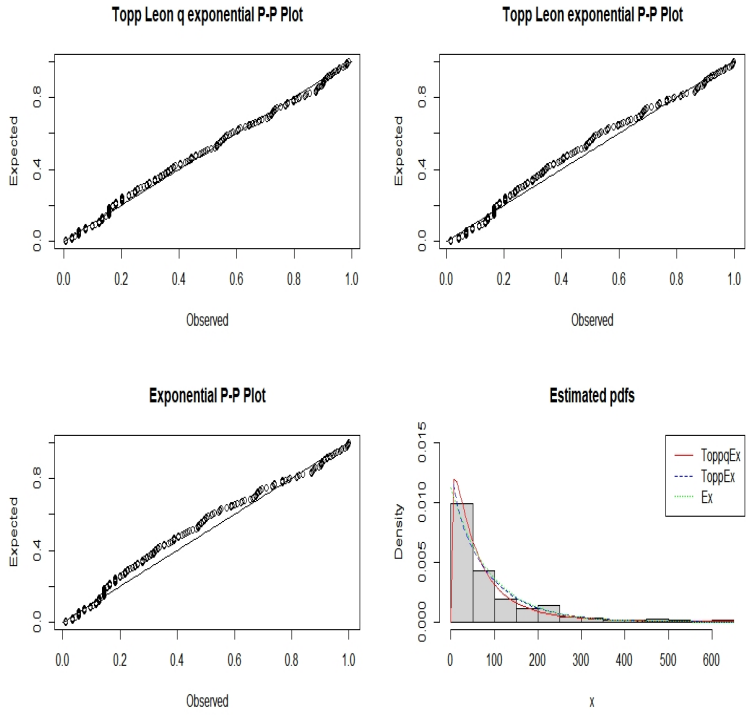

Figure 5: *The P - P plot and estimated pdf of data set.*

According to the Table 8 the type 1 TLqE model is more appropriate as compared to the TLE and exponential distribution.

6. Conclusion and future work

Introduced a quantile function associated with the type 1 Topp-Leone q-exponential distribution. The estimation of parameters of the model using $L-$moments is studied. Also, a reliability test plan was derived on the basis that the lifetime distribution of the test item follows the type 1 TLqE distribution. Besides, we find the minimum sample size needed for the acceptance or rejection of a lot based on percentiles. Some useful tables were provided and applied to establish the test plan. The new test plan is applied to illustrate its use in industrial contexts. We proved empirically the importance and flexibility of the new model in the model building by using a real data set. One can develop a parallel theory for type 2 TLqE distribution using the type 2 beta generated form given in Sebastian et al. [18].

Acknowledgement

The authors have no conflict of interest to declare. The first author would like to thank the Research Council, St Thomas College, Thrissur for the financial assistance for this work under project number F.No.STC/SANTHOME/SEEDMONEY/2020-21/09.

References

[1] Gell-Mann, M. and Tsallis, C. (Eds.) Nonextensive Entropy: Interdisciplinary Applications, Oxford University Press, New York, 2004.

[2] Ghitany M. E. , Kotz, S. And Xie, M. (2005). On some reliability measures and their stochastic orderings for the Topp-Leone distribution, *Journal of Applied Statistics*, 32(7): 715-722.

[3] Hosking, J. R. (1990). $L-$Moments: Analysis and Estimation of Distributions Using Linear Combinations of Order Statistics. *Journal of the Royal Statistical Society: Series B (Methodological)*, 52: 105-124.

[4] Jose, K. K., Joseph, J. (2018). Reliability test plan for the gumbel-unifor m distribution. *Stochastics and Quality Control*, 33(1): 71-81.

[5] Joseph, J., Jose, K. K. (2021). Reliability Test Plan for Gumbel-Par eto Life Time Model. *International Journal of Statistics and Reliability Engineering*, 8(1): 121-131.

[6] Kantam, R. R. L., Rosaiah, K. and Rao, G. S. (2001). Acceptance sampl ing based on life tests: log-logistic model, *Journal of Applied Statistics*, 28 (1): 121-128.

[7] Kotz, S. and Seier, E. (2007). Kurtosis of the Topp-Leone distributions. *Interstat*, 1: 1-15.

[8] Kumarasw amy, P. (1980). Generalized probability density-function for double-bounded random processes. *Journal of Hydrology*, 46: 79-88.

[9] Lee, C., Famo ye, F. and Alzaatr eh, A. Y. (2013). Methods of generating families of univ ariate continuous distributions in the recent decades. *WIREs Comput Stat*, 5: 219-238.

[10] Nadarajah, S. and Kotz, S. (2003). Moments of some J-shaped distributions. *Journal of Applied Statistics*, 30: 311-317.

[11] Nair, N. Unnikrishnan, Sankaran, P. G. and Balakrishnan, N. Quantile-Based Reliability Analysis: Statistics for Industr y and Technology . Springer , Ne w York, 2013.

[12] Papke, L. and Wooldridge, J. (1996). Econometric Methods for Fractional Response Variables with an Application to 401(K) Plan Participation Rates, *Journal of Applied Econometrics*, 11(6): 619-632.

[13] Picoli, S., Mendes, R. S. and Mal acar ne, L. C. (2003). q-exponential, Weibull and q- Weibull distributions: an empirical analysis, *Physica A*, 324(3): 678-688.

[14] Proschan, F. (1963). Theor etical explanation of obser ved decr easing failur e rate. *Technometrics*, 5(3): 375-383.

[15] Rao, S. G., Ghitany , M. E., Kantam, R. R. L. (2009). Reliability Test Plans for Marshall-Olkin Extended Exponential Distribution, *Applied Mathematical Sciences*, 3 (55): 2745-2755.

[16] Sangsanit, Y. and Bodhisuw an, W. (2016). The topp-leone generator of distributions: proper - ties and infer ences. *Songklanakarin Journal of Science and Technology*, 38(5): 537-548.

[17] Sebastian, N. Rasin R. S. and Silviy a P. O. (2019). Topp-Leone Generator Distributions and its Applications, *Proceedings of National Conference on Advances in Statistical Methods*, 127-139.

[18] Sebastian, N., Nair, S. S. and Joseph, D. P. (2015). An Overvie w of the Pathw ay Idea and Its Applications in Statistical and Physical Sciences, *Axioms*, 4(1): 530-553.

[19] Tsallis, C. (1988). Possible generalizations of Boltzmann-Gibbs statistics, *Journal of Statistical Physics*, 52: 479-487.

[20] Topp, C. W. and Leone, F. C. (1955). A family of J-shaped frequency function. *Journal of the American Statistical Association*, 50(269): 209-219.

[21] Wood, A. (1996). Predicting softw are reliability , *IEEE Transactions on Software Engineering*, 22: 69-77.

Single Server Retrial Queueing System with Catastrophe

Neelam Singla [1] and Ankita Garg[2*]

[1] Department of Statistics, Punjabi University, Patiala-India, neelgagan2k3@pbi.ac.in
[2*] Department of Statistics, Punjabi University, Patiala-India, gargankita095@gmail.com

Abstract

The present paper analyses a retrial queueing system with Catastrophe. Primary and secondary customers follow Poisson processes. Inter arrival and service times are Exponentially distributed. Catastrophe occurs on a busy server and follows Poisson process. The server is sent for repair after its failure. The repair times are also Exponentially distributed. Steady state and time dependent solutions for number of customers in the system when the server is idle or busy are obtained. The probability of the server being under repair is obtained. Some performance measures are also evaluated. Numerical results are obtained and represented graphically.

Keywords: Queueing, Retrial, Catastrophe, Repair.

1. Introduction

We have seen in many real life situations that sometimes a customer on arrival does not get the service instantly. So he tries for the service after some random amount of time which is popularly known as retrial. Retrial queue is a model of this kind of system if the server is not free, the customer leaves the service area and joins the virtual queue known as orbit. Thereafter it retries from the orbit after a random amount of time to get service. The queueing systems with these repeated attempts have been used in many field such as telecommunication, computer networks, data transmission, etc. The analysis of such systems lead to the identificatio of a new class of queueing systems known as retrial queueing systems.
For example: In call centers where when customers call, if they are able to reach a live negotiator immediately, they are answered else they repeat the call after a couple of minutes.
The work on retrial queues in its early stages can be found in [1]. In [2] the author discussed some important single server retrial queueing models and represented analytic results. In [3] the single server retrial queue with finit number of sources is analyzed and customer 's arrival distribution, busy period and waiting time process is established. Time dependent probabilities for exact number of arrivals and departures from the system when the server is free or busy are obtained in [4]. An explanation of the retrial queueing system is shown in the following diagram.

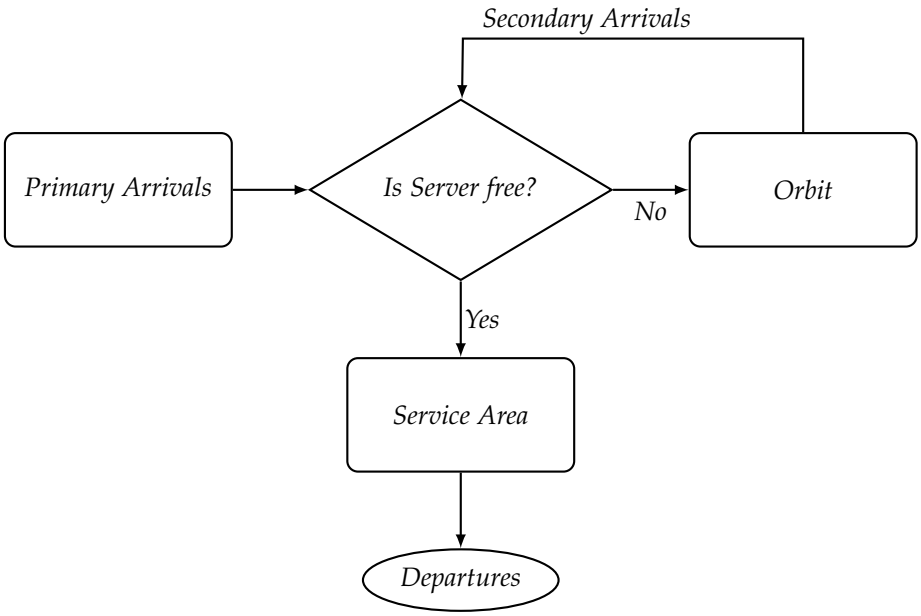

Figure 1: *Basic Structure of Retrial Queueing System*

Recently, a new concept of catastrophe has been introduced in queueing systems. The word catastrophe refers to a sudden, unexpected failure of a machine, computer network, electronic system, communication system, etc. Catastrophes occur randomly, eradicating all customers present in the system and temporarily inactivating the service facilities. Catastrophe resets the system from current state to zero state at random time intervals. Catastrophe may come from outside the system or from another service station. Retrial queueing models with catastrophe have applications in call centers, computer networks and in telecommunication systems that depend on satellites. In population dynamics, catastrophe can be considered as the natural disasters such as floods storms, etc. On the other hand when we talk of catastrophe in queueing systems, it deletes all the customers present there and causes breakdown of the server. A basic example of retrial queueing system with catastrophe is in call centers where if customers are able to reach a live negotiator immediately upon making a call, they are answered else they repeat the call after a couple of minutes. Furthermore, loss of all the customers and inactivation of the server will take place as a result of an incidental power failure or a virus attack. The diagram below shows the retrial queue with catastrophe.

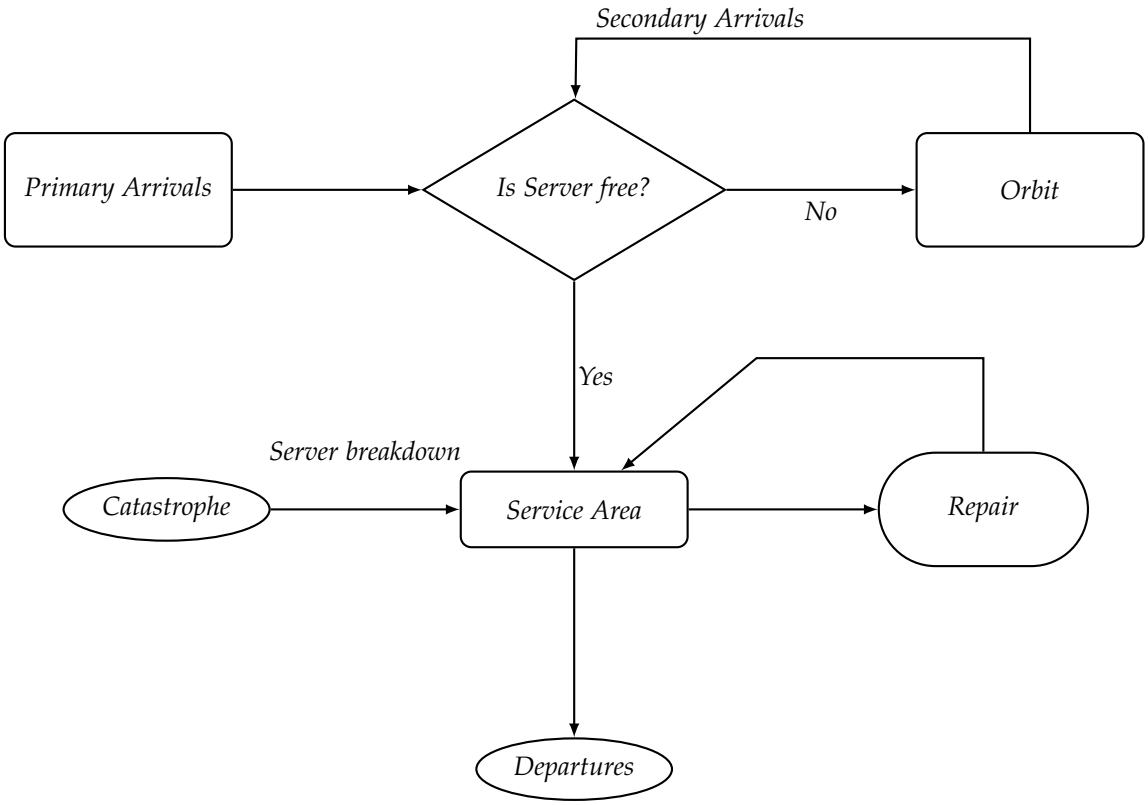

Figure 2: *Basic Structure of a Retrial Queueing System with Catastrophe*

The initial work on catastrophe occurring in a simple Markovian queue could be referred from [5] and [6]. In [7] the author discussed mean queue length and the asymptotic behavior of the probability of server being free. Also the steady state probabilities are obtained. The transient solution for the system with server failure and non-zero repair time on M/M/1 queueing system with catastrophe is obtained by [8] .

In this research paper when a server fails, it is sent for repair immediately and after getting repaired, the server comes back to its working position and the system becomes ready to accept new customers.

The paper has been organized in the following sections.

In section 2 the complete mathematical description of the model is defined Also, the difference-differential equations are derived in this section. Steady-state solution of the model along with the expected number of customers in the system is given in section 3. In section 4 the transient state probabilities and the probability of server being under repair are obtained. In section 5 verificatio of results is given. The numerical results are obtained and represented graphically in section 6. In section 7 the busy period probabilities of system and the server are obtained numerically and presented graphically . Section 8 discusses the conclusion and finall the references are listed.

2. Model Description

In this paper , a single server retrial queueing system with catastrophe is considered. In this system, the customers arrive according to Poisson process. On arrival if a customer find the server busy , he joins the orbit and retries from the orbit. These retrials are considered to be secondary arrivals. Catastrophe occurs on a busy server following Poisson process. It is assumed that the catastrophe occurs only when the system is non-empty and the server is busy . It has no effect on the system when the system is empty . Catastrophe makes system empty and also causes breakdown of the server. Once the system becomes empty and the server breaks down, it

is sent for repair immediately . Further, it is assumed that during the repair time no arrival can take place.

Assumptions : The assumptions underlying the model are listed below.

- Arrival Process: The primary customers arrive at the system according to Poisson process with mean arrival rate λ.
- Retrial Process: The secondary customers arrive at the system according to Poisson process with mean arrival rate θ.
- Service Process: The service times are Exponentially distributed with parameter μ.
- Catastrophe: Catastrophe occur at the system according to Poisson process with rate ξ.
- Repair: The repair time is Exponentially distributed with parameter τ.

The input flow of primary calls, intervals between repetitions, service times, catastrophes and repair times are statistically independent.

Shift operator E is used to increase the value of argument x by h so that $Ef(x) = f(x+h)$, $E^2 f(x) = E[Ef(x)] = E[f(x+h)] = f(x+2h)$ and so on. Here h is the equal interval of spacing. Laplace transformation $\bar{f}(s)$ of $f(t)$ is given by:

$$\bar{f}(s) = \int_0^\infty e^{-st} f(t)dt, \quad Re(s) > 0;$$

The Laplace inverse of

$$\frac{Q(p)}{P(p)} = \sum_{k=1}^{n} \sum_{l=1}^{m_k} \frac{t^{m_k - l} e^{a_k t}}{(m_k - l)!(l-1)!} \times \frac{d^{l-1}}{dp^{l-1}} \left(\frac{Q(p)}{P(p)} \right) (p - a_k)^{m_k} \quad \forall p = a_k, \quad a_i \neq a_k \; for \; i \neq k$$

where

$$P(p) = (p - a_1)^{m_1} (p - a_2)^{m_2} ..... (p - a_n)^{m_n}$$

Q(p) is a polynomial of degree $< m_1 + m_2 + m_3 + ... + m_n - 1$

$$If \;\; L^{-1}\{f(s)\} = F(t) \;\; and \;\; L^{-1}\{g(s)\} = G(t) \;\; then$$
$$L^{-1}\{f(s)g(s)\} = \int_0^t F(u)G(t-u)du = F * G$$

$F * G$ is called the convolution of F and G.

2.1. Notations

$P_{n,0}(t)$ = Probability that there are n customers in the system at time t and the server is free.
$P_{n,1}(t)$ = Probability that there are n customers in the system at time t and the server is busy.
$Q(t)$ = Probability that the server is under repair at time t.
$P_n(t)$ = Probability that there are n customers in the system at time t.

$$P_n(t) = P_{n,0}(t) + P_{n,1}(t) \;\; \forall \; n \geq 0;$$
$$and \qquad P_{n,1}(t) = 0 \;\; for \; n = 0;$$

Initially

$$P_{0,0}(0) = 1; \qquad P_{n,0}(0) = 0, \; n \neq 0; \qquad P_{n,1}(0) = 0, \;\; \forall n; \qquad Q(0) = 0 \; ;$$

2.2. The Difference-Differential equations governing the system are:

$$\frac{d}{dt}P_{n,0}(t) = -(\lambda + n\theta)P_{n,0}(t) + \mu P_{n+1,1}(t) \qquad n \geq 1 \qquad (1)$$

$$\frac{d}{dt}P_{0,0}(t) = -\lambda P_{0,0}(t) + \tau Q(t) + \mu P_{1,1}(t) \qquad (2)$$

$$\frac{d}{dt}P_{n,1}(t) = -(\lambda + \mu + \xi)P_{n,1}(t) + \lambda P_{n-1,0}(t) + \lambda P_{n-1,1}(t)(1 - \delta_{n,1}) + n\theta P_{n,0}(t) \quad n \geq 1 \qquad (3)$$

$$\frac{d}{dt}Q(t) = -\tau Q(t) + \xi \sum_{n=1}^{\infty} P_{n,1}(t) \qquad (4)$$

where

$$\delta_{n,1} = \begin{cases} 1, \text{ when } n = 1 \\ 0, \text{ other wise} \end{cases}$$

3. The steady-state difference equations governing the system

Taking $P_n(t) \to P_n$ and $\frac{d}{dt}P_n(t) \to 0$ as $t \to \infty$

$$(\lambda + n\theta)P_{n,0} = \mu P_{n+1,1} \qquad n \geq 1 \qquad (5)$$

$$\lambda P_{0,0} = \mu P_{1,1} + \tau Q \qquad (6)$$

$$(\lambda + \mu + \xi)P_{n,1} = \lambda P_{n-1,0} + \lambda P_{n-1,1}(1 - \delta_{n,1}) + n\theta P_{n,0} \qquad n \geq 1 \qquad (7)$$

$$\tau Q = \xi \sum_{n=1}^{\infty} P_{n,1} \qquad (8)$$

where

$$\delta_{n,1} = \begin{cases} 1, \text{ when } n = 1 \\ 0, \text{ other wise} \end{cases}$$

3.1. Steady-state solution of the problem

Using $Ef(x) = f(x+1)$, equations (5) and (7) are represented as

$$[(\lambda + (n+1)\theta)E]P_{n,0} - \mu E^2 P_{n,1} = 0 \qquad n \geq 2 \qquad (9)$$

$$[\lambda + ((n+1)\theta)E]P_{n,0} + [\lambda - (\lambda + \mu + \xi)E]P_{n,1} = 0 \qquad n \geq 2 \qquad (10)$$

In order to find the solution of the above system of equations, we need

$$E[\mu(n+1)\theta E^2 - (\lambda(\lambda + (n+1)\theta + \xi) + \theta((n+1)(\mu + \xi)))E + \lambda(\lambda + (n+1)\theta)] = 0 \quad n \geq 2 \qquad (11)$$

The values of $P_{n,0}$ and $P_{n,1}$ are given by

$$P_{n,0} = \sum_{i=0}^{2} a_i z_i^n \qquad n \geq 2$$

$$P_{n,1} = \sum_{i=0}^{2} b_i z_i^n \qquad n \geq 2$$

where z_0, z_1, z_2 are the roots of (11) with $z_0 = 0$ and a_i,b_i, $i = 0, 1, 2$ are the arbitrary constants to be evaluated. Other two roots of the equation (11) are given by

$$z_1, z_2 = \frac{1}{2\mu(\theta + n\theta)}\left\{\left(\lambda(\lambda + (n+1)\theta + \xi) + \theta((n+1)(\mu+\xi))\right) \pm \left[2\theta^2(\mu\xi - \mu\lambda + \xi\lambda) + 2n\theta^2(\mu^2 + \xi^2 + \lambda^2 + 2\mu\xi - 2\mu\lambda + 2\xi\lambda) + 2\lambda^2(2\theta\xi - \mu\theta) + 2n\lambda^2(2\theta\xi + \theta\lambda - \theta\mu) + 2\theta\mu\xi\lambda(n+1) + \lambda^2(\xi^2 + \theta^2 + \lambda^2) + 2\lambda^3(\theta + \xi) + 2\xi^2\theta\lambda(n+1) + \theta^2(\mu^2 + \xi^2)\right]^{1/2}\right\} \quad (12)$$

Clearly the root z_1 is always greater than 1 and the root z_2 is always less than 1. For the convergence of a solution, a root greater than or equal to 1 must be rejected. So when $z_i \geq 1$, a_i and b_i are taken as equal to zero.
Since here z_1 is greater than 1, so we take $a_1 = b_1 = 0$
As $z_0 = 0$ and $a_1 = b_1 = 0$, therefore the values of $P_{n,0}$ and $P_{n,1}$ are given by

$$P_{n,0} = a_2 z_2^n \qquad n \geq 2 \quad (13)$$

$$P_{n,1} = b_2 z_2^n \qquad n \geq 2 \quad (14)$$

From equations (5) and (7) for n=1 the probabilities $P_{1,0}$ and $P_{1,1}$ are given by

$$P_{1,0} = \frac{\mu}{(\lambda+\theta)}P_{2,1} = \frac{\mu}{(\lambda+\theta)}b_2 z_2^2 \quad (15)$$

$$P_{1,1} = \frac{\lambda}{\lambda+\mu+\xi}P_{0,0} + \frac{\mu\theta}{(\lambda+\mu+\xi)(\lambda+\theta)}b_2 z_2^2 \quad (16)$$

By substituting the above values in equation (7) for $n = 2$ and for $n = 3$, we have

$$b_2 z_2^2 = \frac{\mu\lambda}{(\lambda+\theta)(\lambda+\mu+\xi)}\left(1 + \frac{\theta}{\lambda+\mu+\xi}\right)b_2 z_2^2 + \frac{\lambda^2}{(\lambda+\mu+\xi)^2}P_{0,0} + \frac{2\theta}{\lambda+\mu+\xi}a_2 z_2^2 \quad (17)$$

$$b_2 z_2^3 = \frac{\lambda}{\lambda+\mu+\xi}\left(1 + \frac{2\theta}{\lambda+\mu+\xi}\right)a_2 z_2^2 + \frac{\mu\lambda^2}{(\lambda+\theta)(\lambda+\mu+\xi)^2}\left(1 + \frac{\theta}{\lambda+\mu+\xi}\right)b_2 z_2^2 + \frac{3\theta}{\lambda+\mu+\xi}a_2 z_2^3 + \left(\frac{\lambda}{\lambda+\mu+\xi}\right)^3 P_{0,0} \quad (18)$$

On solving equations (17) and (18) we get

$$a_2 = \frac{\left(\frac{\lambda}{\lambda+\mu+\xi}\right)^2\left[\left(\frac{\lambda}{\lambda+\mu+\xi}\right)B - A\right]}{z_2^2\left[2AC - B\left(\frac{\lambda}{\lambda+\mu+\xi}(1+2C) + 3z_2 C\right)\right]}P_{0,0} \quad (19)$$

$$b_2 = \frac{1}{Bz_2^2}\left\{\frac{2C\left(\frac{\lambda}{\lambda+\mu+\xi}\right)^2\left[B\left(\frac{\lambda}{\lambda+\mu+\xi}\right) - A\right]}{2AC - B\left(\frac{\lambda}{\lambda+\mu+\xi}(1+2C) + 3z_2 C\right)} + \left(\frac{\lambda}{\lambda+\mu+\xi}\right)^2\right\}P_{0,0} \quad (20)$$

and the value of $P_{0,0}$ can be found by using the relation

$$P_{0,0} + \sum_{n=1}^{\infty}(P_{n,0} + P_{n,1}) + Q = 1$$

After simplificatio

$$P_{0,0} = \Bigg\{1 + \left(1+\frac{\xi}{\tau}\right)\left(\frac{\lambda}{\lambda+\mu+\xi}\right) + \left(\frac{\mu}{\lambda+\theta} + \left(1+\frac{\xi}{\tau}\right)\left(\frac{\mu\theta}{(\lambda+\theta)(\lambda+\mu+\xi)}\right)\right)$$
$$\left[\frac{2C\left(\frac{\lambda}{\lambda+\mu+\xi}\right)^2\left[B\left(\frac{\lambda}{\lambda+\mu+\xi}\right)-A\right]}{2ABC - B^2\left(\frac{\lambda}{\lambda+\mu+\xi}(1+2C)+3z_2C\right)} + \frac{1}{B}\left(\frac{\lambda}{\lambda+\mu+\xi}\right)^2\right]$$
$$+\frac{1}{1-z_2}\left[\frac{\left(\frac{\lambda}{\lambda+\mu+\xi}\right)^2\left[\left(\frac{\lambda}{\lambda+\mu+\xi}\right)B-A\right]}{\left(2AC - B\left(\frac{\lambda}{\lambda+\mu+\xi}(1+2C)+3z_2C\right)\right)}\right]$$
$$+\frac{1+\frac{\xi}{\tau}}{1-z_2}\left[\frac{2C\left(\frac{\lambda}{\lambda+\mu+\xi}\right)^2\left[B\left(\frac{\lambda}{\lambda+\mu+\xi}\right)-A\right]}{2ABC - B^2\left(\frac{\lambda}{\lambda+\mu+\xi}(1+2C)+3z_2C\right)} + \frac{1}{B}\left(\frac{\lambda}{\lambda+\mu+\xi}\right)^2\right]\Bigg\}^{-1} \tag{21}$$

wher e

$$A = z_2 - \frac{\mu\lambda^2}{(\lambda+\theta)(\lambda+\mu+\xi)^2}\left(1+\frac{\theta}{\lambda+\mu+\xi}\right)$$
$$B = 1 - \frac{\mu\lambda}{(\lambda+\theta)(\lambda+\mu+\xi)}\left(1+\frac{\theta}{\lambda+\mu+\xi}\right)$$
$$C = \frac{\theta}{\lambda+\mu+\xi}$$

Hence by using the values of a_2, b_2 and $P_{0,0}$, the probabilities $P_{n,0}$, $P_{n,1}$ and Q are completely known for various values of n.

3.2. Expected number of customers in the system

Expected number of customers in the system is giv en by

$$L_s = L_{s,0} + L_{s,1}$$

wher e
$L_{s,0}$ denotes the expected number of customers in the system when the ser ver is free.
Ther efor e, by definitio of expectation

$$\begin{aligned} L_{s,0} &= \sum_{n=1}^{\infty} nP_{n,0} \\ &= P_{1,0} + \sum_{n=2}^{\infty} nP_{n,0} \\ &= P_{1,0} + a_2 \sum_{n=2}^{\infty} nz_2^n \\ &= P_{1,0} + a_2 z_2\left[\frac{1}{(1-z_2)^2} - 1\right] \end{aligned} \tag{22}$$

Similarly
$L_{s,1}$ denotes the expected number of customers in the system when the ser ver is busy.

$$L_{s,1} = P_{1,1} + b_2 z_2\left[\frac{1}{(1-z_2)^2} - 1\right] \tag{23}$$

By using (24) and (25)

$$L_s = P_{1,0} + P_{1,1} + (a_2 + b_2)\left(\frac{1}{(1-z_2)^2} - 1\right)z_2$$
$$= P_1 + (a_2 + b_2)\left(\frac{1}{(1-z_2)^2} - 1\right)z_2 \tag{24}$$

4. Laplace transform of difference-differential equations

Using the Laplace transfor mation $\tilde{f}(s)$ of $f(t)$ giv en by

$$\tilde{f}(s) = \int_0^\infty e^{-st} f(t)dt, \quad Re(s) > 0;$$

in the equations (1)-(4) along with the initial conditions, we have

$$(s+\lambda+n\theta)\tilde{P}_{n,0}(s) = \mu\tilde{P}_{n+1,1}(s) \qquad n \geq 1 \tag{25}$$
$$(s+\lambda)\tilde{P}_{0,0}(s) - 1 = \tau\tilde{Q}(s) + \mu\tilde{P}_{1,1}(s) \tag{26}$$
$$(s+\lambda+\mu+\xi)\tilde{P}_{n,1}(s) = \lambda\tilde{P}_{n-1,0}(s) + \lambda\tilde{P}_{n-1,1}(s)(1-\delta_{n,1}) + n\theta\tilde{P}_{n,0}(s) \quad n \geq 1 \tag{27}$$
$$(s+\tau)\tilde{Q}(s) = \xi\sum_{n=1}^{\infty}\tilde{P}_{n,1}(s) \tag{28}$$

wher e

$$\delta_{n,1} = \begin{cases} 1, \text{when } n = 1 \\ 0, \text{other wise} \end{cases}$$

4.1. Transient solution of the Problem

Solving equations (25)-(28) recursiv ely, we have

$$\tilde{P}_{0,0}(s) = \frac{1}{(s+\lambda)} + \frac{\tau}{(s+\lambda)}\tilde{Q}(s) + \frac{\mu}{(s+\lambda)}\tilde{P}_{1,1}(s) \tag{29}$$
$$\tilde{P}_{n,0}(s) = \frac{\mu}{s+\lambda+n\theta}\left[\sum_{k=1}^{n+1}\left(\frac{\lambda}{s+\lambda+\mu+\xi}\right)^{n-k+1}\eta_k'(s)\tilde{P}_{k,0}(s) + \left(\frac{\lambda}{s+\lambda+\mu+\xi}\right)^{n}\tilde{P}_{1,1}(s)\right] \qquad n \geq 1 \tag{30}$$

wher e

$$\eta_k'(s) = \begin{cases} 1 & \text{if } k = 1 \\ 1 + \frac{k\theta}{s+\lambda+\mu+\xi} & \text{if } k = 2 \text{ to } n \\ \frac{k\theta}{s+\lambda+\mu+\xi} & \text{if } k = n+1 \end{cases}$$

$$\tilde{P}_{1,1}(s) = \frac{\lambda}{s+\lambda+\mu+\xi}\left[\frac{1}{(s+\lambda)} + \frac{\tau}{(s+\lambda)}\tilde{Q}(s) + \frac{\mu}{(s+\lambda)}\tilde{P}_{1,1}(s)\right] + \frac{\theta}{s+\lambda+\mu+\xi}\tilde{P}_{1,0}(s) \tag{31}$$
$$\tilde{P}_{n,1}(s) = \sum_{k=1}^{n}\left[\left(\frac{\lambda}{s+\lambda+\mu+\xi}\right)^{n-k}\eta_k'(s)\tilde{P}_{k,0}(s)\right] + \left(\frac{\lambda}{s+\lambda+\mu+\xi}\right)^{n-1}\tilde{P}_{1,1}(s) \qquad n \geq 2 \tag{32}$$

wher e

$$\eta_k'(s) = \begin{cases} 1 & \text{if } k = 1 \\ 1 + \frac{k\theta}{s+\lambda+\mu+\xi} & \text{if } k = 2 \text{ to } n-1 \\ \frac{k\theta}{s+\lambda+\mu+\xi} & \text{if } k = n \end{cases}$$

$$\bar{Q}(s) = \frac{\xi}{(s+\tau)} \sum_{n=1}^{\infty} \bar{P}_{n,1}(s) \tag{33}$$

Taking the Inverse Laplace transfor m of equations of (29)-(33), we have

$$P_{0,0}(t) = e^{-\lambda t} + \tau e^{-\lambda t} * Q(t) + \mu e^{-\lambda t} * P_{1,1}(t) \tag{34}$$

$$\begin{aligned} P_{n,0}(t) = {} & \mu\lambda^n e^{-(\lambda+n\theta)t}\left[\frac{1}{(\mu+\xi)^n} - e^{-(\mu+\xi)t}\sum_{r=0}^{n-1}\frac{t^r}{r!}\frac{1}{(\mu+\xi)^{n-r}}\right] * P_{1,0}(t) + e^{-(\lambda+n\theta)t}\sum_{k=2}^{n}\mu\lambda^{n-k+1} \\ & \left[\frac{1}{(\mu+\xi)^{n-k+1}} - e^{-(\mu+\xi)t}\sum_{r=0}^{n-k}\frac{t^r}{r!}\frac{1}{(\mu+\xi)^{n-k-r+1}}\right] * P_{k,0}(t) + e^{-(\lambda+n\theta)t}\sum_{k=2}^{n}(\mu k\theta)\lambda^{n-k+1} \\ & \left[\frac{1}{(\mu+\xi)^{n-k+2}} - e^{-(\mu+\xi)t}\sum_{r=0}^{n-k+1}\frac{t^r}{r!}\frac{1}{(\mu+\xi)^{n-k-r+2}}\right] * P_{k,0}(t) + e^{-(\lambda+n\theta)t}(n+1)\mu\theta \\ & \left[\frac{1}{(\mu+\xi)} - \frac{e^{-(\mu+\xi)t}}{(\mu+\xi)}\right] * P_{n+1,0}(t) + \mu\lambda^n e^{-(\lambda+n\theta)t}\left[\frac{1}{(\mu+\xi)^n} - e^{-(\mu+\xi)t}\sum_{r=0}^{n-1}\frac{t^r}{r!}\frac{1}{(\mu+\xi)^{n-r}}\right] \\ & * P_{1,1}(t) \qquad\qquad n \geq 1 \end{aligned} \tag{35}$$

$$\begin{aligned} P_{n,1}(t) = {} & \lambda^{n-1}e^{-(\lambda+\mu+\xi)t}\frac{t^{n-2}}{(n-2)!} * P_{1,0}(t) + e^{-(\lambda+\mu+\xi)t}\sum_{k=2}^{n-1}\lambda^{n-k}\frac{t^{n-k-1}}{(n-k-1)!} * P_{k,0}(t) + e^{-(\lambda+\mu+\xi)t} \\ & \sum_{k=2}^{n-1}(k\theta)\lambda^{n-k}\frac{t^{n-k}}{(n-k)!} * P_{k,0}(t) + n\theta e^{-(\lambda+\mu+\xi)t} * P_{n,0}(t) + \lambda^{n-1}e^{-(\lambda+\mu+\xi)t}\frac{t^{n-2}}{(n-2)!} * P_{1,1}(t) \\ & \qquad\qquad n \geq 2 \end{aligned} \tag{36}$$

$$P_{1,1}(t) = \lambda e^{-(\lambda+\mu+\xi)t} * P_{0,0}(t) + \theta e^{-(\lambda+\mu+\xi)t} * P_{1,0}(t) \tag{37}$$

$$Q(t) = \xi e^{-\tau t}\sum_{n=1}^{\infty} P_{n,1}(t) \tag{38}$$

5. Verification of Results

- Summing equations (29)-(33) over n we get,

$$\sum_{n=0}^{\infty}[\bar{P}_{n,0}(s) + \bar{P}_{n,1}(s)] + \bar{Q}(s) = \frac{1}{s}$$

and hence

$$\sum_{n=0}^{\infty}[P_{n,0}(t) + P_{n,1}(t)] + Q(t) = 1$$

which is a verificatio for our results.

6. Numerical Solution and Graphical Representation

The Numerical results are generated using MATLAB programming for the case $\rho = (\frac{\lambda}{\mu}) = 0.8$, $\eta = (\frac{\theta}{\mu}) = 0.9$, $\tau' = (\frac{\tau}{\mu}) = 0.6$, $\xi' = (\frac{\xi}{\mu}) = 0.4$. In follo wing tables, we list some significan probabilities at various time instants.

Table 1: *At time t = 1*

t	$P_{0,0}$	$P_{1,0}$	$P_{2,0}$	$P_{3,0}$	$P_{4,0}$	$P_{5,0}$	$P_{1,1}$	$P_{2,1}$	$P_{3,1}$
1	0.5904	0.0216	0.0033	0.0004	0.0001	0	0.226	0.0701	0.0161

$P_{4,1}$	$P_{5,1}$	Sum
0.0029	0.0005	0.9314

Table 2: *At time t = 5*

t	$P_{0,0}$	$P_{1,0}$	$P_{2,0}$	$P_{3,0}$	$P_{4,0}$	$P_{5,0}$	$P_{1,1}$	$P_{3,1}$	$P_{4,1}$
5	0.3644	0.0556	0.0187	0.0069	0.0032	0	0.1572	0.0489	0.0247

$P_{5,1}$	$Q(t)$	Sum
0.0145	0.2126	0.9067

Table 3: *At time t = 15*

t	$P_{0,0}$	$P_{1,0}$	$P_{3,0}$	$P_{4,0}$	$P_{5,0}$	$P_{1,1}$	$P_{2,1}$	$P_{3,1}$	$P_{4,1}$
15	0.3571	0.0528	0.0078	0.0041	0	0.1514	0.0897	0.0491	0.0274

$P_{5,1}$	$Q(t)$	Sum
0.018	0.2237	0.9811

Table 4: *At time t = 25*

t	$P_{0,0}$	$P_{1,0}$	$P_{2,0}$	$P_{3,0}$	$P_{4,0}$	$P_{5,0}$	$P_{1,1}$	$P_{2,1}$	$P_{3,1}$
25	0.3571	0.0528	0.0189	0.0078	0.0041	0	0.1514	0.0897	0.0491

$P_{4,1}$	$Q(t)$	Sum
0.0274	0.2237	0.982

Table 5: *At time t = 40*

t	$P_{0,0}$	$P_{1,0}$	$P_{2,0}$	$P_{3,0}$	$P_{5,0}$	$P_{1,1}$	$P_{2,1}$	$P_{3,1}$	$P_{4,1}$
40	0.3571	0.0528	0.0189	0.0078	0	0.1514	0.0897	0.0491	0.0274

$P_{5,1}$	$Q(t)$	Sum
0.018	0.2237	0.9959

In the following figures, the probabilities are graphed against time. Figure 3 to figure 5 are plotted for the case $\rho = 0.8$, $\eta = 0.9$, $\tau' = 0.6$, $\xi' = 0.4$.

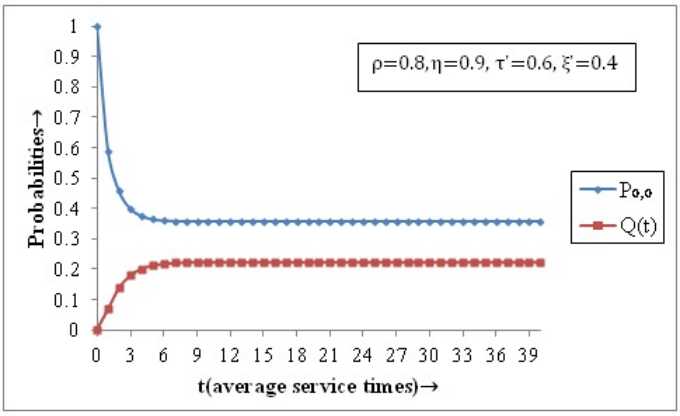

Figure 3: *Probabilities $P_{0,0}$ and $Q(t)$ against average service times t*

In figu e 3, the probabilities $P_{0,0}$ and $Q(t)$ (probability of the server being under repair) are plotted against time t. From the graph, we obser ve that the probability $P_{0,0}$ decr eases rapidly from its initial value 1 at $t = 0$ and ther eafter becomes steady . On the other hand, the probability $Q(t)$ increases in the beginning and then becomes stable.

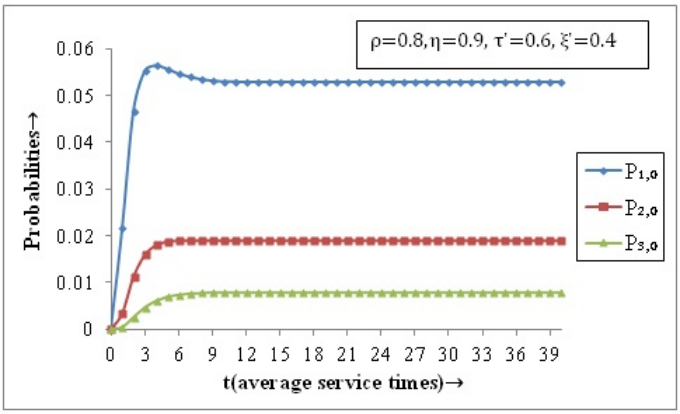

Figure 4: *Probabilities $P_{1,0}$, $P_{2,0}$ and $P_{3,0}$ against average service times t*

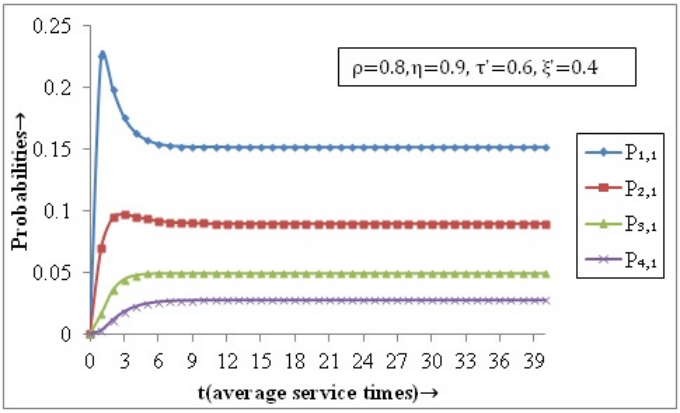

Figure 5: *Probabilities $P_{1,1}$, $P_{2,1}$, $P_{3,1}$ and $P_{4,1}$ against average service times t*

The probabilities $P_{1,0}$, $P_{2,0}$, $P_{3,0}$ are plotted against time t in figu e 4 and the probabilities $P_{1,1}$, $P_{2,1}$, $P_{3,1}$, $P_{4,1}$ are plotted against time t in figu e 5. The graphs clearly indicate that all the

probabilities increase rapidly in the beginning, gradually decline to a certain extent and finall become stable. Also, it can be seen from figu e 4 that the probability of more customers in the system achie ves a lower highest value. In addition, figu e 5 shows that the probability of ser ver being busy attains a lower steady value when there are more customers in the system.

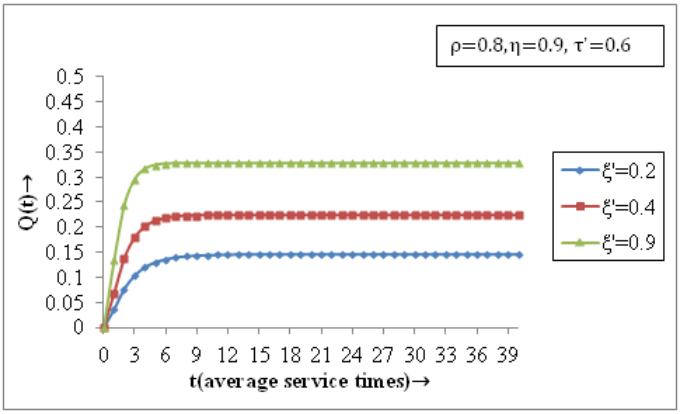

Figure 6: *Effect of change in* ξ' *on probability* $Q(t)$

In figu e 6, we study the effect of change in ξ'(catastr ophe rate per unit ser vice time) on the probability $Q(t)$(probability of ser ver being unde r repair). From the graph it can be seen that whene ver the catastr ophe rate per unit ser vice time increases, the probability $Q(t)$ also increases which is as desir ed.

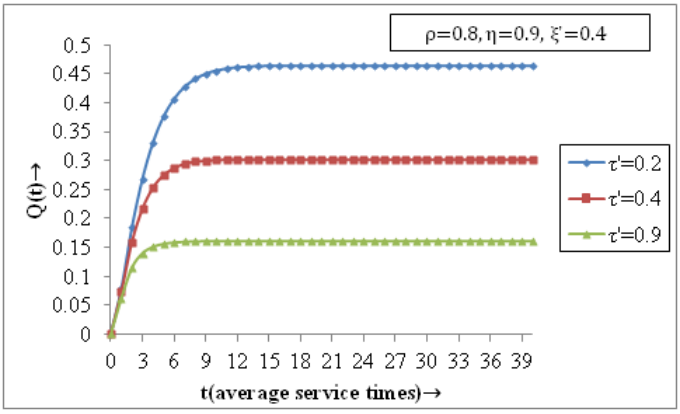

Figure 7: *Effect of change in* τ' *on probability* $Q(t)$

In figu e 7, the effect of change in τ'(repair rate per unit ser vice time) on the probability $Q(t)$ is studied. From the graph it is clearly visible that whene ver the repair rate per unit ser vice time increases, the probability $Q(t)$ decr eases.

7. Busy Period Probabilities

This section discusses the busy period probabilities of ser ver and system.
In ter ms of probability , busy ser vers are deter mined as follo ws:

$$P(Server\ is\ busy) = \sum_{n\geq 1} P_{n,1}(t) \tag{39}$$

And busy systems are deter mined as follo ws:

$$P(System\ is\ busy\ ) = \sum_{n>0} (P_{n,0}(t) + P_{n,1}(t)) + Q(t) \tag{40}$$

7.1. Numerical and Graphical Representation of Busy Period Probabilities

The numerical results are obtained using MATLAB programming and following [9]. The Probabilities of system busy and server busy are obtained for different values of ρ keeping the other parameters constant and are presented in the table below:

Table 6: *Probabilities of system busy and server busy for different values of ρ*

	Probability(System Busy)			Probability(Server Busy)		
t	$\rho = 0.4$	$\rho = 0.6$	$\rho = 0.8$	$\rho = 0.4$	$\rho = 0.6$	$\rho = 0.8$
0	0	0	0	0	0	0
1	0.1916	0.2711	0.341	0.1833	0.2548	0.3156
2	0.2361	0.3283	0.4042	0.212	0.2853	0.3434
3	0.2514	0.3463	0.4203	0.2169	0.2884	0.3432
4	0.2577	0.3525	0.4235	0.2178	0.288	0.3407
5	0.2604	0.3544	0.4229	0.2179	0.2872	0.3387
6	0.2615	0.3548	0.4217	0.2177	0.2865	0.3373
7	0.262	0.3547	0.4207	0.2176	0.2861	0.3366
8	0.2621	0.3546	0.4201	0.2175	0.2859	0.3361
9	0.2622	0.3545	0.4197	0.2175	0.2857	0.3359
10	0.2622	0.3544	0.4194	0.2174	0.2857	0.3357

A graph depicting the probabilities of server and system busy is also included.

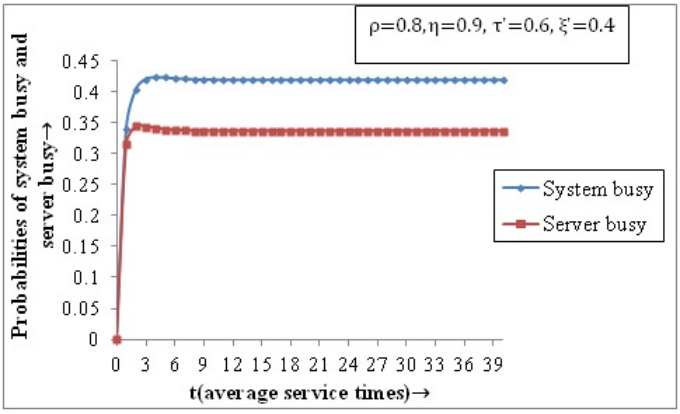

Figure 8: *Probabilities of system busy and server busy against average service times t*

In figure 8, the probabilities of system busy and server busy are plotted against time t for the case $\rho = 0.8$, $\eta = 0.9$, $\tau' = 0.6$, $\xi' = 0.4$. It is clearly visible from the graph that probability of system busy is higher than probability of server busy. Both probabilities increase rapidly in the beginning and then become stable with time.

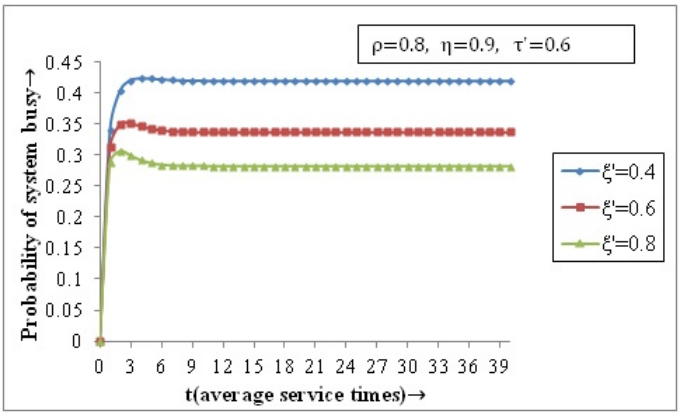

Figure 9: *Probability of system busy for different values of* ξ'

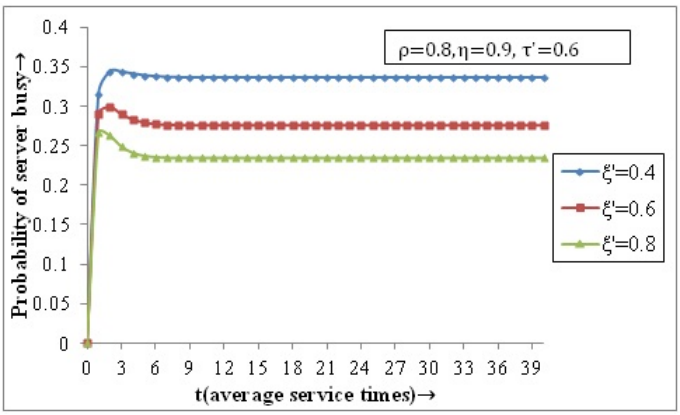

Figure 10: *Probability of server busy for different values of* ξ'

In figures 9 and 10, the probability of system busy and the probability of server busy are plotted respectively against time t for different values of ξ' keeping other parameters constant. As we know when catastrophe occurs, the server breaks down and system becomes empty. So the probability that both system and server remain busy attains lower value for greater values of catastrophe rate per unit service time.

8. Conclusion

We have modeled a single server retrial queueing system with catastrophe to quantify various performance measures and understand characteristics of related systems. The catastrophe has significan impact on businesses, computer networks, etc. It is very important to manage the risk of catastrophe for the smooth functioning of the system. In this paper, the steady-state and transient state probabilities for the number of customers in the system when the server is busy or idle are obtained by solving difference-differential equations. In addition, the probability that server is under repair is also obtained. Some performance measures are given. Numerical solutions and busy period probabilities are obtained by using MATLAB programming and presented graphically. This model is applicable in call centers, computer networks, etc.

References

[1] JW Cohen. Basic problems of telephone traffic theory and the influenc of repeated calls. *Pillips Telecomm. Rev.*, 18(2), 1900.

[2] Tao Yang and James G. C. Templeton. A survey on retrial queues. *Queueing systems*, 2(3): 201–233, 1987.

[3] Gennadi I Falin and Jesus R Artalejo. A finit source retrial queue. *European Journal of Operational Research*, 108(2):409–424, 1998.

[4] Neelam Singla and Sonia Kalra. Performance analysis of a two-state queueing model with retrials. *Journal of Rajasthan Academy of Physical Sciences*, 17:81–100, 2018.

[5] Xiuli Chao. A queueing network model with catastrophes and product form solution. *Operations Research Letters*, 18(2):75–79, 1995.

[6] Antonio Di Crescenzo, Virginia Giorno, Amelia G Nobile, and Luigi M Ricciardi. On the m/m/1 queue with catastrophes and its continuous approximation. *Queueing Systems*, 43(4): 329–347, 2003.

[7] B Krishna Kumar and D Arivudainambi. Transient solution of an m/m/1 queue with catastrophes. *Computers & Mathematics with applications*, 40(10-11):1233–1240, 2000.

[8] B Krishna Kumar, Achyutha Krishnamoorthy, S Pavai Madhesw ari, and S Sadiq Basha. Transient analysis of a single server queue with catastrophes, failures and repairs. *Queueing systems*, 56(3):133–141, 2007.

[9] Brian D Bunday. *Basic queueing theory*. Arnold, 1986.